The role of complex gangliosides in glial cell biology.

Edina Silajdžić

This thesis is submitted to the University of Glasgow in part fulfilment for the degree of Doctor of Philosophy.

November 2007

Division of Clinical Neuroscience
Beatson Laboratories
Garscube Estate
Switchback Road
Glasgow
G61 1BD

بسم الله الرحمن الرحيم

رب يسر ولا تعسر رب تمم بالخير

Acknowledgements

I am extremely grateful to all of the people who have helped me over the past few years. Firstly, I would like to thank my supervisors Prof Sue Barnett and Prof Hugh Willison for giving me the opportunity to work in their labs. I would like to thank all members of N1, past and present, including Ale, Annette, Bob, Debbie, Lynda, Mercedes, Richard, Sarah and Thomas, for making the lab experience so enjoyable. I would also like to thank all the past and present members in Hugh's lab, including Eric, John, Kay, Peter and Sue.

In am also grateful to my adviser Dr Tomoko Iwata, Fiona Fleming for taking care of the mice, all of the technology services for help with microscopes, cutting sections and FACS purification of cells, in particular Margaret O'Prey and Tom Gilbey, Eileen Brown for helping with the epithelial width measurements, John Annan for creating the macros, Colin Nixon for helping me cut sections and Peter McHardy, Iain White and John Adams for assistance with computers.

Finally, I would like to thank my family and friends, especially my Mama, Babo, and Edo, for their endless love, support and encouragement.

Table of contents

Acknowledgements i
Table of contents ii
List of figures vi
List of tables xiii
List of abbreviations xiv
Abstract xvii
Declaration xiii

CHAPTER 1 1
Introduction 1
1.1 Gangliosides 2
1.1.1 Nomenclature, structure and biosynthesis 2
1.1.2 Lipid rafts 6
1.1.3 Function of gangliosides 8
1.1.4 Ganglioside knockout mice 23
1.2 Glial cells 26
1.2.1 Astrocytes 26
1.2.2 Oligodendrocytes 34
1.2.3 Microglia 43
1.2.4 Schwann cells 43
1.3 Myelin 48
1.3.1 Node of Ranvier 49
1.3.2 Paranode 50
1.3.3 Juxtaparanode 51
1.3.4 Internode 52
1.3.5 Role of lipid rafts in myelination 52
1.3.6 Role of gangliosides in myelination 53
1.4 The olfactory system 55
1.4.1 PNS-CNS transitional zone 55
1.4.2 Anatomy of the olfactory system 56
1.4.3 Models of degeneration and regeneration 67
1.5 Aims of the thesis 69
2 CHAPTER 2 71
Methods 71
2.1 Ganglioside knockout mice 72
2.1.1 Generation of α-2,8-sialyltransferase knockout mice 72
2.1.2 Generation of N-acetylgalactosaminyl transferase knockout mice. 74
2.1.3 Generation of double knockout mice 74
2.2 Genotyping of heterozygous and GalNAc T -/- mice 76
2.2.1 Tail tip DNA extraction 76
2.2.2 GM2 primer PCR 76
2.2.3 Labelling with cholera toxin 77
2.3 Tissue culture 77
2.3.1 General tissue culture 77
2.3.2 Olfactory ensheathing cell culture 78
2.3.3 Schwann cell culture 80
2.3.4 Oligodendrocyte precursor cell culture 80
2.3.5 Dissociated spinal cord culture 81
2.4 Assays 82

2.4.1 Proliferation 82
2.4.2 Time-lapse migration 82
2.4.3 Wound assays 83
2.4.4 Axonal density and PLP labelling 85
2.5 Nasal irrigation 86
2.6 Tissue processing 86
2.6.1 Snap frozen sections 86
2.6.2 Frozen sections 86
2.6.3 Paraffin sections 87
2.7 Immunocytochemistry/immunohistochemistry 87
2.7.1 General immunocytochemistry 87
2.7.2 Bromodeoxyuridine immunocytochemistry 89
2.7.3 SMI 31 and AA3 immunocytochemistry 89
2.7.4 O4, NG2 and MBP immunocytochemistry 89
2.7.5 Neurofascin immunocytochemistry 90
2.7.6 Caspr immunocytochemistry 90
2.7.7 Sodium and potassium channel immunocytochemistry 90
2.8 Immunohistochemistry 91
2.8.1 General immunohistochemistry of frozen tissue 91
2.8.2 General immunohistochemistry on paraffin sections 91
2.8.3 PCNA and GFAP immunohistochemistry 92
2.9 Histological staining 93
2.9.1 Haematoxylin and eosin 93
2.10 Quantification of regeneration 94
2.10.1 Olfactory epithelium width assessment 94
2.10.2 Quantification of immunohistochemistry 94
2.10.3 Quantification of cell number 95
2.11 Microscopy 95
2.12 Statistical analysis 95
3 CHAPTER 3 96
Comparison of the proliferative and migratory properties of wild-type and ganglioside-knockout Schwann cells and OECs. 96
3.1 Introduction 97
3.2 Results 99
3.2.1 Mitogenic activity of known glial growth factors 99
3.2.2 Mitogenic effect of increasing acidity 101
3.2.3 Ganglioside expression of Schwann cells and OECs 104
3.2.4 Antigen profile and morphology of wild-type and ganglioside knockout cells 115
3.2.5 Proliferation of wild-type and ganglioside knockout cells 122
3.2.6 Motility of wild-type and ganglioside knockout cells 126
3.3 Discussion 133
3.3.1 Proliferaton of mouse OECs and Schwann cells 133
3.3.2 Ganglioside expression of OECs and Schwann cells 134
3.3.3 Antigen profile and morphology of wild-type and ganglioside knockout OECs and Schwann cells 137
3.3.4 Proliferation of wild-type and ganglioside knockout OECs and Schwann cells 138
3.3.5 Motility of wild-type and ganglioside knockout OECs and Schwann cells 142
3.3.6 Conclusions 143
4 CHAPTER 4 145
Degeneration and regeneration of the olfactory system in wild-type and ganglioside knockout mice 145

4.1 Introduction 146
4.2 Results 147
4.2.1 Ganglioside expression of the olfactory system. 147
4.2.2 Comparison of olfactory epithelial width 158
4.2.3 Preliminary studies of nasal $ZnSO_4$ irrigation 160
4.2.4 Gross morphological changes of the olfactory epithelium 162
4.2.5 Proliferation within the olfactory epithelium 166
4.2.6 Degeneration and regeneration of olfactory axons 169
4.2.7 Synapse formation 174
4.2.8 The astrocytic response 177
4.3 Discussion 179
4.3.1 Ganglioside expression of the olfactory system 179
4.3.2 Comparison of olfactory epithelial width 180
4.3.3 Preliminary studies of nasal $ZnSO_4$ irrigation 180
4.3.4 The response of the olfactory epithelium to nasal $ZnSO_4$ irrigation 182
4.3.5 Proliferation within the olfactory epithelium 183
4.3.6 Olfactory receptor neuron regeneration 185
4.3.7 Synapse formation 186
4.3.8 The astrocytic response 187
4.3.9 Conclusion and future studies 187
5 CHAPTER 5 189
The effect of gangliosides on oligodendrocyte differentiation and axonal-glial interactions *in vitro* 189
5.1 Introduction 190
5.2 Results 191
5.2.1 Differentiation of wild-type and Sia T -/- OPCs 191
5.2.2 Dissociated spinal cord culture: cell composition 192
5.2.3 Comparison of culture media 195
5.2.4 Ganglioside expression of dissociated spinal cord cultures. 200
5.2.5 Comparison of oligodendrocyte differentiation 215
5.2.6 Relationship between oligodendrocytes and axons 220
5.2.7 Comparison of axonal density and PLP staining 224
5.2.8 Localisation of proteins at the node of Ranvier 226
5.2.9 Comparison of astrocyte morphology 227
5.3 Discussion 240
5.3.1 Ganglioside expression of dissociated spinal cord cultures. 240
5.3.2 Differentiation of oligodendrocytes 244
5.3.3 Relationship of oligodendrocytes with axons 248
5.3.4 Comparison of axonal density and myelination 248
5.3.5 Localisation of proteins at the node of Ranvier 251
5.3.6 Conclusion 254
6 CHAPTER 6 257
General Discussion 257
References 266
1 Appendix 310
1.1 Equipment 311
1.2 General Plasticware 311
1.3 Chemicals and reagents 311
1.4 PCR reagents 313
1.4.1 Agarose gel 313
1.4.2 Loading buffer 313
1.4.3 Master Mix 313
1.4.4 PCR primers 314

1.5 Tissue culture reagents 314
1.5.1 10% FBS with heregulin and forskolin (10%HF)..... 314
1.5.2 Bottenstein-Sato's serum free media (DMEM-BS) 314
1.5.3 Collagenase..... 314
1.5.4 Differentiation Medium..... 314
1.5.5 Dubco's Modified Eagle Medium with 10% FBS (10% FBS) 315
1.5.6 Dubco's Modified Eagle Medium with 1% FBS (1% FBS) 315
1.5.7 OEC mitogen media with FBS (OMM+5%FBS) 315
1.5.8 N1 medium 315
1.5.9 Neurobasal/B27..... 315
1.5.10 Plating medium (PM)..... 316
1.5.11 SATO mix..... 316
1.5.12 Soyabean trypsin inhibitor-DNAse (SD)..... 316
1.6 Immunocytochemistry reagents 316
1.6.1 Acid Alcohol 316
1.6.2 Citric Acid Buffer, pH 6.0 316
1.6.3 4% paraformaldehyde..... 316
1.7 Macro: "percentage of BrdU positive nuclei" 317
1.8 Macro: "quantitation of PLP labelling"..... 318

List of Figures

CHAPTER 1

Figure 1.1 Ganglioside structure 4

Figure 1.2 Ganglioside conformation 4

Figure 1.3 Ganglioside biosynthesis pathway showing the effect of knocking out Sia T and GalNAc T genes 5

Figure 1.4 Regulation of growth factor receptors by gangliosides 21

Figure 1.5 Summary of oligodendrogenesis *in vivo*..... 37

Figure 1.6 Ganglioside expression of oligodendrocytes. 38

Figure 1.7 Schematic depiction of the node of Ranvier, paranode, juxtaparanode, and internode. 49

Figure 1.8. Cells of the olfactory epithelium 57

Figure 1.9. Anatomy of the olfactory system. 58

CHAPTER 2

Figure 2.1. Generation of Sia T -/- mice 73

Figure 2.2. Generation of GalNAc T -/- mice 75

Figure 2.3. Image of a wound assay showing how the width of the wound was measured. 85

Figure 2.4. OE width measurements. 94

CHAPTER 3

Figure 3.1 Schwann cell and OEC proliferation under different growth factor conditions..... 102

Figure 3.2 Effect of increasing acidity on Schwann cell and OEC proliferation..... 103

Figure 3.3 Representative images of CTx labelling of OECs. 105

Figure 3.4 Representative images of CTx labelling of Schwann cells. ... 106

Figure 3.5 Representative images of MOG35 labelling of OECs. 107

Figure 3.6 Representative images of MOG35 labelling of Schwann cells. 108

Figure 3.7 Representative images of MOG1 labelling of OECs and Schwann cells..... 109

Figure 3.8. Representative images of OEC and Schwann cell expression of R24..... 110

Figure 3.9. Representative images of MOG30 labelling of OECs and Schwann cells..... 111

Figure 3.10. Representative images of EG2 labelling of OECs and Schwann cells..... 112

Figure 3.11 Representative images of EG3 labelling of OECs and Schwann cells..... 112

Figure 3.12 Ganglioside expression of contaminating cells in OEC cultures 113

Figure 3.13 Ganglioside expression of contaminating cells in Schwann cell cultures. 114

Figure 3.14 Morphology of wild-type and ganglioside knockout OECs grown in DMEM-BS. 116

Figure 3.15 Morphology of wild-type and ganglioside knockout OECs grown in OMM+5%FBS..... 117

Figure 3.16 Morphology of wild-type and ganglioside knockout Schwann cells grown in DMEM-BS. 118

Figure 3.17 Morphology of wild-type and ganglioside knockout Schwann cells grown in 10%HF. 119

Figure 3.18 Antigen profile for wild-type, Sia T -/- and GalNAc T -/- OECs. 120

Figure 3.19. Antigen profile for wild-type, Sia T -/- and GalNAc T -/- Schwann cells..... 121

Figure 3.20. Proliferation of OECs derived from wild-type and ganglioside knockout mice. 124

Figure 3.21. Proliferation of wild-type and ganglioside knockout Schwann cells..... 125

Figure 3.22. Motility of wild-type and ganglioside knockout OECs..... 127

Figure 3.23. Motility of wild-type and ganglioside knockout Schwann cells. 128

Figure 3.24 Motility of wild-type OECs and Schwann cells in a wound assay. 129

Figure 3.25 Representative images of wild-type OEC and Schwann cell motility in a wound assay. 130

Figure 3.26 Motility of wild-type and Sia T -/- OECs and Schwann cells in a wound assay. 131

Figure 3.27 Representative images of wild-type and Sia T -/- OEC and Schwann cell 132

CHAPTER 4

Figure 4.1 The olfactory system of the mouse..... 149

Figure 4.2 CTx labelling of the olfactory system. 151

Figure 4.3 CGM3 labelling of the olfactory system..... 152

Figure 4.4 EG2 labelling of the olfactory system..... 153

Figure 4.5 EG3 labelling of the olfactory system..... 154.

Figure 4.6 MOG1 labelling of the olfactory system. 155

Figure 4.7 MOG30 labelling of the olfactory system. 156

Figure 4.8 MOG35 labelling of the olfactory system. 157

Figure 4.9 Comparison of epithelial width. 159

Figure 4.10 The effect of different $ZnSO_4$ volumes and concentrations on OE width. 161

Figure 4.11 The gross morphological changes in the olfactory epithelium. 163

Figure 4.12 The change in epithelial width in 6 week old wild-type and ganglioside knockout mice. 164

Figure 4.13 The change in epithelial width in 6 month old wild-type and ganglioside knockout mice. 165

Figure 4.14 PCNA labelling in the OE of wild-type and ganglioside knockout mice. 167

Figure 4.15 Comparison of PCNA positive cells in the OE of wild-type and ganglioside knockout mice. 168

Figure 4.16 SMI 31 labelling of 6 week old olfactory tissue. 170

Figure 4.17 The degeneration of axons of the olfactory nerve in 6 week old mice 171

Figure 4.18 The degeneration of olfactory receptor neurons in 6 week old mice. 172

Figure 4.19 The degeneration of olfactory receptor neurons in 6 month old mice. 173

Figure 4.20 Synaptophysin labelling in the glomeruli of 6 week old..... 175

Figure 4.21 The degeneration of synapses in 6 week old wild-type and ganglioside knockout mice. 176

Figure 4.22 The astrocytic response to nasal irrigation in wild-type and ganglioside knockout mice. 178

CHAPTER 5

Figure 5.1 OPCs isolated from Sia T -/- mice did not express A2B5 but were able to differentiate into O4 expressing oligodendrocytes... 193

Figure 5.2 Cell composition of dissociated spinal cord cultures at 7 DIV. 194

Figure 5.3 Antigenic profile of oligodendrocytes in differentiation and neurobasal media. 197

Figure 5.4 Wild-type spinal cord culture at 28 DIV in differentiation and neurobasal media. 198

Figure 5.5 Axonal density and PLL labelling in spinal cord cultures grown in either “differentiation” or “neurobasal” media. 199

Figure 5.6 Ganglioside expression of dissociated spinal cord cultures from wild-type, Sia T -/- and GalNAc T -/- mice. 204

Figure 5.7 A2B5 co-localised with SMI 31, TUJ1, GFAP and NG2 in wild-type cultures at 21 DIV. 205

Figure 5.8 R24 expression in wild-type and GalNAc T -/- cultures at 21 DIV. 206

Figure 5.9 A2B5 and R24 were not expressed by myelinating oligodendrocytes at 28 DIV 209

Figure 5.10 CTx co-localises with SMI 31 in wild-type cultures at 21 DIV. 210

Figure 5.11 CTx co-localised with SMI 31, AA3 and O4 in wild-type cultures at 28 DIV. 211

Figure 5.12 MOG35 co-localised with SMI 31 in wild-type cultures at 21 DIV. 212

Figure 5.13 MOG35 co-localised with AA3 in wild-type cultures at 28 DIV. 213

Figure 5.14 Comparison of oligodendrocyte differentiation. 216

Figure 5.15 Wild-type spinal cord culture at 21 DIV in differentiation medium. 217

Figure 5.16 Sia T -/- spinal cord culture at 21 DIV in differentiation medium. 218

Figure 5.17 GalNAc T -/- spinal cord culture at 21 DIV in differentiation medium. 219

Figure 5.18 Relationship between oligodendrocytes and axons in wild-type cultures. 221

Figure 5.19 Relationship between oligodendrocytes and axons in Sia T -/- cultures. 222

Figure 5.20 Relationship between oligodendrocytes and axons in GalNAc T -/- cultures. 223

Figure 5.21 Axonal density and PLL labelling in wild-type, Sia T -/- and GalNAc T -/- spinal cord cultures. 224

Figure 5.22 Sodium channel clustering at nodes of Ranvier at 28 DIV 225

Figure 5.23 The paranodal localisation of Caspr 226

Figure 5.24 The paranodal localisation of neurofascin 155 228

Figure 5.25 The paranodal and juxtaparanodal localisation of $K_v1.2$ 234

Figure 5.26 Juxtaparanodal localisation of $K_v1.2$ in wild-type cultures at 28 DIV. 236

Figure 5.27 The localisation of Kv1.2 in GalNAc T -/- cultures at 30 and 32 DIV. 237

Figure 5.28 Morphology of astrocytes. 238

Figure 5.29 Representative images of astrocytes located near node of Ranvier in wild-type spinal cord cultures. 239

List of Tables

CHAPTER 2

Table 2.1 Primary antibody list..... 88

Table 2.2 Secondary antibody list..... 88

CHAPTER 3

Table 3.1 Table showing ganglioside expression of OEC and Schwann cells. 104

CHAPTER 4

Table 4.1 Ganglioside expression in the olfactory system. 150

CHAPTER 5

Table 5.1 Summary of gangliosides expression of spinal cord cultures 214

List of Abbreviations

-/-	knockout
A	2'-deoxyadenosine 5'-triphosphate
ACM	astrocyte conditioned medium
AMAN	acute motor axonal neuropathy
ATP	adenosine triphospate
BBB	blood brain barrier
BDNF	brain derived neurotrophic factor
BMP	bone morphogenetic protein
BP	base pair
BrdU	5-bromo-2'-deoxyuridine
BSA	bovine serum albumin
C	2'-deoxycytidine 5'-triphosphate
Ca^{2+}	calcium
Caspr	contactin associated protein
cDNA	cellular deoxyribonucleic acid
Cer	ceramide
CNP	2',3'-cyclic-nucleotide 3'-phosphodiesterase
CNS	central nervous system
CNTF	ciliary neurotrophic factor
CO_2	carbon dioxide
CTx	cholera toxin
DAB	diaminobenzidine
DAPI	4'-6-diamidino-2-phenylindole
DIV	days *in vitro*
DKO	double knockout
DMEM	Dulbecco's Modified Eagle Medium
dNTP	Deoxyribonucleotide triphosphate
DREZ	dorsal root entry zone
DRG	dorsal root ganglion
DTA	diphtheria toxin A
E	embryonic day
ECM	extracellular matrix
EGF	epidermal growth factor
EGFR	epidermal growth factor receptor
E-NCAM	embryonic form of polysialic acid containing N-CAM
ER	endoplasmic reticulum
ERK	extracellular signal-regulated kinase
FACS	Fluorescent Activated Cell Sorting
FAK	focal adhesion kinase
FBS	foetal bovine serum
FGF	fibroblast growth factor
FGFR	fibroblast growth factor receptor
G	2'-deoxyguanosine 5'-triphosphate
GalC	galactocerebroside
GalNAc T	ß1,4-N-acetylgalactosaminyl transferase (GM2/GD2 synthase)
GAP 43	growth associated protein 43kDa
GBC	Globose basal cells
GDNF	glial derived neurotrophic factor
GFAP	glial fibrillary acidic protein
GGF-2	glial growth factor 2
GPI	glycosylphosphatidylinositol

h	hour(s)
HBC	horizontal basal cells
125I	iodine isoform 125
IGF	insulin-like growth factors
K+	potassium
K_v	voltage-gated potassium channels
KO	knockout
L-15	Leibovitz medium
LacCer	lactosylceramide
LIF	leukaemia inhibitory factor
µM	micromoles
MAG	myelin associated glycoprotein
MAPK	mitogen-activated protein kinase
MBP	myelin basic protein
min	minute(s)
mRNA	mitochondrial ribonucleic acid
MS	multiple sclerosis
Na+	sodium
Na_v	voltage-gated sodium channels
NB	Neurobasal medium
N-cadherin	Ca^{2+} dependent cell adhesion molecule
N-CAM	neural cell adhesion molecule
NF155	155kDa isoform of neurofascin
NF186	186kDa isoform of neurofascin
NGF	nerve growth factor
NRG	neuregulin
NT	neurotrophin
OB	olfactory bulb
OE	olfactory epithelium
OEC	olfactory ensheathing cells
OMM	olfactory mitogen medium
OMP	olfactory marker protein
OPCs	oligodendrocyte progenitor cells
ORN	olfactory receptor neurons
$p75^{NTR}$	low affinity neurotrophin receptor p75
PBS	phosphate buffered saline
PC12	pheochromocytoma cell line
PCNA	proliferating cell nuclear antigen
PCR	polymerase chain reaction
PDGF	platelet-derived growth factor
PDGFR	platelet-derived growth factor receptor
PDMP	D,L-threo-1-phenyl-2-decanoylamino-3-morpholino-1-propanol
PI3K	phosphatidylinositol 3´-kinase
PL	proteolipid
PLL	poly-L-lysine
PNS	peripheral nervous system
rpm	revolutions per minute
Sia T	α2,8-sialyl transferase (GD3 synthase)
SC	Schwann cells
T	2'-deoxythymidine 5'-triphosphate
T12.5	12.5 cm^3 tissue culture flask
T25	25 cm^3 tissue culture flask
T3	triiodothyronine
TGFß1	transforming growth factor ß1

TLC	Thin Layer Chromatography
Trk	tropomyosin-related kinase
TTX	tetrodotoxin
UDP	uridine diphosphate
$ZnSO_4$	zinc sulphate

Abstract

Gangliosides are a family of sialic acid-containing glycosphingolipids that are enriched in the nervous system. They are located in the outer leaflet of the plasma membrane within lipid rafts and are thought to be involved in numerous cellular events, including proliferation, differentiation, migration and neurite outgrowth. Gangliosides have also been shown to have neuroprotective actions and have been considered as candidates for the treatment of several neurodegenerative disorders.

In this thesis, the role of gangliosides in glial proliferation, migration and differentiation as well as the regeneration of the olfactory system and myelination were studied using mice lacking enzymes involved in ganglioside biosynthesis. Regeneration of the olfactory system in ganglioside knockout mice was similar to that of wild-type mice. However, proliferation of olfactory ensheathing cells grown on collagen and the migration of Schwann cells grown on laminin or collagen was increased in Sia T -/- mice, which lack b-series gangliosides but have increased levels of a-series gangliosides. These findings suggest that complex gangliosides modulate glial cell function to some extent. However, since the effects observed were subtle, it is possible that simpler gangliosides are able to compensate for the lack of complex gangliosides.

Axonal density and myelination were unaffected in ganglioside knockout mice. However, the localisation of sodium channels at the node of Ranvier and potassium channels at juxtaparanode was retarded in GalNAc T -/- mice lacking all complex gangliosides, suggesting that complex gangliosides modulate the formation of nodes of Ranvier. In addition, GalNAc T -/- mice had significantly lower numbers of NG2 positive early oligodendrocyte progenitors compared to wild-type and Sia T -/- mice, suggesting that complex gangliosides may affect early progenitor differentiation, proliferation or survival.

Declaration

I am the sole author of this thesis. All the work presented in this thesis was performed by myself unless otherwise stated.

CHAPTER 1

Introduction

1.1 Gangliosides

Gangliosides are a class of cell surface glycosphingolipids that are particularly enriched in neuronal and glial membranes. As a result, they are thought to play an important role in the function of the nervous system. Since their discovery in the 1940s by Ernst Klenk (Klenk, 1942), gangliosides have been associated with a number of biological processes. However, very little is known about their role in glial cell biology.

1.1.1 Nomenclature, structure and biosynthesis

Glycosphingolipids are defined by their core oligosaccharide sequence and are divided into ganglio-, hemato-, lacto- and globo-series (Miljan and Bremer, 2002). Gangliosides are a family of anionic glycosphingolipids that carry one or more sialic (neuraminic) acid residues. The sialic acid is usually N-acetyl-neuraminic acid, but can also be N-glycosyl-neuraminic acid (Tettamanti and Riboni, 1994). Gangliosides are ubiquitously expressed in embryonic and adult tissues of vertebrates but are highly enriched in the nervous system (Ledeen *et al.*, 1976). The majority of complex gangliosides are found in the outer leaflet of plasma membranes in structures termed "lipid rafts" (Pande, 2000), such that the polar sugar moiety protrudes into the extracellular space. However, simple gangliosides are ubiquitously distributed to mitochondria, endoplasmic reticulum (ER), Golgi, lysosomes and the plasma membrane (Caputto *et al.*, 1976, Maccioni *et al.*, 1977, Miller-Podraza and Fishman, 1982, Riboni *et al.*, 1994, Trinchera *et al.*, 1990). Gangliosides can be shed from the membrane (Chang *et al.*, 1997) and are also found in non-cell-associated forms in plasma and cerebrospinal fluid (Bergelson, 1995).

The nomenclature commonly used for naming gangliosides was proposed by Svennerholm (1994). Briefly, gangliosides are designated G for ganglioside, followed by a letter M (mono-), D (di-) or T (tri-sialo), indicating the number of sialic acid residues, followed by an arabic numeral to indicate their chromatographic mobility (Svennerholm, 1994). Gangliosides are composed of a hydrophobic ceramide core, immersed in the lipid membrane, linked to an oligosaccharide, bearing one or more sialic acid residues, which extends into the extracellular space (Stults *et al.*, 1989) (Figure 1.1). Gangliosides have a

common minimum-energy conformational structure in which the axis of the oligosaccharide chain is perpendicular to the axis of ceramide (Hakomori, 1986, Stromberg *et al.*, 1991) (Figure 1.2).

Gangliosides are synthesised by the stepwise addition of monosaccharides to lactosylceramide by glycotransferases in the Golgi apparatus and are then transported to the outer leaflet of the plasma membrane (Huwiler *et al.*, 2000). The various expression patterns of gangliosides are determined by the combination of activated glycotransferase genes (Lloyd and Furukawa, 1998). The first ganglioside in the biosynthetic pathway is GM3. GM3 is then modified by either ß1,4-N-acetyl-galactosaminyl transferase (GalNAc T) to produce GM2 and other a-series gangliosides or by α-2,8-sialyltransferase (Sia T) to produce GD3 and other b- and c-series gangliosides (Figure 1.3). These different series are characterised by the number of sialic acid residues attached to the 3-position of the inner galactose moiety: 0-series (zero), a-series (one), b-series (two) and c-series (three sialic acid residues) (Kolter *et al.*, 2002).

The sialic acids on gangliosides can be modified to give a range of different structures. The most common modification in mammals is the addition of O-acetyl esters to the hydroxyl group at the C9 position.

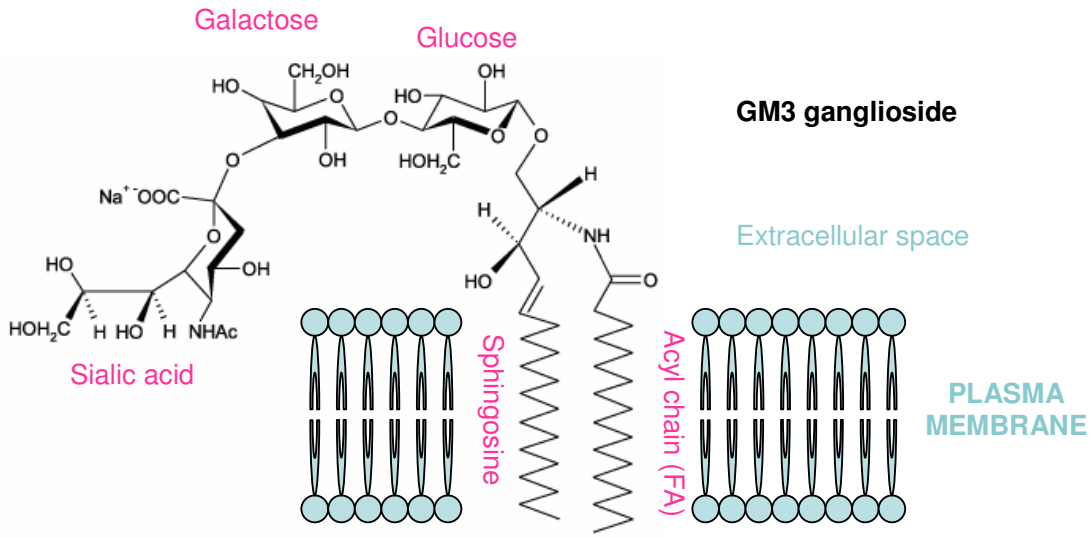

Figure 1.1. Ganglioside structure
Structure of ganglioside GM3 (NeuAcα3Galβ4Glcβ1Cer) showing the lipid ceramide core embedded in the plasma membrane and the carbohydrate group (glucose and galactose) extending into extracellular space. A single sialic (neuraminic) acid group is attached to the carbohydrate group.

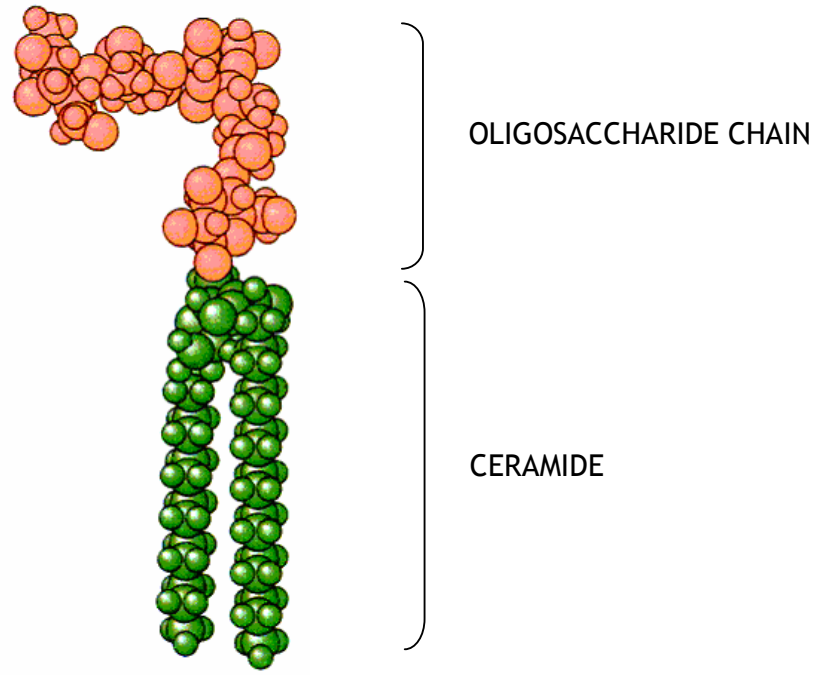

Figure 1.2. Ganglioside conformation.
Minimum-energy model of gangliosides showing that the axis of carbohydrate moiety is perpendicular to the axis of ceramide. Adapted from (Hakomori, 2002).

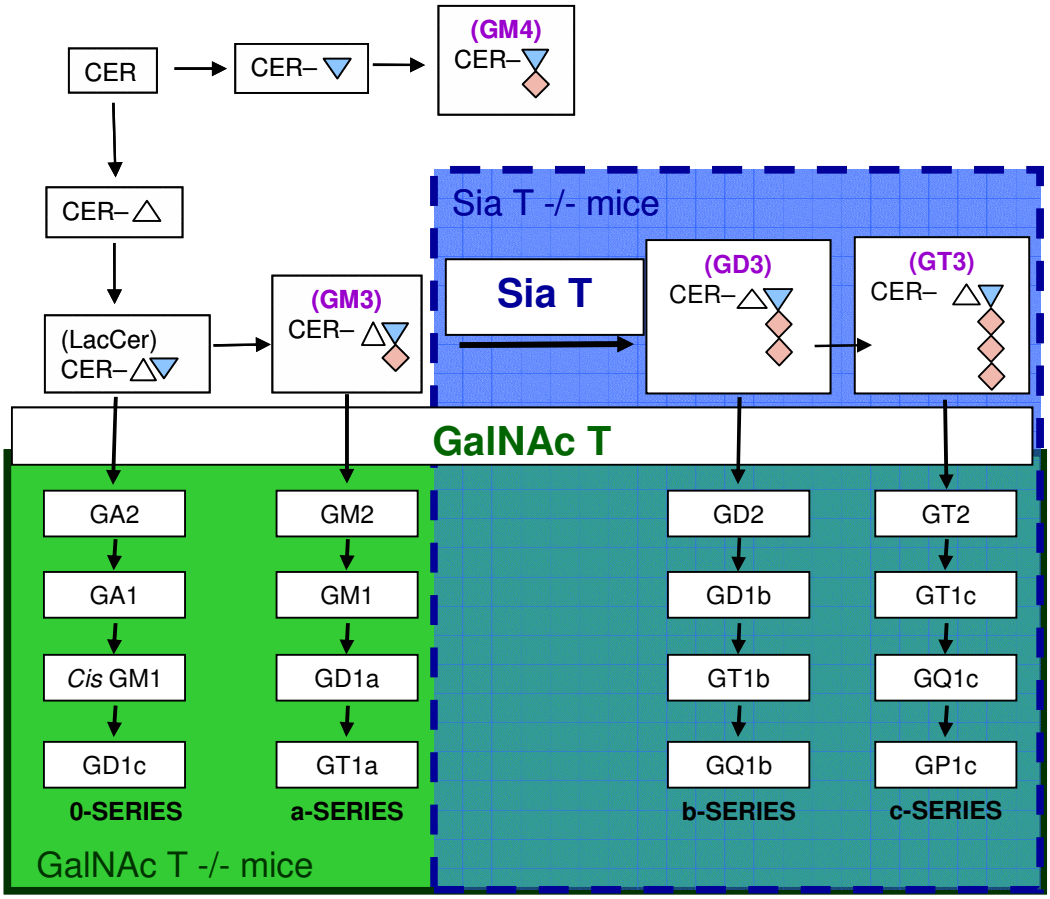

Figure 1.3. Ganglioside biosynthesis pathway showing the effect of knocking out Sia T and GalNAc T genes.
Most gangliosides are derived from glucosyl-ceramide. Addition of galactose to glucosyl-ceramide forms lactosyl-ceramide (LacCer). A 'second sugar substitution' of LacCer, at its' galactose in 3-position by a mono-, bis- or tris-sialic acid residue distinguishes the a-, b- and c-series gangliosides, respectively. Further extension of this ceramide disaccharide by a third monosaccharide leads to the formation of different carbohydrate series.
Disruption of Sia T results in the absence of all b- and c-series gangliosides (dashed box).
Disruption of GalNAc T results in the absence of all complex gangliosides (solid box).
Consequently, double knockout mice will lack all the complex gangliosides within both boxes and express only GM3 and GM4 gangliosides.
CER – ceramide; LacCer – lactosylceramide
△ - glucose; ▽- galactose; ◇ - *N*-acetyl neuraminic acid (sialic acid);
GalNAc T - β1,4-*N*-acetylgalactosaminyl transferase (GM2/GD2 synthase)
Sia T - α2,8-sialyltransferase (GD3 synthase)

1.1.2 Lipid rafts

Gangliosides are not evenly distributed throughout the plasma membrane. Rather, they segregate into unique structures in the exoplasmic leaflet of the lipid bilayer. In the literature these structures are referred to by various terms such as “glycosphingolipid enriched microdomains”, “detergent resistant membranes” and “detergent-insoluble glycolipid-rich domain”. For simplicity, I shall be referring to them as “lipid rafts” throughout this thesis. Lipid rafts are plasma membrane microdomains characterised by a unique lipid environment, enriched in glycosphingolipids and cholesterol, leading to their insolubility in non-ionic detergents. However, some lipid rafts, particularly those enriched in proteolipid/tetraspanin, are independent of cholesterol, are soluble in Triton-X and are termed “glycosynapse” (Hakomori, 2002).

Within lipid rafts, the saturated hydrocarbon chains of glycosphingolipids allow for cholesterol to be tightly intercalated, whereas the plasma membrane surrounding lipid rafts is more fluid, consisting mostly of phospholipids with unsaturated fatty acyl chains, and cholesterol. As a result, lipid rafts form rigid platforms that move around in the lipid bilayer (Schroeder *et al.*, 1994, Brown and London, 1998, , 1997).

Presently, it is unclear as to how the inner leaflet is coupled to the lipid rafts in the outer leaflet. However, it is possible that long chain fatty acids of sphingolipids in the outer leaflet couple the exoplasmic and cytoplasmic leaflets by interdigitation and that transmembrane proteins stabilise this coupling (Simons and Toomre, 2000). It is thought that the inner leaflet is rich in phospholipids with saturated fatty acids and cholesterol (Fridriksson *et al.*, 1999).

Lipid rafts are thought of as platforms coordinating the induction of signalling pathways since they contain many molecules involved in signal transduction, including numerous growth factor receptors (Harder and Simons, 1997, Iwabuchi *et al.*, 1998a). They are important as a site for the interaction between glycolipids and signalling molecules. Lipid rafts can include or exclude proteins to variable extents and many proteins and receptors are constitutively or inducibly localised within them. Proteins and receptors appear as if they are in

dynamic equilibrium, constantly moving in and out of lipid rafts. When separate rafts cluster, receptors and other signalling molecules are exposed to new membrane environments enriched with specific enzymes such as kinases, phosphatases and possibly palmitoylases and depalmitoylases. The phosphorylation state of the receptors can thus be altered, consequently modulating the downstream signalling pathway.

Proteins with raft affinity include growth factor receptors associated with intrinsic tyrosine kinases, glycosylphosphatidylinositol (GPI)-anchored proteins (Brown and London, 1998, Hooper, 1999), doubly acylated proteins, such as Src-family kinases or the α-subunits of heterotrimeric G proteins (Resh, 1999), cholesterol-linked and palmitoylated proteins such as Hedgehog (Rietveld *et al.*, 1999), and transmembrane proteins, especially palmitoylated ones (Brown and London, 1998). Mutational analysis has shown that amino acids in the transmembrane domains near the exoplasmic leaflet are critical for inclusion into lipid rafts (Scheiffele *et al.*, 1997). Acyl lipid modifications, such as palmitoylation and myristoylation, can increase a protein's affinity for rafts, but are not sufficient for raft association (Melkonian *et al.*, 1999, Simons and Toomre, 2000). Cross linking or oligomerisation of proteins also increases their affinity for rafts (Harder *et al.*, 1998). In addition, rafts contain a class of tetraspanin proteins termed proteolipids (PLs) (Kawakami *et al.*, 2002), which were originally described as PL-A, B and C (Folch and Lees, 1951).

Lipid rafts are heterogeneous and contain different ganglioside compositions. For instance, some are GM3-enriched (Iwabuchi *et al.*, 1998b) while others are enriched in GM1 (Schnitzer *et al.*, 1995). The lipid raft hypothesis argues that the heterogeneity of lipid rafts provides important locations for cell signalling processes, having distinct concentrations of specific signalling molecules (Simons and Ikonen, 1997, Brown and London, 1998, Simons and Toomre, 2000, Munro, 2003).

1.1.3 Function of gangliosides

Initially, gangliosides were thought to be inactive components of the plasma membrane. However, ganglioside storage diseases, such as Sandhoff's disease (Sandhoff *et al.*, 1968, Okada *et al.*, 1972), where gangliosides accumulate due to impaired degradation pathways, result in neuronal apoptosis (Huang *et al.*, 1997), progressive loss of motor behaviours and a shortened life span (Sango *et al.*, 1995).

Since gangliosides are present in relatively high concentrations in neural cell membranes (about 5-10% of total membrane lipid), they are thought to play important roles in the function of the nervous system. Numerous studies have been carried out to investigate the function of gangliosides in the nervous system and as a result many diverse functions have been suggested. Gangliosides have been proposed to act as modulators of transmembrane signalling and as a result regulate cell proliferation and induce differentiation (Hakomori, 1990). They have also been implicated in the regulation of apoptosis, migration, neurite outgrowth, cell-cell recognition as well as acting as endogenous ligands for myelin associated glycoprotein (MAG). Gangliosides are also thought to play a role in neuronal regeneration and in the maintenance of myelin. Some of the proposed functions of gangliosides are discussed in more detail below.

1.1.3.1 Proliferation

Gangliosides were the first described tumour-associated antigens and changes in cellular ganglioside composition were associated with altered growth properties (Hakomori, 2000). Following nerve injury, Schwann cells are stimulated to proliferate resulting in regeneration. Myelin basic protein (MBP) and two peptides derived from MBP induce Schwann cell proliferation via GM1 and fibroblast growth factor receptor (FGFR) binding (Tzeng *et al.*, 1999). Furthermore, cholera toxin (CTx), which is known to bind to GM1 ganglioside, is a potent mitogen of Schwann cell proliferation (Moss and Vaughan, 1979). Also, gangliosides GM1, GD1a, GD1b and GT1b stimulate astrocyte proliferation in culture in the absence of serum (Katoh-Semba *et al.*, 1986).

It has also been shown that Sia T gene expression in pheochromocytoma cell line (PC12), which results in the expression of complex b-series gangliosides, causes enhanced proliferation (Fukumoto *et al.*, 2000). Moreover, embryonic fibroblasts generated from sialyltransferase-I (GM3 synthase) knockout mice, lacking all gangliosides, showed increased proliferation (Hashiramoto *et al.*, 2006).

1.1.3.2 Differentiation

Many reports have demonstrated that gangliosides play a role in neuronal differentiation. Exogenously added gangliosides induce neuritogenesis, a typical differentiation phenotype of neuronal cells (Schengrund, 1990, Hakomori, 1990). For instance, exogenous administration of gangliosides to neuro-2A neuroblastoma cells stimulates neurite sprouting and enhances axonal elongation (Roisen *et al.*, 1981). Also, Sia T gene expression in neuro-2A cells, resulting in conversion of simple gangliosides into complex b-series gangliosides, stimulates neurite sprouting and cholinergic differentiation (Kojima *et al.*, 1994). This conversion of simple gangliosides to more complex gangliosides may be required to induce the neuro-2A differentiation (Liu *et al.*, 1997).

Gangliosides also play a role in glial differentiation. Rat astrocytes treated with CTx, which binds to GM1, rapidly convert from a flat polygonal morphology to a stellate morphology (Facci *et al.*, 1988). Ganglioside GM3 enhances the formation of processes by mature oligodendrocytes in culture (Yim *et al.*, 1991). In addition, optimal concentrations of GM3 change the morphology of oligodendrocytes from having a complex network of long processes with a few fine branches to networks of very thick processes near the cell bodies with many more fine processes (Yim *et al.*, 1994). Furthermore, GM3 induces a redistribution of O4 and O1 antigens from cell bodies to a network of thick processes surrounding the cells (Yim *et al.*, 1994). GM3 increases synthesis of sulphatide, galactocerebroside (GalC) and MAG, which are present in initial stages of myelination but has no effect on the synthesis of MBP, which is a major component of compact myelin suggesting that GM3 affects a relatively early stage in the preparation of oligodendrocytes to myelinate (Yim *et al.*, 1994).

1.1.3.3 Apoptosis

Changes in ganglioside concentration, localisation, and composition can lead to the activation of an ER stress response and mitochondrial apoptotic signalling that trigger cell death under physiological or pathological conditions (d'Azzo *et al.*, 2006).

GD3 is a minor ganglioside in normal adult brains (Ellison and de Vellis, 1995, Goldman and Reynolds, 1996, Molander *et al.*, 2000), but is expressed in activated microglia (Andersson *et al.*, 1998, Wolswijk, 1995) and in reactive astrocytes (Kawai *et al.*, 1994). Upon exposure to inflammatory stimuli, microglia secrete GD3, which triggers apoptosis in oligodendrocytes (Simon *et al.*, 2002). It has been shown that GD3 induces opening of the mitochondrial permeability transition pore complex, with the consequent release of apoptogenic factors (Malisan and Testi, 2002).

GD3-mediated apoptosis is cell type specific. Although it has been shown to cause apoptosis in many different cell types, such as oligodendrocytes, many cell types, such as astrocytes, are resistant to GD3-mediated apoptosis (Simon *et al.*, 2002).

1.1.3.4 Cell adhesion and migration

Cell adhesion to extracellular matrix molecules is a crucial step in cell migration. Cell adhesion and migration can either be enhanced or suppressed by gangliosides, depending on the ganglioside species and/or cell type specificity. For instance, GM3 has been shown to increase migration in several cell types, such as in corneal epithelium (Yang *et al.*, 1996), while decreasing migration in others. GM3 and GM2 enhance migration of melanoma cells through artificial basement membrane, while GT1b, GD1b, GT1a and GM1 have no effect, suggesting a possible role for tumour gangliosides during invasion of metastatic tumour cells through basement membrane of the surrounding tissues *in vivo* (Saha *et al.*, 2005). In contrast, suppression of Sia T expression, which results in a marked decrease in the concentration of GD3 and a concomitant increase in GM3, greatly reduces tumour cell migration (Zeng *et al.*, 2000). In addition, GM3 and GT1b inhibit carcinoma cell migration (Wang *et al.*, 2005) , while

membrane GM3 enrichment of retinal Müller glia significantly inhibits fibroblast growth factor (FGF)-induced proliferation and migration, while having much less effect on analogous epidermal growth factor (EGF)-mediated functions (Meuillet *et al.*, 1996).

The simple ganglioside GD3 is considered a marker for cell division and migration during embryonic development (Hilbig *et al.*, 1983). Adhesion of glioma cells to fibronectin, laminin, vitronectin and collagen I is enhanced by exogenous addition of GD3, GM1, GD1a, GD1b or GT1b and, i*n vitro*, gangliosides generally promote glioma cell and foetal brain cell migration while inhibiting their proliferation (Merzak *et al.*, 1995a, Merzak *et al.*, 1995b). A2B5 which binds to gangliosides GT3, O-acetyl GT3 (Dubois *et al.*, 1990, Fenderson *et al.*, 1987) and GQ1c (Kasai and Yu, 1983) inhibits the adhesion of glioma cells to fibronectin, laminin, vitronectin and collagen I (Merzak *et al.*, 1995b) and inhibits glioma cell invasion *in vitro* (Merzak *et al.*, 1994). Moreover, inhibition of ganglioside biosynthesis by an inhibitor of glucosyl-ceramide synthase reduces laminin-mediated attachment and migration in carcinoma cells, but has no effect on fibronectin-mediated attachment and migration (Inokuchi *et al.*, 1990). In contrast, GM3 and GD3 purified from human melanoma tumours impair the migration of Langerhans cells, the first immune barrier against the tumour cells. Also, GD3 and GD2 inhibit melanoma and neuroblastoma cell attachment to collagen, vitronectin, laminin, fibronectin (Cheresh *et al.*, 1986).

A lung cancer cell line transfected with GalNAc T and thus expressing more complex gangliosides showed decreased adhesion to fibronectin as well as reduced migration (Chen *et al.*, 2003). In accordance, GT1b inhibits keratinocyte adhesion and migration on a fibronectin matrix, but does not affect the adhesion or migration of keratinocytes on other matrices such as laminin or collagen IV (Paller *et al.*, 1995). GD3 also inhibits keratinocyte adhesion to fibronectin (Wang *et al.*, 2001a), while endogenous accumulation of GM3 inhibits their adhesion to fibronectin as well as collagen I, IV and VII (Wang *et al.*, 2003). Contrastingly, FGF combined with complex gangliosides GM1, GD1b or GT1b synergistically accelerates endothelial migration (De Cristan *et al.*, 1990).

Granule neurons maintained under thyroid hormone deficient conditions fail to migrate and have reduced levels of GM1 (Chakraborty *et al.*, 1992). In addition,

anti-GM1 antibody inhibits granule neuron migration which suggests that reduced levels of GM1 may be partially responsible for the failure of granule neurons to migrate during development in hypothyroidism (Chakraborty *et al.*, 1992). During T lymphocyte migration GM3- and GM1-enriched lipid rafts redistribute to the leading edge and uropod, respectively, suggesting that these are involved in the redistribution of molecules needed for T cell migration (Gomez-Mouton *et al.*, 2001).

In peroxisome biogenesis disorders, characterised by disturbances in the differentiation of neural cells, such as migration arrest, increased a-series gangliosides GM2, GM1 and GD1a, are observed in fibroblasts of patients, but are absent in normal fibroblasts (Tatsumi *et al.*, 2001). Moreover, GD1a, which is highly expressed in poorly metastatic FBJ-S1 cells, has been shown to inhibit the serum-induced migration capability of highly metastatic FBJ-LL cells and to reduce their adhesion to vitronectin (Hyuga *et al.*, 1997, Hyuga *et al.*, 1999). However, membrane GD1a enrichment of endothelial cells enhances vascular endothelial growth factor (VEGF)-induced proliferation and migration (Lang *et al.*, 2001) and lowers the threshold for VEGF signalling (Liu *et al.*, 2006).

9-O-acetyl GD3 is localised to the membrane of neurons and glial cells and is expressed in regions of cell migration and neurite outgrowth in the developing and adult rat nervous system (Mendez-Otero and Santiago, 2003). In addition, olfactory ensheathing glia express 9-O-acetyl GD3 and their migration is largely impaired by immunoblockage (Calvacante and Santos-Silva, 2003). Furthermore, an *in vivo* study demonstrated that immunoblockage of 9-O-acetyl GD3 can prevent cerebellar granule neuron migration (Santiago *et al.*, 2004).

1.1.3.5 Neurite outgrowth

Gangliosides have also been implicated in the regulation of neurite outgrowth. For instance, MAG binds to GD1a and GT1b to inhibit neurite outgrowth (McKerracher *et al.*, 1994, Mukhopadhyay *et al.*, 1994). In addition, elongation of neurites extended by neurons of embryonic rat dorsal root ganglia explants grown on laminin is halted in the presence of Jones monoclonal antibody which binds to 9-O-acetyl GD3 (Mendez-Otero and Friedman, 1996). Moreover, sialic acid residues on astrocytes regulate neuritogenesis by controlling the assembly

of laminin matrices (Freire *et al.*, 2004). Freire *et al* (2004) showed that embryonic astrocytes supported neuritogenesis with higher efficiency than astrocytes isolated from newborn animals and that this difference in the neuritogenic potential correlated with the organization of the laminin matrices deposited by astrocytes. Films of either a mixture of gangliosides or pure ganglioside GT1b induced formation of matrices of morphological and functional features similar to the matrices deposited by embryonic astrocytes, whereas films of phosphatidylcholine or ganglioside GM1 led to the formation of bulky laminin aggregates that lacked a defined structure similar to matrices deposited by new-born astrocytes (Freire *et al.*, 2004).

1.1.3.6 Myelin stability

MAG is a sialic acid binding lectin that is found selectively on the myelin membranes of Schwann cells and oligodendrocytes directly apposed to the surface of the axon. MAG is a minor constituent of myelin and is thought to mediate axonal-glial interactions (Trapp et al, 1989; Trapp, 1990; Fruttiger et al, 1995; Yin et al, 1998). MAG appears to act both as a ligand for an axonal receptor that is needed for the maintenance of myelinated axons (Schachner and Bartsch, 2000) and as a receptor for an axonal signal that promotes the differentiation, maintenance and survival of oligodendrocytes (Quarles, 2007). MAG also functions as an inhibitor of nerve regeneration acting through a receptor complex involving the Nogo receptor and/or gangliosides containing 2,3-linked sialic acid (Mukhopadhyay *et al.*, 1994, McKerracher *et al.*, 1994).

In order to elicit these physiological effects, MAG is thought to bind to specific targets on the axon of the nerve cell. Studies have demonstrated that gangliosides on the axon surface act as functional MAG ligands (Vyas and Schnaar, 2001, Vyas *et al.*, 2002). MAG binds to the terminal sequence found on the major nerve gangliosides GD1a and GT1b (Collins *et al.*, 1997). Binding of MAG to GD1a and GT1b induces the association of low affinity neurotrophin receptor p75 ($p75^{NTR}$) to lipid rafts and induces signal transduction (Fujitani *et al.*, 2005). Antibody cross-linking of cell surface GT1b, but not GD1a, mimics the effect of MAG, in that neurite outgrowth is inhibited through activation of Rho kinase, which suggests that interaction with GT1b on the neuronal cell surface is a potential mechanism for inhibition of neurite outgrowth by MAG

(Vinson *et al.*, 2001). Accordingly, MAG does not inhibit neurite outgrowth of postnatal cerebellar neurons from mice lacking complex gangliosides such as GD1a and GT1b (Fujitani *et al.*, 2005).

Because of their role as MAG ligands, gangliosides are thought to be important in myelin stability. Indeed, it was found that in mice lacking complex gangliosides, myelin sheaths were not tightly wrapped around the axon and were separated from the axolemma by wide spaces (Ma *et al.*, 2003). Vacuolated nerve fibres, axonal atrophy, redundant myelin sheaths as well as a decrease in the number of myelinated fibres were also observed (Ma *et al.*, 2003). In addition, mice lacking complex gangliosides display progressive and selective loss of MAG from the brain (Sun *et al.*, 2004). Moreover, mice lacking complex gangliosides, mice lacking MAG and mice lacking both MAG and complex gangliosides (double-null mice) exhibit similar neuropathological and behavioural deficits, which supports the hypothesis that MAG binding to gangliosides contributes to long-term axon-myelin stability (Pan *et al.*, 2005). All three exhibited quantitatively and qualitatively similar central and peripheral axon degeneration and nearly identical decreases in axon diameter and neurofilament spacing and displayed similar motor behavioural deficits, with double-null mice only modestly more impaired (Pan *et al.*, 2005).

1.1.3.7 Regeneration

Gangliosides play a role in neurite outgrowth during regeneration as well as during development. Gangliosides also have a neurotrophic role (Schengrund, 1990) and have been administered to experimental animals after generating artificial neurological damage or disorders by mechanical or chemical manipulation (Karpiak, 1984, Karpiak and Mahadik, 1984), by the injection of toxic reagents (Schneider *et al.*, 1992) or by ischemic treatment (Karpiak *et al.*, 1986). These studies showed that exogenously added gangliosides enhance nerve regeneration.

Gangliosides have been shown to prevent glutamate and kainate neurotoxicity in primary neuronal cultures of neonatal rat cerebellum and cortex (Favaron *et al.*, 1988). In addition, ganglioside GT1b prevents neuronal death and promotes regeneration of a lesioned rat hypoglossal nerve (Itoh *et al.*, 2001). GD1b,

GD1a, GQ1b, and GM1 also had the ability to promote regeneration but were not as effective (Itoh *et al.*, 2001). Furthermore, 9-O-acetyl GD3 expression was upregulated during the regeneration of crushed sciatic nerves, suggesting that 9-O-acetyl GD3 may also play a role in neurite outgrowth during regeneration (Mendez-Otero and Santiago, 2003). Moreover, passive transfer of anti-GD1a antibody severely inhibits axon regeneration after peripheral injury in mice (Lehmann *et al.*, 2007).

1.1.3.8 Signalling

Many functional effects of gangliosides are based on their interaction with specific target molecules within lipid rafts. Examples of such interactions include:

(i) Interaction with and activation of signal transducers including Src family kinases and small G-proteins to initiate signal transduction (Sorice *et al.*, 1997, Yamamura *et al.*, 1997, Iwabuchi *et al.*, 1998a, Iwabuchi *et al.*, 1998b);

(ii) Modulation of growth factor receptors with intrinsic tyrosine kinases in order to modulate cell growth (Bremer *et al.*, 1986, Nojiri *et al.*, 1991, Yates *et al.*, 1993, Mutoh *et al.*, 1995, Yates and Rampersaud, 1998)

(iii) Interaction with integrin receptors to modulate cell adhesion and motility (Cheresh *et al.*, 1987, Zheng *et al.*, 1993);

(iv) Formation of complexes with tetraspanins to affect complex formation with integrin or with growth factor receptor (Ono *et al.*, 2001, Kawakami *et al.*, 2002, Toledo *et al.*, 2005);

(v) Carbohydrate-to-carbohydrate interaction with other glycosphingolipids to mediate cell to cell adhesion;

(vi) Acting as receptors for microbial toxins, thus mediating the interaction of microbes with host cells during infection.

1.1.3.9 Regulation of growth factor receptors

Growth factors are proteins which act as signalling molecules between cells. They exert their effects by binding to specific receptors on the surface of their target cells. Growth factors play essential roles in the regulation of a variety of cellular processes such as proliferation and differentiation. Numerous studies report the effects of gangliosides on growth factor receptors. Indeed most, if not all, growth factor receptors have been described as regulated by gangliosides. As mentioned previously, gangliosides are found within lipid rafts, hence why they are thought to play a role in signal transduction. The discovery that growth factor receptor activity can be modulated by gangliosides suggested a mechanism by which they could cause changes in growth and differentiation. The following is a description of the effects of gangliosides on neurotrophin receptor, tropomyosin-related kinase A (TrkA), epidermal growth factor receptor (EGFR), FGFR and platelet-derived growth factor receptor (PDGFR) (Summarised in Figure 1.4).

1.1.3.9.1 Nerve growth factor receptor, TrkA

Nerve growth factor (NGF) is a member of the neurotrophin family of growth factors that includes brain derived neurotrophic factor (BDNF), neurotrophin-3 (NT-3), and NT-4. All neurotrophins bind to $p75^{NTR}$, whereas NGF, BDNF and NT-3 also bind to the high affinity receptors TrkA, TrkB and TrkC, respectively.

A number of studies have been performed to investigate the effects of gangliosides on the function of nerve growth factor receptors. The rat PC12 cell line has been extensively utilised as a differentiation model of neuronal cells, since they show neurite extension following NGF stimulation (Greene and Tischler, 1976). TrkA is a high affinity NGF receptor containing tyrosine kinase activity, which together with $p75^{NTR}$ mediates the effects of NGF. Binding of neurotrophins to TrkA induces activation of the receptor tyrosine kinase, dimerisation and autophosphorylation, and initiates a complex cascade of signal transduction events. Extracellular signal-regulated kinase (Erk) subfamily of structurally related serine–threonine kinases, known as mitogen-activated protein kinases (MAPKs), which convert extracellular stimuli to intracellular signals that control gene expression (Schaeffer and Weber, 1999), is activated in response to TrkA stimulation via the small G proteins, Ras and Rap1 (Grewal *et*

al., 1999). The Erk1 and Erk2 isoforms are thought to mediate some of the survival and differentiative effects of neurotrophins in specific subsets of both peripheral and central neurons (Klesse and Parada, 1999).

Exogenous GM1 tightly binds to TrkA on the surface of PC12 cells and enhances TrkA phosphorylation as well as neurite formation when added with a low concentration of NGF (Mutoh *et al.*, 1995). Also, GM1 enhances NGF-generated TrkA phosphorylation and dimerization (Rabin and Mocchetti, 1995, Farooqui *et al.*, 1997). In addition, GM1 could rescue PC12 cells from apoptotic death induced by serum deprivation (Ferrari *et al.*, 1995). Furthermore, GM1 alone was able to induce the phosphorylation and activation of TrkA and Erks in glioma cells expressing TrkA (Rabin and Mocchetti, 1995).

Duchemin *et al* (2002) demonstrated that GM1 induces tyrosine phosphorylation of TrkA, TrkB and TrkC high-affinity receptors for neurotrophins, and initiates signal transduction resulting in activation of the MEK1/2/Erk1/2 pathway in rat brain slices. However, high concentrations of GM1 (>500 μM) attenuate this response. Other major gangliosides present in brain GD1a, GD1b, GT1b as well as GM2 and GM3 display a similar action when added to brain slices. They also showed that GM1 induces tyrosine phosphorylation of TrkA and Erk1/2 *in vivo* following intracerebroventricular administration (Duchemin *et al*, 2002). In addition, GM1 potentiates the neurotrophic effect of NGF on central cholinergic neurons *in vivo* (Cuello *et al.*, 1989, Fong *et al.*, 1995, Hadjiconstantinou and Neff, 1998).

All of the studies mentioned above show that GM1 induces the phosphorylation of Trks and acts as a neurotrophin mimetic. However, a study using PC12 cells transfected with GM1/GD1b/GA1 synthase cDNA (GM1 overexpressing cells) showed marked alterations in their response to the induced differentiation by NGF and in the activation of signalling molecules (Nishio *et al.*, 2004). These GM1 overexpressing cells did not form neurites after stimulation with NGF. Binding of [^{125}I] NGF was not altered in these cells. However, autophosphorylation of TrkA, dimer formation of TrkA and phosphorylation of Erk1/2 following NGF treatment were markedly suppressed in these cells. This study also revealed dramatic changes in the intracellular localization of TrkA, p75^{NTR}, and Ras in GM1 overexpressing cells. Most of TrkA, p75^{NTR}, and Ras

moved from the raft to the non-raft, whereas GM1 remained in the raft fraction. This means that TrkA is not easily activated outwith lipid rafts in GM1 overexpressing cells, suggesting that appropriate physicochemical circumstances of rafts are required for the early step of its activation. Nishio et al (2004) also showed that *in vitro*, low concentrations of GM1 enhanced TrkA kinase activity, whereas high concentrations of GM1 (>500 μM) suppressed the kinase in a dose-dependent manner.

The difference observed in the effects of exogenous GM1 and cDNA-derived GM1 may be due to several factors:

i) GM1 mediates its effects through interaction with TrkA inside the membrane itself within lipid rafts and although some exogenous GM1 is incorporated into the membrane, it may also directly interact with the extracellular portion of TrkA on the cell surface, producing a different effect.

ii) The expression levels of GM1 or the difference in the duration of the exposure of cells to GM1 may vary, resulting in the different effects on TrkA.

1.1.3.9.2 Epidermal growth factor receptor (EGFR)

EGFR activity is modulated by gangliosides GM1, GM2, GM3, GM4, GD3, GD1a and GT1b (Bremer *et al.*, 1986, Weis and Davis, 1990, Miljan *et al.*, 2002, Slomiany *et al.*, 1992, Li *et al.*, 2001). GD1a, added to certain fibroblasts, followed by prolonged starvation, causes receptor kinase activation rather than down-regulation in response to EGF; this effect was claimed to be triggered by initial activation of cSrc followed by cascades of signalling (Li *et al.*, 2000, Li *et al.*, 2001).

Exogenous addition of GM3 to the culture media of human epidermal carcinoma KB and A431 cells inhibited cell growth. It also inhibited EGF-stimulated EGFR tyrosine phosphorylation in membrane preparations from KB and A431 *in vitro* (Bremer *et al.*, 1986). This inhibition of the EGFR by GM3 appears to be a very early event after ligand binding since tyrosine autophosphorylation of the EGF receptor was inhibited but ligand binding was not (Bremer *et al.*, 1986). Since dimerisation is required for the intermolecular autophosphorylation and activation of the EGFR it is possible that GM3 may inhibit EGFR dimerisation. Miljan et al (2002) showed that GM3 acts as a physiological competitor for EGFR

dimerisation through direct binding to the extracellular domain of the EGFR thus inhibiting EGFR autophosphorylation. Hanai et al (1988) demonstrated that two clones of A431 cells containing different concentrations of GM3 produced different responses to EGF; the clone with the greater GM3 concentration showed a reduced response to EGF (Hanai *et al.*, 1988). Chinese hamster ovary cells, transfected with EGFR and with a reversible defect in ganglioside biosynthesis, showed an inverse correlation between ganglioside content and EGFR kinase activity (Weis and Davis, 1990). Depletion of endogenous gangliosides in cells transfected to overexpress ganglioside catabolic enzymes resulted in enhanced EGFR kinase activity (Meuillet *et al.*, 1999, Zurita *et al.*, 2001). D,L-threo-1-phenyl-2-decanoylamino-3-morpholino-1-propanol (PDMP) is an inhibitor of uridine diphosphate (UDP)-glucose-ceramide glucosyltransferase, which catalyses the transfer of glucose to ceramide in the initial phases of ganglioside synthesis, and is used to deplete total gangliosides from the cell membrane. The addition of PDMP depletes gangliosides, thus reversing the inhibitory effect of exogenous GM3 on EGFR activity (Meuillet *et al.*, 2000).

However, GM3 does not completely attenuate ligand-stimulated signalling for EGFR. Instead it alters the time course of gene expression of EGF-stimulated immediate early genes c–fos and c-jun, shifting the peak expression from 1 h to 20 min (Rebbaa *et al.*, 1996). In PC12 cells EGF stimulates proliferation through a more transient signal, whereas NGF stimulates neural differentiation through a more prolonged signal, therefore a change in the time course of the signal could lead to a change in the final outcome.

Wang and co-workers (2001b) demonstrated that GM3 binds only to glycosylated EGFR in order to inhibit EGFR activation, suggesting that there is a carbohydrate-carbohydrate interaction between GM3 and EGFR within lipid rafts.

1.1.3.9.3 Platelet-derived growth factor receptor (PDGFR)

Platelet derived growth factor (PDGF) exists as 3 isoforms (PDGF-A, -B and –C) and active PDGF is a homo- or heterodimer that acts on one of two receptors, PDGFα-R and PDGFß-R.

Bremer et al (1984) showed that GM1 and GM3 inhibit the PDGF receptor-associated tyrosine kinase, while Van Brocklyn et al (1993) showed that GM1, GM2, GD1a, GD1b, GD3 and GT1b but not GM3 inhibit PDGFR dimerisation and PDGF-dependent cell growth. It is possible that gangliosides inhibit receptor dimerisation by destabilising the dimer through direct binding to the PDGFR, as is the case for GM1 (Mitsuda *et al.*, 2002). Under normal conditions the PDGFR is aggregated in lipid rafts. Mitsuda et al (2002) showed that GM1 regulates the duration of PDGFR-generated signal by altering the intracellular localisation of the PDGFR in Swiss3T3 cells. In cells containing high concentrations of GM1, the PDGF receptor was dispersed from lipid rafts and had a shorter PDGF-induced MAPK signal (Mitsuda *et al.*, 2002). Although gangliosides do not completely attenuate ligand-stimulated signalling for PDGFR in some cases the change in the signal duration can produce a different outcome. In the neuronal cell line SH-SY5Y, PDGF causes proliferation, but in the presence of GM1, PDGF causes neurite outgrowth (Lee *et al.*, 1994).

1.1.3.9.4 Fibroblast growth factor receptor (FGFR)

Fibroblast growth factors, or FGFs, are a family of growth factors crucial for development and any irregularities in their function leads to a range of developmental defects (Amaya *et al.*, 1991, Borland *et al.*, 2001, Coumoul and Deng, 2003). They are involved in many cellular processes including proliferation, migration, differentiation and survival of neurons and glial cells (Thisse and Thisse, 2005). FGF molecules signal through a family of transmembrane receptor tyrosine kinases consisting of 4 members: FGFR1, FGFR2, FGFR3, and FGFR4 (Ornitz *et al.*, 1996). Among the 23 FGF family members, at least 10 different FGFs are expressed in the brain during development in a spatially and temporally regulated manner (Reuss and von Bohlen und Halbach, 2003). The most studied FGF family member is FGF-2 (basic FGF), which activates all known FGFRs.

Interaction of FGFs with cell-surface associated heparan sulphate proteoglycans is required for FGF binding to its receptor (Rapraeger *et al.*, 1991, Yayon *et al.*, 1991), and cells that cannot synthesise heparan sulphate proteoglycans typically do not respond to FGF. The signalling complex at the cell surface is believed to be a ternary complex formed between two identical FGF ligands, two identical

FGFR subunits and either one or two heparan sulphate chains (Kan *et al.*, 1993, Pellegrini *et al.*, 2000, Schlessinger *et al.*, 2000).

Ganglioside modulation of FGF signalling is distinct from that of their modulation of other growth factor signalling in that only FGF interacts directly with a ganglioside (Rusnati *et al.*, 1999). FGFR activity is inhibited by both GM3 (Bremer and Hakomori, 1982) and GM1 (Rusnati *et al.*, 1999), yet the mode of GM3 inhibition differs from that of GM1, because GM1 binds directly to FGF and GM3 does not. Although this data suggests a mechanism in which GM1 blocks FGF binding to the FGFR, inhibiting its activity, another study showed that GM1 could stimulate FGFR activity.

Exogenously added GM1 restored the ability of heparan sulphate-deficient cells to respond to FGF2 (Rusnati *et al.*, 2002), suggesting that GM1 can present FGF to its receptor in a way analogous to that of heparan sulphate proteoglycans. The reason for the difference in the effects of GM1 could be that excess GM1 inhibits FGFR activity through competition with the physiological ligand, whereas physiological levels of GM1 can aid in the activation of FGFR.

GM1 (low concentration)	→	Increased NGF-generated TrkA phosphorylation Increased NGF-dependent neurite formation
GM1 (high concentration)	→	Inhibition of TrkA phosphorylation No neurite formation in response to NGF
GD1a	→	Increased EGF-generated EGFR-phosphorylation
GM3	→	Inhibition of EGF-generated EGFR-phosphorylation Inhibition of EGF-dependent proliferation
GM1 GM2 GM3 GD1a GD1b GD3 GT1b	→	Inhibition of PDGF-generated PDGFR-phosphorylation Inhibition of PDGF-dependent proliferation
GM3	→	Inhibition of FGF-dependent proliferation
GM1 (free)	→	Inhibition of FGF-dependent proliferation (by binding FGF2)
GM1 (membrane)	→	Activation of FGFR (by acting as a co-receptor for FGF2

Figure 1.4. Regulation of growth factor receptors by gangliosides
A summary of the regulation of TrkA, EGFR, PDGFR and FGFR by various gangliosides (listed on the left).

1.1.3.10 Interaction with integrins

Integrins are the major cell surface receptors for extracellular matrix (ECM) ligands, and are widely expressed in many cell types. They comprise a heterodimer of two receptor subunits, termed α and ß, which together form a ligand binding site and have short cytoplasmic domains that assemble a complex of kinases, adaptor proteins, and other signalling molecules following ligand binding. This initiates downstream signalling pathways which have been shown to regulate all fundamental aspects of cell behaviour. Eighteen different α and eight ß subunits generate a significant diversity in ligand binding and signalling properties, thus enabling different ECM environments to regulate distinct aspects of cell behaviour (Hynes, 2002).

Glial cells express a distinct repertoire of integrins. Astrocytes express the collagen/laminin receptor α1ß1, the fibronectin receptor α5ß1, the laminin receptors α6ß1 and α6ß4 and the vitronectin/fibronectin receptors αvß3, αvß5, and αvß8 (Malek-Hedayat and Rome, 1994, Tawil *et al.*, 1993, Tawil *et al.*, 1994, Wagner *et al.*, 1997, Milner *et al.*, 1999). Oligodendrocytes also express a number of integrins which are described in section 1.2.2.3.2.

It has been shown that gangliosides interact with integrin receptors to modulate cell adhesion and motility. Although integrin mediated adhesion to ECM is based on the binding of α and ß receptor subunits to defined peptide sequences of fibronectin, strength of binding is modulated by several factors including association of integrin receptors with adjacent surface membrane gangliosides (Zheng *et al.*, 1993, Cheresh *et al.*, 1987). It has been suggested that GD2 plays an essential role in vitronectin receptor function in human melanoma cells (Cheresh *et al.*, 1987). GT1b and GD3 inhibit keratinocyte adhesion to fibronectin and migration by blocking the interaction of fibronectin with α5ß1 integrin via a carbohydrate-carbohydrate interaction with α5ß1 integrin (Wang *et al.*, 2001a). GM3 also inhibits keratinocyte adhesion and migration on fibronectin but is unable to directly bind to α5ß1 (Wang *et al.*, 2003). Instead, GM3 blocks the interaction of α5ß1 integrin with matrix metalloproteinase-9 (Wang *et al.*, 2003), which facilitates migration by proteolytic degradation of matrices such as fibronectin, laminin, and collagen IV (Amano *et al.*, 2001,

Bannikov *et al.*, 2002, Thant *et al.*, 2000). Furthermore, expression of GT1b or GM3 in carcinoma cells inhibits urokinase-type plasminogen activator (uPA)-dependent cell migration by preventing the association of uPA receptor with α5β1 integrin or uPA receptor/α5ß1 with EGFR, respectively (Wang *et al.*, 2005). It has also been shown that optimal concentrations of GM3 enhance α5ß1 integrin-dependent adhesion of a carcinoma cell line to fibronectin, whereas GM3 concentrations above the optimal range decrease adhesion (Zheng *et al.*, 1993).

Integrin receptors are often found associated with tetraspanins and integrin-tetraspanin complexes are found within lipid rafts (Kazui *et al.*, 2000, Mannion *et al.*, 1996, Ono *et al.*, 2001, Kawakami *et al.*, 2002). Gangliosides form complexes with tetraspanins to affect complex formation with integrins (Ono *et al.*, 2001, Kawakami *et al.*, 2002, Toledo *et al.*, 2005). It has been shown that GM3 inhibits tetraspanin CD9-facilitated cell motility in various cell lines (Ono *et al.*, 2001). In addition, GM3 promotes the interaction of CD9 with α3 integrin in lipid rafts, leading to inhibition of laminin-5-dependent cell motility (Kawakami *et al.*, 2002). It has also been shown that GM2 suppresses cell adhesion via fibronectin-integrin interaction since cells expressing GM2 attached more slowly to fibronectin and exhibited reduced phosphorylation of focal adhesion kinase (FAK) downstream of integrins (Chen *et al.*, 2003). Furthermore, GM3 and tetraspanins CD9 and CD81 affect the functional interaction between integrins and FGFR within lipid rafts and consequently affect FGF-independent proliferation of fibroblasts (Toledo *et al.*, 2005).

1.1.4 Ganglioside knockout mice

To assess the function of gangliosides, the following knockout mice have been generated (Figure 1.3):

1.1.4.1 α-2,8-sialyltransferase knockout

α-2,8-sialyltransferase knockout (Sia T -/-) mice were created by knocking out Sia T, the enzyme which converts the first ganglioside, GM3, to GD3 and is thus responsible for generating all b- and c-series gangliosides (Kawai *et al.*, 2001, Okada *et al.*, 2002). These mice lack all b- and c-series gangliosides and have

slightly increased levels of a-series gangliosides (Okada *et al.*, 2002). Despite the deletion of b- and c-series, the Sia T -/- mice had an intact gross morphology (Kawai *et al.*, 2001, Okada *et al.*, 2002) and there was no observable demyelination (Kawai *et al.*, 2001). Furthermore, the mice had normal motor functions, learning and memory (Okada *et al.*, 2002). Sia T -/- mice were also fertile, had normal growth and had no behavioural abnormalities (Kawai *et al.*, 2001). These results suggest that the remaining a-series gangliosides compensate for the lack of b- and c-series gangliosides. However, the knockout mice exhibited reduced regeneration of axotomised hypoglossal nerves compared with wild-type (Okada *et al.*, 2002), which supports previous work showing that b-series gangliosides may be important in the repair of the nervous system. Despite earlier evidence implicating GD3 in apoptosis, Sia T -/- mice did not display an apoptosis related phenotype (Okada *et al.*, 2002).

1.1.4.2 N-acetylgalactosaminyl transferase knockout

GalNAc T knockout (GalNAc T -/-) mice were created by knocking out GalNAc T, the enzyme which catalyses the conversion of GM3 to GM2, GD3 to GD2, and GT3 to GT2, hence preventing the synthesis of all complex a-, b- and c-series gangliosides, respectively (Takamiya *et al.*, 1996). In contrast to wild-type mice, sciatic nerves and brains of GalNAc T -/- mice lacked the four major nervous system gangliosides, GM1, GD1a, GD1b and GT1b (Sun *et al.*, 2004, Susuki *et al.*, 2007a, Takamiya *et al.*, 1996). Instead, GalNAc T -/- mice have increased levels of simple gangliosides GM3, O-acetyl GD3 and GD3 (Susuki *et al.*, 2007a). Histological analysis of the brain tissue at 10 weeks old showed that the GalNAc T -/- mice had a normal morphology and no difference in the myelin structure or synapse formation. The mice also had normal memory and motor functions and were normal in gross behaviour. There was a decreased conduction velocity from the tibial nerve to the somatosensory cortex, but not to the lumbar spine, suggesting a role for gangliosides in neural function (Takamiya *et al.*, 1996). These results were surprising because gangliosides were expected to play important roles in the development of the nervous system.

However, an independent strain of GalNAc T -/- mice generated by Sheikh *et al* (1999b) displayed axonal degeneration in both optic and sciatic nerves.

Furthermore, there was a decrease in myelination in the central nervous system (CNS), as demonstrated by a 2-fold increase in the number of unmyelinated fibres as well as an increase in the mean diameter of unmyelinated fibres. It was also observed that there was ongoing demyelination and remyelination in the peripheral nervous system (PNS). There was also evidence of doubly myelinated axons and redundant myelin loops indicating dysregulation in CNS myelination (Sheikh *et al.*, 1999b). Unusual myelin anomalies are also seen in MAG knockout mice (Bartsch, 1996). GalNAc T -/- mice also display dysregulation of MAG expression in that MAG levels decrease to about 30% of normal levels as the mice age (Sun *et al.*, 2004). This further supports the evidence that gangliosides may be endogenous MAG ligands.

Another study showed that adult mice expressing only GM3 and GD3 developed significant and progressive behavioural neuropathies, including deficits in reflexes, strength, coordination and balance (Chiavegatto *et al.*, 2000). In addition, there was significant incidence of tremor and catalepsy in twelve month old GalNAc T -/- mice (Chiavegatto *et al.*, 2000).

1.1.4.3 Double knockout mice

By crossbreeding the Sia T -/- mice and GalNAc T -/- mice, double knockout mice (DKO) have been generated that express only the GM3 simple ganglioside (Inoue *et al.*, 2002, Kawai *et al.*, 2001). DKO mice contained similar amounts of total brain ganglioside but reduced levels of lipid-linked sialic acid compared with wild-type and single knockout mice. In contrast to the single knockout mice, double mutant mice had an extremely high mortality rate: 92% had died during the observation period of 36 weeks (Kawai *et al.*, 2001). Kawai et al (2001) also found that DKO mice were susceptible to audiogenic seizures, which in most cases resulted in death.

However, the cause of premature death of the DKO mice is now not thought to be due to the audiogenic seizures since another study showed that 12- and 18-week old mice did not have seizures when treated with various audiogenic stimuli (Inoue *et al.*, 2002).

DKO mice generated by Inoue and colleagues (2002) developed a characteristic skin lesion that appeared mostly on the face of the mutant mice 25 weeks after

birth or later. The lesions are thought to be triggered by the reduced sensitivity of the sensory nerve due to nerve degeneration, leading to over-scratching (Inoue *et al.*, 2002). Inoue et al (2002) showed that degeneration of peripheral nerves in DKO mice was more prominent than in the single mutants.

1.2 Glial cells

Glial cells exist alongside neurons in the nervous system where they perform many different structural and supporting functions. Glial cells can be divided into two subtypes: microglia and macroglia. The macroglia comprise many subtypes including astrocytes, oligodendrocytes and Schwann cells. The nervous system consists of a central and a peripheral component. The CNS contains the brain and the spinal cord, whereas the PNS contains all the nerves which connect the rest of the body to the spinal cord and the brain. The PNS and CNS contain different glial populations. The CNS contains oligodendrocytes, astrocytes and microglia, whereas the main PNS glia are the Schwann cells. Oligodendrocytes are glia responsible for myelination of neuronal axons in the CNS while Schwann cells are responsible for myelination in the PNS. Astrocytes are not involved in producing myelin; however they perform many other important functions which will be discussed later. The olfactory system, which spans both the CNS and the PNS, contains a further glial population, called olfactory ensheathing cells (OECs).

1.2.1 Astrocytes

Differences in the cellular composition between the PNS and the CNS involve many cells, the most significant being the astrocytes. Astrocytes comprise 25% of the total CNS cells, making them the most abundant cell type within the CNS (Eng *et al.*, 1992). Anatomical studies show that they are generally stellate in shape with long, branching processes which interact with neuronal, glial, and endothelial cells. Differentiated astrocytes can be identified both *in vitro* and *in vivo* by the expression of glial fibrillary acidic protein (GFAP) (Bignami *et al.*, 1972), the major constituent of glial intermediate filaments (Schachner *et al.*, 1977, Eng, 1985).

Classically, astrocytes *in vivo* have been classified into two types which are distinct in morphology and distribution. Protoplasmic astrocytes, which have short, thick, highly branched processes, are mostly found in the grey matter. Fibrous astrocytes, which have long, thin, less branched processes, are found in the white matter (Wilkin *et al.*, 1990, Somjen, 1988). Astrocytes are very heterogeneous and exhibit regional variations (Shinoda *et al.*, 1989, Wilkin *et al.*, 1990).

1.2.1.1 Type-1 and type-2 astrocytes

Studies in cultures of white matter have characterised two types of astrocytes (type-1 and -2), which develop from two distinct precursor cells (Raff *et al.*, 1984a). In cultures of grey matter only type-1 astrocytes are seen (Raff *et al.*, 1983a). Type-1 astrocytes of the optic nerve are thought to develop from optic stalk cells (Small *et al.*, 1987) beginning several days before birth (Miller *et al.*, 1985), whereas type-2 astrocytes are thought to develop postnatally (Miller *et al.*, 1985) from oligodendrocyte precursor cells, which can differentiate into type-2 astrocytes in culture media containing 10% serum (Levi *et al.*, 1986, Raff *et al.*, 1983b).

Both type-1 and -2 astrocytes express GFAP but differ in morphology, growth characteristics and ganglioside expression (Raff *et al.*, 1983a, Raff, 1989). Type-1 astrocytes are morphologically similar to fibroblasts in that they are flat and sheet-like and proliferate in culture (Raff *et al.*, 1983a). In contrast, type-2 astrocytes divide infrequently, appear similar to neurons or oligodendrocytes, and bear numerous processes (Raff *et al.*, 1983a). Type-1 astrocytes are positive for rat neural antigen 2, whereas type-2 astrocytes do not express this antigen (Bartlett *et al.*, 1981).

It is unclear how the *in vitro* classification corresponds with the *in vivo* classification. The morphologies and regional origins of type-1 and type-2 astrocytes suggest that these two cell types may correspond to protoplasmic and fibrous astrocytes *in vivo*, respectively. Tetanus toxin-binding, A2B5 and GFAP positive cells (type-2 astrocytes) were found in cell suspensions prepared from freshly dissected white matter tracts but not from freshly dissected grey matter of developing rats (Raff *et al.*, 1983a). However, the optic nerve is composed

entirely of white matter and is generally thought to contain astrocytes that are almost exclusively of the fibrous type (Vaughn and Peters, 1967). Yet cultures of developing optic nerve contained many type-1 astrocytes. So the argument that type-1 astrocytes correspond to protoplasmic astrocytes of the grey matter is an oversimplification. Miller and colleagues (1985) showed that type-1 astrocytes (GFAP+/A2B5-) first appear in the optic nerve at embryonic day 16 (E16), oligodendrocytes (GFAP-/GalC+) at birth (E21) and type-2 astrocytes (GFAP+/A2B5+) at postnatal day 7. They also showed that type-2 astrocytes did not develop from type-1 astrocytes *in vivo*, suggesting that the two types of astrocytes develop from two serologically distinct precursor cells (Miller *et al.*, 1985). However, Skoff et al, (1990, 1991) showed that only one wave of astrocyte development exists and did not observe the second wave of astrocyte development following the development of oligodendrocytes (Skoff, 1990, Skoff and Knapp, 1991). They conclude that separate lineages exist for astrocytes and oligodendrocytes during postnatal development and suggest that there is no compelling *in vivo* evidence for a bipotential progenitor cell that generates both oligodendrocytes and astrocytes (Skoff, 1990, Skoff and Knapp, 1991). Furthermore, labelled oligodendrocyte precursor cells transplanted into neonatal rat brains develop into oligodendrocytes but not type-2 astrocytes (Espinosa de los Monteros *et al.*, 1993). Therefore, another possibility is that type-1 astrocytes represent those in the brain, whereas type-2 astrocytes may be an artefact of culture.

1.2.1.2 Ganglioside expression of astrocytes

As mentioned above, cultured type-1 and type-2 astrocytes differ in their ganglioside content. Type-2 astrocytes are positive for A2B5, which labels gangliosides GT3, O-acetyl GT3 (Farrer and Quarles, 1999) and GQ1c, and tetanus toxin which binds to gangliosides GD1b and GT1 (Van Heyningen, 1963), whereas type-1 astrocytes are negative for both (Raff *et al.*, 1983a, Murakami *et al.*, 1999). GM3 is the major ganglioside expressed in cultured type-1 astrocytes, whereas in type-2 astrocytes it is GM3 and GD3 (Murakami *et al.*, 1999). Numerous studies have found GM3 to be the predominant ganglioside in cultured rodent astrocytes (Asou and Brunngraber, 1983, Asou *et al.*, 1989b, Asou *et al.*, 1989a, Sbaschnig-Agler *et al.*, 1988), whereas in human tissue little or no GM3 is found on astrocytes (Satoh *et al.*, 1996, Marconi *et al.*, 2005).

Surprisingly many studies have shown that astrocytes do not contain the major brain ganglioside GM1 on their cell surface both in rodents (Asou and Brunngraber, 1983, Yamamoto *et al.*, 2007, Asou *et al.*, 1989a, Asou *et al.*, 1989b, Sbaschnig-Agler *et al.*, 1988) and in human foetal astrocytes (Satoh *et al.*, 1996). In contrast, a study of adult human brain tissue found GM1 and GD1b to be expressed on all astrocytes (Marconi *et al.*, 2005) and a study in mouse foetal astrocytes found GM1 expression to be regulated by the cell cycle, with maximal expression during G0/G1 phase (Majoul *et al.*, 2002). In addition, GM1 is found on the nuclear envelope of astrocytes and is thought to be involved in the regulation of nuclear calcium (Xie *et al.*, 2004, Ledeen and Wu, 2006).

Marconi *et al* (2005) found that GD3 is expressed on less than 20% of astrocytes in adult human tissue. In contrast, Kawai *et al* (1999b, , 1999a) found that normal astrocytes in adult human tissue do not express GD3, instead they find that GD3 is expressed in the cytoplasm of reactive and neoplastic astrocytes. It was found that in young and adult mouse brain, both normal and reactive astrocytes express GD3 (Cammer and Zhang, 1996). GD3 is also expressed in cultured rat astrocytes (Kawashima *et al.*, 1996) and in small population of cultured human foetal astrocytes (Satoh and Kim, 1995, Satoh *et al.*, 1996).

Other gangliosides expressed on astrocytes include GM2, GD2 and GM4 in foetal human brains (Satoh *et al.*, 1996), and GM4 in chicken cerebellum (Ozawa *et al.*, 1993).

1.2.1.3 Function of astrocytes

Astrocytes are the housekeeping cells of the CNS, maintaining and supporting its normal functions. As such, they are involved in maintaining pH homeostasis and local ion concentrations such as potassium (K^+) and calcium (Ca^{2+}), as well as regulating the extracellular volume within the CNS (Sykova *et al.*, 1992). The regulation of brain energy metabolism is under the control of an intimate dialogue between astrocytes and neurons (Escartin *et al.*, 2006). Astrocytes provide neurons with glucose and metabolic substrates, while removing neuronal waste such as metabolic byproducts.

The glia limitans, which is the outermost layer of nervous tissue of the CNS, directly under the pia mater, arises from astrocytes (Yonezawa *et al.*, 2003).

Ends of astrocyte processes, known as perivascular end feet, contact the basement membrane under the pia mater, where they seal off the CNS through tight association of these processes, forming the glia limitans (Peters *et al.*, 1991).

In addition, densely packed astrocyte processes surround endothelial cells of CNS capillaries and venules that form the blood brain barrier (BBB) (Janzer, 1993, Goldstein, 1988). This barrier protects the brain by preventing the entry of numerous large molecules, such as proteins and toxic substances from the blood. BBB function is induced , maintained, regulated and repaired by astrocytes (Janzer, 1993).

Following injury to the CNS, astrocytes become reactive, undergoing morphological changes and expressing distinct markers from resting astrocytes (Ridet *et al.*, 1997). They respond to injury by becoming hypertrophic, migrating and proliferating around the affected region to form a glial scar, thus sealing off the damaged area (Eng and Ghirnikar, 1994). Although the astrocytes act to preserve the integrity of the host tissue, the glial scar appears to limit the regenerative capacity of the CNS (Fawcett, 1997), inhibiting regeneration of severed axons (Davies *et al.*, 1997).

1.2.1.4 Perinodal astrocytes

It is well established that perinodal astrocyte processes are closely associated with nodes of Ranvier in the CNS (Waxman, 1986, Black and Waxman, 1988), suggesting that, in addition to the axon and oligodendrocyte, astrocytes participate in the formation of mature CNS nodes. Electron microscopic studies of the feline spinal cord demonstrated that processes extend from astrocyte cell bodies to approach the node of Ranvier where they come into close association with the bare nodal segment of the axon (Hildebrand, 1971a, 1971b). This association has subsequently been confirmed in rabbit corpus callosum (Waxman and Swadlow, 1976), rat optic nerve (Hildebrand and Waxman, 1984, Waxman and Black, 1984, ffrench-Constant *et al.*, 1986) and guinea pig (Raine, 1984), rat (Sims *et al.*, 1985) and lower vertebrate (Bodega *et al.*, 1987) spinal cord. Some of these studies showed that perinodal astrocyte processes travel many

micrometers to contact the nodal axon membrane (Hildebrand, 1971b, Waxman and Black, 1984, Waxman and Sims, 1984, Raine, 1984).

It could be argued that the presence of astrocyte processes at nodes is due to the abundance of astrocytes within the CNS, with astrocyte processes merely occupying the space between adjacent oligodendrocytes within the perinodal region. However, the relationship between astrocyte processes and the sodium channel-rich axon membrane at the node seems to be highly specific. Sims *et al* (1985) reduced the population of astrocytes and oligodendrocytes in the dorsal funiculus of the spinal cord by irradiation, resulting in the minimisation of random glial-axonal interactions and myelination of only a limited number of axons. Despite the low numbers of astrocytes, the nodes of Ranvier that were formed within the irradiated cord were invariably associated with astrocyte processes, and in some instances the astrocyte process bypassed unmyelinated axons as it extended to become associated with a node (Sims *et al.*, 1985).

The interaction between perinodal astrocyte processes and nodal membrane is likely to be mediated by cell adhesion molecules since J1, a glycoprotein involved in neuron-astrocyte adhesion (Kruse *et al.*, 1985), is concentrated at the interface between the axon and perinodal astrocyte processes at nodes of Ranvier (ffrench-Constant *et al.*, 1986).

Several suggestions have been put forward with regard to the role of perinodal astrocytes, including the formation of nodal gap substance and regulation of the extracellular ionic environment (Hildebrand, 1971a, 1971b). Charged molecules, such as potassium K^+, are released into the extracellular space during neuron firing and need to be removed in order to maintain the electrical homeostasis. Astrocytes can buffer the excess K^+ released by neurons (Sykova *et al.*, 1992). Astrocytes form gap junctions amongst themselves (Gutnick *et al.*, 1981, Massa and Mugnaini, 1982), which allow them to distribute charged molecules among the resulting syncytia.

Cultured astrocytes have been shown to express functional ion channels, including voltage-sensitive sodium channels (Na_v) (Barres *et al.*, 1988, Bevan *et al.*, 1985, Nowak *et al.*, 1987). Moreover, immuno-ultrastructural studies have demonstrated that white matter astrocytes express Na_v on the plasmalemma of the perinodal process as well as the cytoplasm (Black *et al.*, 1989a, Black *et al.*,

1989b). Whereas neurons express Na_v most intensely in the axon membrane, astrocyte Na_v are heterogeneously distributed within the cytoplasm and are also associated with some regions of astrocyte plasmalemma (Black *et al.*, 1989a, Black *et al.*, 1989b). In addition, perinodal astrocyte processes display more intense Na^+ channel immunoreactivity than astrocyte processes at the glia limitans and surrounding blood vessels (Black *et al.*, 1989b). Therefore, it is possible that perinodal astrocytes complement neuronal perikaryal Na_v synthesis and axonal transport by functioning as extra-neuronal sites for the synthesis of Na_v, which are subsequently transferred to the axon membrane at nodes of Ranvier (Bevan *et al.*, 1985).

1.2.1.5 Calcium waves and the tripartite synapse

Astrocytes exhibit a form of communication based on the propagation of transient rises in cytosolic free Ca^{2+}, termed "calcium waves" (Cornell-Bell *et al.*, 1990, Charles *et al.*, 1991, Cornell-Bell and Finkbeiner, 1991, Duffy and MacVicar, 1995, Finkbeiner, 1992). These calcium waves can be initiated by neuronal synaptic activity (Dani *et al.*, 1992, Porter and McCarthy, 1996, Kang *et al.*, 1998). Calcium waves are thought to be mediated via the diffusion of inositol triphosphate through gap junctions (Finkbeiner, 1992) as well as through the extracellular release of adenosine triphospate (ATP), and consequent activation of purinergic receptors on other cells (Arcuino *et al.*, 2002, Cotrina *et al.*, 1998, Hassinger *et al.*, 1996, Newman, 2001). These astrocytic Ca^{2+} variations can cause the release of the excitatory neurotransmitter glutamate, which then signals to adjacent neurons (Hassinger *et al.*, 1995, Parpura *et al.*, 1994, Pasti *et al.*, 1997) and modulates synaptic transmission (Araque *et al.*, 1998a, Araque *et al.*, 1998b, Kang *et al.*, 1998, Parpura and Haydon, 2000). Astrocytes also modulate synaptic transmission by removing neurotransmitters, such as glutamate, gamma amino butyric acid (GABA) and acetylcholine, from the synaptic cleft (Schousboe *et al.*, 1992, Bergles *et al.*, 1999, Smit *et al.*, 2001).

The discovery of the existence of bidirectional communication between glial cells and neurons gave rise to a new concept, the tripartite synapse, in which the synapse is formed by three mutually interacting elements: the presynaptic

terminal, the postsynaptic membrane and the surrounding astrocytes (Araque *et al.*, 1999, Carmignoto, 2000).

1.2.1.6 Astrocytes and myelination

Growth factors influence oligodendrocyte differentiation and myelination as described in section 1.2.2.3.1 and astrocytes are known to secrete many of these factors including FGF2 (Araujo and Cotman, 1992), PDGF (Richardson *et al.*, 1988), ciliary neurotrophic factor (CNTF) (Stockli *et al.*, 1989), NGF (Furukawa *et al.*, 1986, Houlgatte *et al.*, 1989) and NT-3 (Rudge *et al.*, 1992), suggesting that astrocytes could be indirectly involved in myelination.

Recent evidence suggest that astrocytes promote myelination by mature oligodendrocytes in an activity-dependent manner (Ishibashi *et al.*, 2006). Ishibashi et al (2006) stimulated dorsal root ganglion (DRG) neurons, co-cultured with mature oligodendrocytes and astrocytes, with a pattern of electrical activity know to stimulate ATP release from axons and found that myelination increased 3-fold on axons firing action potentials compared with unstimulted controls, or axons stimulated in the presence of tetrodotoxin (TTX), which blocks sodium-dependent action potentials. Treatment of these co-cultures with a non-hydrolysable form of ATP, 2MeSATP, also resulted in significantly more myelinated axons per field of view. A search of the literature for factors that might affect myelination after OPCs have differentiated to a promyelinating phenotype led them to cytokine leukaemia inhibitory factor (LIF). To test the hypothesis that ATP might promote myelination through an LIF-dependent mechanism, Ishibashi *et al* added antibodies against LIF to co-cultures treated with 2MeSATP and found that the increase in myelin induced by 2MeSATP was blocked by the presence of antibody blocking LIF activity. Addition of antibody against LIF alone had no effect on myelination indicating that the effects of endogenous LIF on myelination require activation of P2 receptors. They then measured the concentration of LIF in these cultures to determine if LIF was released when axons were stimulated to fire action potentials and found that the concentration of LIF was significantly increased following stimulation. Since astrocytes are a probable source of LIF, Ishibashi *et al* tested this and showed that electrical activity in axons increased the level of mRNA for LIF in astrocytes. In addition, this increase in LIF mRNA due to electrical stimulation

was inhibited in the presence of apyrase, an enzyme that rapidly degrades extracellular ATP, supporting the hypothesis that the increase in LIF mRNA in astrocytes growing on electrically active DRG axons is dependent upon release of ATP from axons. In summary, Ishibashi *et al* showed that electrical activity in premyelinated axons increases myelination after oligodendrocyte precursors mature to a promyelinating stage by the activity dependent release of ATP from axons, which acts in a paracrine manner on astrocytes to release LIF and stimulate myelination at this later stage of development.

1.2.2 Oligodendrocytes

Oligodendrocytes are the myelinating cells of the CNS (Bunge, 1968). They extend multiple processes that wrap concentrically around the axons to form the insulating myelin sheath. Electron microscopy shows that they have a characteristic electron-dense cytoplasm containing few if any intermediate filaments but large numbers of microtubules (Raff *et al.*, 1983b). They have a small cell body and a large number of branching processes, which enable them to ensheath and myelinate fifteen axons on average, as well as surround neuronal cell bodies in the grey matter.

1.2.2.1 Development of oligodendrocytes

Like most other CNS neural cells, oligodendrocytes derive from cells of the neural tube (Warf *et al.*, 1991). It is thought that they arise from ventral subsets of multi-potential neuroepithelial precursors cells in the ventricular zone of the brain and spinal cord (Pringle and Richardson, 1993, Woodruff *et al.*, 2001); although there is evidence that a subset of oligodendrocytes arise from radial glia in the dorsal spinal cord (Fogarty *et al.*, 2005). In the oligodendrocyte lineage there is a progression of cells from immature to mature states and each stage is demarcated by distinct morphological, biochemical, and behavioural characteristics (Figure 1.5) (Hardy and Reynolds, 1991, Pfeiffer *et al.*, 1993).

The earliest cells in the oligodendrocyte lineage are early oligodendrocyte progenitor cells (OPCs), which label with the antibody A2B5 (Raff *et al.*, 1984b). Early OPCs are bipolar or unipolar with a large cell body (Raff *et al.*, 1984b).

They are first detected at E12 to 14 in the rat and can be identified by expression of the PDGFα-R (Pringle *et al.*, 1992), as well as mRNA for myelin genes 2',3'-cyclic-nucleotide 3'-phosphodiesterase (CNP) (Yu *et al.*, 1994) and DM20, an isoform of proteolipid protein (PLP) (Timsit *et al.*, 1995). Early OPCs also express the sulphated proteoglycan, NG2 (Nishiyama *et al.*, 1996) and the embryonic form of polysialic acid containing neural cell adhesion molecule (E-NCAM or PSA-NCAM), thought to be involved in their migration (Zhang *et al.*, 2004). OPCs are thought to arise from NG2-positive pre-OPCs (Baracskay *et al.*, 2007). Although early OPCs constitutively differentiate into oligodendrocytes, under the influence of different signals they can give rise to type-2 astrocytes (Raff *et al.*, 1983b), type-1 astrocytes and neurons (Kondo and Raff, 2000), suggesting that they have stem like properties. Early OPCs divide and migrate, populating most of the CNS during early development. At birth, early OPCs are evenly distributed throughout the CNS and begin to proliferate and differentiate (Nishiyama *et al.*, 1996).

These early OPCs differentiate into late OPCs (also known as pro-oligodendrocytes), which are committed to the oligodendrocyte linage and are post migratory but still proliferative (Warrington *et al.*, 1993). Late progenitors are multipolar and begin to express antigens that are recognised by the antibody O4 (Bansal *et al.*, 1992, Sommer and Schachner, 1981). Antigens which are recognised by the O4 antibody include seminolipid (Bansal *et al.*, 1989), prooligodendrocyte antigen (Bansal *et al.*, 1992) and galactosulphatide that subsequently becomes a structural component of myelin (Sommer and Schachner, 1981). In the presence of correct differentiation factors, late OPCs differentiate into pre-myelinating oligodendrocytes (also known as immature oligodendrocytes) (Trapp *et al.*, 1997). However, some late OPCs remain undifferentiated and persist in the adult CNS (Wolswijk and Noble, 1989, Shi *et al.*, 1998, Dawson *et al.*, 2003). Adult OPCs differ from neonatal OPCs in that their motility, proliferation and time course of differentiation are all significantly slower (Dawson *et al.*, 2000, Dawson *et al.*, 2003, Wolswijk and Noble, 1989).

Pre-myelinating oligodendrocytes develop a few days before myelination starts (Trapp *et al.*, 1997). Structurally, the morphology of pre-myelinating oligodendrocytes is more complex in that they extend multiple processes. They

lose the expression of A2B5, NG2 and PDGFαR, but continue to express antigens labelled with the O4 antibody (Raff *et al.*, 1984b). Pre-myelinating oligodendrocytes express GalC, the major glycolipid in myelin (Raff *et al.*, 1978b, Ranscht *et al.*, 1982), as well as low levels of myelin-related proteins such as MAG, MBP, DM20 and CNP (Reynolds *et al.*, 1989).

In the absence of axons to ensheath, pre-myelinating oligodendrocytes form broad membranous sheets that have been suggested to represent early stages of myelin formation (Reynolds *et al.*, 1989). *In vivo*, pre-myelinating oligodendrocytes have a limited lifespan of 2 to 3 days before they differentiate into myelinating oligodendrocytes (also known as mature oligodendrocytes) or undergo apoptosis. Contact between pre-myelinating oligodendrocytes and axons induces the expression of myelin proteins such as PLP and myelin oligodendrocyte glycoprotein (MOG) and the wrapping of oligodendrocyte processes around the axon to form the myelin sheath (Pfeiffer et al, 1993). Differentiation of a pre-myelinating oligodendrocyte to a myelinating oligodendrocyte is characterised by maturation from a nonpolarised to a polarised cell: as myelination begins, the myelin proteins are targeted to specific membrane domains (Trapp *et al.*, 1997). Pre-myelinating oligodendrocytes that fail to contact an axon undergo programmed cell death (Barres *et al.*, 1992, Trapp *et al.*, 1997).

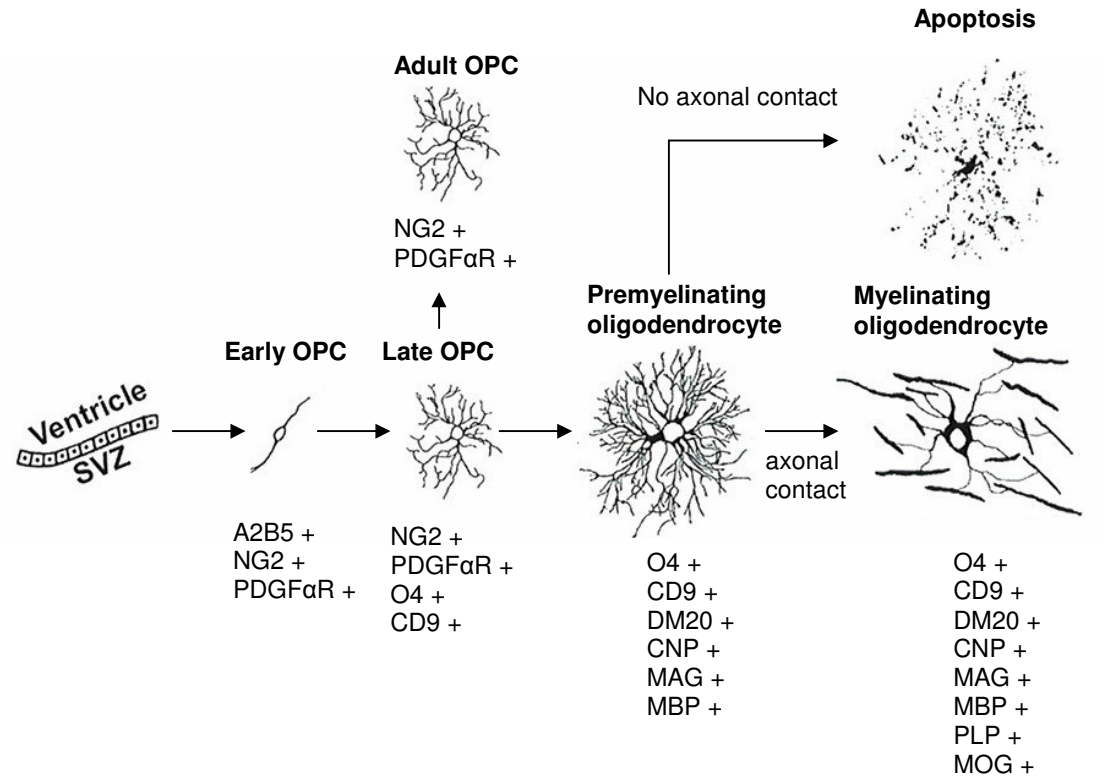

Figure 1.5. Summary of oligodendrogenesis *in vivo*.
Oligodendrocyte progenitor cells (OPCs) originate in the subventricular zone (SVZ), migrate and populate the CNS as early OPCs. Early OPCs give rise to late OPCs which, in turn, give rise to premyelinating oligodendrocytes. Upon contact with axons, premyelinating oligodendrocytes differentiate into myelinating oligodendrocytes. Those that fail to contact an axon die by apoptosis. Some of the phenotypic markers for each stage are listed. Adapted from (Trapp *et al.*, 1997). A2B5 recognises gangliosides GT3 and O-acetyl GT3; NG2 recognises a sulphated proteoglycan; PDGFαR is platelet derived growth factor receptor alpha; O4 recognises seminolipid, sulfatide and prooligodendrocyte antigen; CD9 is a tetraspanin proteolipid; DM20 is an isoform of proteolipid protein; CNP is 2',3'-cyclic-nucleotide 3'-phosphodiesterase; MAG is myelin associated glycoprotein; MBP is myelin basic protein; PLP is proteolipid protein.

1.2.2.2 Ganglioside expression of oligodendrocytes

Oligodendrocytes express different gangliosides during different stages of development (Figure 1.6). It has been shown *in vitro* that an OPC cell line CG-4 expresses different gangliosides during distinct differentiation stages (Schnaar *et al.*, 1996). OPCs in culture express ganglioside GT3 and O-acetyl GT3, antigens that react with A2B5 antibody (Farrer and Quarles, 1999). Both of these gangliosides are down-regulated as OPCs differentiate into oligodendrocytes; however, they continue to be expressed when they differentiate into type 2 astrocytes (Farrer and Quarles, 1999). Moreover, OPCs also express 9-O-acetyl

GD3, which is also expressed in type 2 astrocytes but down-regulated in oligodendrocytes (Farrer and Quarles, 1999).

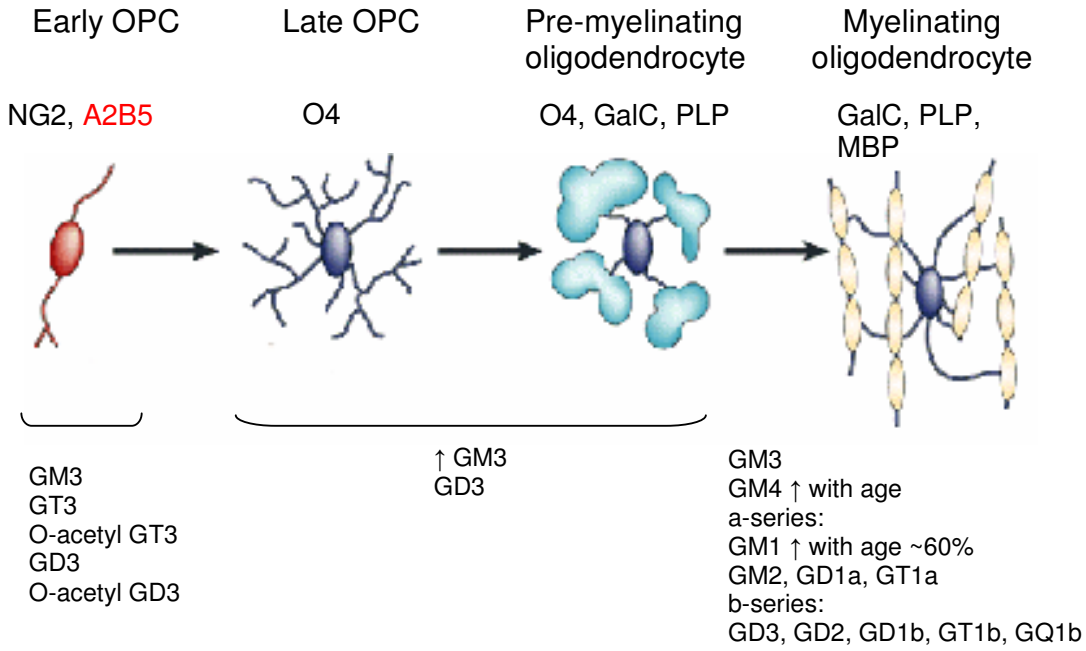

Figure 1.6. Ganglioside expression of oligodendrocytes.
Gangliosides expressed during distinct stages of oligodendrocyte differentiation are listed below the representative drawings of each stage. Early OPCs express gangliosides simple gangliosides GM3, GT3, O-acetyl GT3, GD3 and O-acetyl GD3. Late OPCs continue to express GD3 and have increased levels of GM3, but do not express GT3, O-acetyl GT3 and O-acetyl GD3. Myelinating oligodendrocytes continue to express GM3 and GD3, have increased expression of GM4 and GM1 and express GM2, GD1a, GT1a, GD2, GD1b, GT1b and GQ1b. The above is a summary of data found in several journals looking at ganglioside expression of oligodendrocytes and myelin (Farrer and Quarles, 1999, Yim *et al.*, 1994, Yim *et al.*, 1995, Yu and Yen, 1975, Cochran *et al.*, 1982).

1.2.2.3 Factors affecting oligodendrocytes

Myelination of the CNS requires a precise regulation of proliferation, migration, survival, and differentiation of the oligodendrocyte lineage cells. Accordingly, the behaviour of OPCs and oligodendrocytes is tightly regulated by growth factors and extracellular matrix molecules (Barres and Raff, 1994, Kiernan *et al.*, 1996, Orentas and Miller, 1998).

1.2.2.3.1 Growth factors

OPCs in culture proliferate in response to a number of different growth factors such as PDGF, FGFs, insulin-like growth factors (IGFs) and neuregulin (NRG)

(McMorris and Dubois-Dalcq, 1988, Richardson *et al.*, 1988, Bogler *et al.*, 1990, Canoll *et al.*, 1996). The onset of differentiation in OPCs and oligodendrocytes is thought to be controlled by a combination of cell intrinsic factors and extrinsic environmental signals. Differentiation is the default pathway for OPCs in the absence of mitogens. As a result, the availability of growth factors such as PDGF, IGF-1 and FGF-2 is likely to play a role in the onset of differentiation (Barres and Raff, 1994, Goddard *et al.*, 1999).

Astrocytes and neuronal cell bodies provide mitogenic, migratory, and survival signals to the OPCs (Noble *et al.*, 1988, Barres *et al.*, 1992, Fruttiger *et al.*, 2000) by releasing PDGF (Richardson *et al.*, 1988, Yeh *et al.*, 1991), which is recognised by the PDGF α receptor (PDGFαR) expressed on the surface of OPCs (Pringle *et al.*, 1992). PDGF stimulates migration of OPCs by enhancing motility (Noble *et al.*, 1988) and by acting as a chemotactic agent (Armstrong *et al.*, 1990). PDGF is also a potent survival factor for OPCs (Barres *et al.*, 1992), and the limited supply of PDGF in the normal CNS may act to keep OPC proliferation under tight control and allow cell cycle exit and differentiation (van Heyningen *et al.*, 2001). As OPCs differentiate into pre-myelinating oligodendrocytes, they downregulate PDGFαR (Hall *et al.*, 1996) and become unresponsive to PDGF (Hart *et al.*, 1989, Gard and Pfeiffer, 1993).

FGF2 stimulates OPC proliferation and migration *in vitro* and inhibits terminal differentiation (Bogler *et al.*, 1990, Milner *et al.*, 1997a, Osterhout *et al.*, 1997). FGF2 also upregulates PDGFαR and co-operates with PDGF to induce proliferation and inhibit differentiation of OPCs (Bogler *et al.*, 1990, McKinnon *et al.*, 1990). In contrast to OPCs, where it causes proliferation and migration, in mature oligodendrocytes FGF2 causes *Mbp* gene downregulation, loss of myelin compaction as well as demyelination of axons (Fressinaud *et al.*, 1995, Grinspan *et al.*, 1996b, Bansal and Pfeiffer, 1997, Butt and Dinsdale, 2005a, 2005b). In addition, FGF2 knockout mice showed increased OPC differentiation and oligodendrocyte repopulation of experimentally demyelinated white matter compared with wild-type mice (Armstrong *et al.*, 2002). Consequently, FGF2 has been proposed to play a role in the pathogenesis of demyelination and the failure of remyelination in experimental models of multiple sclerosis (MS).

Neuregulins are a large family of proteins related to EGF that contain an EGF-like domain critical to their activity (Buonanno and Fischbach, 2001) and activate the ErbB family of tyrosine kinase receptors, which includes ErbB1 (the EGF receptor), ErbB2, ErbB3 and ErbB4. Neurons, astrocytes and oligodendrocytes all secrete neuregulins (Meyer and Birchmeier, 1994, Raabe *et al.*, 1997, Francis *et al.*, 1999) and cells of the oligodendrocyte lineage express ErbB2, ErbB3, and ErbB4 (Canoll *et al.*, 1996). Neuregulins appear to be necessary for the formation of oligodendrocytes (Vartanian *et al.*, 1999) and are a potent survival factor for cells of the oligodendrocyte lineage (Canoll *et al.*, 1996, Fernandez *et al.*, 2000, Flores *et al.*, 2000). A soluble isoform of neuregulin-1, glial growth factor 2 (GGF-2), is mitogenic for both $O4^+$ late OPCs and $GalC^+$ pre-myelinating oligodendrocytes *in vitro*, promotes survival of late OPCs (Canoll *et al.*, 1996), and strongly inhibits oligodendrocyte maturation into MBP^+ myelinating oligodendrocytes (Canoll *et al.*, 1999, Canoll *et al.*, 1996). On the other hand, neuregulin/ErbB2 is required for the terminal differentiation of oligodendrocytes and for development of myelin (Park *et al.*, 2001, Kim *et al.*, 2003), suggesting that, like other growth factors, neuregulins play different roles during different stages of oligodendrocyte differentiation.

Oligodendrocytes also express neurotrophin receptors TrkA and TrkC. NT-3 is involved in oligodendrocyte development and promotes the survival and proliferation of OPCs (Barres *et al.*, 1994, Barres *et al.*, 1993b, Cohen *et al.*, 1996, Kumar *et al.*, 1998)

Both OPCs and oligodendrocytes express insulin and IGF receptors (Baron-Van Evercooren *et al.*, 1991). Astrocytes secrete IGF-1 (Chernausek, 1993), whereas neurons have been shown to secrete IGF-1 (Schechter *et al.*, 1995) and insulin (Schechter *et al.*, 1994). Insulin, IGF-1 and IGF-2 promote survival of OPCs (Barres *et al.*, 1992, Barres *et al.*, 1993b, Cui *et al.*, 2005). IGF-1 also promotes the proliferation of OPCs (McMorris and Dubois-Dalcq, 1988), is a mitogenic co-factor for FGF-2 and NT-3 (Barres *et al.*, 1993b, Barres and Raff, 1994), and promotes the differentiation of oligodendrocytes into mature $GalC^+$ cells (McMorris and Dubois-Dalcq, 1988, McMorris *et al.*, 1986, Goddard *et al.*, 1999).

1.2.2.3.2 Extracellular matrix molecules and integrins

ECM molecules bind to integrin receptors which form a transmembrane linkage between the ECM and the cytoskeleton and signal to the inside of the cell (Hynes, 1992, Diamond and Springer, 1994). Interaction between growth factor and integrin signalling pathways provides a mechanism for integration of short-range ECM signalling and long-range growth factor signalling in OPCs.

Oligodendrocytes express 5 integrins: the laminin receptor α6ß1, as well as αvß1, αvß3, αvß5 and αvß8, all of which bind vitronectin (Milner and ffrench-Constant, 1994, Milner *et al.*, 1997b), fibronectin, and a number of other extracellular and cell surface ligands containing the Arg-Gly-Asp (RGD) recognition sequence. Integrins α6ß1 and αvß8 are expressed throughout oligodendrocyte development, whereas αvß1, αvß3 and αvß5 are expressed sequentially during development (Milner and ffrench-Constant, 1994, Milner *et al.*, 1997b) and are thought to be involved in oligodendrocyte migration, proliferation and differentiation, respectively (Blaschuk *et al.*, 2000). The differential expression and activation of integrins has been proposed to regulate growth factor signalling and influence multiple aspects of oligodendrocyte development and myelination (Baron *et al.*, 2005).

In vitro studies have demonstrated a role for αvß1 integrin in PDGF mediated migration of OPCs (Milner *et al.*, 1996). The mitogenic effects of PDGF are mediated through the PDGFαR and the activation of αvß3 integrin (Baron *et al.*, 2002). While physiological concentrations of PDGF (1 ng/ml) are not sufficient to directly promote OPC proliferation, they do so indirectly via activation of integrin αvß3 that leads to increased affinity for PDGF (Baron *et al.*, 2002).

As OPCs differentiate into oligodendrocytes, the major role of the PDGFαR is to provide a survival signal for newly formed oligodendrocytes (Barres *et al.*, 1992, Calver *et al.*, 1998). The PDGF generated survival signal is amplified by α6ß1 integrin signalling via Fyn tyrosine kinase and the phosphatidylinositol 3´-kinase (PI3K) pathway in response to laminins expressed on the target axons, thereby providing a mechanism for the target dependence of oligodendrocyte survival (Colognato *et al.*, 2002, Colognato *et al.*, 2004).

It has been shown that oligodendrocyte membranes contain lipid rafts (Taylor *et al.*, 2002) and that PDGFαR and α6β1 integrin are localised in lipid rafts of newly differentiated oligodendrocytes (Baron *et al.*, 2003). Laminin-2 induces the co-localization of integrin α6β1 and the PDGFαR within the same raft domain and enhances PI3K signalling in response to PDGF (Baron *et al.*, 2003). This localisation is important for normal survival signalling, because depletion of lipid rafts increases oligodendrocyte apoptosis and inhibits PI3K signalling, whereas integrin activation increases raft localization and rescues the effects of both raft depletion and PDGF removal on survival and PI3K signalling (Decker and ffrench-Constant, 2004). In contrast, integrin αvβ3, which is associated with PDGFαR in OPCs and is part of the signalling pathway by which PDGF stimulates proliferation, is not present in lipid rafts of differentiated oligodendrocytes (Baron *et al.*, 2002). Thus the integrin associated with the PDGFαR determines the response to PDGF. Lipid rafts provide a favourable environment for growth factor-mediated integrin activation and the localisation of different integrins in lipid rafts at different stages of differentiation allows for switching of growth factor responses.

A similar change in response occurs with NRG signalling following axonal contact. NRG binding to ErbB receptors on OPCs stimulates survival and proliferation via a PI3K dependent pathway, whereas following axonal contact α6β1-laminin interactions trigger a switch to a MAPK signalling pathway that enhances survival and differentiation of more mature oligodendrocytes (Colognato *et al.*, 2002, Colognato *et al.*, 2004). β1 integrins are also implicated in myelin membrane formation following axonal contact (Relvas *et al.*, 2001, Colognato *et al.*, 2004, Olsen and ffrench-Constant, 2005). Thus association of growth factors with integrins provides a mechanism for contact dependent regulation of oligodendrocyte development.

1.2.2.3.3 Axon-oligodendrocyte interactions

In vitro, OPCs have the intrinsic potential to differentiate into oligodendrocytes even in the absence of axons, demonstrated by their ability to form myelin membrane-like sheets and the expression of myelin structural proteins (Reynolds *et al.*, 1989). In contrast, myelination *in vivo* requires a high level of specificity and requires axonal signals (Barres and Raff, 1999). The establishment of axon-glial contact during development is critical for the onset of myelination, with

the axon providing important signalling cues to the oligodendrocytes (Barres and Raff, 1999). In turn, the myelinating oligodendrocytes regulate axonal diameter and induce increased phosphorylation of neurofilaments (Sanchez *et al.*, 1996, Yin *et al.*, 1998). Axon derived survival signals regulate oligodendrocyte cell number and ensure that the oligodendrocyte population is precisely matched to the surface area of axons to be myelinated. This is achieved both by increasing the proliferation of OPCs (Wood and Bunge, 1986, Gard and Pfeiffer, 1990, Hardy and Reynolds, 1993, Barres and Raff, 1993) and by increasing oligodendrocyte survival (Barres *et al.*, 1993a, Frost *et al.*, 1999, Fernandez *et al.*, 2000).

Axons and oligodendrocytes are mutually dependent, both during development and in the adult, and the integrity of the axon-glial unit requires continual bidirectional signalling between the oligodendrocyte and the axon. The precise nature of the signals involved in axonal-oligodendrocyte interaction is not fully understood and may involve both soluble factors released from the axon and/or contact-dependent signalling following attachment of the oligodendrocyte to the axonal surface.

1.2.3 Microglia

Microglia are the immune cells of the CNS, and can act as phagocytes, cleaning up CNS debris. They are ontogenetically related to mononuclear phagocytes (Kreutzberg, 1996). Resting microglia are small cells with short, branched processes that comprise approximately 5% of the CNS glia. Microglia become activated upon injury and mainly function as phagocytes, although they also play other roles involved in tissue repair and neural regeneration.

1.2.4 Schwann cells

Schwann cells are the main peripheral nerve glial cells. Mature Schwann cells are traditionally classified according to their morphological relationship with axons into two different phenotypes: myelinating and non-myelinating Schwann cells. Like their CNS equivalents, the oligodendrocytes, myelinating Schwann cells insulate large diameter axons by producing myelin sheaths. However, whereas one oligodendrocyte can envelop approximately fifteen axonal internodes, the Schwann cell only envelops one axonal internode belonging to

the neuron to which it is associated. Schwann cell myelin differs to oligodendrocyte myelin in that it contains different proteins. The major peripheral myelin protein is P_0, whereas the central myelin contains PLP. Non-myelinating Schwann cells typically ensheath bundles of axons which are less than 1 μm in diameter without forming a myelin sheath (Jessen and Mirsky, 1991). Myelinating and non-myelinating Schwann cells can be distinguished by their antigenic phenotype. Both myelinating and non-myelinating Schwann cells express O4 (Mirsky *et al.*, 1990). Myelinating Schwann cells also express high levels of glycolipid GalC as well as myelin-related proteins including P_0, peripheral myelin protein 22kDa, MAG and MBP. Non-myelinating Schwann cells express GFAP, growth associated protein 43kDa (GAP 43), $p75^{NTR}$ as well as adhesion molecules L1, neural cell adhesion molecule (N-CAM), and Ca^{2+} dependent cell adhesion molecule (N-cadherin) (Mirsky *et al.*, 1986, Jessen *et al.*, 1990, Curtis *et al.*, 1992).

1.2.4.1 Development of Schwann cells

The majority of Schwann cells originate directly from the neural crest (Jessen and Mirsky, 1992, Le Douarin *et al.*, 1991), along with other glial cells of the PNS, peripheral neurons and melanocytes. Some Schwann cells are derived from boundary cap cells (Maro *et al.*, 2004), which in turn derive from the neural crest (Niederlander and Lumsden, 1996).

The generation of Schwann cells from the neural crest involves two intermediate cell types: Schwann cell precursors and immature Schwann cells (Mirsky and Jessen, 1999). Schwann cell precursors, which do not express S100 and lack a basal lamina, are detected in rat peripheral nerves at embryonic days (E) 14 and 15. These are dependent upon axonal signals for survival (Jessen *et al.*, 1994). Immature Schwann cells which form from the precursor cells can be observed from E17 until the time of birth (Jessen *et al.*, 1994, Dong *et al.*, 1995, Dong *et al.*, 1999). Immature Schwann cells envelop unmyelinated axons and form a basal lamina. Schwann cells require axonal contact to drive their differentiation from immature Schwann cells to myelinating or non-myelinating mature Schwann cells (Mirsky and Jessen, 1999).

Myelinating Schwann cells begin to form from the time of birth, whereas the non-myelinating Schwann cells appear later. Schwann cells are able to interchange between myelinating and non-myelinating phenotypes. In addition, mature Schwann cells are able to return to a cell type similar to the immature phenotype (Mirsky and Jessen, 1996) and to redifferentiate to the mature phenotype following re-establishment of appropriate axonal contact.

Schwann cell development is, in part, regulated by neuregulins. Neuregulins influence survival and proliferation of Schwann cells (Grinspan *et al.*, 1996a, Trachtenberg and Thompson, 1996). Inactivation of the neuregulin receptor ErbB3 (Garratt *et al.*, 2000) or the reduction of neuregulin-1 (Michailov *et al.*, 2004) results in reduced myelin sheath thickness which suggests that neuregulins also play a role in myelination of peripheral nerves.

1.2.4.2 Function of Schwann cells

Schwann cells provide an interface between the axon and the surrounding tissue. As mentioned above, Schwann cells produce the myelin sheath which allows saltatory conduction of nerve impulses. Schwann cells also play important roles in the development of the nerves (Mirsky *et al.*, 2002) and are thought to be responsible for the regenerative properties of the PNS. Schwann cells also provide the cellular scaffolds for regeneration in the nerve tracts and sprouting axons at neuromuscular junctions (Son *et al.*, 1996).

Following injury to the peripheral nerve, nerve fibres distal to the lesion undergo a calcium-mediated process called Wallerian degeneration (Waller, 1850). The axon and the surrounding myelin fragment as the nerve degenerates in an anterograde fashion, leaving behind Schwann cells inside the basal lamina that surrounded the original nerve. Schwann cells are able to survive without axonal contact because they are maintained by an autocrine mechanism involving IGF-2, PDGF-BB and NT-3 (Meier *et al.*, 1999).

The degeneration is followed by removal and recycling of axonal and myelin derived material to prepare the environment for subsequent axonal growth by the regenerating nerve. An initial role of Schwann cells is to help remove the degenerated axonal and myelin debris and then pass it on to macrophages. Once the axon and the myelin degenerate, the remaining denervated Schwann cells

are stimulated to proliferate within the basal lamina, forming columns of Schwann cells known as endoneurial tubes or bands of Büngner (Torigoe *et al.*, 1996, Burnett and Zager, 2004). These act as conduits for the regenerating axons. The basal lamina is comprised of collagen, fibronectin and laminin produced by Schwann cells (Baron-Van Evercooren *et al.*, 1986). Both fibronectin and laminin are potent substrates for neurite outgrowth (Cohen *et al.*, 1987, Humphries *et al.*, 1988). The axonal and myelin debris (Salzer and Bunge, 1980, Salzer *et al.*, 1980a, Salzer *et al.*, 1980b) as well as invading macrophages which have phagocytosed myelin (Baichwal *et al.*, 1988) stimulate proliferation of denervated Schwann cells within the bands of Büngner.

The presence of Schwann cells is the critical factor in peripheral nerve regeneration. This has been demonstrated in experiments where the nerve is frozen, killing the Schwann cells while leaving the basal lamina intact. When this nerve is grafted onto a proximal stump in a host animal, regeneration through the graft is only possible when it is accompanied by Schwann cells. If the invasion of live Schwann cells into the nerve graft is prevented by cytotoxic agents, axons fail to regenerate (Hall, 1986).

Denervated Schwann cells have a similar phenotype to that of non-myelinating Schwann cells (Guenard *et al.*, 1996), but express higher levels of GAP 43 and lower levels of glycolipids GalC and sulphatide (Mirsky and Jessen, 1996). They express large numbers of growth factors and cytokines including neurotrophins such as NT-4/5, neuregulins (Raabe *et al.*, 1996), NGF, BDNF (Yamamoto *et al.*, 1993); transforming growth factor ß1 (TGFß1); and glial derived neurotrophic factor (GDNF) which have been shown to attract and nourish axons in the distal nerve stump (Fu and Gordon, 1997). They also express a number of cell adhesion molecules that are believed to promote axonal regeneration and sprouting including N-CAM, L1 (Martini *et al.*, 1994), integrins and N-cadherin (Bixby *et al.*, 1988).

1.2.4.3 Ganglioside expression of Schwann cells

Numerous studies examining the Schwann cell expression of gangliosides have been performed, however, they have yielded conflicting results. The major ganglioside expressed by neonatal Schwann cells appears to be GM3 (Farrer and

Quarles, 1996). Levison and McCarthy (Levison and McCarthy, 1989) found that in culture, GD3 was expressed by peripheral neurons and fibroblasts but not Schwann cells and that the intensity of GD3 labelling on neuronal processes was diminished at sites contacted by Schwann cells (Levison and McCarthy, 1989). In contrast, GD3 was found to expressed on the surface of Schwann cells and at nodes of Ranvier in peripheral nerves (Usuki *et al.*, 2006). Two studies have found that Schwann cells derived from neonatal rat sciatic nerve label with CTx suggesting they express GM1 (Brockes *et al.*, 1979, Raff *et al.*, 1979), whereas another similar study showed that neonatal rat Schwann cell cultures do not express GM1 (Okada *et al.*, 1982). The finding that CTx is mitogenic for neonatal rat Schwann cells suggests that rat Schwann cells express GM1 (Raff *et al.*, 1978a). In addition, MBP induces Schwann cell proliferation via an interaction with GM1 (Tzeng *et al.*, 1995, Tzeng *et al.*, 1999). Furthermore, a study of mature, myelinating Schwann cells found that low amounts of GM1 are found on the Schwann cell internodal surfaces but that GM1 is primarily localised on specialised Schwann cell structures in the nodal region in rat peripheral nerves (Ganser *et al.*, 1983). Another study using GM1 immunofluorescence of adult rat spinal roots by Molander *et al* (1997) confirmed that GM1 is confined to Schmidt-Lanterman's incisures, myelin sheath paranodal end segments and to some extent the abaxonal Schwann cell cytoplasm. Also, some studies have found that Schwann cells express GD1a (Santafe *et al.*, 2005) whereas others have found that it is expressed by axons but not Schwann cells (Ho *et al.*, 1999).

1.2.4.4 Integrin expression by Schwann cells

In peripheral nerves Schwann cells interact with axons and extracellular matrix in order to ensheath and myelinate axons during development and regeneration. These interactions are likely to be mediated by adhesion molecules, including integrins, which mediate cell-cell and cell-extracellular matrix interactions. Studies have shown that Schwann cells express the following integrin receptors: α1β1, α2β1, α5β1, α6β1, α7β1, α6β4, αvβ3 and αvβ8 (Milner *et al.*, 1997a).

Collagen/laminin receptor α1β1 is expressed in large amounts in undifferentiated Schwann cells in contact with axons (Fernandez-Valle *et al.*, 1994) and only at very low levels on myelinating Schwann cells (Stewart *et al.*, 1997). Fibronectin receptor α5β1 is expressed on Schwann cells during

peripheral nerve development and during regeneration (Lefcort *et al.*, 1992). The laminin receptor α6β1 is expressed on migrating Schwann cells before birth (Dubovy *et al.*, 2001, Previtali *et al.*, 2003b). Undifferentiated Schwann cells in contact with axons express large amounts of α6β1 (Fernandez-Valle *et al.*, 1994), although it is constitutively expressed by Schwann cells even in the absence of axonal contact (Einheber *et al.*, 1993). The laminin-2 receptor, α7β1, which is expressed on Schwann cells postnatally, is the last laminin receptor expressed by differentiating Schwann cells (Chernousov *et al.*, 2007, Previtali *et al.*, 2003a).

α6β4 is expressed at the abaxonal surface of myelinating Schwann cells, opposite the Schwann cell basal lamina (Feltri *et al.*, 1994, Niessen *et al.*, 1994). α6β4 expression is axonally regulated and is irrespective of myelin formation, although it dramatically increases at the onset of myelination (Einheber *et al.*, 1993, Niessen *et al.*, 1994). αvβ8 is expressed by Schwann cells, and is a receptor for fibrin, which derives from fibrinogen infiltrating into peripheral nerve following injury (Chernousov and Carey, 2003).

1.3 Myelin

Schwann cell and oligodendrocyte processes wrap around axons to form an electrically insulating membrane known as myelin, which reduces current flow across the axonal membrane and increases resistance. The myelin sheath is interrupted at regular intervals by gaps, called nodes of Ranvier, where axonal electrical excitation is confined (Sherman and Brophy, 2005). Because the cytoplasm of the axon is electrically conductive, and because the myelin inhibits charge leakage through the membrane, depolarisation at one node of Ranvier is sufficient to elevate the voltage at a neighboring node to the threshold for initiation of a nerve impulse. As a result, nerve impulses, known as action potentials, travel along the axon by jumping from node to node, which greatly increases the rate and efficiency of nerve impulse propagation. This mode of action potential propagation is termed saltatory conduction.

The myelin sheath and the underlying axon are organised into discrete molecular structural and functional domains, which include the node of Ranvier, paranodal and juxtaparanodal regions and the internode (Salzer, 2003) (Figure 1.7). Each

domain contains unique complexes of molecules, both on the axonal surface and within the myelin sheath (Menon *et al.*, 2003). Axon-glial interactions are critical for the formation of these domains which allow saltatory conduction to take place.

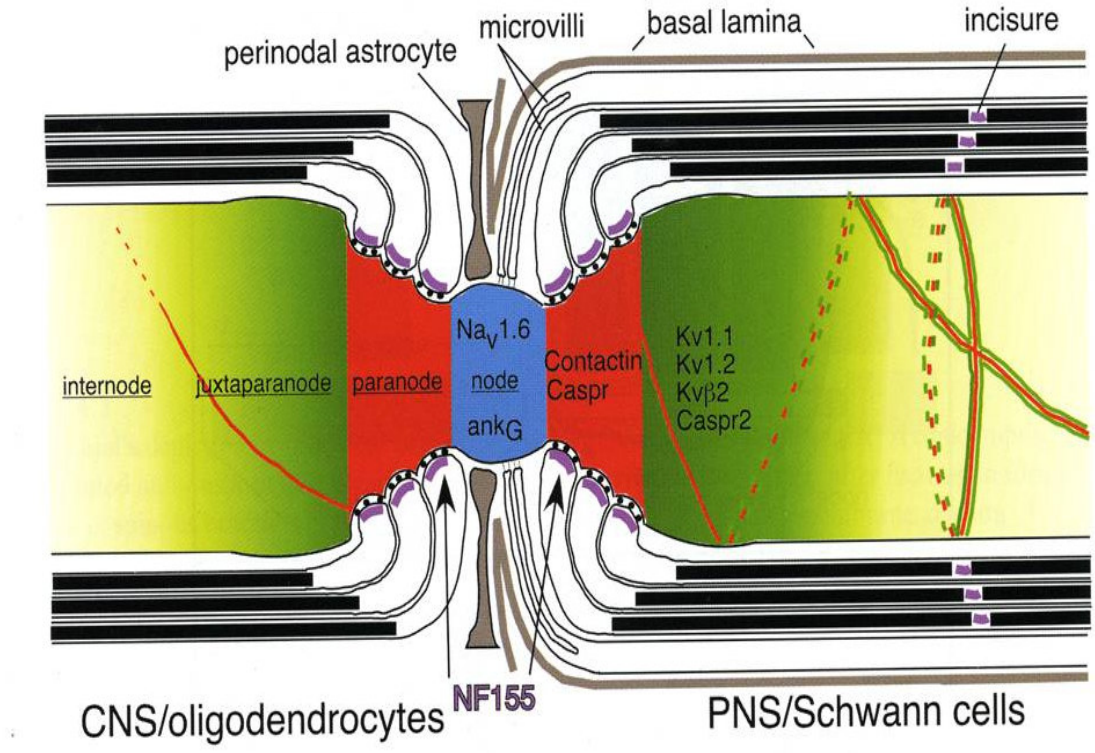

Figure 1.7. Schematic depiction of the node of Ranvier, paranode, juxtaparanode, and internode.
The left hand side panel depicts CNS myelin whereas the right hand side panel depicts PNS myelin. Axonal membrane in each domain is characterised by their expression of a different set of molecules in both the PNS and the CNS. Voltage-gated sodium channels are concentrated at nodes of Ranvier, while shaker-type voltage-gated potassium channels are concentrated at juxtaparanodes. The axonal cell adhesion molecules, contactin and caspr, and the glial cell adhesion molecule, neurofascin 155, are essential components of paranodal junctions. Adapted from (Arroyo and Scherer, 2000). In the PNS, components of the paranode and juxtaparanode extend into the internode as a thin spiral apposed to the inner mesaxon (red and green lines).

1.3.1 Node of Ranvier

The nodes of Ranvier contain clusters of voltage dependent Na^+ channels (Na_v) in the axonal membrane that are essential for the generation of action potentials (Rasband *et al.*, 1999a, Rasband and Trimmer, 2001). During development the main subtype of Na_v at node of Ranvier is $Na_v1.2$, which is replaced by $Na_v1.6$ in the adult CNS (Kaplan *et al.*, 2001). Na_v are molecular complexes that consist of a pore-forming α subunit and ancillary ß subunits. Na_v interact with other

molecules at the node to form macromolecular complexes. They form a complex with the cell adhesion molecules neuron-glia related CAM (Nr-CAM) and neurofascin 186 (NF186) and this complex is stabilised by association with the cytoskeletal adapter protein ankyrin G and the actin binding protein spectrin ßIV located in the axoplasm (Kordeli *et al.*, 1995, Davis *et al.*, 1996, Berghs *et al.*, 2000). Perinodal astrocyte processes and the ECM molecules tenascin-R, tenascin-C and phosphacan are also present within the perinodal space and may further stabilise nodal molecular complexes. Na_v are initially continuously distributed along axons, but eventually become clustered within nodes of Ranvier. Contact with Schwann cells induces clustering of sodium channels along the axons of peripheral neurons *in vitro* and *in vivo* (Joe and Angelides, 1992, Dugandzija-Novakovic *et al.*, 1995, Vabnick *et al.*, 1996). Similarly oligodendrocytes are crucial in inducing clustering of sodium channels in central neurons *in vitro* and *in vivo* (Kaplan *et al.*, 1997). Accordingly, rats lacking oligodendrocytes form very few Na^+ channel clusters (Kaplan *et al.*, 1997). Induction of Na_v clustering is independent of paranodal oligodendrocyte contact (Kaplan *et al.*, 1997, Jenkins and Bennett, 2002, Ishibashi *et al.*, 2003, Dupree *et al.*, 2005) and seems to be triggered by a protein released by oligodendrocytes (Kaplan *et al.*, 1997).

Na_v accumulate at the ends of the developing myelin sheath and as two adjacent internodal regions elongate, Na_v clusters fuse, forming the node of Ranvier. Potassium channels (K_v) are then excluded from the nodal region by the developing paranodal region and localise beneath the myelin sheath (Vabnick and Shrager, 1998). Based on the sequential appearance of antigens in developing nerves, NF186 and ankyrin G appear to be instrumental in the formation of the node and the recruitment of Na^+ channels to the node (Davis *et al.*, 1996, Lambert *et al.*, 1997, Jenkins and Bennett, 2002, Koticha *et al.*, 2006). Indeed, nodes of Ranvier fail to form correctly in NF186 deficient mice (Sherman *et al.*, 2005)

1.3.2 Paranode

Paranodes are the predominant interaction sites between myelinating glia and the axon. At paranodes, the lateral edge of the myelin sheath spirals around the axon forming a septate-like axoglial junction that provides a barrier to ion flow

within the axon. These septate-like paranodal junctions are important for the establishment of saltatory conduction because they separate Na^+ channels at the node from K^+ channels at the juxtaparanode (Rios *et al.*, 2003). The disruption of paranodal junctions results in mislocalisation of both Na^+ and K^+ channels, suggesting that they function as a diffusion barrier restricting the lateral mobility of membrane proteins (Bhat *et al.*, 2001, Boyle *et al.*, 2001, Rios *et al.*, 2003, Sherman *et al.*, 2005). Autotypic junctions also form between the paranodal loops themselves including tight junctions and gap junctions (Spiegel and Peles, 2002).

Glial and axonal membranes have distinct molecular specialisations at the paranodes. The 155 kDa isoform of neurofascin (NF155), a member of the L1 family of cell adhesion molecules, is expressed exclusively by oligodendrocytes. It is localised at the paranodes of myelinated nerves where the oligodendrocyte processes attach to the axon (Tait *et al.*, 2000). The axonal proteins contactin and contactin associated protein (Caspr) form a cis complex in the axolemma at the paranode (Einheber *et al.*, 1997, Rios *et al.*, 2000). The caspr/contactin complex binds to NF155, forming a critical component of the axo-glial paranodal junction (Charles *et al.*, 2002). In the PNS, the paranodes are enriched in gangliosides GD1b and GQ1b (Chiba *et al.*, 1993, Kusunoki *et al.*, 1993).

The proper assembly of the paranodes depends on many factors including protein–protein interactions and protein–lipid interactions. Caspr fails to localise to paranodes in shiverer mice lacking the myelin protein MBP as well as in mice lacking glycolipids GalC and sulphatide, which are involved in the formation of lipid rafts (Dupree *et al.*, 1998, Dupree *et al.*, 1999, Rasband *et al.*, 1999a). Paranodal junctions are also severely disrupted in both Caspr and contactin deficient mice (Bhat *et al.*, 2001, Boyle *et al.*, 2001). Furthermore, paranodes are completely absent in mice lacking NF155, suggesting that NF155 is critical for the formation of paranodes (Sherman *et al.*, 2005).

1.3.3 Juxtaparanode

The juxtaparanodal region is located adjacent to the innermost paranodal loop and forms the most lateral edge of the internodal compact myelin. Delayed rectifier Shaker type potassium channels Kv1.1 , Kv 1.2 and Kvβ2.1 are highly

enriched in the juxtaparanodal region and are thought to promote membrane repolarisation and maintenance of internodal resting potential (Rasband *et al.*, 1999b, Rasband and Trimmer, 2001). In the axolemma of the juxtaparanode K_v co-localise with the adhesion molecules caspr-2, structurally similar to Caspr found at the paranodes, and transient axonal protein (TAG-1) (Poliak *et al.*, 2003, Traka *et al.*, 2003). Caspr 2 and TAG-1 form a complex in the axonal membrane, which interacts with TAG-1 present on the glial membrane. This complex is essential for the accumulation of K_v at the juxtaparanode (Poliak *et al.*, 2001, Poliak *et al.*, 2003, Traka *et al.*, 2003).

1.3.4 Internode

The internodal region consists of compact myelin surrounding the axon and no specific molecular complexes have been described in this region. In the PNS components of the paranode and juxtaparanode, including Caspr-2, K_v, NF155 and TAG-1 extend into the internode as a thin spiral apposed to the inner mesaxon but this is not thought to occur in the CNS (Arroyo *et al.*, 2001, Traka *et al.*, 2003).

1.3.5 Role of lipid rafts in myelination

Lipid rafts have been implicated in protein sorting and as sites for signalling in the plasma membrane. It has been hypothesised that oligodendrocytes may adopt a mechanism of co-clustering proteins destined for myelination with lipid rafts during sorting and transport from the trans-Golgi network (Kim *et al.*, 1995). A study looking at the association of known myelin proteins with lipid rafts found that approximately 40% of non-compact myelin proteins CNP and MOG were selectively associated with lipid rafts, suggesting that they may have both non-active, and functionally active lipid raft-associated forms in the membrane (Kim and Pfeiffer, 1999).

As mentioned above, NF155 is required for the establishment of the paranodal axo-glial junctions. NF155 is recruited to lipid rafts during oligodendrocyte development (Maier *et al.*, 2005). It is not located in lipid rafts in cultured premyelinating oligodendrocytes but becomes raft associated during its progressive localisation to paranodes (Schafer *et al.*, 2004). Conditions

resembling the perturbation of the blood brain barrier, such as alteration of the extracellular matrix, interfere with NF155 raft association. In oligodendrocytes cultivated on poly-L-lysine, NF155 is recruited to lipid rafts during development and becomes enriched in secondary and tertiary processes, whereas in those grown on fibronectin the localisation and raft association of NF155 is perturbed and inhibits the molecular differentiation of oligodendrocytes. It has been demonstrated that efficient raft-association of NF155 is essential for the assembly of the paranodal junction and that reduced association of NF155 to lipid rafts is accompanied by the disassembly of the paranodal junction and thus contributes to the demyelination process in MS (Maier *et al.*, 2007). In MS lesions, the association of NF155 with lipid rafts was reduced, indicating that membrane association of NF155 was generally affected (Maier *et al.*, 2007).

GalC and its sulphated derivative, sulphatide, are major myelin galactolipids and are essential components of lipid rafts. It has been shown that these myelin galactolipids are important for paranode stability (Dupree *et al.*, 1998, Dupree *et al.*, 1999, Honke *et al.*, 2002, Ishibashi *et al.*, 2002, Marcus *et al.*, 2002) and may contribute to maintenance of axo-glial contacts by promoting the stabilisation of NF155 in lipid rafts (Schafer *et al.*, 2004). In accordance with this, mutant animals lacking PLP, GalC or sulphatide have disrupted paranodal junctions and have significantly reduced levels of raft-associated NF155 (Schafer *et al.*, 2004).

1.3.6 Role of gangliosides in myelination

Gangliosides are abundant on glial and neuronal cell membranes but their precise functions in the nervous system remain largely undefined. GalNAc T -/- mice that lack all complex gangliosides have a reduced conduction velocity (Takamiya *et al.*, 1996), which is indicative of myelination defects since it is myelin which facilitates saltatory conduction and greatly increases conduction velocity. A subsequent study in 4 to 10 week old GalNAc T -/- mice found morphological changes in the nerve fibre tracts of the spinal cord (Ma *et al.*, 2003). Specifically, the number of degenerated axons and unmyelinated fibres were markedly increased (Ma *et al.*, 2003). Ma *et al* (2003) also observed loosened myelin sheaths and myelin sheaths separated from axons by wide spaces. In addition, 12 to 16-week old GalNAc T -/- mice have decreased

myelination and axonal degeneration in optic and sciatic nerves (Sheikh *et al.*, 1999b). Furthermore, 8 to 12-month old GalNAc T -/- mice develop motor dysfunction (Chiavegatto *et al.*, 2000). These findings indicate that complex gangliosides are important for the maintenance of myelin and the integrity of nerve fibres.

Gangliosides have been shown to be important in the maintenance of paranodal junctions and ion channel clusters. It has been shown that antibodies to GM1 ganglioside label paranodal regions (Susuki *et al.*, 2007a). Autoantibodies to gangliosides GM1 and GD1a are thought to disrupt nodes of Ranvier in peripheral motor nerves and cause an axonal subtype of Guillain-Barré syndrome, termed acute motor axonal neuropathy (AMAN) (Hughes and Cornblath, 2005), an autoimmune neuropathy characterised by acute limb weakness. In addition, nodes of Ranvier are abnormally lengthened in ventral roots from early AMAN cases (Griffin *et al.*, 1996). Also, in a Guillain-Barré disease model, anti-GM1 antibodies bind to the nodal region, causing abnormally lengthened node of Ranvier (Susuki *et al.*, 2007b). This leads to the disruption of paranodal axoglial junctions, resulting in the disruption or disappearance of nodal Na^+ channel clusters (Susuki *et al.*, 2007b).

GalNAc T -/- mice lacking all complex gangliosides, including GM1 and GD1a, also have altered paranodal junctions, broadened Na^+ channel clusters, and mislocalisation of juxtaparanodal K^+ channels at the paranodes (Susuki *et al.*, 2007a). In these mice, immunostaining of Caspr and NF155 was reduced and some paranodal loops failed to attach to the axolemma in both peripheral and central nervous nerves (Susuki *et al.*, 2007a). Moreover, abnormal immunostaining at paranodes became more prominent with age (Susuki *et al.*, 2007a). These defects were more prevalent in ventral than dorsal roots, and less frequent in Sia T -/- mice lacking b-series gangliosides but with excess a-series gangliosides such as GM1 and GD1a (Susuki *et al.*, 2007a). Susuki *et al* (2007) also found slower nerve conduction and reduced nodal Na_v current in GalNAc T -/- peripheral motor nerves. In addition, the amounts of Caspr and NF155 in lipid rafts were reduced in GalNAc T -/- brains (Susuki *et al.*, 2007a). Earlier, Shafer et al (2004) showed that NF155 inclusion into lipid rafts occurs during paranode formation. These findings suggest that gangliosides are lipid

raft components that play important roles in stabilising neuron-glia interactions at paranodal junctions.

1.4 The olfactory system

The olfactory system is the sensory system is involved in the perception of odours. In mammals, odorants are inhaled through the nose where they interact with an odorant receptor located in the cilia of the olfactory receptor neurons (ORNs) (Farbman, 1990). ORNs transduce molecular features of the odorants into electrical signals which then travel along the olfactory nerve into the olfactory bulb.

1.4.1 PNS-CNS transitional zone

The PNS is able to support axonal outgrowth throughout life. In contrast, most CNS tissues can only support axonal outgrowth during development. This is exemplified by the dorsal root crush model. The dorsal root entry zone (DREZ) is a transitional zone between the CNS and the PNS and has been widely used to study the regenerative capacity of the nervous system. It is the region at which the dorsal roots enter the spinal cord and exemplifies the difference in the regenerative capacities of the two divisions of the nervous system. Cell bodies of the primary neurons lie in the dorsal root ganglia and they have a single axon which projects one branch peripherally and one branch centrally, to form the dorsal roots (Ramer *et al.*, 2001). Following a crush lesion of a dorsal root, the damaged axons are able to regrow through the Schwann cell environment of the PNS but they come to an abrupt halt when they reach the boundary between the PNS and the CNS, the DREZ (Carlstedt *et al.*, 1989).

The olfactory system is also a transitional zone between the PNS and the CNS (Doucette, 1991). Olfactory receptor neurons are one of the only populations of neurons to undergo neurogenesis throughout the lifetime of an organism, both as a result of natural turnover and in response to injury (Graziadei and Graziadei, 1979, Farbman, 1990). Unlike at the DREZ, new ORNs are generated from basal cells in the PNS environment of the olfactory epithelium (OE) and are able to re-enter the olfactory bulb and reform synapses with second order neurons in the CNS (Schwob, 2002).

1.4.2 Anatomy of the olfactory system

The two major components of the primary olfactory system are the olfactory mucosa which is located in the nasal cavity in the PNS and the olfactory bulb which is located in the CNS (Figure 1.8). The olfactory mucosa is composed of the OE and the lamina propria (LP). The nasal cavity also contains the respiratory epithelium. In addition, the trigeminal, vagus and glossopharyngeal nerves all have chemoreceptive free endings in the mucosal lining of the respiratory tract.

Olfactory epithelium is a pseudostratified columnar epithelium which lies in the posteriodorsal region of the nasal cavity. In humans it occupies an area of 1 cm^2, however in macrosmatic animals where the sense of smell is of paramount importance such as rodents, this area is increased by the presence of elaborate turbinates that extend from the lateral wall of the nasal cavity. The olfactory epithelium develops from the olfactory placode, a localised epithelial thickening that develops at E10 in rats, at the rostrolateral region of the embryonic head (Brunjes and Frazier, 1986, De Carlos *et al.*, 1995). The olfactory epithelium is composed of three main cell types: the sustentacular cells, ORNs and basal cells (Figure 1.9).

The lamina propria is a layer of loose connective tissue which lies beneath the epithelium. It contains Bowman's glands and OECs which ensheath ORNs as they travel from the olfactory epithelium to the olfactory bulb (Au and Roskams, 2003). The connective tissue is made up of various cell types including: fibroblasts, macrophages, pericytes, endothelial cells, smooth muscle cells from the lining of the blood vessels and Schwann cells that ensheath nerves that innervate the blood vessels (Barnett and Chang, 2004).

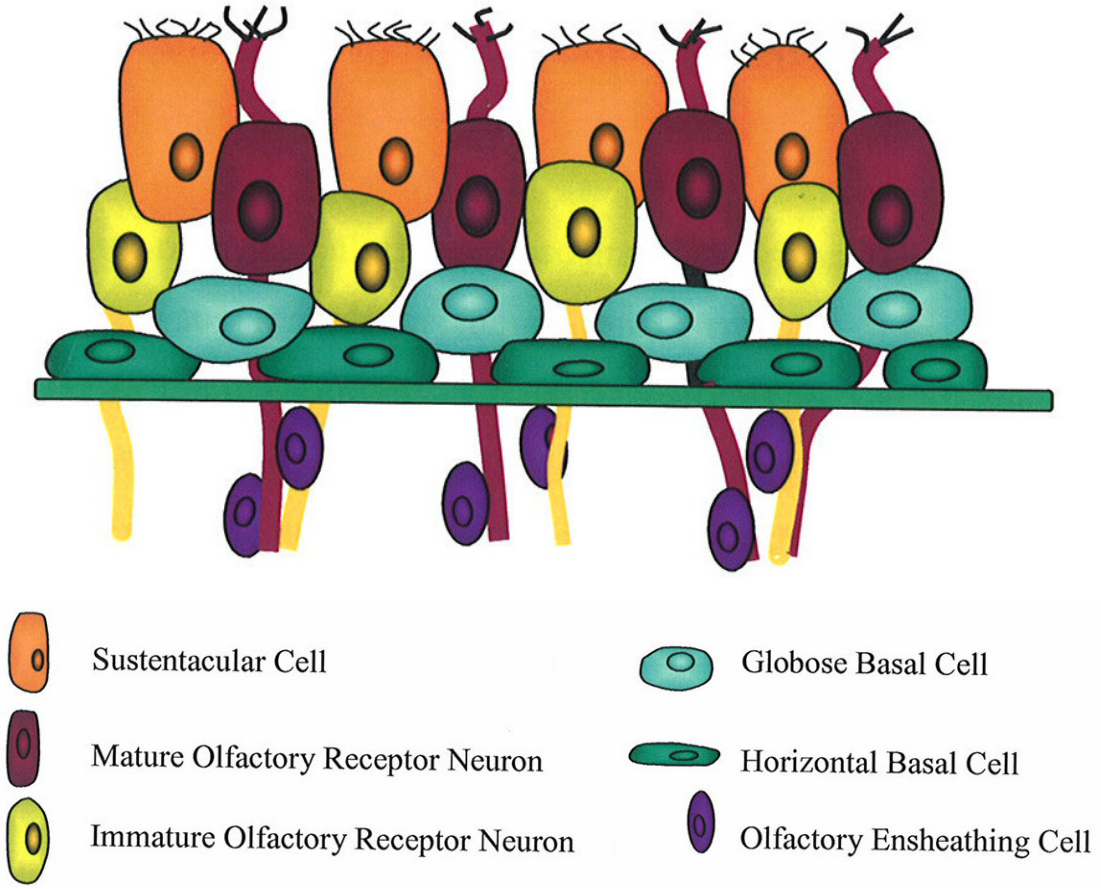

Figure 1.8. Cells of the olfactory epithelium
The olfactory epithelium contains the following cell types: sustentacular cell, immature olfactory receptor neurons, mature olfactory receptor neurons, globose basal cells and horizontal basal cells. Olfactory ensheathing cells are located in the lamina propria.

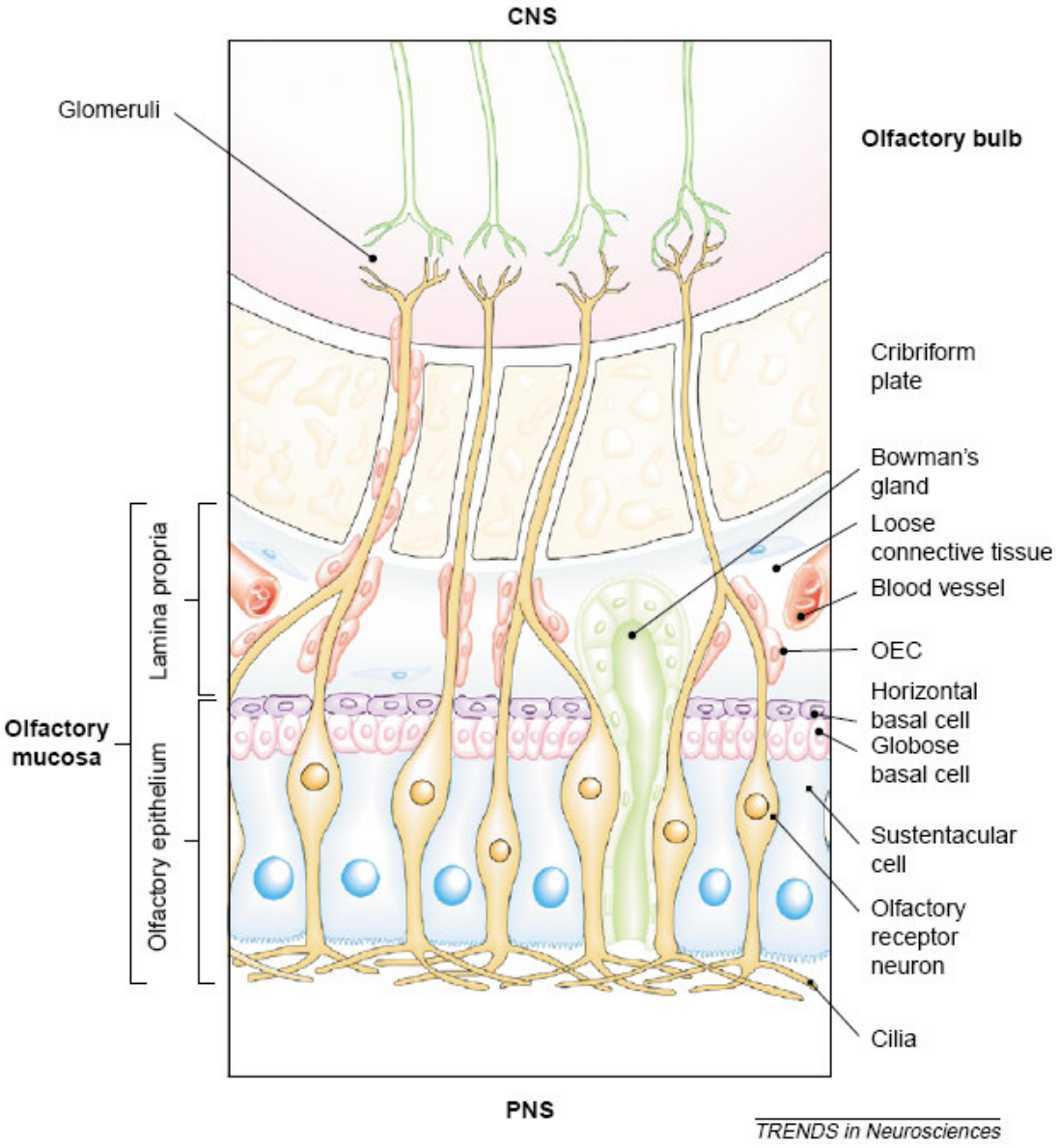

Figure 1.9. Anatomy of the olfactory system.
The olfactory system contains both PNS and CNS components. The olfactory mucosa, which contains the olfactory epithelium and the lamina propria, is located within the PNS, whereas the olfactory bulb is in the CNS. Cells of the olfactory epithelium are described in figure 1.8. Lamina propria consists of loose connective tissue and olfactory ensheathing cells, which ensheath bundles of olfactory receptor neurons as they travel from the olfactory epithelium to the olfactory bulb. The connective tissue within lamina propria contains many cell types such as fibroblasts, macrophages, pericytes, endothelial cells, smooth muscle cells from the lining of the blood vessels and Schwann cells that ensheath nerves that innervate the blood vessels. Figure taken from (Barnett and Chang, 2004).

1.4.2.1 Sustentacular cells

Sustentacular cells are supporting columnar epithelial cells that are similar to Müller cells in the retina (Pixley, 1992) and compose 15 to 25% of the total cell population of the olfactory epithelium (Weiler and Farbman, 1998). They possess numerous microvilli and much ER (Farbman and Buchholz, 1992). Sustentacular cells are thought to be involved in detoxification, due to the presence of a prominent cytochrome P-450 system, as well as in processing of odorants (Schwob and Mozell, 1999, Carr *et al.*, 1990), regulating the ionic composition of the mucus (Getchell *et al.*, 1984) and providing a structural, supportive matrix (Getchell *et al.*, 1984).

1.4.2.2 Olfactory receptor neurons

ORNs are bipolar neurons which project an apical dendrite to the surface of the epithelium, where it expands into a ciliated dendritic knob and a basal axon through the epithelium and underlying basal lamina. ORN axons are small in diameter, approximatey 0.2 μm and therefore unmyelinated. Upon exiting the base of the epithelium ORN axons form fascicles, which comprise the olfactory nerve, the first cranial nerve. The olfactory nerve projects through foramina in the cribiform plate of the ethmoid bone to enter the CNS at the olfactory bulbs. Mature ORNs are characterised by the expression of 19 kDa cytoplasmic protein, the olfactory marker protein (OMP) (Margolis, 1982). OMP is also expressed in other small groups of neurons throughout the CNS (Baker *et al.*, 1989). The function of OMP has not been fully elucidated, although it is known to cause an increase in the proliferation of both neural progenitors and sustentacular cells (Farbman *et al.*, 1998). OMP-null mice have an ultrastructurally normal epithelium and bulb, however, they have an impaired physiological response to odour stimuli (Buiakova *et al.*, 1996). Mature ORNs have both an axon and a dendrite, whereas immature ORNs lack a dendrite and are characterised by the expression of GAP 43 (Verhaagen *et al.*, 1989, Meiri *et al.*, 1991).

1.4.2.3 Basal cells

There are two classes of basal cell within the olfactory epithelium, globose and horizontal basal cells. Globose basal cells (GBCs) are the most mitotically active

cells within the epithelium. They label with antibodies to the putative glycolipids GBC-1, 2 and 3 (Goldstein and Schwob, 1996). They are located beneath the immature ORNs in the epithelium and above the horizontal basal cells (HBCs).

The HBCs are located at the base of the epithelium, immediately above the basement membrane, are flattened in shape and are characterised by the expression of cytokeratins 5 and 14 (Holbrook *et al.*, 1995). It has been proposed that they function as intermediate signalling cells, transmitting information regarding the status of the ORN population to the GBCs causing them to respond accordingly (Holbrook *et al.*, 1995).

As mentioned previously, ORNs undergo constant replacement from progenitors residing in the olfactory epithelium, the identity of which has been the subject of some contention, both the HBCs and GBCs having been contenders. It now appears, however, that GBCs are the neuronal progenitors since they have a faster turnover rate than HBCs (Holbrook *et al.*, 1995, Huard and Schwob, 1995). Lineage studies using replication-incompetent retroviral vectors encoding heritable markers also suggest that GBCs are neuronal precursors (Caggiano *et al.*, 1994, Schwob *et al.*, 1994a). Not only are they neuronal precursors, but they have also been demonstrated in certain circumstances to generate sustentacular cells, cells of the Bowman's glands and ducts as well as HBCs (Huard *et al.*, 1998).

Neurogenesis in the olfactory epithelium is under the regulation of a negative feedback, mature ORNs feeding-back to inhibit the further differentiation of basal cells. *In vivo* studies have shown the rate of proliferation of GBCs increases if the death of the ORNs is induced, whereas it decreases if ORNs are protected from damage (Farbman, 1990). *In vitro* data also supports this theory, proliferative colonies of olfactory progenitors being inhibited when grown in the presence of differentiated ORNs (Mumm *et al.*, 1996). This feedback is regulated by the bone morphogenetic proteins (BMPs), which are members of the TGFβ superfamily that play important roles in neurogenesis. In cell culture, BMP-2, 4 and 7 decreased the number of proliferating olfactory progenitors and inhibited the differentiation of ORNs, due to the proteolysis of Mash 1 (Shou *et*

al., 1999) and all three are expressed in the olfactory system *in vivo* (Shou *et al.*, 2000).

There are two different classes of GBCs. One population expresses the transcription factor Mash 1 and functions as transient amplifying cells (Gordon *et al.*, 1995) whereas the other expresses the transcription factor neurogenin 1 and functions as immediate neuronal precursors (Gordon *et al.*, 1995, Cau *et al.*, 1997). This has been confirmed using transgenic animals. In Mash 1 null mutant mice, olfactory progenitors are not produced, while in neurogenin 1 null mutant mice, progenitors are produced but differentiation is blocked (Cau *et al.*, 2002).

1.4.2.4 Bowman's glands

Bowman's glands produce a layer of mucus that constantly washes over the surface of the epithelium, removing odorant molecules (Schwob and Mozell, 1999). The ducts of Bowman's glands extend from the lamina propria, through the epithelium to the luminal surface.

1.4.2.5 Olfactory ensheathing cells

OECs are a unique class of macroglial cell which straddle the divide between the glia of the CNS and the PNS. They ensheath the thin non-myelinated axons of the ORNs from their peripheral origin in the olfactory mucosa across the cribiform plate and into the olfactory nerve layer of the ipsilateral olfactory bulb within the CNS. The cytoplasmic processes of OECs enfold bundles of unmyelinated ORN axons, with OEC perikarya aligning along the length of the fascicles (Ramon-Cueto and Avila, 1998).

OECs share similarities with both astrocytes and Schwann cells and although in the past they have been considered to be variants of both types of glia (Doucette, 1984, Chuah and Au, 1991), they are now regarded as a unique glial cell. OECs have a different developmental origin to neural crest derived PNS glia and neuroectoderm derived CNS glia, originating instead from the olfactory placode.

OEC that share many properties with the well characterised rat OECs have been identified in the human olfactory system (Barnett *et al.*, 2000). Human OECs

were shown to have a similar flattened morphology and demonstrated immunoreactivity for $p75^{NTR}$, although no E-NCAM positive cells were observed. They were also capable of remyelinating experimentally created demyelinated lesions (Barnett *et al.*, 2000).

1.4.2.5.1 Properties in vivo

OEC characteristics include fusiform morphology, indented nuclei, electron dense cytoplasm, and scattered intermediate filaments (Doucette, 1984). Morphologically, OECs *in vivo* appear most similar to non-myelinating Schwann cells since they both ensheath small diameter axons (<1 μm) without forming myelin sheaths. OECs are often compared to non-myelinating Schwann cells because they have many things in common. For instance, OECs express laminin (Liesi, 1985), L1 (Miragall *et al.*, 1988), vimentin (Ramon-Cueto and Nieto-Sampedro, 1992) and $p75^{NTR}$ (Barnett *et al.*, 1993), as do non-myelinating Schwann cells (Bunge *et al.*, 1986, Jessen and Mirsky, 1991, Ramon-Cueto and Nieto-Sampedro, 1992).

However, OECs differ from Schwann cells in many ways. Although both cell types express GFAP, OECs express the central type whereas Schwann cells express peripheral GFAP (Barber and Dahl, 1987, Jessen *et al.*, 1990). Unlike both myelinating Schwann cells and non-myelinating Schwann cells (Jessen and Mirsky, 1991), OECs do not express GalC (Barnett *et al.*, 1993). Also, unlike Schwann cells, OECs do not have a basal lamina apart from where they form part of the glia limitans at the surface of the olfactory bulb and form end-feet on blood vessels (Doucette, 1984). They also differ from non-myelinating Schwann cells in the number of axons they ensheath. Non-myelinating Schwann cells ensheath approximately 20 axons entrenched in separate furrows, whereas individual OECs embrace bundles of up to 200 axons separated by a few cytoplasmic processes (Franklin and Barnett, 1997).

1.4.2.5.2 Properties in vitro

OECs are a heterogeneous population *in vitro* with respect to morphology and express different markers depending on the conditions in which they are grown, time in culture and the age of the tissue donor. In culture, OECs also have an antigenic phenotype most akin to non-myelinating Schwann cells (Barnett *et al.*, 1993).

When OECs are maintained in serum-free conditioned medium from confluent type-1 astrocytes, known as astrocyte conditioned medium (ACM) (Noble and Murray, 1984), two phenotypes are observed with either Schwann cell-like or astrocyte-like properties (Pixley, 1992, Franceschini and Barnett, 1996). Astrocyte-like OECs have a flattened morphology and express E-NCAM, fibrous GFAP and weak levels or no $p75^{NTR}$. The Schwann cell-like OECs have a spindle-like morphology, lack E-NCAM, and express diffuse GFAP and high levels of $p75^{NTR}$ (Franceschini and Barnett, 1996, Yan and Johnson, 1988). Intermediate phenotypes are observed, even in an established clonal cell line, supporting the opinion that they are derived from a common precursor (Franceschini and Barnett, 1996). Manipulation of culture conditions can vary these expression patterns, although S100 (glial low molecular weight Ca^{2+} binding protein) appears to be expressed by all OECs *in vitro* and *in vivo* (Ramon-Cueto and Avila, 1998).

A combination of the growth factors forskolin, heregulin ß1 and FGF2, known as olfactory mitogen medium (OMM), in addition to ACM, which contains type III neuregulin-1 (Pollock *et al.*, 1999), was found to be the most mitogenic condition for OECs (Alexander *et al.*, 2002, Yan *et al.*, 2001). Subsequent tissue culture work has also revealed that the addition of medium containing 10% foetal bovine serum (FBS) to this mixture, in a 1:1 ratio, augments the mitogenic effect. Other factors found to be mitogenic for OECs are NGF and hepatocyte growth factor (Chuah and Teague, 1999).

1.4.2.5.3 OECs and regeneration

The unique restorative capacity of the olfactory system may be due to the supportive glial cell environment provided by the presence of the OECs since OECs express a number of growth promoting molecules (Schwob, 2002). Vimentin is the main constituent of OEC intermediate filaments (Franceschini and Barnett, 1996). This protein is normally expressed by astrocytes during development (Bignami *et al.*, 1982) but this expression is shifted to GFAP as astrocytes become non-permissive to axonal growth (Carlstedt *et al.*, 1987, Ramon-Cueto and Avila, 1998). Vimentin being a major constituent of adult OECs suggests that OECs maintain an immature growth-permissive phenotype. OECs also express nestin (Doucette, 1993). Nestin is an intermediate filament protein that is used as a marker for precursor cells in the CNS and the presence

of nestin within OECs is perhaps a reflection of the cellular plastic potential of these cells.

Williams *et al* (2004) showed that following damage to the olfactory epithelium, OECs appear to maintain their architecture and act as a conduit for regenerating olfactory nerve axons. The plasma membranes of OECs contain a number of adhesion molecules such as L1 (Miragall *et al.*, 1988), E-NCAM (Franceschini and Barnett, 1996), fibronectin, laminin and type IV collagen (Doucette, 1996, Kafitz and Greer, 1997). These adhesion molecules could guide regenerating axons. In addition, OECs also produce and secrete growth factors such as PDGF, NGF, FGF and BDNF (Woodhall *et al.*, 2001). Barnett and colleagues (1993) detected neonatal OEC expression of $p75^{NTR}$ while others report CNTF and CNTF receptor-α expression (Wewetzer *et al.*, 2001). Expression of such factors may contribute to the persisting regenerative properties of the olfactory system.

Furthermore, a number of experiments have demonstrated that the OEC is responsible for the olfactory system's ability to regenerate. Following transection of a segment of adult rat spinal cord, a guidance channel containing Schwann cells was placed between the spinal cord stumps with OECs injected into either end of this channel. This resulted in OEC migration into the channel and the passage of regenerating axons through the channel (Ramon-Cueto *et al.*, 1998) with recovery of forepaw function (Imaizumi *et al.*, 1998). In the absence of OEC injection few axons were capable of exiting the channel.

The cells of the primary olfactory system express a large number of growth factors, which may contribute to the regenerative properties of the region. The following growth factors have been shown to be expressed in the olfactory epithelium: NGF (Williams and Rush, 1988, Aiba *et al.*, 1993), BDNF (Buckland and Cunningham, 1999), FGF2 (Goldstein *et al.*, 1997), IGFI and II (Ayer-le Lievre *et al.*, 1991, Federico *et al.*, 1999), GDNF (Buckland and Cunningham, 1999), TGFα (Farbman and Buchholz, 1996) and type I NRG heregulin (Salehi-Ashtiani and Farbman, 1996). Cells of the olfactory epithelium also express the following growth factor receptors: TrkA, TrkB and TrkC (Roskams *et al.*, 1996), FGFR (Mackay-Sima and Chuahb, 2000), EGFR (Farbman, 1994, Holbrook *et al.*, 1995) as well as neuregulin receptors ErbB2, ErbB3 and ErbB4 (Salehi-Ashtiani and Farbman, 1996, Perroteau *et al.*, 1998, Lindholm *et al.*, 2002). There is some

disagreement within the literature regarding the presence of $p75^{NTR}$ in the epithelium, some investigators reporting it to be expressed in basal cells (Roskams *et al.*, 1996) whilst others describe a lack of expression (Gong *et al.*, 1994).

In vitro data indicates that the survival and differentiation of ORNs are likely to be under the control of many different, interacting growth factors. It has been suggested that NGF acts indirectly via OECs to act as a survival factor for ORNs, although this effect was only sustained for 10 days (Mahanthappa and Schwarting, 1993), and NT3 prevented apoptosis of mature ORNs (Holcomb *et al.*, 1995). PDGF-AB has also been shown to promote the survival of ORNs (Newman *et al.*, 2000). It has also been shown that NGF, BDNF and NT-3 act together to induce c-fos expression and increase the number of differentiating ORNs (Roskams *et al.*, 1996).

FGF2 is mitogenic for GBCs (DeHamer *et al.*, 1994), while TGFα and EGF stimulate the proliferation of HBCs (Getchell *et al.*, 2000, Farbman, 1994) and sustentacular cells (Farbman and Buchholz, 1996). IGF1 also stimulates the proliferation of neuronal precursors (Pixley *et al.*, 1998), although they do not express the receptors (Pixley *et al.*, 1998).

As mentioned earlier, in most areas of the brain 9-O-acetyl GD3 staining of pathways of axon outgrowth disappears as soon as the axons reach their target axons. However, in the primary olfactory system the expression of 9-O-acetyl GD3 begins at E13, when the olfactory epithelium and the migratory mass are intensely stained and at E19, the immunoreactivity disappears from the olfactory epithelium but remains in a few fascicles and some glomeruli of the olfactory bulb in the newborn and the adult (Mendez-Otero and Ramon-Cueto, 1994). This suggests the expression of 9-O-acetyl GD3 by ORN axons and/or migrating cells may facilitate axonal outgrowth during development and may be involved in the formation of new glomeruli in the mature olfactory bulb (Mendez-Otero and Ramon-Cueto, 1994).

1.4.2.6 The olfactory bulb

The olfactory bulbs are located ventral to the orbital surfaces of the frontal lobes and are highly distinctive due to their laminated structure. They derive

from the neural tube (Hinds, 1968). The outer layer of the bulb, termed the olfactory nerve layer, is comprised solely of axons of the ORNs and their associated glial cells. The glomerular layer is immediately adjacent to the outer nerve layer and consists of round structures termed glomeruli, where the axons of the ORNs synapse onto dendrites of interneurons and projection neurons (Meisami and Sendera, 1993). Glomeruli are dense collections of interweaving processes that are demarcated by the cell bodies of interneurons and glia.

There are believed to be at least 3 morphologically distinct types of periglomerular interneurons. Two types, the periglomerular cells, and the external or superficial tufted cells, send dendrites into the glomeruli, forming dendrodendritic synapses with both the ORNs and projection neurons. The third type, the short axon cells, have processes that do not enter the glomeruli (Kosaka *et al.*, 1998). At ORN terminals both GABA acting on presynaptic $GABA_B$ receptors (Bonino *et al.*, 1999) and dopamine acting on presynaptic D2 receptors (Hsia *et al.*, 1999) act as inhibitory neurotransmitters. Glutamate acting via NMDA (N-methyl-D-aspartate) and AMPA (α-amino-3-hydroxy-5-methyl-4-soxazolepropionic acid)/kainite receptors acts as an excitatory neurotransmitter.

There are two types of output neuron in the olfactory bulb, the mitral and tufted cells (Kishi *et al.*, 1982, Macrides and Schneider, 1982). The cell bodies of the tufted neurons are located in the wide external plexiform layer along with those of the periglomerular interneurons, whereas the cell bodies of the mitral neurons form the adjacent narrow mitral cell layer. Mitral cells are large neurons, approximately 20-30µm in diameter and are normally arranged in single layer. Next to the mitral cell layer is the internal plexiform layer, which is also very narrow and contains many processes. The granule cell layer contains the cell bodies of the most numerous interneurons in the bulb, the granule cells, which are approximately 5-10µm in diameter. Granule cells lack axons, sending their dendrites into the external plexiform layer where they form dendro-dendritic synapses with mitral and tufted cells. It is through these connections that lateral inhibition of the output neurons occurs, an important mechanism in odour discrimination (Isaacson and Strowbridge, 1998).

Both of the populations of interneurons in the bulb, the periglomerular and granule cells also undergo neurogenesis throughout life, are replaced from progenitors in the subependymal layer (Altman, 1969, Lois *et al.*, 1996). These originate in the subventricular zone of the lateral ventricles (Lois *et al.*, 1996) and migrate to the olfactory bulb via the rostral migratory stream.

Axons of the mitral and the tufted cells form the olfactory tract which projects to the cortex and the contralateral olfactory bulb. In turn, the olfactory bulbs receive afferent connections from many different areas of the brain (Parent, 1996).

1.4.3 Models of degeneration and regeneration

The unique regenerative property of the primary olfactory system can be exploited experimentally to study regeneration. Several techniques have been employed to induce the degeneration and subsequent regeneration of the olfactory system, some of which are outlined below.

1.4.3.1 Physical lesioning

Transection of the olfactory nerve within the PNS portion of the olfactory system has been widely used to induce retrograde degeneration and apoptosis of ORNs (Graziadei and Monti Graziadei, 1980, Doucette *et al.*, 1983). The degeneration of ORNs following transection is rapid, starting 15 to 24 hours following transection and is complete after 10 days (Graziadei and Monti Graziadei, 1980). The axons of regenerated ORNs reach the glomeruli after 25 to 30 days (Graziadei and Monti Graziadei, 1980, Doucette *et al.*, 1983) and the olfactory epithelium reacquires a population of mature ORNs similar to controls after 60 to 90 days (Graziadei *et al.*, 1980). This technique mimics inherent degeneration of ORNs that happens throughout life in that it does not damage any cell types within the epithelium other than mature ORNs. However, this method damages the tissue surrounding the axons, producing scar tissue, which does not occur during normal turnover. Also, when the axons are cut within the olfactory nerve layer, which is in the CNS, the axons are unable to grow through the resulting scar (Doucette *et al.*, 1983).

1.4.3.2 Chemical lesioning

A number of different chemicals have been directly administered into the olfactory epithelium to induce degeneration including triton X-100 (Verhaagen *et al.*, 1990, Turner and Perez-Polo, 1993), colchicine (Rochel and Margolis, 1980, Suzuki, 1998), methyl bromide (Schwob *et al.*, 1995, Schwob *et al.*, 1999) and zinc sulphate ($ZnSO_4$) (Matulionis, 1975, Williams *et al.*, 2004). The advantage of chemical lesioning is that, apart from the epithelium, it does not affect any other tissue in the olfactory system. Application of colchicine causes the disaggregation of microtubules and thus results in the degeneration of ORNs and GBCs, while HBCs and sustentacular cells remain unaffected (Suzuki, 1998). Triton X-100 treatment causes the least damage to the olfactory epithelium resulting in faster regeneration (Rochel and Margolis, 1980). Chemical lesioning using methyl bromide and $ZnSO_4$ causes the degeneration of all cell types within the epithelium except the basal cells which remain attached to the underlying basal lamina.

Although $ZnSO_4$ has been used extensively to cause the degeneration of the ORNs, it is reported to produce varying degrees of damage. In some studies it was only 25% effective, while in others it caused "irreversible damage" (Rochel and Margolis, 1980). However, Williams *et al* (2004) showed that following $ZnSO_4$ treatment, degeneration in the epithelium is reproducible and rapid, with regeneration following after 4 days, and being morphologically complete by 5 weeks.

Inhalation of methyl bromide over 6 hours causes the destruction of ORNs and sustentacular cells in 90% of epithelium (Schwob *et al.*, 1995). There is an increase in the number of proliferating cells 24 to 48 hours following methyl bromide treatment, which returns to normal levels between 4 to 6 weeks. Immature ORNs start to appear 3 days later, while the mature ORNs and sustentacular cells first appear 1 to 2 weeks after treatment. ORNs begin to extend axons after 1 week and these reach the glomeruli after 2 weeks (Schwob *et al.*, 1999). The olfactory system returns to normal 2 months after methyl bromide treatment (Schwob *et al.*, 1995, Schwob *et al.*, 1999).

1.4.3.3 Removal of the target

The surgical removal of olfactory bulbs is known as bulbectomy. Removal of the synaptic targets of ORNs by bulbectomy results in apoptosis of ORNs which peaks after two days (Holcomb *et al.*, 1995, Calof *et al.*, 1996). Five to six days after target deprivation, the width of the olfactory epithelium is reduced to a minimum (Holcomb *et al.*, 1995). There is also an increase in the proliferation of ORNs progenitors in the epithelium (Schwartz Levey *et al.*, 1991, Nan *et al.*, 2001). However, the lifespan of the newly generated ORNs is reduced to approximately 10 days (Carr and Farbman, 1993), and the majority of ORNs within the regenerating epithelium remain in an immature state, unable to extend dendrites (Verhaagen *et al.*, 1990). This suggests that ORNs are dependent on factors from the olfactory bulbs for their survival and maturation (Schwob *et al.*, 1992). In adults, the cavity previously occupied by the bulb becomes filled with scar tissue, preventing the newly regenerated axons from making contact with the brain (Butler *et al.*, 1984, Hendricks *et al.*, 1994). In neonates, younger than postnatal day 13, there is the forward displacement of the frontal lobes into the vacant space left by the bulbs, which is innervated by the regenerating axons to form glomeruli-like structures (Butler *et al.*, 1984, Evers *et al.*, 1996).

1.5 Aims of the thesis

Many functions have been attributed to gangliosides such as, migration and axonal outgrowth, proliferation, differentiation and repair. I was interested in these functions in relation to ascertaining the role gangliosides play in glial cells. Specifically, this thesis will address the role of complex gangliosides in the biology of OECs and Schwann cells in order to gain a better understanding of these two glial cells. I will initially compare the ganglioside expression of OECs and Schwann cells followed by a comparison of proliferation and migration of OECs and Schwann cells obtained from wild-type and ganglioside knockout mice.

Previous studies have shown that exogenously added gangliosides enhance peripheral nerve regeneration. In addition, Sia T -/- mice have reduced regeneration of axotomised hypoglossal nerves compared with wild-type. There have also been numerous studies suggesting that gangliosides play a role in

migration and neurite extension. It was, therefore, interesting to compare regeneration in ganglioside knockout and wild-type mice. The olfactory system was chosen for the regeneration experiments because it is a constantly regenerative tissue and it contains both PNS and CNS components. Unlike most CNS tissue, the olfactory system regenerates throughout life – after damage the olfactory receptor neuron axons can, with the help of the OECs, grow back into the CNS and form synapses. This makes the olfactory system an ideal system to study regeneration. I shall first examine the ganglioside expression of the olfactory system using immunocytochemistry. In order to study the degeneration and regeneration of the olfactory system, I shall use an established method whereby the olfactory receptor neurons are destroyed using $ZnSO_4$. I shall look at several markers to track and compare the degeneration and regeneration of the olfactory system in wild-type and ganglioside knockout mice.

During the development of the CNS, oligodendrocyte precursor cells progress through migratory and proliferative stages before differentiating into myelin-forming oligodendrocytes. Gangliosides are differentially expressed throughout oligodendrocyte differentiation suggesting they may play a role in oligodendrocyte differentiation. I will initially study differentiation in oligodendrocytes isolated from wild-type and Sia T -/- optic nerves. In order to study the role of gangliosides in myelination, I shall compare oligodendrocyte differentiation, myelination and axonal density in dissociated spinal cord cultures, which contain a mixture of cells including oligodendrocytes, axons and astrocytes, isolated from wild-type, Sia T -/- and GalNAc T -/- mice.

2 CHAPTER 2

Methods

2.1 Ganglioside knockout mice

Three types of ganglioside knockout mice were used in this project: α-2,8-sialyltransferase knockout (Sia T -/-), N-acetylgalactosaminyl transferase knockout (GalNAc T -/-) and double knockout (DKO) mice lacking both Sia T and GalNAc T genes (Figure 1.3). Ganglioside knockout mice were obtained from Koichi Furukawa and were generated as described below.

2.1.1 Generation of α-2,8-sialyltransferase knockout mice

Carried out by (Okada *et al.*, 2002)

α-2,8-sialyltransferase (Sia T) gene knockout mice were generated as described in Okada et al, 2002. Briefly, the chromosomal Sia T gene was cloned from the λgt11 phage genomic library using a radiolabeled fragment of α-2,8-sialyltransferase cDNA, clone pD3T-31, as a probe. The α-2,8-sialyltransferase gene was mapped as described in Furukawa et al, 1996, using restriction enzyme digestion, Southern blotting using Sia T cDNA probes and sequencing of exon regions. *In situ* hybridisation was performed to distinguish the Sia T gene from pseudo-genes. The identity of the gene was confirmed based on the correspondence of the gene assignment between humans and mice. The targeting plasmid was constructed containing a neomycin-resistant gene inserted between the *Bal*I and *Acc*I sites in exon 1 of the gene, and a 9.5-kb gene fragment was used as a targeting vector as shown in (Figure 2.1.A). The diphtheria toxin A gene was attached to eliminate nonhomologous recombinants as described previously (Aizawa et al, 1990). Homologous recombination was confirmed by Southern blotting using a probe, generating 4.5- and 2.8-kb fragments by *Bam*HI and 4.6- and 3.1-kb fragments by *Hind*III digestion in the wild-type and the recombinant allele, respectively, as shown in (Figure 2.1.B)."

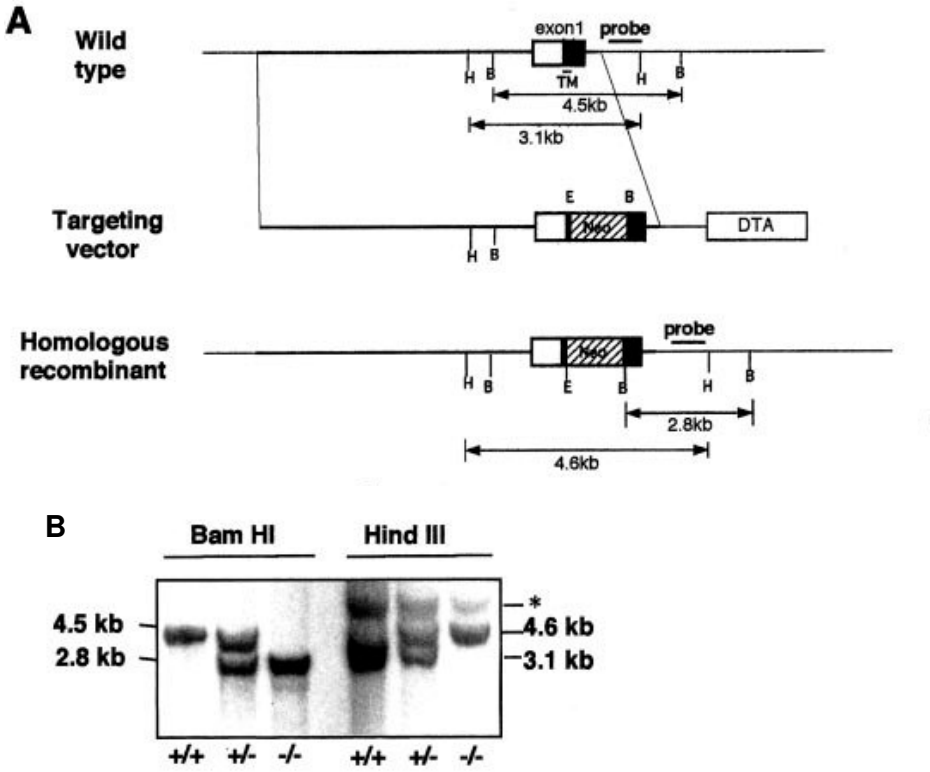

Figure 2.1. Generation of Sia T -/- mice (Modified from Okada et al, 2002).
(A) The strategy of the mouse Sia T gene knockout with a targeting vector. "Wild type" represents the normal genomic structure of mouse Sia T gene. Exon 1 is shown as a box on the line with the filled box representing coding regions. The middle line is the "Targeting vector" into which the neomycin-resistant gene was inserted between the *Eco*RI and BamHI sites in exon 1 of the gene (the text states the neo^r is inserted between the *Bal*I and *Acc*I sites in exon 1 of the gene but the figure shows it is inserted between E and B). The diphtheria toxin A fragment (DTA) gene was ligated on the 3' terminus across the vector backbone for negative selection. The lower line labelled "Homologous recombinants" shows the structure of the Sia T gene after a correct targeting event. The bold line labelled "probe" represents the *Hind*III fragment used as a probe to identify gene targeting events. Predicted sizes (kb) of *Bam*HI and *Hind*III-digested fragments hybridising to this probe are shown.
(B) Example of Southern blot analysis of F2 mice showing the homologous recombination as presented in A. Using *Bam*HI and *Hind*III-digested DNA, the wild-type allele gave a 4.5 and 4.6-kb band and the recombinant allele gave a 2.8 and 3.1-kb band, respectively. +/+ indicates wild-type lanes, +/- indicates heterozygous lanes, -/- indicates homozygous mutant lanes.
Abbreviations: TM, transmembrane; Neo, Neomycin resistant gene; DTA, diphtheria toxin A fragment gene; B, *Bam*HI; H, *Hind*III; E, *Eco*RI

2.1.2 Generation of N-acetylgalactosaminyl transferase knockout mice

Carried out by (Takamiya *et al.*, 1996).

N-acetylgalactosaminyl transferase (GalNAc T) gene knockout mice were generated as described in Takamiya et al, 1996. Briefly, the BALB/c mouse genomic library was screened with a 2.1-kb XbaI fragment of mouse cDNA (clone pTm3-5, (Takamiya *et al.*, 1995)) to isolate the chromosomal GalNAc T gene. The neomycin-resistant gene with phospoglycerate kinase-1 gene promoter and without poly(A)+ addition signal was inserted into the HindIII site in exon 4 as shown in (Figure 2.2.A). The targeting vector (24nM) was linearised with NotI and was mixed with embryonic stem (ES) cell suspension (1 x 107), then electroporated at 0.25 kV, 960 µF, using a Bio-Rad Genepulser. G418 was added to the medium 48 hours after electroporation at the concentration of 150 µg/ml. The G418-resistant clones were isolated after 7 to 8 days and subjected to screening for homologous recombination by PCR. The sense primer was 5'-TCGTGCTTTACGGTATCGCCGCTCCCGATT-3' in 3' terminus of the neomycin-resistant gene, and the antisense primer was 5'-GGGTGTGGCGGCATACATCT-3' in the intron of the GalNAc T gene. The following PCR protocol was used: one cycle of 95°C (2 min), 55°C (1 min), 74°C (5 min), thereafter 35 cycles of 94°C (1 min), 60°C (30 sec), 74°C (1.5 min). Homologous recombinant clones gave a 1.1-kb fragment. Two chimeric males derived from ES cell lines D-120 and G-193, respectively, transmitted the GalNAc T mutation to progeny. Mice heterozygous for the disrupted GalNAc T gene were mated, and homozygous mutant progeny were identified by PCR and Southern blot analysis of DNA isolated from mouse tails.

2.1.3 Generation of double knockout mice

Sia T and GalNAc T knockouts were mated to produce double knockout (DKO) mice lacking both Sia T and GalNac T. Because GalNac T -/- males are sterile, Sia T -/- females were mated with GalNAc T heterozygous males. This produced litters containing Sia T -/-, heterozygous and DKO mice. Therefore, the genotypes of the offspring were screened for the two genes using DNA extraction

and PCR and mice which lacked both Sia T and GalNac T (ie DKO mice) were used in the experiments.

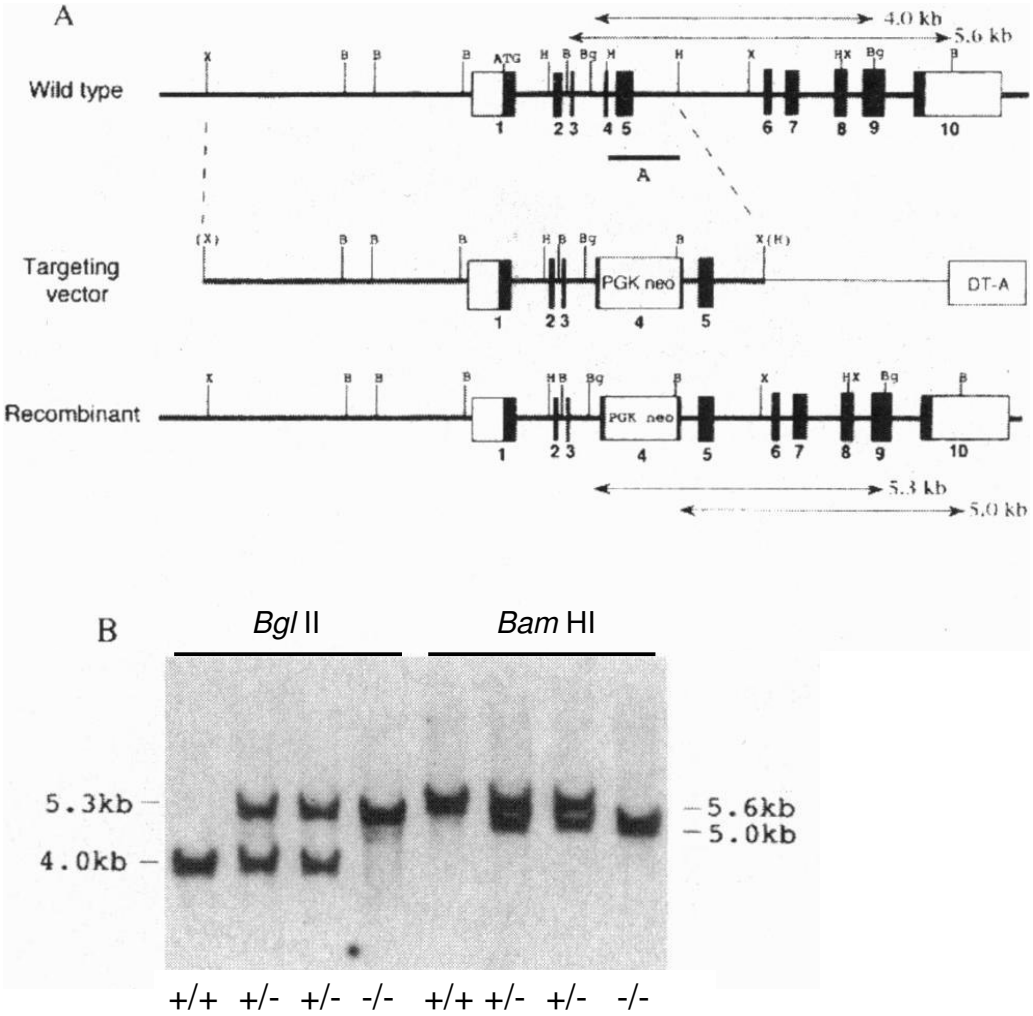

Figure 2.2. Generation of GalNAc T -/- mice (Modified from Takamiya et al, 1996.)
(A) Strategy for disruption of the mouse GalNAc T gene. "Wild type" represents the normal genomic structure of mouse GalNAc T gene. Exons 1 to 10 are shown as a box on the line with filled boxes representing coding regions. The translation initiation site is indicated as ATG. The middle line is the "Targeting vector" which was linearized at unique *Not*I site. In this vector, neomycin-resistant gene (PGK neo) was inserted into the *Hind*III site in exon 4. The DTA gene with MC1 promoter was ligated on the 3' terminus across the vector backbone for negative selection. The lower line labelled "Recombinant" shows the structure of the GalNAc T gene after a correct targeting event. PCR was used in the identification of homologous recombinants. The bold line labelled "A" represents the 800-bp *Hind*III fragment used as a probe to identify gene targeting events. Predicted sizes (kb) of *Bgl*II and *Bam*HI-digested fragments hybridising to this probe are shown. Abbreviations for restriction enzyme sites: X, *Xho*I; B, *Bam* HI; H, *Hind*III; Bg, *Bgl*II.
(B) Example of Southern blot analysis of F2 mice. The genomic DNA extracted from the tail was digested with *Bgl*II or *Bam*HI, and hybridised with the shown probe under high stringency. Using BglII or BamHI digested DNA, the wild-type allele gave a 4.0-kb, 5.6kb band and the recombinant allele gave a 5.3-kb and 5.0-kb band, respectively. +/+ indicates wild-type lanes, +/- indicates heterozygous lanes, -/- indicates homozygous mutant lanes

2.2 Genotyping of heterozygous and GalNAc T -/- mice

GalNAc T -/- were bred by mating GalNAc T -/- females with GalNAc T heterozygous males. Adult mice were genotyped by extracting DNA from the tails of the mice followed by PCR, whereas the embryos and the neonates were genotyped by labelling with CTx.

2.2.1 Tail tip DNA extraction

DNA was extracted using a PureGene Mouse Tail Kit (Gentra Systems) containing a cell lysis solution, a protein precipitation solution and a DNA hydration solution. Five 1 mm tail tip segments were cut on clean Parafilm using a disposable scalpel and were added to an autoclaved 1.5 ml eppendorf containing 300 µl of cell lysis solution. Proteinase K (1.5 µl of 20 mg/ml stock) was added to the eppendorf and the contents were mixed and incubated for 2 hours at 55ºC. The sample was cooled to room temperature, 100 µl of protein precipitation solution was added and the tube contents were mixed by inverting the eppendorfs 10 times. The sample was centrifuged at 12 500 rpm for 3 minutes. The supernatant was added to an autoclaved 1.5 ml eppendorf containing 300 µl of 100% isopropanol (2-propanol) and the tube was inverted until the DNA became visible. The samples were centrifuged at 12 500 rpm for 3 minutes, the supernatant was poured off and 300 µl of 70% ethanol was added to the DNA pellet. The sample was centrifuged at 12 500 rpm for 3 minutes and the ethanol removed. The tubes were inverted and placed on absorbent paper to dry out for 1 hour. The sample was rehydrated by adding 50 µl DNA hydration solution to the dried pellet and was left to go into solution.

2.2.2 GM2 primer PCR

The master mix was made up as described in the appendix. 4 µl of extracted DNA was mixed with 21 µl master mix in a 0.5 ml PCR tube. The following PCR protocol was used: one cycle of 95ºC (3 min), 60ºC (1 min), 72ºC (2 min), then 35 cycles of 94ºC (1 min), 57ºC (30 sec), 72ºC (1 min) and a final step of 72 ºC (10 min). As a positive control a sample was made up containing 4 µl heterozygous DNA (made up as described in section 2.2.1) and 21 µl master mix.

A negative control sample was made up containing 4 µl distilled water and 21 µl master mix.

2% agarose gel was made up as described in the appendix and was poured into the tank and left to set. A 100 bp DNA ladder was placed in the first well of the gel. The loading buffer was made up as described in the appendix and 1.5 µl was added to the 25 µl PCR mixture. 8 µl of sample containing the loading gel was placed into a well of the agarose gel. The gel was run for approximately 30 minutes and was taken out and photographed using a Syngene Bioimaging System.

2.2.3 Labelling with cholera toxin

To determine the genotype of neonatal mice or embryos from which the cells were derived, the cells from each mouse or embryo were cultured separately and were stained with CTx. 2.5 µg/ml of FITC labelled cholera toxin was added to the live cells in PBS for 30 minutes at room temperature. The cells were then fixed with 4% paraformaldehyde for 10 minutes, and then mounted in Vectashield containing 4'-6-diamidino-2-phenylindole (DAPI), which forms fluorescent complexes with double-stranded DNA, and hence labels nuclei. GalNAc T -/- tails and cells were negative for CTx whereas the heterozygous tails and cells were positive.

2.3 Tissue culture

2.3.1 General tissue culture

Primary cell cultures of Schwann cells, olfactory ensheathing cells and oligodendrocyte precursor cells and dissociated spinal cord cultures were cultured as described below. All cell cultures were grown in 12.5 cm^3 (T12.5) and 25 cm^3 (T25) culture flasks, and 24-well culture plates. All dishes and coverslips were coated in poly-L-lysine solution (PLL, 13.3 µg/ml in distilled water; Sigma). PLL was added to the dishes in a volume sufficient to cover the bottom for at least 30 minutes at 37ºC, washed in distilled water (dH_2O) and left to air-dry in a tissue culture hood before use.

All cells were maintained in a humidified incubator at 37°C with 7% carbon dioxide in the appropriate medium depending on the cell type. Cells grown in T12.5 flasks, T25 flasks or in 24-well plates were fed with 3 ml, 4 ml and 0.5 ml of media respectively, and were fed three times a week, by removing half of the media, and replacing with fresh media. All fresh media and tissue culture reagents were filtered through a 0.22 µm filter.

Cell cultures were passaged as follows: first, cells were washed in pre-warmed (37ºC) phosphate-buffered saline (PBS), and then 1.5 ml of pre-warmed PBS containing 0.1% trypsin was added for 2 minutes at 37ºC, with frequent agitation to assist cell detachment. The PBS-trypsin containing the cell suspension was then transferred to a 15 ml falcon tube, and trypsin activity inhibited by addition of 10 ml of 1%FBS (foetal bovine serum (FBS) in Dulbecco's Modified Eagle Medium (DMEM)). The suspension was centrifuged at 1200 rpm for 6 minutes. The resulting pellet was resuspended in fresh media and re-plated onto dishes as required.

In some instances, the number of cells was counted before plating down. This was done by placing 10 µl of the resuspended pellet in a haemocytometer and counting the number of cells within the 4x4 grid under a light microscope, and multiplying this by 10^4 to give the total number of cells/ml.

2.3.2 Olfactory ensheathing cell culture

Olfactory ensheathing cells (OECs) were obtained from olfactory bulbs of 7 day old mice of mixed sex. Instruments were sterilised using 100% ethanol. Mice were decapitated and olfactory bulbs dissected as follows; the skin on the head was sterilised with 100% ethanol and removed to expose the skull. The skull was cut on either side of the head to a point between the eyes and above the nose and was peeled back to exposed the brain. The olfactory bulbs (OB) were removed by cutting the olfactory tracts connecting them to the forebrain. OBs were placed in 4 ml Leibovitz medium containing 50 µg/ml gentamicin (L-15). OBs were finely chopped using a sterile scalpel in order to increase the reactive surface for enzymatic digestion. The tissue was then digested in 0.5 ml of 1.33% collagenase in L-15 for 30 min at 37°C. 0.5 ml of SD (soybean trypsin inhibitor-0.52mg/ml; bovine pancreas DNAse-0.04mg/ml; bovine serum albumin-3.0

mg/ml) was added to inhibit the enzymatic activity and a single cell suspension was made by passing five times through a 5ml pipette and once through 21G and 23G needles. The dissociated cells were transferred into a 15 ml falcon tube, washed in 10 ml of 1%FBS, centrifuged for 6 min at 12000 rpm, resuspended in olfactory mitogen medium (containing FGF2, forskolin, heregulin and astrocyte conditioned media) with 10%FBS (OMM+5%FBS) and plated in PLL-coated T25 tissue culture flasks at a density of 6 to 8 OBs per flask. Fresh OMM+5%FBS was replaced every 3 to 4 days.

Approximately a week later, the cells were purified using Fluorescent Activated Cell Sorting (FACS) and the $p75^{NTR}$ antibody (Abcam). Mixed olfactory bulb cells were trypsinised, resuspended in 10%FBS containing $p75^{NTR}$ antibody (1:800) and incubated on ice for 3 hours. Cells were washed twice in 10 ml of 1% FBS and then resuspended in 10%FBS containing goat anti rabbit IgG-FITC (1:100) and incubated for 45 min on ice. The cells were again washed twice in 10ml of 1%FBS, then resuspended in 4 ml of 1%FBS. The resuspended cells were poured through a 70 µm cell strainer to ensure that clumps of cells did not cause blockages in the FACS machine, and transferred to a polystyrene round bottom 5ml tube. Cell sorting was carried out by Tom Gilbey. A 'FACSVantage SE' sorter was used to purify the cells by exciting the fluorophores with a 488 nm argon laser at 100-150 mW. The sort windows were set in order to firstly separate live cells from dead cells and debris by size (forward scattering of light) and granularity (side scatter). The gated cells were plotted on a SSC-FL1 dot plot and the $p75^{NTR}$ positive, FITC cells were sorted. Purified cells were collected in a second polystyrene round bottom 5 ml tube, containing 4 ml of 1%FBS and then centrifuged for 6 min at 1200 rpm. The resulting pellet was resuspended in 100 µl of OMM+5%FBS and plated as a strip in the centre of a PLL-coated T12.5 tissue culture flask. After 30 min 4 ml of OMM+5%FBS was added and the cells were maintained in OMM+5%FBS medium.

A small aliquot of each sort was plated onto PLL-coated coverslips to assess the purity of cells. This was carried out by immunolabelling for $p75^{NTR}$ and cultures which were over 95% pure were used in subsequent experiments.

2.3.3 Schwann cell culture

Schwann cells were obtained from sciatic nerves of 7 day old mice of mixed sex, killed by decapitation. The skin on the back of the hind legs was sterilised and removed to reveal the muscles. The muscles were separated to reveal the sciatic nerves, which were dissected and cells dissociated as described for OECs. The cells were then resuspended in 10%FBS containing heregulin and forskolin (10%HF) and plated in T25 tissue culture flasks at a density of 12 to 16 sciatic nerves per flask. Fresh 10%HF was replaced every 3 to 4 days. Around one week after culture, Schwann cells were separated from contaminating fibroblasts by selective trypsination whereby the Schwann cells were selectively removed from the flask using a low concentration of trypsin (0.02%), leaving the contaminating fibroblasts behind. The trypsinised cells were added to a 15 ml falcon, washed in 10 ml of 1%FBS, centrifuged at 1200rpm for 6 min and the resulting pellet reconstituted in 10%HF and plated in T12.5 tissue culture flasks.

Schwann cell purity was assessed by plating an aliquot of cells onto coverslips and immunolabelling with anti- $p75^{NTR}$ and cultures over 90% pure were used in subsequent experiments.

2.3.4 Oligodendrocyte precursor cell culture

Oligodendrocyte precursor cells (OPCs) were obtained from optic nerves of 7 day old mice of mixed sex. The optic nerves were dissected and pooled in L-15, cut into small pieces using a scalpel and digested in 1.33% collagenase in Leibovitz medium for 15 min at 37°C. 75 µl of 2.5% trypsin was then added and the mixture was incubated for a further 15min. The reaction was terminated by adding SD. The tissue was triturated 5 times through an 18G needle and then a 21G needle in order to generate a single cell suspension. The cells were washed in 10 ml 1%FBS and centrifuged for 6 min at 12000 rpm, resuspended in DMEM-BS containing 20 ng/ml PDGF and FGF and plated in PLL-coated 13mm coverslips in a 24-well tissue culture plate.

2.3.5 Dissociated spinal cord culture

An *in vitro* myelinating culture system was generated from dissociated spinal cords from E13.5 mouse embryos. A pregnant female mouse at E13.5 was killed by overdose of CO_2, followed by cervical dislocation. The hair covering the abdomen was sterilised using 100% ethanol. The skin and the tissue in the middle of the abdomen were cut and the uterus was removed and placed in L-15. The foetuses were extruded, decapitated about 3mm rostral to the cervical flexure and the umbilical cord cut. The skin and the tissue on the back of the foetus covering the spinal cord were removed gently using sterile forceps and the spinal cords were cut just above the hind legs and removed. The meninges were stripped, dorsal root ganglia removed and the spinal cords placed in 1 ml HBSS without calcium and magnesium.

The cords were chopped lightly with a sterile scalpel then collected in 1 ml HBSS without calcium and magnesium. 1 ml of 0.25% trypsin and 100 µl of 1% collagenase were added and the mixture incubated for 15 min at 37ºC. 2ml SD was added to stop the reaction. The tissue was allowed to sink to the bottom and excess liquid was removed leaving behind approximately 1 ml. The tissue fragments were broken down by gentle trituration through a glass Pasteur pipette. The tissue was transferred into a 15 ml falcon tube, 5 ml plating medium added and centrifuged for 5 min at 800 rpm. The supernatant was removed and the cells reconstituted in plating medium to achieve a live cell count of 1,500,000/ml (approximately 5ml for 5 cords).

The cells were counted and 100 µl of the cell suspension, containing 150,000 cells, was plated onto PLL-coated coverslips in a 30 mm diameter petri dish, containing three 13 mm coverslips. The cells were left to attach for approximately 2 h at 37ºC. 200 µl of plating media see appendix for composition) and 500µl of either differentiation or neurobasal/B27 media (see appendix for composition) was added and the cells subsequently maintained in either differentiation or neurobasal/B27 media. In cultures where differentiation media was used insulin was withdrawn from this media after 12 DIV.

2.4 Assays

2.4.1 Proliferation

5-bromo-2'-deoxyuridine (BrdU) uptake was used as an indicator of cell proliferation in order to assess the proliferation rates of wild-type and ganglioside knockout OECs and Schwann cells on different substrates. OECs and Schwann cells were cultured and purified 5 to 7 days later as described above. Two to five days after purification, cells were plated onto coverslips coated with 10 µg/ml PLL, laminin or collagen in PBS (all from Sigma).
400 µl of PLL, laminin or collagen was added to the coverslips for 4 hours at 37ºC. The coverslips were washed three times in PBS and were not allowed to dry out before the addition of cells.

OECs and Schwann cells were plated onto coated coverslips at a density of 10,000 cells per well, and left to adhere overnight. Media was changed the following day to DMEM-BS or the optimal medium for each cell type and two days after plating 20 µM of BrdU, which is incorporated by cells synthesising DNA (Gratzner, 1982), was added. Cells were immunolabelled for anti-BrdU 16 h after BrdU addition as described in section 1.3.2.

Proliferation was measured as the percentage of DAPI nuclei which have taken up BrdU. Fifteen images at x10 magnification were taken of each coverslip and using a macro devised by John Annan (described in the Appendix 1.7 Macro: "percentage of BrdU positive nuclei") in a programme called Image J, the number of DAPI positive and BrdU positive nuclei were counted and the percentage of BrdU uptake was calculated for each image. The macro counts the number of blue (DAPI) nuclei, the number of green (BrdU) nuclei and the number of nuclei which are positive for both. Experiments were carried out in duplicate and were performed at least three times (n=3).

2.4.2 Time-lapse migration

To compare migration speeds of wild-type and ganglioside knockout OECs and Schwann cells on different substrates, cells were imaged using time-lapse microscopy and their migration speeds assessed. Wells of a 24-well plate were

coated with PLL, laminin or collagen (as outlined above). OECs and Schwann cells were cultured and purified 5 to 7 days later as described above. Two to five days after purification, cells were plated onto coated wells at a density of 5,000 cells per well in their optimal medium, and left to adhere overnight. Media was changed the following day to DMEM-BS or the optimal medium for each cell type and a day later time-lapse imaging of the cells was performed.

Time-lapse imaging of cells was performed using an Axiovert S100 microscope or an Axioplan 200 microscope connected to a computer, using a programme called AndorIQ. The 24-well plate was placed under the microscope within a box heated to 37ºC and was connected to a supply of CO_2. Three fields of view were chosen per well at x10 magnification. Images were taken at 3 min intervals, for a period of 5 hours. The position of the cell body was measured for each time point using a programme called Tracker, and an average speed of migration for each cell was calculated. 15 cells were tracked from each field of view. Experiments were carried out in duplicate and were performed at least three times (n=3).

2.4.3 Wound assays

To assess migration, a wound assay was performed where 30,000 wild-type or ganglioside knockout OECs or Schwann cells were plated onto PLL, laminin or collagen coated wells. Media was changed the following day to DMEM-BS or the optimal medium for each cell type and the cells were maintained in these media until they reached confluence. Once the cells reached confluence, a single scratch wound was made in the middle of the well using a micropipette tip.

The 24-well plate was then placed under the microscope within a box heated to 37ºC and was connected to a supply of CO_2. Time-lapse imaging of cells was performed using an Axiovert S100 microscope or an Axioplan 200 microscope connected to a computer, using a programme called AndorIQ. Three fields of view were chosen by the user per wound at x10 magnification. Images were taken at 30 min intervals, for a period of 24 hours. The width of the wound was measured using ImageJ: the distance between the opposing edges of the wound was measured at five points within each field of view and the time taken for the wound to close was noted. In the instances where the wound had not closed by

24 hours, the width of the wound was measured at 24 hours and the distance travelled per hour was calculated (Figure 2.3). Experiments were carried out in duplicate and were performed at least three times (n=3).

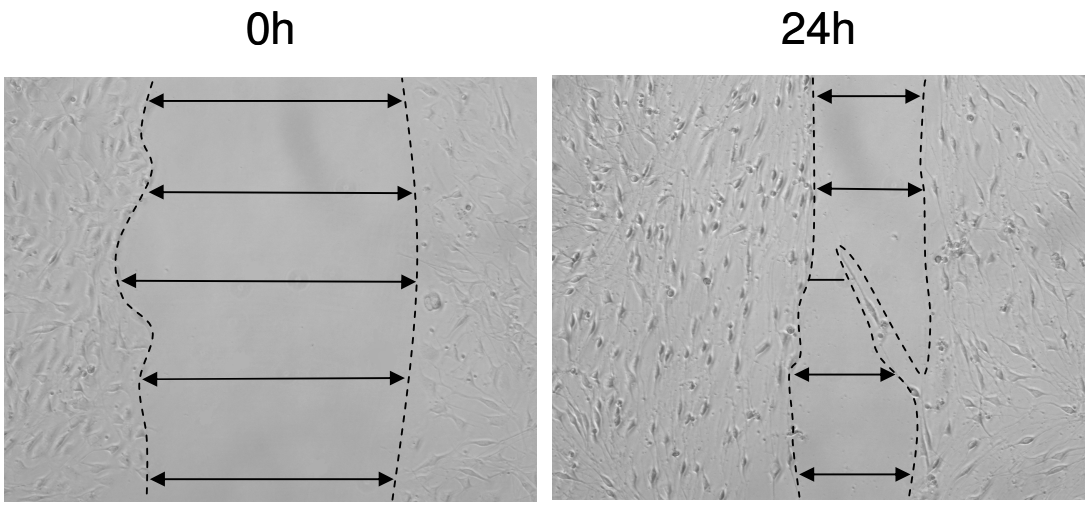

Figure 2.3. Image of a wound assay showing how the width of the wound was measured. The width between two cell fronts was measured at five points along the length of the wound, at 0 and 24 hours and was divided by 24 to obtain the migration speed which was expressed as the distance travelled (in micrometers) per hour.

2.4.4 Axonal density and PLP labelling

Axonal density and the extent of PLP labelling in dissociated spinal cord cultures derived from wild-type or ganglioside knockout mice was compared after 21 and 28 days *in vitro* (DIV). Axons were labelled using the antibody SMI 31, which detects a phosphorylated epitope in phosphorylated neurofilament H and, to a lesser extent, neurofilament M, and immunocytochemically reacts with thick and thin axons. Myelin was labelled with the AA3 antibody, which recognizes proteolipid protein (PLP), one of the major structural proteins in CNS myelin, and its functionally distinct DM20 isoform. Nine images were taken of each coverslip at x10 magnification. These images were analysed using image J to calculate the area (in pixels) of axonal staining and the background. Using this information it was possible to calculate the percentage area occupied by axons for each image. Using Adobe Photoshop Elements, the PLP labelling was traced and using a macro devised by John Annan (described in the Appendix 1.8 Macro: "quantitation of PLP labelling") in ImageJ, the area (in pixels) occupied by myelin in each image was measured. Using the area of axons and the area of PLP labelling, the percentage area of axons labelled with PLP was calculated for each image. Three separate experiments were carried out in triplicate and the mean was calculated for each experiment (n=3).

2.5 Nasal irrigation

Wild-type, Sia T -/-, GalNAc T -/- and DKO adult mice were lightly anaesthetized by inhalation with halothane. 20µl of autoclaved 10% zinc sulphate made up in distilled water was administered into the left nostril using a DNA pipette tip. Control animals were administered 20 µl of distilled water, also into the left nostril. The right hand side nostril in both experimental and control animals was not irrigated

At least five experimental animals and two control animals of each genotype were sacrificed by transcardial perfusion at each of the following time points: 1, 4 and 7 days and 3 and 9 weeks. Animals were firstly anaesthetized by inhalation with 3% halothane, 200 cc/min oxygen and 500 cc/min N_2O. Animals were perfused through the left ventricle with 20 ml heparinised saline (1000 units/ml), followed by fixation with 20ml 4% paraformaldehyde in PBS. All animal studies were performed under a Home Office licensing protocol.

Olfactory bulb and the olfactory mucosa were dissected out together and placed in 4% paraformaldehyde.

2.6 Tissue processing

2.6.1 Snap frozen sections

Tissue for ganglioside immunocytochemistry was embedded in OCT immediately after dissection, frozen on dry ice and stored at -20ºC. 10 µm thick sections were cut onto Vectabond coated slides and stored at -20ºC.

2.6.2 Frozen sections

Tissue for cryosectioning was fixed in 4% paraformaldehyde in PBS for 4 hours at 4ºC before cryoprotecting overnight in 30% sucrose in PBS, at 4ºC. Tissue was then embedded in OCT, frozen on dry ice and stored at -20ºC. 15 µm thick sections were cut onto Vectabond coated slides and stored at -20ºC.

2.6.3 Paraffin sections

Tissue for paraffin embedding was fixed overnight in 4% paraformaldehyde in PBS at 4ºC and processed for embedding using an automated processor (carried out by Tom Gilby and Margaret O'Prey). It was passed through increasing concentrations of alcohol and into melted paraffin wax before being embedded in paraffin wax. Surface decalcification was achieved by placing tissue blocks for 30 minutes at room temperature in a suspension of 200 g of sodium chloride in 50ml distilled water and 2 ml concentrated hydrochloric acid. Tissue blocks were rinsed in distilled water and 10 µm longitudinal sections were cut with a microtome onto Vectabond coated slides and stored at room temperature (some of the tissue was cut by Colin Nixon and Tom Gilby).

2.7 Immunocytochemistry/immunohistochemistry

For details of antibodies see table 1.1 and 1.2 (primary and secondary antibody lists).

2.7.1 General immunocytochemistry

Cells for immunolabelling were plated onto PLL-coated coverslips contained within 24-well plates or 35 mm diameter petri dishes as described above. In order to immunolabel the cells, the coverslips were taken out and any remaining media was blotted on tissue paper. Between all steps the coverslips were washed in PBS and any remaining media blotted onto tissue paper. Primary and secondary antibodies were made up in PBS at the concentrations indicated in Tables 1.1 and 1.2. 50 µl of primary antibody was added for 45 min at room temperature. The primary antibody was washed off and 50 µL of secondary antibody was added for 30 min. Cells were washed and fixed by adding 100 µl ice cold methanol per coverslip for 15 min at -20°C. In the case of intracellular antigens the fixation step is performed before incubating with primary antibody. After a final wash the coverslips were mounted using Vectashield containing DAPI.

Table 1.1 Primary antibody list

ANTIBODY	CLASS	DILUTION	SOURCE
β tubulin isotype III; TUJ1	IgG2a	1:500	Covance
A2B5 hybridoma	IgM	1:1	Gift from Mark Noble
AA3	Anti-rat	1:10	Hybridoma;Yamamura, 1991
BrdU	IgG1	1:20	DakoCytomation
CGM-3	IgM	20 μg/ml	Prof. Hugh Willison
caspr	Anti-rabbit	1:1000	Dr Ori Peles
contactin	Anti-human	neat	Dr Ori Peles
EG-2	IgG3	50 μg/ml	Prof. Hugh Willison
EG-3	IgG1	50 μg/ml	Prof. Hugh Willison
Gap43	IgG2a	1 in 5000	SigmaAldrich
GFAP	Anti-rabbit	1:100	DakoCytomation
$K_v1.2$	Anti-rabbit	1:100	Alomone Laboratories
MBP	Anti-rat	1:200	Serotec
MOG-1	IgG3	90 μg/ml	Prof. Hugh Willison
MOG-30	IgG3	160 μg/ml	Prof. Hugh Willison
MOG-35	IgG2b	20 μg/ml	Prof. Hugh Willison
Na_v (pan)	IgG1	1:100	SigmaAldrich
NG2	Anti-rabbit	1:200	Chemicon
Nestin	IgG1	1:200	Chemicon
Neurofascin 155	Anti-rabbit	1:200	Dr Ori Peles
O4 hybridoma	IgM	1:1	Sommer & Schachner, 1981
OMP	Anti-goat	1:500	Wako
$p75^{NTR}$	Anti-rabbit	1:800	Abcam
PCNA	IgG2a	1:20,000	Santa Cruz
R24	IgG3	1:100	Prof. Hugh Willison
SMI 31	IgG1	1:1500	Sternberger monoclonals
Synaptophysin	IgG1	1:400	Sigma
Thy 1.2	IgM	1:10	Serotec

Table 1.2 Secondary antibody list

ANTIBODY	CONJUGATE	DILUTION	SOURCE
Goat anti mouse IgG1	FITC; TRITC	1:100	Southern Biotech
Goat anti mouse IgG1	Alexa Fluor: 488, 555, 647	1:600	Molecular Probes
Goat anti mouse IgG2a	FITC; TRITC	1:100	Southern Biotech
Goat anti mouse IgG2b	FITC; TRITC	1:100	Southern Biotech
Goat anti mouse IgG3	FITC; TRITC	1:100	Southern Biotech
Goat anti mouse IgM	FITC; TRITC	1:100	Southern Biotech
Goat anti rabbit IgG	FITC; TRITC	1:100	Southern Biotech
Goat anti rabbit IgG	Alexa Fluor: 488, 555	1:600	Molecular Probes
Goat anti rat IgG	FITC; TRITC	1:100	Southern Biotech
Goat anti rat IgG	Alexa Fluor: 488, 555, 647	1:600	Molecular Probes
Donkey anti goat IgG	FITC	1:100	Southern Biotech
Goat anti human IgG, Fc_γ	Cy3	1:500	Jackson Labs
Rabbit anti mouse IgG	Biotinylated	1:300	DakoCytomation
Goat anti rabbit IgG	Biotinylated	1:300	DakoCytomation

2.7.2 Bromodeoxyuridine immunocytochemistry

The cells were fixed with ice-cold methanol for 10 min at -20ºC, washed in PBS and further fixed with 0.2% paraformaldehyde for 1 min at room temperature. They were washed in PBS, and 0.07 M sodium hydroxide was added for 10 min at room temperature. The cells were washed in PBS, and anti-BrdU (1:20) was added for 45 min at room temperature. The primary antibody was washed off using PBS and goat anti mouse IgG1-FITC (1:100) was added for 30 min at room temperature. The coverslips were mounted with Vectashield containing DAPI.

2.7.3 SMI 31 and AA3 immunocytochemistry

Cells were fixed in 4% paraformaldehyde for 15 minutes, washed in PBS, permeabilised with 0.5% triton X-100 in PBS for 15 minutes and blocked using a blocking buffer (0.2% pig skin gelatine and 0.1% triton X-100 in PBS) for 20 minutes at room temperature. Primary antibodies AA3 (1:10) and SMI 31 (1:1,500), diluted in blocking buffer, were added overnight at 4ºC, washed in PBS and the secondary antibodies goat anti rat-FITC (1:100) and goat anti mouse IgG1-TRITC (1:100) diluted in blocking buffer were added for 30 minutes at room temperature. The coverslips were mounted with Vectashield containing DAPI.

2.7.4 O4, NG2 and MBP immunocytochemistry

Spinal cord cultures were rinsed briefly in DMEM and the primary antibodies O4 (1:1) and NG2 (1:200), diluted in DMEM, were applied for 45 minutes at room temperature. The coverslips were washed in DMEM and the secondary antibodies goat anti mouse IgM-TRITC (1:100) and goat anti rabbit-AF488 (1:600), diluted in DMEM, were added for 30 minutes. The coverslips were washed in DMEM and fixed in 4% paraformaldehyde for 15 minutes, washed in PBS, permeabilised with 0.5% triton X-100 in PBS for 15 minutes and blocked using a blocking buffer (0.2% pig skin gelatine and 0.1% triton X-100 in PBS) for 20 minutes at room temperature. MBP (1:100) diluted in blocking buffer was added for 45 minutes at room temperature, washed in PBS and the secondary antibody goat anti rat-AF647 (1:600) diluted in blocking buffer was added for 30 minutes at room temperature. The coverslips were mounted with Vectashield containing DAPI.

2.7.5 Neurofascin immunocytochemistry

Cells were fixed with 4% paraformaldehyde for 10 minutes, washed in PBS, fixed in Bouins fixative for 1 minute and washed in PBS. Cells were blocked using a blocking solution (0.2% triton X-100, 10% normal goat serum and 1% glycine in PBS) for 40 minutes at room temperature. The cells were washed in PBS and the primary antibodies neurofascin 155 (1:200), SMI 31 (1:1,500) and AA3 (1:10) diluted in blocking solution were added overnight at 4ºC, washed in PBS and the secondary antibodies goat anti rabbit-alexa488 (1:600), goat anti mouse IgG1-alexa647 (1:600) and goat anti rat-alexa555 (1:600) diluted in blocking solution were added for 30 minutes at room temperature. The coverslips were mounted with Vectashield containing DAPI.

2.7.6 Caspr immunocytochemistry

Cells were fixed with 4% paraformaldehyde for 10 minutes, washed in PBS, fixed in methanol for 10 minutes at -20˚C and washed in PBS. Cells were blocked using a blocking solution (0.1% triton X-100, 10% normal goat serum and 1% glycine in PBS) for 40 minutes at room temperature. The cells were washed in PBS and the primary antibodies caspr (1:1000), SMI 31 (1:1,500) and AA3 (1:10) diluted in blocking solution were added overnight at 4ºC, washed in PBS and the secondary antibodies goat anti rabbit-alexa488 (1:600), goat anti mouse IgG1-alexa647 (1:600) and goat anti rat-alexa555 (1:600) diluted in blocking solution were added for 30 minutes at room temperature. The coverslips were mounted with Vectashield containing DAPI.

2.7.7 Sodium and potassium channel immunocytochemistry

Cells were fixed with 100% methanol for 6 minutes at -20ºC, were permeabilised using 5% NGS & 1% Triton X for 1 hour at room temperature, and were blocked using 5% NGS for 1 hour at room temperature. Sodium channel antibody (Na_v,1:100) and potassium channel antibody (K_v, 1:100) in 5% NGS were added overnight at 4ºC, excess was washed off using PBS and the secondary antibodies goat anti mouse IgG1- alexafluor 488 (1:600) for Na_v and anti rabbit-alexafluor555 (1:600) for K_v in 5% NGS were added for 1h at room temperature. The coverslips were mounted with Vectashield containing DAPI.

2.8 Immunohistochemistry

2.8.1 General immunohistochemistry of frozen tissue

The tissue was circled with a hydrophobic pen and incubated for 1 hour at room temperature in blocking solution containing 2% bovine serum albumin (BSA) and 10% normal animal sera (corresponding to the animal in which the secondary antibody to be used was raised in) in PBS. The sections were incubated in primary antibody in blocking solution overnight at 4ºC. The excess antibody was removed by washing in PBS twice for 5 minutes with agitation. Sections were incubated in the relevant fluorescent secondary antibody in blocking solution for an hour at room temperature and excess antibody removed by washing in PBS twice for 5 minutes on a rocker. Sections were mounted in Vectashield containing DAPI.

2.8.2 General immunohistochemistry on paraffin sections

Paraffin embedded sections were cleared in histoclear for 15 minutes and rehydrated through a graded series of ethanol solutions (100% and 70%) and water.

2.8.2.1 Immunofluorescence

Following clearing and rehydration, the tissue was circled with a hydrophobic pen and incubated for 1 hour at room temperature in blocking solution containing 2% BSA and 10% normal animal sera (corresponding to the animal in which the secondary antibody to be used was raised in) in PBS. The sections were incubated in primary antibody in blocking solution overnight at 4ºC. The excess antibody was removed by washing in PBS twice for 5 minutes with agitation. Sections were incubated in the relevant fluorescent secondary antibody in blocking solution for an hour at room temperature and excess antibody removed by washing in PBS twice for 5 minutes on a rocker. Sections were mounted in Vectashield containing DAPI.

2.8.2.2 Immunohistochemistry

Following clearing and rehydration, endogenous peroxidases were inhibited by incubating sections in 3% hydrogen peroxide in methanol for 30 minutes at room temperature. Sections were then washed for 5 minutes in running water and for 5 minutes in PBS with agitation. The tissue was circled with a hydrophobic pen and incubated for 1 hour at room temperature in blocking solution containing 2% BSA and 10% normal animal sera (corresponding to the animal in which the secondary antibody to be used was raised in) in PBS. The sections were incubated in primary antibody in blocking solution overnight at 4ºC. The excess antibody was removed by washing in PBS twice for 5 minutes with agitation. Sections were incubated in the relevant biotinylated secondary antibody in blocking solution for an hour at room temperature and excess antibody removed by washing in PBS twice for 5 minutes on a rocker. Avidin (1:400) in PBS was added for 45 minutes at room temperature. Sections were washed twice for 5 minutes in PBS with agitation and a solution of diaminobenzidine (DAB) was added to the sections for 5 minutes. DAB was washed off in running water and the sections dehydrated, cleared and mounted in Histomount. Negative control sections were performed in parallel where the primary antibody was omitted to ensure that staining observed was not due to non-specific binding of the secondary antibody to the tissue.

2.8.3 PCNA and GFAP immunohistochemistry

Following clearing and rehydration, endogenous peroxidases were inhibited by incubating sections in 3% hydrogen peroxide in methanol for 30 minutes at room temperature. Sections were then washed for 5 minutes in running water and for 5 minutes in PBS with agitation. The tissue was circled with a hydrophobic pen and incubated for 1 hour at room temperature in blocking solution containing 2% BSA and 10% normal goat serum in PBS. The sections were incubated in GFAP antibody (1:400) in blocking solution overnight at 4ºC. The excess antibody was removed by washing in PBS twice for 5 minutes with agitation. The biotinylated goat anti-rabbit secondary antibody (1:300) in blocking solution was added for 1 hour at room temperature. Excess antibody was removed by washing in PBS twice for 5 minutes on a rocker. Avidin was added for 45 minutes at room temperature at a concentration of 1 in 400 in PBS. Sections were washed twice

for 5 minutes in PBS with agitation and a solution of DAB was added to the sections for 5 minutes. DAB was washed off in running water and PBS. The sections were placed in citric acid buffer and were microwaved on high for 10 minutes, then left to cool down for an hour. The tissue was incubated for 1 hour at room temperature in blocking solution containing 2% BSA and 10% normal rabbit serum in PBS. The sections were incubated in the proliferating cell nuclear antigen (PCNA) antibody at a concentration of 1 in 10,000 in blocking solution overnight at 4ºC. Sections were then washed twice for 5 minutes in PBS with agitation and the biotinylated rabbit anti-mouse secondary antibody (1:300) in blocking solution was added for 1 hour at room temperature. Excess antibody was removed by washing in PBS twice for 5 minutes on a rocker. Avidin was added for 45 minutes at room temperature at a concentration of 1 in 400 in PBS. Sections were washed twice for 5 minutes in PBS with agitation and a solution of Vector SG was added to the sections for 5 minutes. Vector SG was washed off in PBS for 5 minutes and water for 20 minutes. The sections were dehydrated, cleared and mounted in Histomount.

2.9 Histological staining

2.9.1 Haematoxylin and eosin

Sections were stained with routine histological stains haematoxylin and eosin (H&E) to study the general features of the tissue. Paraffin embedded sections were cleared in Histoclear for 15 minutes and rehydrated through a graded series of ethanol solutions (100% and 70%) and water. Sections were placed in haematoxylin for 1 minute, washed in water, and blued in Scott's Tap Water Substitute. Excess haematoxylin was removed by immersion in acid alcohol (1% concentrated HCl in 70% ethanol). The sections were washed and placed in eosin for 10 seconds, rinsed in water, dehydrated through a series of alcohols and cleared in Histoclear.

2.10 Quantification of regeneration

2.10.1 Olfactory epithelium width assessment

Sections 10, 20 and 30 from each animal were stained with H & E and sections of the olfactory epithelium were photographed using a light microscope at x20 magnification. Measurements of the control and experimental olfactory epithelial width were taken at right angles from the basement membrane to the luminal surface of the epithelium using Image J. A measurement was taken at 20 µm intervals along the length of the epithelium as shown in Figure 2.4. Width results from mice of the same age, genotype and time point of perfusion were averaged out and analysed using ANOVA analysis of variance in Minitab. Eileen Brown did some of the OE width measurements.

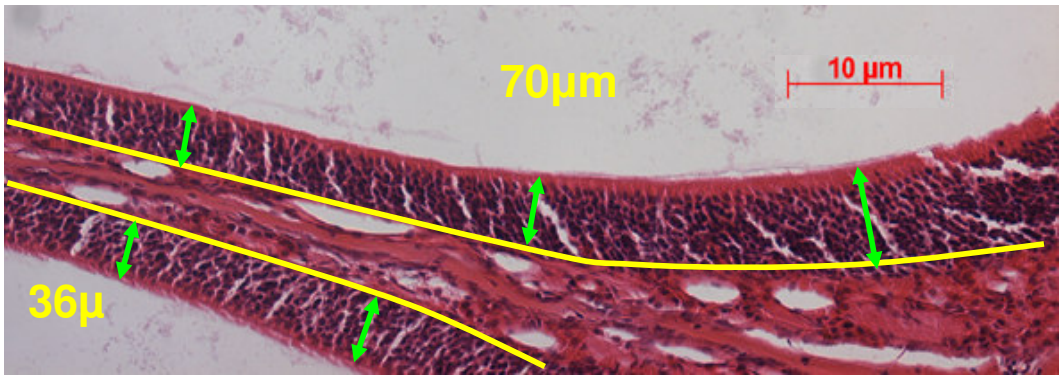

Figure 2.4. OE width measurements.
Image of olfactory epithelium showing how the olfactory epithelium width was measured at intervals of 20 µm along the length of the epithelium.

2.10.2 Quantification of immunohistochemistry

Relative optical density for synaptophysin and SMI 31 (phosphorylated neurofilament) immunohistochemistry was measured using ImageJ. Images for each antibody were taken at 40x magnification at the same microscope light intensity. For SMI 31, 3 sections were used for each time point and Mean Gray Value (MGV) measurements were taken at 25 random areas along the olfactory nerve. For anti-synaptophysin, 3 sections were used for each time point and 3 MGV measurements were taken from each of 10 randomly selected glomeruli. Background levels were determined by taking MGV measurements from

unlabelled areas. The mean background MGV was subtracted from the mean MGV of the positive areas to give the relative optical density value.

2.10.3 Quantification of cell number

To quantify the number of proliferating cells within the olfactory epithelium, cells expressing PCNA within the olfactory epithelium were counted. 3 sections were used for each time point and counts were made from 10 random areas along the length of the epithelium. The number of cells was divided by the length of the olfactory epithelium to give the number of cells per mm of olfactory epithelium.

2.11 Microscopy

Confocal microscopy was carried out using an Olympus Fluoview FV1000 confocal microscope at 10 and 40 x magnifications. Images of nodal regions were taken using an Olympus Fluoview FV1000 confocal microscope at 60x magnification with a zoom of 3 or using a Leica TCS SP2 confocal at 63x magnification. Other microscopy was carried out using Zeiss Axioskop and Zeiss Axioplan microscopes at x40 magnification.

2.12 Statistical analysis

To compare values between groups, data were analysed by one-way analysis of variance (ANOVA) using MINITAB, to determine if at least two of the populations had significantly different means. Experimental means were compared to controls using Dunnett's two-tailed t-test, to allow for multiple comparisons.

All values were expressed as the mean +/- standard error of the mean (SEM). *p*-values were displayed using three levels of statistical significance ($p < 0.001$, $p < 0.01$ and $p < 0.05$). Values below 0.05 were considered significant, and were indicated in figures by the presence of an asterisk.

All experiments were performed in triplicate and repeated three times, unless otherwise stated, and the mean from each individual experiment was used to calculate the final mean value.

3 CHAPTER 3

Comparison of the proliferative and migratory properties of wild-type and ganglioside-knockout Schwann cells and OECs.

3.1 Introduction

It is a well established fact that the CNS is unable to regenerate following injury. This is due to a number of factors such as the presence of inhibitory myelin components, the presence of inhibitory guidance molecules and the formation of a glial scar. CNS glia play a major role in the normally abortive regeneration of CNS axons, due most likely both to the presence of inhibitory molecules as well as the lack of sufficient growth promoting molecules (Reier and Houle, 1988, Hoke and Silver, 1994, Gebicke-Haerter *et al.*, 1996, Moore and Thanos, 1996, Frisen, 1997, Ridet *et al.*, 1997).

The olfactory system is exceptional in that it is one of the few CNS regions that can support neurogenesis throughout life (Farbman, 1990). Olfactory receptor neurons detect odours and relay this information to the brain. These neurons die as a result of injury or normal cell turnover and are replaced by new neurons generated from putative stem cells in the olfactory epithelium (Schwob, 2002). The regenerative property of the olfactory system is thought to be partially due to the permissive nature of the glial cells found only in the olfactory system, namely the olfactory ensheathing cells (OECs). OECs provide ensheathment for small C fibres within both the CNS and PNS portions of the olfactory nerve (Doucette, 1984, Doucette, 1993, Raisman, 1985). It is thought that OECs act as conduits, guiding the axons of newly generated ORNs through the PNS environment of the olfactory mucosa and into the CNS environment of the olfactory bulb (Williams *et al.*, 2004).

Several studies have described the ganglioside expression in the olfactory system (Chiba *et al.*, 1997, Hofteig *et al.*, 1981, Ohsawa, 1989, Ohsawa and Shumiya, 1991, Suchy *et al.*, 1988, Valdes-Gonzalez *et al.*, 2001). GM4, GM3, GM2, GM1, GD1a, GD3, GD1b, GT1b and GQ1b have been shown to be expressed in the fish and human olfactory nerve (Chiba *et al.*, 1997, Hofteig *et al.*, 1981). In mouse olfactory bulbs, GM3 was characteristically more concentrated than in the other brain regions (Ohsawa and Shumiya, 1991). Mouse olfactory bulbs also express GM1, GD1a, GT1b and GD1b (Ohsawa and Shumiya, 1991).

Gangliosides have been shown to affect proliferation and migration in a number of different cell types. Gangliosides can not only stimulate but also inhibit cell

growth and motility, and their effect depends both on the structure of their carbohydrate chains and the type of cell. For instance, Sia T expression in PC12 cells led to decreased expression of a-series ganglioside, GM1 and increased expression of b-series gangliosides, GD1b and GT1b, and resulted in increased cell growth (Fukumoto *et al.*, 2000) and motility (Kamimura *et al.*, 2005). Swiss 3T3 cells almost exclusively express the simplest ganglioside, GM3 (Kamimura *et al.*, 2005). Swiss 3T3 cells transfected with GalNAc T express the a-series ganglioside GM1, which results in decreased proliferation (Mitsuda *et al.*, 2002). Sia T expression in Swiss 3T3 led to the expression of b-series ganglioside GD3 and increased cell motility. However, unlike in PC12 cells where increased b-series gangliosides resulted in increased proliferation, increased b-series gangliosides in Swiss 3T3 cells had no effect on their growth (Kamimura *et al.*, 2005).

Prior to studying the role of gangliosides in the olfactory system, the role of gangliosides in the biology of the olfactory system glia, the OECs, as well as the related cell type, Schwann cells, was studied. Although OECs are a unique cell type, they share many cellular and molecular properties with peripheral myelinating cells, Schwann cells. These include molecular markers, morphological phenotype in culture and responsiveness to growth-promoting molecules.

Many strategies have been employed in order to promote CNS regeneration. One of these is glial cell transplantation. OECs and Schwann cells have both been proposed as candidates for transplant-mediated repair. Although OECs and Schwann cells share many features in common, there are several differences which are important when considering their suitability as candidates for transplant mediated repair. For instance, OECs are able to freely migrate and co-exist with astrocytes, whereas Schwann cells have a limited ability to migrate in the presence of astrocytes and induce a reactive phenotype in astrocytes. A better understanding of the biology of OECs and Schwann cells may aid in their use for CNS repair. With this in mind, the aim of the present study was to examine the biological properties of glial cells isolated from wild-type and ganglioside knockout mice.

Glial cells were grown from wild-type and ganglioside knockout mice. Initially, the proliferation of mouse OECs and Schwann cells was compared using different culture conditions in order to determine their optimal growth conditions. The ganglioside expression of these cells was assessed by immunocytochemistry and subsequent experiments were performed to determine what role, if any, gangliosides play in the modulation of OEC and Schwann cell migration and proliferation.

3.2 Results

3.2.1 Mitogenic activity of known glial growth factors

Schwann cells and OECs were obtained from sciatic nerves and olfactory bulbs of 7 day old mice, respectively. They were purified as described in the methods section in order to remove any contaminating cells and only cultures which were more than 95% pure were used in the experiments.

The growth response of glial cells isolated from mice and rats was initially observed. It was clear that rodent cells had different growth requirements *in vitro* since Schwann cells and OECs isolated from mice grew much slower than comparable rat cells. For instance, olfactory bulbs purified from 4 rats, plated into a T25 flask would become confluent within a few days and if split between two T25 flasks would again grow and become confluent within a few days. In contrast, olfactory bulbs purified from 6 mice, plated into a T25 flask would take a lot longer to become confluent and if split between two T25 flasks would not reach confluence again. The mouse cells were maintained for up to 2 months and although they proliferated initially, eventually they stopped proliferating. In order to identify mitogenic factors that would enable the expansion of purified mouse Schwann cells and OECs *in vitro* for further studies, the effect of a range of growth factors, previously identified Schwann cell and OEC mitogens, was examined: BDNF, EGF, FGF, forskolin, heregulin, IGF-1, NT-3, PDGF and TGFβ (Alexander *et al.*, 2002, Dong *et al.*, 1997, Levi *et al.*, 1995, Ramon-Cueto and Avila, 1998, Yan *et al.*, 2001, Zhang *et al.*, 1995, Pollock *et al.*, 1999). Due to the small number of viable cells recovered following mouse OEC or Schwann cell purification only one concentration of each growth factor

was tested as shown in Figure 3.1. The concentrations used were higher than those used previously in the literature (Pollock *et al.*, 1999).

To observe the effects of the individual growth factors, these were added to serum- and growth factor-free DMEM-BS medium. The mitogenic activity of individual growth factors was compared to that of DMEM-BS, 10% FBS in DMEM-BS, and well-established rat OEC and Schwann cell media, OMM+5%FBS (Alexander *et al.*, 2002) and 10%HF, respectively (Figure 3.1). Mitogenic activity was quantified using an assay of DNA synthesis based on immunocytochemical detection of nuclear BrdU incorporation of cells having entered the S phase during a set period of exposure to this agent (Gratzner, 1982). Approximately 10,000 purified OECs or Schwann cells were plated onto PLL-coated coverslips and were maintained overnight in OMM+5%FBS and 10%HF, respectively, then exposed to the appropriate medium.

As shown in Figure 3.1 (B) BrdU uptake in mouse Schwann cells grown in serum-free medium was not significantly increased compared to DMEM-BS in response to the following single mitogens: BDNF, EGF, NT-3 or TGFβ. A selection of single mitogens significantly increased Schwann cell proliferation compared to serum-free medium, DMEM-BS. These include: PDGF ($p < 0.01$), IGF-1 ($p < 0.05$), heregulin ($p < 0.001$), forskolin ($p < 0.05$) and FGF ($p < 0.001$). Schwann cells grown in 10%FBS or OMM+5%FBS also proliferated significantly better than in serum-free medium ($p < 0.001$). None of the single mitogens increased Schwann cell proliferation above the level achieved by maintaining the cells in 10%HF.

OECs do not proliferate in response to forskolin or NT-3 alone as shown in Figure 3.1 (A). Most other mitogens tested, including EGF ($p < 0.01$), FGF ($p < 0.01$), BDNF, heregulin, IGF-1, PDGF and TGFβ ($p < 0.05$), increased the proliferation of OECs to above base levels. OECs grown in 10%FBS ($p < 0.05$) as well as 10%HF ($p < 0.01$) also showed significantly greater proliferation than those grown in serum-free media. However, none of the other media tested increased OEC proliferation to above the level achieved by maintaining the cells in OMM+5%FBS. In subsequent experiments, OECs were grown in OMM+5%FBS (olfactory mitogen medium containing FGF2, forskolin, heregulin, and astrocytes conditioned medium and an equal volume of 10% foetal bovine serum), while Schwann cells were grown in 10%HF (10% FBS 20 ng/ml heregulin and 2 μM forskolin).

Purified mouse OECs and Schwann cells proliferated slowly in control medium DMEM-BS (Figure 3.1); the percentage of OECs incorporating BrdU over a 16 hour exposure was 20.98 ± 6 whereas the percentage of Schwann cells incorporating BrdU over a 16 hour period was 6.5 ± 1.94. However, this difference was not statistically significant. Mouse OECs had higher proliferation rates than Schwann cells under most of the growth factor conditions used: 10%FBS ($p < 0.01$), 10%HF ($p < 0.05$), BDNF ($p < 0.001$), EGF ($p < 0.001$), FGF ($p < 0.001$), forskolin ($p < 0.001$), heregulin ($p < 0.01$), IGF-1 ($p < 0.001$), NT-3 ($p < 0.001$), PDGF ($p < 0.01$), and TGFβ ($p < 0.001$).

3.2.2 Mitogenic effect of increasing acidity

As mentioned previously, it was observed that OECs and Schwann cells derived from mice did not grow as well as comparable cells derived from rats. Several parameters can alter the growth of cells including available growth factors, cell density, osmolality and pH.

To determine if any of these factors would improve growth and identify the optimal growth conditions for mouse Schwann cells and OECs the effect of increasing the acidity of tissue culture media on their proliferation was investigated. Increasing the percentage of CO_2 in the air lowers the pH of the culture media making it more acidic. Purified OECs and Schwann cells were grown in 5, 7 or 10% CO_2 for 48 hours and the incorporation of BrdU, which is added to the culture media 16 hours before the end of the experiment, was compared. Cell nuclei were visualised with DAPI and cells that had incorporated BrdU were recognised by an anti-BrdU antibody. Proliferation rate was expressed as the proportion of total cells that were BrdU-positive.

Increasing the concentration of CO_2 the cells were maintained in, and thereby lowering the pH of the media, did not significantly affect the proliferation of either Schwann cells or OECs (Figure 3.2). For this reason, the cells were subsequently maintained in incubators containing 7% CO_2 in OMM+5%FBS (OEC) or 10%HF (Schwann cells). It can be seen in Figures 3.1 and 3.2 that OEC proliferation was generally higher than Schwann cell proliferation, suggesting that the two cell types require different growth conditions.

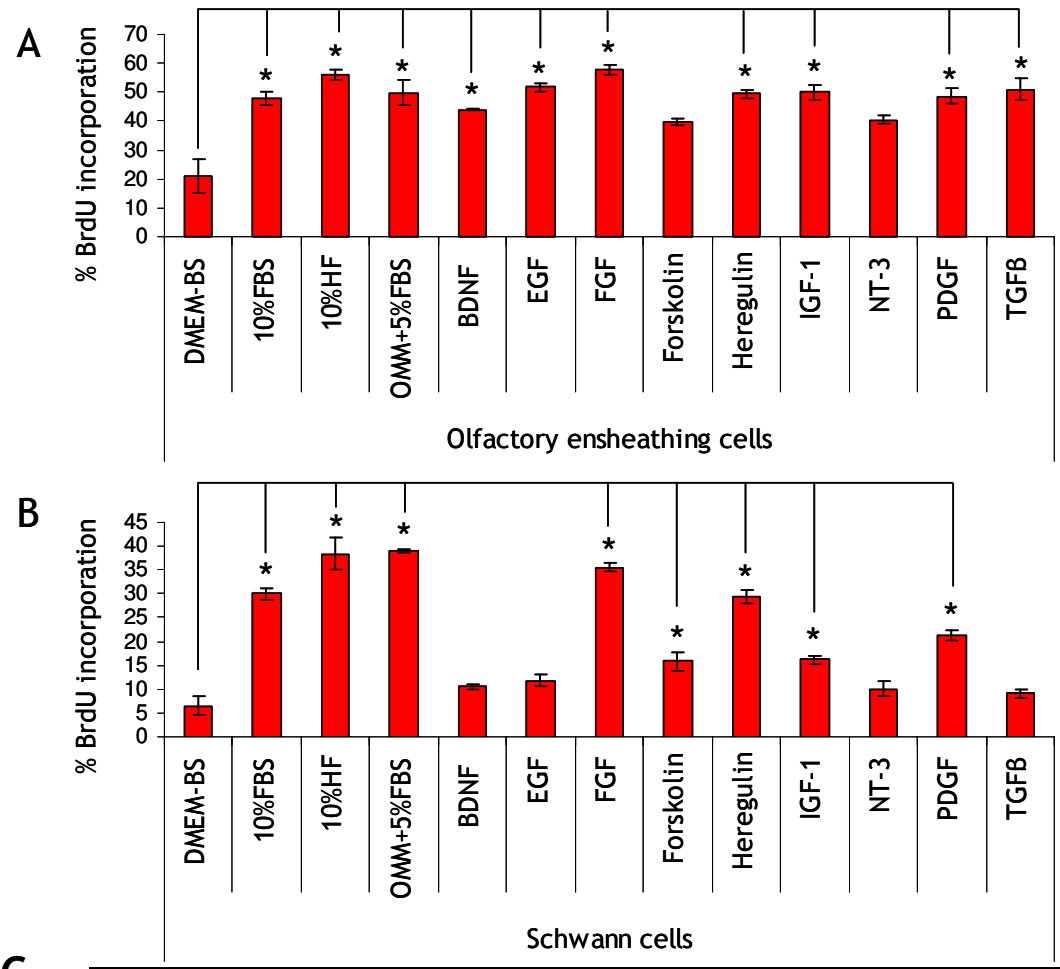

C

Abbreviation	Contents
DMEM-BS	See Appendix for contents
10%FBS	10% foetal bovine serum and 100 mM glutamine in DMEM
10%HF	"10%FBS"; 2 µM forskolin; 20 ng/ml heregulin
OMM+5%FBS	5% FBS; 500 ng/ml FGF2; 50 ng/ml heregulin; 0.5 nM forskolin; 20% ACM in DMEM-BS
BDNF	20 ng/ml brain derived neurotrophic factor in DMEM-BS
EGF	20 ng/ml epidermal growth factor in DMEM-BS
FGF	50 ng/ml fibroblast growth factor in DMEM-BS
Forskolin	20 µg/ml forskolin in DMEM-BS
Heregulin	20 ng/ml heregulin in DMEM-BS
IGF-1	20 ng/ml insulin-like growth factor-1 in DMEM-BS
NT-3	20 ng/ml neurotrophin-3 in DMEM-BS
PDGF	5 ng/ml platelet-derived growth factor in DMEM-BS
TGFβ	20 ng/ml transforming growth factor β in DMEM-BS

Figure 3.1. Schwann cell and OEC proliferation under different growth factor conditions. Schwann cells and OECs isolated from 7 day old mice were purified after approximately 7 DIV and plated onto glass coverslips (10,000 cells per coverslip) in 10%HF and OMM+5%FBS, respectively. They were left to attach overnight, washed with DMEM-BS and treated with various growth factors in DMEM-BS for 48h. Twenty micromolar of BrdU was added for the last 16h of the experiment. Proliferating cells were visualised by indirect immunolabelling with an anti-BrdU antibody, and nuclei were visualised with DAPI. The mean OEC proliferation rates expressed as the percentage of BrdU positive nuclei are displayed in A. The mean Schwann cell proliferation rates are displayed in B. Each point represents the mean ± SEM (n=3); (*) $p < 0.05$. The table in C explains the abbreviations used in the graphs and shows the concentration of each growth factor used.

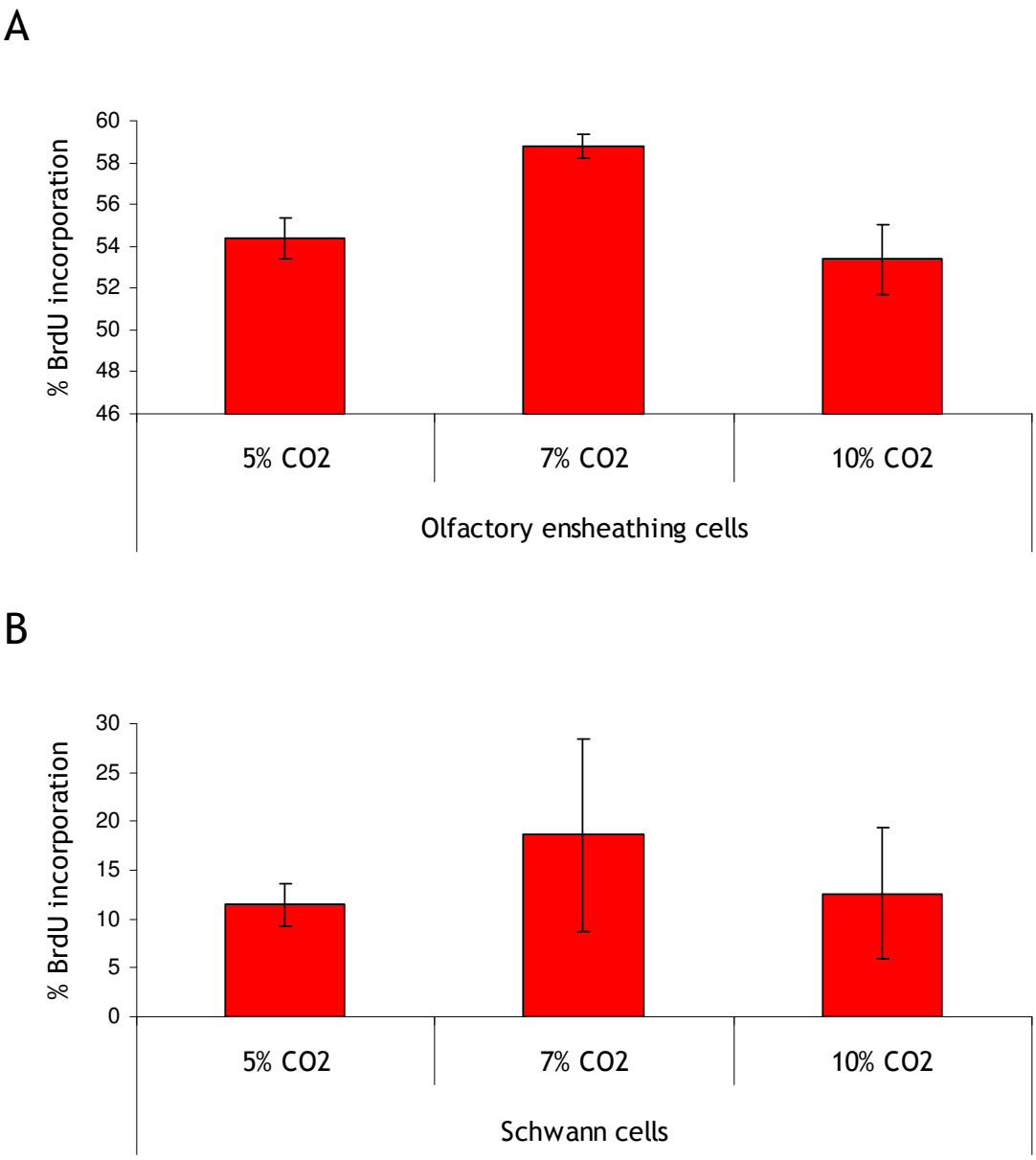

Figure 3.2. Effect of increasing acidity on Schwann cell and OEC proliferation.
Purified Schwann cells and OECs from 7 day old mice were plated on PLL-coated coverslips at a density of approximately 10,000 cells per coverslip. Schwann cells were maintained in 10%HF and OECs in OMM+5%FBS throughout the experiment. The cells were allowed to attach overnight in incubators containing 7% CO_2, then washed with DMEM-BS and fresh media added. They were maintained in 5%, 7% or 10% CO_2 for 48 hours. Twenty micromolar of BrdU was added for the last 16 h of the experiment and the percentage of cells expressing BrdU was assessed by indirect immunocytochemistry using an anti-BrdU antibody, to label proliferating nuclei and DAPI to visualise all nuclei. Increasing the CO_2 concentration and thereby increasing the acidity did not significantly alter the growth of either Schwann cells or OECs. (A) displays the mean proliferation rates in OECs expressed as % of BrdU incorporation and (B) displays the data for Schwann cells. Each point represents the mean ± SEM (n=3).

3.2.3 Ganglioside expression of Schwann cells and OECs

To assess if ganglioside expression varied in OECs and Schwann cells, the ganglioside expression of OECs and Schwann cells isolated from 7 day old mice was examined by immunocytochemistry. Antibodies used were a gift from Prof. Willison's lab. The antibodies used were EG2 which binds to gangliosides GT1a, GD1b, GT1b and GQ1b; EG3 which recognises GT1a and GQ1b; MOG1 which is specific for GD1b; MOG30 which is specific for GQ1b; MOG35 which specifically binds to GD1a; and R24 which binds to GD3, GT1a and GQ1b. CTx, which binds to GM1, was also used. The results are summarised in Table 3.1.

OECs and Schwann cells have a similar ganglioside expression in that the major gangliosides expressed *in vitro* by both cell types are a-series complex gangliosides GM1 (Figure 3.3 and 3.4) and GD1a (Figure 3.5 and 3.6). The majority of $p75^{NTR}$-immunoreactive OECs and Schwann cells double-labelled with MOG35, which binds to GD1a or CTx which binds to GM1. The intensity of CTx and MOG35 in both Schwann cells and OECs was heterogeneous. The contaminating cells in OEC and Schwann cell cultures also expressed GM1 and GD1a (Figure 3.12 and 3.13).

Marker	Binds to ganglioside:		OEC	SC
	a-series	b-series		
CTx	GM1		80-100% positive	80-100% positive
EG2	GT1a +++	GD1b ++ ; GT1b +++; GQ1b ++	negative	<1% positive
EG3	GT1a ++++	GQ1b +++	negative	0-5% positive
MOG1		GD1b ++++	<1% positive	<1% positive
MOG30		GQ1b +++	negative	<1% positive
MOG35	GD1a ++++		80-100% positive	80-100% positive
R24	GT1a ++	GQ1b ++ ; GD3 +++	<5% positive	<5% positive

Table 3.1. Table showing ganglioside expression of OEC and Schwann cells
OECs and Schwann cells purified from 7 day old mice were maintained in known optimal conditions, namely OMM+5%FBS or 10%HF, respectively, and labelled with antibodies which bind to gangliosides and FITC-labelled CTx which binds to ganglioside GM1, after 7 to 14 days *in vitro*. In instances where the antibodies labelled less than 1% of the cells, the labelled cells morphologically resembled OECs or Schwann cells and were $p75^{NTR}$-positive. Anti-ganglioside reactivities: optical density >0.1 ≤0.5 (+); >0.5 ≤1.0 (++); >1.0 ≤1.5 (+++); >1.5 (++++).

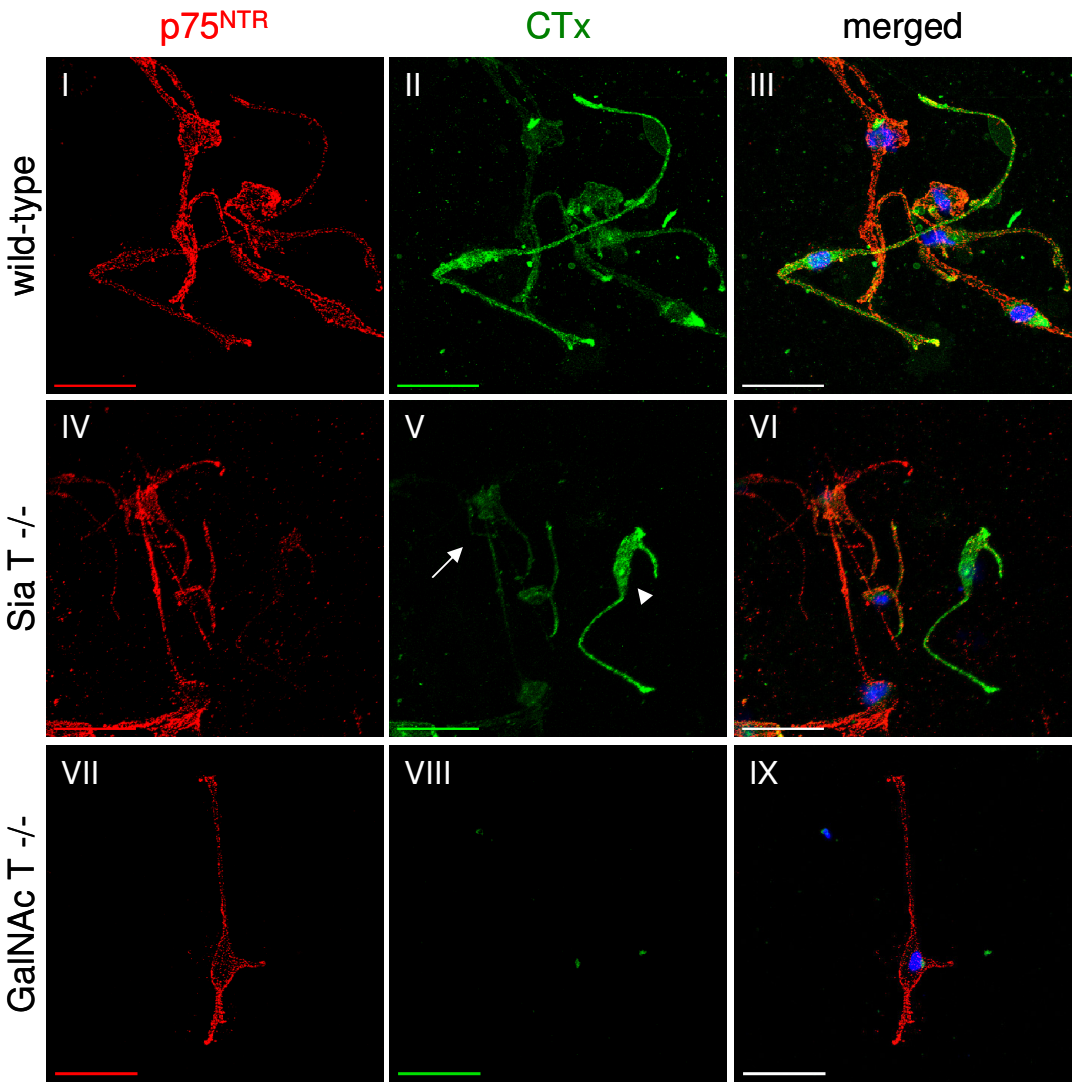

Figure 3.3. Representative images of CTx labelling of OECs.
Purified OECs from 7 day old wild-type (I-III), Sia T -/- (IV-VI) and GalNAc T -/- mice (VII-IX) were labelled with CTx (green) and p75^{NTR} (red). Nuclei were visualised with DAPI (blue). I, IV and VII illustrate the p75^{NTR} immunoreactivity; II, V and VIII illustrate the CTx immunoreactivity; III, VI and IX illustrate the merged images. CTx binds to ganglioside GM1, whereas p75^{NTR} identifies OECs. The majority of wild-type and Sia T -/- OECs express GM1 as demonstrated by the double-labelling of p75^{NTR} with CTx. The intensity of CTx labelling is heterogeneous: in some cells the immunoreactivity is strong (arrowhead) whereas in others it is weak (arrow) (V). GalNAc T -/- mice lack all a-series gangliosides and therefore do not express GM1 as demonstrated by the lack of CTx labelling (VIII). Scale bar = 50 μm.

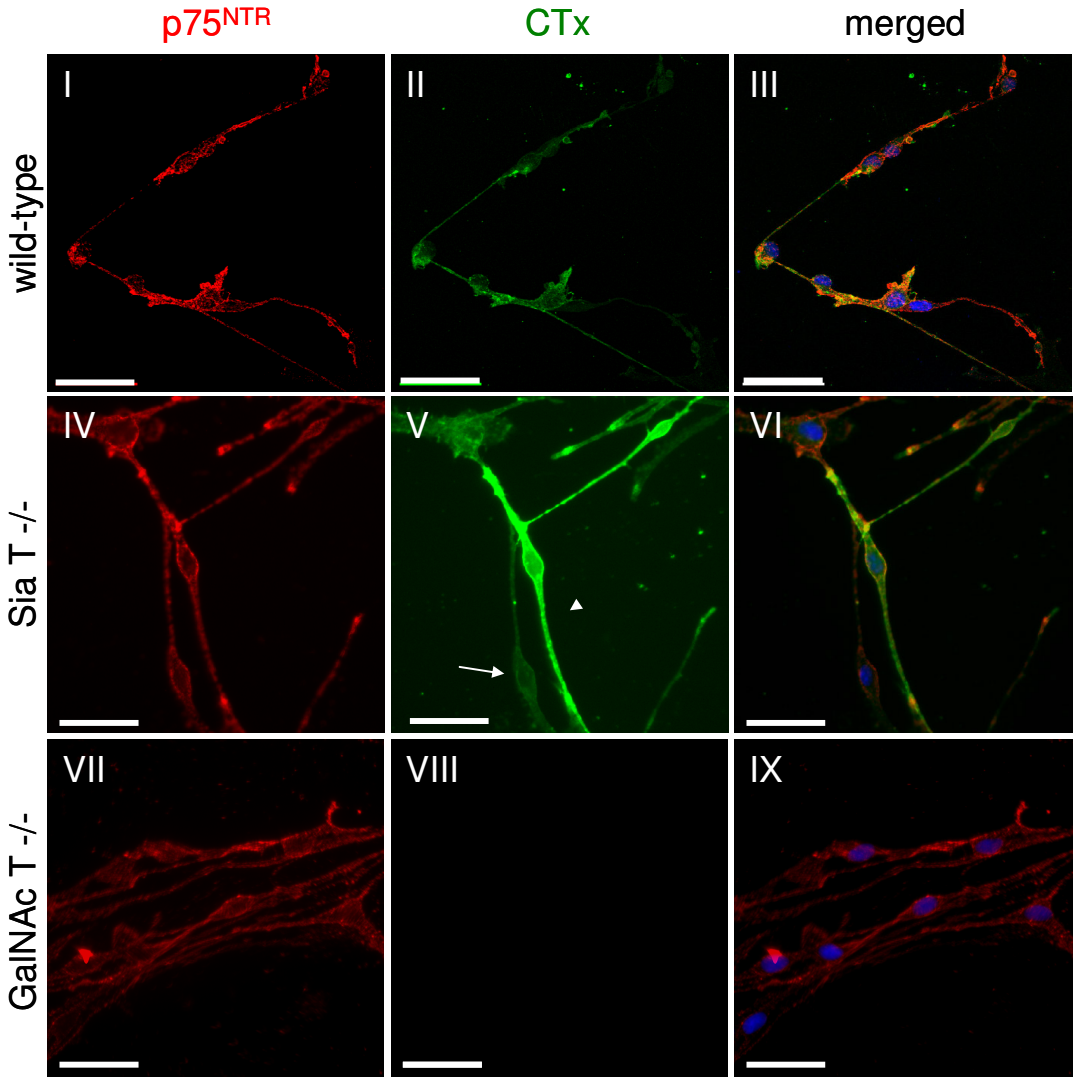

Figure 3.4. Representative images of CTx labelling of Schwann cells.
Purified Schwann cells from 7 day old wild-type (I-III), Sia T -/- (IV-VI) and GalNAc T -/- mice (VII-IX) were labelled with CTx (green) and $p75^{NTR}$ (red). Nuclei were visualised with DAPI (blue). I, IV and VII show the $p75^{NTR}$ immunoreactivity; II, V and VIII show the CTx immunoreactivity; III, VI and IX show the merged images. CTx binds to ganglioside GM1, whereas $p75^{NTR}$ identifies Schwann cells. The majority of wild-type and Sia T -/- Schwann cells express GM1 as demonstrated by the double-labelling of $p75^{NTR}$ with CTx. The intensity of CTx labelling is heterogeneous: in some cells the immunoreactivity is strong (arrowhead) whereas in others it is weak (arrow) (V). Note that the brightness in image V was digitally increased to reveal the weaker staining. GalNAc T -/- mice lack all a-series gangliosides and therefore do not express GM1 as demonstrated by the lack of CTx labelling (VIII). I-III scale bar = 50 μm; IV-IX scale bar = 20 μm.

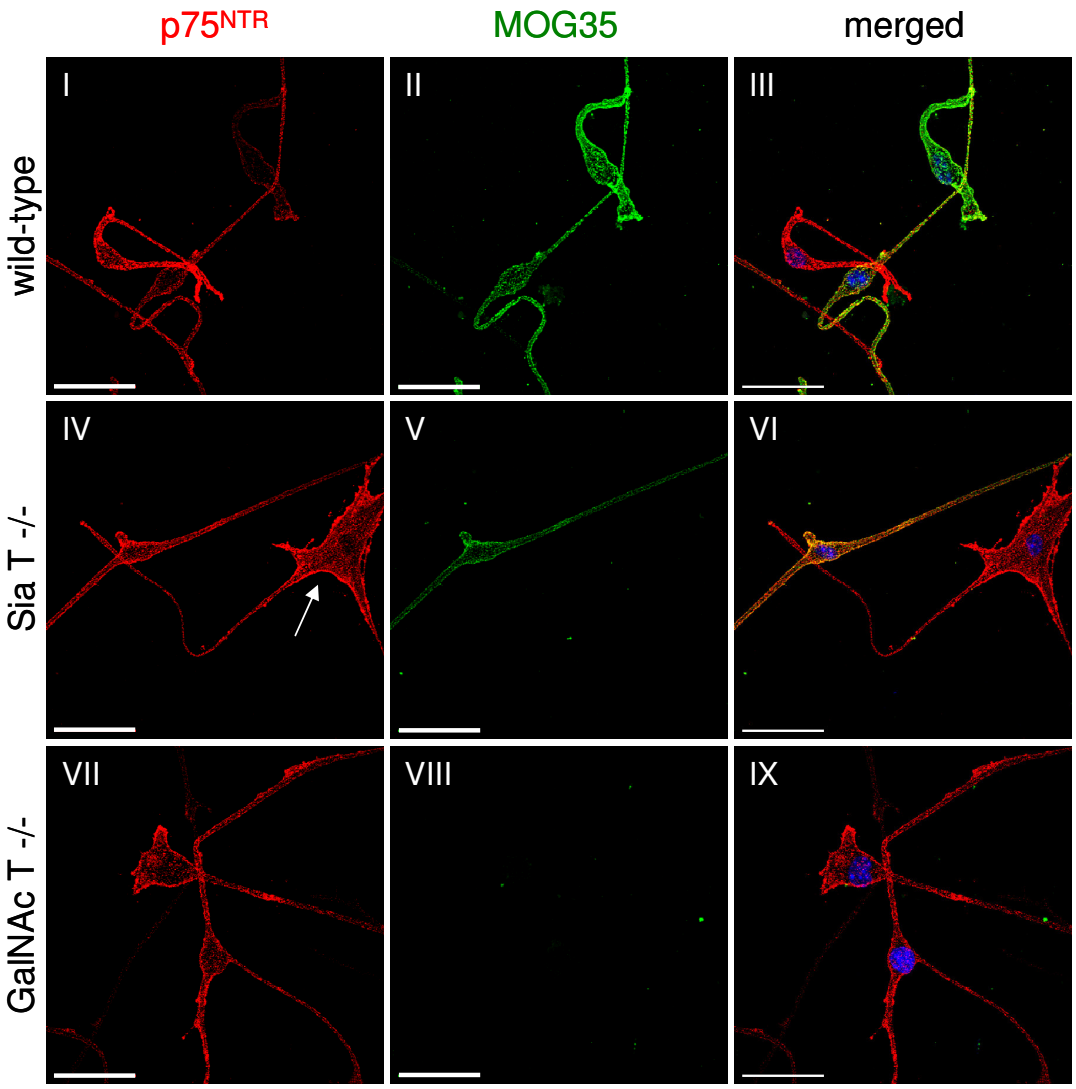

Figure 3.5. Representative images of MOG35 labelling of OECs.
Purified OECs from wild-type (I-III), Sia T -/- (IV-VI) and GalNAc T -/- mice (VII-IX) were labelled with MOG35 (green) and $p75^{NTR}$ (red). Nuclei were visualised with DAPI (blue). I, IV and VII show the $p75^{NTR}$ immunoreactivity; II, V and VIII show the MOG35 immunoreactivity; III, VI and IX show the merged images. MOG35 binds to ganglioside GD1a, whereas $p75^{NTR}$ identifies OECs. Majority of wild-type and Sia T -/- OECs express GD1a as demonstrated by the double-labelling of $p75^{NTR}$ with MOG35, however some OECs do not express MOG35 (arrow) (IV). GalNAc T -/- mice lack all a-series gangliosides and therefore do not express GD1a as demonstrated by the lack of MOG35 labelling (VIII). Scale bar = 50 μm.

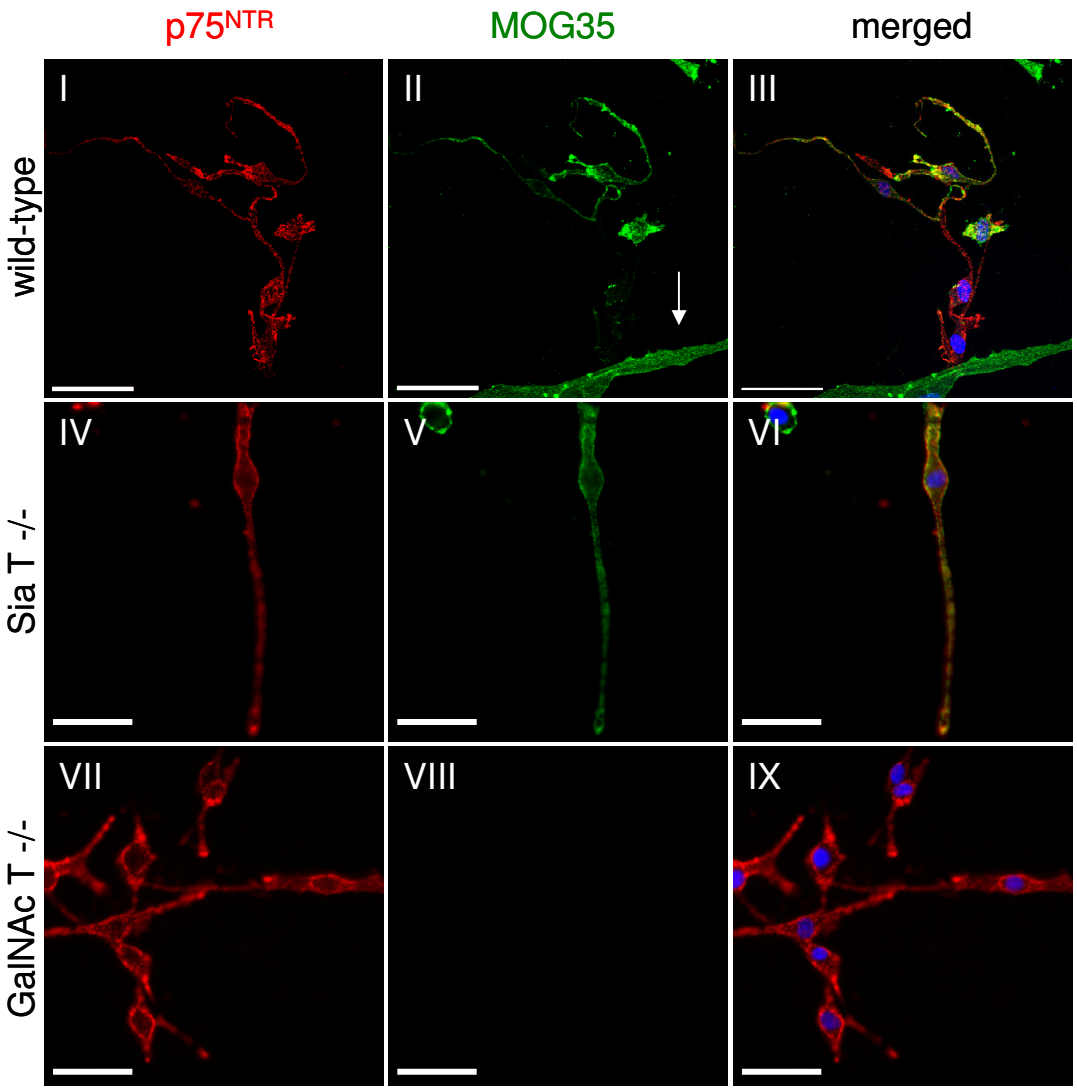

Figure 3.6. Representative images of MOG35 labelling of Schwann cells.
Purified Schwann cells from wild-type (I-III), Sia T -/- (IV-VI) and GalNac T -/- mice (VII-IX) were labelled with MOG35 (green) and $p75^{NTR}$ (red). Nuclei were labelled with DAPI (blue). I, IV and VII show the $p75^{NTR}$ immunoreactivity; II, V and VIII show the MOG35 immunoreactivity; III, VI and IX show the merged images. MOG35 binds to ganglioside GD1a, whereas $p75^{NTR}$ identifies Schwann cells. Majority of wild-type and Sia T -/- OECs express GD1a as demonstrated by the double-labelling of $p75^{NTR}$ with MOG35. Contaminating fibroblast also label with MOG35 (arrow) (II). GalNAc T -/- mice lack all a-series gangliosides and therefore do not express GD1a as demonstrated by the lack of MOG35 labelling. I-III scale bar = 50 μm; IV-IX scale bar = 20 μm.

A very small proportion of both Schwann cells and OECs (less than 1%) expressed ganglioside GD1b which is recognised by the antibody MOG1 (Figure 3.7). This was not due to the contaminating cells since the positive cells co-labelled with $p75^{NTR}$. A small percentage of both OECs and Schwann cells (less than 5%) labelled with the marker R24 which binds to GD3 and several complex gangliosides. A similar proportion of GalNAc T -/- cells, which lack all complex gangliosides, labelled with R24 (Figure 3.8). The contaminating cells in OEC and Schwann cell cultures also labelled with MOG1 and R24 (Figure 3.12 and 3.13).

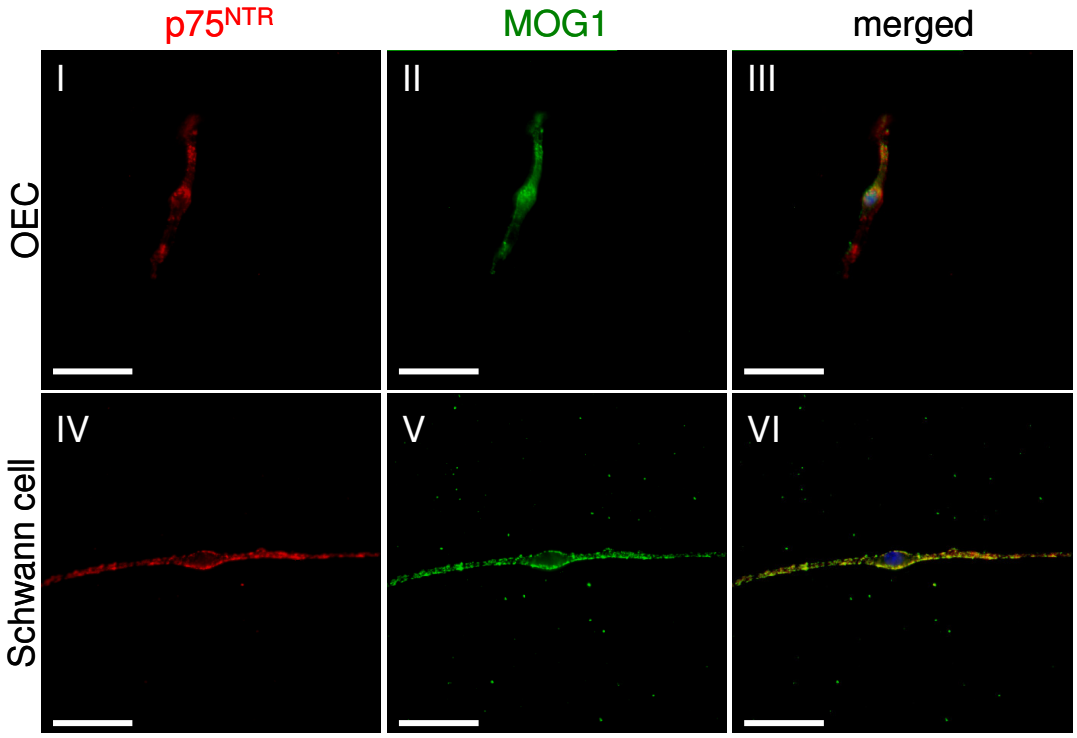

Figure 3.7. Representative images of MOG1 labelling of OECs and Schwann cells.
Purified wild-type OEC (I-III) and Schwann cells (IV-VI) were labelled MOG1 (green) and $p75^{NTR}$ (red). Nuclei were visualised with DAPI (blue). I and IV show the $p75^{NTR}$ immunoreactivity; II and V show the MOG1 immunoreactivity; III and VI show the merged images. Less than 1% of wild-type $p75^{NTR}$ immunoreactive Schwann cells and OECs double labelled with MOG1, which binds to ganglioside GD1b. Scale bar = 20 µm.

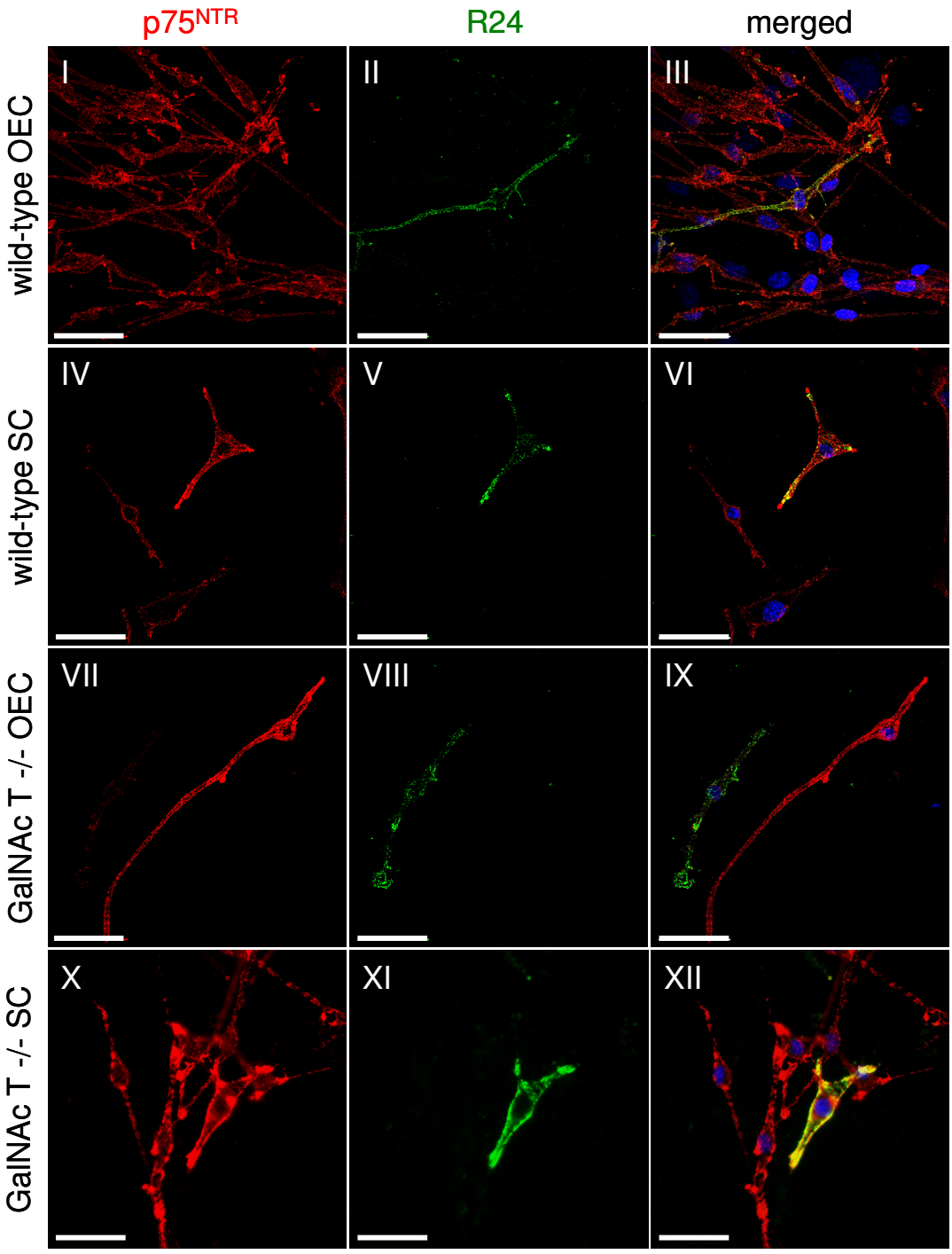

Figure 3.8. Representative images of OEC and Schwann cell expression of R24. Purified wild-type and GalNAc T -/- OECs and Schwann cells were double labelled with $p75^{NTR}$ (red) and R24 (green). I-III wild-type OEC; IV-VI wild-type Schwann cells; VII-IX GalNAc T -/- OEC; X-XII GalNAc T -/- Schwann cells. R24 labels gangliosides GT1a, GQ1b and GD3. Since GalNAc T -/- lack all complex gangliosides, the R24 labelling in GalNAc T -/- cells is due to R24 binding to simple ganglioside GD3. Nuclei were visualised with DAPI. I-IX Scale bar = 50 µm; X-XII scale bar = 20 µm.

There was a slight difference in the ganglioside expression between OECs and Schwann cells. A very small proportion of Schwann cells were positive for MOG30, EG2 and EG3 (less than 1%), whereas OECs were negative for all three (Figures 3.9, 3.10 and 3.11, respectively). The EG2, EG3 and MOG30 labelling in Schwann cell cultures was not due to the contaminating fibroblasts since the positive cells also labelled with $p75^{NTR}$.

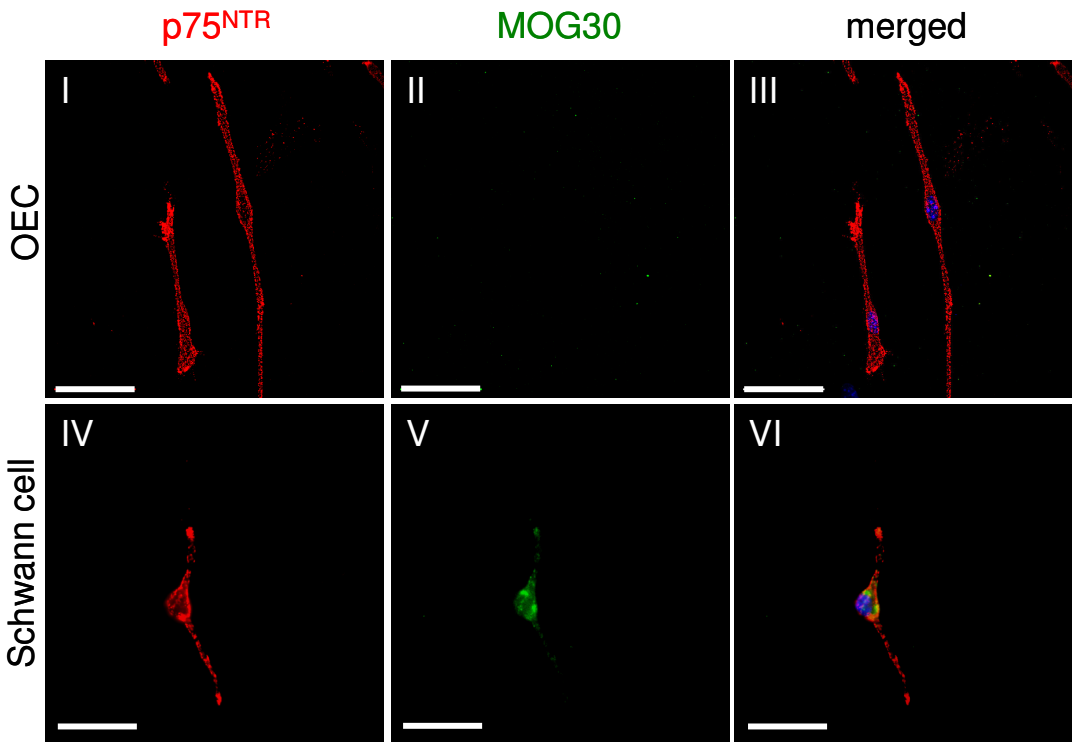

Figure 3.9. Representative images of MOG30 labelling of OECs and Schwann cells. Purified OECs (I-III) and Schwann cells (IV-VI) from 7 day old wild-type mice were double labelled with $p75^{NTR}$ (red) and MOG30 (green). Nuclei were visualised with DAPI (blue). Merged images are shown in images III and VI. All of the $p75^{NTR}$ positive OECs were negative for MOG30. Less than 1% of Schwann cells were positive for MOG30, which binds to ganglioside GQ1b. I-III scale bar = 50μm; IV-VI scale bar = 20 μm.

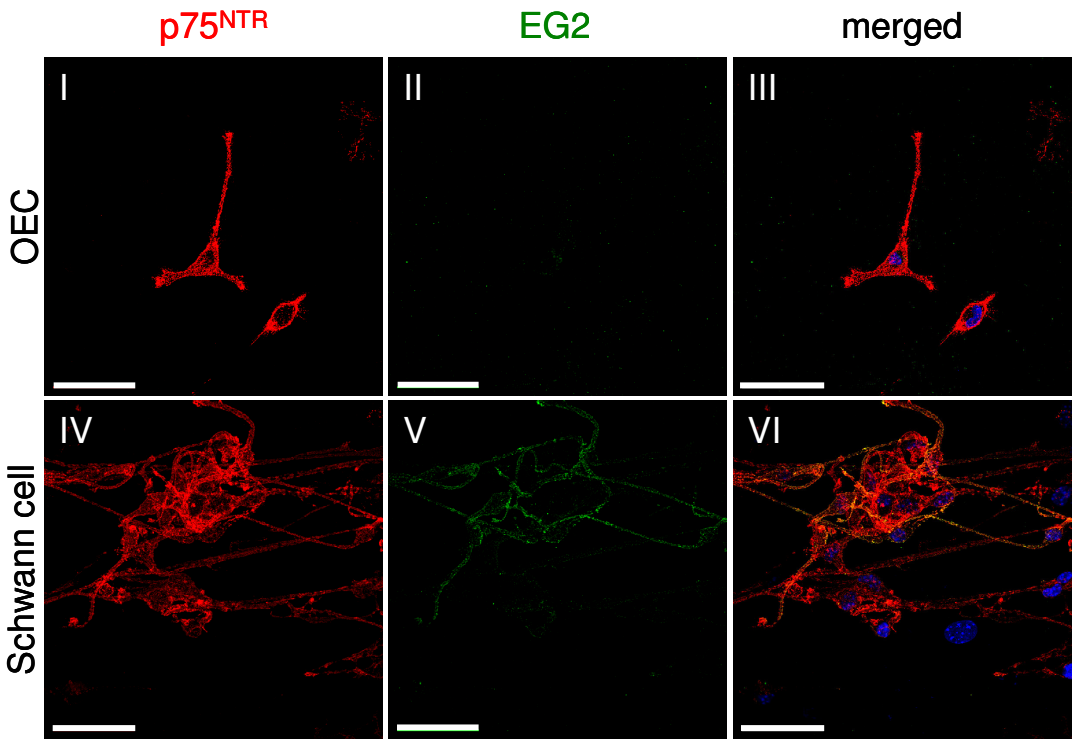

Figure 3.10. Representative images of EG2 labelling of OECs and Schwann cells. Purified wild-type OECs (I-III) and Schwann cells (IV-VI) were labelled with $p75^{NTR}$ (red) and EG2 (green). Nuclei were visualised with DAPI (blue). III and VI show the merged images. $p75^{NTR}$ labels OECs and Schwann cells; EG2 labels gangliosides GT1a, GD1b, GT1b and GQ1b. All of the $p75^{NTR}$ OECs were negative for EG2, whereas less than 1% of $p75^{NTR}$ immunoreactive Schwann cells were also EG2 immunoreactive. Scale bar = 50 μm.

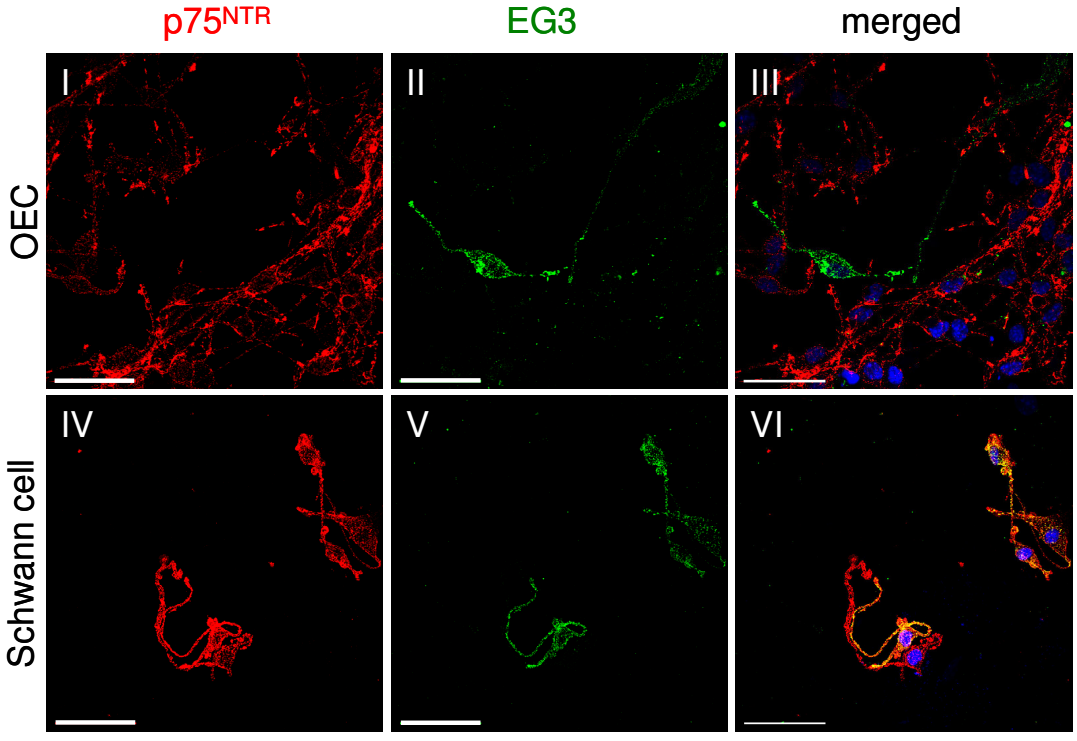

Figure 3.11. Representative images of EG3 labelling of OECs and Schwann cells. Purified wild-type OECs (I-III) and Schwann cells (IV-VI) were labelled with $p75^{NTR}$ (red) and EG3 (green). Nuclei were visualised with DAPI (blue). III and VI show the merged images. $p75^{NTR}$ labels OECs and Schwann cells; EG3 labels gangliosides GT1a and GQ1b. All of the $p75^{NTR}$ OECs were negative for EG3, whereas less than 1% of $p75^{NTR}$ immunoreactive Schwann cells were also EG3 immunoreactive. Scale bar = 50 μm.

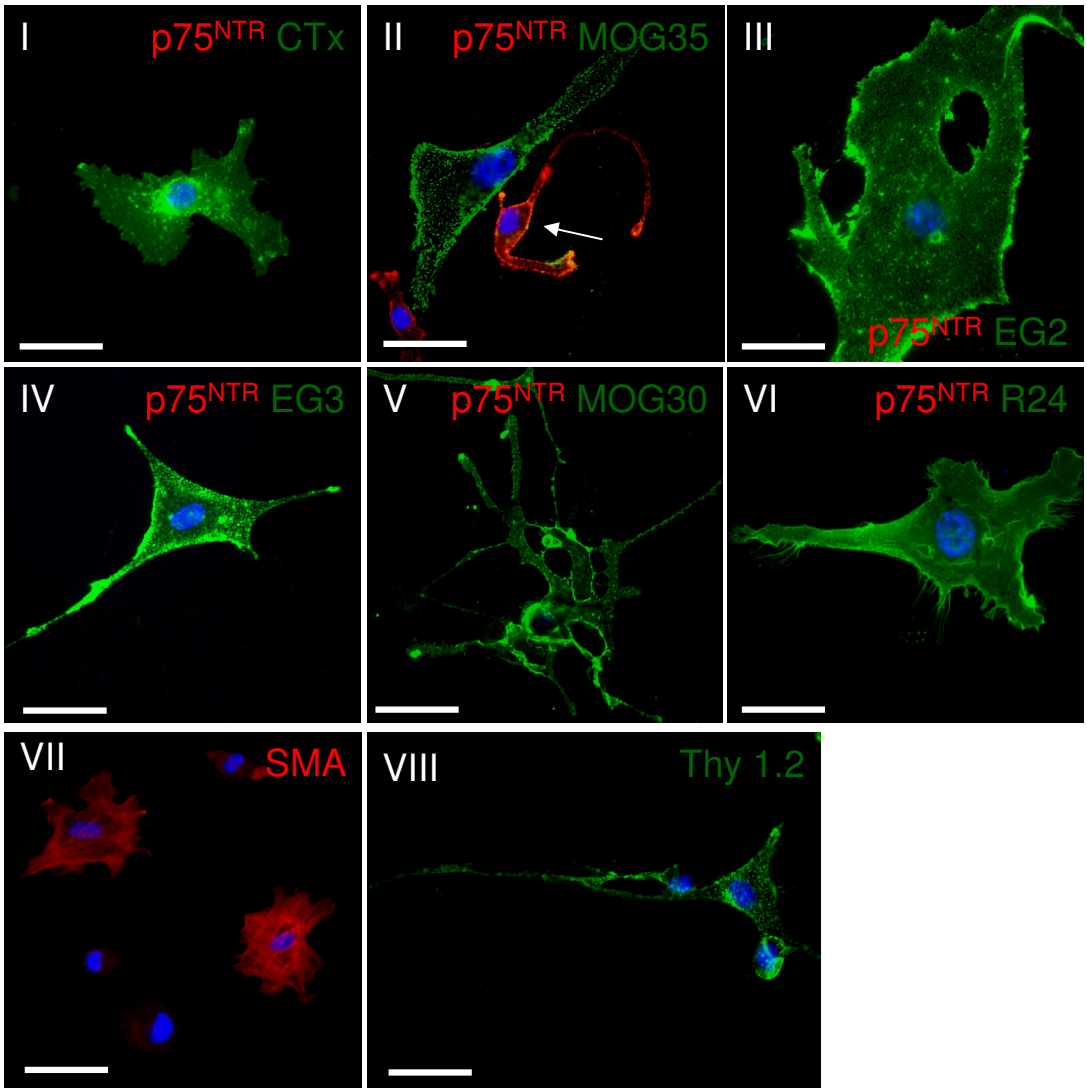

Figure 3.12. Ganglioside expression of contaminating cells in OEC cultures.
Mixed olfactory bulb cultures from wild-type mice were labelled with $p75^{NTR}$ (red, I-VI) and the following ganglioside markers (green): CTx (I), MOG35 (II), EG2 (III), EG3 (IV), MOG30 (V) and R24 (VI). OECs purified from 7-day old wild-type olfactory bulbs contain less than 5% of contaminating cells. These contaminating cells differ in morphology from the OECs and are $p75^{NTR}$ negative. These contaminating cells express gangliosides, SMA (red, VII) and Thy 1.2 (green, VIII). Note the difference in morphology between $p75^{NTR}$ positive OECs (arrow) and the $p75^{NTR}$ negative cell in II. Nuclei were visualised with DAPI (blue). Scale bar = 20 μm

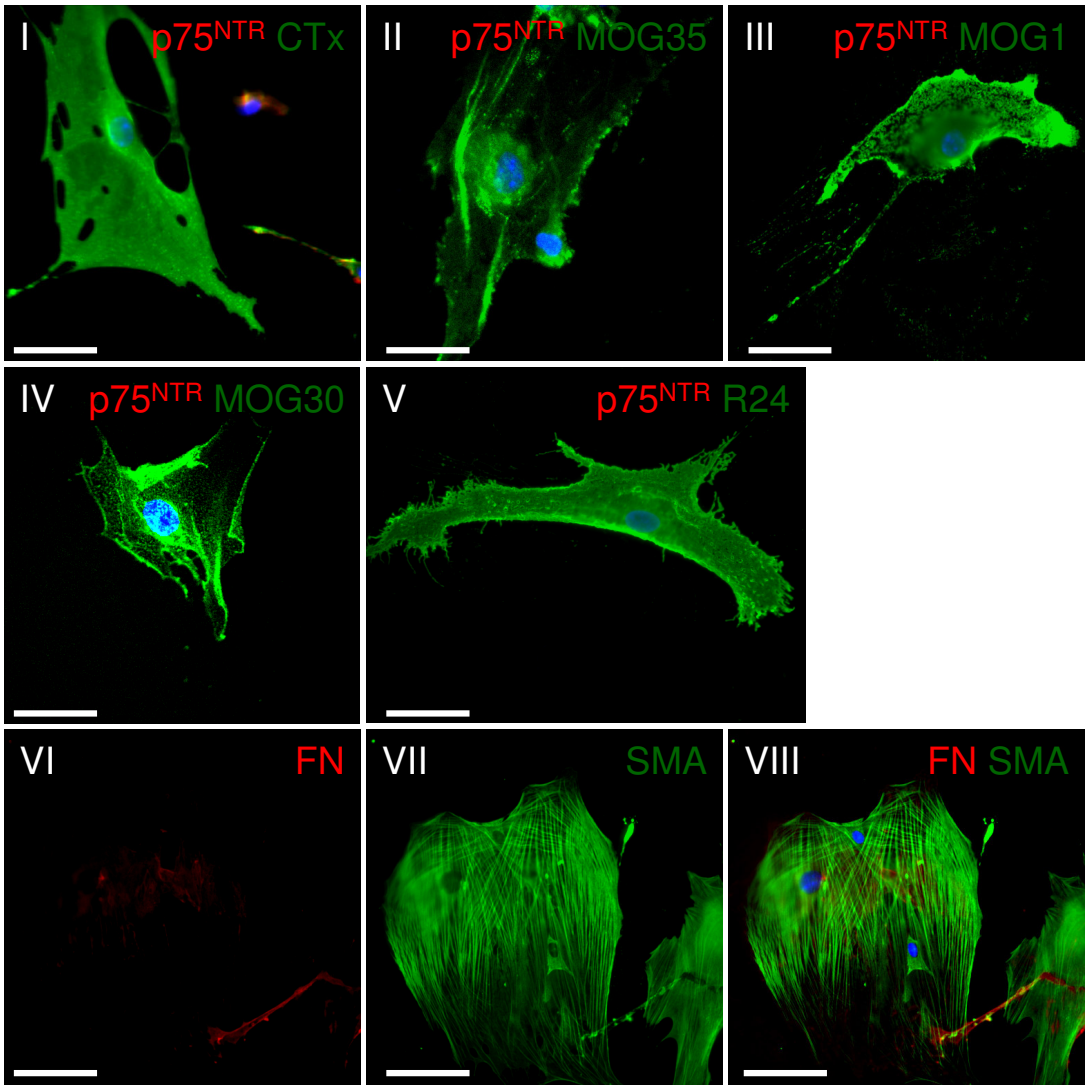

Figure 3.13. Ganglioside expression of contaminating cells in Schwann cell cultures. Mixed sciatic nerve cultures from wild-type mice were labelled with $p75^{NTR}$ (red, I-VI) and the following ganglioside markers (green): CTx (I), MOG35 (II), MOG1 (III), MOG30 (IV), and R24 (V). Schwann cells purified from 7-day old wild-type sciatic nerves contain less than 5% of contaminating cells. These contaminating cells differ in morphology from the Schwann cells and are $p75^{NTR}$ negative. These contaminating cells express gangliosides, as well as, fibronectin (red, VI) and SMA (green, VII). Nuclei were labelled with DAPI. VIII shows the merged SMA and fibronectin image. Scale bar = 20 μm.

3.2.4 Antigen profile and morphology of wild-type and ganglioside knockout cells

Having shown that both OECs and Schwann cells express complex gangliosides, the aim was to investigate the role gangliosides play in the biology of OECs and Schwann cells. Firstly, the morphology of wild-type and ganglioside knockout OECs and Schwann cells was compared on PLL, laminin and collagen (Figure 3.14-3.17).

Examination by phase contrast microscopy of the morphology of OECs and Schwann cells after re-plating on culture dishes coated with PLL, laminin or collagen showed that the appearance of cells varied depending on the type of growth surface and whether they were grown in the presence or absence of serum and growth factors. However, the morphological characteristics of ganglioside knockout OECs and Schwann cells grown on PLL or ECM components collagen IV and laminin were similar to wild-type cells.

In serum and growth factor-free medium, DMEM-BS, both OECs and Schwann cells extended two or three long processes which were sometimes branched (Figures 3.14 and 3.16, respectively), while those grown in the presence of serum and growth factors had comparably shorter processes and appeared flatter (Figures 3.15 and 3.17, respectively).

OECs and Schwann cells grown on laminin (Figures 3.14 to 3.17 II, V and VIII), both in the presence and absence of serum and growth factors, had much longer processes than those grown in PLL and collagen.

Secondly, the antigen profile of OECs and Schwann cells obtained from wild-type, Sia T -/- and GalNAc T -/- mice was examined (Figure 3.18 and 3.19). It was found that ganglioside knockout cells had the same antigen profile as the wild-type cells with all genotypes expressing $p75^{NTR}$, nestin and GFAP.

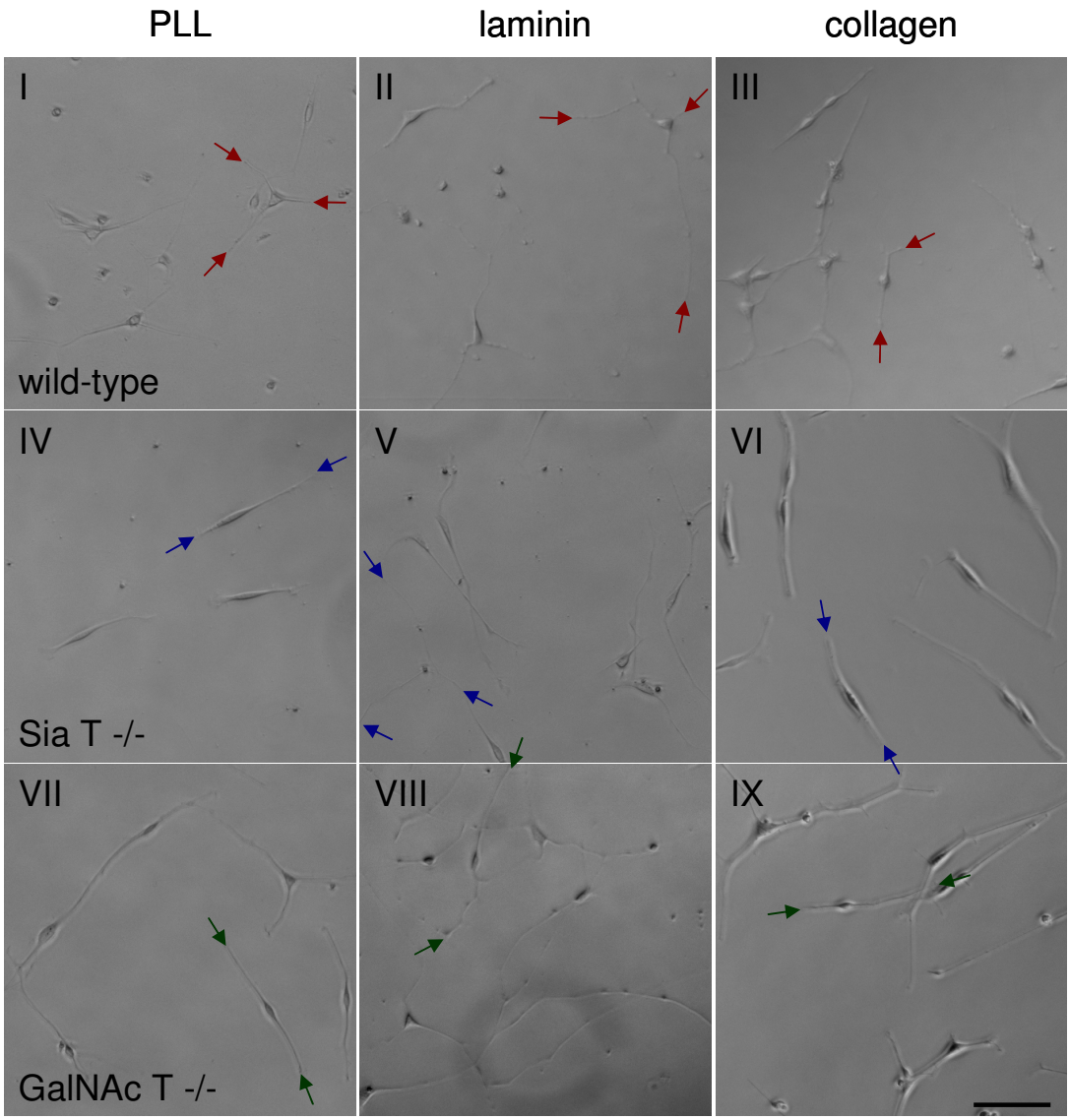

Figure 3.14. Morphology of wild-type and ganglioside knockout OECs grown in DMEM-BS. Wild-type (I-III), Sia T -/- (IV-VI) and GalNAc T -/- (VII-IX) OECs were trypsinised from parent cultures, and re-plated at low density on wells coated with PLL (I, IV & VII) , laminin (II, V & VIII) or collagen (III, VI & IX) as described in the Methods section. Cells were left to attach overnight in OMM+5%FBS. This was replaced by growth factor- and serum free medium, DMEM-BS, and phase contrast images were taken 48 hours later. In each image, a cell was chosen as an example and arrows were used to show where its processes end. These representative images show that there was no difference in the morphology of OECs derived from wild-type, Sia T -/- and GalNAc T -/- mice. Scale bar = 100 µm.

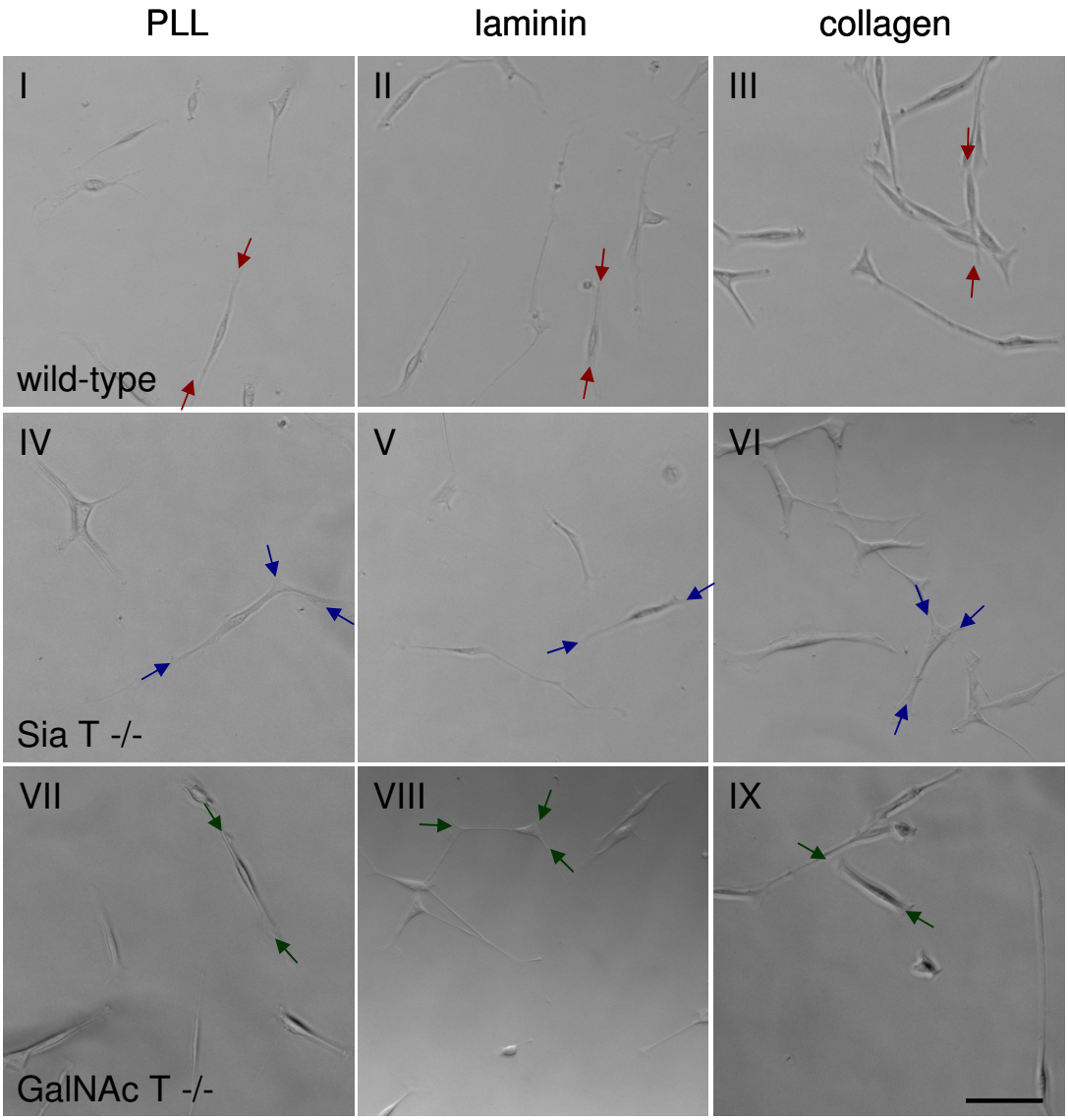

Figure 3.15. Morphology of wild-type and ganglioside knockout OECs grown in OMM+5%FBS. Wild-type (I-III), Sia T -/- (IV-VI) and GalNAc T -/- (VII-IX) OECs were trypsinised from parent cultures, and re-plated at low density on wells coated with PLL (I, IV & VII) , laminin (II, V & VIII) or collagen (III, VI & IX) as described in the Methods section. Cells were maintained in OMM+5%FBS. Phase contrast images were taken 48 hours after plating. In each image, a cell was chosen as an example and arrows were used to show where its processes end. Scale bar = 100 µm.

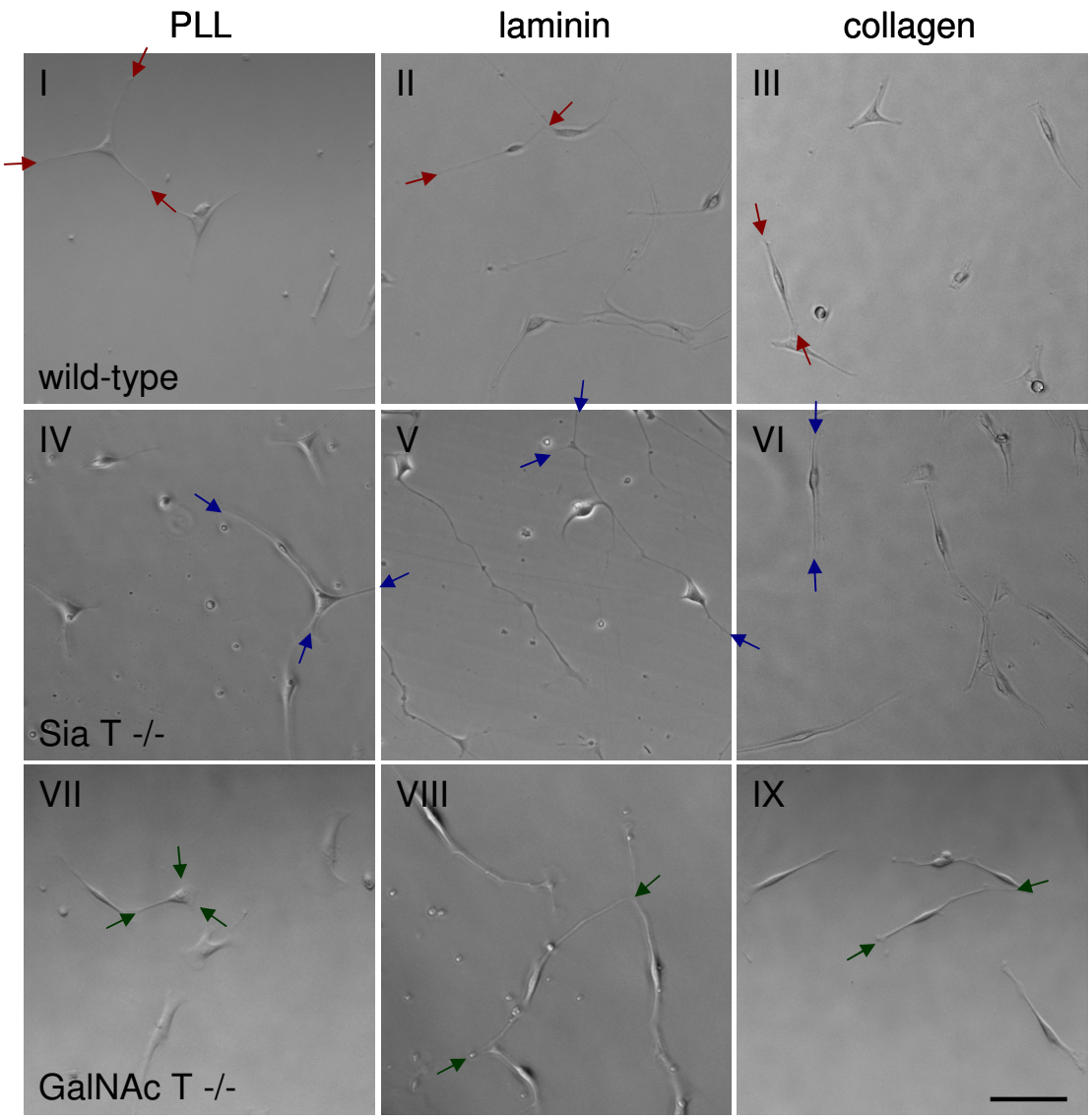

Figure 3.16. Morphology of wild-type and ganglioside knockout Schwann cells grown in DMEM-BS.
Wild-type (I-III), Sia T -/- (IV-VI) and GalNAc T -/- (VII-IX) Schwann cells were trypsinised from parent cultures, and re-plated low density on wells coated with PLL (I, IV & VII) , laminin (II, V & VIII) or collagen (III, VI & IX) as described in the Methods section. Cells were left to attach overnight in 10%HF. This was replaced by growth factor- and serum free medium, DMEM-BS, and phase contrast images were taken 48 hours later. In each image, a cell was chosen as an example and arrows were used to show where its processes end. The round cells in III are cells which had detached from the substrate. Scale bar = 100 µm.

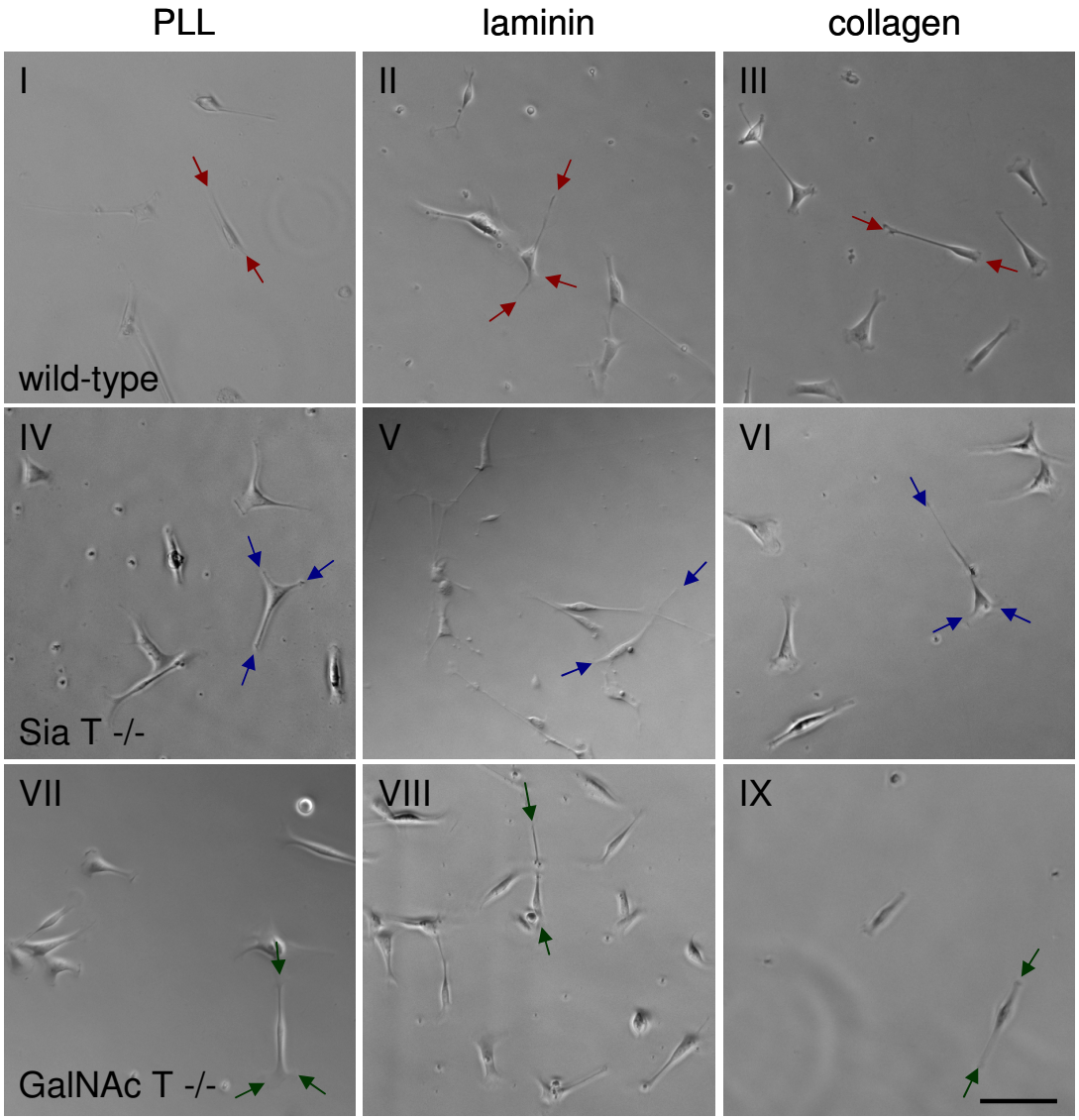

Figure 3.17. Morphology of wild-type and ganglioside knockout Schwann cells grown in 10%HF. Wild-type (I-III), Sia T -/- (IV-VI) and GalNAc T -/- (VII-IX) Schwann cells were trypsinised from parent cultures, and re-plated at low density on wells coated with PLL (I, IV & VII) , laminin (II, V & VIII) or collagen (III, VI & IX) as described in the Methods section. Cells were maintained in 10%HF. Phase contrast images were taken 48 hours after plating. In each image, a cell was chosen as an example and arrows were used to show where its processes end. Scale bar = 100 µm.

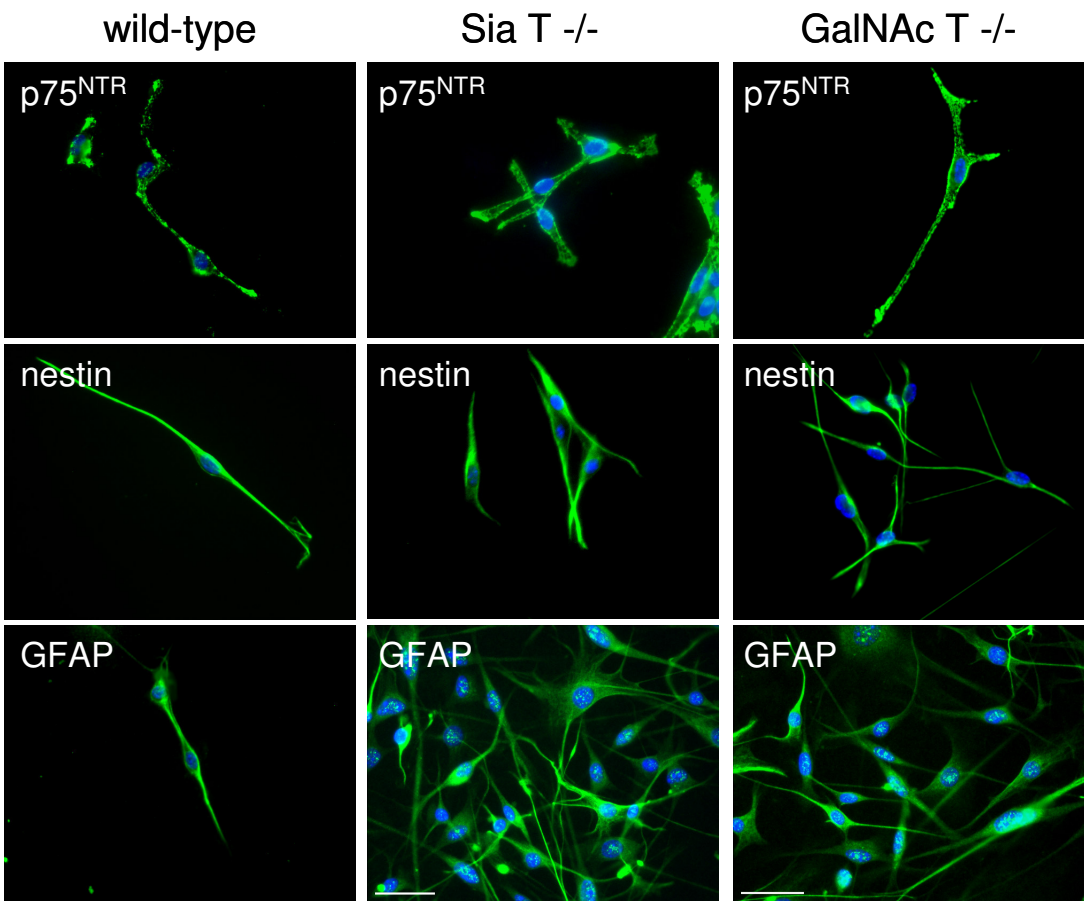

Figure 3.18. Antigen profile for wild-type, Sia T -/- and GalNAc T -/- OECs.
Purified OECs from 7-day old wild-type, Sia T -/- and GalNAc T -/- mice were labelled with typical OEC markers $p75^{NTR}$, nestin and GFAP. The antigen profile was similar in all three genotypes. Nuclei are labelled with DAPI (blue). Scale bar = 20 μm.

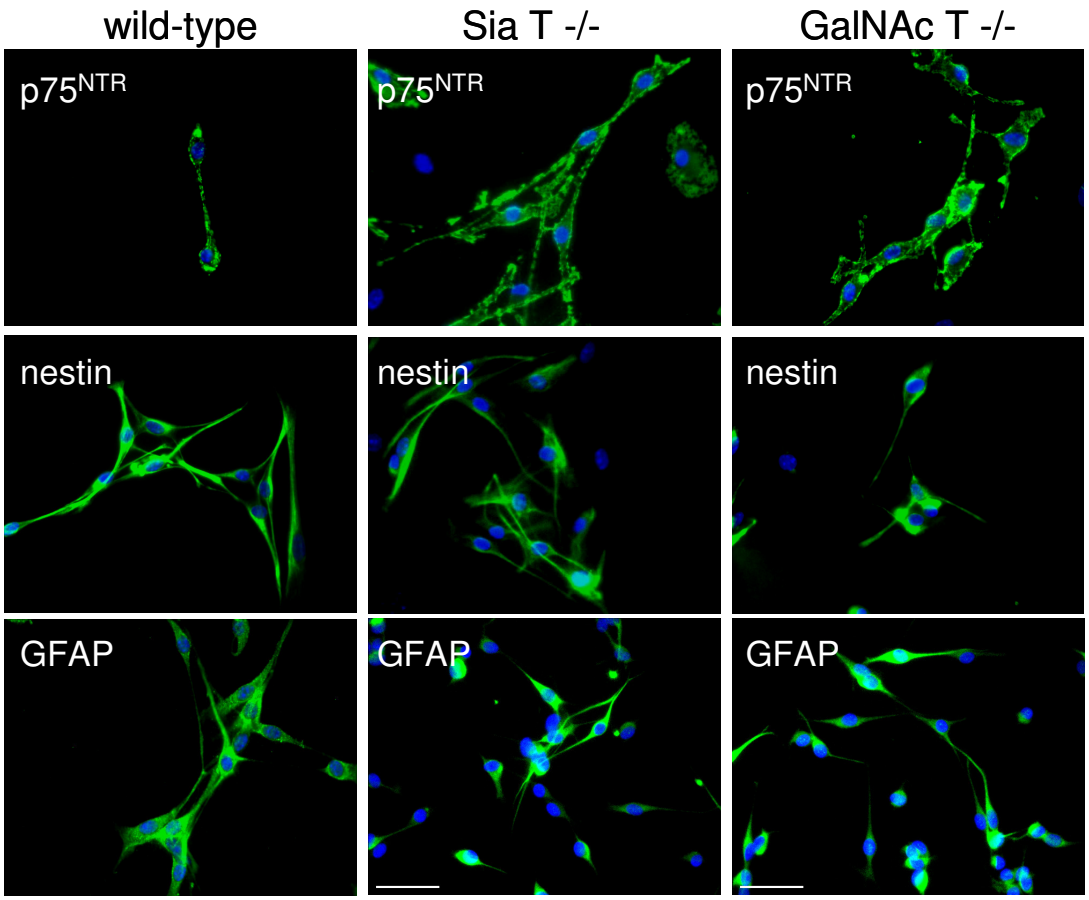

Figure 3.19. Antigen profile for wild-type, Sia T -/- and GalNAc T -/- Schwann cells.
Purified Schwann cells from 7 day old wild-type, Sia T -/- and GalNAc T -/- mice were labelled with typical Schwann cell markers $p75^{NTR}$, nestin and GFAP. The antigen profile was similar in all three genotypes. Nuclei are labelled with DAPI (blue). Scale bar = 20 μm.

3.2.5 Proliferation of wild-type and ganglioside knockout cells

As it has been shown that gangliosides can interact with growth factor receptors and integrins to modulate cell function (Cheresh *et al.*, 1987, Zheng *et al.*, 1993), the growth and motility of OECs and Schwann cells was investigated on different substrates in the presence or absence of growth factors. The proliferation of wild-type, Sia T -/- and GalNAc T -/- OECs and Schwann cells was therefore compared on PLL, laminin and collagen in media with or without growth factors. OECs and Schwann cells were isolated from the olfactory bulbs and sciatic nerves of 7 day old mice, respectively. The cells were purified as described in the methods section and after approximately 7 DIV, the purified cells were trypsinised and re-plated onto PLL, collagen or laminin coated coverslips at a density of around 10,000 cells per coverslip. The cells were maintained in their respective optimal growth media (OECs in OMM+5%FBS and Schwann cells in 10%HF) overnight to allow them to attach. The following day, the cells were washed in DMEM-BS and the cells were subsequently maintained in either serum- and growth factor-free medium (DMEM-BS), or in media containing growth factors (OMM+5%FBS for OECs and 10%HF for Schwann cells). BrdU was added for the last 16 hours of the experiment. Finally, the cells were fixed and stained with an anti-BrdU antibody to label the proliferating cells, and DAPI to label the nuclei. Proliferation rates are presented as the percentage of cells which have taken up BrdU over the 16 hour period. Each experiment was performed in duplicate and a minimum of 1000 cells was counted per coverslip.

It was found that the proliferation of OECs derived from ganglioside knockout mice did not differ from wild-type OEC proliferation in serum- and growth factor-free medium. Furthermore, in serum- and growth factor-free medium, wild-type and ganglioside knockout OECs proliferated at a similar rate on all three substrates.

OECs from all three genotypes had significantly higher proliferation rates when grown in OMM+5%FBS regardless of substrate ($p < 0.05$). In addition, Sia T -/- OECs proliferated significantly better on laminin compared with PLL when grown in the presence of growth factors ($p < 0.05$). Ganglioside knockout OECs grown on PLL and laminin had similar proliferation rates to wild-type OECs. However,

Sia T -/- OECs had a higher proliferation ($p < 0.05$) compared with wild-type and GalNAc T -/- OECs when grown on collagen in OMM+5%FBS (Figure 3.20).

As with the OECs, Schwann cells proliferated better on all substrates in media containing growth factors compared with DMEM-BS ($p < 0.05$). In contrast to OECs, Sia T -/- Schwann cells did not proliferate better on laminin when grown in media containing growth factors: Schwann cell proliferation was similar on all three substrates. Also in contrast to OECs, ganglioside knockout Schwann cells had similar proliferation rates to wild-type Schwann cells on all three substrates in both serum- and growth factor-free medium (DMEM-BS) and in medium containing growth factors (10%HF) (Figure 3.21).

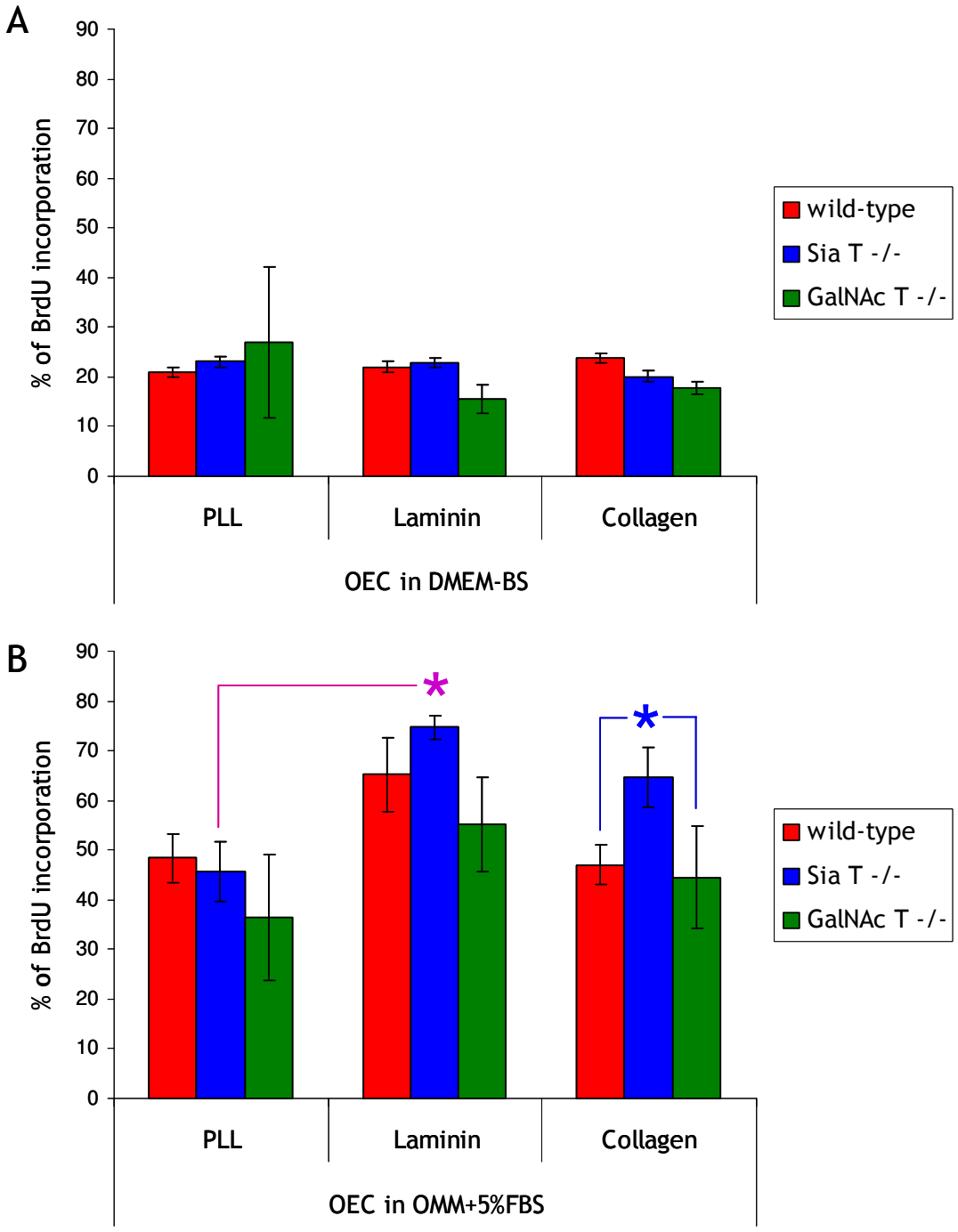

Figure 3.20. Proliferation of OECs derived from wild-type and ganglioside knockout mice. A comparison was made of the proliferation of OECs purified from 7 day old wild-type, Sia T -/- and GalNAc T -/- mice grown in serum- and growth factor-free medium, DMEM-BS (A) or OMM+5%FBS (B) on PLL, laminin and collagen. OECs cultured from wild-type and ganglioside knockout mice have similar proliferation rates on all three substrates when grown in DMEM-BS. OECs proliferation was significantly higher in medium containing growth factors. OECs derived from ganglioside knockout mice grown on PLL and laminin in OMM+5%FBS had similar proliferation rates to OECs derived from wild-type mice. Sia T -/- OECs grown in OMM+5%FBS on collagen had increased proliferation compared with WT cells ($p < 0.05$). Each point represents the mean ± SEM (n=3). Sia T -/- OECs proliferate better on laminin compared with PLL ($p < 0.01$, pink *). Sia T -/- OEC grown on collagen have a higher proliferation rate that wild-type and GalNAc T -/- OECs ($p < 0.05$, blue *).

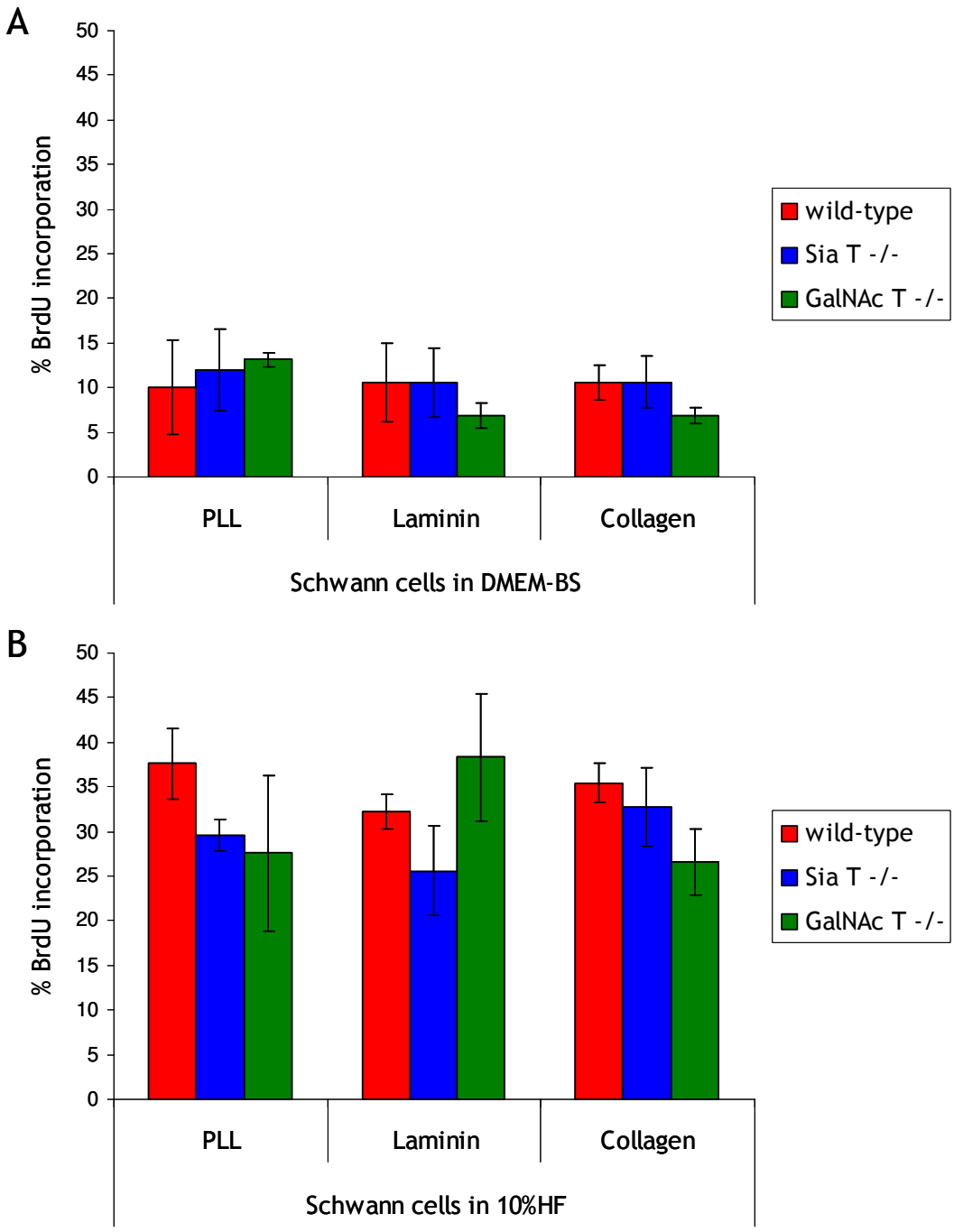

Figure 3.21. Proliferation of wild-type and ganglioside knockout Schwann cells.
A comparison was made of the proliferation of Schwann cells purified from 7 day old wild-type, Sia T -/- and GalNAc T -/- mice grown in serum- and growth factor-free medium, DMEM-BS (A) or 10%HF (B) on PLL, laminin and collagen. The proliferation of Schwann cells was significantly higher in medium containing growth factors. Schwann cells obtained from ganglioside knockout mice had similar proliferation rates in both DMEM-BS and 10%HF on all three substrates. Each point represents the mean ± SEM (n=3).

3.2.6 Motility of wild-type and ganglioside knockout cells

In order to test whether gangliosides play a role in OEC and Schwann cell motility, the motility of wild-type and ganglioside knockout cells was measured using time-lapse microscopy. OECs and Schwann cells were isolated from the olfactory bulbs and sciatic nerves of 7 day old mice, respectively. The cells were purified as described in the methods section and after approximately 7 DIV, the purified cells were plated onto PLL, collagen or laminin coated wells at a density of around 5,000 cells per well for the migration experiments and 30,000 cells per well for the wound assay experiments. The cells were maintained in their respective optimal growth media (OECs in OMM+5%FBS and Schwann cells in 10%HF) overnight to allow them to attach. The following day the cells were washed in DMEM-BS and were subsequently maintained in either serum- and growth factor-free medium (DMEM-BS), or in media containing growth factors (OMM+5%FBS for OECs and 10%HF for Schwann cells).

No difference was observed in the motility of cells between wild-type and ganglioside knockout OECs (Figure 3.22) and Schwann cells (Figure 3.23) using an assay where the migration of individual cells plated at low density was measured. The greatest migration velocities were achieved on laminin in all genotypes tested in medium with or without growth factors ($p < 0.05$). Whereas the proliferation of OECs and Schwann cells increased in the presence of growth factors, the motility of both cell types was unaffected by the presence of growth factors (Figure 3.22 and 3.23).

Using a wound assay it was observed that the migration of wild-type OECs and Schwann cells was again similar in medium with or without growth factors (Figure 3.24 and 3.25). Because it was difficult to obtain a confluent layer of cells for the wound assay in the medium lacking growth factors, it was decided to study the migration of ganglioside knockout cells using wound assays only in the presence of growth factors. When the cells were plated at high density and a wound was made, Sia T -/- Schwann cells grown on laminin and collagen exhibited a significantly higher wound healing migration compared with wild-type cells ($p < 0.05$).

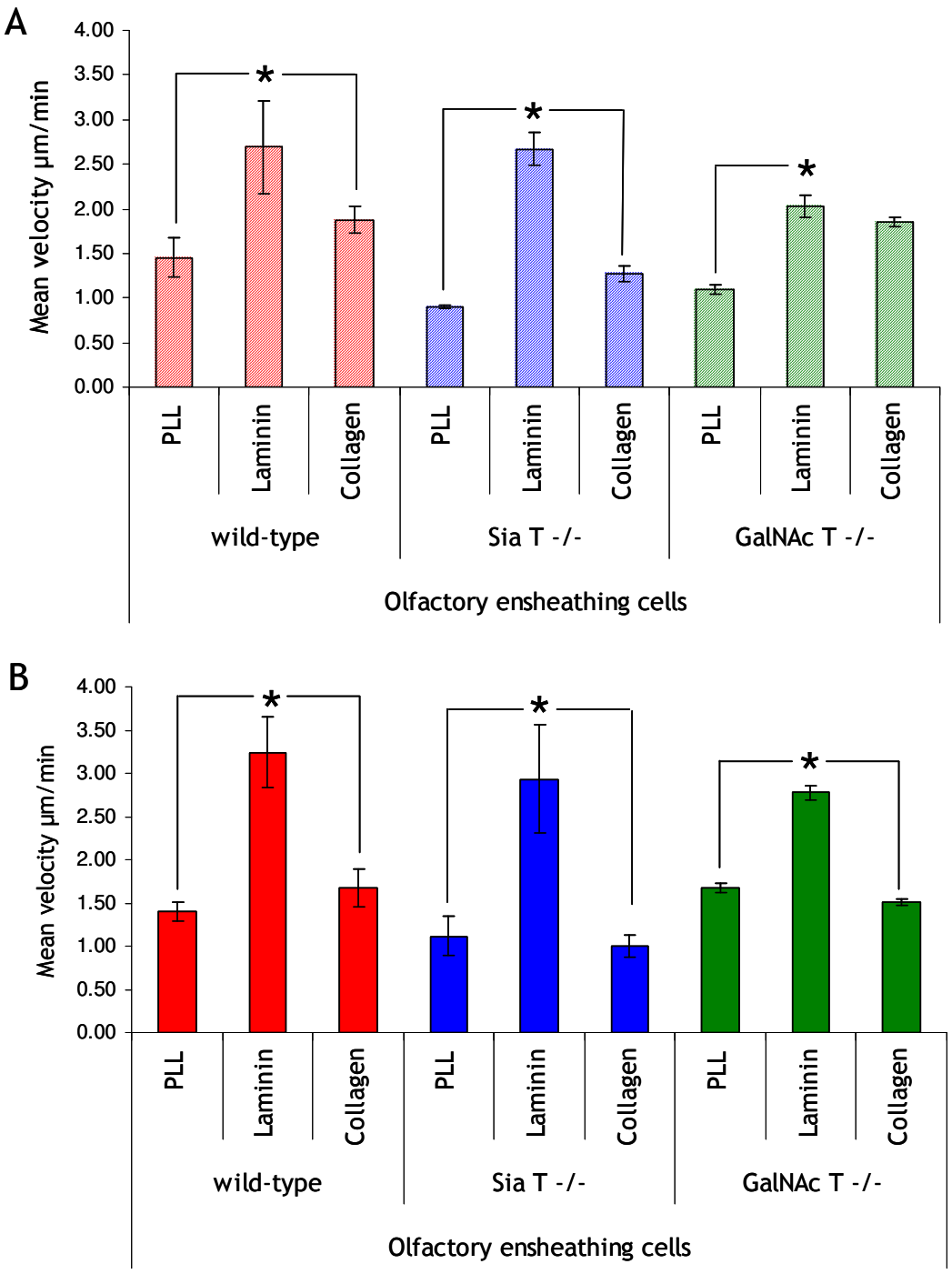

Figure 3.22. Motility of wild-type and ganglioside knockout OECs.
The motility of OECs isolated from wild-type and ganglioside knockout mice was compared in medium containing no growth factors, DMEM-BS (A) and in optimal growth media, OMM+5%FBS (B) on PLL, laminin and collagen. Wild-type and ganglioside knockout OECs have similar migration profiles, with all cells migrating faster on laminin. The presence of growth factors in the culture medium did not affect the motility of OECs. Each point represents the mean ± SEM (n=3).

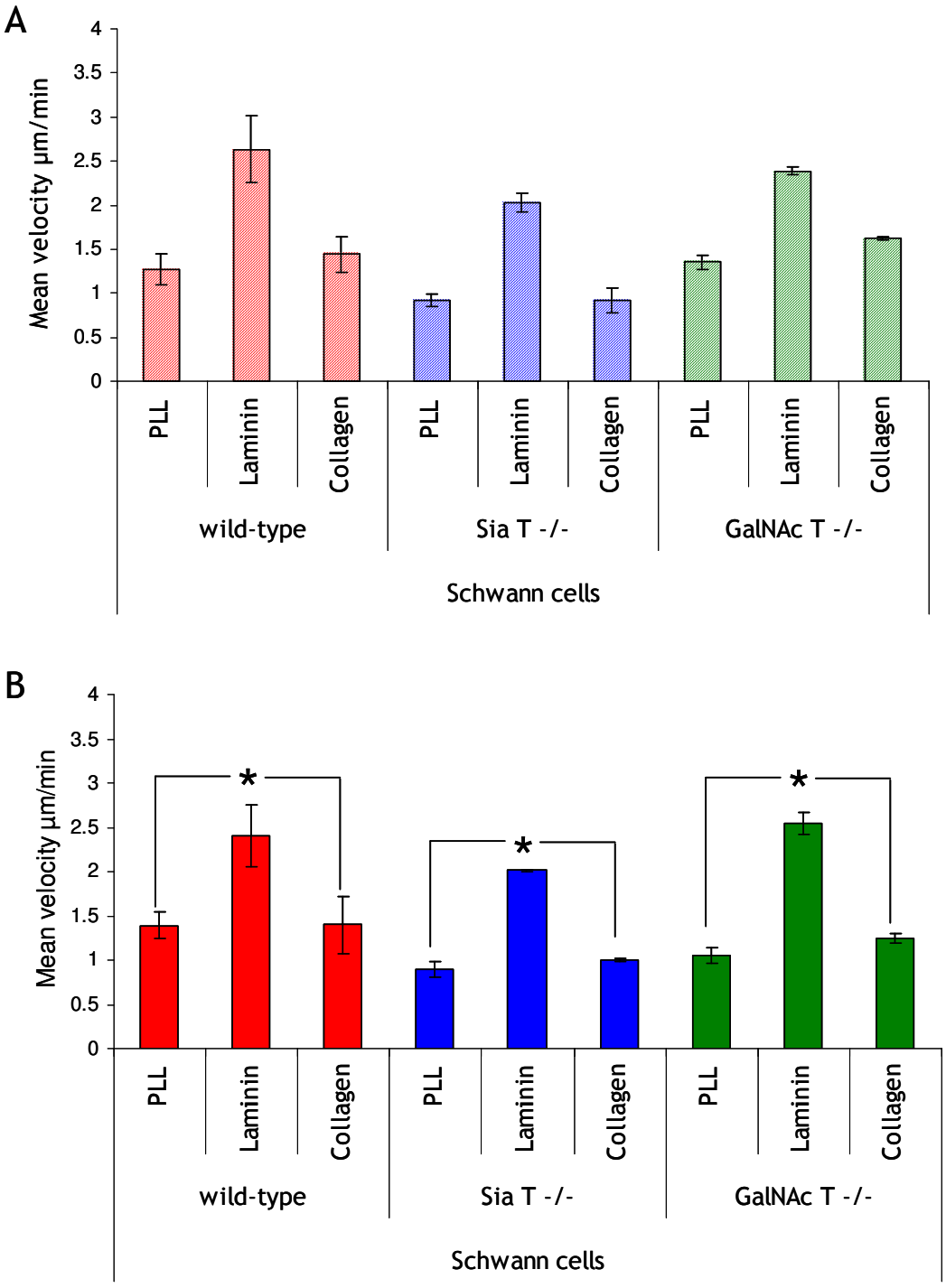

Figure 3.23. Motility of wild-type and ganglioside knockout Schwann cells.
The motility of Schwann cells from wild-type and ganglioside knockout mice was compared in medium containing no growth factors, DMEM-BS (A) and in optimal growth media, 10%HF (B) on PLL, laminin and collagen. Wild-type and ganglioside knockout Schwann cells have similar migration profiles, with all cells migrating faster on laminin. Schwann cell motility was similar in the presence and absence of growth factors. Each point represents the mean ± SEM (n=3).

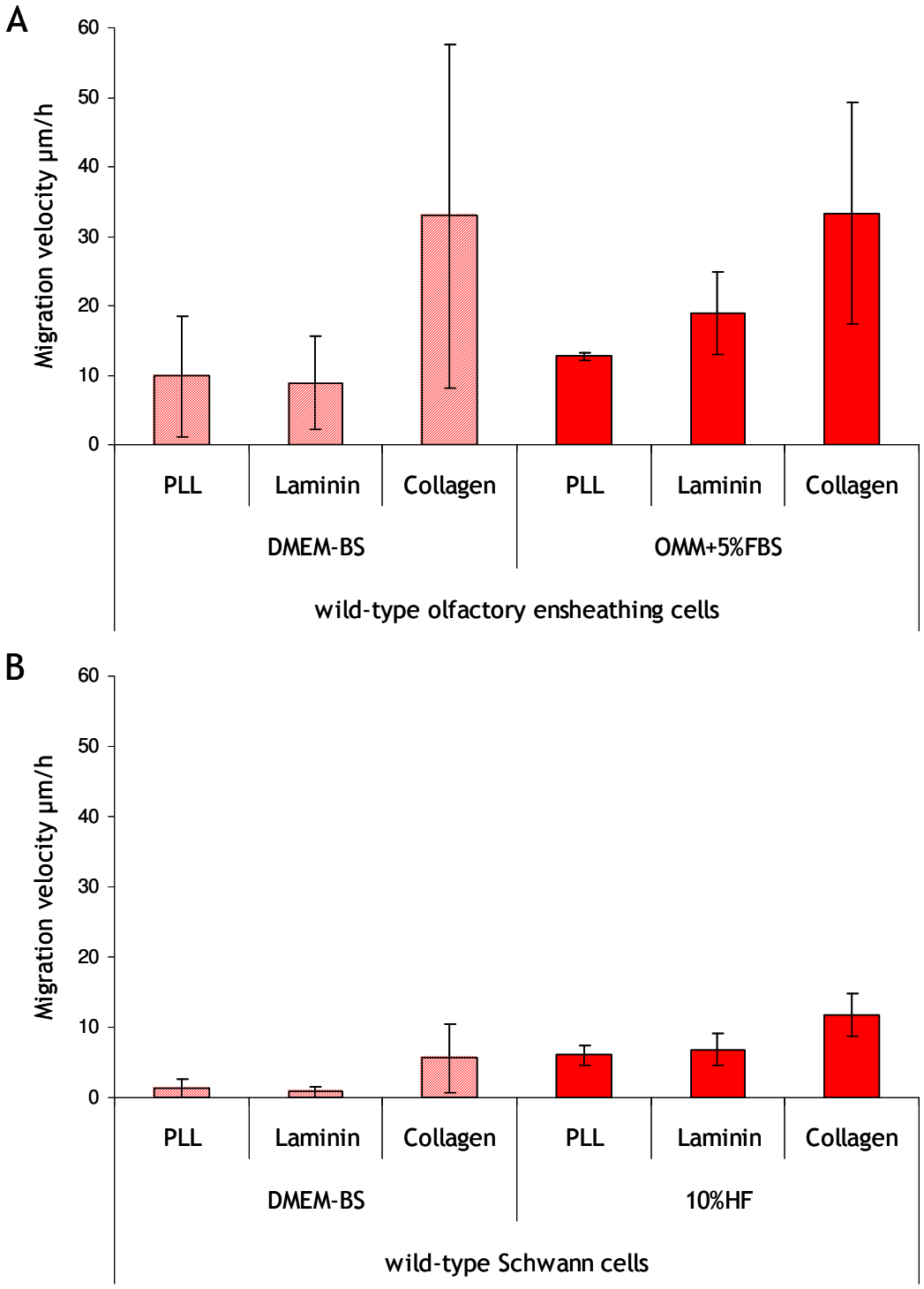

Figure 3.24. Motility of wild-type OECs and Schwann cells in a wound assay.
The motility of OECs (A) and Schwann cells (B) isolated from wild-type mice was compared in medium containing no growth factors (DMEM-BS) and in optimal growth media (OMM+5%FBS for OECs and 10%HF for Schwann cells) on PLL, laminin and collagen. A scratch was made using a pipette tip on a layer of confluent cells thus creating a gap between two confluent cell layers. The cells were washed with PBS to remove any cell debris and the two cell fronts growing towards each other were filmed using time-lapse microscopy over a period of 24 hours. The distance travelled between the two cell fronts was measured over time. The motility of OECs and Schwann cells was similar in medium with and without growth factors. Each point represents the mean ± SEM (n=3).

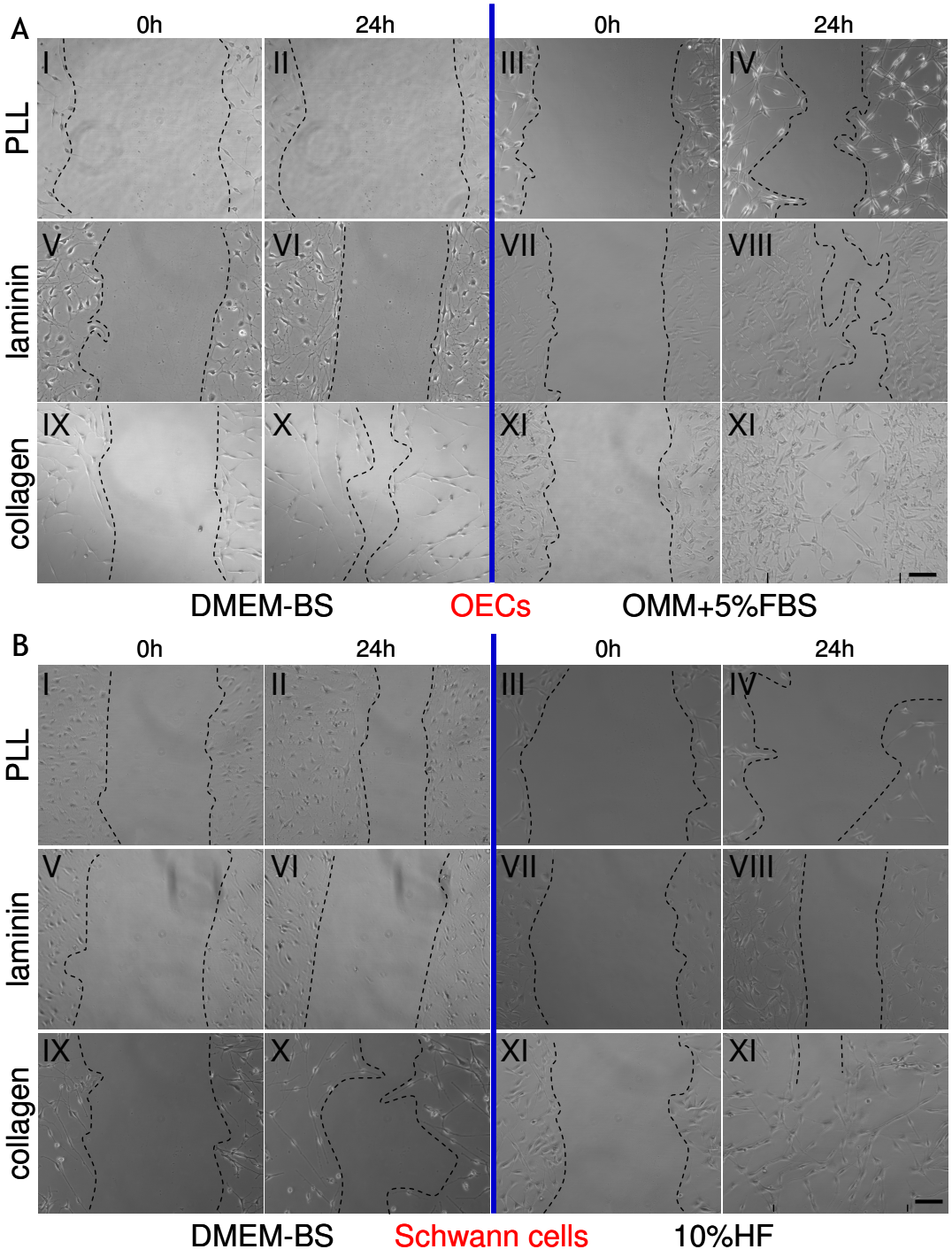

Figure 3.25. Representative images of wild-type OEC and Schwann cell motility in a wound assay.

The motility of OECs (A) and Schwann cells (B) from wild-type mice was compared in medium containing no growth factors, DMEM-BS, and in optimal growth media (OMM+5%FBS for OEC; 10%HF for Schwann cells) on PLL (I-IV), laminin (V-VIII) and collagen (IX-XI). A scratch was made using a pipette tip on a layer of confluent cells thus creating a gap between two confluent cell layers. The cells were washed with PBS to remove any cell debris and the two cell fronts growing towards each other were filmed using time-lapse microscopy over a period of 24 hours. The distance travelled between the two cell fronts was measured over time. Scale bar = 100 µm.

p

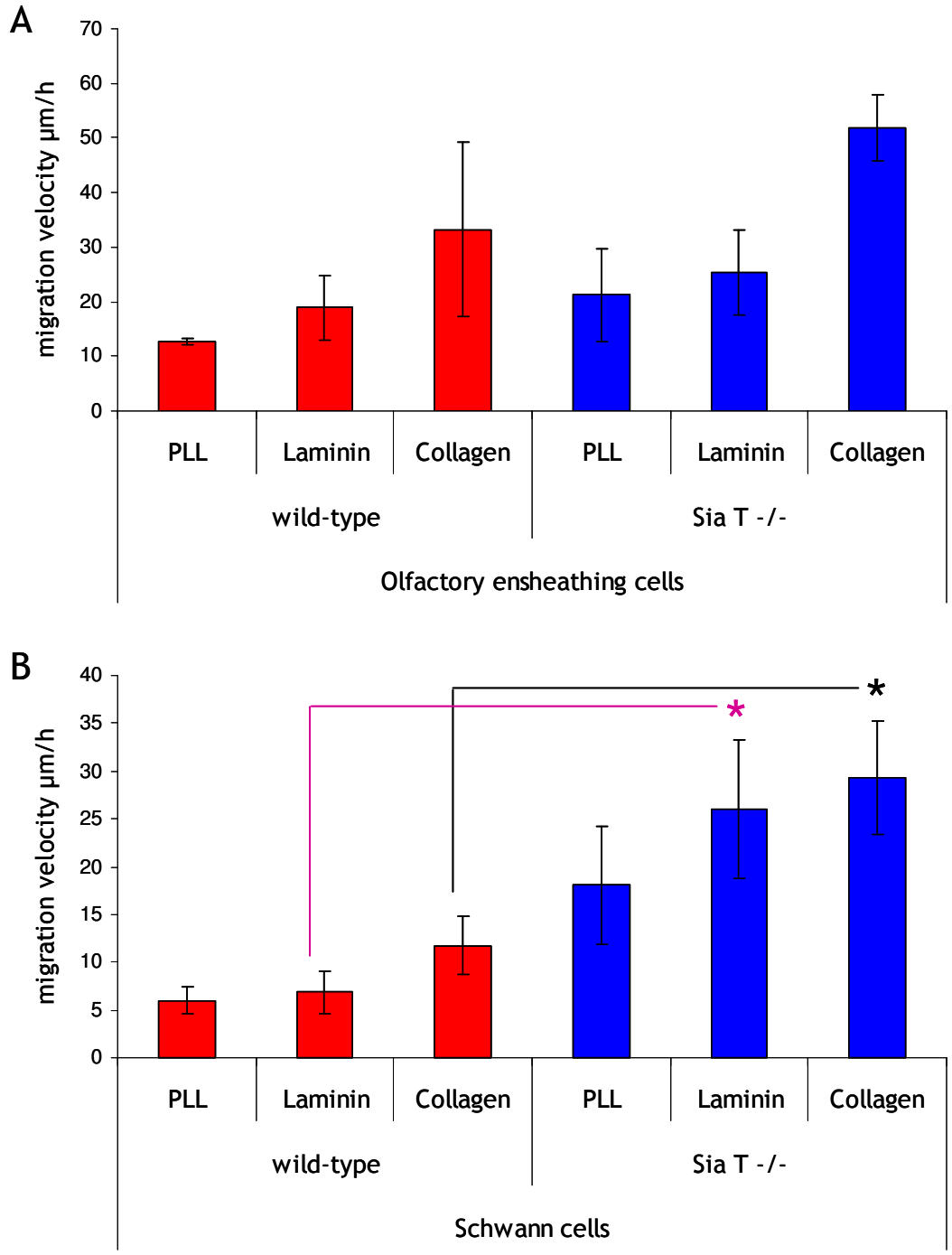

Figure 3.26. Motility of wild-type and Sia T -/- OECs and Schwann cells in a wound assay. Confluent OECs (A) and Schwann cells (B) from wild-type and Sia T -/- mice, grown on PLL, laminin or collagen were used in the wound assays to compare their migration rates. A scratch was made using a pipette tip on a layer of confluent cells thus creating a gap between two confluent cell layers. The cells were washed with PBS to remove any cell debris and the two cell fronts growing towards each other were filmed using time-lapse microscopy over a period of 24 hours. The rate of change of distance between the two cell fronts was measured over time. Sia T -/- Schwann cells had significantly higher motility compared with wild-type cells on laminin ($p < 0.05$) and collagen ($p < 0.05$). Each point represents the mean ± SEM (n=3).

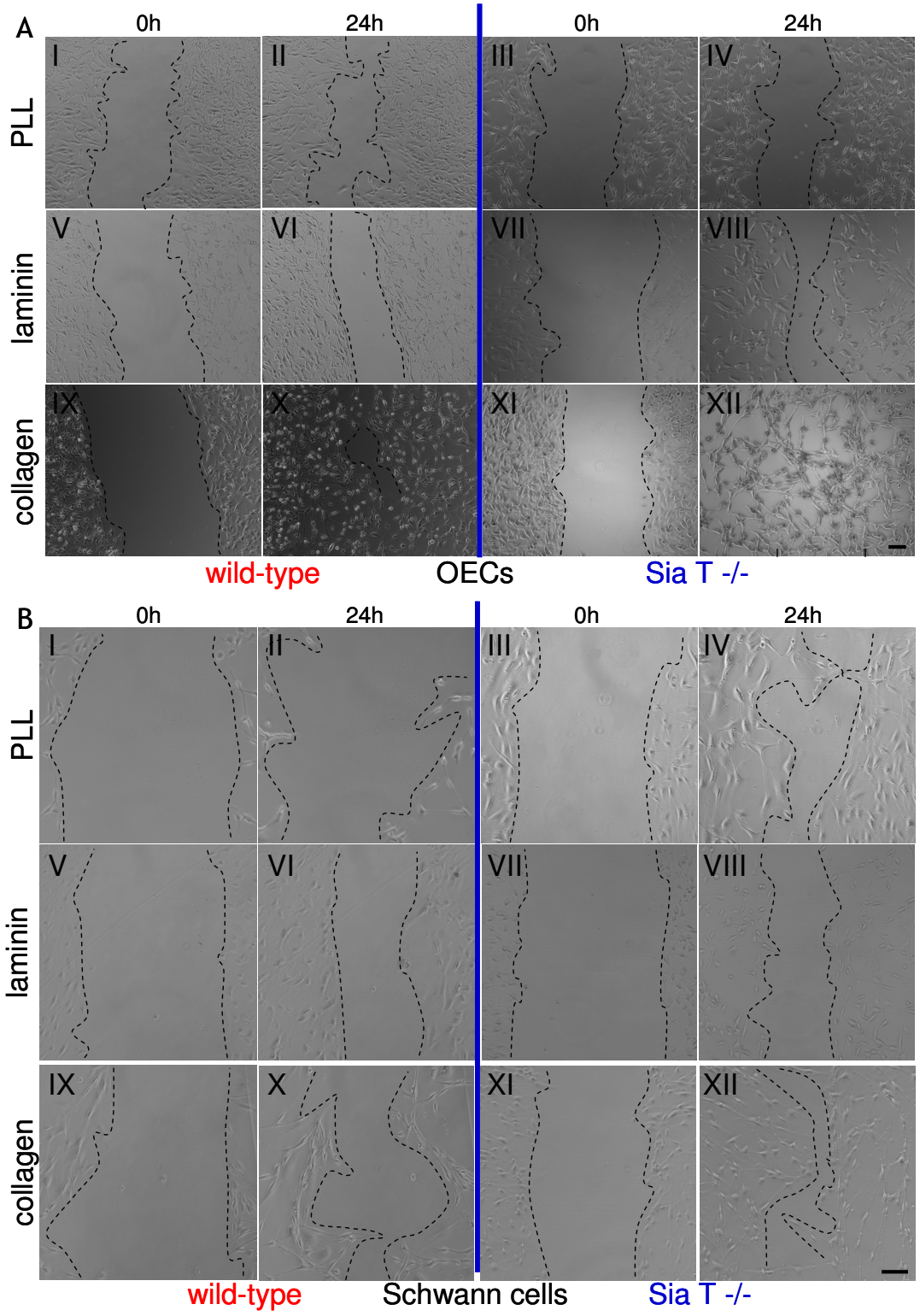

Figure 3.27. Representative images of wild-type and Sia T -/- OEC and Schwann cell motility in a wound assay.
The motillity of OECs (A) and Schwann cells (B) from wild-type and Sia T -/- mice was compared in optimal growth media (OMM+5%FBS for OEC; 10%HF for Schwann cells) on PLL (I-IV), laminin (V-VIII) and collagen (IX-XI) using a wound assay described in the Methods section. Scale bar = 100 µm.

3.3 Discussion

3.3.1 Proliferaton of mouse OECs and Schwann cells

This study showed that mouse OECs and Schwann cells had a similar basal rate of division, but that there was a notable difference in their mitogenic response to the addition of growth factors. Namely, OECs proliferated significantly better than Schwann cells in response to serum, 10%HF and individual growth factors. Among the growth factors tested, OECs had higher proliferation rates than Schwann cells in response to BDNF, EGF, FGF, forskolin, heregulin, IGF-1, NT-3, PDGF, and TGFβ. The difference in the response to growth factors between OECs and Schwann cells gives further weight to the argument that they are two distinct cell types.

It has been shown that in rat Schwann cell cultures, FGF and PDGF are mitogenic only in the presence of agents which elevate intracellular levels of cAMP, as well as, either serum (Davis and Stroobant, 1990), IGF1, IGF2 (Stewart *et al.*, 1996) or high concentrations of insulin (Stewart *et al.*, 1991). However, in this study it was found that some single growth factors, including FGF and PDGF, were mitogenic for mouse Schwann cells. Despite this, mouse Schwann cells and OECs failed to proliferate as well as rat cells when a combination of growth factors was used. Rat OECs and Schwann cells maintained under the conditions used in the present study continued to proliferate and increase in cell number while mouse OECs and Schwann cells maintained under identical conditions only proliferated initially. This suggests that mouse cells differ in their mitogenic requirements from rat cells.

Previous studies have reported an inherent species difference in growth requirements between mouse and rat cells. For instance, Svendsen *et al* (1997) showed that mouse neural precursors can self renew and remain pluripotent for over 50 days, whereas rat neural precursor cells began to undergo apoptosis after 28 days in culture. Ray and Gage (2006) also found major differences between rat and mouse progenitor proliferation in response to various substrates, growth factors and heparin. In addition, the present study showed that spinal cord cultures obtained from embryonic mice could be maintained on PLL (see Chapter 5) whereas other studies have shown rat spinal cord cultures

maintained under the same conditions did not survive well on PLL (Sorensen *et al.*, 2008).

The reason why mouse OECs and Schwann cells did not continue to proliferate is not known, but presumably it is due to some imbalance of factors or deficiency in the culture environment. Future experiments could test different combinations of growth factors, hormones and substrates to find their optimal growth conditions.

3.3.2 Ganglioside expression of OECs and Schwann cells

Several studies have examined the ganglioside content of Schwann cells both *in vitro* and *in vivo*. In contrast, I have not found any reports in the literature describing the ganglioside expression of OECs. Although many studies have examined Schwann cell ganglioside expression, the results were variable. For instance, two studies found that Schwann cells derived from neonatal rat sciatic nerve label with CTx suggesting they express GM1 (Brockes *et al.*, 1979, Raff *et al.*, 1979), whereas another similar study showed that neonatal rat Schwann cell cultures do not express GM1 (Okada *et al.*, 1982). In agreement with the first two studies, the present study showed that CTx labelled the majority of neonatal mouse Schwann cells isolated from sciatic nerves. This is supported by the findings that CTx is mitogenic for neonatal rat Schwann cells (Raff *et al.*, 1978a) and that MBP induces Schwann cell proliferation via an interaction with GM1 (Tzeng *et al.*, 1995, Tzeng *et al.*, 1999). In addition, a study of mature, myelinating Schwann cells found that low amounts of GM1 are found on Schwann cell internodal surfaces but that GM1 is primarily localized on specialised Schwann cell structures in the nodal region in rat peripheral nerves (Ganser *et al.*, 1983). Another study using GM1 immunofluorescence of adult rat spinal roots by Molander *et al* (1997) confirmed that GM1 is confined to Schmidt-Lanterman's incisures, myelin sheath paranodal end segments and to some extent the abaxonal Schwann cell cytoplasm.

Neuraminidase converts GD1a and GT1b (and other complex gangliosides) to GM1. The study by Ganser *et al* (1983) also found that the amount of CTx binding to Schwann cells increases when the nerve fibres are treated with neuraminidase suggesting that the enzyme is converting polysialogangliosides to

GM1. Since Schwann cells do not bind tetanus toxin (Fields *et al.*, 1978, Brockes *et al.*, 1979, Raff *et al.*, 1979) which recognises gangliosides GD1b, GT1b, GQ1b (Holmgren *et al.*, 1980) it is possible that this polysialoganglioside is GD1a. This would be in agreement with the present study where it was found that the majority of Schwann cells expressed GD1a. Also, in mouse muscle, an antibody which binds to GM2, GD1a and GM1b was found presynaptically in Schwann cells (Santafe *et al.*, 2005) and since GM2 is rarely found in normal mouse Schwann cells (Watabe *et al.*, 2001), the staining is likely due to either GD1a or GM1b. However, in humans anti-GD1a antibody is associated with axonal but not demyelinating forms of Guillain-Barré syndrome, which would suggest that human Schwann cells do not express GD1a (Ho *et al.*, 1999). These contrasting results might be due to species differences in ganglioside expression.

Using Thin Layer Chromatography (TLC) it was found that the major ganglioside in normal peripheral nerves is GD1a, whose expression is reduced in *trembler* mutant mice (Harpin *et al.*, 1982) which have a defect of PNS myelination related to impairment in Schwann cell differentiation (Aguayo *et al.*, 1977) and increased Schwann cell proliferation (Perkins *et al.*, 1981). The same study also showed that the Trembler mutant peripheral nerves had increased levels of the simple ganglioside GM3 (Harpin *et al.*, 1982). Another study using TLC in Schwann cells isolated from neonatal rat dorsal root ganglia showed that the simple ganglioside GM3 is the major glycolipid in these cells (Farrer and Quarles, 1996). It remains possible that mouse Schwann cells also contain GM3 as their major ganglioside, however, this possibility was not investigated in the present study.

Halstead *et al* (Halstead *et al.*, 2005) showed that GD3 antibodies induced perisynaptic Schwann cell death, suggesting that mouse perisynaptic Schwann cells express GD3. The present study found that less than 5% of neonatal mouse sciatic nerve Schwann cells labelled with R24, which mainly binds to GD3 as well as complex gangliosides GT1a and GQ1b. GalNAc T -/- Schwann cells, which lack all complex gangliosides also labelled with R24 suggesting that the R24 staining in Schwann cells is due to the simple ganglioside GD3. Therefore, it is possible that GD3 expression is particular to perisynaptic Schwann cells but not other Schwann cell types.

The present study has shown that Schwann cells and OECs have a similar ganglioside expression profile which is unsurprising since these two cell types have many markers in common. However, a very small percentage of Schwann cells (less than 1%), but not OECs labelled with EG2, EG3 and MOG30. EG2 binds to GT1a, GD1b, GT1b and GQ1b, EG3 binds to GT1a and GQ1b and MOG30 is specific for ganglioside GQ1b. It is likely that the ganglioside expressed by a very small proportion of Schwann cells but not OECs is GQ1b, since all three markers, which bind to Schwann cells but not OECs, bind to this ganglioside. However, previous studies in cultured rat Schwann cells showed that tetanus toxin, which binds to GD1b, GT1b and GQ1b (Holmgren *et al.*, 1980), does not bind to Schwann cells (Brockes *et al.*, 1979, Fields *et al.*, 1978, Raff *et al.*, 1979). It is possible that these contrasting results are due to a species difference in ganglioside expression.

As mentioned above, some of the anti-ganglioside antibodies used bound to less than 1% of the cells. Since these cells also labelled with $p75^{NTR}$ it is likely that they are OECs or Schwann cells and not the contaminating cells present in the cultures. The reason why such a small proportion of cells labelled with certain antibodies is unclear. It is possible that OECs or Schwann cells express particular gangliosides during different phases of the cell cycle. An example of this is seen in mouse foetal astrocytes where GM1 expression was found to be regulated by the cell cycle, with maximal expression during G0/G1 phase (Majoul *et al.*, 2002). Alternatively, it is possible that the small proportion of cells that are labelling with particular anti-ganglioside antibodies are senescent or are undergoing apoptosis. Future studies could test this possibility, by double-labelling OECs and Schwann cells with anti-ganglioside antibodies and apoptotic markers, such as annexin V, Apolipoprotein C-1, BM-1/JIMRO, BV2 or senescence markers such as senescence-associated ß-galactosidase.

To confirm the ganglioside expression of OECs and Schwann cells, gangliosides could be extracted from primary cultures and the ganglioside content examined by TLC and tandem mass spectrometry.

Therefore, to summarise, the main gangliosides expressed in cultured wild-type mouse OECs and Schwann cells are GM1 and GD1a. Sia T -/- mice lack all b-series gangliosides and as a result have slightly increased levels of a-series

gangliosides (Okada *et al.*, 2002). It is therefore likely that Sia T -/- OECs and Schwann cells will have slightly higher levels of GM1 and GD1a. In contrast, GalNAc T -/- mice lack all complex gangliosides (Takamiya *et al.*, 1996) and accordingly, as shown in the present study, GalNAc T -/- OECs and Schwann cells do not express GM1 and GD1a. Consequently, the lack or excess of GM1 and GD1a in ganglioside knockout OECs and Schwann cells would be expected to have an impact on the biology of these cells.

3.3.3 Antigen profile and morphology of wild-type and ganglioside knockout OECs and Schwann cells

Previous studies have demonstrated that the addition of gangliosides to glia and neuronal cell lines alters the morphology of these cells (Facci *et al.*, 1987, Hefti *et al.*, 1985, Morgan and Seifert, 1979, Rybak *et al.*, 1983, Skaper *et al.*, 1986, Sobue *et al.*, 1988, Spero and Roisen, 1984). Astrocytes cultured in serum normally assume a flat, epithelioid morphology. The addition of a mixture of gangliosides containing GM1, GD1a, GD1b and GT1b or pure gangliosides GM1 and GD1a to cultures of dissociated rat septal cells caused the astrocytes within these cultures to change from a flat to a process bearing morphology as visualised by GFAP immunocytochemistry (Hefti *et al.*, 1985). Skaper *et al* (1986) showed that the addition of CTx, which binds GM1, to neonatal rat astrocytes, changed their morphology from a flat to a stellate shape but in contrast to the previous study, the addition of GM1 did not alter the morphology of astrocytes. Moreover, the addition of GM1, GD1a, GD1b or GT1b to these cultures blocked or reversed the effect of CTx addition to astrocytes (Skaper *et al.*, 1986).

Sobue *et al* (1988) showed that the addition of GM1, GM3 or a ganglioside mixture containing GM1, GD1a, GD1b and GT1b caused Schwann cells to extend extremely long processes. Contrary to this, in the present study, Sia T -/- Schwann cells and OECs, which have increased levels of GM1 and GD1a and GalNAc T -/- Schwann cells and OECs, which lack GM1 and GD1a, did not differ morphologically from wild-type cells.

It is possible that exogenously added gangliosides act differently from membrane associated gangliosides and therefore no change in morphology is seen when the amount of membrane bound gangliosides is altered in ganglioside knockout cells.

This suggests that experiments consisting of the addition of gangliosides, while valuable, may not always adequately address the physiological role of gangliosides and that studies in knockout mice may be better at assessing the physiological role of gangliosides. To test the possibility that exogenously added gangliosides act differently from membrane-associated gangliosides, future studies could examine the morphology of OECs and Schwann cells following the addition of GM1 and CTx to cultures to see if a change in morphology is observed.

The present study found that the wild-type and ganglioside knockout cells had the same antigen profile. However, the number of markers examined in the present study was limited. Future studies could examine the antigen expression of wild-type and ganglioside knockout OECs and Schwann cells in more detail. For example, the expression of O4 which labels both OECs (Barnett *et al*., 1993) and non-myelinating Schwann cells (Mirsky et al., 1990) could be examined. In addition, OECs express several adhesion molecules such as such as L1 (Miragall et al., 1988), E-NCAM (Franceschini and Barnett, 1996), fibronectin, laminin and type IV collagen (Doucette, 1996, Kafitz and Greer, 1997), whose expression could be examined. Finally, the expression of GAP 43 and adhesion molecules L1, N-CAM, and N-cadherin (Mirsky et al., 1986, Jessen et al., 1990, Curtis et al., 1992), which are normally found on non-myelinating Schwann cells could be compared between wild type and ganglioside knockout cells.

3.3.4 Proliferation of wild-type and ganglioside knockout OECs and Schwann cells

The present study found that the lack of complex gangliosides in GalNAc T -/- mice did not affect the proliferation of OECs or Schwann cells but that a lack of b-series gangliosides and a concurrent increase in a-series gangliosides in Sia T -/- mice led to increased proliferation of OECs maintained on collagen in the presence of growth factors.

The fact that the proliferation of GalNAc T -/- OECs and Schwann cells did not differ from wild-type cells may be due to increased levels of the simple gangliosides, such as GM3 and GD3, compensating for the lack of complex gangliosides or it may be that complex gangliosides are not involved in modulating OEC proliferation. Therefore it is likely that in Sia T -/- mice an excess of a-series gangliosides leads to increased OEC proliferation on collagen in the presence of growth factors. These findings suggest that physiological levels of gangliosides do not modulate the proliferation of OECs and Schwann cells grown on PLL, laminin or collagen IV. To examine whether the increased proliferation in Sia T -/- OECs was due to increased levels of a-series gangliosides GM1 and GD1a, future studies should examine the proliferation of wild-type and GalNAc T -/- OECs on collagen following the exogenous addition of GM1 and/or GD1a.

Numerous studies have demonstrated the effect of gangliosides on the proliferation of various cell types (Section 1.1.3.3 in the Introduction). For instance, the addition of GM1, GM3 or a mixture of gangliosides containing GM1, GD1a, GD1b and GT1b reduced the baseline proliferation of cultured rat Schwann cells (Sobue *et al.*, 1988). In contrast, CTx acts as a mitogen for cultured Schwann cells by binding to GM1 (Raff *et al.*, 1978a). MBP and MBP peptides interact with GM1 and FGFR to induce Schwann cell and astrocyte proliferation (South *et al.*, 2000, Tzeng *et al.*, 1995, Tzeng *et al.*, 1999).

Since OECs and Schwann cells express gangliosides GD1a and GM1, which have been shown to modulate proliferation in Schwann cells and other cell types, it was interesting to examine the effect of increased and decreased levels of these gangliosides in Sia T -/- and GalNAc T -/- mice, respectively, on OEC and Schwann cell proliferation. Yet, the present study found that the proliferation rate of Schwann cells was unaffected in ganglioside knockout mice. Therefore, in contrast to a study which showed that the addition of GM1 or GD1a reduced proliferation of Schwann cells and reduced their response to growth factors (Sobue *et al.*, 1988), excess endogenous GM1 and GD1a in Sia T -/- mice did not reduce the proliferation of Schwann cells. Although some added gangliosides do incorporate into the membrane, this difference could be due to free gangliosides having a different mechanism of action than endogenous, membrane bound gangliosides. Similarly, the lack of GM1 and GD1a in GalNAc T -/- mice did not

increase proliferation of Schwann cells, suggesting that the increase in simple gangliosides may be sufficient to compensate for the lack of these complex gangliosides. It would, therefore, be interesting to examine if mouse Schwann cells do indeed express the simple ganglioside GM3 and to see if the GD3-expressing Schwann cells are more mitotically active, since both of these simple gangliosides have been shown to modulate the proliferation of various cell types. However, it is also possible that studies where exogenous gangliosides are added can be misleading and are not useful for elucidating the physiological effects of gangliosides.

It was surprising that ganglioside knockout OECs behaved differently from ganglioside knockout Schwann cells, since their ganglioside profile was so similar. The present study showed that Sia T -/- OECs had increased proliferation rate compared with wild-type and GalNAc T -/- when cultured on collagen IV, but only when grown in the presence of growth factors. It is possible that this difference is due to OECs and Schwann cells expressing other gangliosides which were not labelled for in the present study. To examine this possibility, future studies should examine the ganglioside content of OECs and Schwann cells in more detail. Alternatively, it may be that gangliosides play different roles in these two cell types as it has been observed before that the effect of gangliosides on proliferation can depend on the cell type (Kamimura *et al.*, 2005).

Another possibility is that the difference in the proliferation of Sia T -/- OECs and Schwann cells which has been observed is due to different growth factors present in the culture media. Indeed, gangliosides have been shown to modulate most, if not all, growth factor receptors and to interact with integrins (Sections 1.1.3.1 and 1.1.3.2 in the Introduction). Schwann cells were maintained in their optimal proliferation medium containing 10% serum, heregulin and forskolin, whereas OECs were maintained in their optimal growth medium, which contains 5% serum, heregulin, forskolin, FGF and ACM. To test if the differences in the proliferation of Sia T -/- OECs and Schwann cells is different because they are grown in different media, the proliferation of OECs and Schwann cells grown on collagen in both OEC media and Schwann cell media should be compared.

It is possible that the increased proliferation in Sia T -/- OECs could be due to an interaction between the a-series gangliosides and FGF or some other growth factor present within ACM. To test this, OECs and Schwann cells could be grown in medium containing only DMEM-BS and FGF2 or DMEM-BS and ACM.

Because OECs and Schwann cells were grown in different media it is difficult to directly compare the effect of gangliosides on their proliferation. This is not only due to the presence of different growth factors which gangliosides can interact with but also the fact that there may be gangliosides present in the serum or ACM. Gangliosides can be shed from the membrane (Chang *et al.*, 1997) and are also found in non-cell-associated forms in plasma (Bergelson, 1995). It is thus possible that the OEC media contains gangliosides from the serum and those shed from astrocytes in the ACM, whereas Schwann cell media, which contains more serum, may also contain serum gangliosides. To enable a direct comparison of the effects of gangliosides on the proliferation of OECs and Schwann cells, future studies should examine the proliferation of OECs and Schwann cells in media that does not contain serum or ACM, such as OMM, which contains DMEM-BS and a combination of the growth factors forskolin, heregulin ß1 and FGF2.

The fact that Sia T -/- OECs proliferate significantly better on extracellular matrix substrates, collagen IV and laminin, and not on non-specific substrate PLL, suggests that this effect may be due to an interaction between gangliosides, integrins and growth factors or growth factor receptors. To be able to investigate this further, the integrin expression of OECs would first need to be characterised, and the proliferation of OECs grown on corresponding substrates assessed in the presence of individual growth factors.

Studies have shown that Schwann cells express several laminin or collagen receptors, such as the integrins α1ß1, α2ß1, α6ß1, α7ß1 and α6ß4 (Milner *et al.*, 1997a). In the present study, it was shown that a lack of complex gangliosides has no effect on the proliferation of Schwann cells on PLL, laminin or collagen IV which may suggest that gangliosides do not interact with collagen or laminin receptors to modulate Schwann cell proliferation. However, Schwann cells express other integrin receptors such as the fibronectin receptor (α5ß1), the vitronectin receptor (αvß3) and the fibrin receptor (αvß8). Therefore, future

studies could examine the proliferation of Schwann cells on substrates such as extracellular matrix, fibronectin or vitronectin.

3.3.5 Motility of wild-type and ganglioside knockout OECs and Schwann cells

Gangliosides are thought to modulate cell adhesion and motility by interacting with integrin receptors (Cheresh *et al.*, 1987, Zheng *et al.*, 1993) and many studies have demonstrated their involvement in the migration of several cell types (Section 1.1.3.6 in the Introduction). It was therefore decided to study the motility of wild-type and ganglioside knockout OECs and Schwann cells using two assays. Their migration was examined on the non-specific substrate PLL and on extracellular matrix substrates laminin and collagen IV which bind to integrins present on Schwann cells (Milner *et al.*, 1997a). No difference was observed in the motility of wild-type and ganglioside knockout OECs and Schwann cells plated at low density, which suggests that complex gangliosides are not required for cell movement per se. However, in a wound assay, Sia T -/- Schwann cells had a significantly greater migration velocity compared to wild-type cells when grown on extracellular matrix substrates laminin and collagen IV but not on PLL.

The contrasting results obtained by the two assays may be due to cell interactions since OECs and Schwann cells plated at low density will only interact with the substrate whereas those in the wound assay are in a confluent cell layer and will therefore be interacting not just with the substrate but also with each other. In addition, a dense population of cells may secrete more growth factors, which could have an autocrine effect on their motility.

The fact that an increase in Sia T -/- Schwann cell motility is observed on laminin and collagen IV but not PLL indicates the involvement of integrins. Future studies should, therefore, examine the signalling involved in the increased motility. Future studies should also examine the motility of OECs and Schwann cell on other substrates such as fibronectin and vitronectin which bind to integrins expressed on Schwann cells.

Sia T -/- Schwann cells lack all b-series gangliosides but have increased levels of a-series gangliosides. Future studies should examine the motility of GalNAc T -/-

Schwann cells using the wound assay: since these cells lack all a-series gangliosides it might be predicted that their motility would be reduced. However, if no difference is observed in the motility of Schwann cells obtained from GalNAc T -/- mice, it will indicate that physiological levels of gangliosides do not modulate Schwann cell motility and that the effect seen in Sia T -/- are due to an excess of a-series gangliosides.

The present study did not find a difference in the migration between wild-type and ganglioside knockout OECs, which is surprising since OECs and Schwann cells express similar gangliosides. This may be due to a different ganglioside expressed on one cell but not the other that was not detected in the present study or it may be the case that the same gangliosides play different roles in the two cell types. The different behaviour of ganglioside knockout OECs and Schwann cells in terms of migration and proliferation supports the argument that they are two different cell types. However, as was the case for the proliferation experiments, to make a proper comparison, future studies could compare the motility of OECs and Schwann cells grown in the same medium.

The findings of the present study suggest that gangliosides are not essential for OEC and Schwann cell motility. However, future studies should examine the directed migration of these cells by examining their migration on different ECM substrates towards different chemoattractants.

3.3.6 Conclusions

In conclusion, in this chapter it has been demonstrated that a change in the amount/type of gangliosides does affect the proliferation and migration of OECs and Schwann cells to some degree. No significant difference is seen with GalNAc T -/- cells which lack all complex gangliosides but rather with Sia T -/- cells which lack b-series gangliosides and instead have higher levels of a-series gangliosides. Since the major gangliosides expressed by OECs and Schwann cells are a-series gangliosides GM1 and GD1a, it is possible that an increase in these gangliosides results in the increased proliferation and migration of Sia T -/- cells observed on certain substrates. Further experiments involving the addition of GM1 and GD1a to wild-type and GalNAc T -/- cells or the addition of antibodies against GM1 and GD1a to Sia T -/- cells would be needed to clarify these

observations. However, the findings of this study suggest that gangliosides are not likely to be involved in the proliferation and motility of OECs or Schwann cells.

This conclusion may seem surprising because numerous studies have shown that gangliosides modulate proliferation and migration in so many cell types. However, this conclusion is supported by the fact that both Sia T -/- and GalNAc T -/- mice have no obvious developmental defects. Since migration and proliferation are paramount during development, it is more likely that gangliosides do not play a big role in modulating these functions. This suggests that studies where gangliosides or antibodies that bind to gangliosides are added to cells may not show the physiological role of gangliosides and that studies where gangliosides are removed are more likely to reveal the role of gangliosides.

Initially, I had planned to also examine the role of gangliosides in the apoptosis of OECs and Schwann cells because gangliosides are thought to be involved in the apoptosis of several cell types (Section 1.1.3.3 in the Introduction). However, due to time constraints, this was not possible. Finally, future studies should examine the proliferation and migration of OECs and Schwann cells in DKO mice which only express the simple ganglioside GM3, as this should clarify the role of complex gangliosides in the biology of these cells.

4 CHAPTER 4

Degeneration and regeneration of the olfactory system in wild-type and ganglioside knockout mice

4.1 Introduction

The peripheral nervous system (PNS) is able to support axonal outgrowth throughout life, whereas most central nervous system (CNS) tissues can only support axonal outgrowth during development. Unlike most of the CNS, the primary olfactory system continually generates new neurons throughout life. This unique regenerative property of the primary olfactory system can be exploited experimentally to study CNS regeneration.

Gangliosides seem to play a role in neurite outgrowth during regeneration as well as during development (Constantine-Paton *et al.*, 1986, Mendez-Otero and Constantine-Paton, 1990, Mendez-Otero and Santiago, 2003, Mendez-Otero *et al.*, 1988). The Jones antibody binds to O-acetylated gangliosides GD3 and GQ1c (Bonafede *et al.*, 1989). Using Jones antibody immunolabelling, Mendez-Otero et al (Mendez-Otero and Ramon-Cueto, 1994) showed that its expression coincides with pathways of axon extension in the brain during development. This expression was downregulated in all areas of the brain after axons reached their destination except in the olfactory system where its expression continued into adulthood, suggesting that O-acetylated gangliosides may play a role in the regenerative capacity of the olfactory system. However, a recent study in Sia T -/- mice showed that the inhibition of neuronal migration by Jones antibody is not due to its binding to O-acetylated gangliosides (Yang *et al.*, 2007). Therefore, it is possible that the Jones antibody immunolabelling seen by Mendez-Otero *et al* (Mendez-Otero and Ramon-Cueto, 1994) in rats may, in fact, not be due to O-acetylated ganglioside expression.

Many studies have shown that exogenously added gangliosides enhance peripheral nerve regeneration. Furthermore, Sia T -/- mice exhibited reduced regeneration of axotomised hypoglossal nerves compared with wild type (Itoh *et al.*, 2001).

It was shown in the previous chapter that OECs *in vitro* express complex gangliosides GM1 and GD1a. Williams et al (Williams *et al.*, 2004) showed that OECs act as conduits for the regenerating axons. Extracellular matrix molecules are also involved in axonal guidance. Since gangliosides interact with integrins,

the receptors for extracellular matrix molecules, it is possible that the gangliosides expressed on OECs play a role in this guidance.

In the present study the regeneration of the olfactory system, which contains both central and peripheral nervous system components, was examined following zinc sulphate ($ZnSO_4$) treatment in wild-type and ganglioside knockout mice. $ZnSO_4$ destroys olfactory receptor neurons, which, with time, grow back from the putative stem cells in the olfactory epithelium (OE) and with the help of the OECs, their axons find their way back to the olfactory bulb and re-form synapses with second order neurons. This allowed the examination of the effect of gangliosides on the proliferation of the putative stem cells, neurite outgrowth and synapse formation. Because many of the defects observed in ganglioside knockout mice are amplified with age, two age groups were examined in the present study: young adult (6 weeks old) and adult (6 months old).

4.2 Results

4.2.1 Ganglioside expression of the olfactory system.

The expression of major brain gangliosides GM1, GD1a, GD1b, GT1b and GQ1b in the olfactory system of 6-week old mice was examined by immunocytochemistry using the following antibodies: CTx, CGM-3, EG2, EG3, MOG1, MOG30 and MOG35. Paraffin-embedded olfactory tissue was initially stained with histological stains haematoxylin and eosin (H & E) to observe its general morphology and to demonstrate the regions imaged in the subsequent figures, namely glomeruli, olfactory nerve and the olfactory mucosa (Figure 4.1).

The majority of gangliosides tested for were expressed in the wild-type olfactory system with the exception of MOG35 as summarised in Table 4.1. As a control, Sia T -/- and GalNAc T -/- tissue was also labelled to look at their expression of major brain gangliosides. CTx, which binds to GM1, labelled all of the regions examined in wild-type and Sia T -/- mice: glomeruli, olfactory nerve, lamina propria (LP) and OE (Figure 4.2). GalNAc T -/- olfactory system did not label with CTx since it lacks all a-series gangliosides (Figure 4.2). CGM3 labelling was observed in all three genotypes, although the labelling was less prevalent in Sia T -/- and GalNAc T -/- mice (Figure 4.3). CGM3 recognises sulphatide as well as

gangliosides GD3, GT1a and GQ1b which could account for the immunolabelling observed in Sia T -/- and GalNAc T -/- mice. Whereas CTx appeared to label all of the cells in the regions examined (Figure 4.2), CGM3 labelling was localised to particular cell types (Figure 4.3). In addition, CGM3 labelled cells in the glomeruli, olfactory nerve and LP but not the OE (Figure 4.3). EG2, EG3, MOG1 and MOG30 labelled wild-type but not Sia T -/- or GalNAc T -/- tissue (Figure 4.4 to 4.7). EG2, which binds to GT1a, GD1b, GT1b and GQ1b, appeared to label majority of cells in wild-type glomeruli and the LP but did not label any cells in the OE (Figure 4.4). EG3, which binds to gangliosides GT1a and GQ1b, appeared to label the majority of gangliosides in the glomeruli, and rarely labelled cells in the LP (Figure 4.5). EG3 did not label the OE (Figure 4.5). EG3 labelling in the olfactory system is likely to be due to GQ1b and not GT1a since Sia T -/- tissue, which has increased levels of a-series gangliosides such as GT1a, did not label with this antibody (Figure 4.5). However, EG3 did label cells in the LP underlying respiratory epithelium. This is confirmed by immunolabelling with MOG30, which specifically binds to GQ1b. Like EG3, MOG30 labelled the majority of cells in the glomeruli, but did not label cells in the olfactory nerve or the olfactory mucosa (Figure 4.7). MOG1, which specifically binds to GD1b, appeared to label the majority of cells in the glomeruli and the olfactory nerve and labelled some cells in the LP and OE (Figure 4.6). In addition, MOG1 labelled cells in the LP associated with the respiratory epithelium (Figure 4.6).

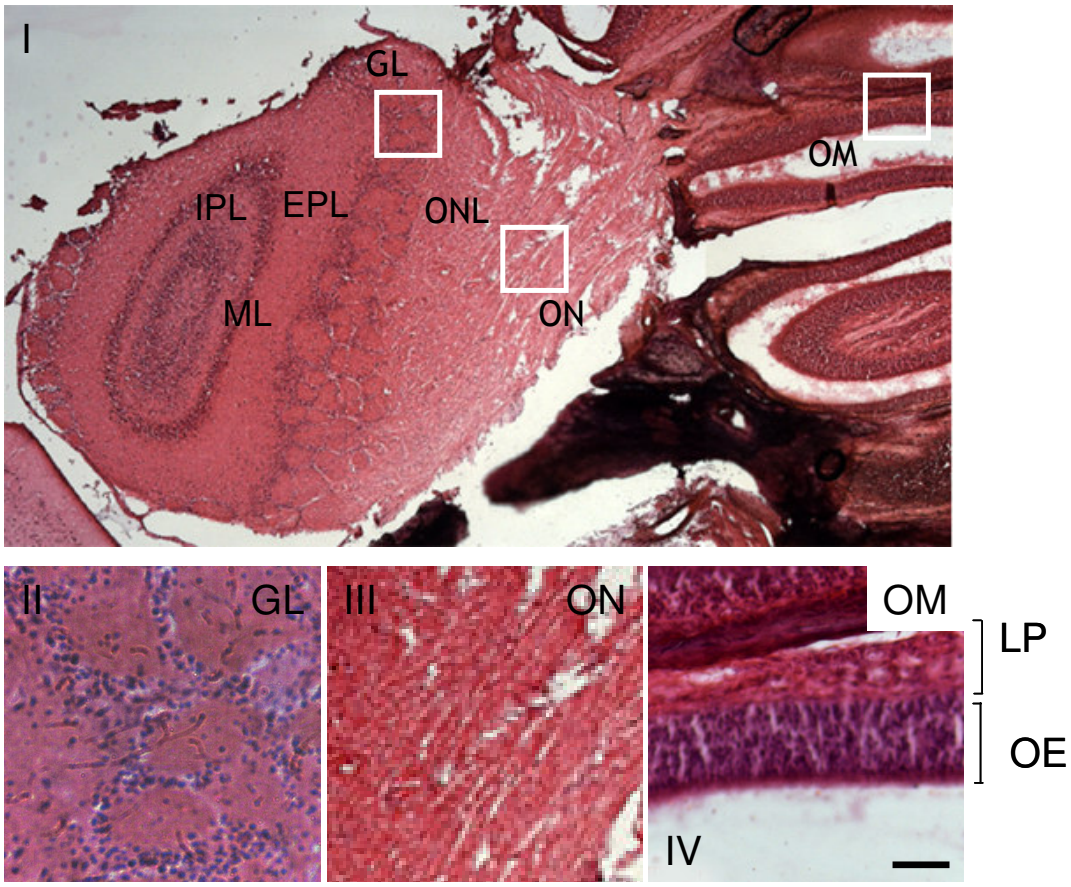

OM	Olfactory mucosa
OE	Olfactory epithelium
LP	Lamina propria
ON	Olfactory nerve
ONL	Olfactory nerve layer
GL	Glomerular layer
EPL	External plexiform layer
ML	Mitral cell layer
IPL	Internal plexiform layer

Figure 4.1. The olfactory system of the mouse.
Parasagittal sections of decalcified, paraffin-embedded olfactory system tissue were stained with haematoxylin and eosin (H & E). This enabled visualisation of the olfactory bulb in the CNS and olfactory mucosa in the PNS as well as the olfactory nerve connecting the two (I). The parts of the olfactory system imaged in Figures 4.2 to 4.8 are shown in II to IV: glomeruli (II), olfactory nerve (III) and the olfactory mucosa (IV), which contains the olfactory epithelium and the lamina propria.

Marker	Binds to ganglioside:		wild-type				Sia T -/-				GalNAc T -/-			
	a-series	b-series	olfactory epithelium	lamina propria	olfactory nerve layer	glomeruli	olfactory epithelium	lamina propria	olfactory nerve layer	glomeruli	olfactory epithelium	lamina propria	olfactory nerve layer	glomeruli
CTx	GM1		+	+	+	+	+	+	+	+	-	-	-	-
CGM-3	GT1a ++	GD3 ++ GQ1b +++	-	+	+	+	-	+	+	+	+	+	+	+
EG2	GT1a +++	GD1b ++ GT1b +++ GQ1b ++	-	+	+	+	-	-	-	-	-	-	-	-
EG3	GT1a ++++	GQ1b +++	-	+	+	+	-	-	-	-	-	-	-	-
MOG1		GD1b ++++	+	+	+	+	-	-	-	-	-	-	-	-
MOG30		GQ1b +++	-	-	-	+	-	-	-	-	-	-	-	-
MOG35	GD1a ++++		-	-	-	-	-	-	-	-	-	-	-	-

Table 4.1. Ganglioside expression in the olfactory system.
Unfixed, frozen olfactory system sections from 6 week old wild-type, Sia T -/- and GalNAc T -/- mice were labelled with antibodies which bind to gangliosides and FITC-labelled cholera toxin which binds to ganglioside GM1. Anti-ganglioside reactivities: optical density >0.1 ≤0.5 (+); >0.5 ≤1.0 (++); >1.0 ≤1.5 (+++); >1.5 (++++). Note, the intensity of CTx labelling was higher in Sia T -/- mice.

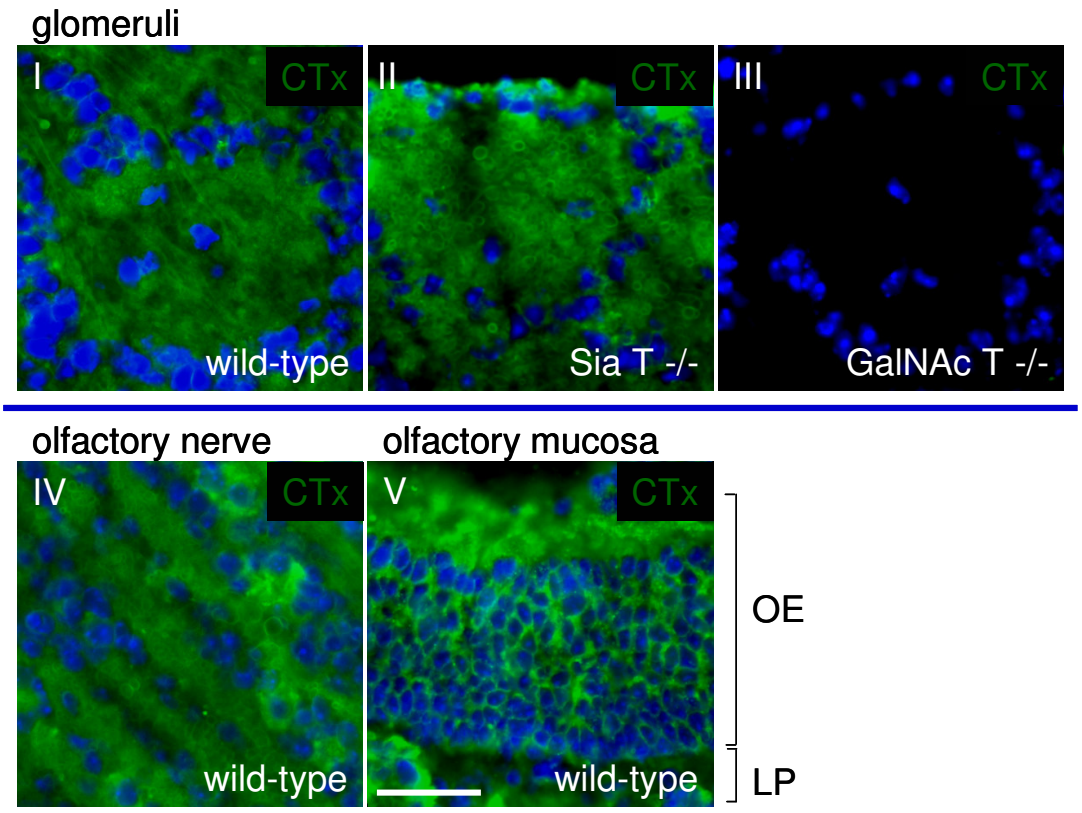

Figure 4.2. CTx labelling of the olfactory system.
Olfactory system tissue from 6 week old wild-type (I, IV and V), Sia T -/- (II) and GalNAc T -/- (III) mice was labelled with CTx, which binds to a-series ganglioside GM1. CTx labelled the majority of cells in the glomeruli, olfactory nerve and olfactory mucosa of wild-type and Sia T -/- mice but not GalNAc T -/- tissue. Refer to Figure 4.1 for orientation. Scale bar = 100 µm.

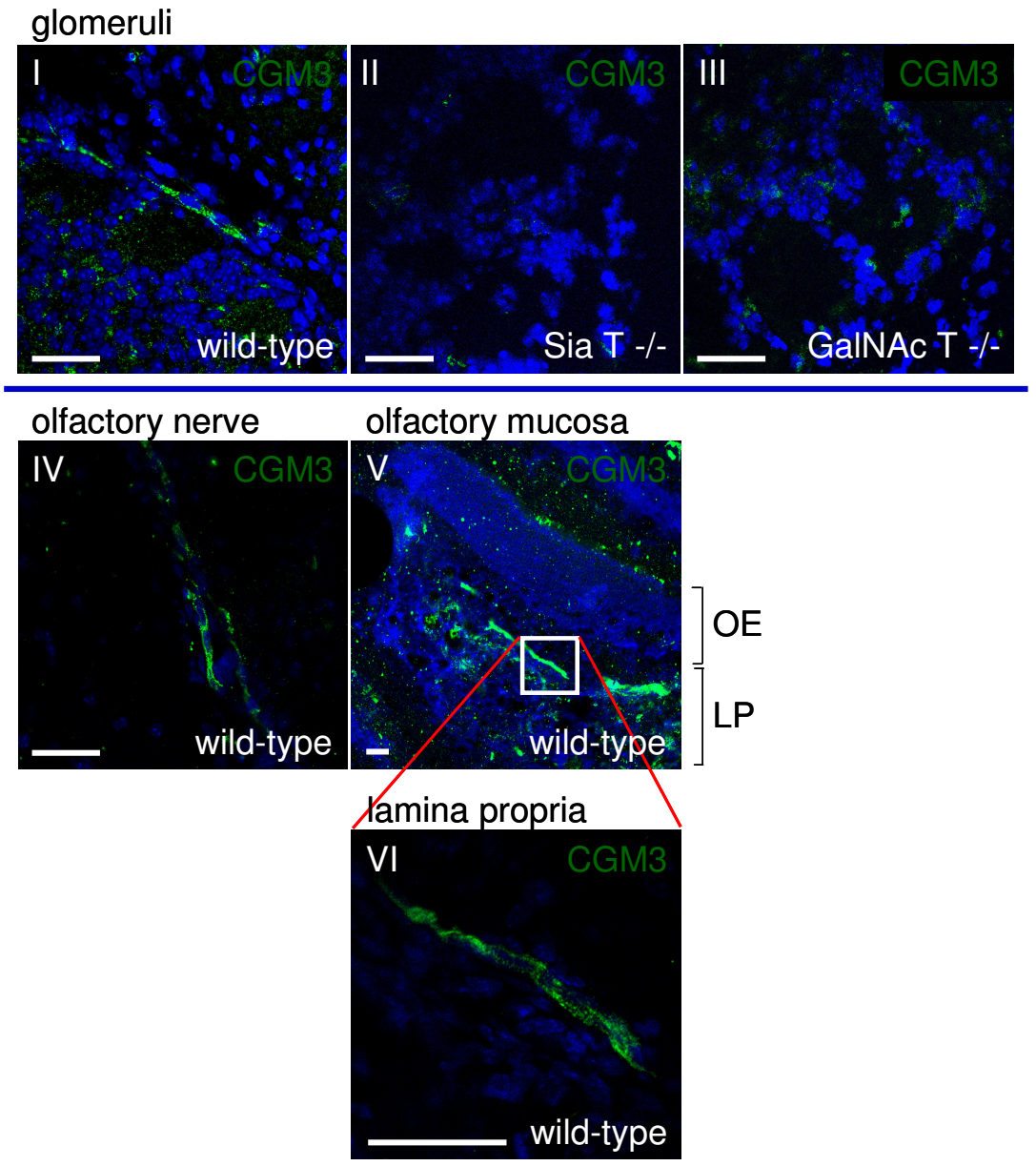

Figure 4.3. CGM3 labelling of the olfactory system.
Olfactory system tissue from 6 week old wild-type (I, IV to VI), Sia T -/- (II) and GalNAc T -/- (III) mice was labelled with CGM-3, which binds to a-series ganglioside GT1a, b-series gangliosides GD3 and GQ1b and sulphatide. CGM3 labelled the majority of cells in the glomeruli of wild-type mice (I), few cells in the glomeruli of Sia T -/- (II) and GalNAc T -/- (III) mice and olfactory nerve (IV) and lamina propria (V and VI) of wild-type mice. Refer to Figure 4.1 for orientation. Scale bar = 50 μm.

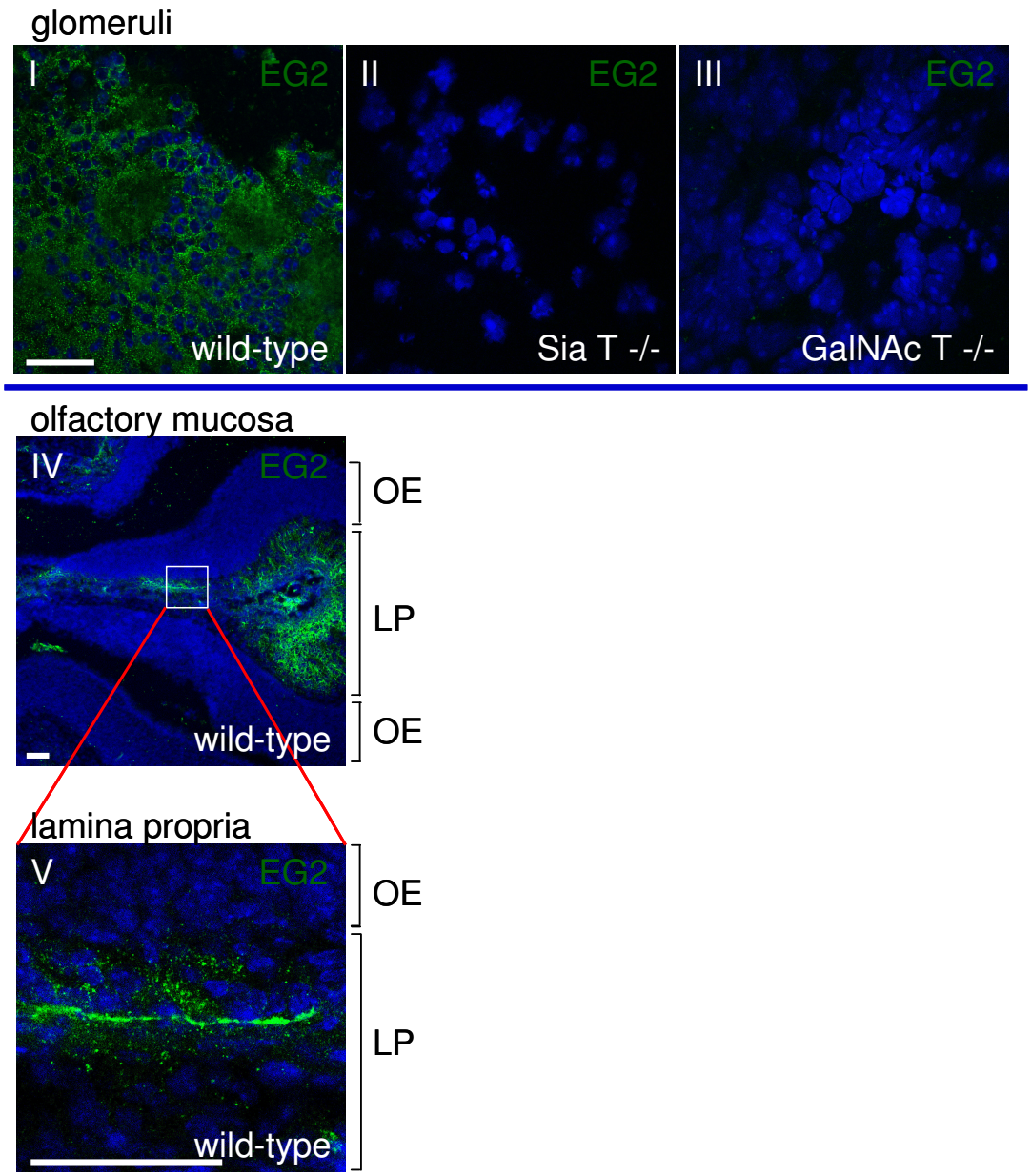

Figure 4.4. EG2 labelling of the olfactory system
Olfactory system tissue from 6 week old wild-type (I, IV and V), Sia T -/- (II) and GalNAc T -/- (III) mice was labelled with EG2, which binds to a-series ganglioside GT1a, and b-series gangliosides GD1b, GT1b and GQ1b. EG2 labelled the majority of cells in the glomeruli (I) and lamina propria (IV and V) of wild-type mice, but did not label Sia T -/- (II) or GalNAc T -/- (III) tissue. Refer to Figure 4.1 for orientation. Scale bar = 50 μm.

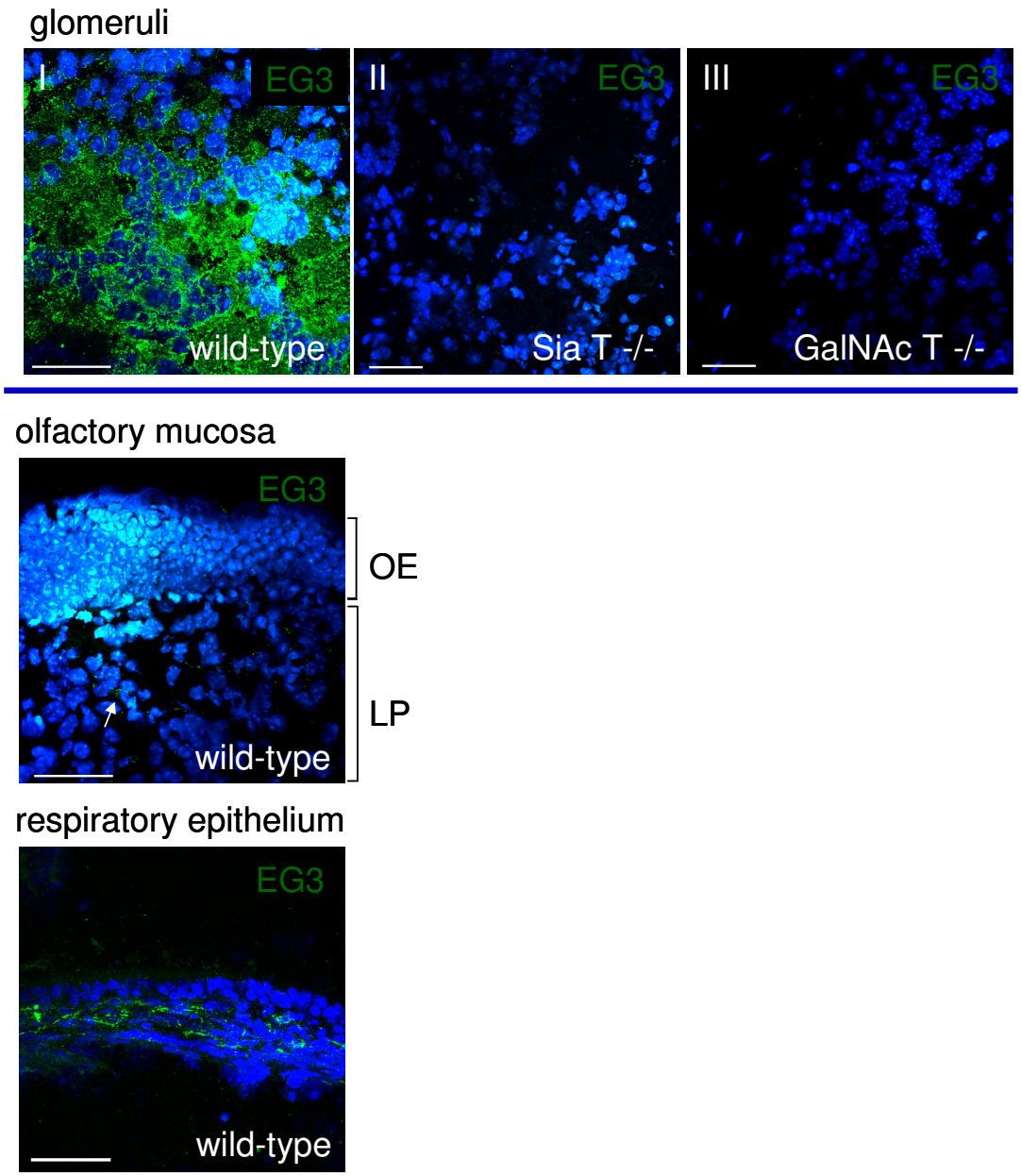

Figure 4.5. EG3 labelling of the olfactory system.
Olfactory system tissue from 6 week old wild-type (I, IV and V), Sia T -/- (II) and GalNAc T -/- (III) mice was labelled with EG3, which binds to a-series ganglioside GT1a, and b-series ganglioside GQ1b. EG3 labelled the majority of cells in the glomeruli of wild-type mice (I), but did not label Sia T -/- (II) or GalNAc T -/- (III) tissue. While EG3 rarely labelled cells in the lamina propria underlying the OE (IV), it labelled the majority of cells in the lamina propria associated with respiratory epithelium (V). Refer to Figure 4.1 for orientation. Scale bar = 50 µm.

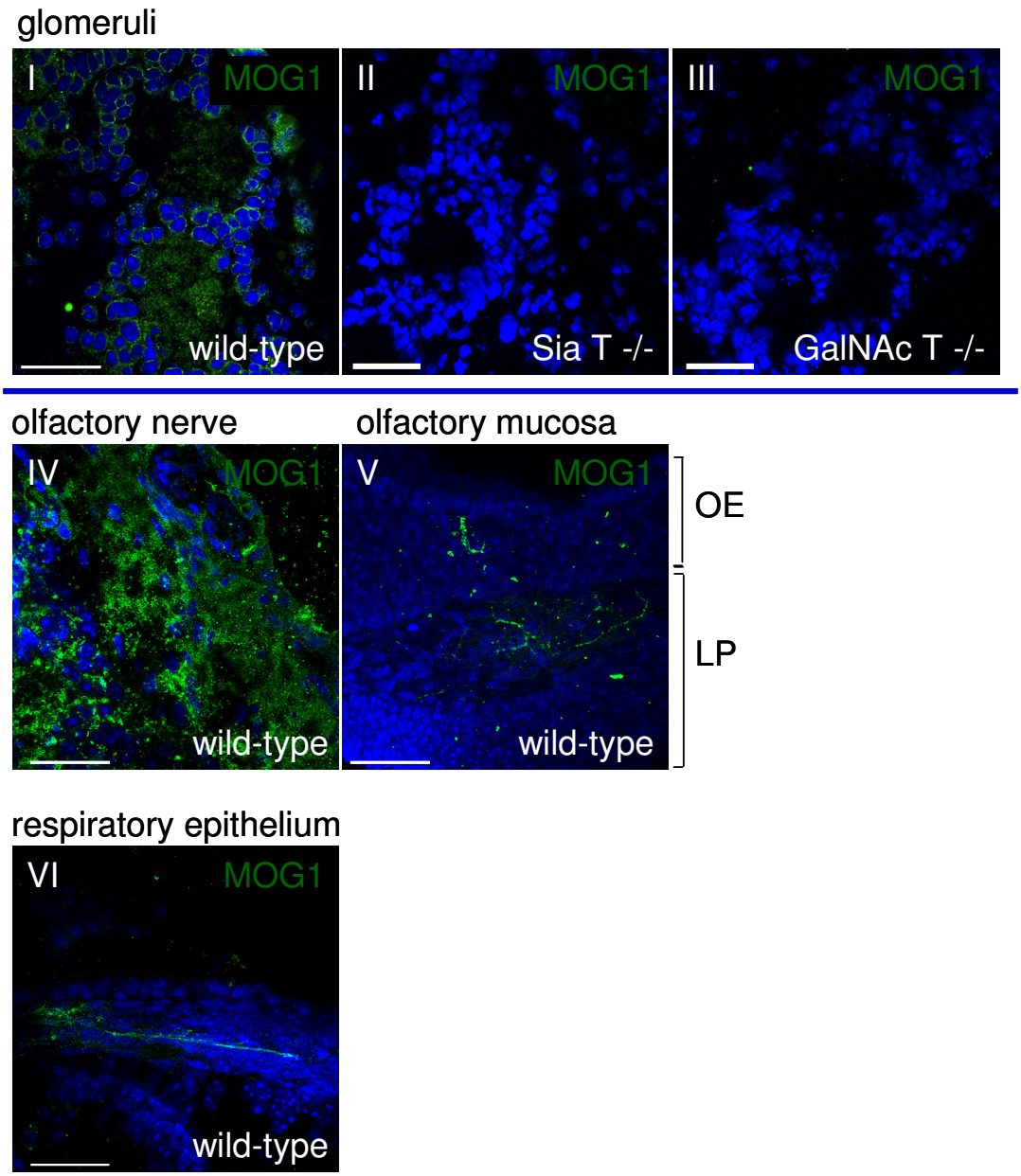

Figure 4.6. MOG1 labelling of the olfactory system.
Olfactory system tissue from 6 week old wild-type (I, IV to VI), Sia T -/- (II) and GalNAc T -/- (III) mice was labelled with MOG1, which binds to b-series ganglioside GD1b. GD1b was found in the glomeruli (I), olfactory nerve (IV), OE (V) and lamina propria associated with both OE (V) and respiratory epithelium (VI) of wild-type mice. MOG1 did not label Sia T -/- (II) and GalNAc T -/- (III) tissue. Refer to Figure 4.1 for orientation. Scale bar = 50 μm.

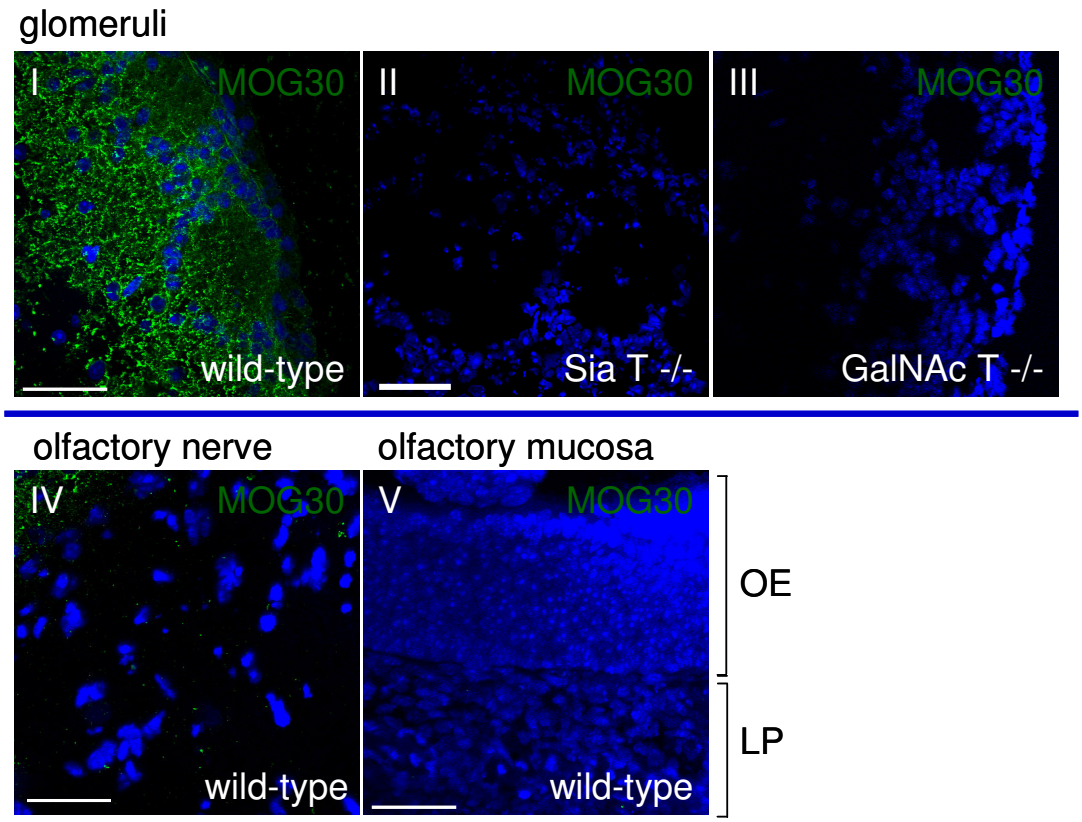

Figure 4.7. MOG30 labelling of the olfactory system.
Olfactory system tissue from 6 week old wild-type (I, IV to VI), Sia T -/- (II) and GalNAc T -/- (III) mice was labelled with MOG30, which binds to b-series ganglioside GQ1b. GQ1b was found in the glomeruli (I) of wild-type mice. Olfactory nerve (IV), and olfactory mucosa of wild-type mice were negative for MOG30. MOG30 did not label Sia T -/- (II) and GalNAc T -/- (III) tissue. Refer to Figure 4.1 for orientation. Scale bar = 50 µm.

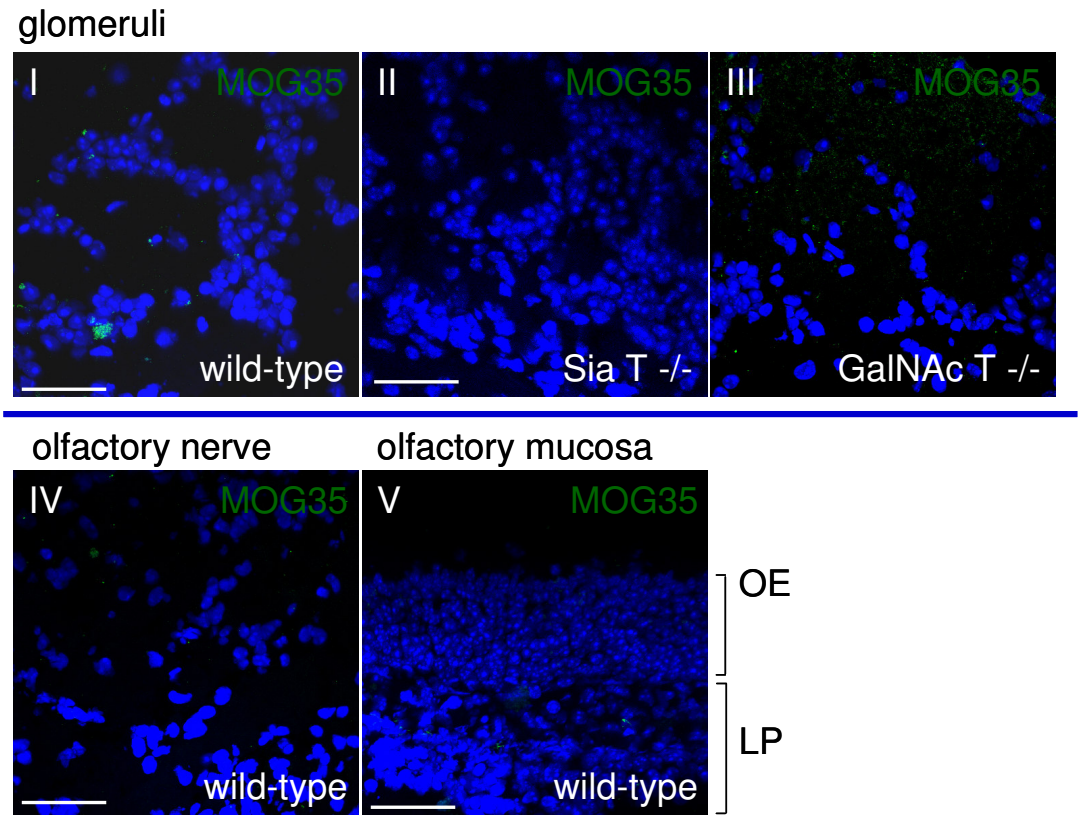

Figure 4.8. MOG35 labelling of the olfactory system.
Olfactory system tissue from 6 week old wild-type (I, IV & V), Sia T -/- (II) and GalNAc T -/- (III) mice was labelled with MOG35, which binds to a-series ganglioside GD1a. However, all sections were negative for GD1a. Refer to Figure 4.1 for orientation. Scale bar = 50 µm.

4.2.2 Comparison of olfactory epithelial width

To investigate whether the lack or the overexpression of gangliosides had an effect on the anatomy of the olfactory system, the olfactory widths of wild-type and ganglioside knockout mice were compared. The OE is a pseudo-stratified columnar (cuboidal) epithelium that has been well characterised. It contains three main cell types: olfactory receptor neurons, sustentacular cells and basal cells, which can be distinguished by their morphology, position within the epithelium and the expression of a number of cellular markers. The width of the OE is therefore a good indication of whether the cell composition is normal. The epithelial widths of wild-type and ganglioside knockout mice were measured using ImageJ from frozen olfactory tissue sections labelled with H & E. All 4 genotypes (wild-type, Sia T -/-, GalNAc T -/- and DKO) were found to have a mean epithelial width of between 60 and 80 μm, suggesting no difference during development (Figure 4.9).

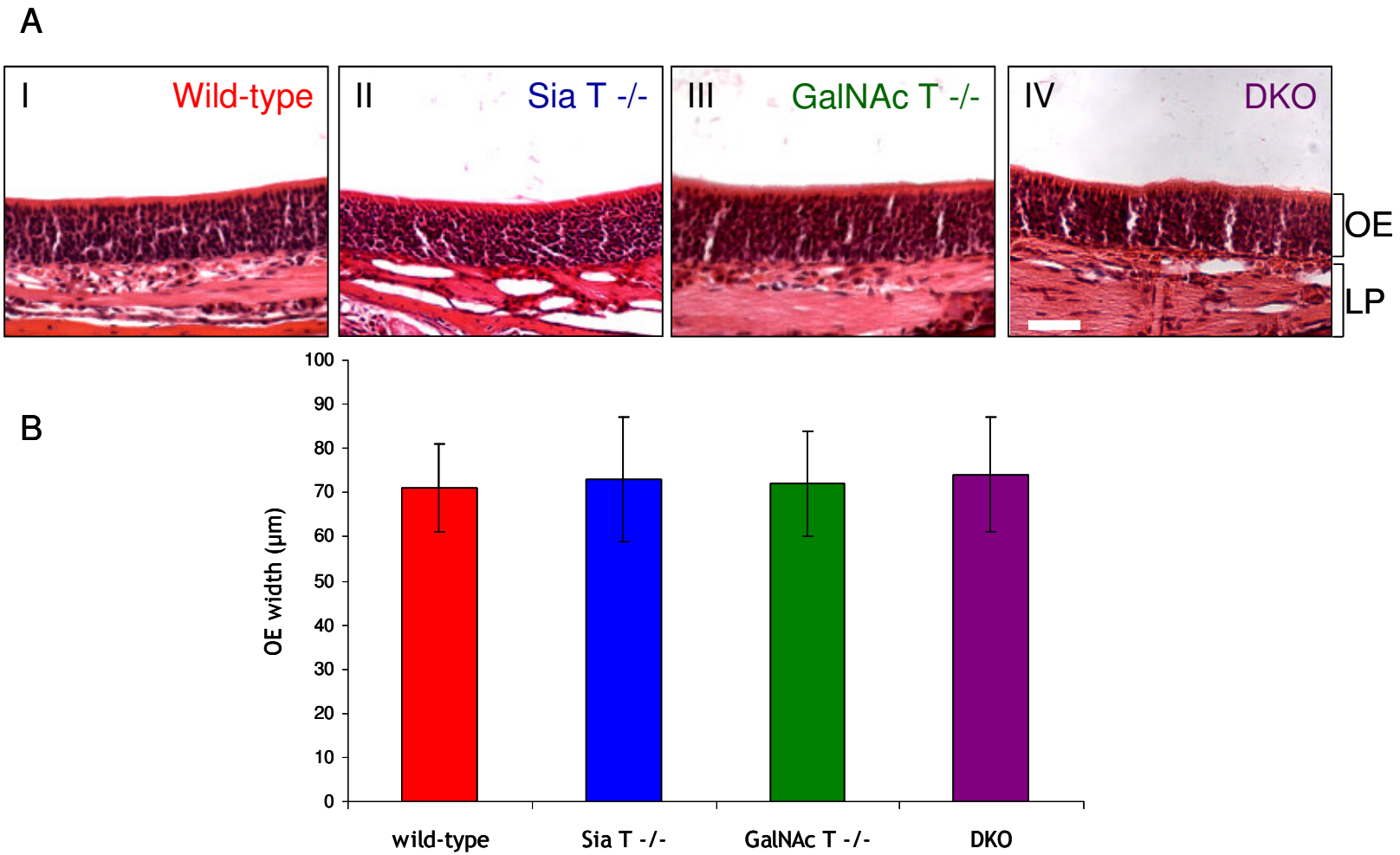

Figure 4.9. Comparison of epithelial width.
Frozen sections of the olfactory system were cut and stained with H & E and the width of the epithelium was measured using ImageJ. A: Representative images show the control olfactory epithelium from wild-type (I), Sia T -/- (II), GalNAc T -/- (III) and double knockout (IV) mice. B: Bar chart of the control epithelial widths from wild-type, Sia T -/-, GalNAc T -/- and DKO mice. OE = olfactory epithelim. LP = lamina propria. Scale bar = 50 µm.

4.2.3 Preliminary studies of nasal $ZnSO_4$ irrigation

Preliminary studies were performed to test the concentration of $ZnSO_4$ to use in the subsequent intranasal deafferentation experiments. A literature search revealed that various volumes and concentrations of $ZnSO_4$ have been used to induce damage to the olfactory epithelium in mice including: 1 to 2 µl of 4% $ZnSO_4$ into each nostril (Edwards *et al.*, 1972), 100 µl of 5% $ZnSO_4$ into one nostril (Margolis *et al.*, 1974), three drops of 1% ZnSO4 into each nostril, three times at 24-hour (Matulionis, 1975) or 30-minute (Matulionis, 1976) intervals, and 20 µl of 10% $ZnSO_4$ (Ducray *et al.*, 2002). The following concentrations and volumes of $ZnSO_4$ were tested in the present study: 20, 50 and 100 µl of 0.5% $ZnSO_4$, 20, 50 and 100 µl of 5% $ZnSO_4$ and 20 µl 10% $ZnSO_4$ (Figure 4.10). As can be seen in the representative images in Figure 4.10, 20 and 50 µl of 0.5% $ZnSO_4$ caused no damage, whereas 100 µl only slightly damaged the OE. 20 µl of 5% $ZnSO_4$ caused no damage, 50 µl damaged the top layers of cells in the OE and 100 µl of 5% $ZnSO_4$ completely destroyed all of the cells within the OE. 20 µl of 10% $ZnSO_4$ destroyed most of the cells in the OE apart from the bottom layer of cells. In subsequent experiments, the left nasal cavity of wild-type and ganglioside knockout mice was irrigated with 20 µl of 10% $ZnSO_4$ as described in the methods section since mice recovered better after lower volumes of $ZnSO_4$ were used and 20 µl of 10% $ZnSO_4$ sufficiently damaged the OE.

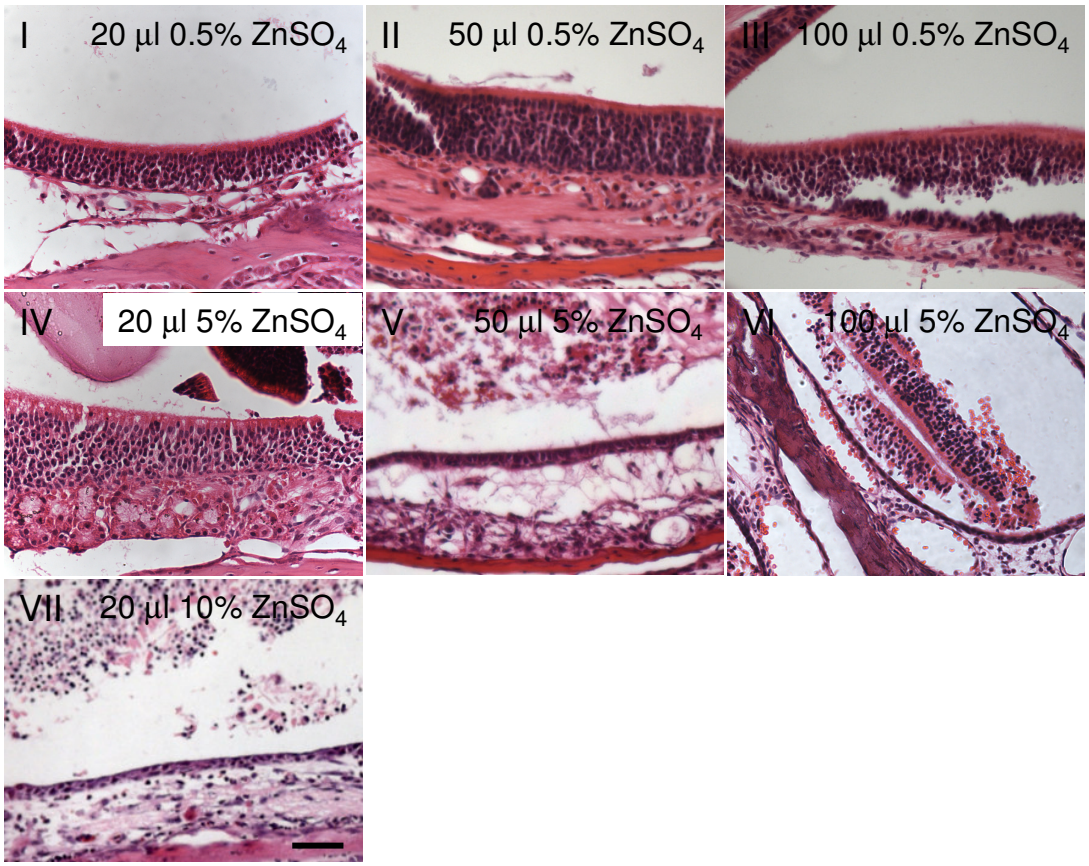

Figure 4.10. The effect of different $ZnSO_4$ volumes and concentrations on OE width. Representative H & E images showing the effects of using 20, 50 or 100 µl of 0.5 % $ZnSO_4$ (I to III, respectively), 20, 50 or 100 µl of 5% $ZnSO_4$ (IV to VI, respectively) and 20 µl of 10% $ZnSO_4$ (VII). Preliminary experiments were performed to determine the optimal $ZnSO_4$ volume and concentration to use in subsequent experiments. Various concentrations and volumes of $ZnSO_4$ were administered to the left nasal cavity of 6 week old wild type mice. The following day, the mice were sacrificed, perfused with 4% paraformaldehyde and the OE dissected. Sections of the OE were labelled with H & E to assess the extent of OE damage caused by different concentrations and volumes of $ZnSO_4$. The aim was to destroy all cells of the OE except the bottom layer of cells (the globose and horizontal basal cells). 20, 50 or 100 µl of 0.5% $ZnSO_4$ or 20 and 50 µl of 5% $ZnSO_4$ were not sufficient to destroy all cells in the OE leaving only the bottom layer of cells, whereas 100 µl of 5% ZnSO4 destroyed all the cells, including the basal cell layer. 20 µl of 10% $ZnSO_4$ was sufficient to destroy all cells except for the basal cells (VII). Scale bar = 50 µm.

4.2.4 Gross morphological changes of the olfactory epithelium

One day after irrigation with 10% $ZnSO_4$, very few cells remained, much of the epithelium having dissociated from the underlying basement membrane (Figure 4.11, I to IV). The nasal lumen was filled with many lytic and necrotic cells. Seven days after irrigation (Figure 4.11, V to VIII) the epithelium began to increase in width, a process which continued for the proceeding 9 weeks. Although the epithelium began to regenerate as soon as 4 days after irrigation, the organised structure displayed in the control tissue did not start to reappear until 3 weeks after irrigation and sometimes did not reappear even 9 weeks following $ZnSO_4$ treatment. Moreover, 9 weeks following $ZnSO_4$ treatment (Figure 4.11, IX to XI), the majority of OE had not regenerated to the original width in wild-type and ganglioside knockout mice. This was the case in wild-type and ganglioside knockout mice both at 6 weeks and 6 months of age.

The width of the OE was measured at each time point from the basement membrane to the top of the epithelium in 6 week old (Figure 4.12) and 6 month old (Figure 4.13) wild-type and ganglioside knockout mice. The average width of the control epithelium was around 45 µm in both wild-type and ganglioside knockout mice in both age groups (Figure 4.12 and 4.13). The OE width decreased dramatically following $ZnSO_4$ treatment, and was reduced to around 10 µm after one day in wild-type and ganglioside knockout mice. By day 4, the epithelium had begun to increase in width and continued to do so until the last time point examined (week 9). However, 9 weeks following $ZnSO_4$ treatment the width of the OE was only 50% of that of the untreated tissue in wild-type and ganglioside knockout tissue in both age groups. As can be seen in Figure 4.12 and 4.13 (B), the unilateral irrigation with $ZnSO_4$ occasionally caused a bilateral lesion as has been described previously (Chuah *et al.*, 1995). This was probably due to leakage through the nasal septum.

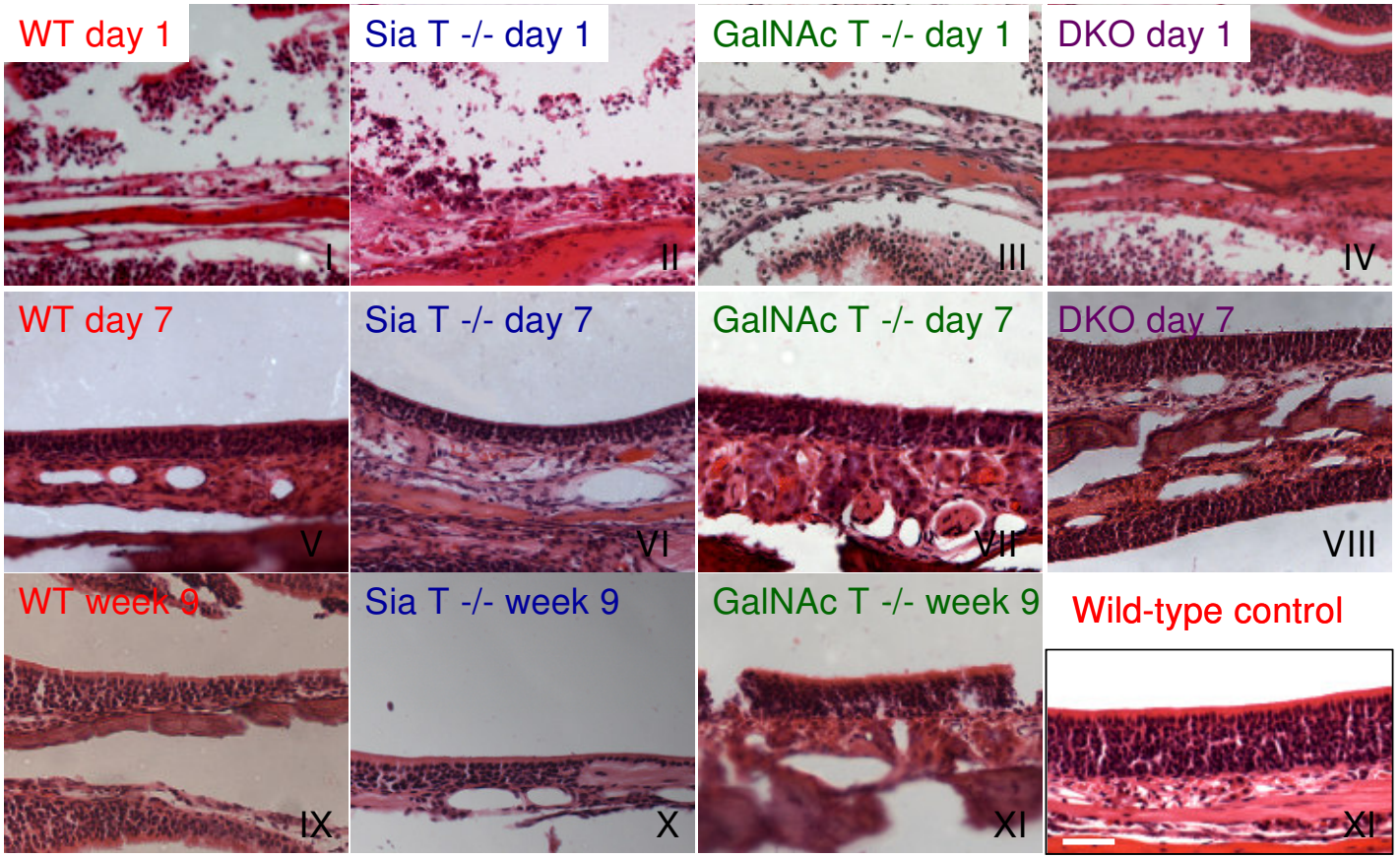

Figure 4.11. The gross morphological changes in the olfactory epithelium.
The effects of nasal irrigation to the olfactory system were initially investigated by studying the changes to the olfactory epithelium in paraffin embedded tissue from wild-type (I, V and IX), Sia T -/- (II, VI and X), GalNAc T -/- (III, VII and XI) and double knockout (IV and VIII) tissue stained by H & E. An example of untreated olfactory epithelium from a wild-type mouse is shown in XII for comparison. After 1 day (I to IV), most of the cells of the epithelium had gone from the underlying basal lamina, leaving very few cells attached. At this time the nasal cavity was seen to contain a lot of cellular debris. By the 7th day (V to VIII), the epithelium already appeared to increase in width. However, 9 weeks after treatment (IX to XI) the olfactory epithelium had not regained its organised appearance (compare with control sections in Figure 4.9). Scale bar = 50 µm.

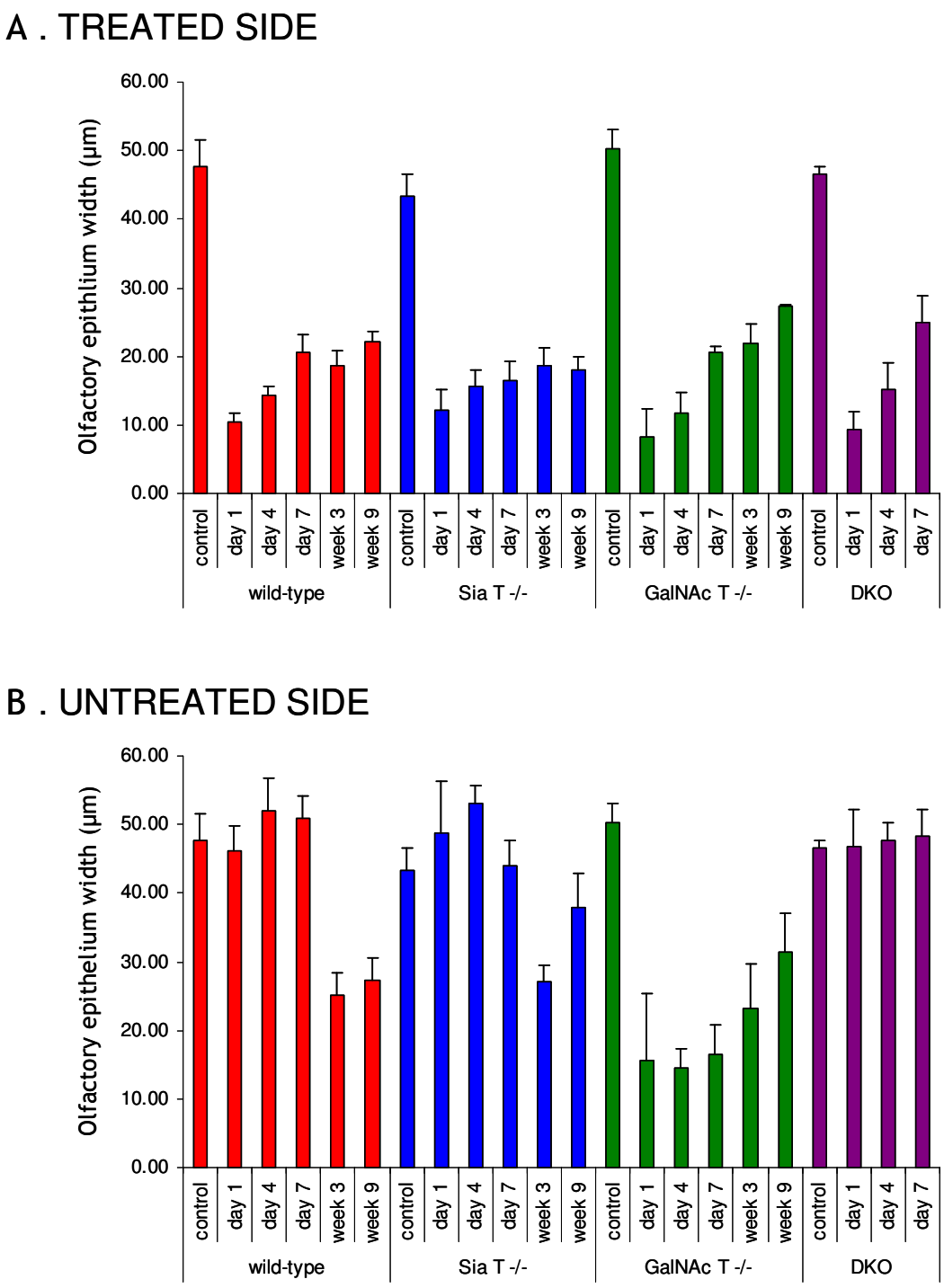

Figure 4.12. The change in epithelial width in 6 week old wild-type and ganglioside knockout mice.

The width of the OE was measured from the basement membrane to the lumen and was found to have dramatically decreased following $ZnSO_4$ treatment, from around 45 µm in untreated tissue to around 10 µm one day after $ZnSO_4$ irrigation. OE widths were measured from the treated (A) and untreated (B) side of the olfactory system. However, the untreated side could not be used as an internal control since occasionally the untreated side also became damaged. Each point represents the mean ± SEM (n=3).

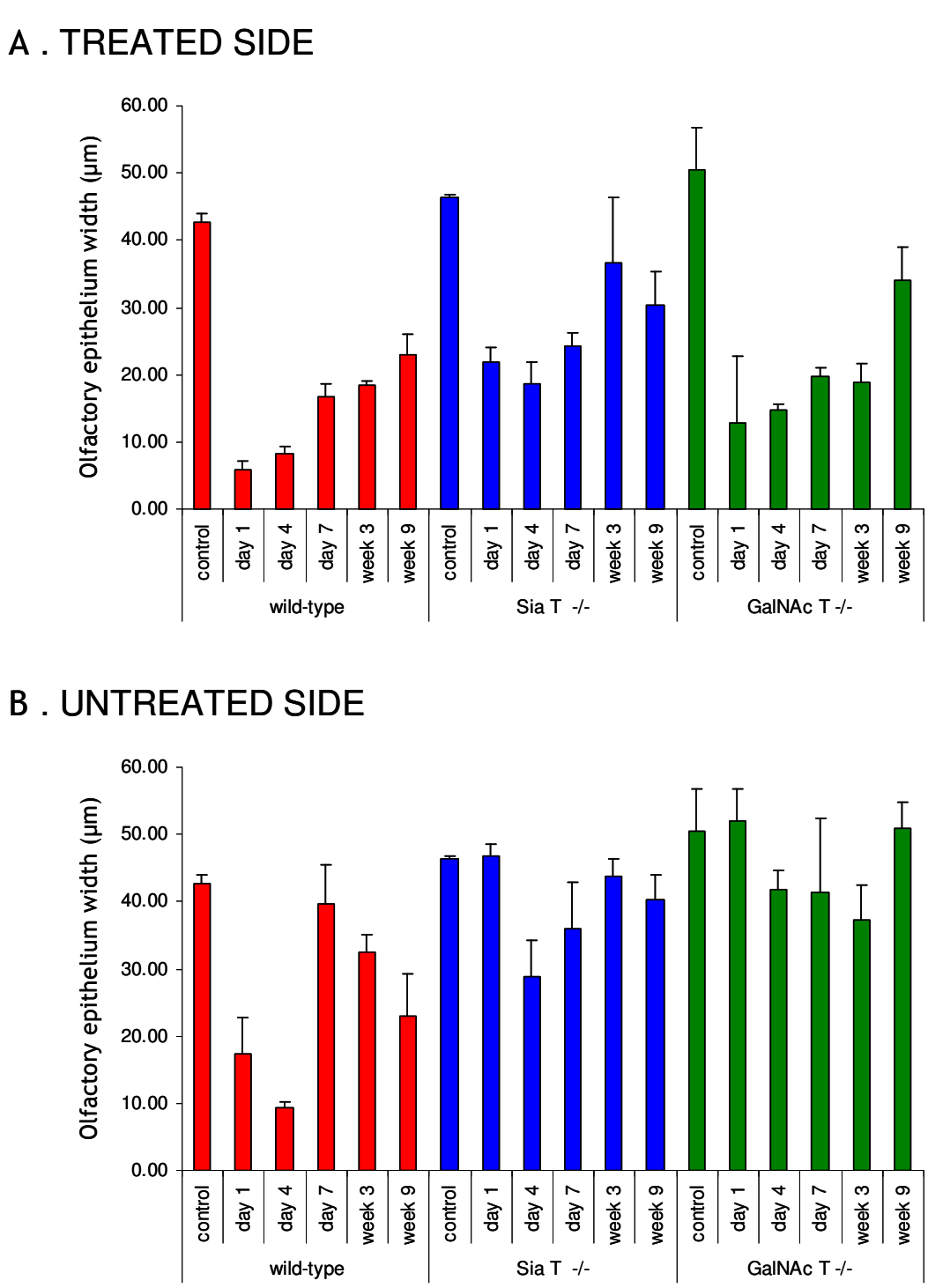

Figure 4.13. The change in epithelial width in 6 month old wild-type and ganglioside knockout mice.
The width of the OE was measured from the basement membrane to the lumen and was found to have dramatically decreased following $ZnSO_4$ treatment, from around 45 µm in untreated tissue to around 10 µm one day after $ZnSO_4$ irrigation. OE widths were measured from the treated (A) and untreated (B) side of the olfactory system. However, the untreated side could not be used as an internal control since occasionally the untreated side also became damaged. Each point represents the mean ± SEM (n=3).

4.2.5 Proliferation within the olfactory epithelium

It was shown in the previous chapter that *in vitro*, OECs isolated from Sia T -/- mice had a higher proliferation rate than OECs isolated from wild-type and GalNAc T -/- mice, when grown on collagen in the presence of growth factors. In this chapter, the aim was to examine if gangliosides play a role in the proliferation of the putative stem cells following destruction of the OE. An antibody to proliferating cell nuclear antigen (PCNA) was used to label cells in the S phase of the cell cycle in the OE, in paraffin embedded tissue from 6 week old mice (Figure 4.14). In control tissue, labelled cells were present as a single, discontinuous layer. Due to their location and shape the majority of positive cells were presumed to be globose basal cells (GBCs). One day following $ZnSO_4$ treatment, PCNA positive cells were visible as a single layer of cells, and by 7 days after irrigation, many of the cells of the regenerating OE were labelled.

The numbers of PCNA positive cells were quantified in tissue from 6 week old mice by counting the numbers of immunoreactive cells per mm of epithelium (Figure 5.15). In control tissue, the average number of PCNA positive cells per mm of epithelium was 45 +/- 6 in all four genotypes at both age groups. One day after $ZnSO_4$ treatment, there was a decrease in the number of PCNA positive cells, followed by an increase 4 days after treatment. After 9 weeks, the level of PCNA positive cells returned to control levels.

Levels of PCNA positive cells in Sia T -/- and GalNAc T -/- mice followed the pattern seen in wild-type mice, however, DKO mice had a significantly higher number of PCNA positive cells seven days after $ZnSO_4$ treatment (Figure 5.14 panel D).

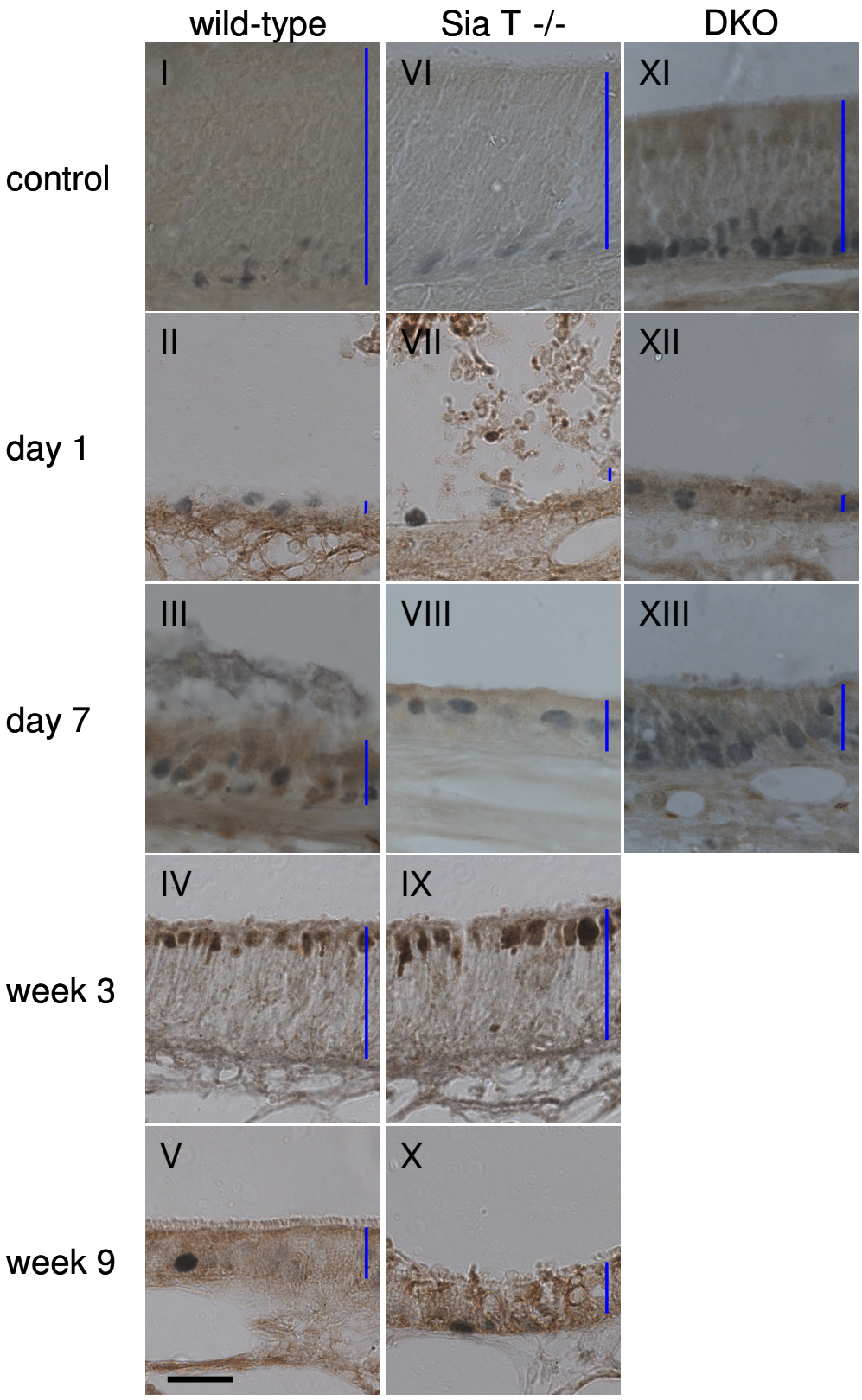

Figure 4.14. PCNA labelling in the OE of wild-type and ganglioside knockout mice.
In order to detect proliferating cells, sections of the olfactory mucosa were labelled with an antibody against PCNA. Representative images from 6 week old wild-type (I-V), Sia T -/- (VI-X) and DKO (XI-XIII) mice are shown. In untreated tissue of all the genotypes examined, PCNA-positive cells were seen as a narrow band along the base of the epithelium. Four days after $ZnSO_4$ irrigation, many of the cells across the regenerating epithelium were immunoreactive for PCNA and by week 9, the PCNA immunoreactivity was again confined to the base of the epithelium. The blue line shows the width of the olfactory epithelium. Scale bar = 20 μm

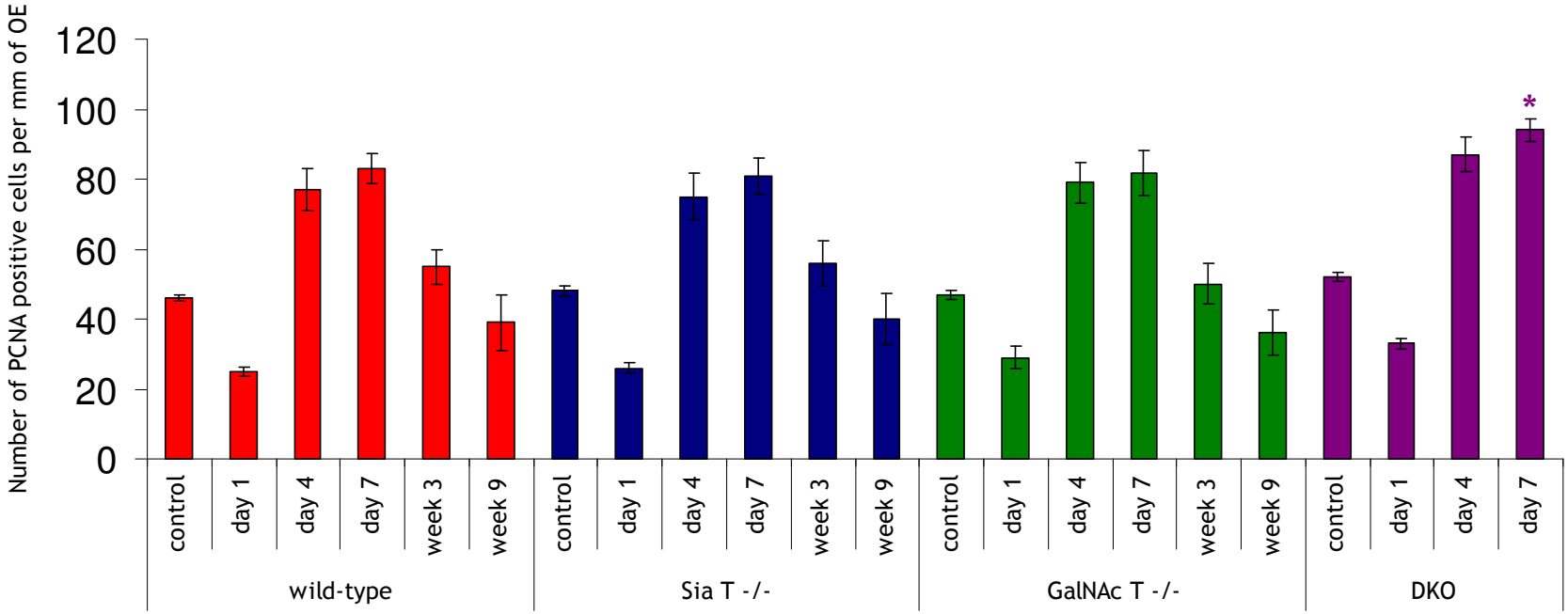

Figure 4.15. Comparison of PCNA positive cells in the OE of wild-type and ganglioside knockout mice.
To examine the role of gangliosides in the proliferation of basal cells of the olfactory epithelium following $ZnSO_4$ treatment, sections of the olfactory mucosa were labelled with an antibody against PCNA that detects proliferating cells. The number of cells expressing PCNA within the OE was quantified per mm. Each point represents the mean ± SEM (n=3). The number of proliferating cells in control, untreated olfactory epithelium was similar in all four genotypes examined. Following nasal irrigation, there was a decrease, followed by an increase in the number of proliferating cells in wild-type, Sia T -/-, GalNAc T -/- and DKO mice. By week 9, the number of PCNA positive cells was again decreased. DKO tissue had a greater number of proliferating cells 7 days following $ZnSO_4$ treatment compared to wild-type and the single knockouts (* $p < 0.05$).

4.2.6 Degeneration and regeneration of olfactory axons

To study the role of gangliosides in axonal regrowth from the PNS to the CNS the expression of SMI 31 was compared during degeneration and regeneration of the olfactory system (Figure 4.16 and 4.17). SMI 31 binds to phosphorylated neurofilament, the major cytoskeletal component of axons. The expression of phosphorylated neurofilament was examined both in the lamina propria where the axons first come out and in the olfactory nerve just before the axons reach the olfactory bulb. The representative images are from wild-type tissue but a similar pattern was seen in all genotypes of 6 week old mice. Subsequently, an antibody against olfactory marker protein (OMP) was obtained and was used to specifically label olfactory receptor neurons (Figures 4.18 and 4.19). In control tissue, axons projected in an orderly manner in the olfactory nerve and were intensely stained with both SMI 31 and anti-OMP. SMI 31 immunoreactivity was completely diminished as soon as one day after $ZnSO_4$ treatment, whereas OMP immunoreactivity remained until at least the 4^{th} day following $ZnSO_4$ treatment, suggesting that axons of olfactory receptor neurons become de-phosphorylated prior to degenerating. As shown in Figure 4.16 and 4.18, SMI 31 and OMP labelling began to reappear 3 weeks after $ZnSO_4$ treatment and by week 9 the extent of labelling was similar to that in untreated mice. However, this was not always the case and some sections remained SMI 31 or OMP negative even after 9 weeks (not shown) suggesting that the extent of axonal regeneration was not uniform. In contrast, in 6 month old wild-type, Sia T -/-, GalNAc T -/- mice only the control tissue labelled with SMI 31, whereas all of the time points following $ZnSO_4$ treatment were negative. Accordingly, anti-OMP immunoreactivity showed that in 6 month old mice olfactory receptor neurons had not regenerated even 9 weeks following $ZnSO_4$ treatment. This showed that the regeneration in the younger mice was a lot better than in the older mice. The pattern in ganglioside knockout mice was the same as that observed in wild-type tissue in both age groups.

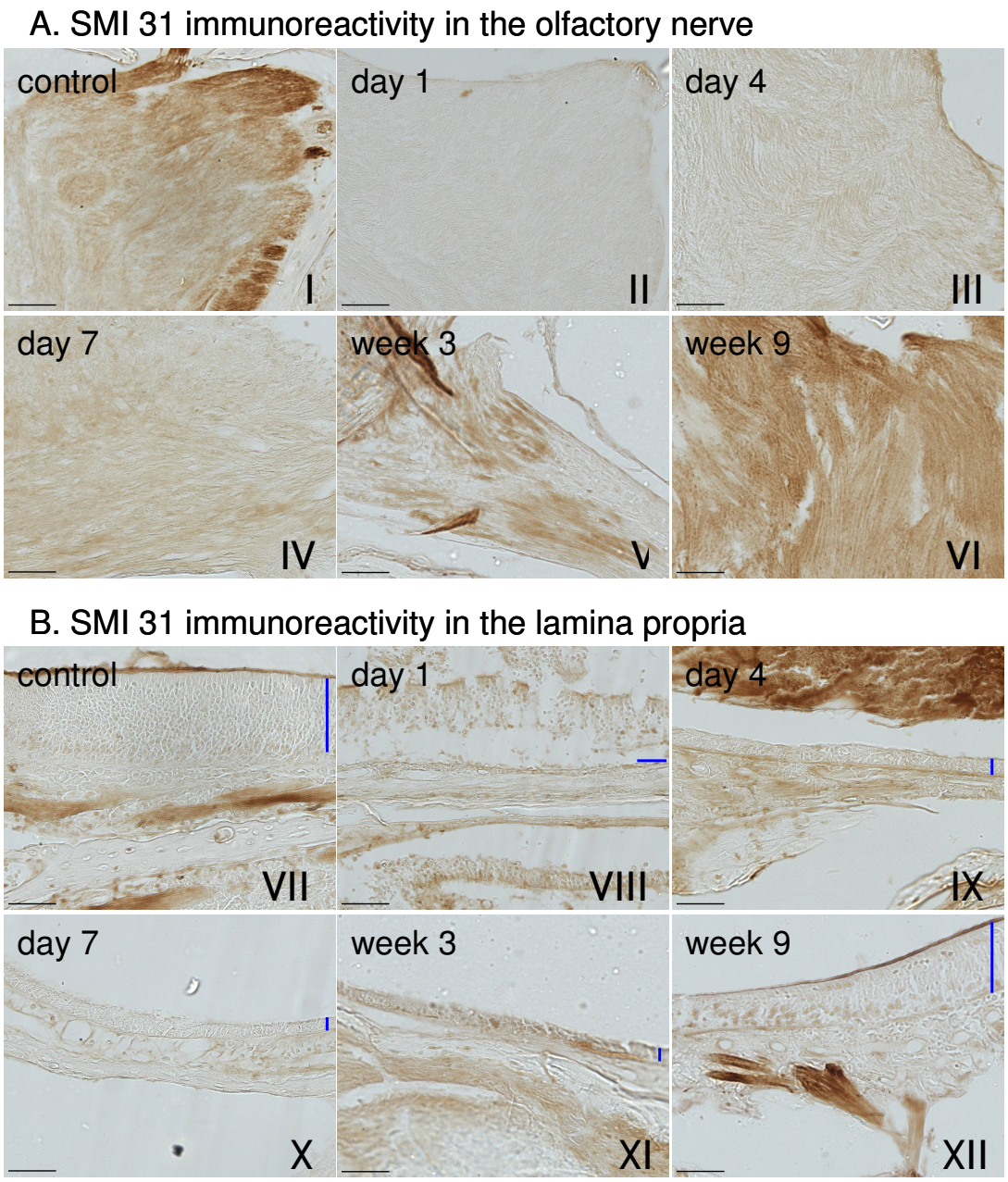

Figure 4.16. SMI 31 labelling of 6 week old olfactory tissue.
To examine the role of gangliosides in neurite extension of olfactory receptor neurons during regeneration of the olfactory system, tissue from 6 week old wild-type mice was labelled with SMI 31, an antibody that recognises phosphorylated neurofilament (I-XII). In control tissue (I & VII), axons of the olfactory receptor neurons were strongly labelled with SMI 31, however following $ZnSO_4$ treatment there was an immediate loss of SMI 31 immunoreactivity (II & VIII). This was accompanied by a loss of structural integrity of the projection from the olfactory epithelium (VIII). SMI 31 staining began to reappear after 3 weeks, along with the return of structure of the nerve (V, XI). Representative images are shown of olfactory nerve (A) and olfactory mucosa (B) from 6 week old wild-type mice, however a similar pattern was observed in 6 week old Sia T -/- and GalNAc T -/- mice. The blue lines delineate the OE, showing its width. Scale bar = 50 µm.

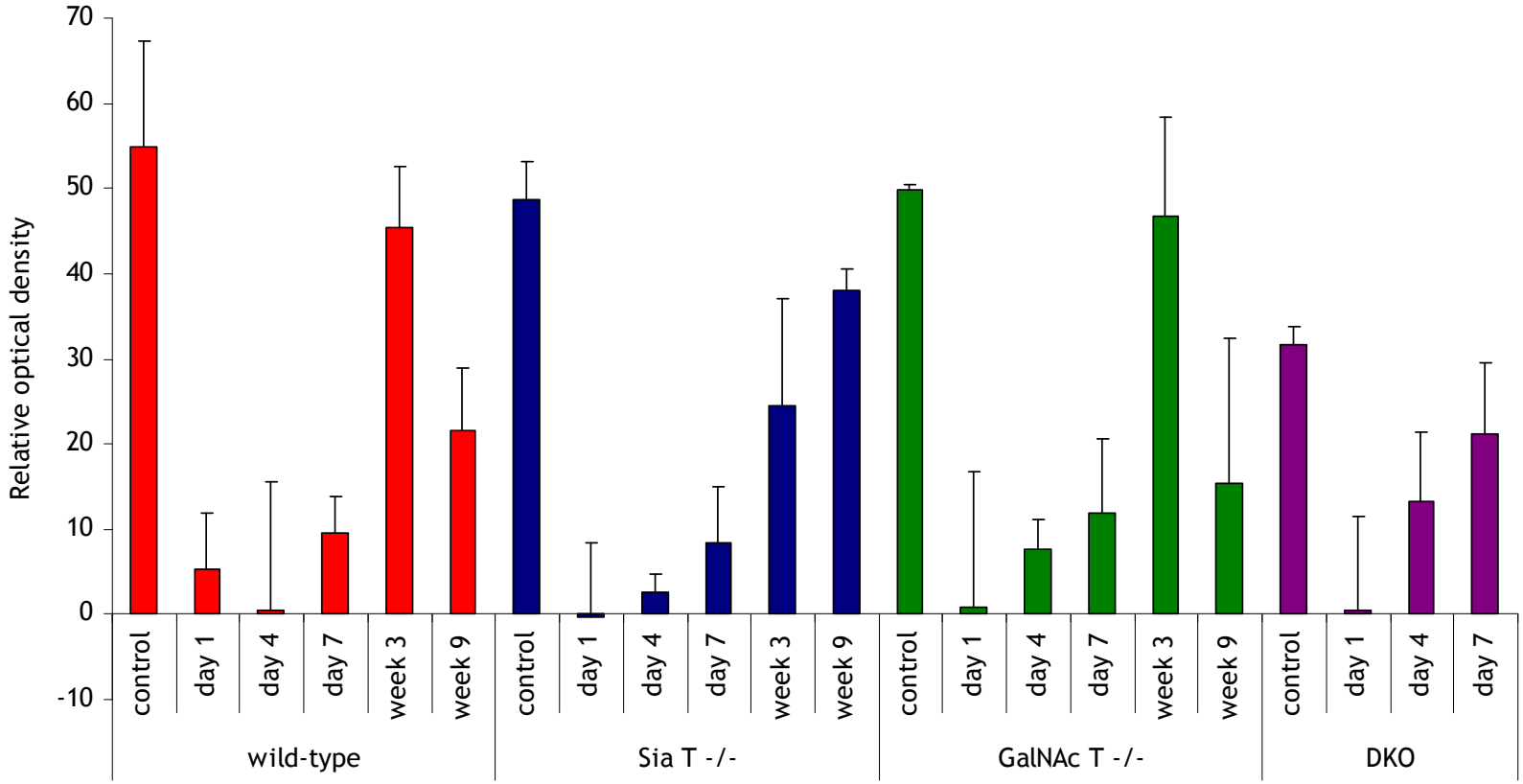

Figure 4.17. Quantitation of SMI 31 labelling during degeneration and regeneration of ORNs in the olfactory nerve in 6 week old mice.
To examine the role of gangliosides in neurite extension during olfactory receptor neuron regeneration following $ZnSO_4$ treatment, sections of the olfactory system were labelled with SMI 31, an antibody that recognises phosphorylated neurofilament. The loss of axons was quantified by measuring optical density of the SMI 31 staining in the olfactory nerve of wild-type, Sia T -/-, GalNAc T -/- and DKO mice. Each point represents the mean ± SEM (n=3). One day after $ZnSO_4$ irrigation the intensity of staining was completely diminished. The intensity of SMI 31 labelling began to increase after 7 days and continued to increase. It can be seen that 3 and 9 weeks after treatment the intensity of labelling had reached control levels in some sections, however as can be seen from the error bars the labelling was extremely variable. A similar pattern was observed in all four genotypes tested.

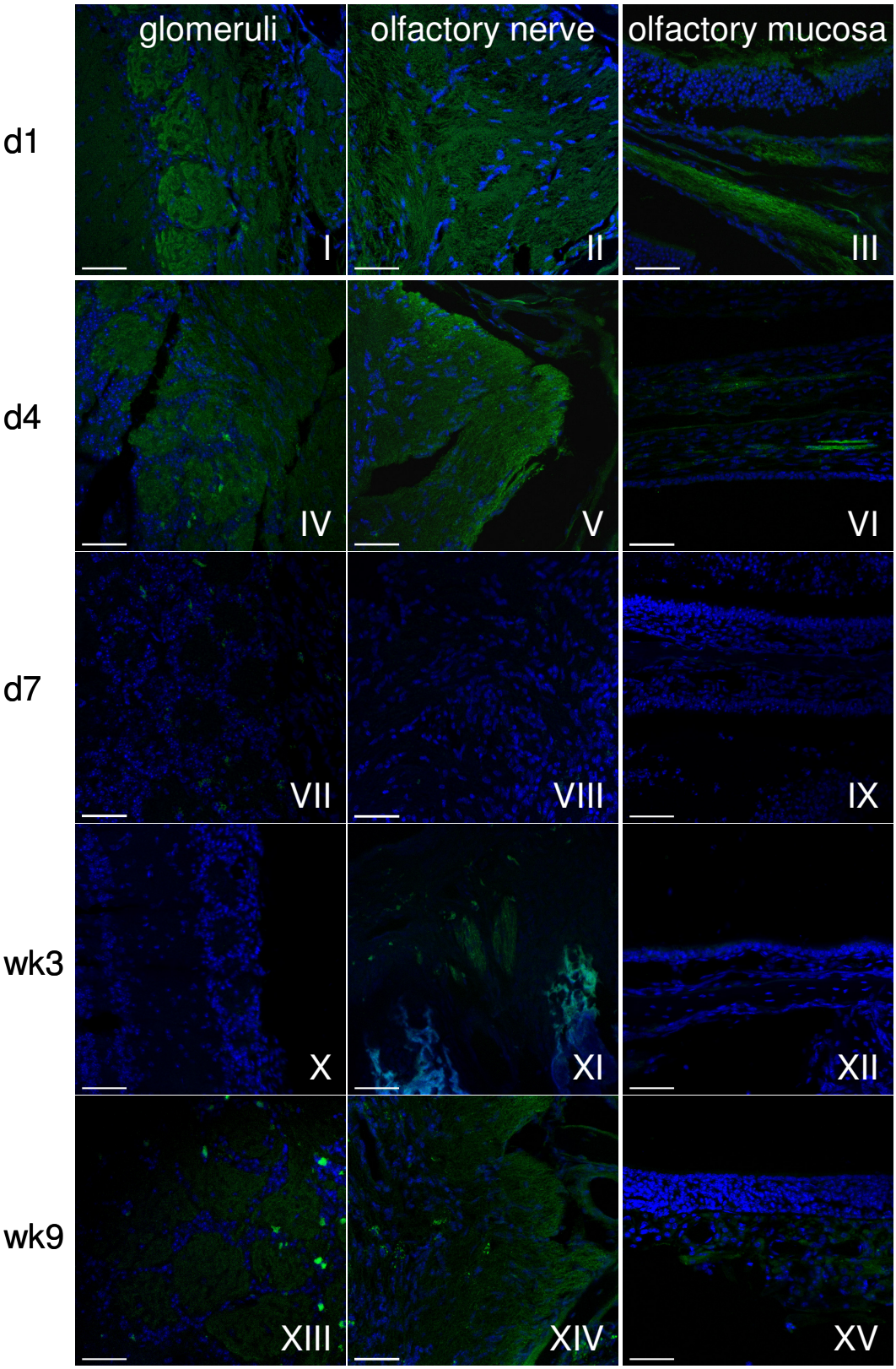

Figure 4.18. The degeneration and regeneration of ORNs in 6 week old mice.
To examine the role of gangliosides in neurite extension during the regeneration of the olfactory system after $ZnSO_4$ treatment, sections were labelled with an anti-OMP antibody that specifically recognises olfactory receptor neurons. The representative images show glomeruli (I, IV, VII, X & XIII), olfactory nerve (II, V, VIII, XI, XIV) and olfactory mucosa (III, VI, IX, XII & XV) from 6 week old wild-type mice, labelled with anti-OMP (green) and DAPI (blue) to show the cell nuclei. In untreated tissue, ORNs were strongly labelled with anti-OMP (not shown) and this labelling remained until 4 days following $ZnSO_4$ treatment (IV-VI). 7 days following $ZnSO_4$ treatment, the OMP labelling had diminished (VII-IX). 9 weeks after $ZnSO_4$ treatment, the OMP labelling reappeared in some sections (XIII-XV). Scale bar = 50 μm.

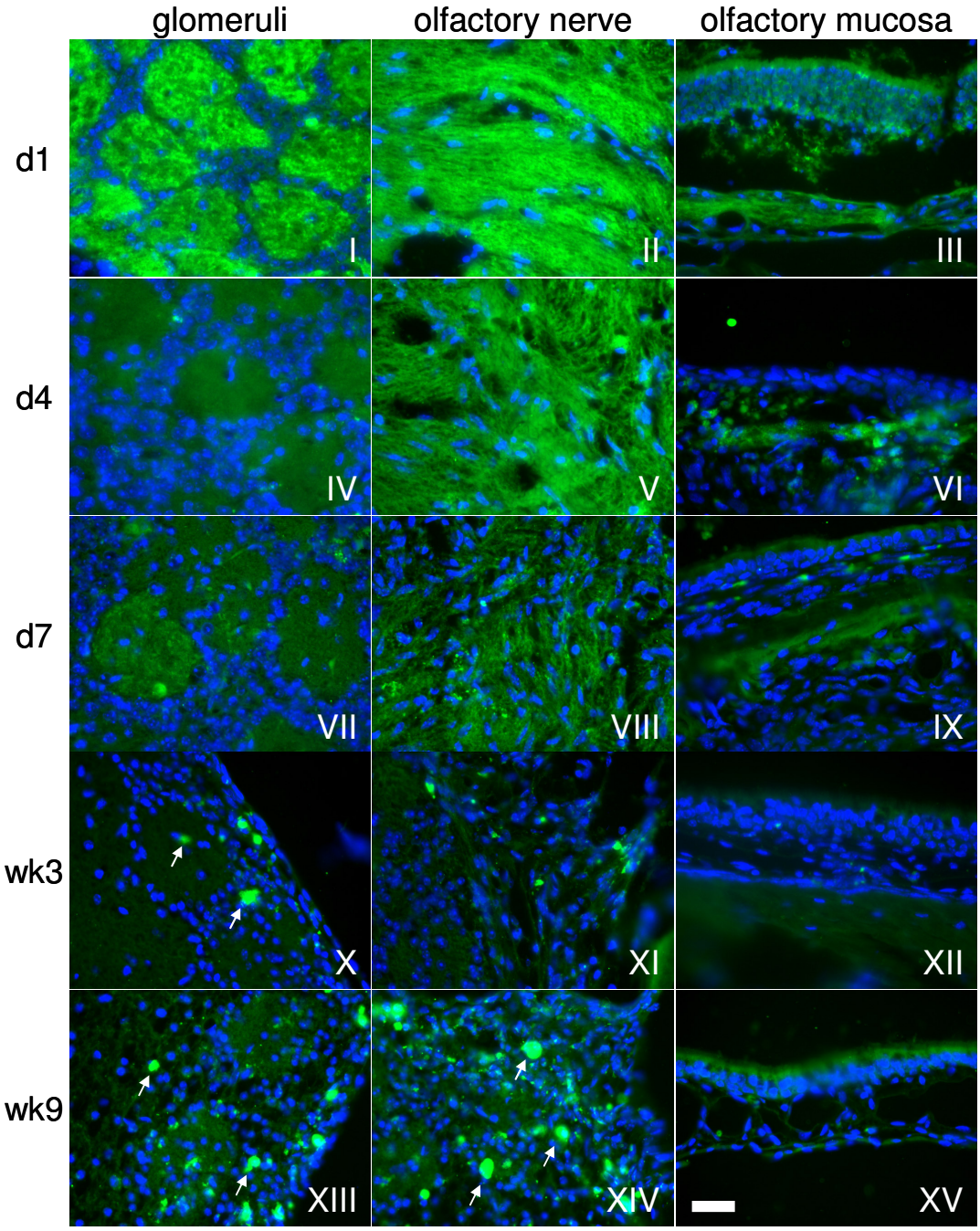

Figure 4.19. The degeneration of olfactory receptor neurons in 6 month old mice.
To examine the role of gangliosides in neurite extension during the regeneration of the olfactory system after $ZnSO_4$ treatment, sections were labelled with an anti-OMP antibody that specifically recognises olfactory receptor neurons. The representative images show glomeruli (I, IV, VII, X & XIII), olfactory nerve (II, V, VIII, XI, XIV) and olfactory mucosa (III, VI, IX, XII & XV) from 6 month old wild-type mice, labelled with anti-OMP (green) and DAPI (blue) to show the cell nuclei. In control tissue, axons of the olfactory receptor neurons were strongly labelled with OMP (not shown) and this labelling remained initially following $ZnSO_4$ treatment (I-VI). However, seven days following $ZnSO_4$ treatment OMP labelling decreased (VII-IX) and was not regained 9 weeks after $ZnSO_4$ nasal irrigation, as can be seen in images XIII-XV. Arrows in X, XIII and XIV show non-specific staining. Scale bar = 100 μm.

4.2.7 Synapse formation

To examine the role of gangliosides in synapse formation in the olfactory system, immunohistochemistry was performed using an antibody to synaptophysin, a synaptic vesicle membrane protein (Figure 4.20). In control tissue, glomeruli could clearly be identified around the periphery of the olfactory bulbs and were intensely and uniformly labelled with synaptophysin. One day after ZnSO4 treatment, glomeruli were similar in appearance to untreated glomeruli, however, by the fourth day following treatment, they had lost much of the characteristic circular appearance and were no longer evenly labelled with synaptophysin. This loss of synaptophysin labelling continued and even after nine weeks was not recovered suggesting that in the present study, the olfactory receptor neurons do not re-form synapses.

The changes in the intensity of synaptophysin labelling were quantified by measuring optical density as described in the methods section (Figure 4.21). The optical density decreases immediately following $ZnSO_4$ treatment and is never regained. The pattern observed in 6 week old wild-type mice was also observed in ganglioside knockout mice in both age groups examined.

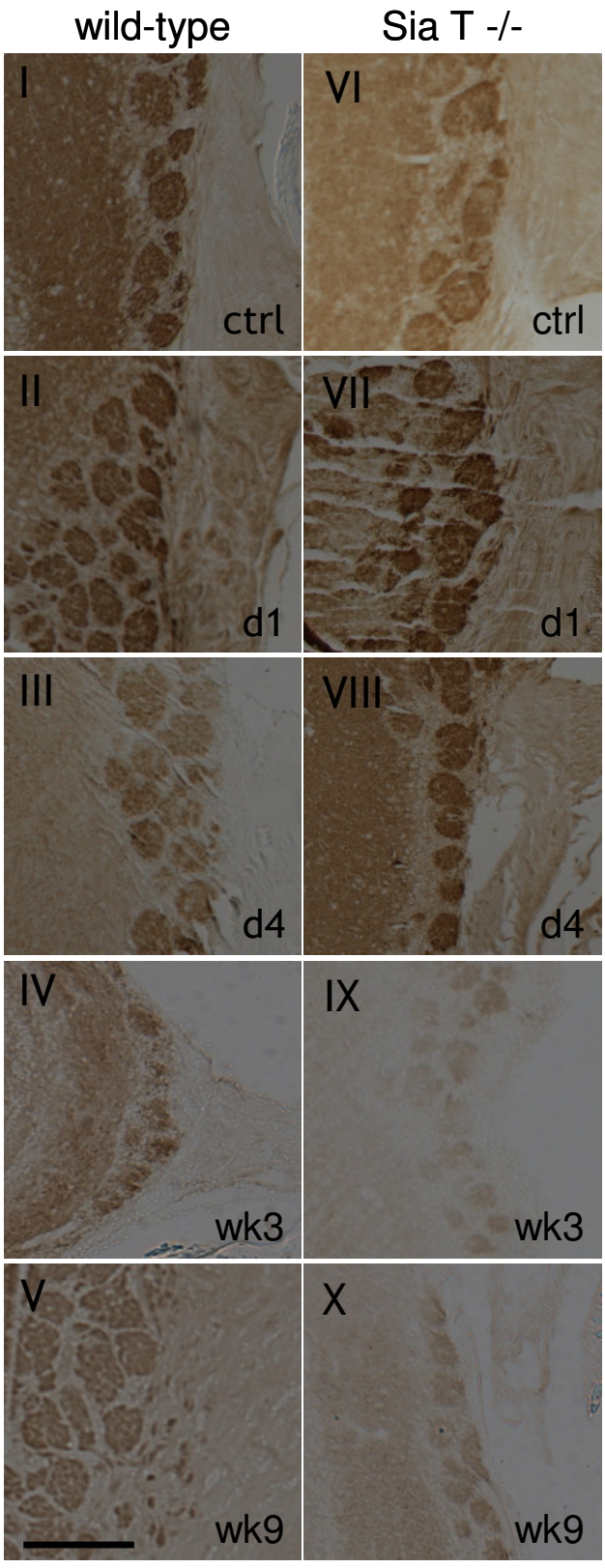

Figure 4.20. Synaptophysin labelling in the glomeruli of 6 week old mice.
To examine the role of gangliosides in synapse formation during olfactory system regeneration, immunohistochemistry was carried out with an antibody against synaptophysin. Representative images from wild-type (I-V) and Sia T -/- (VI-X) mice, 1 day (II & VII), 4 days(III & VIII), 3 weeks (IV & IX) and 9 weeks (V & X) after $ZnSO_4$ treatment are shown. In control, untreated tissue (I & VI), the glomeruli of the olfactory bulb were seen as circular, densely-labelled structures. Three weeks after $ZnSO_4$ treatment (IV & IX) their distinctive round appearance was no longer evident and the synaptophysin labelling was less intense. The synaptophysin labelling continued to decrease and was not regained 9 weeks after the initial damage (V & X). Scale bar = 200 μm

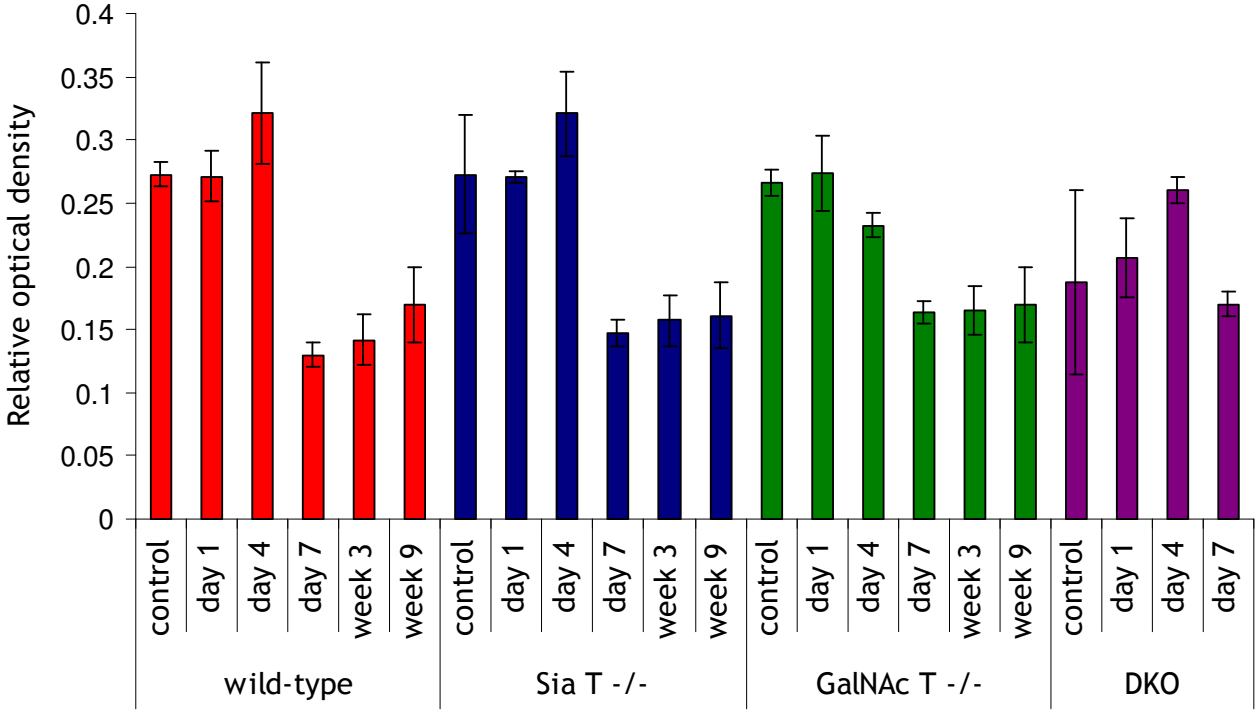

Figure 4.21. The degeneration of synapses in 6 week old wild-type and ganglioside knockout mice.
To examine the role of gangliosides in synapse formation during olfactory system regeneration following nasal irrigation with ZnSO4, olfactory bulb sections from 6 week old wild-type, Sia T -/-, GalNAc T -/- and DKO were labelled with an antibody to the synaptic vesicle membrane protein synaptophysin. Optical density measurements were taken to quantify the loss of intensity of synaptophysin labelling in glomeruli of wild-type, Sia T -/-, GalNAc T -/- and DKO mice. Each point represents the mean ± SEM (n=3). The loss in synaptophysin immunoreactivity was not evident until 7 days following $ZnSO_4$ treatment and continued until the last time point examined (week 9).

4.2.8 The astrocytic response

The astrocytic response in the olfactory bulb was detected using an antibody against glial fibrillary acidic protein (GFAP) and PCNA (Figure 4.22), in order to observe two features of astrocytosis: an increase in GFAP expression and proliferation.

In the control tissue, typical, non-proliferating, GFAP-positive astrocytes were present in the glomerular layer. Following $ZnSO_4$ treatment, GFAP-labelling became more intense and the astrocytes began to express PCNA. This continued up to week 3 after treatment. After 9 weeks following treatment the GFAP expression was similar to that observed in control tissue and the astrocytes no longer labelled with PCNA. The same pattern was observed in wild-type, Sia T -/- and GalNAc T -/- tissue in both age groups. Representative images for wild-type and Sia T -/- tissue obtained from 6 week old mice are shown in Figure 4.22.

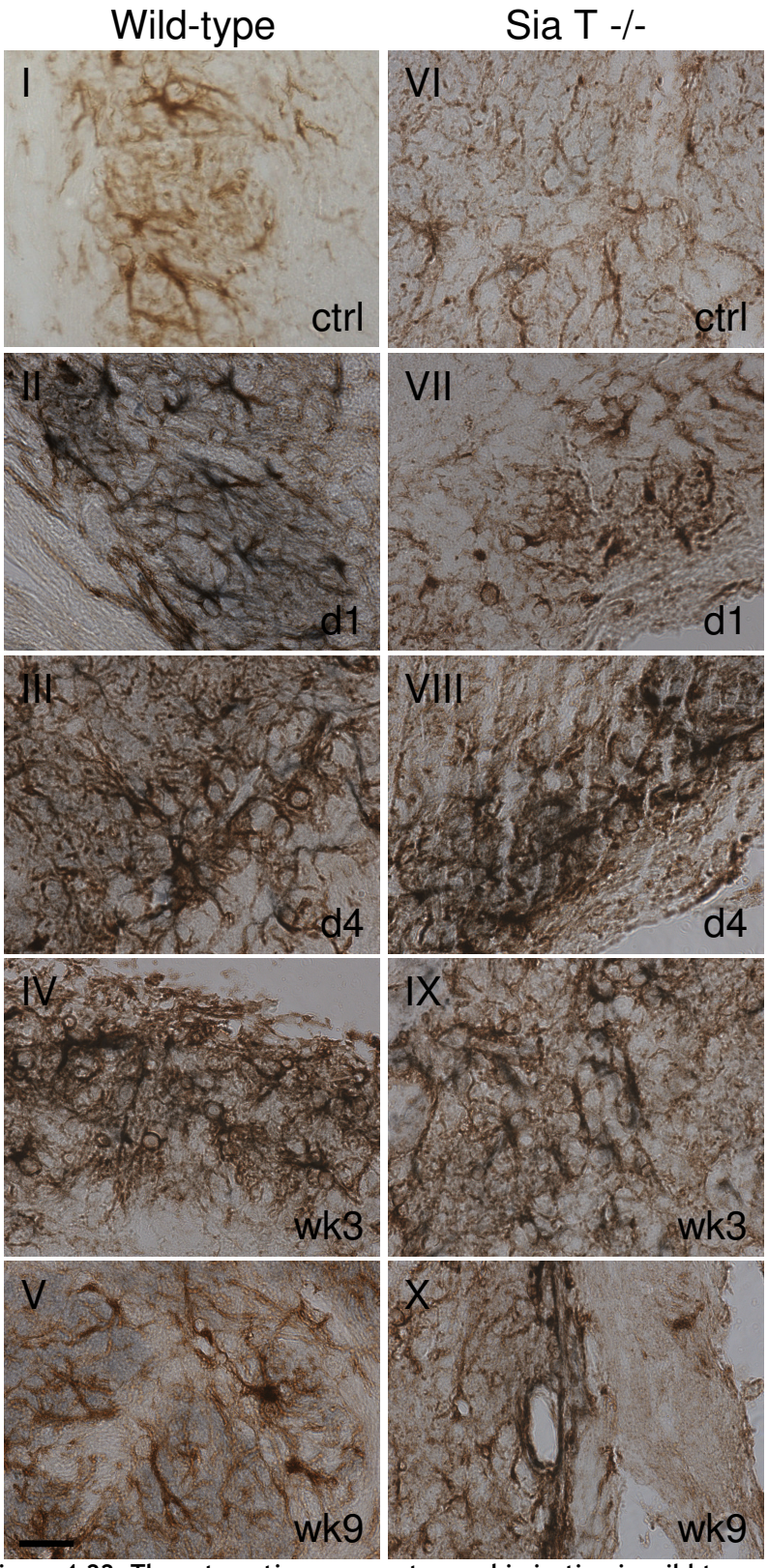

Figure 4.22. The astrocytic response to nasal irrigation in wild-type and ganglioside knockout mice. The astrocytic response to damage caused by $ZnSO_4$ was assessed with double immunohistochemistry using anti-GFAP (brown) and anti-PCNA (black). Representative images show wild-type (I-V) and Sia T -/- (VI-X) tissue from 6 week old mice labelled with anti-GFAP and anti-PCNA 1 day (II and VII), 4 days (III and VIII), 3 weeks (IV and IX) and 9 weeks (V and X) following $ZnSO_4$ treatment. In control, untreated tissue (I and VI), GFAP positive astrocytes could be seen in the glomerular layer, although none double labelled with PCNA. There was an increased expression of GFAP following $ZnSO_4$ treatment and the GFAP-positive cells were double labelled with PCNA. This astrocytosis persisted up to 3 weeks after $ZnSO_4$ treatment. After 9 weeks the majority of astrocytes had stopped proliferating and the expression of GFAP was similar to that seen in the untreated tissue. Scale bar = 20 μm.

4.3 Discussion

4.3.1 Ganglioside expression of the olfactory system

The initial aim of this study was to characterise the expression of major brain gangliosides GM1, GD1a, GD1b, GT1b and GQ1b in the olfactory system of 6-week old mice. This would ascertain whether there was justification to carry out further studies on the regeneration of the olfactory system in ganglioside knockout mice.

Using immunofluorescent labelling with various anti-ganglioside antibodies, it was found that the olfactory system of wild-type mice expresses all of the gangliosides examined apart from GD1a. This was surprising because GD1a is one of the major brain gangliosides. GD1a is found on axons and is thought to act as a ligand for MAG (Collins et al., 1997). In addition, the same antibody labelled axons in cultures of dissociated spinal cord (Figure 5.12). It is thus very unlikely that GD1a is not present in the olfactory system. Therefore, it is more likely that for some unknown reason the antibody used in the present study did not detect GD1a in the olfactory system. Future studies should confirm the ganglioside content of the OB and the OM should by extracting gangliosides form the OB and the OM and analysing them by TLC and tandem mass spectrometry.

The results of the present study also showed that the olfactory system of GalNAc T -/- mice lacked all a-series gangliosides, whereas the olfactory system of Sia T -/- mice lacked all b-series gangliosides but had higher levels of a-series gangliosides. Both the lack and the excess of particular gangliosides may have an effect on the degeneration or the regeneration of the olfactory system.

Future studies should examine in more detail the ganglioside expression of the various cell types within the olfactory system by double labelling with anti-ganglioside antibodies and antibodies that recognise the specific cells types. For instance, sections of the OB and OM could be double labelled with anti-ganglioside antibodies and OMP which recognises ORNs or GBC-1 which recognises the globose basal cells.

4.3.2 Comparison of olfactory epithelial width

The patterns of distribution of gangliosides during different stages of development, as well as their abundance in neural cells gave rise to the idea that gangliosides must play important roles in many biological processes in the nervous system. Until the emergence of ganglioside knockout mice, most investigations into the biological role of gangliosides consisted of addition of gangliosides or inhibitors of their synthesis to cells in culture. These studies suggested that gangliosides modulate many functions at the cellular level but could not address the physiological roles of gangliosides at the level of the whole organism.

To investigate whether the lack or the overexpression of gangliosides had an effect on the anatomy of the olfactory system, the present study compared the olfactory epithelium widths of wildtype and ganglioside knockout mice. The width of the olfactory epithelium, which is composed of several cell layers whose structure is very organised, was measured as an indication of the development of the tissue. The mean epithelial width in ganglioside knockout mice did not differ from that of wild-type mice which suggests that a change in the ganglioside expression does not affect the development of the OE. This means that any changes in the epithelial width in the ganglioside knockout mice that may be observed in the regeneration study would be due to lack of regeneration.

4.3.3 Preliminary studies of nasal $ZnSO_4$ irrigation

In order to study the role of gangliosides in the degeneration and regeneration of the olfactory system, an established method was used where the ORNs and other cells in the OE are destroyed by $ZnSO_4$. The biggest difficulty in this study was establishing the optimal volume and concentration of $ZnSO_4$ to use in order to induce the right amount of OE damage. It was decided to keep the volume low, since higher volumes were detrimental to the health of the mice, and preliminary studies indicated that 20 µl of $ZnSO_4$ would be sufficient to induce destruction of the cells of the olfactory epithelium. However, all the results of the present study suggest that this concentration was too high since in most

instances it also destroyed the basal cells which are needed in order for the olfactory epithelium to regenerate.

Therefore, with hindsight, 20 µl of 10% ZnSO4 was too strong and destroyed too many basal cells which suggests that more concentrations should have been tested in the preliminary studies. If I was to repeat this study I would try different volumes of 5% $ZnSO_4$ to determine which damaged the OE enough to destroy all cells, leaving only the basal cells. From the preliminary studies it can be seen that 50 µl of 5% $ZnSO_4$ damaged the top layers of cells in the OE, whereas 100 µl of 5% $ZnSO_4$ completely destroyed all of the cells within the OE. I would therefore irrigate the left nasal cavity of 6 month old wild-type mice with 60, 70 and 80 µl of 5% $ZnSO_4$. However, rather than adding it all at once, it would be better to add it in several stages because large volumes were detrimental to the health of the mice. For instance, I would irrigate the nasal cavity with 2 x 10 µl of 5% $ZnSO_4$ and an hour later, after the mouse has had time to recover, add another 2 x 10 µl, and an hour later another 2 x 10 µl of 5% $ZnSO_4$.

In addition, rather than examining the tissue one day after irrigation, preliminary studies should have also looked at a later time point to examine how much of the tissue had regenerated. For instance, mice could have been sacrificed three weeks following $ZnSO_4$ treatment to determine the extent of regeneration, by labelling the tissue with H & E to measure OE width, OMP, to observe the regeneration of ORNs and synaptophysin to examine if the synapses had re-formed. Subsequent experiments should only be performed once it was demonstrated that a certain volume and concentration of $ZnSO_4$ reproducibly caused enough damage to destroy all cells of the OE except the basal cells and that three weeks later all the cells of the OE had regenerated and that ORNs had reformed synapses with the second order neurons in the OB.

With hind-sight the number of mice used in the present study was too large. Because many of the neurological defects seen in the single knockouts were age related, I would not study regeneration in the younger age group and would concentrate on the older age group. This would mean leaving out the DKO mice but if a difference in the regeneration of the 6 month old single knockouts was seen, another study could compare the regeneration of, for example, 3 week old

wild-type and DKO mice which would allow the examination of regeneration as far as 4 weeks following $ZnSO_4$ treatment. This is because, according to the Home Office licence, DKO mice cannot be kept after 7 weeks of age.

However, concentrating on one age group would cut the numbers down considerably allowing an additional time point. The time points used in the present study were 1, 4, 7, 21 and 63 days following $ZnSO_4$ irrigation. This meant that there was a big gap between 7 and 21 days during which the tissue was still in the process of regeneration. Therefore, it would be beneficial to add a time point at 14 days after $ZnSO_4$ treatment. In addition, because of variability the number of mice per time point could be increased to six. Finally, instead of embedding the tissue in paraffin, I would freeze the tissue instead because this would allow the use of more antibodies.

4.3.4 The response of the olfactory epithelium to nasal $ZnSO_4$ irrigation

To examine the role of gangliosides in the degeneration and regeneration of the olfactory system following ZnSO4 irrigation, I first compared the OE width, which is an indication of the degeneration and regeneration of the ORNs and other cells present in the olfactory epithelium. One day after ZnSO4 treatment, the OE is reduced to one cell layer thick or in some places completely destroyed. Over time the OE grows back, however after 9 weeks it does not reach control levels. In wild-type and ganglioside knockout mice, the olfactory epithelium reaches only 50% of the control value, suggesting incomplete regeneration. This indicates that the concentration of ZnSO4 used was too strong, and that not enough basal cells survived the treatment to differentiate and repopulate all the cells of the OE.

The respiratory epithelium is a ciliated, pseudo-stratified epithelium which functions to warm and humidify the incoming air. It is located anterior to the olfactory epithelium in the nasal cavity. There have been numerous reports in the literature that damage to the OE is, to a certain extent, irreversible, and results in the partial replacement of olfactory epithelium with respiratory epithelium (Schwob et al., 1995, Schwob et al., 1999). Indeed, replacement of olfactory epithelium by respiratory epithelium is observed with naturally occurring rhinitis (Smith, 1938a), ZnSO4 irrigation (Harding et al., 1977, Smith,

1938b), and injection of 3-methyl indole either alone (Turk et al., 1987) or in combination with methyl bromide inhalation (Schwob et al., 1994b). Schwob et al (Schwob et al., 1995) showed that where neurogenesis fails, the epithelium changes to respiratory in character, as defined by the presence of ciliated columnar cells and the absence of microvillar capped sustentacular cells. From the results of the present study, it would appear that a significant fraction of olfactory epithelium became respiratory epithelium, which meant that it if gangliosides did play a role in the regeneration of the olfactory system it may not be detected. The severity of initial injury correlates with the degree of replacement and it was evident from the H & E staining of the olfactory mucosa that in the present study many parts of the epithelium were destroyed down to the basal lamina, thus leading to the destruction of the entire population of putative stem cells.

A closer inspection of at the graphs showing the OE measurements (Figures 4.12 and 4.13) reveals that in some instances, the olfactory epithelium in the untreated side was also damaged and that there is variability between the extent of damage between time-points. The observation that the amount of OE damage was not uniform, suggests that the amount of OE damage varied between treatment days because mice that were treated at the same time were generally used for the same time-point. In other words, if I had treated five wild-type mice one day, all five would be sacrificed on, for example, the fourth day following irrigation. However, it may have been better to sacrifice one mouse a day after the irrigation, one four days later, one seven days later and so on. This may help reduce variability between time-points. In addition, increasing the number of mice used per time point may compensate for some of the variability. Finally, optimising the concentration of ZnSO4, so that it did not damage too many basal cells in the treated side of the OE, and did not damage the untreated side would allow an examination of the role of gangliosides in OE degeneration and regeneration and would allow the untreated side to be used as an internal control.

4.3.5 Proliferation within the olfactory epithelium

Numerous studies have suggested a role for gangliosides in the proliferation of various cell types (section 1.1.3.1 in the Introduction). In addition, gangliosides

are thought to be involved in regeneration. In the olfactory system, when the ORNs are destroyed, they grow back from the putative stem cells in the olfactory epithelium. Because the regeneration of the olfactory system depends on the proliferation and the differentiation of the putative stem cells, it was decided to examine if gangliosides play a role in the proliferation of the putative stem cells following destruction of the OE.

An antibody to PCNA, a protein involved in DNA synthesis (Mathews *et al.*, 1984), was used to label proliferating cells. PCNA occurs in cells during the last 5% of the G1 phase and the first 35% of the S phase of the cell cycle (Paunesku *et al.*, 2001), and is widely used to label those cells undergoing proliferation (Hill-Felberg *et al.*, 1999).

The present study showed that in the control, untreated tissue, the proliferation of cells in the basal layer of the OE was similar in wild-type and ganglioside knockout mice. This suggests that gangliosides do not modulate the proliferation of the two classes of basal cell within the olfactory epithelium, the globose and horizontal basal cells, during development.

Yet, seven days after the destruction of the olfactory epithelium by $ZnSO_4$, levels of PCNA positive cells were significantly higher in DKO mice compared with wild-type and the single knockout mice. Neurogenesis in the olfactory epithelium is under the regulation of a negative feedback, mature ORNs feeding-back to inhibit the further differentiation of basal cells. Indeed, the proliferation of GBCs increases if the death of the ORNs is induced, whereas it decreases if ORNs are protected from damage (Farbman, 1990). Therefore, the increased level of proliferation of basal cells in DKO mice suggests that the signalling between ORNs and basal cells, which regulates the proliferation rate of globose basal cells, is altered in the absence of complex gangliosides.

However, the proliferation of cells in the basal layer in Sia T -/- and GalNAc T -/- mice was similar to that in wild-type mice. GalNAc T -/- mice lack all complex gangliosides and have higher levels of simple gangliosides GM3, GD3 and GT3, whereas DKO mice only have the simple ganglioside GM3. Therefore, the lack of complex gangliosides in GalNAc T -/- mice has no effect on the proliferation of basal cell, possibly because increased levels of GD3 and GT3 can compensate for the lack of complex gangliosides.

Because of their location, proliferating cells were presumed to be basal cells. In order to identify categorically the cells that were undergoing proliferation, future experiments could involve double-labelling studies.

4.3.6 Olfactory receptor neuron regeneration

To assess the role of gangliosides in axonal regrowth from the PNS to the CNS the expression of SMI 31, which binds to phosphorylated neurofilament, and OMP, which labels ORNs, was examined in wild-type and ganglioside knockout mice during degeneration and regeneration of the olfactory system. It was found that in wild-type and ganglioside knockout mice, one day after $ZnSO_4$ treatment, the axons of the ORNs were still present but had become de-phosphorylated, and after seven days had degenerated. In 6 week old wild-type and ganglioside knockout mice some regeneration of the ORNs was evident 3 weeks after $ZnSO_4$ irrigation, however by 9 weeks most of the ORNs had not regenerated. In the 6 month old wild-type and ganglioside mice, no regeneration of the ORNs was observed following $ZnSO_4$ irrigation.

Despite a remarkable regenerative capacity, recovery of the mammalian olfactory epithelium can fail in severely injured areas, which subsequently reconstitute as aneuronal respiratory epithelium, which is a form of metaplasia (Jang et al., 2003). Jang et al (2003) showed that in areas of olfactory epithelium in which GBC are preserved, they multiply and reconstitute the cells of the epithelium, however, in areas where the GBCs are also destroyed, the epithelium is repopulated, in part, by cells arising from Bowman's glands.

As a result of olfactory epithelium becoming replaced by aneuronal respiratory epithelium, the population of reinnervating fibres was less and consequently the olfactory bulb remained denervated even 9 weeks following $ZnSO_4$ treatment, as shown by the OMP immunolabelling. As was shown using SMI 31 phosphorylated neurofilament immunolabelling, some areas of the olfactory bulb are re-innervated, however, in the majority of cases this was not the case. It is also important to note that the damage to the olfactory epithelium was not uniform throughout the olfactory mucosa and that although some areas were rendered acellular by the treatment, there were areas that were spared damaged altogether. Therefore, the neurofilament labelling observed following

treatment is either due to regenerated olfactory receptor neurons or the olfactory receptor neurons which were not damaged.

Due to lack of regeneration, the role of gangliosides in neurite outgrowth during regeneration could not be examined in the present study. However, being a constantly regenerative tissue, the olfactory system is a good system to study regeneration and studies in Sia T -/- mice have indicated that these mice have impaired PNS regeneration (Itoh et al., 2001). In addition, gangliosides have been shown to be neurotrophic (Schengrund, 1990). Hence, future studies should asses the role of gangliosides in neurite outgrowth following damage of the olfactory epithelium using an improved, and more reproducible method of damaging the olfactory epithelium.

4.3.7 Synapse formation

Glomeruli of the olfactory bulb are dense collections of synapses. In the present study, the role of gangliosides in synapse formation during regeneration of the olfactory system following $ZnSO_4$ treatment was examined by labelling olfactory bulb tissue from wild-type and ganglioside knockout mice with an antibody to the synaptic vesicle membrane protein, synaptophysin, which has previously been used to identify synaptic degeneration (Meller et al, 1994). It was found that synapses began to deteriorate four days after $ZnSO_4$ treatment, and are not re-formed even as late as 9 weeks after the initial injury in wild-type and ganglioside knockout mice.

The optical density of the synaptophysin immunohistochemistry, unlike that of the neurofilament, did not decrease to the same extent. Whereas the loss of neurofilament staining was almost complete, the staining of synaptophysin decreased to around 50% of the control level. This is because, firstly, the glomeruli not only contain ORN synapses, but also second order neuron and interneuron synapses and secondly, some ORNs may have survived the treatment.

These results suggest that 9 weeks following $ZnSO_4$ treatment, the ORNs do not regenerate sufficiently to re-form synapses with second order neurons in the olfactory bulb. As a result, it is not possible to draw any conclusions on the role of gangliosides in synapse formation in the olfactory system.

4.3.8 The astrocytic response

Reactive astrocytosis is one of the first consequences of injury to the CNS and is a process characterised by the proliferation and hypertrophy of astrocytes within the vicinity of damage. Reactive astrocytes are thought to impede regeneration. The astrocytic response in the olfactory bulb was detected using an antibody against GFAP and PCNA, in order to observe two features of astrocytosis: an increase in GFAP expression and proliferation.

In control tissue, non-proliferating, GFAP-positive astrocytes were present in the glomerular layer. However, nasal irrigation with $ZnSO_4$ lead to a rapid astrocytosis within the olfactory bulb, astrocytes both proliferating and becoming hypertrophic, as shown by double immunohistochemistry with GFAP and PCNA. This was observed between and surrounding the glomeruli and in the outer region of the external plexiform layer beginning after 4 days and continuing 3 weeks after $ZnSO_4$ treatment. 9 weeks following initial damage, the astrocytes were no longer proliferating and the levels of GFAP labelling were comparable to untreated tissue. There was no difference in the astrocytic response to damage between wild-type and ganglioside knockout mice, which suggests that gangliosides are not involved in reactive astrocytosis.

4.3.9 Conclusion and future studies

Due to the destruction of the putative stem cells and subsequent failure of the epithelium to regenerate, it was not possible to properly examine the aims of the study, namely the role of gangliosides in the proliferation of putative stem cell, neuronal outgrowth, or synapse formation. Although some differences were observed, due to the low n-number and high variability these differences were not significantly different. Most of the results obtained from 6 week old mice suggest that at this age, the regeneration of ganglioside knockout mice is similar to that of wild-type but as the regeneration in all genotypes was incomplete it is difficult to draw any conclusions.

However, if the experiment was repeated in older mice with a more suitable concentration of $ZnSO_4$ and a higher number of mice per time-point, it may be possible to properly assess the role of gangliosides in all the processes involved

in the degeneration and regeneration of the olfactory system. Moreover, if complete regeneration was achieved, it would be worthwhile to examine other aspects of the regenerative process such as the formation of immature ORNs, which are characterised by the expression of the phosphoprotein GAP43 (Verhaagen *et al.*, 1989), dendritic changes in the glomeruli, and the inflammatory cell response. Finally, the response of the OECs, which are thought to facilitate regeneration in the olfactory system should be studied in wild-type and ganglioside knockout mice by examining the expression of in vivo OEC markers such as the calcium binding protein S100, which is primarily localised to the cytoplasm of glial cells (Fano *et al.*, 1995), GFAP (Barber *et al.*, 1987), O4 and $p75^{NTR}$ (Au *et al.*, 2003).

5 CHAPTER 5

The effect of gangliosides on oligodendrocyte differentiation and axonal-glial interactions *in vitro*

5.1 Introduction

Myelin facilitates saltatory conduction by restricting sodium currents to nodes of Ranvier and reducing the capacitance of the internodal axonal membrane thereby ensuring rapid and efficient action potential propagation. The molecular architecture of axons and myelin sheaths are specialised for this function. Myelinated axons are divided into four functional regions: nodes of Ranvier, paranodes, juxtaparanodes, and internodes (Poliak and Peles, 2003). Nodes of Ranvier contain clusters of voltage-gated sodium channels (Na_v) in the axonal membrane that are important for the generation of action potentials (Rasband *et al.*, 1999a, Rasband and Trimmer, 2001). The paranodal axonal membrane contains cell adhesion molecules contactin-associated protein (Caspr) (Einheber *et al.*, 1997, Peles *et al.*, 1997) and contactin, while cell adhesion molecule neurofascin 155 (NF155) is present in the paranodal glial membrane. These cell adhesion molecules are important components of paranodal axo-glial junctions: NF155 interacts with a Caspr-contactin complex and thus links glial and axonal membranes at the paranodes (Charles *et al.*, 2002). Caspr and NF155 are associated with lipid rafts. Paranodal axo-glial junctions are important for ion channel clustering and rapid action potential propagation in myelinated nerve fibres. Shaker-type voltage-gated potassium channels (K_v) are localised to juxtaparanodes. In order for the saltatory conduction to occur, it is essential that proteins such as Caspr, NF155, Na_v and K_v assemble in a correct fashion.

Several studies have found that mice lacking complex gangliosides have myelination defects suggesting that they are important for the maintenance of myelin and the integrity of nerve fibres (Chiavegatto *et al.*, 2000, Ma *et al.*, 2003, Sheikh *et al.*, 1999b, Takamiya *et al.*, 1996). Gangliosides are also thought to be important in the maintenance of nodal architecture (Susuki *et al.*, 2007a) and GD1a and GT1b may be important in myelin stability due to their role as MAG ligands. Since GalNAc T -/- mice lack GT1a and GT1b and Sia T -/- mice lack GT1b, it is possible that the absence of these MAG ligands may lead to a decrease in the stability of myelinated axons and the subsequent axonal degeneration.

Oligodendrocytes are the myelinating glia of the CNS and have been shown to differentially express gangliosides. Myelination is paramount for the proper

conduction of neural impulses and failure of oligodendrocytes to re-myelinate is a problem in neurological diseases such as multiple sclerosis (MS). Although oligodendrocyte progenitor cells (OPCs) are present within MS lesions they fail to myelinate the axons (Chang *et al.*, 2000, Chang *et al.*, 2002). Maier et al (Maier *et al.*, 2005) showed that raft association of NF155 was reduced in spinal cord experimental allergic encephalomyelitis rats and that fibronectin perturbed localisation and raft association of NF155 and inhibited the morphological differentiation of oligodendrocytes, suggesting that changes in the extracellular matrix can inhibit re-myelination. Studying the myelination process may help explain the apparent inability of some oligodendrocytes within MS lesions to contribute to the repair process.

To examine further the role of gangliosides in axonal integrity, myelination and interaction between glia and axons, myelinating cultures isolated from spinal cords of E13.5 wild-type and ganglioside knockout mice were utilised. Initially, ganglioside expression of cell types present within spinal cord cultures was examined. Next, the role of gangliosides in the differentiation of oligodendrocytes in the absence or presence of axons was investigated. Subsequently, the effect of gangliosides on axonal survival, myelination and the localisation of nodal proteins was studied.

5.2 Results

5.2.1 Differentiation of wild-type and Sia T -/- OPCs

C-series gangliosides GT3 and O-acetyl GT3 are expressed in the early stage of oligodendrocyte differentiation. As Sia T -/- mice lack these gangliosides the aim of the present study was to investigate if oligodendrocyte precursor cells (OPCs) isolated from 7-day old Sia T -/- mice differentiated into O4 expressing oligodendrocytes. GalNAc T -/- mice which lack all complex gangliosides but have an excess of simple gangliosides such as GT3 and O-acetyl GT3 were not included in this study because GalNAc T -/- litters are a combination of knockout and heterozygous pups, and therefore the optic nerve had to be cultured individually from each pup and then pooled only after the tissue had been genotyped. However, due to the small volume of tissue obtained from optic

nerves, it is not feasible to culture them individually hence why this experiment was not performed using GalNAc T -/- mice.

The antibody A2B5, which is expressed before O4 during oligodendrocyte differentiation, was used to detect c-series gangliosides GT3 and O-acetyl GT3. As shown in Figure 5.1 A, wild-type early OPC expressed A2B5 when maintained in DMEM-BS containing FGF and PDGF. In contrast, Sia T -/- OPCs maintained under the same conditions did not express A2B5 as shown in Figure 5.1 B. When the growth factors were removed, OPCs isolated from Sia T -/- mice, differentiated into multiprocessed O4-expressing oligodendrocytes as can be seen in Figure 5.1 B. Subsequently, myelin membrane was evident (Figure 5.1 B). When maintained in medium containing serum they differentiate into type-2 astrocytes (Figure 5.1 B).

These findings suggest that, in the absence of axons, c-series gangliosides do not affect oligodendrocyte differentiation.

5.2.2 Dissociated spinal cord culture: cell composition

The next objective was therefore to investigate the effect of gangliosides on oligodendrocyte differentiation in the presence of axons and subsequently, glial-axonal interaction. For this purpose, dissociated spinal cord cultures from E13.5 mice were utilised. These cultures contain a mixture of cells including astrocytes, OPCs, neurons and microglia as can be seen in Figure 5.2. Using this culture system, a series of events can be studied over time including neuronal survival, neurite extension and the ensheathment and myelination of axons by endogenous oligodendrocytes in the culture (Sorensen *et al.*, 2008).

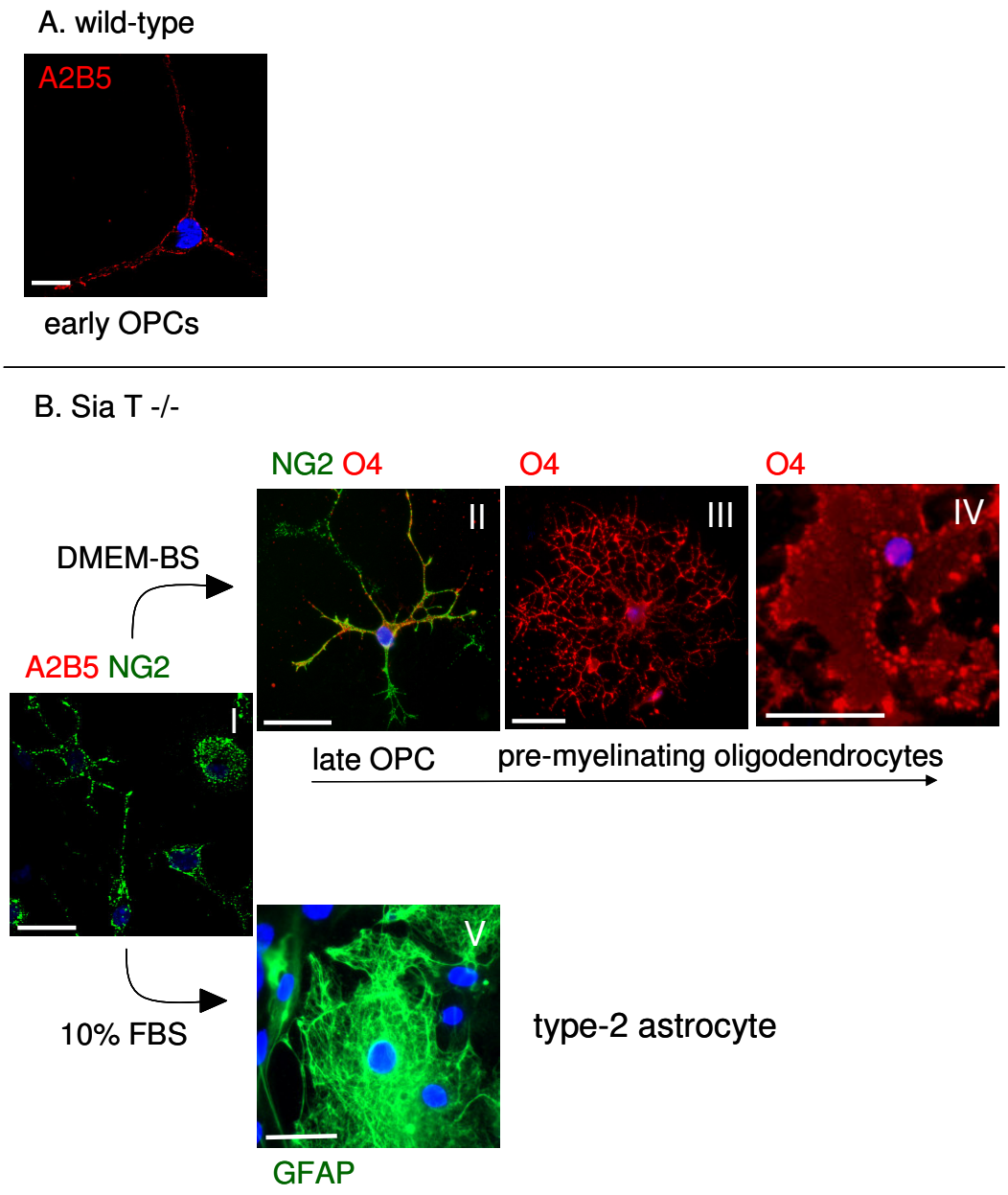

Figure 5.1. OPCs isolated from Sia T -/- mice did not express A2B5 but were able to differentiate into O4 expressing oligodendrocytes.
(A) Early OPCs isolated from wild-type P7 mice expressed the marker, A2B5. OPCs grown in DMEM-BS with no added growth factors differentiated into oligodendrocytes, whereas those grown in 10% FBS differentiated into type-2 astrocytes. (B) Early OPCs isolated from P7 Sia T -/- mice, labelled with NG2 (I), were negative for A2B5, however, their differentiation into O4-expressing oligodendrocytes (II-IV) or type-2 astrocytes (V) was unaffected. Scale bars = 50 μm

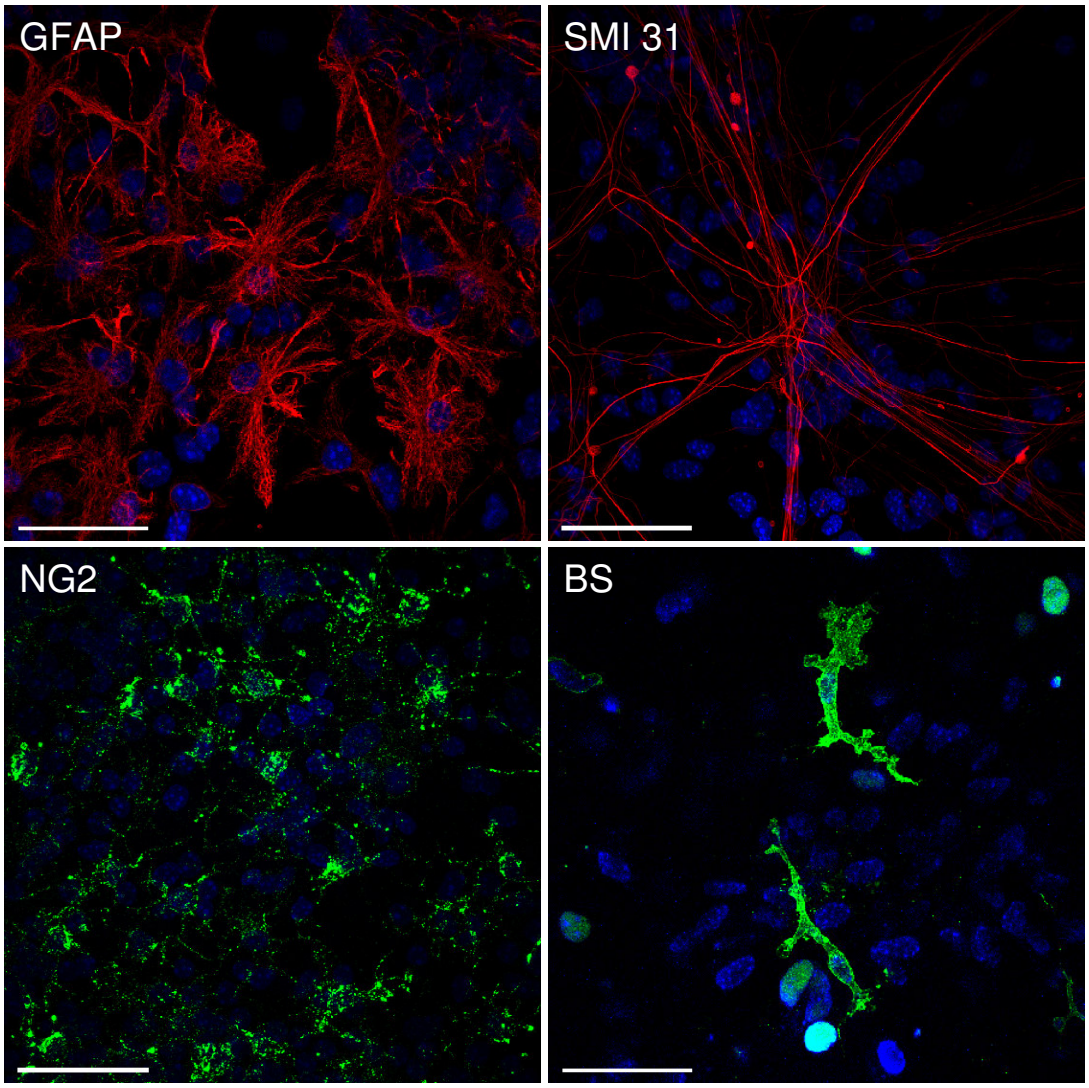

Figure 5.2. Cell composition of dissociated spinal cord cultures at 7 DIV.
Spinal cord cultures from wild-type E13.5 mice were labelled with various markers to elucidate their cellular composition. Astrocytes (GFAP, red), neurons (SMI 31, red) and OPCs (NG2, green) were the main cells present in these cultures. There was also a small number of microglia (BS lectin, green). Cell nuclei were labelled with DAPI (blue). Scale bars = 50 μm.

5.2.3 Comparison of culture media

Neurobasal B27 (NB) is a medium commonly used for the study of axonal glial interaction and myelination (Brewer *et al.*, 1993); www.invitrogen.com). However, according to Thomson *et al* (2006), who compared NB with a serum-free defined medium "differentiation medium", myelination was better in cultures maintained in differentiation media. These two media were therefore compared to optimise conditions for myelination in wild-type and Sia T -/- spinal cord cultures.

To compare the antigenic differentiation of oligodendrocytes grown in either differentiation or NB media, the cultures were labelled with antibodies to antigens expressed at different stages of oligodendrocyte differentiation (NG2, O4 and MBP) at 21 and 28 DIV. NG2 positive cells correspond to early OPCs; cells which label with both NG2 and O4 correspond to late OPCs; cells which are only O4 positive are intermediate between the late OPCs and pre-myelinating oligodendrocyte stage; O4- and MBP- positive cells are pre-myelinating oligodendrocytes and cells which are only MBP positive are myelinating oligodendrocytes (see Introduction Figure 1.5). Figure 5.3 shows the proportion of cells immunoreactive for NG2, NG2/O4, O4, O4/MBP and MBP in wild-type and Sia T -/- cultures after 21 and 28 DIV. No significant difference was found in the proportion of cells immunopositive for NG2, O4, and MBP alone or in combination between cultures grown in differentiation medium and cultures grown in NB medium. Representative images of wild-type spinal cord cultures at 28 DIV grown in differentiation medium and NB medium (Figure 5.4) showed that although there was no difference in the proportion of cells labelled with oligodendrocyte lineage markers, the cells differed morphologically. O4-positive cells grown in differentiation medium had a dense network of secondary and tertiary processes. In contrast, O4-positive cells grown in NB medium were less branched, containing mostly primary processes with few secondary processes. Those that were not in contact with axons seemed to produce myelin-like membrane.

Next, the effect of the two different media, differentiation versus NB, on neuronal survival and axonal density were examined. Axon density, expressed as the percentage of SMI 31-immunoreactivity per given area, was calculated for

embryonic spinal cord cultures plated onto PLL at 21 and 28 DIV. The percentage of axons that were myelinated was assessed using the antibody AA3, which binds to PLP/DM20 and recognises compact myelin. There was no significant difference in axonal density or the myelination of these between cultures grown in differentiation medium or in NB medium as illustrated in Figure 5.4 (panel B). Since the morphology of oligodendrocytes maintained in differentiation medium was more similar to that described in the literature (Trapp et al, 1997), subsequent cultures were grown in differentiation medium.

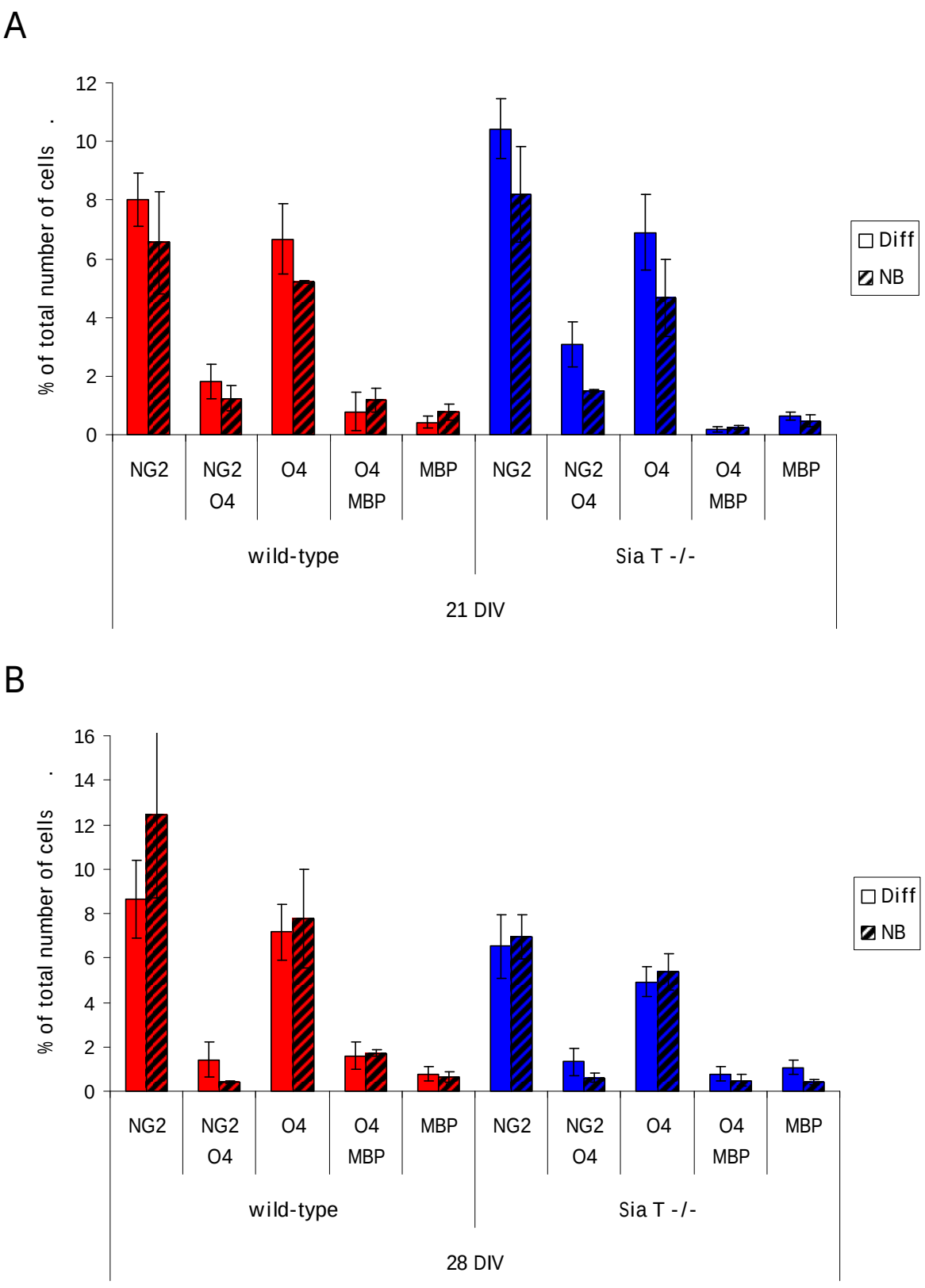

Figure 5.3. Antigenic profile of oligodendrocytes in differentiation and neurobasal media.

Wild-type and Sia T -/- dissociated spinal cord cultures were grown in either differentiation or neurobasal media, and were stained with markers of the oligodendrocyte lineage at 21 (A) and 28 DIV (B): NG2, O4 and MBP. The graphs represent the percentage of total cells positive for NG2, NG2/O4, O4, O4/MBP and MBP in spinal cord cultures grown in either differentiation or neurobasal B27 medium. There was no significant difference in the proportion of cells expressing antigens recognised by these antibodies alone or in combination between the two culture media. Diff = differentiation medium, NB = neurobasal medium with B27 supplement. Each point represents the average ± SEM (n=3).

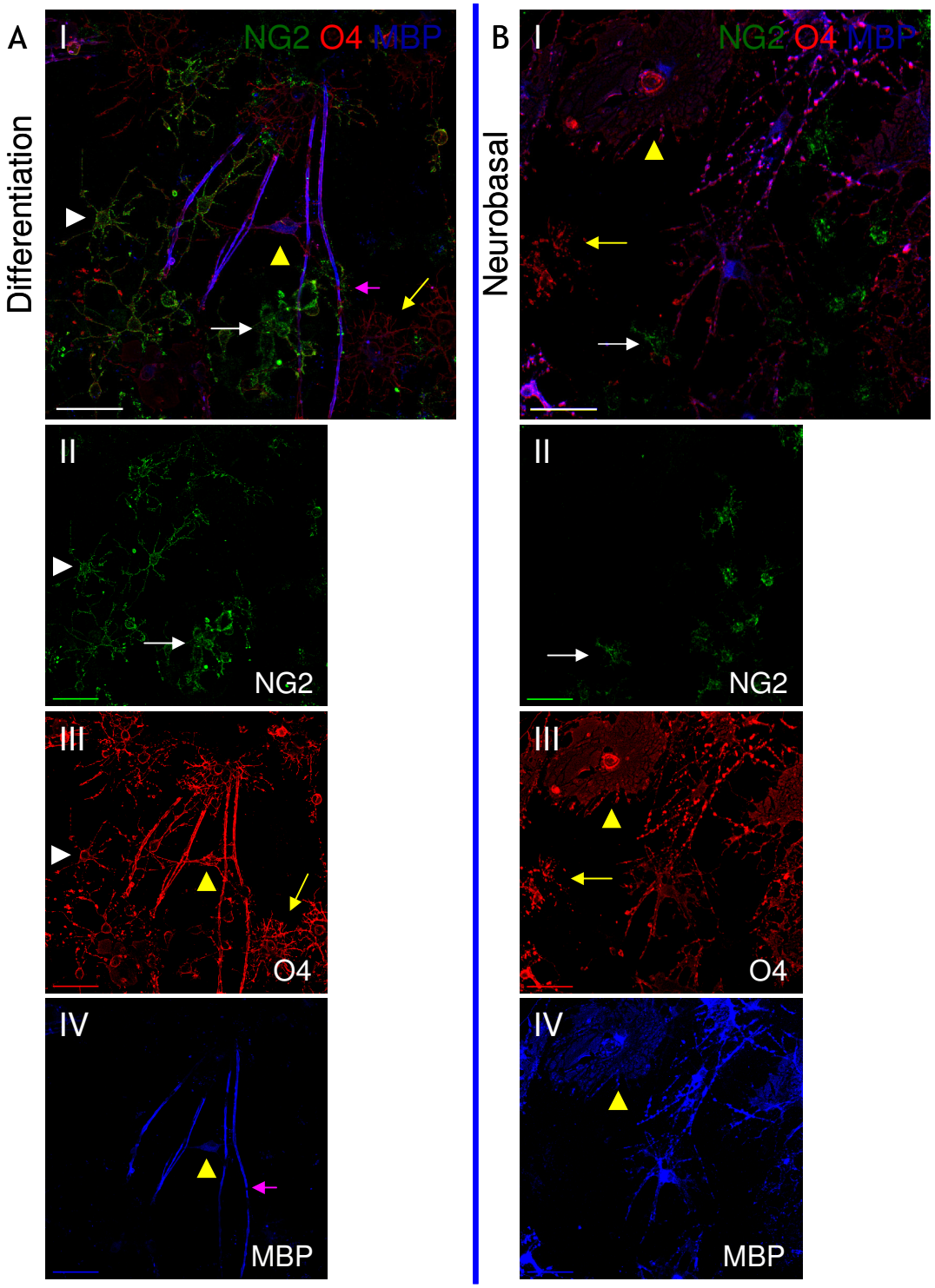

Figure 5.4. Wild-type spinal cord culture at 28 DIV in differentiation and neurobasal media. Representative image of wild-type spinal cord culture at 28 DIV grown in differentiation (A) and neurobasal (B) media and immunolabelled with NG2 (green, II), O4 (red, III) and MBP (blue, IV). The merged image is shown in I, while II to IV show the individual markers. Examples of following can be seen in these images: NG2+ early OPCs (white arrow), NG2+/O4+ late OPCs (white arrowhead), O4+ oligodendrocytes (yellow arrow), and O4+/MBP+ pre-myelinating oligodendrocytes (yellow arrowhead). Note that in cultures maintained in differentiation medium, NG2+ cells are branched with primary and secondary processes and O4+ cells have a dense network of primary, secondary and tertiary processes. Also, the O4+/MBP+ staining resembles myelin formed following contact with axons and there is a break in the MBP staining resembling a node of Ranvier (pink arrow). In cultures maintained in neurobasal medium, the processes of NG2+ and O4+ cells appear to be shorter compared with those seen in differentiation medium. Also, some O4+/MBP+ labelling resembles myelin membranes formed by oligodendrocytes which have failed to contact an axon. Scale bar = 50 μm.

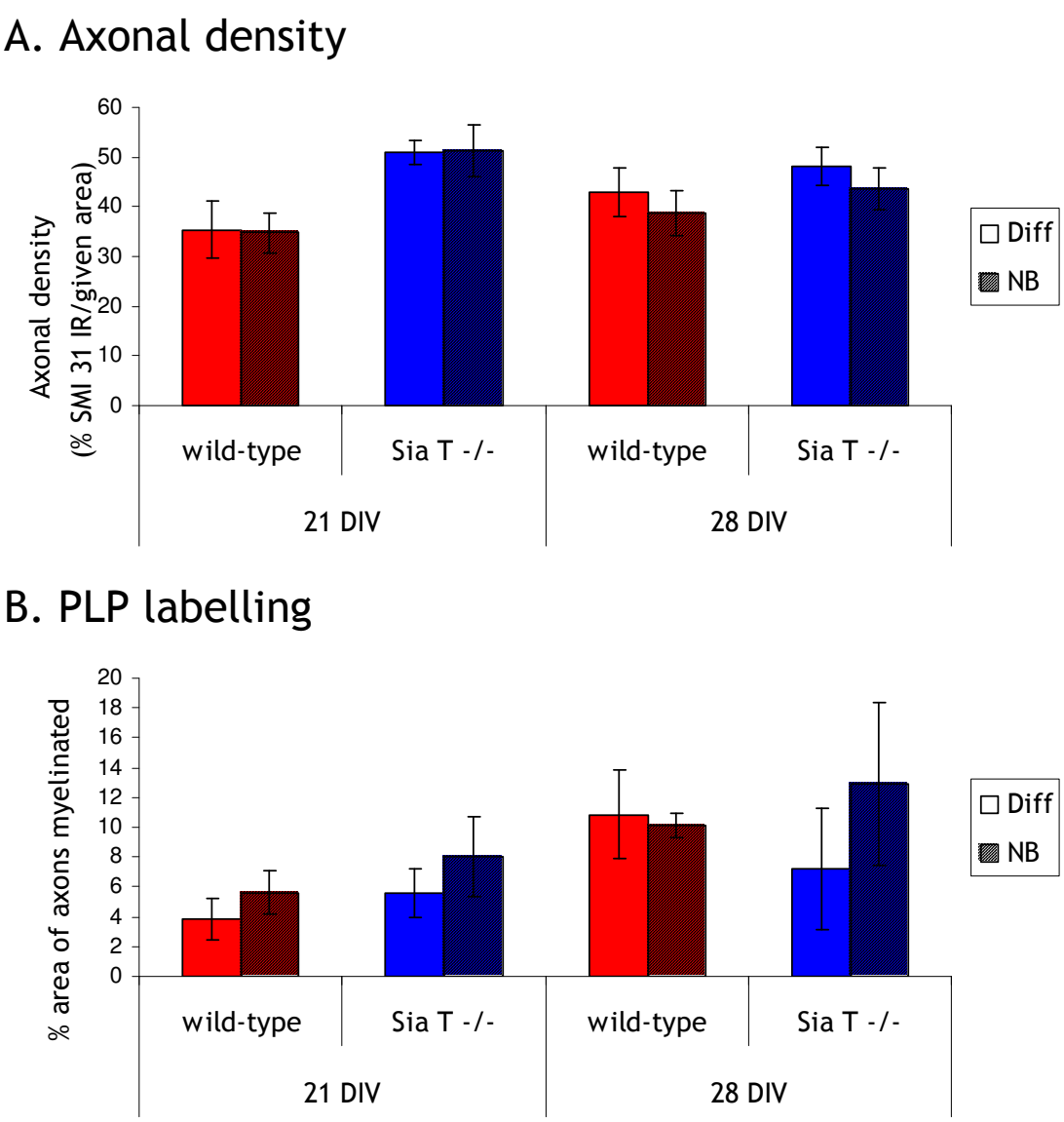

Figure 5.5. Axonal density and PLP labelling in spinal cord cultures grown in either "differentiation" or "neurobasal" media.
Spinal cord cultures isolated from wild-type and Sia T -/- mice and maintained in either differentiation or neurobasal media were labelled with an axonal marker, SMI 31, and PLP expression was revealed by staining for AA3. Axonal survival was gauged by measuring axonal density (A) and was found to be similar in both media. In addition, the percentage of axonal area covered by myelin (B) was not significantly different between cultures maintained in differentiation or neurobasal media. Each point represents the average ± SEM (n=3).

5.2.4 Ganglioside expression of dissociated spinal cord cultures.

Having established the optimal medium for myelination of axons in the dissociated spinal cord cultures, the ganglioside content of these cultures was examined. Before studying the role of gangliosides in myelination and glial-axonal interaction, it was important to demonstrate which gangliosides were expressed by cells present in the culture system. Four ganglioside markers were chosen for this purpose: A2B5 and R24, which bind to simple gangliosides GT3, O-acetyl GT3 and GD3 and are differentially expressed during oligodendrocyte differentiation; CTx, which binds to the major brain ganglioside GM1; and MOG35, which is an antibody against ganglioside GD1a, the axonal ligand for MAG.

All of the antigens labelled by the antibodies used in this study were found in wild-type dissociated spinal cord cultures (Figure 5.6). A2B5, which binds to c-series gangliosides GT3 and O-acetyl GT3, was found in GalNAc T -/- cultures, where the intensity was slightly higher compared to wild-type, but no positive immunoreactivity was found in Sia T -/- cultures which lack all c-series gangliosides (Figure 5.6). To examine more specifically which cell types within the spinal cord cultures (astrocytes, oligodendrocytes or neurons) expressed antigens recognised by A2B5 at 21 DIV, the cultures were double labelled with A2B5 and one of the following antibodies: SMI 31, which is specific for phosphorylated epitopes on the heavy neurofilament peptide and to a lesser extent medium neurofilament peptide; TUJ1, which binds to the neuron specific Class III β-tubulin; NG2, which labels early OPCs; or GFAP, which binds to astrocytes (Figure 5.7). A2B5 showed co-localisation with TUJ1 and SMI 31 as shown in Figure 5.7 suggesting that neurites express gangliosides. A2B5 was also expressed by OPCs as shown by its co-expression with NG2 (Figure 5.7). While the majority of GFAP positive cells were negative for A2B5 (type-1 astrocytes), some were co-labelled with A2B5, indicating the presence of type-2 astrocytes (Figure 5.7). A similar pattern of co-localisation was found between A2B5 and SMI 31, TUJ1, NG2 and GFAP in cultures isolated from GalNAc T -/- mice.

R24, which binds to gangliosides GD3, GT1a and GQ1b was expressed in wild-type and GalNAc T -/- cultures, but not in Sia T -/- cultures (Figure 5.6). Sia T -

/- mice lack all b-series gangliosides including GD3 and GQ1b, while GalNAc T -/- mice lack all complex gangliosides including GT1a and GQ1b but have increased levels of GD3. The R24 positive staining in GalNAc T -/- cultures is therefore due to R24 recognising the simple b-series ganglioside GD3 (Figure 5.6). R24 expression was stronger and more prevalent in GalNAc T -/- cultures than in wild-type. To ascertain which cell type within the wild-type spinal cord cultures expressed R24 at 21 DIV, the cultures were double labelled with R24 and one of the following antibodies: NG2, O4, which labels oligodendrocytes, SMI 31 or GFAP (Figure 5.8). As shown in Figure 5.8, R24 was co-expressed in NG2 positive cells indicating that OPCs express at least some of the gangliosides recognised by this antibody. In addition, R24 was expressed in some, but not all, O4 positive oligodendrocytes: oligodendrocytes which were R24 negative were generally multi-processed and appeared to be in a later stage of the oligodendrocyte differentiation than R24 positive O4 cells (Figure 5.8). While the majority of GFAP positive cells were negative for R24 (Figure 5.8), there were a few examples of R24 co-expression with GFAP, albeit rare. Furthermore, the GFAP/R24 positive cells had a different morphology from other GFAP-positive cells as their GFAP staining was diffuse as opposed to fibrous as shown in Figure 5.8. R24 and SMI 31 did not co-localise, indicating that axons containing phosphorylated neurofilaments do not express the gangliosides recognised by this antibody (GD3, GT1a, GQ1b).

To examine to which cell type the increased R24 expression seen in GalNAc T -/- cultures was localised, these were double labelled with R24 and one of the following antibodies: NG2, GFAP, or SMI 31 (Figure 5.8). The increased R24 immunolabelling in GalNAc T -/- cultures appeared to resemble axons, so it was surprising that the majority of SMI 31 positive axons were negative for R24 (Figure 5.8). However, when using the TUJ1 antibody, which labels both axons and dendrites, co-staining with R24 was evident as shown in Figure 5.8 (panel D). This suggests that GD3 was expressed in axons containing non-phosphorylated neurofilament and dendrites and to a lesser extent in axons containing phosphorylated neurofilament recognised by SMI 31. As in the wild-type cultures, GalNAc T -/- cultures also showed that R24 was expressed by cells early in the oligodendrocyte lineage as shown in Figure 5.8 (Panel F). Unlike in wild-type cultures, none of the astrocytes in GalNAc T -/- cultures were positive for R24 as shown in Figure 5.8 (panel J).

To examine whether myelinating oligodendrocytes expressed gangliosides recognised by A2B5 and R24, spinal cord cultures were co-labelled with AA3 after 28 DIV (Figure 5.9). It was found that myelinating oligodendrocytes as recognised by AA3, were negative for both A2B5 and R24 as shown in Figure 5.9.

Immunoreactivity for CTx, which binds to GM1 was apparent in wild-type and Sia T -/- cultures but not GalNAc T -/- cultures as shown in Figure 5.6. Furthermore, in Sia T -/- cultures the intensity of the reactivity appeared to be slightly higher than in wild-type. This may be due to an increase in the expression of a-series ganglioside GM1, in Sia T -/- mice. As CTx specifically binds to a-series ganglioside GM1, it is not expressed in GalNAc T -/- cultures which lack all a-series gangliosides (Figure 5.6). To determine which cell types within the spinal cord cultures expressed GM1 at 21 DIV, wild-type cultures were double labelled with CTx and one of the following markers: O4, GFAP or SMI 31 (Figure 5.10). GFAP positive astrocytes did not express GM1 as shown in Figure 5.10. After 21 DIV CTx was not expressed in O4 positive oligodendrocytes (Figure 5.10). Contrastingly, after 28 DIV the O4 positive oligodendrocytes did co-express CTx (Figure 5.11), suggesting that GM1 expression is switched on in the more mature phenotype. AA3 positive oligodendrocytes were also positive for CTx (Figure 5.11). The majority of SMI 31 positive axons co-labelled with CTx after 21 DIV, however, at day 28, this was not always the case as shown in Figure 5.11. Although in many instances CTx labelling was found throughout the myelinated axon, it was sometimes expressed near nodes of Ranvier in the paranodal region (Figure 5.11). A similar pattern was seen in cultures isolated from Sia T -/- mice.

MOG35, which is specific for a-series ganglioside GD1a, was expressed in wild-type and Sia T -/- cultures but not in GalNAc T -/- cultures as these lack all a-series gangliosides (Figure 5.6). To elucidate which cell types express GD1a in the wild-type and Sia T -/- spinal cord cultures, these were double labelled with MOG 35 and one of the following antibodies: SMI 31, O4 or GFAP at 21 DIV (Figure 5.12). GD1a was expressed on many, but not all, SMI 31 positive axons as shown in Figure 5.12 (panel A). GFAP positive astrocytes were negative for MOG35 as shown in Figure 5.12 (panel C). O4 positive oligodendrocytes did not express MOG 35 as shown in Figure 5.12 (panel B), however, AA3 positive

oligodendrocytes co-expressed MOG35 as illustrated in Figure 5.13. In addition, an unidentified cell type expressed MOG35 as shown in Figure 5.12 (panel D).

To summarise, various cell types (neurons, oligodendrocytes and astrocytes) within the spinal cord cultures expressed gangliosides investigated in this study, although some at different stages of development (see Table 5.1).

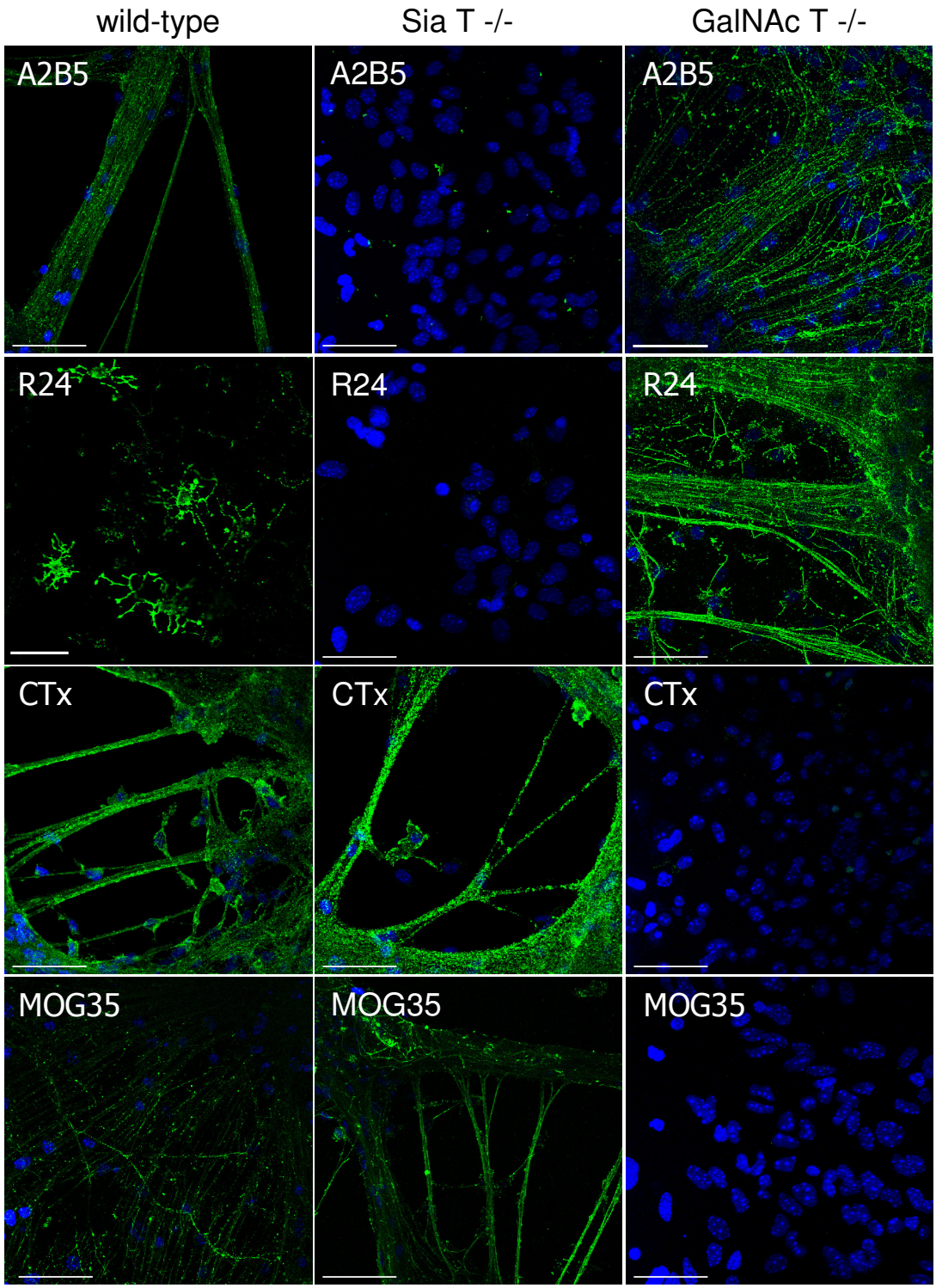

Figure 5.6. Ganglioside expression of dissociated spinal cord cultures from wild-type, Sia T -/- and GalNAc T -/- mice.
Dissociated spinal cord cultures from wild-type, GD3 S -/- and GalNAc T -/- mice were stained with CTx and antibodies A2B5, R24 and MOG35 at 21 DIV. Wild-type and GalNAc T -/- cultures were positive for A2B5, which binds c-series gangliosides GT3 and O-acetyl GT3, whereas Sia T -/- cultures lack all c-series gangliosides and therefore do not label with this antibody. Wild-type and GalNAc T -/- cultures express R24, although the staining in GalNAc T -/- is stronger and more prevalent, suggesting an upregulation of b-series ganglioside GD3 which is labelled with R24. Sia T -/- mice lack all b-series gangliosides and therefore do not label with R24. Wild-type and Sia T -/- cultures label with CTx and MOG35 which label a-series gangliosides GM1 and GD1a, respectively. GalNAc T -/- lack all a-series gangliosides and therefore do not label with these two markers. Nuclei were labelled with DAPI (blue). Scale bar = 50 μm.

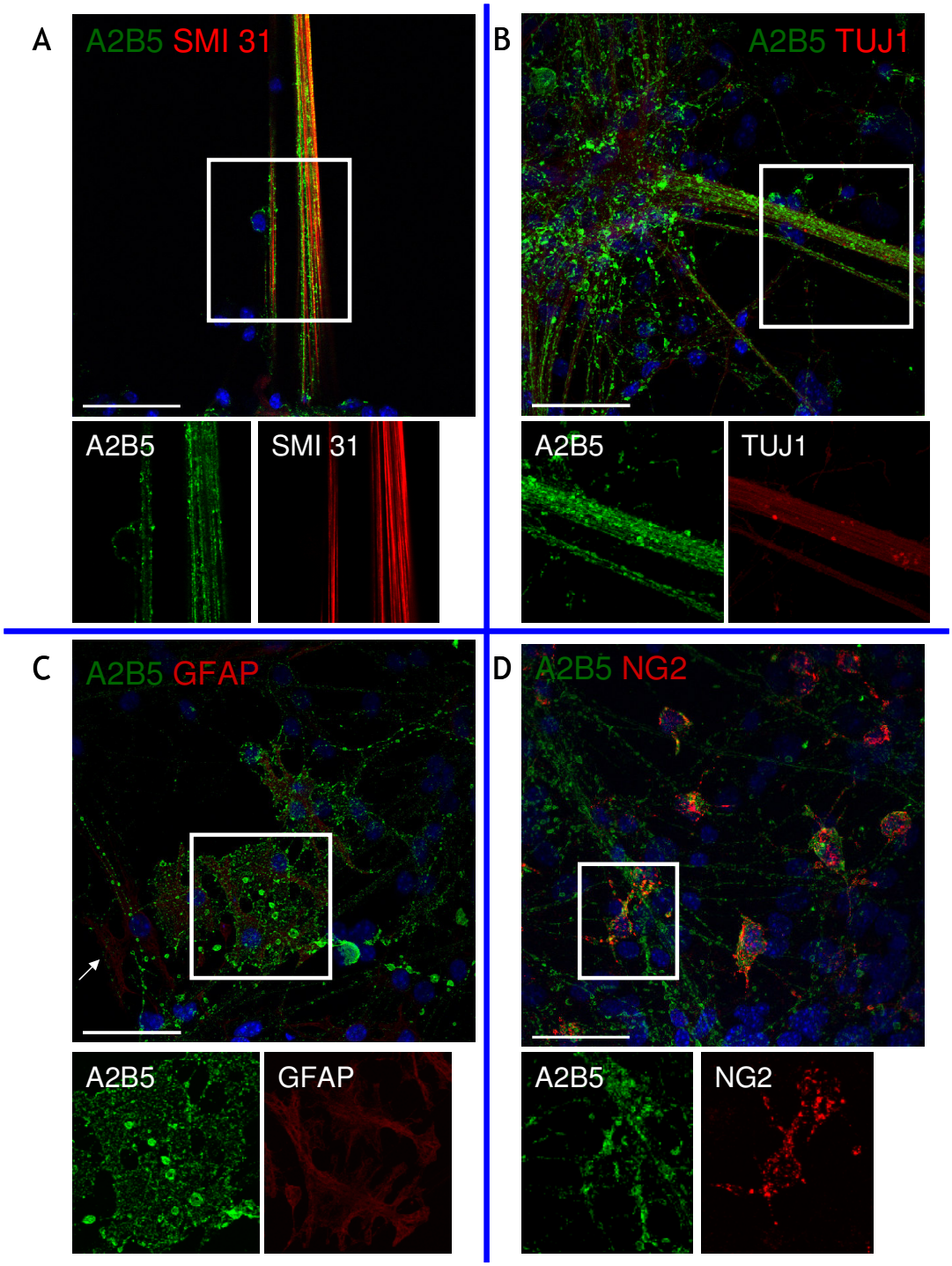

Figure 5.7. A2B5 co-localised with SMI 31, TUJ1, GFAP and NG2 in wild-type cultures at 21 DIV.
Wild-type spinal cord cultures were double labelled with A2B5 and one of the following markers after 21 DIV: SMI 31 (A), TUJ1 (B), GFAP (C) and NG2 (D). The co-localisation of A2B5 with SMI 31 and TUJ1 in spinal cord cultures indicated that spinal cord neurons express gangliosides GT3 and/or O-acetyl GT3, both of which are A2B5 antigens. A2B5 staining co-localised with NG2 which indicated that OPCs express GT3 and/or O-acetyl GT3. The majority of GFAP positive astrocytes within spinal cord cultures were A2B5 negative (arrow), suggesting they are type-1 astrocytes. However, a subset of GFAP positive astrocytes was also labelled with A2B5 suggesting they are type-2 astrocytes. Nuclei were labelled with DAPI (blue). Scale bar = 50 μm.

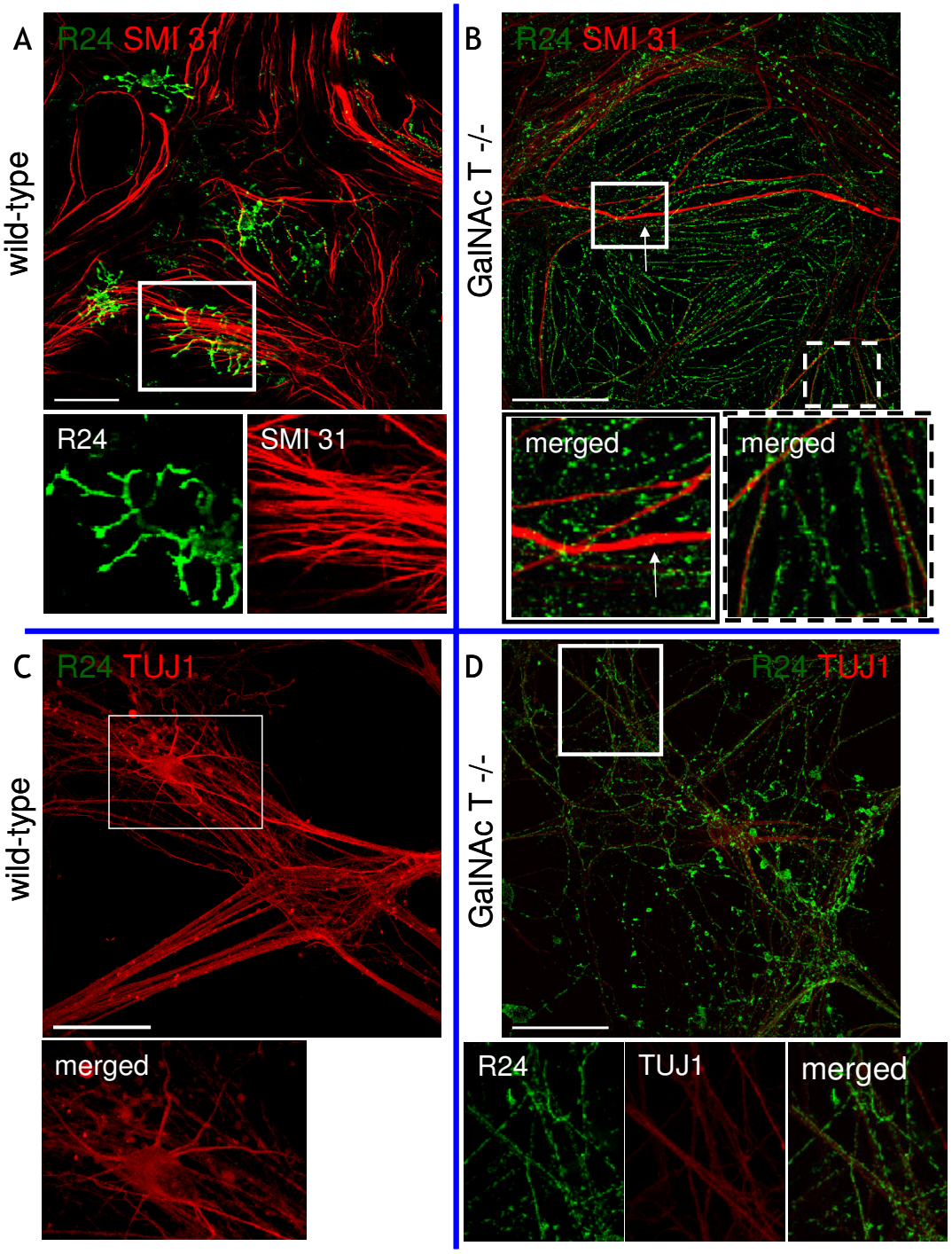
A
R24 SMI 31
wild-type
R24
SMI 31
B
R24 SMI 31
GalNAc T -/-
merged
merged
C
R24 TUJ1
wild-type
merged
D
R24 TUJ1
GalNAc T -/-
R24
TUJ1
merged

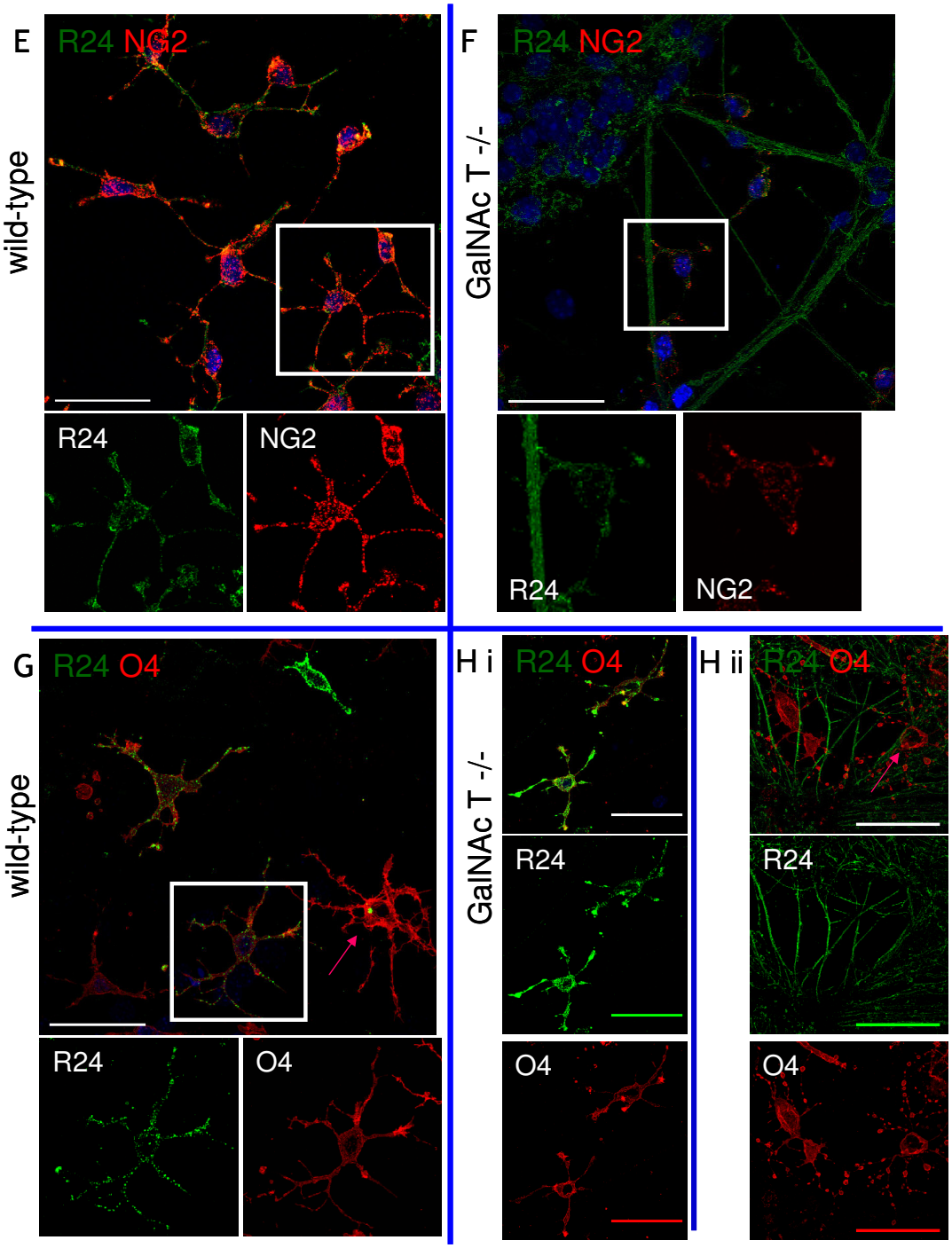
E
R24 NG2
wild-type
R24
NG2
F
R24 NG2
GalNAc T -/-
R24
NG2
G
R24 O4
wild-type
R24
O4
H i
R24 O4
GalNAc T -/-
R24
O4
H ii
R24 O4
R24
O4

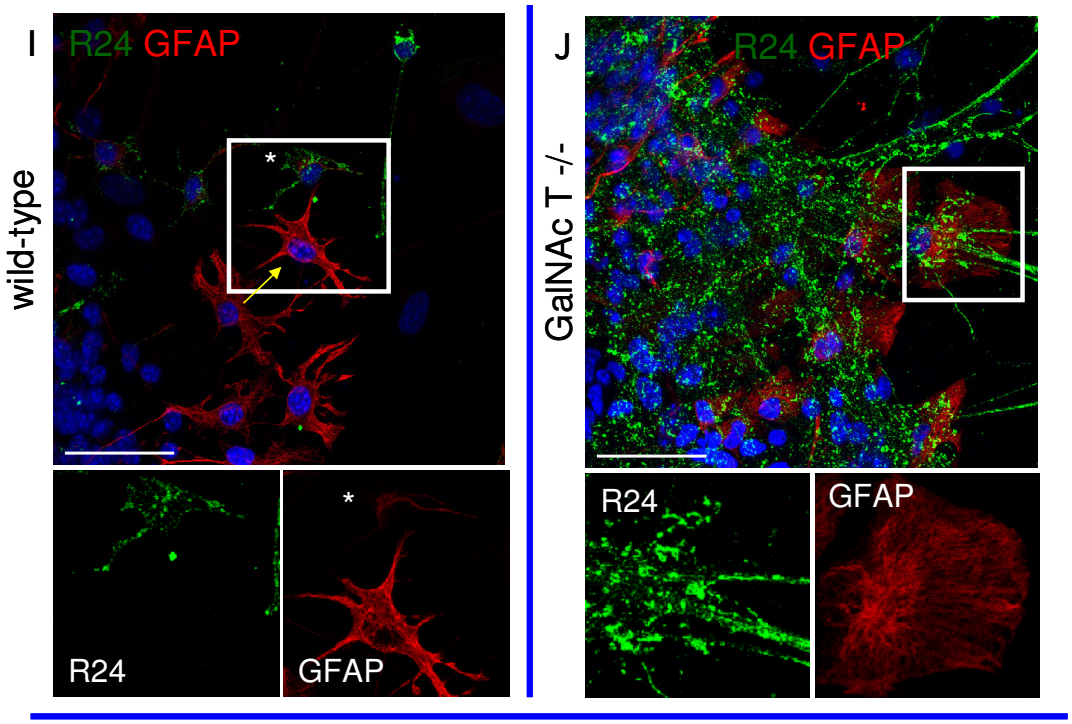

Figure 5.8. R24 expression in wild-type and GalNAc T -/- cultures at 21 DIV.
Wild-type (A, C, E, G and I) and GalNAc T -/- (B, D, F, H and J) spinal cord cultures were double labelled with R24 and one of the following markers after 21 DIV: SMI 31 (A and B), TUJ1 (C and D), NG2 (E and F), O4 (G and H) and GFAP (I and J). Wild-type neurites were negative for both SMI 31 and TUJ1, whereas GalNAc T -/- neurites expressed the simple ganglioside GD3 as indicated by the co-localisation of R24 with SMI 31 (dashed box in B) and TUJ1. However, not all SMI 31 positive axons expressed GD3 (white arrow in B). The co-localisation of R24 with NG2 in these cultures indicated that OPCs express gangliosides recognised by this antibody. O4 positive oligodendrocytes in the early stages of oligodendrocyte lineage expressed R24 (G and H i), while those with an extensive network of processes that appeared to be in the later stages of differentiation were R24 negative (pink arrow in G and H ii). While a subset of GFAP-positive astrocytes within wild-type spinal cord cultures were R24 immunoreactive (*), the majority were R24 negative (yellow arrow). All of the GFAP positive astrocytes within GalNAc T -/- cultures were R24 negative, suggesting these are type-1 astrocytes. Nuclei were labelled with DAPI (blue). Scale bar = 50 μm.

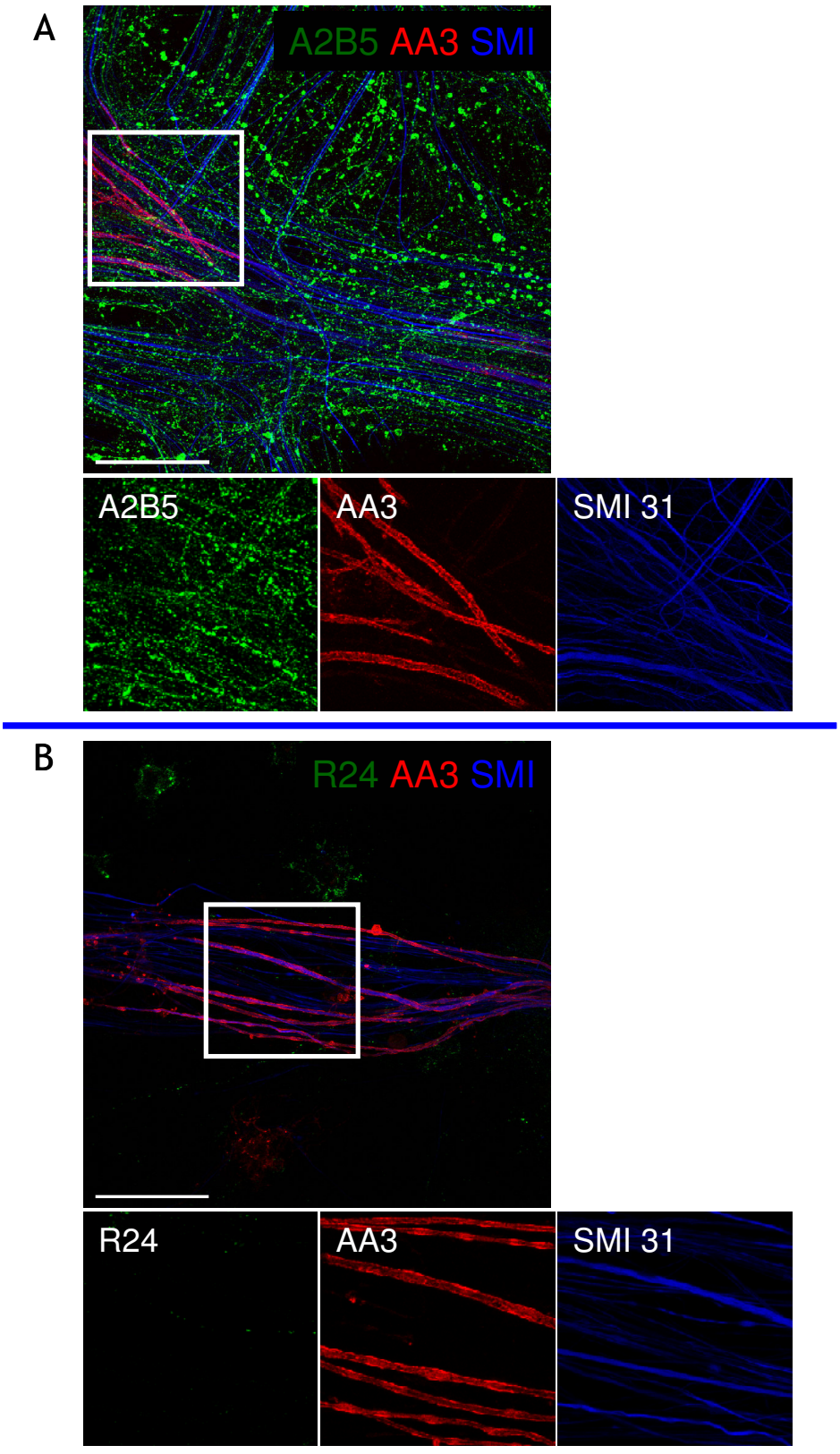

Figure 5.9. A2B5 and R24 were not expressed by myelinating oligodendrocytes at 28 DIV. Wild-type spinal cord cultures were triple labelled with AA3, SMI 31 and either A2B5 (A) or R24 (B) after 28 days in culture. A2B5 and R24 did not co-localise with AA3 suggesting that myelinating oligodendrocytes did not express simple gangliosides GT3, O-acetyl GT3 or GD3. Scale bar = 50 µm.

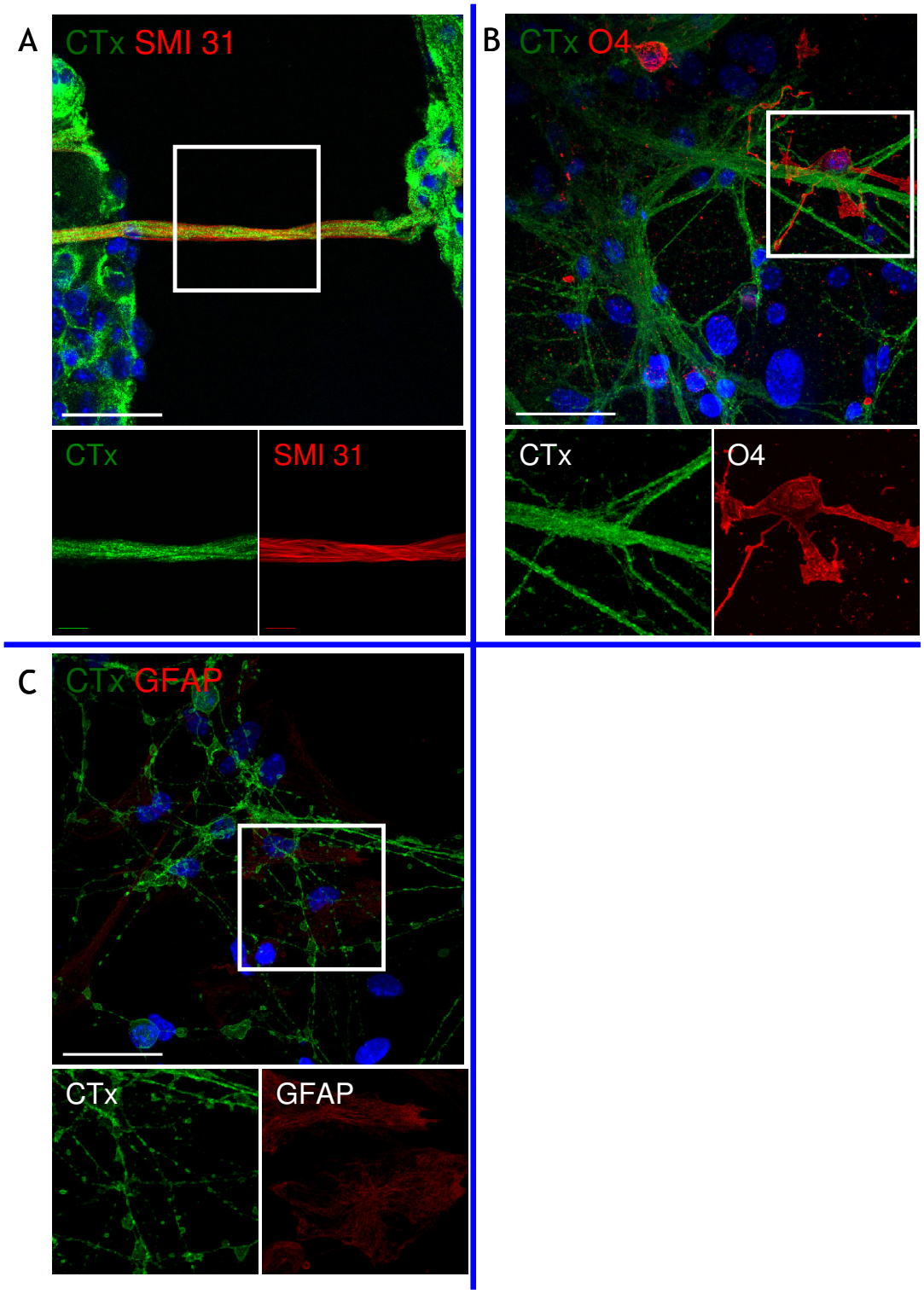

Figure 5.10. CTx co-localises with SMI 31 in wild-type cultures at 21 DIV.
Wild-type spinal cord cultures were double labelled with CTx, which specifically binds ganglioside GM1, and one of the following markers after 21 DIV: SMI 31 (A), O4 (B) and GFAP (C). The co-localisation of CTx with SMI 31 in these cultures indicated that phosphorylated neurofilament expresses GM1. All of the GFAP positive astrocytes and O4 positive oligodendrocytes within these cultures were CTx negative at 21 DIV. Nuclei were labelled with DAPI (blue). Scale bar = 50 µm.

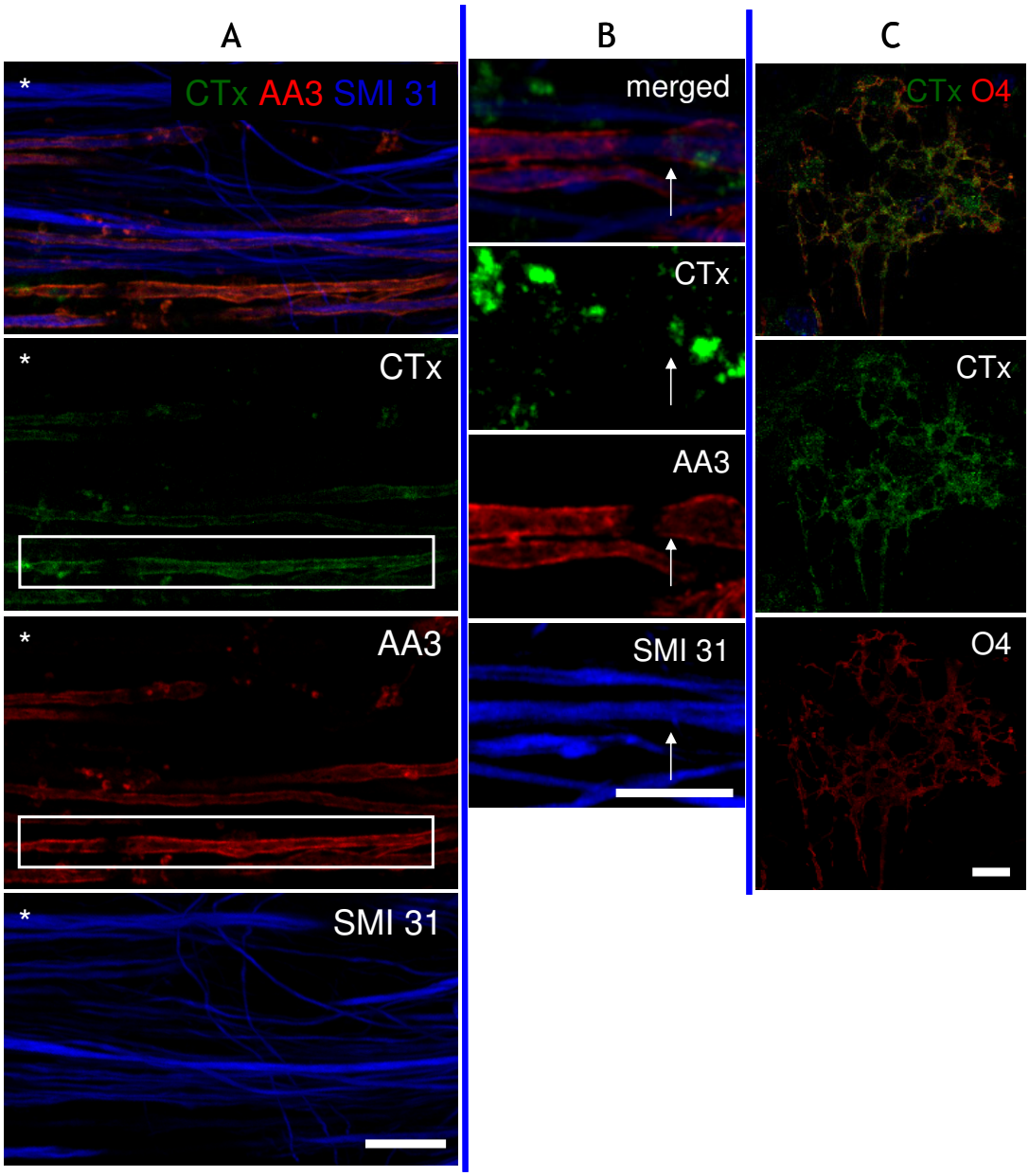

Figure 5.11. CTx co-localised with SMI 31, AA3 and O4 in wild-type cultures at 28 DIV. Wild-type spinal cord cultures were double labelled with CTx and the following markers after 28 DIV: SMI 31 and AA3 (A and B) or O4 (C). CTx expression changed between 21 and 28 DIV in that O4 positive oligodendrocytes which were in the late stage of differentiation became CTx positive whereas fewer SMI 31 positive axons showed CTx-immuoreactivity. (*) shows an SMI 31 positive axon which was negative for CTx. Also, at 28 DIV CTx was co-localised with AA3, which recognises myelin (box). However, in some instances CTx labelling was not observed throughout the myelin, but rather in the paranodal region (arrow). Nuclei were labelled with DAPI (blue). Scale bar = 10 µm.

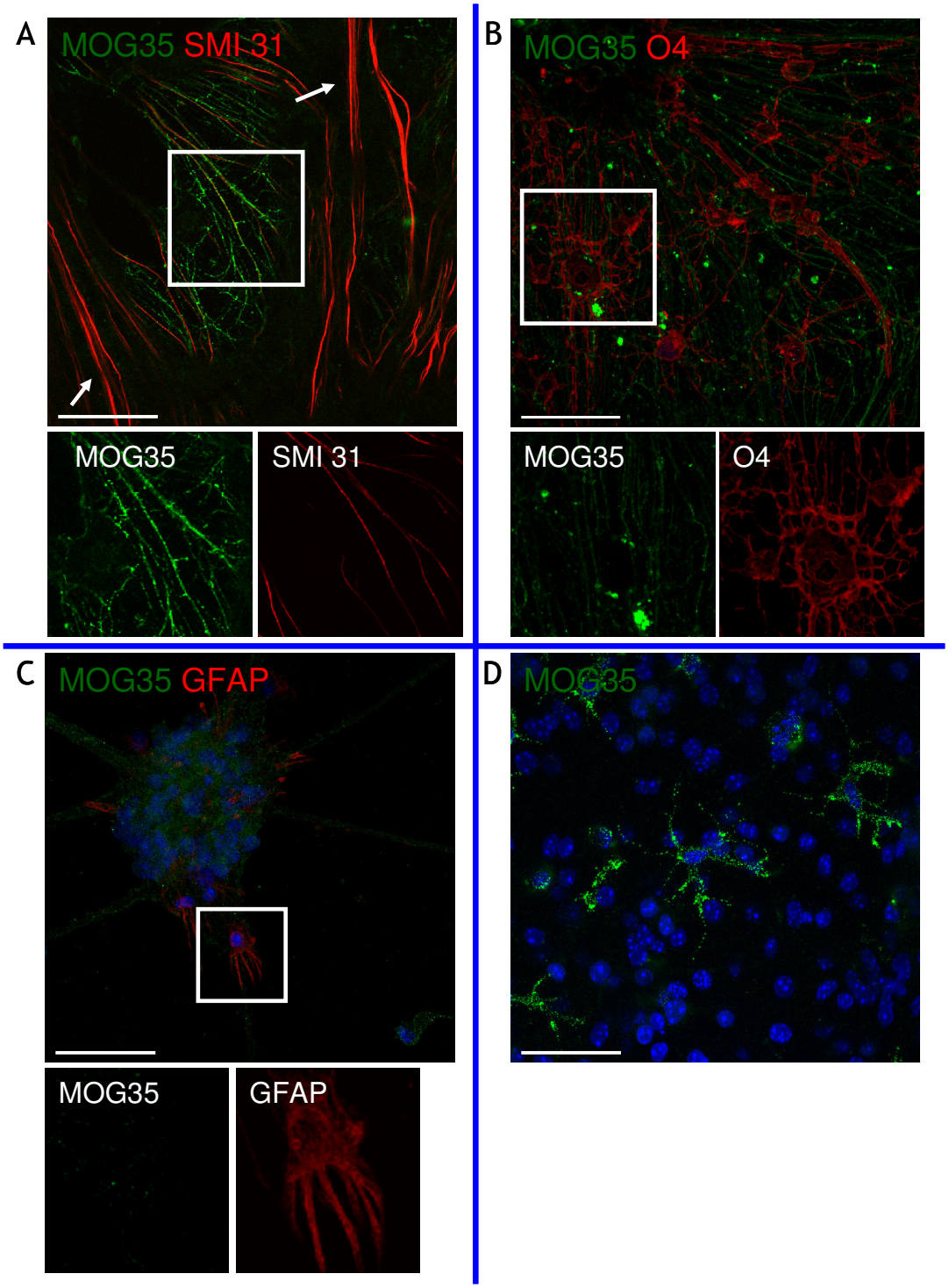

Figure 5.12. MOG35 co-localised with SMI 31 in wild-type cultures at 21 DIV.
Wild-type spinal cord cultures were double labelled with MOG35 and one of the following markers after 21 DIV: SMI 31 (A), O4 (B) or GFAP (C). Oligodendrocytes and astrocytes did not express GD1a since O4 and GFAP did not co-localise with MOG 35. Some SMI 31 positive axons expressed GD1a, whereas others did not (arrow). There were MOG35 positive cells which did not label with SMI 31, O4 or GFAP (D). Nuclei were labelled with DAPI (blue). Scale bar = 50 µm.

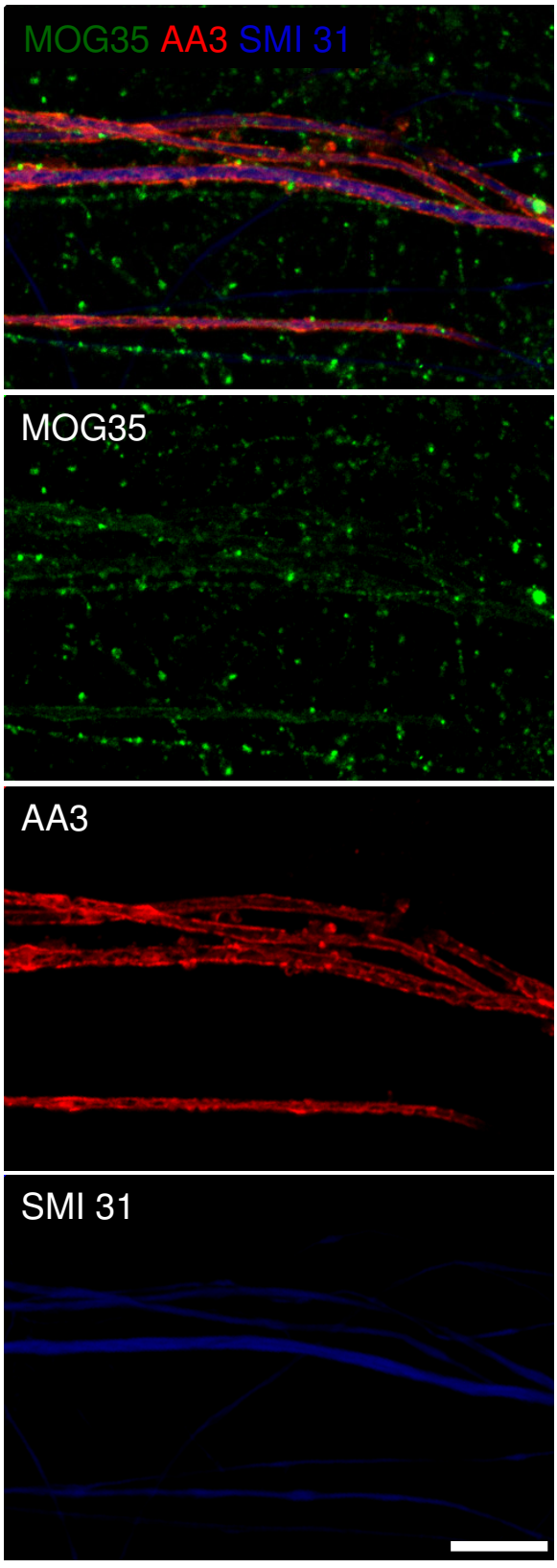

Figure 5.13. MOG35 co-localised with AA3 in wild-type cultures at 28 DIV.
Wild-type spinal cord cultures were triple labelled with AA3, SMI 31 and MOG35 after 28 days in culture. MOG35 co-localised with AA3 suggesting that myelinating oligodendrocytes expressed simple gangliosides GD1a. Scale bar = 10 µm.

Marker	Binds to ganglioside:			wild-type				Sia T -/-				GalNAc T -/-			
	a-series	b-series	c-series	neurites (SMI 31, TUJ1)	astrocytes (GFAP)	OPCs (NG2)	oligodendrocytes (O4, AA3)	neurites (SMI 31, TUJ1)	astrocytes (GFAP)	OPCs (NG2)	oligodendrocytes (O4, AA3)	neurites (SMI 31, TUJ1)	astrocytes (GFAP)	OPCs (NG2)	oligodendrocytes (O4, AA3)
A2B5			GT3 O-acetyl GT3 GQ1c	+	+ *	+	-	-	-	-	-	+	+ *	+	-
CTx	GM1			+	-	-	+ ▫	+	-	-	+ ▫	-	-	-	-
MOG35	GD1a			+	-	-	+ •	+	-	-	+ •	-	-	-	-
R24	GT1a	GD3 GQ1b		-	+ *	+	+ ~	-	-	-	-	+	-	+	+ ~

Table 5.1. Table showing ganglioside expression in dissociated spinal cord cultures.
Summary of ganglioside expression of cells in dissociated spinal cord cultures. Wild-type neurons expressed gangliosides recognised by A2B5, CTx and MOG35, Sia T -/- neurons expressed gangliosides recognised by CTx and MOG35, and GalNAc T -/- neurons expressed gangliosides recognised by A2B5 and R24. Only a small number of wild-type astrocytes expressed gangliosides recognised by A2B5 and R24 (*), Sia T -/- astrocytes were negative for all markers studied, while a small number of GalNAc T -/- labelled with A2B5 (*). Wild-type and GalNAc T -/- OPCs were positive for A2B5 and R24, whereas Sia T -/- OPCs were negative for all markers studied. A subset of wild-type and Sia T -/- O4 positive oligodendrocytes which appeared to be in a late stage of oligodendrocyte differentiation and AA3 positive oligodendrocytes labelled with CTx (▫). AA3 positive oligodendrocytes in wild-type and Sia T -/- cultures also labelled with MOG35 (•). A subset of O4 positive oligodendrocytes which appeared to be in an early stage of oligodendrocyte differentiation were also positive for R24 in wild-type and GalNAc T -/- cultures(~).

5.2.5 Comparison of oligodendrocyte differentiation

The remarkably distinctive ganglioside expression on differentiating oligodendrocytes suggests that they may play a functional role in oligodendrocyte differentiation. To investigate this further, oligodendrocytes were labelled with markers found at different stages of oligodendrocyte differentiation, namely NG2, O4 and MBP.

Spinal cord cultures from wild-type and ganglioside knockout mice were labelled with NG2, O4, and MBP as well as DAPI at 21 and 28 DIV. Images were taken at x40 magnification and the number of immunopositive cells quantified from these. Representative images for wild-type, Sia T -/- and GalNAc T -/- cultures at 21 DIV are shown in Figure 5.15, 5.16 and 5.17, respectively. The representative images show that all three markers can be present in these cultures at the same time.

The total number of DAPI positive nuclei was counted as well as the number of cells only labelled with NG2 ($NG2^+$); cells which co-labelled with NG2 and O4 ($NG2^+O4^+$); cells which only labelled with O4 ($O4^+$); cells which co-labelled with O4 and MBP ($O4^+MBP^+$); and cells which were only labelled with MBP (MBP^+). The results are represented as the percentage of each cell type out of the total number of cells (Figure 5.14).

It was found that spinal cord cultures from wild-type and Sia T -/- mice had a similar proportion of each cell type: $NG2^+$ early OPCs, $NG2^+O4^+$ late OPCs, $O4^+$ oligodendrocytes, $O4^+MBP^+$ premyelinating oligodendrocytes and MBP^+ myelinating oligodendrocytes. In other words, the differentiation of oligodendrocytes from OPCs to myelinating oligodendrocytes was unaffected in mice lacking b- and c-series, but containing increased levels of a-series gangliosides.

GalNAc T -/- cultures had a significantly lower proportion of $NG2^+$ early OPCs compared with wild-type and Sia T -/- cultures ($p=0.000$), but had similar levels of $NG2^+O4^+$ late OPCs, $O4^+$ oligodendrocytes, $O4^+MBP^+$ premyelinating oligodendrocytes and MBP^+ myelinating oligodendrocytes. Therefore, to summarise, the lack of complex, but increased simple gangliosides in GalNAc T -/- cultures affects an early stage of differentiation in the oligodendrocytes

lineage, the differentiation of early OPCs into late OPCs, but has no affect on the later stages of oligodendrocytes differentiation.

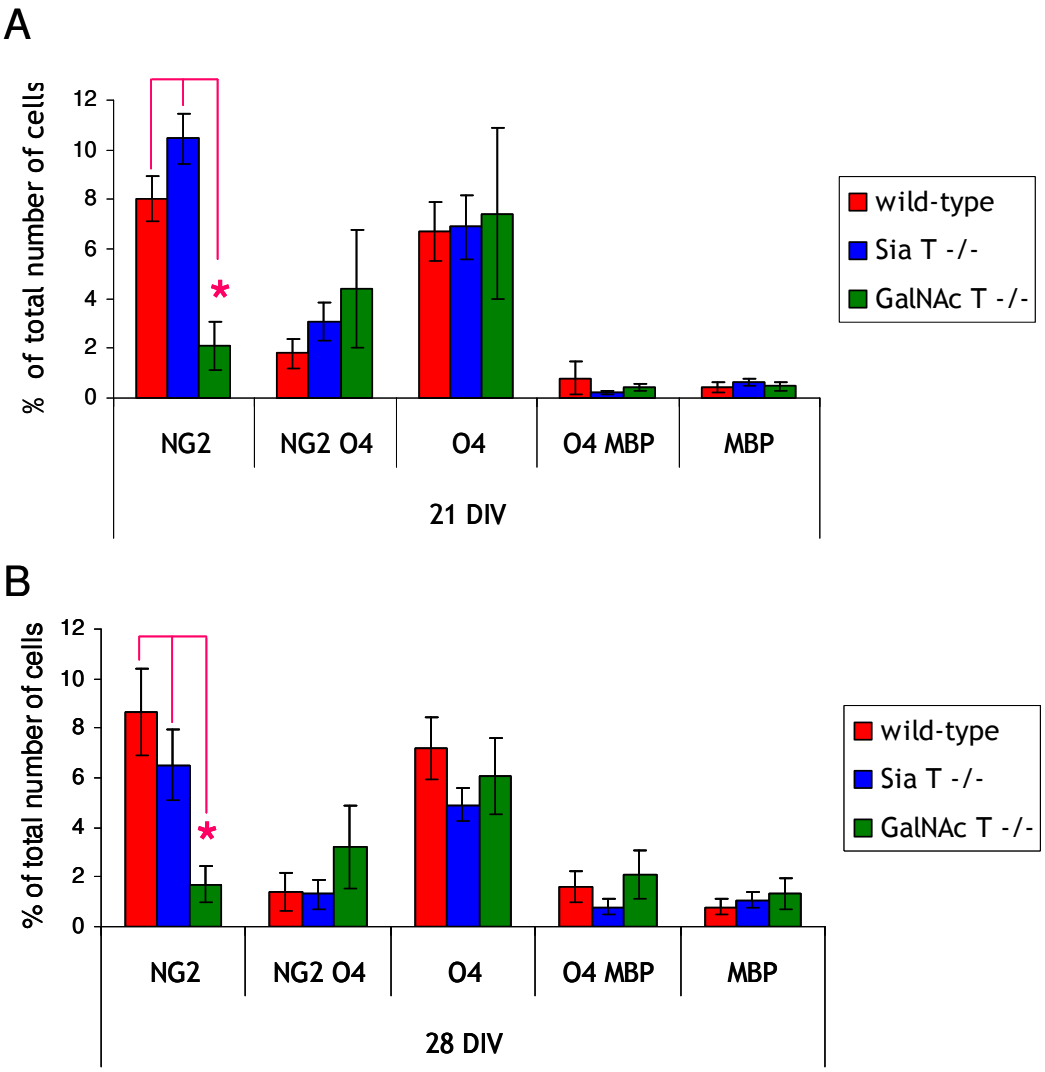

Figure 5.14. Comparison of oligodendrocyte differentiation.
Wild-type, Sia T -/- and GalNAc T -/- spinal cord were labelled with markers NG2, O4 and MBP at 21 (A) and 28 DIV (B) to capture different stages of oligodendrocyte differentiation. Cells which were only NG2 positive ($NG2^+$) correspond to early OPCs; cells which were both NG2 and O4 positive ($NG2^+O4^+$) are late OPCs; cells which were only O4 positive ($O4^+$) are intermediate between the late OPC and the premyelinating oligodendrocyte stage; cells which were O4 and MBP positive ($O4^+MBP^+$) correspond to the premyelinating oligodendrocytes and cells which were only MBP positive (MBP^+) are the myelinating oligodendrocytes. The table shows that there was no significant difference in the proportion of cells double labelled with NG2 and O4; O4 alone; O4 and MBP; and MBP alone in ganglioside knockout mice compared with wild-type. However, GalNAc T -/- mice had a significantly lower proportion of cells labelled with NG2 alone which indicated that they have a lower proportion of early OPCs when the spinal cord was cultured *in vitro*. (*) $p < 0.001$.

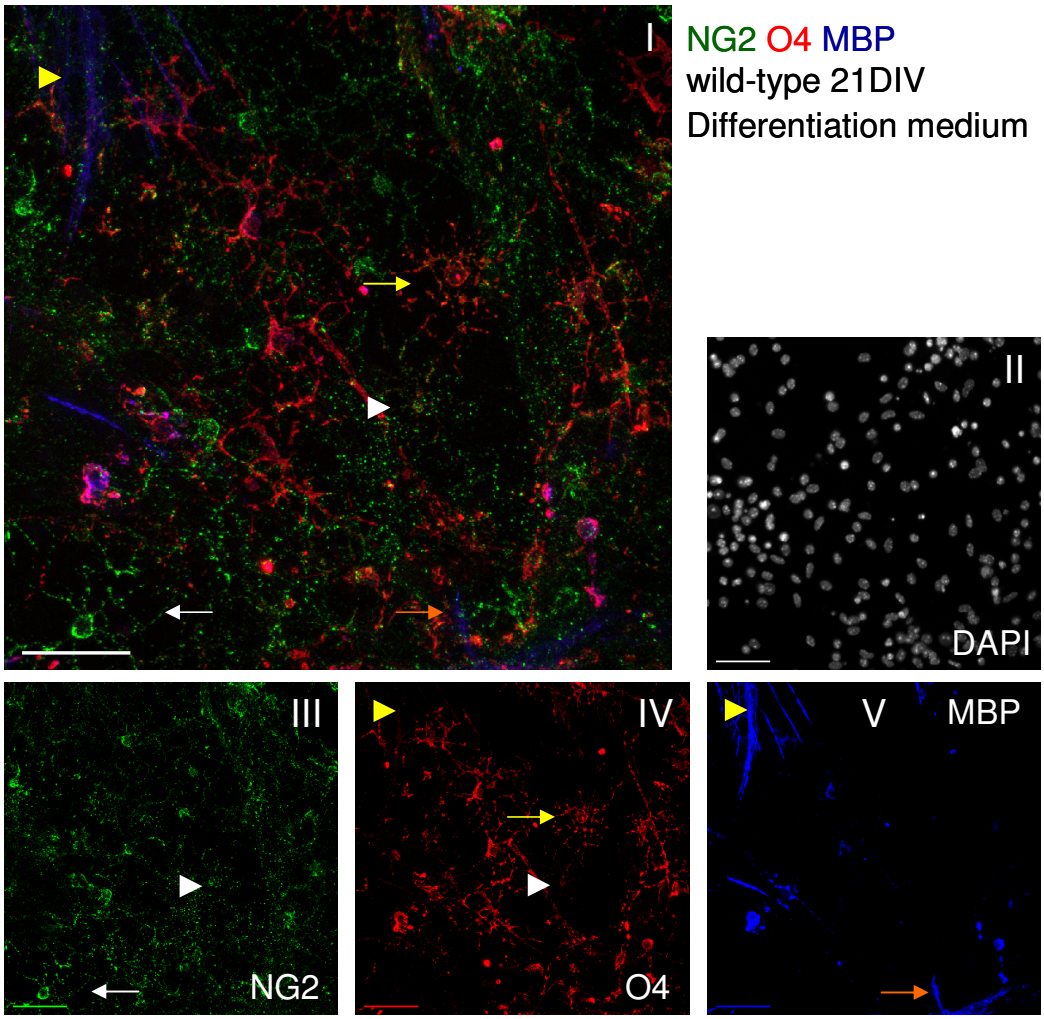

Figure 5.15. Wild-type spinal cord culture at 21 DIV in differentiation medium. Representative image of wild-type spinal cord cultures at 21 DIV grown in differentiation media, immunolabelled with NG2 (green, III), O4 (red, IV) and MBP (blue, V). The merged image is shown in I, while III to V show the individual markers. Nuclei were labelled with DAPI (white, II). Examples of following can be seen in this image: NG2+ early OPCs (white arrow), NG2+/O4+ late OPCs (white arrowhead), O4+ oligodendrocytes (yellow arrow), O4+/MBP+ pre-myelinating oligodendrocytes (yellow arrowhead), and MBP+ myelinating oligodendrocytes (orange arrow). Note that NG2+/O4+ and O4+ cells were multi processed. Scale bar = 50 µm.

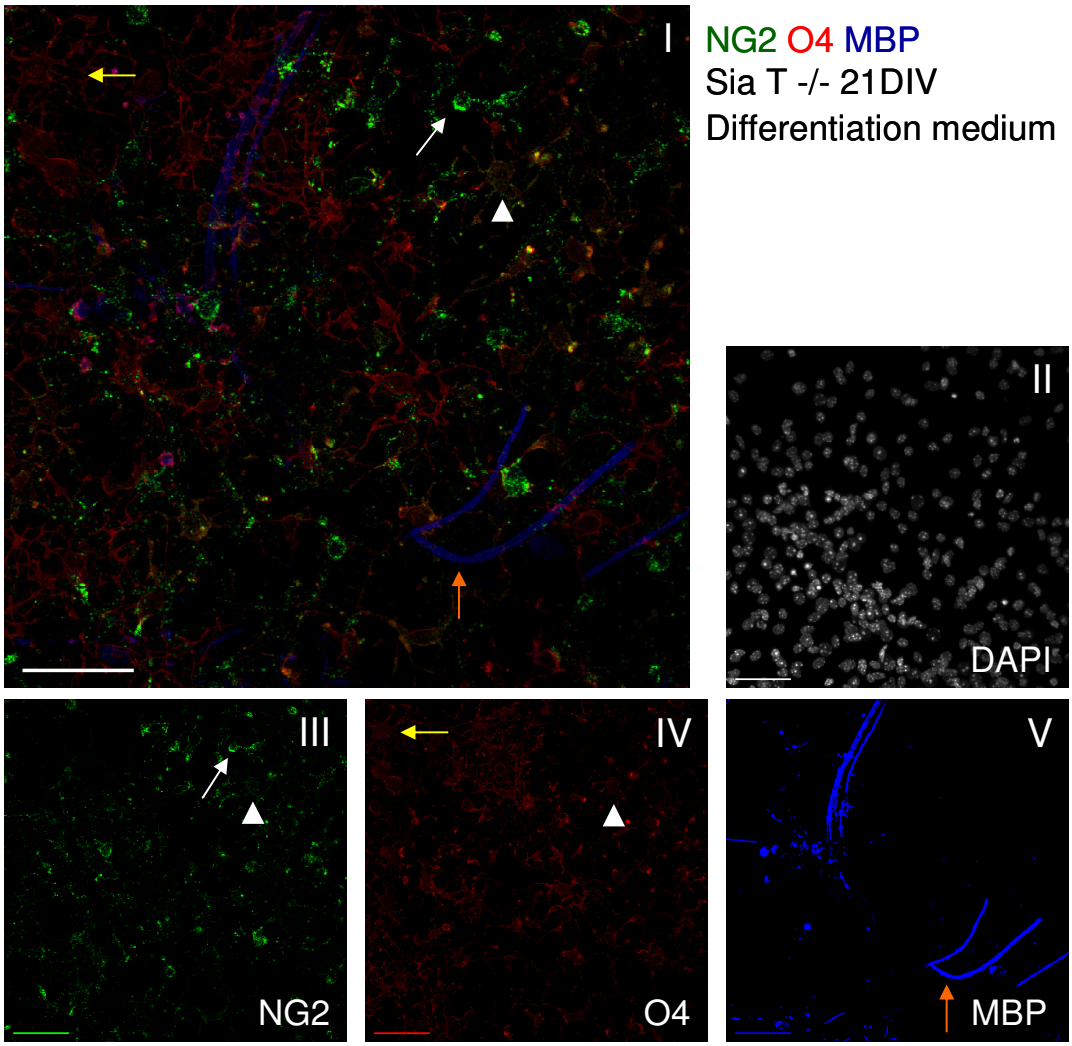

Figure 5.16. Sia T -/- spinal cord culture at 21 DIV in differentiation medium.
Representative image of Sia T -/- spinal cord culture at 21 DIV grown in differentiation medium, immunolabelled with NG2 (green, III), O4 (red, IV) and MBP (blue, V). The merged image is shown in I, while III to V show the individual markers. Nuclei were labelled with DAPI (white, II). Examples of following can be seen in this image: NG2+ early OPCs (white arrow), NG2+/O4+ late OPCs (white arrowhead), O4+ oligodendrocytes (yellow arrow), and MBP+ myelinating oligodendrocytes (orange arrow). Note that the NG2+/O4+ and O4+ cells had many branched processes. Scale bar = 50 μm.

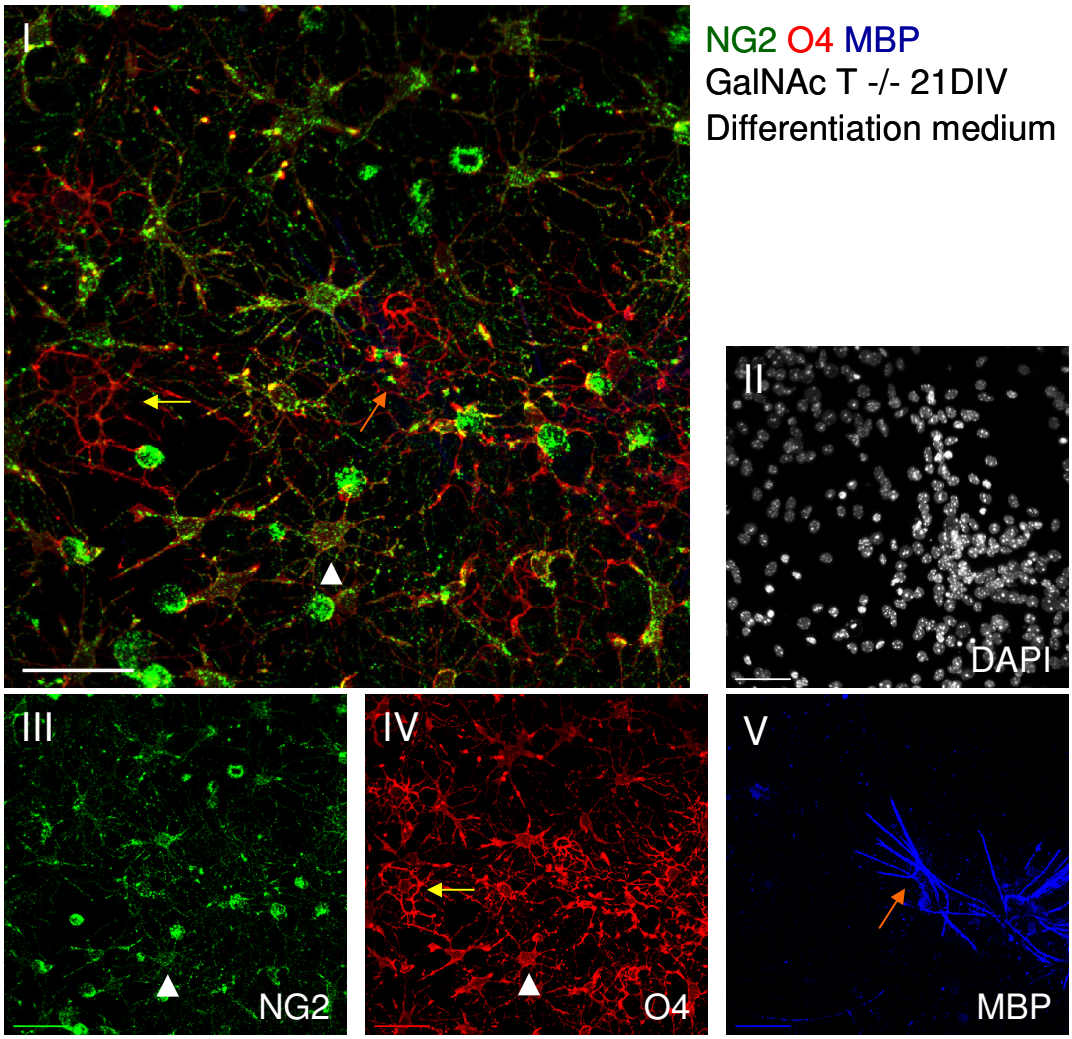

Figure 5.17. GalNAc T -/- spinal cord culture at 21 DIV in differentiation medium. Representative image of GalNAc T -/- spinal cord culture at 21 DIV grown in differentiation medium, immunolabelled with NG2 (green, III), O4 (red, IV) and MBP (blue, V). The merged image is shown in I, while III to V show the individual markers. Nuclei were labelled with DAPI (white, II). Examples of following can be seen in this image: NG2+/O4+ late OPCs (white arrowhead), O4+ oligodendrocytes (yellow arrow), and MBP+ myelinating oligodendrocytes (orange arrow). Scale bar = 50 µm.

5.2.6 Relationship between oligodendrocytes and axons

It has so far been shown that neurites and glia found in the spinal cord cultures differentially express gangliosides. This, however, appeared to have no major effect on the differentiating properties of the oligodendrocytes. To investigate whether the lack of gangliosides affects the relationship between glia and axons, the interaction between oligodendrocytes and axons in spinal cord cultures was studied by confocal microscopy after 7, 14, 21 and 28 days in culture. Earlier stages of oligodendrocyte differentiation were visualised using the O4 antibody, and later using the AA3 antibody. Axons were visualised using SMI 31 (Figures 5.19 – 5.21).

The interaction between oligodendrocytes and axons appeared to be similar when comparing wild-type and ganglioside knockout cultures (Figures 5.19 – 5.21). After 7 DIV the O4 positive oligodendrocytes had few processes. After 14 DIV, many of the oligodendrocytes were multiprocessed and some of their processes were contacting an axon. After 21 DIV, many of the oligodendrocytes expressed AA3, and some myelin was seen wrapped around the axons. The nodes of Ranvier were not evident at this stage; however, after 28 DIV the nodes of Ranvier were more abundant.

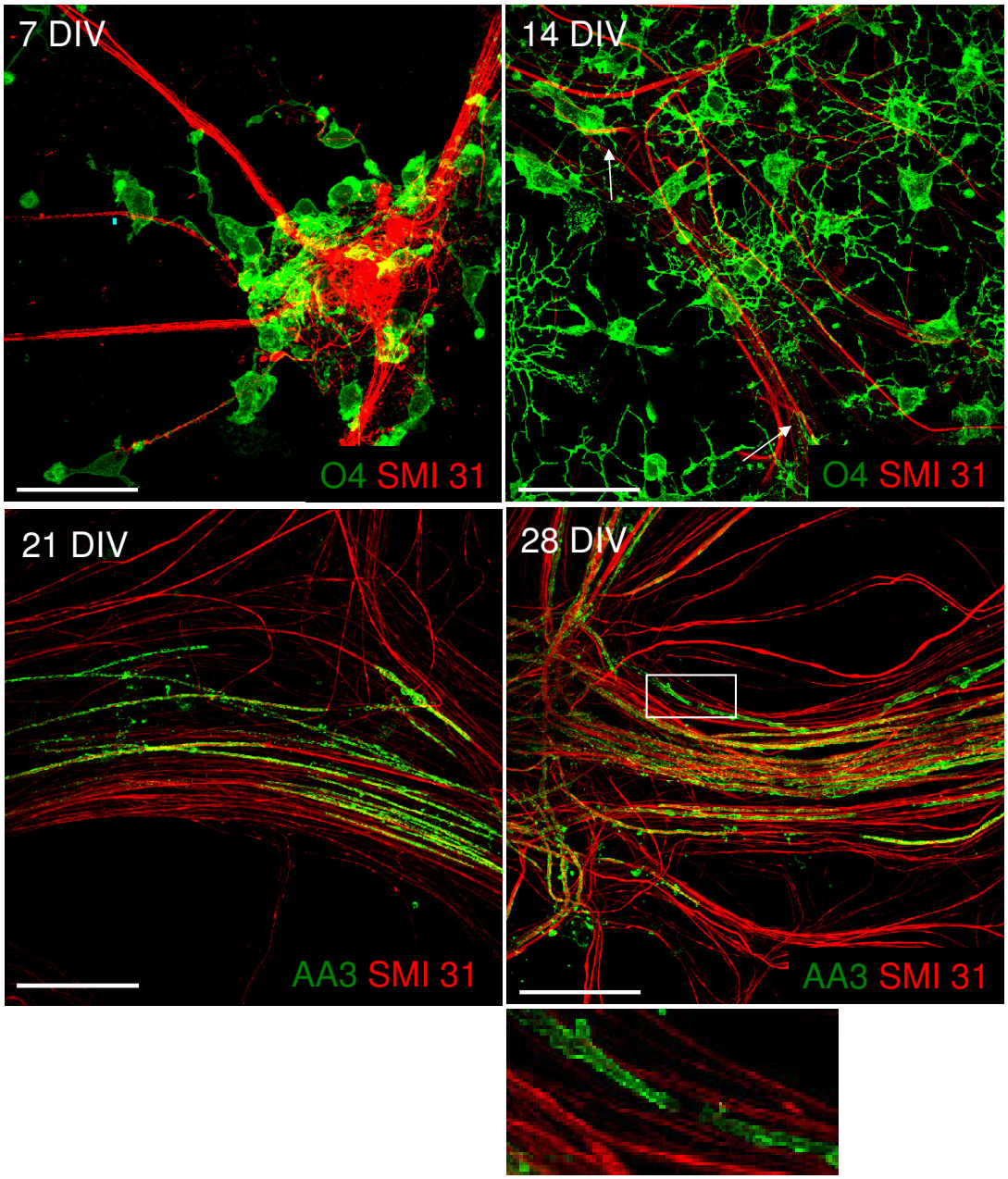

Figure 5.18. Relationship between oligodendrocytes and axons in wild-type cultures. Wild-type spinal cord cultures were co-labelled with O4 (green) and SMI 31 (red) after 7 and 14 DIV as well as AA3 (green) and SMI 31 (red) after 21 and 28 days in culture to observe the relationship between oligodendrocytes and axons. At 7 DIV, oligodendrocytes had very few processes and were located near axons. By 14 DIV oligodendrocytes had developed extensive networks of processes and began to contact and ensheath the axons (arrows). At 21 and 28 DIV it could be seen that oligodendrocytes were in close contact with the axons and were forming myelin. In addition, at 28 DIV, the myelin sheaths appeared to be interrupted by nodes of Ranvier. Scale bars = 50μm.

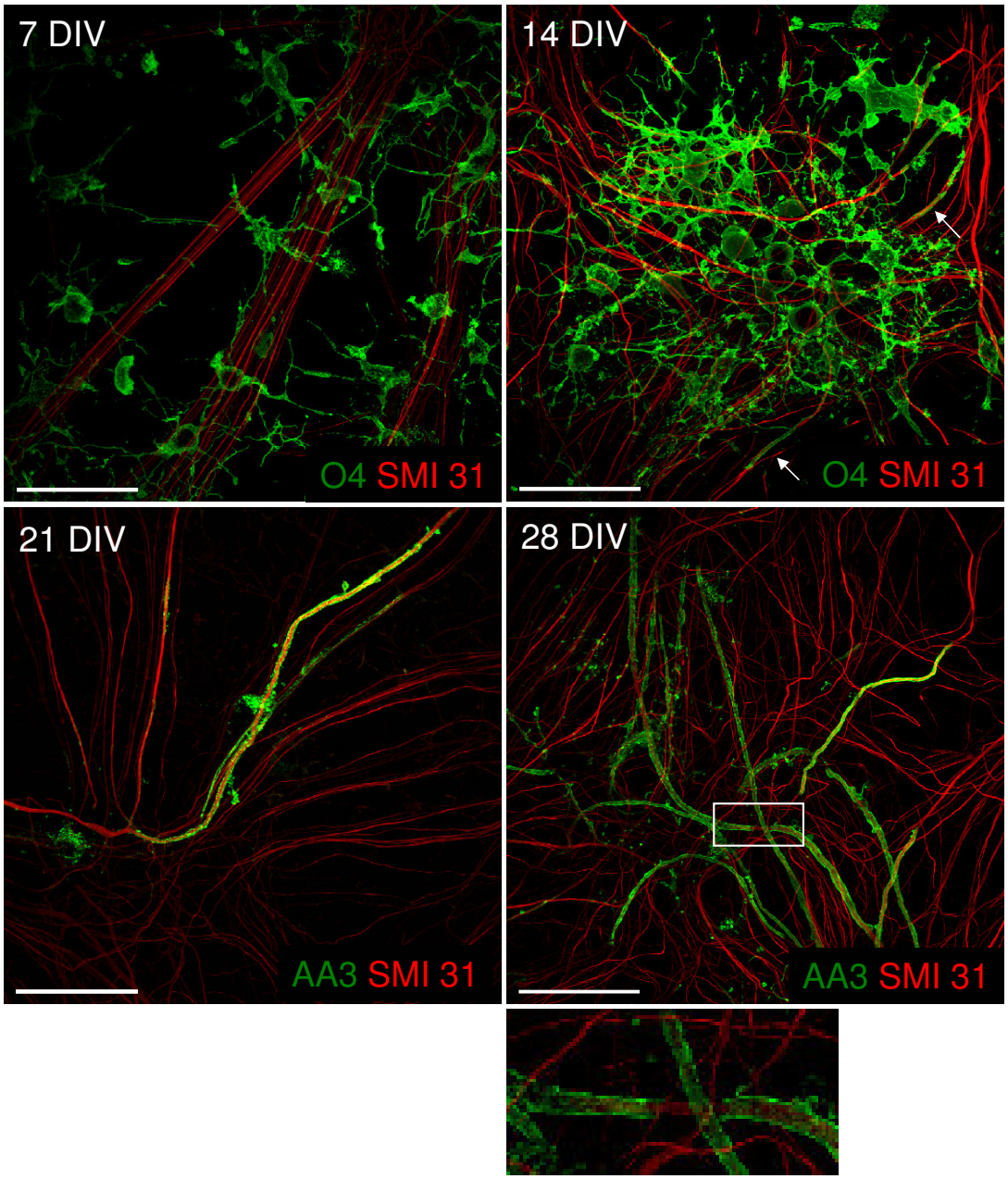

Figure 5.19. Relationship between oligodendrocytes and axons in Sia T -/- cultures.
Sia T -/- spinal cord cultures were co-labelled with O4 (green) and SMI 31 (red) after 7 and 14 DIV as well as AA3 (green) and SMI 31 (red) after 21 and 28 days in culture to observe the relationship between oligodendrocytes and axons. Sia T -/- oligodendrocytes differentiated and began to myelinate axons in a similar manner to that described for wild-type cultures (Figure 5.18). Scale bars = 50μm.

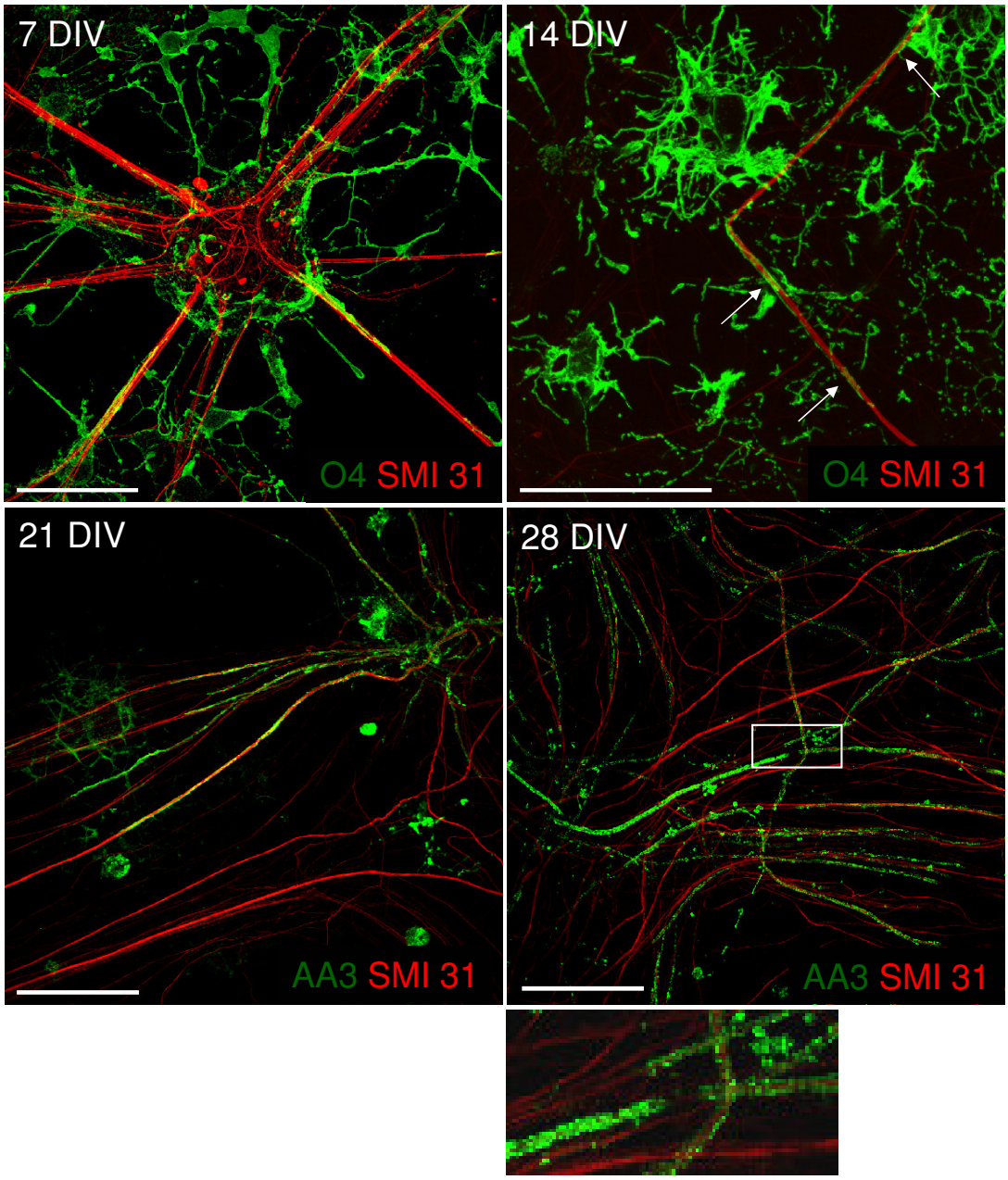

Figure 5.20. Relationship between oligodendrocytes and axons in GalNAc T -/- cultures. GalNAc T -/- spinal cord cultures were co-labelled with O4 (green) and SMI 31 (red) after 7 and 14 DIV as well as AA3 (green) and SMI 31 (red) after 21 and 28 days in culture to observe the relationship between oligodendrocytes and axons. GalNAc T -/- oligodendrocytes differentiated and began to myelinate axons in a similar manner to that described for wild-type cultures (Figure 5.18). Scale bars = 50μm.

5.2.7 Comparison of axonal density and PLP staining

The studies using confocal microscopy showed no obvious difference in the interplay between axons and oligodendrocytes as a result of altering the ganglioside expression. The next aim was therefore to investigate the myelinating properties of wild-type, Sia T -/- and GalNAc T -/- oligodendrocytes. For this purpose spinal cord cultures were double-labelled with an axonal marker SMI 31 and the AA3 antibody that recognises PLP at 21 and 28 days in culture (Figure 5.21). Axonal density was quantified using Image J by determining the area of SMI 31 immunoreactivity as a percentage of the total area of the image. The percentage of axons expressing PLP was calculated by measuring the immunoreactivity associated with AA3, dividing it by the area obtained for axonal density and multiplying it by a 100. The percentage of axons within a given area and the percentage of these expressing PLP is shown in Figure 5.21.

After 21 days in culture axonal density was significantly higher in Sia T -/- cultures compared to GalNAc T -/- and wild type cultures ($p < 0.05$), however, by 28 DIV axonal density was similar in all three genotypes. Thus, although the increase in a-series and the lack of b- and c-series gangliosides in axons of Sia T -/- mice initially lead to increased axonal density, this increase was not sustained. Furthermore, in agreement with the observation that oligodendrocyte differentiation was unaffected in Sia T -/- cultures, PLP labelling was also unaffected in Sia T -/- cultures, again suggesting that increased a-series and lack of b- and c-series gangliosides does not affect oligodendrocyte differentiation and axonal myelination.

The lack of complex gangliosides in GalNAc T -/- mice did not have an effect on axonal development either. However, the percentage of axons expressing PLP after 21 DIV was significantly lower in GalNAc T -/- ($p < 0.05$). However, after 28 DIV the difference was no longer statistically significant. This suggests that the lack of complex gangliosides and the concomitant increase in simple gangliosides, leads to delayed expression of PLP but levels are restored to those similar to wild-type by 28 DIV.

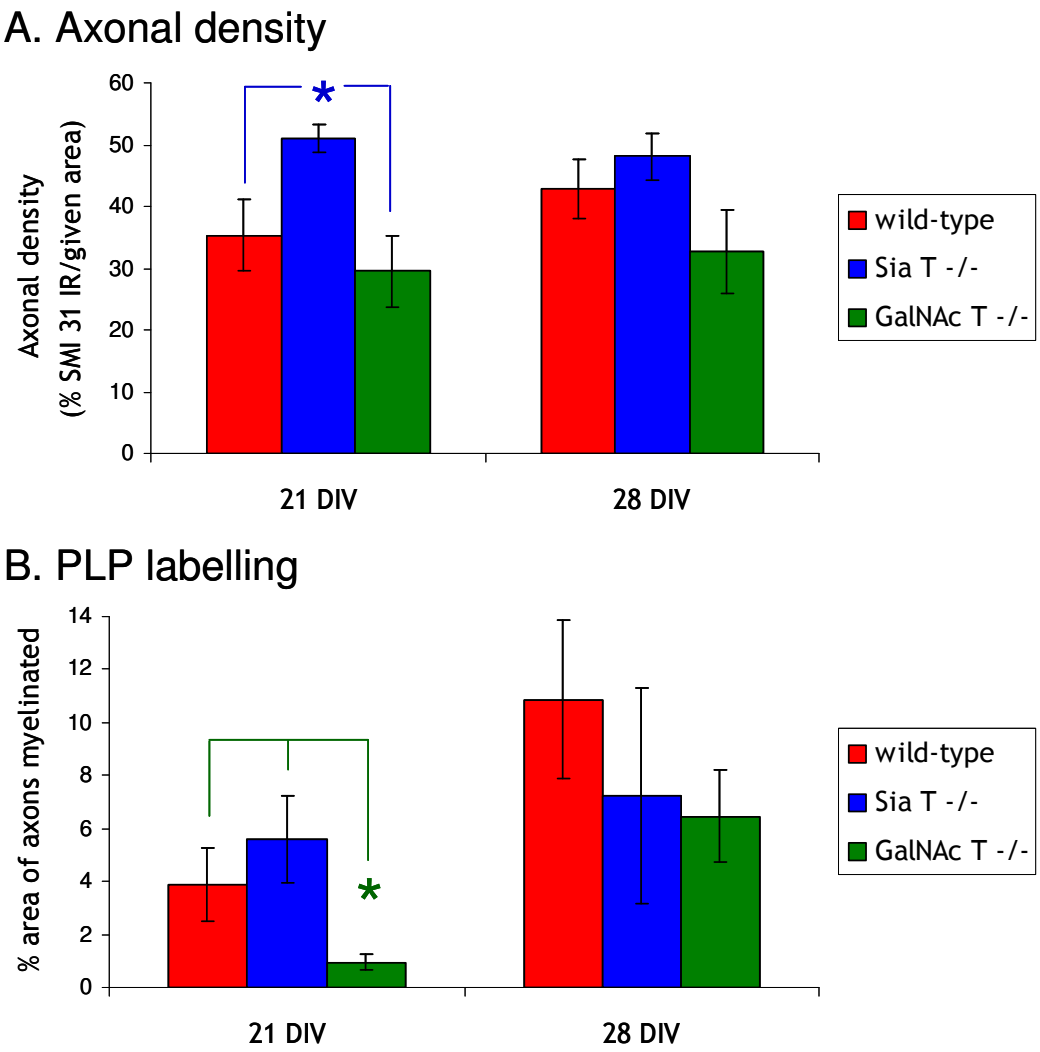

Figure 5.21. Axonal density and PLP labelling in wild-type, Sia T -/- and GalNAc T -/- spinal cord cultures.
Axonal density (A) and PLP labelling (B) of wild-type, Sia T -/- and GalNAc T -/- spinal cord cultures maintained in differentiation medium at 21 and 28 days in culture. Spinal cord cultures from wild-type and ganglioside knockout mice were labelled with SMI 31 to detect axons and AA3 to detect PLP expression at 21 and 28 DIV. The percentage axons within a given area and the percentage area of axons labelled with AA3 was measured as described in the Methods section. At 21 DIV, Sia T -/- cultures showed increased axonal density compared with wild-type and GalNAc T -/- cultures (blue *; $p = 0.029$), however, by 28 DIV the axonal density was similar in all cultures. At 21 DIV, PLP labelling was significantly lower in GalNAc T -/- cultures (green *; $p = 0.045$), however, at 28 DIV the percentage of myelinated axons was similar in all three genotypes.

5.2.8 Localisation of proteins at the node of Ranvier

As shown in Figures 5.19 to 5.21, after 28 DIV the myelin internodes were interrupted by what appeared to be node of Ranvier. To examine whether gangliosides play a role in node of Ranvier formation the localisation of NF155 and Caspr at the paranodes, Na_v at the nodes of Ranvier and K_v at the juxtaparanodes was investigated. Wild-type, Sia T -/- and GalNAc T -/- cultures were triple labelled with AA3 to detect myelin, Na_v antibody and one of the following antibodies: $K_v1.2$, Caspr or NF155. Cultures were also labelled with an antibody against $K_v1.1$, however, none of the cultures were positive for this antibody.

As shown in Figure 5.22, Na_v were distributed continuously throughout the axonal membrane in unmyelinated axons, however, in myelinated axons containing nodes of Ranvier, the Na_v immunoreactivity was confined to the node. As shown in Figure 5.22 (panel C) GalNAc T -/- cultures sometimes had sodium channels distributed throughout the axonal membrane as well as concentrated at the nodes of Ranvier. This did not occur in wild-type and Sia T -/- cultures.

The distribution of Caspr and NF155 immunoreactivity was found to be confined to the paranodal region, on either side of the sodium channel. This pattern was similar in all three genotypes as shown in Figures 5.24 and 5.25, respectively.

In wild-type and Sia T -/- myelinated fibres, $K_v1.2$ immunolabelling was located at the paranodal and juxtaparanodal regions as shown in Figure 5.25 (panels A and B, respectively). Although, in some wild-type myelinated fibres $K_v1.2$ were beginning to confine to only the juxtaparanodal regions as demonstrated in Figure 5.26.

In contrast to wild-type and Sia T -/- cultures, the $K_v1.2$ immunolabelling in GalNAc T -/- cultures after 28 DIV was either spread throughout the myelinated axon as shown in Figure 5.25 (panel C), was co-localised with Na_v at the node of Ranvier or was only observed on one side of the node of Ranvier in the paranodal and juxtaparanodal regions as shown in Figure 5.29 (panel D). However, as can be seen in Figure 5.27, at 30 and 32 DIV in GalNAc T -/- cultures K_v labelling is also localised in the paranodal and juxtaparanodal regions.

In summary, in wild-type and Sia T -/- mice Caspr, neurofascin 155, K_v1.2, and Na_v were localised as would be expected based on *in vivo* observations. However, in GalNAc T -/- myelinated axons K_v1.2 immunoreactivity was not confined to the paranodal and juxtaparanodal regions until 30 to 32 DIV. Instead, it was spread throughout the axonal membrane and was only beginning to localise at the juxtaparanode at 28 DIV. These results suggest that the assembly of nodal proteins is retarded in the absence of complex gangliosides.

5.2.9 Comparison of astrocyte morphology

Several studies have shown that the addition of exogenous gangliosides can alter the morphology of astrocytes (Hefti et al, 1985; Skaper et al, 1986; Facci et al, 1987). To determine whether the morphology of astrocytes was different in ganglioside knockout mice compared with wild-type, astrocytes were labelled with GFAP and their morphology studied using confocal microscopy. As shown in figure 5.28, the morphology of astrocytes was similar in all genotypes. It has also been shown that processes of perinodal astrocytes are in close association with the node of Ranvier. To determine if perinodal astrocytes were present in spinal cord cultures, these were triple labelled with AA3 to visualise myelin, SMI 31 to visualise axons and GFAP to visualise astrocytes (Figure 5.29). Although astrocytes were present near nodes of Ranvier, it was not possible to determine by confocal microscopy whether their processes were associated with nodes of Ranvier (see Figure 5.29).

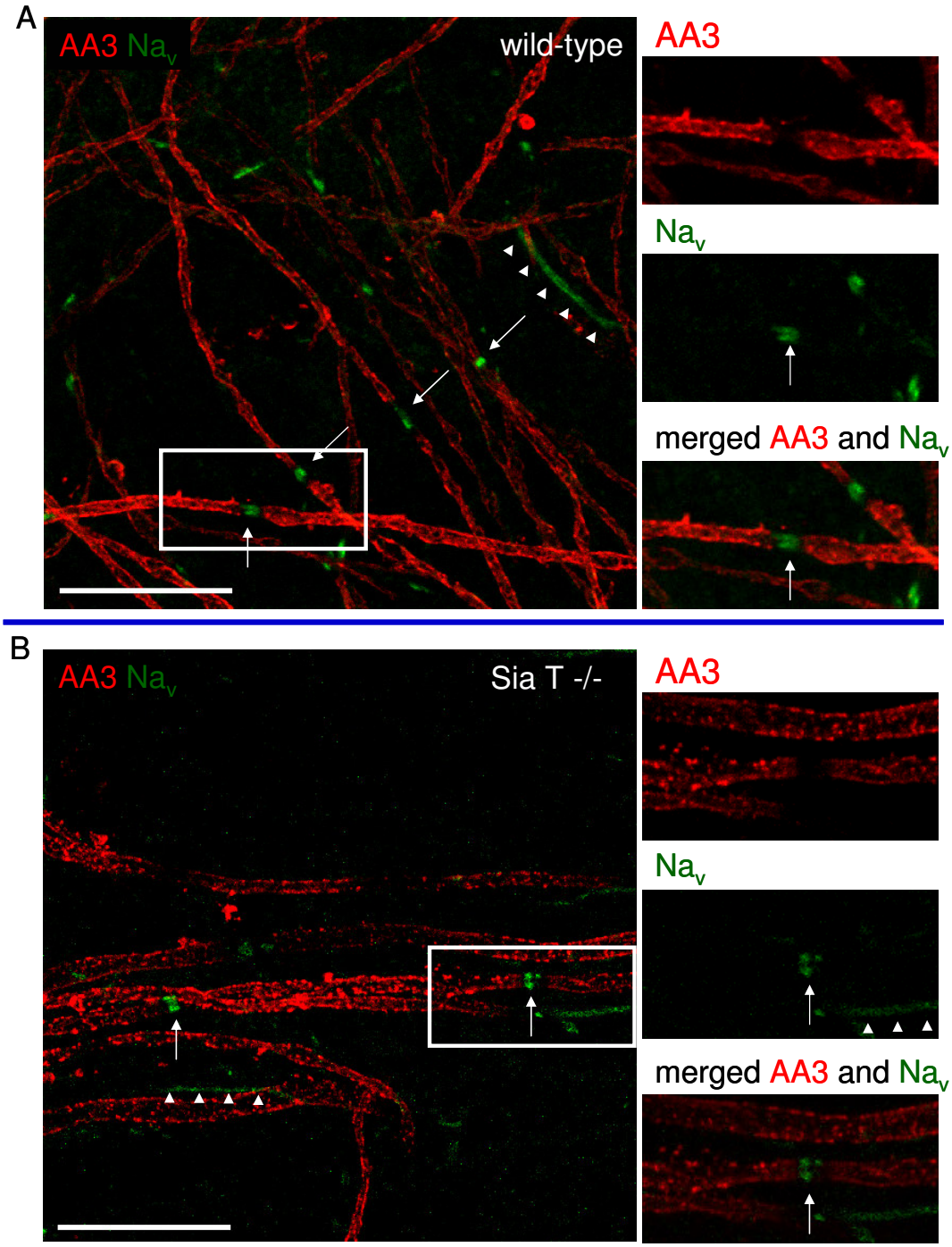
A
AA3 Nav
wild-type
AA3
Nav
merged AA3 and Nav
B
AA3 Nav
Sia T -/-
AA3
Nav
merged AA3 and Nav

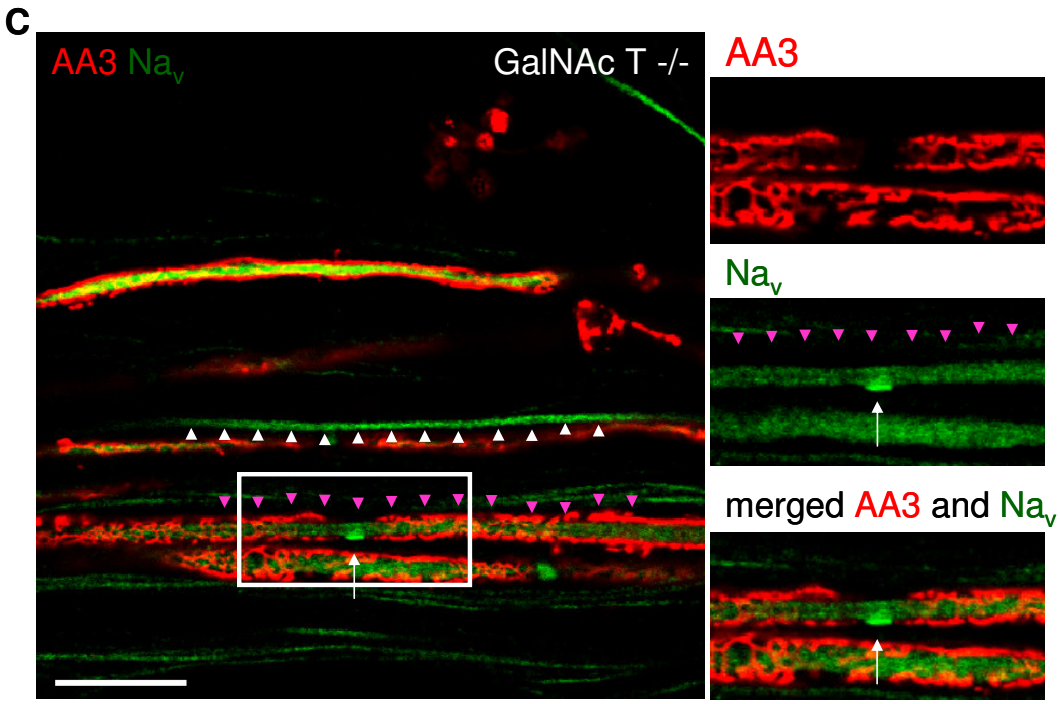

Figure 5.22. Sodium channel clustering at nodes of Ranvier at 28 DIV.
Wild-type (panel A), Sia T -/- (panel B) and GalNAc T -/- (panel C) spinal cord cultures were labelled with AA3 (red), which recognises compact myelin, and an antibody against voltage dependent sodium channels (Na_v; green). In unmyelinated fibres Na_v staining was observed throughout the axonal membrane (white arrowheads). In myelinated fibres in wild-type and Sia T -/- cultures, Na_v clustering is displayed at nodes of Ranvier (white arrows). Although GalNAc T -/- cultures displayed Na_v clustering at node of Ranvier (Figures 5.25 and 5.26), it was also observed that some myelinated fibres in GalNAc T -/- cultures showed Na_v immunoreactivity throughout the axonal membrane (pink arrowheads) as well as at the node of Ranvier. However, the occurrence of the latter was not quantified. Scale bar = 20 µm.

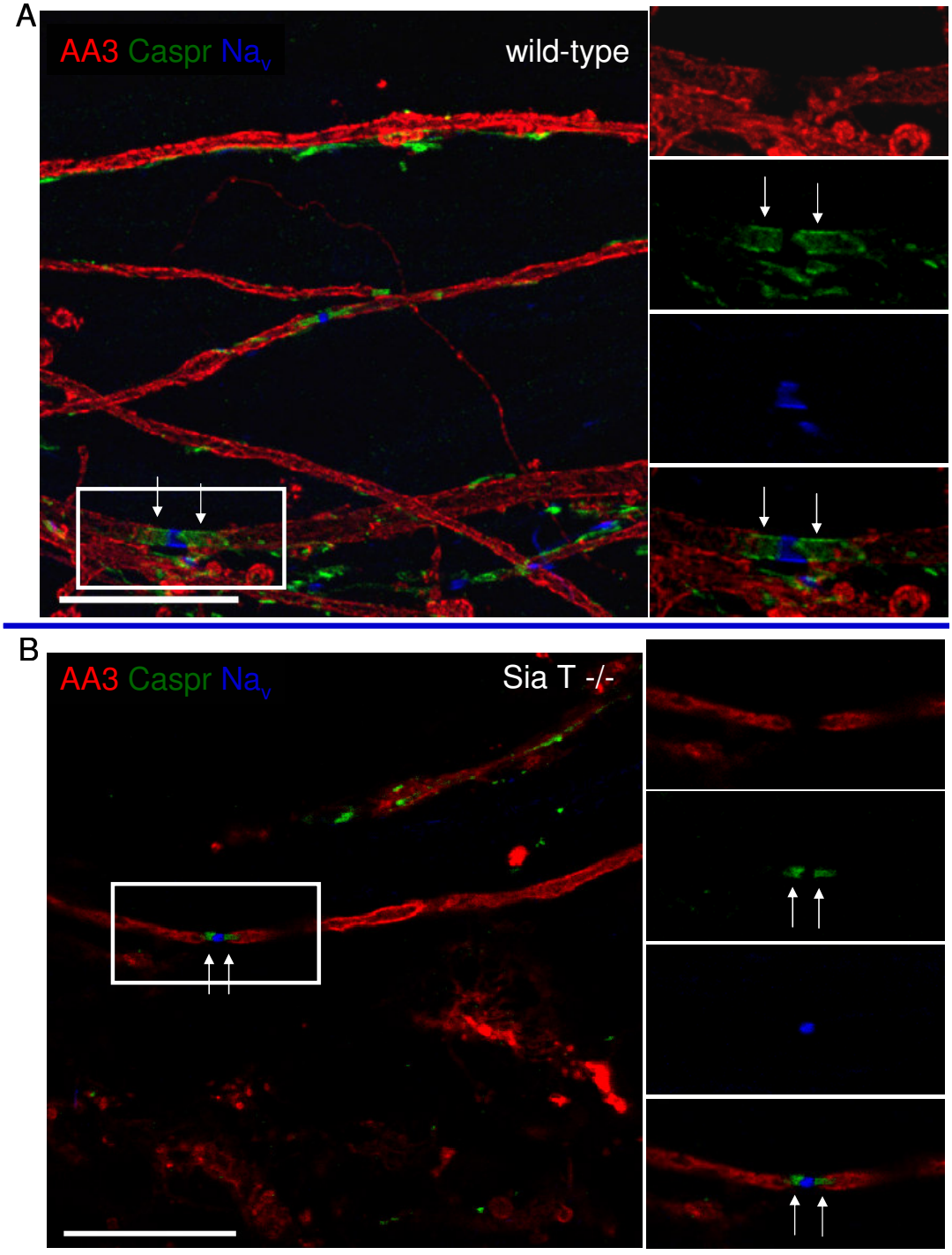
A
AA3 Caspr Na$_v$
wild-type
B
AA3 Caspr Na$_v$
Sia T -/-

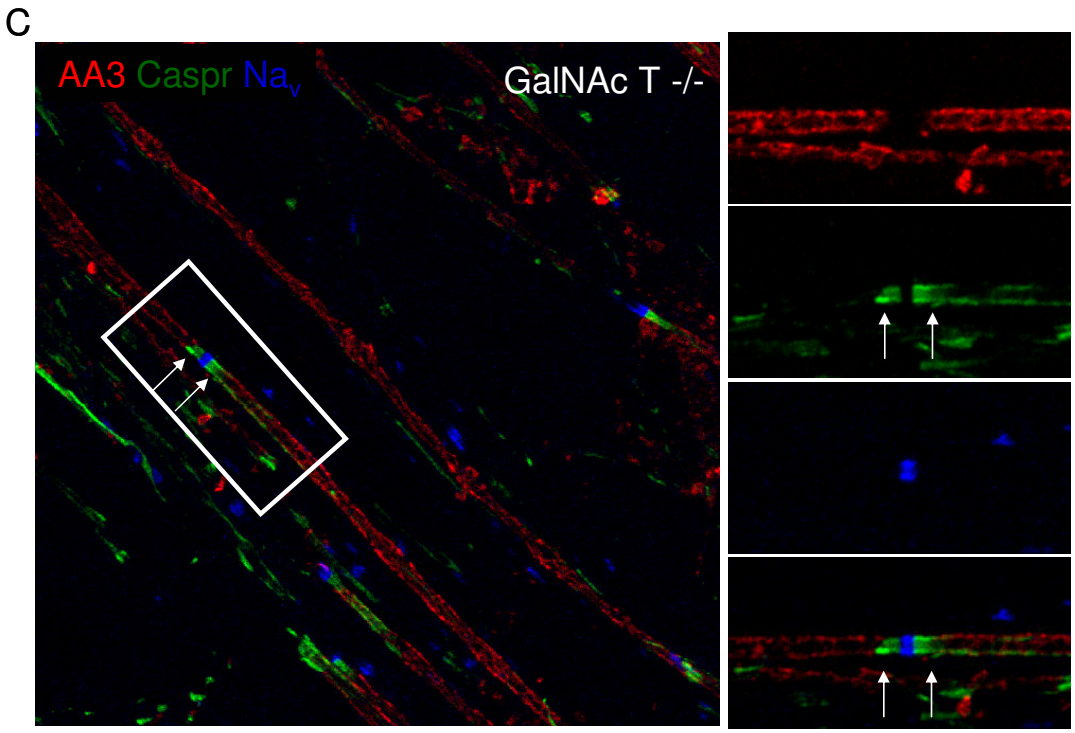

Figure 5.23. The paranodal localisation of Caspr
Wild-type (panel A), Sia T -/- (panel B) and GalNAc T -/- (panel C) spinal cord cultures were labelled with AA3 (red), which recognises compact myelin, Na_v (blue) to show the node of Ranvier and Caspr (green) at 28 DIV. It was observed that Caspr was localised at the paranodes of myelinated fibres in all three genotypes (white arrows). Scale bar = 20 µm.

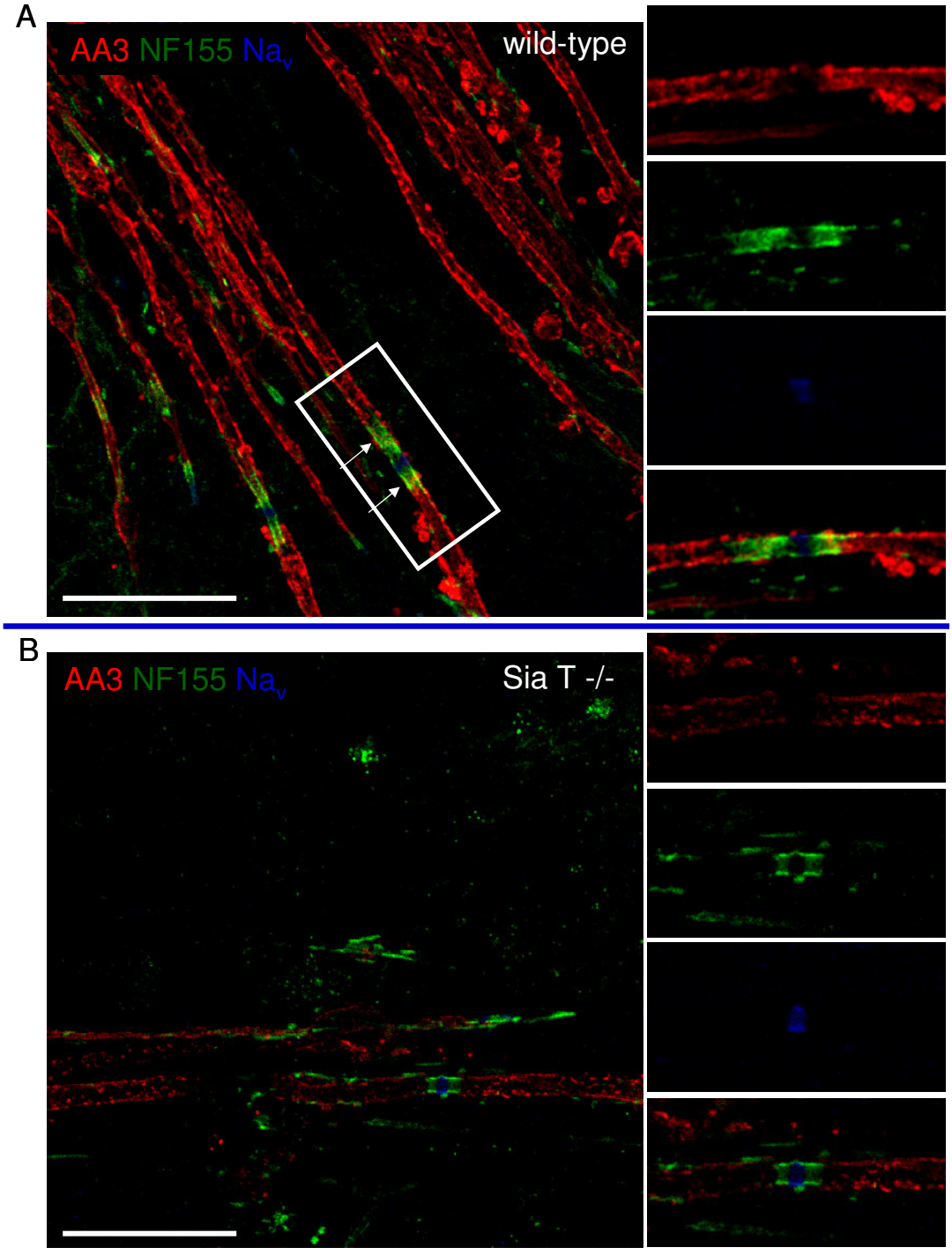
A
AA3 NF155 Nav
wild-type
B
AA3 NF155 Nav
Sia T -/-

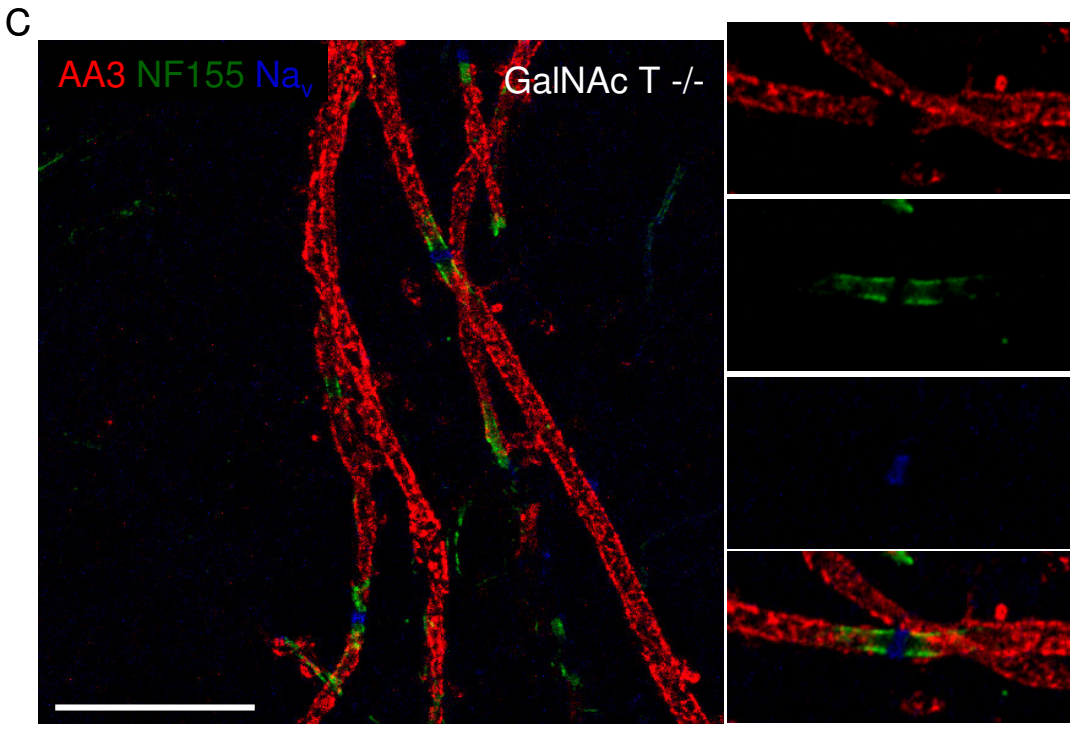

Figure 5.24. The paranodal localisation of neurofascin 155
Wild-type (panel A), Sia T -/- (panel B) and GalNAc T -/- (panel C) spinal cord cultures were labelled with AA3 (red), which recognises compact myelin, Na_v (blue) to show the node of Ranvier and neurofascin 155 (green) at 28 DIV. It was observed that neurofascin was localised at the paranodes of myelinated fibres in all three genotypes (white arrows). Scale bar = 20 µm.

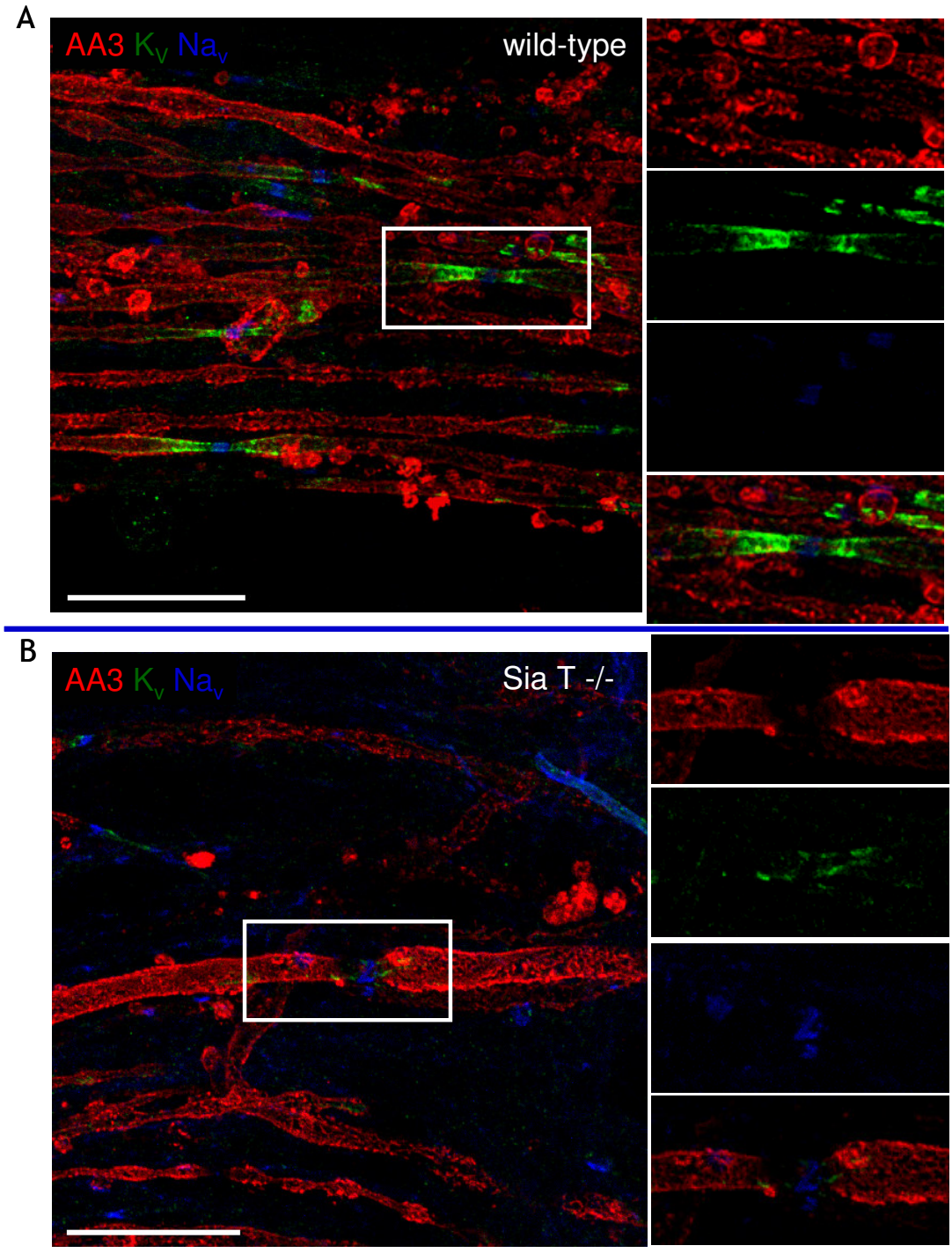
A
AA3 K_v Na_v
wild-type
B
AA3 K_v Na_v
Sia T -/-

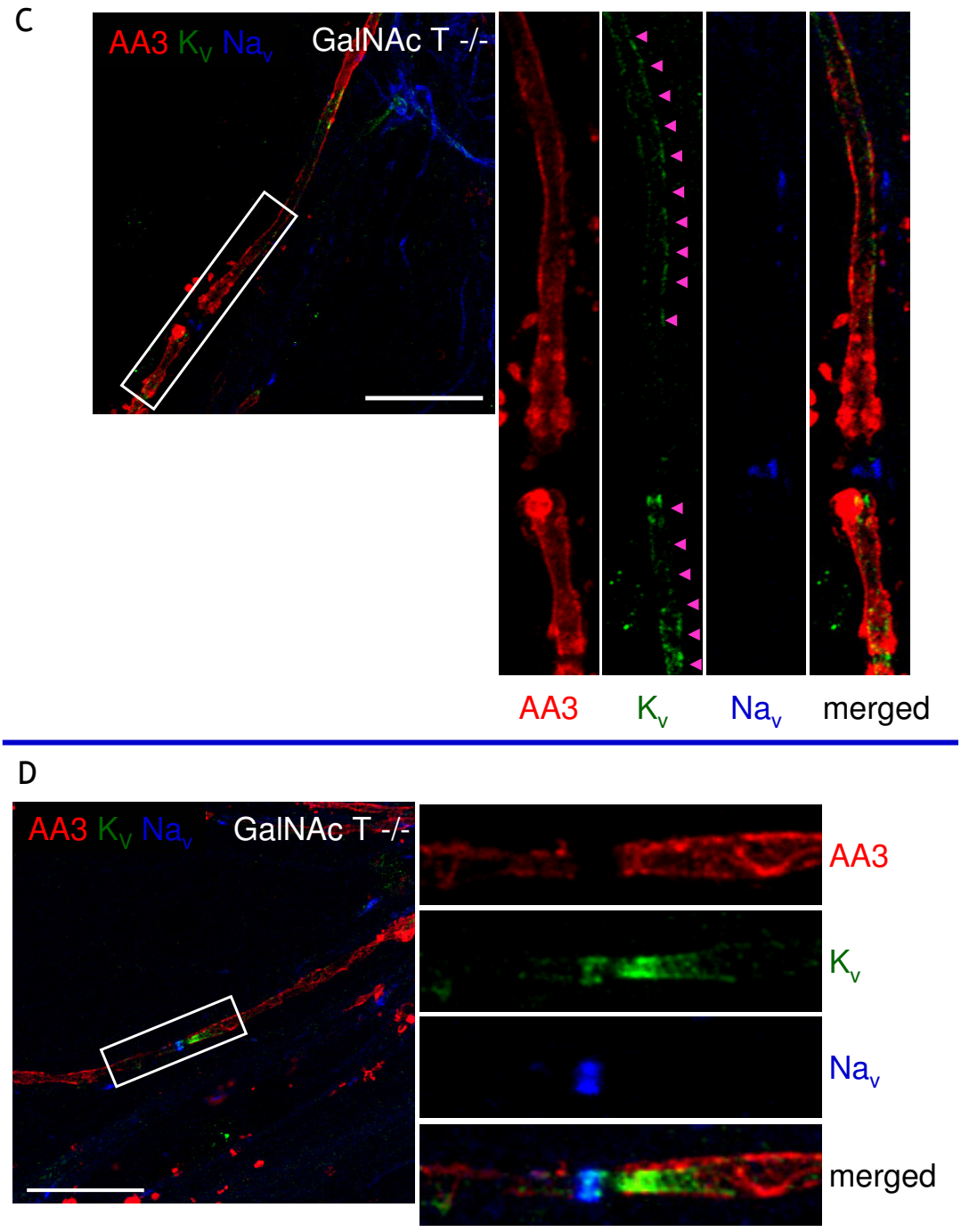

Figure 5.25. The paranodal and juxtaparanodal localisation of $K_v1.2$
Wild-type (panel A), Sia T -/- (panel B) and GalNAc T -/- (panel C and D) spinal cord cultures were labelled with AA3 (red), which recognises compact myelin, Na_v (blue) to show the node of Ranvier and $K_v1.2$ (green) at 28 DIV. In wild-type and Sia T -/- cultures, $K_v1.2$ was seen in the paranodal and juxtaparanodal area, however, in GalNAc T -/- cultures, the localisation of $K_v1.2$ was disturbed. Instead of being only localised to the paranodes and juxtaparanodes, K_v were also spread throughout the axonal membrane (C) and node of Ranvier (D). Scale bar = 20 µm.

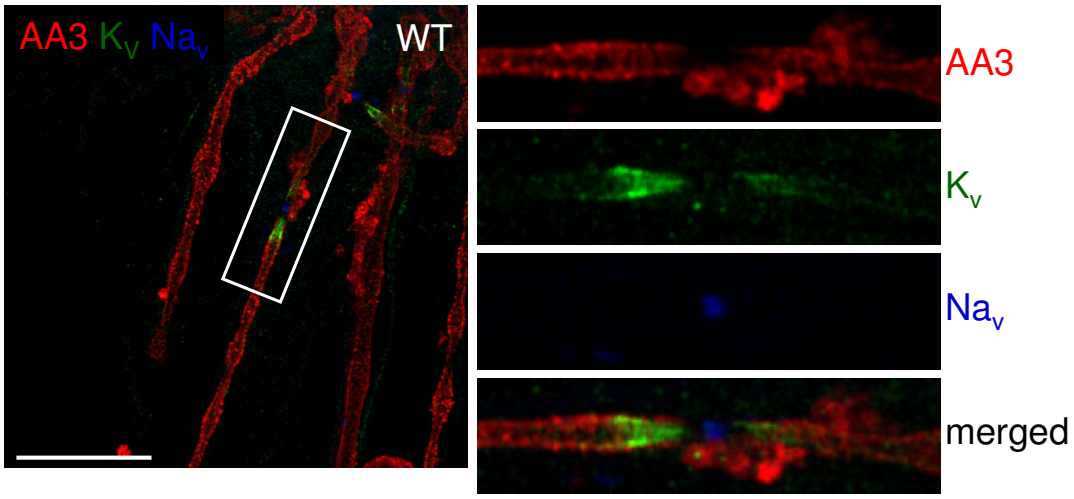

Figure 5.26. Juxtaparanodal localisation of K_v1.2 in wild-type cultures at 28 DIV.
Wild-type spinal cord cultures were labelled with AA3 (red), which recognises compact myelin, Nav (blue) to show the node of Ranvier and K_v1.2 (green) at 28 DIV. As shown in Figure 5.25, at 28 DIV, K_v was localised at paranodes and juxtaparanodes in the majority of wild-type myelinated fibres, however, occasionally K_v labelling was starting to localise to only the juxtaparanode. Scale = 20 µm.

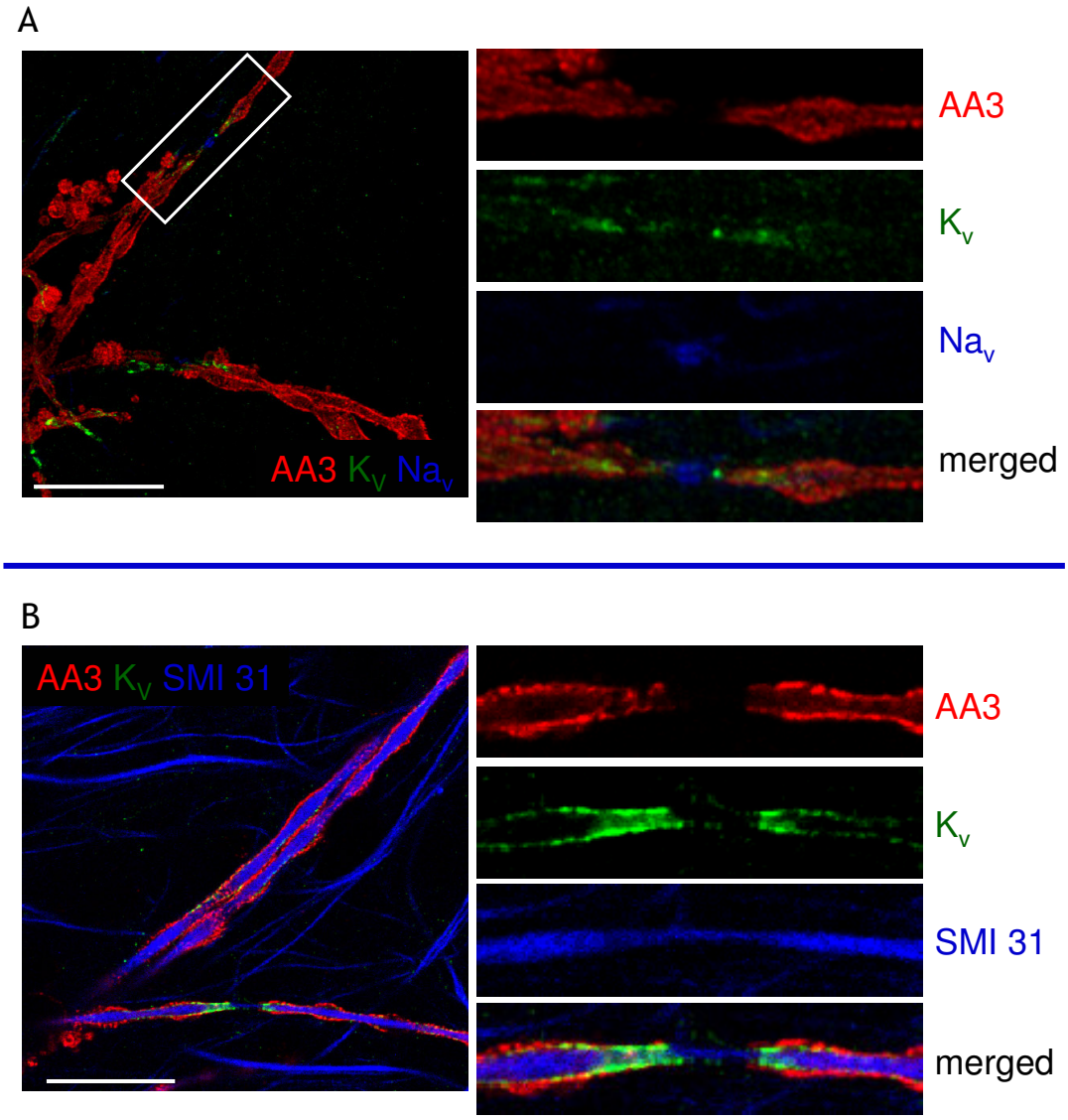

Figure 5.27. The localisation of Kv1.2 in GalNAc T -/- cultures at 30 and 32 DIV. GalNAc T -/- spinal cord cultures were labelled with AA3 (red), which recognises compact myelin, Nav (blue) to show the node of Ranvier and K_v1.2 (green) at 30 DIV (panel A) and AA3 (red), SMI 31 (blue) to show the axons and K_v1.2 at 32 DIV (panel B). As shown in Figure 5.25, at 28 DIV in GalNAc T -/- cultures, K_v were spread throughout the axonal membrane, however, by 30 to 32 DIV K_v labelling was localised to the paranode and juxtaparanode. In other words, at 30 to 32 DIV, the K_v labelling in GalNAc T -/- cultures resembled that of wild-type and Sia T -/- cultures at 28 DIV. Scale bar = 20 µm.

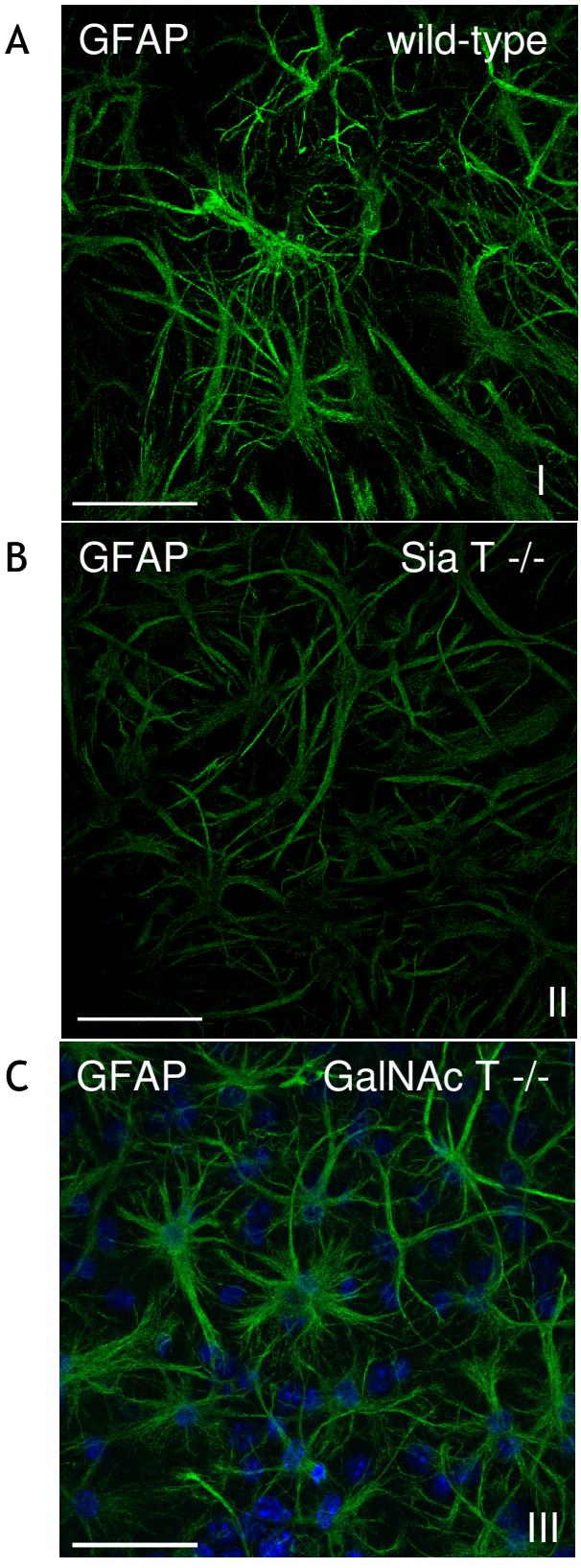

Figure 5.28. Morphology of astrocytes.
Spinal cord cultures obtained from wild-type (I), Sia T-/- (II) and GalNAc T -/- (III) mice were labelled with the typical astrocyte marker GFAP and DAPI to show cell nuclei (in III) to investigate if the morphology of astrocytes differed between wild-type and ganglioside knockout mice. It was found that there was no difference in astrocyte morphology between wild-type and ganglioside knockout mice. Scale bar = 50 μm.

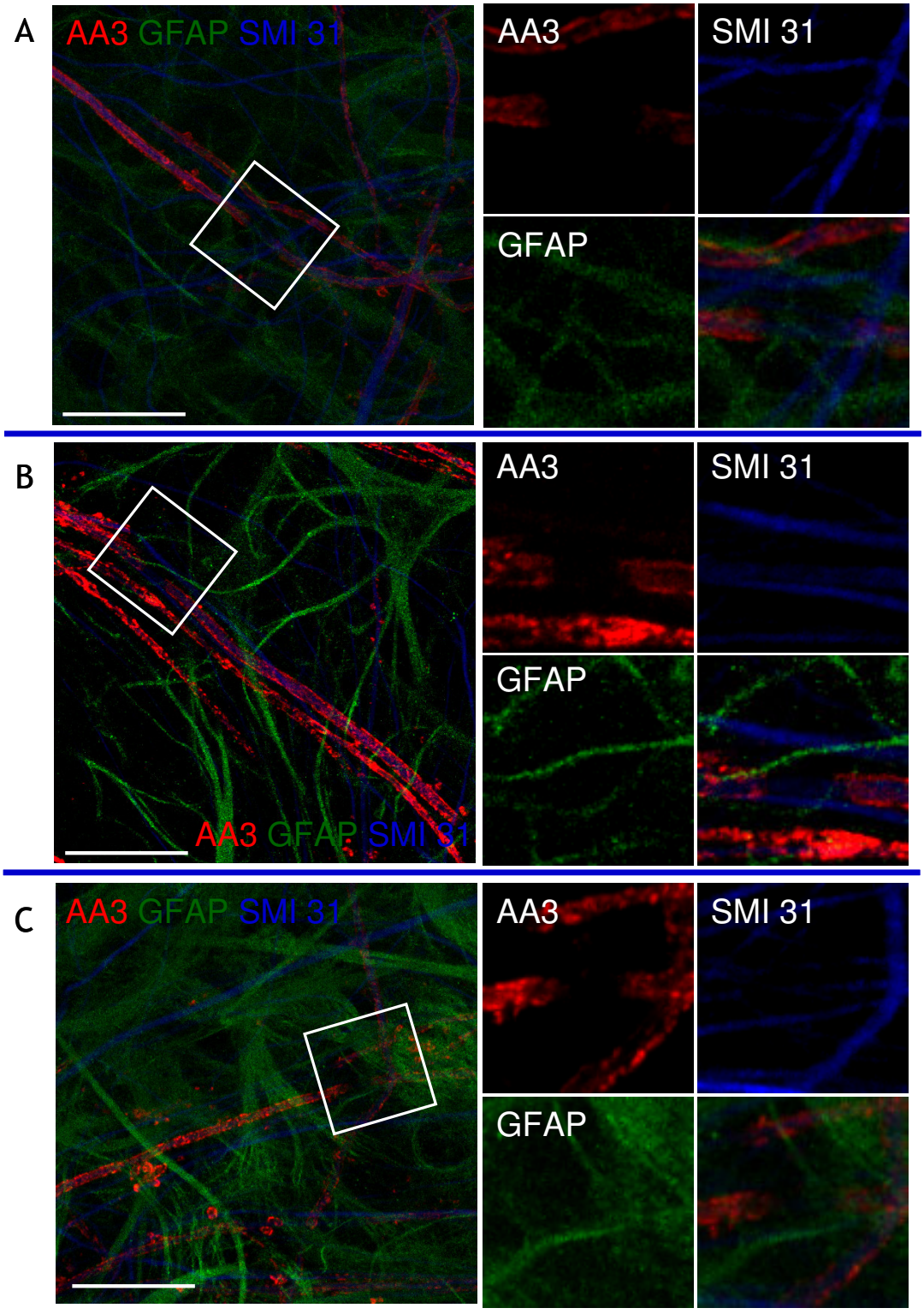

Figure 5.29. Representative images of astrocytes located near node of Ranvier in wild-type spinal cord cultures.
To investigate whether astrocyte processes were associated with node of Ranvier of Ranvier in spinal cord cultures, wild-type cultures were labelled with GFAP to visualise astrocytes, AA3 to visualise compact myelin and SMI 31 to visualise axons. Although the astrocytes processes were found near nodes of Ranvier it was not possible to determine whether they were in contact. Scale bar = 20 µm.

5.3 Discussion

5.3.1 Ganglioside expression of dissociated spinal cord cultures.

The The main aim of this study was to characterise the ganglioside expression of the main cell types present within dissociated spinal cord cultures, namely astrocytes, neurons, and oligodendrocytes. This would then allow us to ascertain if there was differential expression between the various cell types and also whether there was justification to carry out further studies on the various cell types from the ganglioside transgenic mice.

Initially, the optimal culture conditions for these cultures were investigated. Two media were tested which had subtle differences in their composition, to ensure I had optimal conditions for myelination. Thomson *et al* (2006) found that myelin formation was better in differentiation medium and was not promoted by Neurobasal medium with B27 supplement. Although the present study did not find any difference in axonal growth or myelination between cultures maintained in the two media, it was decided to perform subsequent experiments using cultures maintained in differentiation medium. The cultures were initially established in serum-rich plating medium, and were subsequently fed using serum-free differentiation medium such that the concentration of serum declined with each feeding so that, by 10–12 days in vitro, it was less than 1% (Thomson *et al*., 2006).

5.3.1.1 Ganglioside expression of OPCs and oligodendrocytes

During nervous system development OPCs progress through a series of morphologically and immunohistochemically distinct differentiation steps, starting as proliferating and migrating progenitor cells and leading to mature myelinating oligodendrocytes. Out of the four markers tested, OPCs, as labelled by the antibody NG2, were positive for A2B5 and R24 but negative for CTx and MOG35. As OPCs matured into oligodendrocytes, their ganglioside expression changed. Mature myelinating oligodendrocytes no longer labelled with A2B5 and R24 and instead labelled with CTx and MOG35. This is in agreement with previous studies looking at ganglioside expression of oligodendrocytes, which

also found that their ganglioside expression differs during different stages of development.

Farrer and Quarles (1999) showed that OPCs in culture express ganglioside GT3, O-acetyl GT3 and 9-O-acetyl GD3, all of which are down-regulated as OPCs differentiate into oligodendrocytes but continue to be expressed when they differentiate into type-2 astrocytes. This is in agreement with the present study, where it was found that A2B5, which binds to GT3 and O-acetyl GT3 (Fenderson et al., 1987, Dubois et al., 1990) co-labelled with the OPC marker NG2 and astrocyte marker GFAP, but not myelinating oligodendrocyte marker AA3. Yim et al (1994, , 1995) showed that GD3 and GM3 are major gangliosides in OPCs, with GM3 synthesis increasing dramatically as OPCs differentiate to mature oligodendrocytes, whereas the level of GD3 remained relatively constant as the cells differentiated to mature oligodendrocytes. The present study did not investigate the expression of the simple ganglioside GM3. In agreement with Yim et al, the present study demonstrated that GD3 was expressed in both NG2 positive OPCs as well as O4 positive oligodendrocytes.

Yu and Yen (1975) showed that GM1 is the major ganglioside in mouse myelin and that it increases with age. This was confirmed by Cochran et al (1982) who also showed that mouse myelin contained 59.6% GM1, 4.7% GM4, 4.2% GD3, 4.8% GD2, 8% GD1b, 4.2% GT1b, 2.6% GQ1b, 0.3% GM3, 3.6% GM2, 8% GD1a and 4.8% GT1a. This is partly in agreement with the present study where it was found that myelinating oligodendrocytes contained GM1 and GD1a, however in contrast to the study by Cochran et al (1982), the present study did not observe co-localisation of AA3 with R24, which binds to GD3.

Ganglioside expression of oligodendrocytes suggests that simple gangliosides, GT3 and GD3 that are recognised by A2B5 and R24, respectively, and are found on OPCs, are more likely to be involved in modulating functions such as proliferation and migration. Whereas complex gangliosides, GM1 and GD1a that are recognised by CTx and MOG35, respectively, and are found on mature oligodendrocytes, are more likely to be involved in modulating functions such as myelination and node of Ranvier formation.

5.3.1.2 Ganglioside expression of astrocytes

Type-2 astrocytes are positive for A2B5 antibody labelling (Farrer and Quarles, 1999), whereas type-1 astrocytes are negative (Raff et al., 1983a, Murakami et al., 1999). Type-2 astrocytes also express GD3 (Murakami et al., 1999). The present study demonstrated that the majority of astrocytes within spinal cord cultures are A2B5 negative although some A2B5 positive astrocytes were also present. In addition, very few spinal cord astrocytes labelled with R24, which binds to GD3. This indicates that the majority of astrocytes in spinal cord cultures are type-1 astrocytes. The present study also found that astrocytes in spinal cord cultures did not express GM1 or GD1a, which is in agreement with previous studies that have shown that rodent astrocytes do not contain GM1 on their cell surface (Asou and Brunngraber, 1983, Yamamoto et al., 2007, Asou et al., 1989a, Asou et al., 1989b, Sbaschnig-Agler et al., 1988). In contrast, it was demonstrated that adult human brain tissue expressed GM1 and GD1b on all astrocytes (Marconi et al., 2005) and a study in mouse foetal astrocytes found GM1 expression to be regulated by the cell cycle, with maximal expression during G0/G1 phase (Xie et al., 2004, Ledeen and Wu, 2006). Kawai et al (1999b, 1999a) reported that normal astrocytes in adult human tissue lack GD3 expression, but instead GD3 is expressed in the cytoplasm of reactive and neoplastic astrocytes. It is possible that the astrocytes which labelled with R24 in the present study are reactive astrocytes. In contrast to the present study, it was found that in young and adult mouse brain, both normal and reactive astrocytes express GD3 (Cammer and Zhang, 1996), which may indicated that astrocytes have a different ganglioside expression in vivo and in vitro. Moreover, in contrast to the present study GD3 was found to be expressed in cultured rat astrocytes (Kawashima et al., 1996), which might be due to a species difference.

To confirm the ganglioside expression of astrocytes, primary astrocyte cultures could be obtained (differentiated from neurospheres isolated from the corpus striatum), gangliosides extracted and the ganglioside content examined by thin layer chromatography and tandem mass spectrometry.

5.3.1.3 Ganglioside expression of spinal cord neurons

The present study found that neurons present in dissociated spinal cord cultures isolated from wild-type mice labelled with A2B5, which binds to gangliosides GT3, O-acetyl GT3 (Dubois et al., 1990, Fenderson et al., 1987) and GQ1c (Kasai and Yu, 1983), CTx, which binds to GM1 and MOG35, which binds to GD1a. A2B5 was originally thought to bind only to neurons in chick CNS and PNS tissues (Eisenbarth et al., 1979), and was found to bind to the majority of neurons in cultures of a variety of vertebrate CNS tissues (Berg and Schachner, 1982, Schnitzer and Schachner, 1982), which is in agreement with the present study. In agreement with the present study, numerous studies have shown that neurons express GM1 on their cell surface both in situ and in vitro (Asou et al., 1983, Okada et al., 1982). Vyas et al (2002) showed that GD1a is expressed on the cell surface of nerves, which is in accordance with the present study. Furthermore, gangliosides GD1a and GT1b, which are present on the surface of axons, act as functional ligands for MAG and play a role in MAG-mediated inhibition of neurite outgrowth (Vyas et al., 2002). However, in contrast to other studies (Molander et al., 1997, Sheikh et al., 1999a, Susuki et al., 2007b), the present study did not observe the localisation of GM1 at paranodes. These contrasting results may reflect differences in antibodies used or experimental methods. In previous studies the animals were perfused with paraformaldehyde prior to dissection (Molander et al., 1997, Sheikh et al., 1999a, Susuki et al., 2007b) and the tissue permeabilised with Triton X (Molander et al., 1997, Susuki et al., 2007b), whereas in the present study, the ganglioside labelling was performed on unfixed cultures without the use of detergents, which could account for the different results. Indeed, it has been found that the fixation method can greatly influence the apparent localisation of gangliosides (Schwarz and Futerman, 1997). Autoantibodies to GM1 and GD1a attack the nodal region and cause AMAN, which is usually restricted to peripheral motor nerve fibres (Hughes and Cornblath, 2005). The present study did not observe the presence of GD1a at paranodes of cultured spinal cord neurons, so it is possible that GD1a is only present near nodes of Ranvier in peripheral nerves.

The present study revealed that axons in wild-type spinal cord cultures were R24 negative whereas GalNAc T -/- axons were R24 positive suggesting that in wild-type axons GD3 is converted into more complex gangliosides.

Because ganglioside knockout mice have altered paranodal junctions, broadened Na^+ channel clusters, and mislocalisation of juxtaparanodal K^+ channels at the paranodes (Susuki et al., 2007a), it is important to examine the ganglioside expression of axons and oligodendrocytes at and around the nodes of Ranvier in more detail. Different staining protocols should be tested to examine the ganglioside expression of myelinated axons in spinal cord cultures at 28 and 32 DIV at which point many of the myelinated axons contain nodes of Ranvier.

5.3.1.4 Summary of ganglioside expression

The initial aim of this study was to investigate the role of gangliosides in the final step of oligodendrocyte differentiation, the myelination of axons. As demonstrated by immunocytochemistry in this study and by others, ganglioside composition undergoes significant changes during oligodendrocyte development. This could potentially have an impact on the myelination of axons by oligodendrocytes. It has also been shown that axons express gangliosides on their cell surface, and these gangliosides may also play a role in the myelination process. Finally, although astrocytes are not directly involved in the myelination process, it has been shown that astrocytes promote myelination by mature oligodendrocytes in an activity dependent manner (Ishibashi et al., 2006) and the close association of perinodal astrocyte processes with nodes of Ranvier suggests that they may play a functional role. Astrocytes also express numerous gangliosides (described in section 1.2.1.2), which could affect their function.

5.3.2 Differentiation of oligodendrocytes

The present study found that the antigenic differentiation of oligodendrocytes was similar in all three genotypes with one major exception being that GalNAc T -/- mice had lower numbers of the more immature NG2+O4- OPCs.

The differentiation of Sia T -/- OPCs into oligodendrocytes was unaffected in optic nerve and spinal cord cultures despite the lack of many of the gangliosides normally present in OPCs. This would suggest that b-series ganglioside GD3 which is present in OPCs and oligodendrocytes in wild-type cultures but absent in Sia T -/- cultures and c-series gangliosides GT3 and O-acetyl GT3, which are

present in wild-type OPCs but absent in Sia T -/- OPCs, do not play a role in the differentiation in the early or late stages of the oligodendrocyte lineage.

Reduced numbers of NG2+O4- early OPCs in GalNAc T -/- could be due to several factors. The increased amount of simple gangliosides GM3, GD3 and GT3 in GalNAc T -/- cultures may drive the differentiation into NG2+O4+ oligodendrocytes. It can be seen in figure 5.14 that GalNAc T -/- cultures do have higher levels of NG2+O4+ cells compared with wild-type and Sia T -/- cultures (although this increase is not statistically different), which would support this argument. Indeed Yu et al (Yu et al., 1994) have shown that increased level of GM3 enhances the differentiation of OPCs towards premyelinating oligodendrocytes.

Alternatively, it may be that the increased amount of simple gangliosides leads to a reduction in the proliferation or survival of OPCs. The spinal cord cultures were maintained in the presence of insulin, which is a survival factor for oligodendrocytes (Barres et al., 1992), after which the insulin is withdrawn. It may be possible that GalNAc T -/- early OPCs are less resistant to the withdrawal of insulin. Due to time constraints it was not possible to perform proliferation or apoptosis assays to examine whether the lack of NG2+ OPCs in GalNAc T -/- cultures was due to reduced proliferation or increased cell death. However, it was observed that GalNAc T -/- cultures at 7 DIV did not appear to have lower levels of NG2+ OPCs compared with wild-type which would suggest that reduced early OPC numbers in GalNAc T -/- mice at 21 and 28 DIV may be due to either reduced proliferation or increased apoptosis.

GalNAc T -/- knockouts have decreased myelination in the optic nerve and demyelination in the sciatic nerve (Sheikh et al., 1999a). It has been shown that adult brains also contain a pool of OPCs which could be used to produce myelinating oligodendrocytes. Future studies could examine whether GalNAc T -/- mice contain lower number of “adult OPCs” in vivo. If this is the case, inadequate remyelination in GalNAc T -/- mice may be the result of a reduced number of OPCs. It is possible that the lack of OPCs means that when myelin deteriorates, there are not enough OPCs present to differentiate and form myelinating oligodendrocytes in order to replace the damaged myelin.

The present study has demonstrated a reduction in OPCs in GalNAc T -/- cultures which have increased levels of GD3. This may reflect the pathology of MS as it has been reported that plaques have high levels of GD3 (Yu et al., 1974). Thus the increased GD3 in MS plaques may cause decreased proliferation or increased apoptosis of OPCs which may contribute to the failure of OPCs to remyelinate the demyelinated axons.

To try and interpret the reason for lower numbers of the NG2+/O4- OPCs future studies could examine the differentiation of oligodendrocytes in GalNAc T -/- mice in more detail in the presence and in the absence of axons. In this study, I compared the differentiation of wild-type, GalNAc T -/- and Sia T -/- oligodendrocytes in the presence of axons, at 21 and 28 DIV. It would be beneficial to repeat this experiment at earlier time-points (for example, after 1, 7 and 14 DIV) to assess if the numbers of NG2+O4- early OPCs in GalNAc T -/- mice are lower initially or if this develops over time.

In this project I studied the differentiation of wild-type and Sia T-/- optic nerve oligodendrocytes in the absence of axons. The low number of oligodendrocytes obtained from the optic nerve limited the number and the type of experiments that could be carried out and meant that I could only examine wild-type and Sia T -/- oligodendrocytes. In order to examine the role of gangliosides in oligodendrocyte biology in more detail a method of generating large numbers of mouse oligodendrocytes is needed. This could be achieved by culturing OPCs isolated from neonatal mouse spinal cord using a method previously described (Thomson *et al.*, 1999). This method could be used to obtain not only wild-type and Sia T -/- cultures, but also GalNAc T -/- and DKO cultures because each spinal cord could be cultured separately and the genotype examined by labelling with CTx. This would allow a more detailed examination of the role of gangliosides in oligodendrocyte differentiation in the absence of axons, by comparing antigen expression, morphology and by measuring process extension as previously described (Sorensen *et al.*, 2008). This would show whether GalNAc T -/- cultures also had lower numbers of NG2+O4- early OPCs in the absence of axons.

Having shown that b- and c-series gangliosides do not play a role in the differentiation of oligodendrocytes, the next step would be to examine whether

gangliosides expressed in migratory and proliferative OPCs modulate these processes. Using OPCs isolated from neonatal spinal cord, proliferation and differentiation of oligodendrocytes obtained from wild-type and ganglioside knockout mice could be compared using flow cytometry as described previously (Lu *et al.*, 2008). Alternatively, oligodendrocyte proliferation could be examined by Ki67 or BrdU immunolabelling.

OPC migration is controlled by a combination of short-range attractants and repellents, such as tenascin, ephrin and anosmin-1 as well as long-range chemoattractants and chemorepellents, such as chemokines, growth factors and semaphorins. The role of each of these factors can differ depending on the location and during the course of development, probably due to changes in the receptor repertoire of OPCs and to environmental co-factors. Numerous in vitro studies have suggested that gangliosides play a modulatory role in cell migration and adhesion, however, the fact that ganglioside knockout mice develop normally suggests that compensatory mechanisms and/or molecular or functional substitutions must exist. It is likely that gangliosides do not directly influence OPC migration but rather that they modulate the effects of other molecules. Indeed, it has been shown that an interaction of tenascin-R with cell surface disialogangliosides mediates a selective inhibition of integrin-dependent cell adhesion to fibronectin in vitro (Probstmeier *et al.*, 1999). Since GD3-positive OPCs are highly motile, it would be interesting to examine the migration of OPCs obtained from ganglioside knockout mice, especially from the double knockout mice. Since gangliosides are thought to modulate the function of most growth factors, it would be interesting to examine the migration of OPCs in response to PDGF and FGF, both of which are chemoattractant for OPCs. To examine the interaction between gangliosides, integrins and tenascin-R, OPC adhesion and migration would have to be examined on different substrates such as PLL, laminin, fibronectin and vitronectin, in the presence and absence of tenascin. Moreover, if gangliosides do play a role in OPC migration, future studies should investigate whether gangliosides interact with any of the other molecules involved in OPC migration, such as NG2, netrin or PSA-NCAM.

Due to time constrains, I was not able to repeat any of the experiments using cultures obtained from double knockout mice as these animals are poor breeders and produce low numbers of homozygous pups. The simpler gangliosides are, to

some extent, able to compensate for the lack of complex gangliosides, which makes it more difficult to interpret results obtained from single knockouts because it is hard to dissect out whether a particular result is due to the lack of particular gangliosides or the excess of others. Therefore, experiments in double knockout mice which only express GM3, should shed more light on the role of ganglioside in oligodendrocyte proliferation, migration and differentiation in the absence or presence of axons.

5.3.3 Relationship of oligodendrocytes with axons

The mixed spinal cord cultures used in these experiments seem to follow in vivo development, allowing the in vitro study of several stages of neural development (Hardy and Friedrich, 1996, Sherman and Brophy, 2005, Trapp et al., 1997). The early phase of development is characterised by neuronal survival and axon/neurite extension and OPCs proliferation. This is followed by OPC differentiation from a premyelinating cell with many, highly branched processes into a myelinating cell with fewer processes and the ensheathment/myelination of axons and their formation of nodes of Ranvier (Sorensen *et al.*, 2008).

The present study showed that the relationship between oligodendrocytes and axons prior to the formation of node of Ranvier was similar in wild-type and ganglioside knockout mice. This suggests that the early interaction of oligodendrocytes with axons is not modulated by gangliosides. However, this experiment needs to be repeated in the double knockout mice because it is possible that, in the single knockouts, the simpler gangliosides are able to compensate for the lack of complex gangliosides.

5.3.4 Comparison of axonal density and myelination

The effect of knocking out gangliosides on neuronal survival and the density of axons was examined using embryonic spinal cord cultures plated on PLL. Axonal density (% SMI 31-immunoreactivity/given area) was found to be significantly higher in Sia T -/- cultures at 21 DIV but is similar in all genotypes at 28 DIV. The transient increase in neurite extension in Sia T -/- cultures may be due to the lack of b- or c- series gangliosides or the increased levels of a-series gangliosides. To determine which, axonal density measurements need to be

carried out in double knockout mice: if the axonal density is increased in double knockout mice then it would suggest that it is the lack of b-series gangliosides, rather than the increase in a-series gangliosides that is responsible for the transient increase in axonal density.

It has been shown that MAG inhibits neurite outgrowth by binding to GT1a and GT1b (McKerracher et al., 1994, Mukhopadhyay et al., 1994). It is possible that increased a-series gangliosides on Sia T -/- neurons initially lead to increased neurite outgrowth and survival, but once oligodendrocytes begin to express MAG, it inhibits further neurite outgrowth. Future studies should examine the MAG expression in wild-type and ganglioside knockout cultures at several time-points (for example 7, 14, 21, and 28 DIV) and measure the axonal density at the same time-points to examine if there is a correlation between MAG expression and the reduction of axonal density in Sia T -/- cultures.

Sia T -/- cultures lack the ganglioside O-acetyl GD3 which is associated with elongation of neurites. It has been shown that neurite outgrowth in neurons of embryonic rat dorsal root ganglia explants grown on laminin is halted in the presence of Jones monoclonal antibody which binds to 9-O-acetyl GD3 (Mendez-Otero and Friedman, 1996). This would suggest that Sia T -/- which lack O-acetyl GD3 would have decreased neurite outgrowth. However, Yang et al (Yang et al., 2007) found that Jones antibody had the same effect on wild-type and Sia T -/- neurons which lack O-acetyl GD3, suggesting that its effects on neurite outgrowth are not mediated by O-acetyl GD3 binding, which explains why we have not seen a reduced neurite outgrowth in Sia T -/- cultures in the present study.

PLP labelling was found to be lower in GalNAc T –/- mice at 21 DIV, however, by 28 DIV, it was similar in all genotypes. This finding suggests that complex gangliosides may play a role in the initiation of myelination. GalNAc T -/- mice lack all complex gangliosides but have excess of simple gangliosides such as GM3. It was shown that excess GM3 drives the differentiation of oligodendrocytes toward the premyelinating stage (Yim et al., 1994, Yim et al., 1995). As seen from the ganglioside expression of oligodendrocytes, simpler gangliosides are present in the early stages of oligodendrocytes differentiation and are replaced by complex gangliosides such as GM1 and GD1a in the later

stages of differentiation. The results of the present study suggest that without these complex gangliosides, the differentiation of premyelinating oligodendrocytes into myelinating oligodendrocytes is slower.

To test whether the decreased PLP labelling in GalNAc T -/- mice is due to increased levels of simple gangliosides or the lack of complex gangliosides, this experiment needs to be repeated in double knockout mice. If the level of PLP labelling is also decreased in double knockout mice it would suggest that the decreased levels of PLP labelling are more likely to be due to the decreased levels of a-series gangliosides, although the possibility that it's due to increased levels of GM3 could not be excluded.

There could be several reasons for the decreased myelination in GalNAc T -/- cultures at 21 DIV. Axonal density is similar in wild-type and GalNAc T -/- cultures at 21 DIV which suggests that the reason for reduced myelination in GalNAc T -/- cultures at 21 DIV may be a reduction in oligodendrocyte process extension or in oligodendrocyte numbers, rather than a lack of axons. The reduced myelination in GalNAc T -/- mice may also be due to an inhibitory contact-mediated mechanism between axons and oligodendrocytes. Alternatively, GalNAc T -/- oligodendrocytes could be more responsive to a secreted inhibitory factor that prevents myelination, or there may be a delay in GalNac T -/- axons secreting a premyelinating factor. Future studies should elucidate the mechanism in more detail.

In the present study, I used PLP labelling as an indicator of the extent of myelination. However, this gives no indication of whether the myelin is compacted and well formed at the ultrastructural level. To examine myelination in more detail, future experiments should use electron microscopy to compare the quality of myelin produced in wild-type cultures with that of ganglioside knockout cultures. This would allow the measurement of myelin thickness and would show up any myelination defects.

Studies have shown that synapse formation and the development of electrical activity promotes myelination. Future studies could compare the effect of electrical activity on myelination in wild-type and ganglioside knockout mice by adding tetrodotoxin, which blocks action potentials or α-scorpion toxin, which increases axonal firing (Demerens *et al.*, 1996).

As shown in the present study, neuronal survival and myelination were good in both wild-type and ganglioside knockout cultures maintained in differentiation medium on non-specific substrate PLL. It is interesting to note that in rat cultures neuron survival was poor past one to two weeks and that myelinated axons were observed rarely in rat embryonic spinal cord cultures grown on PLL under the same conditions (Sorensen *et al.*, 2008), which highlights the different growth requirements for mouse and rat cells.

5.3.5 Localisation of proteins at the node of Ranvier

The mature molecular organisation of the membrane of myelinated axons includes clusters of Nav1.6 at nodes, Caspr and NF155 forming paranodal junctions and aggregations of Kv1.2 in juxtaparanodal regions.

The present study showed that Caspr and NF155 localisation was unaffected in both Sia T -/- and GalNAc T -/- mice. In addition, the distribution of Na_v at developing nodes of Ranvier formed in Sia T -/- dissociated spinal cord cultures by differentiating oligodendrocytes was found to be similar to that observed at wild-type nodes. K_v localisation in Sia T -/- spinal cord cultures was also similar to that observed in wild-type cultures. These findings suggest that GM1 or GD1a, which are found on Sia T -/- axons, may play important stabilising roles at paranodal junctions in spinal cord neurons.

As at wild-type nodes (Bhat, 2003, Girault and Peles, 2002, Poliak and Peles, 2003, Salzer, 2002), the populations of channels in Sia T -/- cultures were sharply delimited, with Na_v clustered at the nodal axolemma and K_v channels at the paranodal and juxtaparanodal region. In wild-type and Sia T -/- cultures, no Na_v were detected beneath the myelin sheath in the internodes, in accordance with the observation that Na_v are present only in low density beneath the myelin sheath in normal axons (Waxman and Ritchie, 1993).

However, in GalNAc T -/- cultures, Na_v were often observed throughout the myelinated axon, resembling the Na_v labelling in unmyelinated axons. Furthermore, the localisation of K_v to paranodal and juxtaparanodal regions was delayed in GalNAc T -/- cultures compared with wild-type. Rather at 28 DIV, when Kv were localised to the paranodal and juxtaparanodal regions in wild-type cultures, in GalNAc T -/- cultures, the K_v were observed throughout the

membrane or were clustered at the node of Ranvier. These abnormalities in distribution are absent in nodes of Ranvier formed in Sia T -/- and wild-type cultures.

Kv are generally not observed in the nodal axolemma (Mi et al., 1995, Wang et al., 1993). Instead, they are aggregated within juxtaparanodal domains, and their segregation to this region is dependent on intact paranodal axo-glial junctions (Rasband, 2004, Rasband et al., 1999b). In the absence of intact paranodal junctions, Kv1 channels can encroach into paranodal and even nodal domains, leading to abnormalities in conduction parameters (Bhat et al., 2001, Boyle et al., 2001, Coetzee et al., 1996, Dupree et al., 1998). Since K_v are localised in paranodal and juxtaparanodal regions in wild-type and Sia T -/- cultures, it would suggest that the paranodal axo-glial junctions are not properly formed, despite Caspr and NF155 being present at their correct locations at the paranodes. K_v localisation in wild-type and Sia T -/- mice showed a similar pattern as previously reported (Poliak et al., 2001, Susuki et al., 2007a, Vabnick et al., 1999).

The present in vitro study is partly in agreement with the in vivo observations in ganglioside knockout mice (Susuki et al., 2007a). Susuki et al (2007) observed broadened Na^+ channel clusters and found that the localisation of K_v to juxtaparanodes was slower in GalNAc T -/- mice during development. The same study found that immunostaining of Caspr and NF155 was reduced in both peripheral and central nervous nerves, which became more prominent with age (Susuki et al., 2007a). This is in contrast to the present study where no difference was found in the immunolabelling of Caspr and NF155 between wild-type and ganglioside knockout mice. Susuki *et al* observed myelination and nodal defects in Sia T -/- mice, however these defects were less frequent in Sia T -/- mice compared with GalNAc T -/- mice (Susuki et al., 2007a). In contrast, the present study found no difference between wild-type and Sia T -/- in terms of myelination and the formation of nodes of Ranvier.

However, Susuki et al (2007a) found that paranodal junctions and ion channel clusters were disrupted in ventral rather than in dorsal roots from GalNAc-T -/- mice, suggesting that the composition or contribution of gangliosides at paranodal structures may differ between peripheral motor and sensory nerve

fibers. The neurons in the dissociated spinal cord cultures examined in the present study are most likely to be motor neurons. Therefore, it is possible that no abnormalities are observed in Sia T -/- cultures for this reason. Our findings do not exclude the possibility that defects may be present in Sia T -/- sensory neurons.

Studies in sciatic nerve (Boiko et al., 2001) and optic nerve (Boiko et al., 2001, Jenkins and Bennett, 2002, Kaplan et al., 2001, Rios et al., 2003) have demonstrated that $Na_v1.2$ is distributed along premyelinated axons and is transiently present at immature nodes in these tracts. $Na_v1.2$ is subsequently replaced by $Na_v1.6$, which was shown to be the predominant isoform at mature nodes of Ranvier in both the PNS and CNS (Caldwell et al., 2000). The Na_v antibody used in the present study recognises all known vertebrate sodium channels, so it was not possible to distinguish which subtype of sodium channel was present in the spinal cord cultures. Future studies could include an examination of the subtype of sodium channel present at the nodes of Ranvier in wild-type and ganglioside knockout mice.

It has been shown that the axonal membrane also undergoes a sequential transformation during development. In the PNS, cell adhesion molecules such as neurofascin 155 are the first molecules to appear at prospective nodes, followed by ankyrin G isoforms and Na_v (Lambert et al., 1997). Finally clusters of Kv1.1 and Kv1.2 channels appear after clusters of Na_v channels and ankyrin G are well established (Vabnick and Shrager, 1998, Vabnick et al., 1999). The K_v channels gradually become sequestered in the juxtaparanodal region, where they are thought to be electrically isolated from the nodes. The fact that myelinating cultures from GalNAc T -/- mice show normal distribution of Caspr and NF155 and sometimes Na_v but not K_v at 28 DIV suggests that the assembly of the molecular components in and around the node of Ranvier is slower in these mice compared with wild-type. This raises the question whether the retarded temporal expression in GalNAcT -/- cultures is specific to Na_v and K_v or is it the case that that the assembly of all the proteins is slower in GalNAc T -/- mice. In other words, it is possible that the expression of Caspr and neurofascin 155 is also slowed in GalNAc T -/- but the time points that were chosen in the present study were too late to observe this. This question could be answered by

examining the expression of neurofascin 155 and Caspr at time points between 21 and 28 DIV.

Since abnormalities in the assembly of nodal proteins were less frequent in Sia T -/- mice lacking GD1b and GT1b and since the major gangliosides in Sia T -/- mice are GM1 and GD1a (Okada *et al*., 2002), it suggests that GM1 or GD1a play a role in the formation of node of Ranvier. However, changes due to other minor gangliosides or excess of a-series gangliosides such as GM1 and GD1a cannot be excluded.

The findings of the present study show that gangliosides do play a role in the assembly of node of Ranvier. However, from previous studies in adult ganglioside knockout mice, it would appear that gangliosides are more important in the maintenance than the development of myelinated axons. Finally, it is possible that the concurrent increase in simple gangliosides that goes hand-in-hand with knocking out complex gangliosides has a compensatory role during development, and minimises the detrimental effects of knocking out complex gangliosides. Due to time restrictions it was not possible to carry out studies on double knockout mice in the present study. However, it would be interesting to repeat these experiments using double knockout mice which lack all gangliosides apart from the simplest ganglioside GM3. It is possible that much more severe effects would be observed.

5.3.6 Conclusion

In the present study, dissociated spinal cord cultures have been validated as a good model for studying oligodendrocytes differentiation, neurite outgrowth and myelination since temporal changes in these cultures can mirror developmental events in vivo.

Cells of the oligodendrocyte lineage in dissociated spinal cord cultures express simple b- and c-series gangliosides GD3 and GT3 in the early stages of differentiation and with time the ganglioside expression profile changes to express a-series gangliosides GM1 and GD1a. The majority of astrocytes were negative for all four markers tested in this study, however, a subset of astrocytes labelled with A2B5 and R24, revealing the presence of type-2

astrocytes in these cultures. Axons of spinal cord neurons expressed gangliosides recognised by A2B5, as well as GM1 and GD1a.

The major finding of the present study are that GalNAc T -/- cultures lacking all complex gangliosides contain significantly lower number of early OPCs, have decreased myelination initially and that Na_v and K_v channel assembly to the node of Ranvier and juxtaparanode, respectively, is slower compared to wild-type and Sia T -/- mice. In contrast, no abnormalities were observed in Sia T -/- cultures which lack all b-series gangliosides, with the exception of initially higher axonal density compared with wild-type and GalNAc T -/- cultures.

Previous studies have shown that astrocytes express gangliosides and that they can promote myelination of CNS axons (Blakemore and Crang, 1989; Blakemore *et al.*, 2003, Franklin *et al.*, 1991, Ishibashi *et al.*, 2006, Sorensen *et al.*, 2008). Therefore, future studies should examine in more detail the role of astrocytes in myelination in wild-type and ganglioside knockout mice.

It has been shown that gangliosides modulate cellular events by interacting with integrins or growth factor receptors. These cultures could be used to examine the interaction of gangliosides with growth factors by comparing the effects of the addition of growth factors. To investigate whether the effects of knocking out gangliosides observed in the present study involve integrin signalling, future studies could include a more detailed investigation into the effect of other substrates, such as laminin, extracellular matrix or fibronectin and the addition of antibodies to specific integrins. Gangliosides have been shown to be localised in lipid rafts, which are thought to be sites of cell signalling. It is possible that the myelination defects observed in ganglioside knockout mice are due to the altered ganglioside composition of the lipid raft which may affect cell signalling. Therefore, future studies should examine lipid raft association of molecules involved in myelination in wild-type and ganglioside knockout.

Future studies should investigate signalling and should be aimed at examining whether gangliosides are a trophic axonal signal that signals oligodendrocytes to differentiate or are the gangliosides present on oligodendrocyte used in cell-to-cell interaction in the cross-talk between oligodendrocytes and axons. These questions could be addressed by setting up co-cultures of neurons from wild-type mice (without other cells) and glia (oligodendrocytes and astrocytes) from

knockout mice and vice versa similar to co-cultures described previously (Chan *et al*, 2004, Lubetzki *et al*., 1993, Mi *et al*., 2005, Wang *et al*., 2007).

6 CHAPTER 6

General Discussion

Ganglioside enrichment in neural cells (neurons and glia) has led to investigations into their role in nervous system function. As a result, gangliosides have been implicated in the neurobiology of diseases, and in the regulation of many cellular and molecular properties. However, most studies have focused on the role of gangliosides in neuronal function. The aim of my thesis was to investigate ganglioside function in glial cell biology by using wild-type and ganglioside knockout mice. I initially studied detailed cellular properties of olfactory ensheathing cells (OECs) and Schwann cells followed by the role of gangliosides in the regeneration of the olfactory system and in oligodendrocyte differentiation and myelination using an embryonic spinal cord culture system.

Central nervous system (CNS) pathologies are often very debilitating due to the inability of the CNS to undergo repair following damage. Examples of such pathologies include chronic neurodegenerative diseases such as Parkinson's disease and Alzheimer's disease, and disorders characterised by cell death or loss of key neural pathways such as spinal cord injury and ischemic stroke. Although neuronal degeneration and death are the ultimate consequences of these pathological processes, alterations in the function of surrounding glial cells are key features in the progression of many of these diseases.

Numerous potential therapies are being investigated at present to promote repair of the damaged CNS, ranging from use of cellular transplantation to mediate repair and remyelination, to growth factor delivery to improve survival rates of neurons and promote axonal outgrowth, and use antibodies or pharmacological agents against inhibitory factors. The findings that neuronal accumulation of gangliosides in lysosomal storage diseases profoundly influenced the development and differentiation of neurons (Purpura and Suzuki, 1976) and that the addition of exogenous gangliosides could promote the regrowth of damaged neurons (Ceccarelli *et al.*, 1976) prompted studies to examine the potential use of exogenous gangliosides as therapeutic agents for neurological diseases.

Subsequent studies have demonstrated that gangliosides can affect multiple neuronal populations including dopaminergic, cholinergic, glutamatergic, serotonergic and noradrenergic neurons (Hadjiconstantinou and Neff, 1998).

Several preclinical studies have reported acute neuroprotective and longer-term neuroregenerative effects of GM1 in experimental models of ischemia and injury (Agnati *et al.*, 1983, Bose *et al.*, 1986, Ceccarelli *et al.*, 1976, Di Gregorio *et al.*, 1984, Fass and Ramirez, 1984, Gorio, 1988, , 1986, Gorio *et al.*, 1980, Gorio *et al.*, 1984a, Gorio *et al.*, 1984b, Itoh *et al.*, 1999, Itoh *et al.*, 2001, Karpiak, 1984, Karpiak *et al.*, 1987, Kojima *et al.*, 1984, Lainetti *et al.*, 1998, Ledeen, 1984, Pope-Coleman *et al.*, 2000, Ramirez *et al.*, 1987a, Ramirez *et al.*, 1987b, Roisen *et al.*, 1981, Rybak *et al.*, 1983, Sabel *et al.*, 1987, Sabel *et al.*, 1984a, Sabel *et al.*, 1984b, Sabel and Stein, 1986, Skaper and Leon, 1992, Toffano *et al.*, 1984a, Toffano *et al.*, 1983, Walker, 1991, Wang *et al.*, 1995). For instance, administration of GM1 in experimental models of Parkinson's disease in rodents and primates, stimulated the regeneration of dopaminergic neurons in the substantia nigra and ameliorated the abnormal motor responses (Fadda *et al.*, 1993, Hadjiconstantinou and Neff, 1988, Pope-Coleman *et al.*, 2000, Raiteri *et al.*, 1985, Schneider *et al.*, 1992, Toffano *et al.*, 1983, Toffano *et al.*, 1984b). These pre-clinical findings led to a small clinical trial of GM1 in patients with Parkinson's disease. These patients responded to the treatment with an overall improvement of motor function, including decreased rigidity and bradykinesia (Schneider, 1998, Schneider *et al.*, 1998) which demonstrates the usefulness of GM1 as a treatment for Parkinson's disease.

A small clinical trial designed to investigate the efficacy of GM1 in patients with cervical and thoracic spinal cord injury suggested that GM1 had the ability to enhance recovery of lower extremities after 1 year (Geisler *et al.*, 1991). This led to a larger scale trial to further investigate the efficacy of low and high dose GM1 following standard treatment with methylprednisolone (Geisler *et al.*, 2001). However, despite GM1 demonstrating improved rates of recovery, along with improved bladder/bowel function, sacral sensation, and anal contraction over the first 3 months post-injury the prospectively planned analysis at 6 months was negative (Geisler *et al.*, 2001).

However, Sia T -/- mice, which lack b-series gangliosides, but have increased levels of a-series gangliosides such as GM1, have reduced regeneration of axotomised hypoglossal nerves compared with wild-type. Since numerous studies have demonstrated the neuroprotective role of GM1 it is surprising that mice which have increased levels of GM1 have decreased regeneration. In order

to understand better the role of gangliosides in regeneration, I compared regeneration of the olfactory system in wild-type and gangliosides knockout mice.

The olfactory system was chosen for this study since it has a great capacity for repair. Olfactory receptor neurons (ORNs) are constitutively replaced throughout life. Because they are in direct contact with the outside environment, they are susceptible to damage from airborne toxins and pathogens (Farbman and Buchholz, 1992) and as a result require continual neurogenesis. This regenerative capacity has often been utilised in studies of regeneration following experimental damage. Many different experimental methods have been used to induce damage in the olfactory system, each with advantages and disadvantages. The transection of the olfactory nerve leads to the retrograde degeneration of mature ORNs, however this method compromises the natural structure of the system and does not damage any of the other cells in the olfactory epithelium including immature ORNs which have not yet extended an axon. The removal of olfactory bulbs also causes the degeneration of ORNs, however the cells are unable to fully mature without a target. In contrast, irrigation of the nasal cavity with zinc sulphate ($ZnSO_4$) results in the rapid degeneration of all cell types of the olfactory epithelium (OE) and is more akin to naturally occurring sequence of events. Williams *et al* (Williams *et al.*, 2004) showed that $ZnSO_4$ irrigation is a reliable method of inducing ORN degeneration and regeneration in the rat. However, other studies have found that this method is partially irreversible (Burd, 1993, Ducray *et al.*, 2002, Harding *et al.*, 1978). In this study, I have observed similar results in that the OE regenerated to about 50% of the control value. It may be that $ZnSO_4$ irrigation is more reliable in rats than in mice.

I have shown that complex gangliosides are present in the normal adult olfactory system. However, I did not observe reduced regeneration in ganglioside knockout cells compared with wild-type. This may be due to the simpler gangliosides being able to compensate for the lack of complex gangliosides. Alternatively, it may be the case that excess of the simpler gangliosides has a neuroprotective role. On the other hand, it may be possible that the method we used was too harsh in that it did not lead to complete regeneration and as a result, any subtle changes in the regeneration capacity in ganglioside knockout

mice may be missed. A milder method of causing damage to the OE might lead to better regeneration of the mouse olfactory system and may be better for studying the effect of gangliosides on the degeneration and regeneration of the olfactory system.

As mentioned above, one of the strategies for repair is cell transplantation. A range of cells have been studied for cellular transplantation including oligodendrocyte precursor cells (OPCs), neural stem cells, Schwann cells and OECs. It is becoming clear that no single strategy will be sufficient to repair spinal cord injury and many studies have a multi-strategy approach such as cell transplantation combined with the addition of growth factors or agents which reduce inhibitory signals. Therefore, a potential treatment for CNS repair could be the addition of gangliosides such as GM1, as well as transplantation of cells such as OECs or Schwann cells. In that case, it would be important to understand the effect gangliosides have on the transplanted cells.

For this reason, I compared the cellular properties of OECs and Schwann cells isolated from wild-type and ganglioside knockout mice. I have shown that the majority of OECs and Schwann cells express a-series gangliosides GM1 and GD1a. Subtle effects were seen in cells obtained from ganglioside knockout mice. For example, OECs isolated from Sia T-/- mice grown on collagen in the presence of growth factors had faster proliferation compared to OECs isolated from wild-type and GalNAc T-/- mice. This suggests that the increase in GM1 and GD1a due to the lack of Sia T -/- may be mediating this effect. Furthermore, since the effect on proliferation was only seen on collagen IV in the presence of growth factors and not on PLL or laminin, it suggests that there is an interaction between these gangliosides and integrins. However, it is difficult to identify the mechanism by which this occurs since there are no known specific collagen IV-binding integrins which do not also interact with laminin. Cell adhesion to collagen IV is mediated by integrins α1β1 and α2β1, however these integrins also bind to laminin (Ruoslahti, 1991). It would, thus, be interesting to examine the signalling involved in mediating the increased proliferation in OECs isolated from Sia T -/- mice.

My experiments also revealed differences in the properties of OECs and Schwann cells isolated from Sia T -/- mice. For instance, Sia T-/- derived OECs had a

greater proliferation rate than Sia T-/- derived Schwann cells. However, this may be difficult to analyse since OECs and Schwann cells were grown in their optimal growth media, which are different. OEC medium (OMM+5%FBS) contains additional factors to Schwann cell medium (10%HF) including astrocyte conditioned medium (ACM) and FGF2 and less foetal bovine serum. ACM contains numerous growth factors including FGF2 (Araujo and Cotman, 1992), PDGF (Richardson *et al.*, 1988), TGFβ (Saad *et al.*, 1991), CNTF (Stockli *et al.*, 1989), NGF (Furukawa *et al.*, 1986, Houlgatte *et al.*, 1989) and NT-3 (Rudge *et al.*, 1992). So the differential growth of the two glial cells may reflect these growth factor differences. If this is the case, it might be that an interaction between gangliosides, integrins and growth factors is responsible for the increase in the proliferation of Sia T -/- OECs. It has been shown in oligodendrocytes that interaction between gangliosides, integrins and growth factors can affect the response of cells: laminin-2 induces the co-localisation of integrin α6β1 and the PDGFαR within the same raft domain and enhances PI3K signalling in response to PDGF (Baron *et al.*, 2003). Also, the fact that Sia T -/- OECs do not show an increase in proliferation when grown in the medium without growth factors, also suggests an interaction between gangliosides and growth factors.

On the other hand the difference observed in the response of OECs and Schwann cells to the depletion of b-series gangliosides and increase in a-series gangliosides may be due to OECs and Schwann cells expressing different integrins. Final differentiation of Schwann cells and myelination requires the synthesis and assembly of ECM molecules, such as laminins and type IV collagen, to form a basal lamina (Bunge, 1993, Bunge *et al.*, 1986, Eldridge *et al.*, 1989, Eldridge *et al.*, 1987, Fernandez-Valle *et al.*, 1993). Non-myelinating Schwann cells express α1β1 (a collagen and laminin receptor) and α6β1 (a unique laminin receptor). Not a lot is known about the integrin expression of OECs. However, they do express the β1 subunit (Au and Roskams, 2003, Pastrana *et al.*, 2006) and the α6 subunit co-localises with $p75^{NTR}$ in the outer nerve layer suggesting that OECs express α6. The α6 subunit is thought to be involved in neuronal migration, neurite outgrowth, and axon guidance during olfactory development (Whitley *et al.*, 2005). Since no reports have been published on the integrin expression of OECs, it would be interesting to characterise the integrin expression of OECs to examine if the different effects of gangliosides on the

proliferation and migration of OECs and Schwann cells are due to the interaction of gangliosides with different integrins.

A common feature seen in chronic neurodegenerative diseases is apoptosis, a form of programmed cell death believed to be caused by secondary injury processes (Bossy-Wetzel *et al.*, 2004). Ganglioside GD3 mediates apoptosis in some cell types, including oligodendrocytes. It would have been interesting to compare the survival of OECs and Schwann cells derived from wild-type, Sia T -/- (which lack GD3) and GalNAc T -/- (which have increased levels of GD3) mice to determine if GD3 plays a role in their survival. However, due to time constraints this was not possible.

Multiple sclerosis (MS) is a chronic inflammatory disease of the CNS white matter, thought to result from an autoimmune attack against autoantigens within the myelin sheath. It is the most common disabling neurological condition affecting young adults, with 85,000 sufferers in the United Kingdom. Disease onset usually occurs in young adults and is more common in women. The prevalence of MS varies from country to country and is much more prevalent in northern Europe, continental North America and Ausralasia than in countries near the equator (Rosati, 2001). Climate, diet, geomagnetism, toxins, sunlight exposure, genetic factors, and infectious diseases have all been discussed as possible reasons for these regional differences. Environmental factors during childhood may play an important role in the development of MS later in life (Marrie, 2004). Pathological characteristics of MS include the loss of oligodendrocytes, demyelination and neurodegeneration (Kalman *et al.*, 2007). Although initially spontaneous remyelination occurs in many MS lesions, the repair process eventually fails (Chari, 2007). Understanding oligodendrocyte differentiation and the myelination process may help to develop strategies to promote myelin repair.

Recent findings suggest that gangliosides play a role in myelination and assembly and maintenance of nodes of Ranvier (Susuki *et al.*, 2007a). To examine the role of gangliosides in oligodendrocyte differentiation, myelination and the formation of node of Ranvier, I used embryonic spinal cord cultures obtained from wild-type, Sia T -/-and GalNAc T -/- mice. The spinal cord cultures revealed several changes in ganglioside knockout mice compared with wild-type. There was a big

difference in the number of NG2 positive cells between wild-type and GalNAc T -/- cultures which suggests that the GalNAc T -/- cultures have less progenitor cells. If this is also true *in vivo*, it would mean that adult GalNAc T -/- mice would have reduced numbers of adult progenitors which would affect remyelination. It has been shown that adult GalNAc T -/- mice have myelination defects (Chiavegatto *et al.*, 2000, Ma *et al.*, 2003, Sheikh *et al.*, 1999b, Takamiya *et al.*, 1996). The reason for the reduced number of progenitors in GalNAc T -/- mice could be that the lack of complex gangliosides or the rise in simple gangliosides GD3 and GT3, which are predominantly expressed in OPCs, somehow speeds up the differentiation of OPCs into more mature oligodendrocytes or results in decreased proliferation or survival of OPCs.

Another difference observed in GalNAc T -/- mice was in the reduced localisation of sodium channels to the node of Ranvier. This is in agreement with studies performed by Susuki *et al* (Susuki *et al.*, 2007a), which show that lack of complex gangliosides affects nodal stability. No difference was observed between wild-type and Sia T -/- cultures suggesting that b-series gangliosides are not vital for oligodendrocyte differentiation, myelination or the formation of node of Ranvier. This study also demonstrates that dissociated spinal cord culture is a useful model for studying myelination *in vitro*.

Although studies in ganglioside knockout mice may not lead directly to treatment of diseases such as MS, it is nevertheless important to examine their contribution to the maintenance of the nervous system. The determination of normal functions of gangliosides should eventually enable an understanding of how they participate in pathological states such as neurodegenerative disorders. The more we understand about the nervous system function the easier it will be to come up with repair strategies when things go wrong.

In conclusion, the comparison of glial cells isolated from wild-type and knockout mice lacking complex gangliosides suggest that gangliosides are not essential in glial cell development and differentiation; however, they do seem to be important in the maintenance of the nervous system. Indeed, babies born with a defect in the ganglioside biosynthesis pathway develop epileptic seizures within the first year of life associated with developmental stagnation and blindness (Simpson *et al.*, 2004), supporting the idea that gangliosides play an important

role in nervous system maintenance and stability. Finally, future studies in mice lacking all ganglio-series gangliosides (Yamashita *et al.*, 2005) should contribute much more to the understanding the physiological role of gangliosides in the nervous system.

References

AGNATI, L. F., FUXE, K., CALZA, L., BENFENATI, F., CAVICCHIOLI, L., TOFFANO, G. & GOLDSTEIN, M. (1983) Gangliosides increase the survival of lesioned nigral dopamine neurons and favour the recovery of dopaminergic synaptic function in striatum of rats by collateral sprouting. *Acta Physiol Scand,* 119, 347-63.
AGUAYO, A. J., ATTIWELL, M., TRECARTEN, J., PERKINS, S. & BRAY, G. M. (1977) Abnormal myelination in transplanted Trembler mouse Schwann cells. *Nature,* 265, 73-5.
AIBA, T., MORI, J. & NAKAI, Y. (1993) Nerve growth factor (NGF) and its receptor in rat olfactory epithelium. *Acta Otolaryngol Suppl,* 506, 37-40.
ALEXANDER, C. L., FITZGERALD, U. F. & BARNETT, S. C. (2002) Identification of growth factors that promote long-term proliferation of olfactory ensheathing cells and modulate their antigenic phenotype. *Glia,* 37, 349-64.
ALTMAN, J. (1969) Autoradiographic and histological studies of postnatal neurogenesis. IV. Cell proliferation and migration in the anterior forebrain, with special reference to persisting neurogenesis in the olfactory bulb. *J Comp Neurol,* 137, 433-57.
AMANO, S., AKUTSU, N., MATSUNAGA, Y., NISHIYAMA, T., CHAMPLIAUD, M. F., BURGESON, R. E. & ADACHI, E. (2001) Importance of balance between extracellular matrix synthesis and degradation in basement membrane formation. *Exp Cell Res,* 271, 249-62.
AMAYA, E., MUSCI, T. J. & KIRSCHNER, M. W. (1991) Expression of a dominant negative mutant of the FGF receptor disrupts mesoderm formation in Xenopus embryos. *Cell,* 66, 257-70.
ANDERSSON, L. M., FREDMAN, P., LEKMAN, A., ROSENGREN, L. & GISSLEN, M. (1998) Increased cerebrospinal fluid ganglioside GD3 concentrations as a marker of microglial activation in HIV type 1 infection. *AIDS Res Hum Retroviruses,* 14, 1065-9.
ARAQUE, A., PARPURA, V., SANZGIRI, R. P. & HAYDON, P. G. (1998a) Glutamate-dependent astrocyte modulation of synaptic transmission between cultured hippocampal neurons. *Eur J Neurosci,* 10, 2129-42.
ARAQUE, A., PARPURA, V., SANZGIRI, R. P. & HAYDON, P. G. (1999) Tripartite synapses: glia, the unacknowledged partner. *Trends Neurosci,* 22, 208-15.
ARAQUE, A., SANZGIRI, R. P., PARPURA, V. & HAYDON, P. G. (1998b) Calcium elevation in astrocytes causes an NMDA receptor-dependent increase in the frequency of miniature synaptic currents in cultured hippocampal neurons. *J Neurosci,* 18, 6822-9.
ARAUJO, D. M. & COTMAN, C. W. (1992) Basic FGF in astroglial, microglial, and neuronal cultures: characterization of binding sites and modulation of release by lymphokines and trophic factors. *J Neurosci,* 12, 1668-78.
ARCUINO, G., LIN, J. H., TAKANO, T., LIU, C., JIANG, L., GAO, Q., KANG, J. & NEDERGAARD, M. (2002) Intercellular calcium signaling mediated by point-source burst release of ATP. *Proc Natl Acad Sci U S A,* 99, 9840-5.
ARMSTRONG, R. C., HARVATH, L. & DUBOIS-DALCQ, M. E. (1990) Type 1 astrocytes and oligodendrocyte-type 2 astrocyte glial progenitors migrate toward distinct molecules. *J Neurosci Res,* 27, 400-7.
ARMSTRONG, R. C., LE, T. Q., FROST, E. E., BORKE, R. C. & VANA, A. C. (2002) Absence of fibroblast growth factor 2 promotes oligodendroglial repopulation of demyelinated white matter. *J Neurosci,* 22, 8574-85.
ARROYO, E. J. & SCHERER, S. S. (2000) On the molecular architecture of myelinated fibers. *Histochem Cell Biol,* 113, 1-18.
ARROYO, E. J., XU, T., POLIAK, S., WATSON, M., PELES, E. & SCHERER, S. S. (2001) Internodal specializations of myelinated axons in the central nervous system. *Cell Tissue Res,* 305, 53-66.

ASOU, H. & BRUNNGRABER, E. G. (1983) Absence of ganglioside GM1 in astroglial cells from 21-day old rat brain: immunohistochemical, histochemical, and biochemical studies. *Neurochem Res,* 8, 1045-57.
ASOU, H., BRUNNGRABER, E. G. & JENG, I. (1983) Cellular localization of GM1-ganglioside with biotinylated choleragen and avidin peroxidase in primary cultured cells from rat brain. *J Histochem Cytochem,* 31, 1375-9.
ASOU, H., HIRANO, S. & KOHSAKA, S. (1989a) Changes in ganglioside composition and morphological features during the development of cultured astrocytes from rat brain. *Neurosci Res,* 6, 369-75.
ASOU, H., HIRANO, S. & UYEMURA, K. (1989b) Ganglioside composition of astrocytes. *Cell Struct Funct,* 14, 561-8.
AU, E. & ROSKAMS, A. J. (2003) Olfactory ensheathing cells of the lamina propria in vivo and in vitro. *Glia,* 41, 224-36.
AYER-LE LIEVRE, C., STAHLBOM, P. A. & SARA, V. R. (1991) Expression of IGF-I and -II mRNA in the brain and craniofacial region of the rat fetus. *Development,* 111, 105-15.
BAICHWAL, R. R., BIGBEE, J. W. & DEVRIES, G. H. (1988) Macrophage-mediated myelin-related mitogenic factor for cultured Schwann cells. *Proc Natl Acad Sci U S A,* 85, 1701-5.
BAKER, H., GRILLO, M. & MARGOLIS, F. L. (1989) Biochemical and immunocytochemical characterization of olfactory marker protein in the rodent central nervous system. *J Comp Neurol,* 285, 246-61.
BANNIKOV, G. A., KARELINA, T. V., COLLIER, I. E., MARMER, B. L. & GOLDBERG, G. I. (2002) Substrate binding of gelatinase B induces its enzymatic activity in the presence of intact propeptide. *J Biol Chem,* 277, 16022-7.
BANSAL, R. & PFEIFFER, S. E. (1997) FGF-2 converts mature oligodendrocytes to a novel phenotype. *J Neurosci Res,* 50, 215-28.
BANSAL, R., STEFANSSON, K. & PFEIFFER, S. E. (1992) Proligodendroblast antigen (POA), a developmental antigen expressed by A007/O4-positive oligodendrocyte progenitors prior to the appearance of sulfatide and galactocerebroside. *J Neurochem,* 58, 2221-9.
BANSAL, R., WARRINGTON, A. E., GARD, A. L., RANSCHT, B. & PFEIFFER, S. E. (1989) Multiple and novel specificities of monoclonal antibodies O1, O4, and R-mAb used in the analysis of oligodendrocyte development. *J Neurosci Res,* 24, 548-57.
BARACSKAY, K. L., KIDD, G. J., MILLER, R. H. & TRAPP, B. D. (2007) NG2-positive cells generate A2B5-positive oligodendrocyte precursor cells. *Glia,* 55, 1001-10.
BARBER, P. C. & DAHL, D. (1987) Glial fibrillary acidic protein (GFAP)-like immunoreactivity in normal and transected rat olfactory nerve. *Exp Brain Res,* 65, 681-5.
BARNETT, S. C., ALEXANDER, C. L., IWASHITA, Y., GILSON, J. M., CROWTHER, J., CLARK, L., DUNN, L. T., PAPANASTASSIOU, V., KENNEDY, P. G. & FRANKLIN, R. J. (2000) Identification of a human olfactory ensheathing cell that can effect transplant-mediated remyelination of demyelinated CNS axons. *Brain,* 123 (Pt 8), 1581-8.
BARNETT, S. C. & CHANG, L. (2004) Olfactory ensheathing cells and CNS repair: going solo or in need of a friend? *Trends Neurosci,* 27, 54-60.
BARNETT, S. C., HUTCHINS, A. M. & NOBLE, M. (1993) Purification of olfactory nerve ensheathing cells from the olfactory bulb. *Dev Biol,* 155, 337-50.
BARON-VAN EVERCOOREN, A., GANSMULLER, A., GUMPEL, M., BAUMANN, N. & KLEINMAN, H. K. (1986) Schwann cell differentiation in vitro: extracellular matrix deposition and interaction. *Dev Neurosci,* 8, 182-96.
BARON-VAN EVERCOOREN, A., OLICHON-BERTHE, C., KOWALSKI, A., VISCIANO, G. & VAN OBBERGHEN, E. (1991) Expression of IGF-I and insulin receptor genes in

the rat central nervous system: a developmental, regional, and cellular analysis. *J Neurosci Res,* 28, 244-53.
BARON, W., COLOGNATO, H. & FFRENCH-CONSTANT, C. (2005) Integrin-growth factor interactions as regulators of oligodendroglial development and function. *Glia,* 49, 467-79.
BARON, W., DECKER, L., COLOGNATO, H. & FFRENCH-CONSTANT, C. (2003) Regulation of integrin growth factor interactions in oligodendrocytes by lipid raft microdomains. *Curr Biol,* 13, 151-5.
BARON, W., SHATTIL, S. J. & FFRENCH-CONSTANT, C. (2002) The oligodendrocyte precursor mitogen PDGF stimulates proliferation by activation of alpha(v)beta3 integrins. *Embo J,* 21, 1957-66.
BARRES, B. A., CHUN, L. L. & COREY, D. P. (1988) Ion channel expression by white matter glia: I. Type 2 astrocytes and oligodendrocytes. *Glia,* 1, 10-30.
BARRES, B. A., HART, I. K., COLES, H. S., BURNE, J. F., VOYVODIC, J. T., RICHARDSON, W. D. & RAFF, M. C. (1992) Cell death and control of cell survival in the oligodendrocyte lineage. *Cell,* 70, 31-46.
BARRES, B. A., JACOBSON, M. D., SCHMID, R., SENDTNER, M. & RAFF, M. C. (1993a) Does oligodendrocyte survival depend on axons? *Curr Biol,* 3, 489-97.
BARRES, B. A. & RAFF, M. C. (1993) Proliferation of oligodendrocyte precursor cells depends on electrical activity in axons. *Nature,* 361, 258-60.
BARRES, B. A. & RAFF, M. C. (1994) Control of oligodendrocyte number in the developing rat optic nerve. *Neuron,* 12, 935-42.
BARRES, B. A. & RAFF, M. C. (1999) Axonal control of oligodendrocyte development. *J Cell Biol,* 147, 1123-8.
BARRES, B. A., RAFF, M. C., GAESE, F., BARTKE, I., DECHANT, G. & BARDE, Y. A. (1994) A crucial role for neurotrophin-3 in oligodendrocyte development. *Nature,* 367, 371-5.
BARRES, B. A., SCHMID, R., SENDNTER, M. & RAFF, M. C. (1993b) Multiple extracellular signals are required for long-term oligodendrocyte survival. *Development,* 118, 283-95.
BARTLETT, P. F., NOBLE, M. D., PRUSS, R. M., RAFF, M. C., RATTRAY, S. & WILLIAMS, C. A. (1981) Rat neural antigen-2 (RAN-2): a cell surface antigen on astrocytes, ependymal cells, Muller cells and lepto-meninges defined by a monoclonal antibody. *Brain Res,* 204, 339-51.
BARTSCH, U. (1996) Myelination and axonal regeneration in the central nervous system of mice deficient in the myelin-associated glycoprotein. *J Neurocytol,* 25, 303-13.
BERG, G. J. & SCHACHNER, M. (1982) Electron-microscopic localization of A2B5 cell surface antigen in monolayer cultures of murine cerebellum and retina. *Cell Tissue Res,* 224, 637-45.
BERGELSON, L. D. (1995) Serum gangliosides as endogenous immunomodulators. *Immunol Today,* 16, 483-6.
BERGHS, S., AGGUJARO, D., DIRKX, R., JR., MAKSIMOVA, E., STABACH, P., HERMEL, J. M., ZHANG, J. P., PHILBRICK, W., SLEPNEV, V., ORT, T. & SOLIMENA, M. (2000) betaIV spectrin, a new spectrin localized at axon initial segments and nodes of ranvier in the central and peripheral nervous system. *J Cell Biol,* 151, 985-1002.
BERGLES, D. E., DIAMOND, J. S. & JAHR, C. E. (1999) Clearance of glutamate inside the synapse and beyond. *Curr Opin Neurobiol,* 9, 293-8.
BEVAN, S., CHIU, S. Y., GRAY, P. T. & RITCHIE, J. M. (1985) The presence of voltage-gated sodium, potassium and chloride channels in rat cultured astrocytes. *Proc R Soc Lond B Biol Sci,* 225, 299-313.
BHAT, M. A. (2003) Molecular organization of axo-glial junctions. *Curr Opin Neurobiol,* 13, 552-9.

BHAT, M. A., RIOS, J. C., LU, Y., GARCIA-FRESCO, G. P., CHING, W., ST MARTIN, M., LI, J., EINHEBER, S., CHESLER, M., ROSENBLUTH, J., SALZER, J. L. & BELLEN, H. J. (2001) Axon-glia interactions and the domain organization of myelinated axons requires neurexin IV/Caspr/Paranodin. *Neuron,* 30, 369-83.
BIGNAMI, A., ENG, L. F., DAHL, D. & UYEDA, C. T. (1972) Localization of the glial fibrillary acidic protein in astrocytes by immunofluorescence. *Brain Res,* 43, 429-35.
BIGNAMI, A., RAJU, T. & DAHL, D. (1982) Localization of vimentin, the nonspecific intermediate filament protein, in embryonal glia and in early differentiating neurons. In vivo and in vitro immunofluorescence study of the rat embryo with vimentin and neurofilament antisera. *Dev Biol,* 91, 286-95.
BIXBY, J. L., LILIEN, J. & REICHARDT, L. F. (1988) Identification of the major proteins that promote neuronal process outgrowth on Schwann cells in vitro. *J Cell Biol,* 107, 353-61.
BLACK, J. A., FRIEDMAN, B., WAXMAN, S. G., ELMER, L. W. & ANGELIDES, K. J. (1989a) Immuno-ultrastructural localization of sodium channels at nodes of Ranvier and perinodal astrocytes in rat optic nerve. *Proc R Soc Lond B Biol Sci,* 238, 39-51.
BLACK, J. A. & WAXMAN, S. G. (1988) The perinodal astrocyte. *Glia,* 1, 169-83.
BLACK, J. A., WAXMAN, S. G., FRIEDMAN, B., ELMER, L. W. & ANGELIDES, K. J. (1989b) Sodium channels in astrocytes of rat optic nerve in situ: immuno-electron microscopic studies. *Glia,* 2, 353-69.
BLAKEMORE, W. F. & CRANG, A. J. (1989) The relationship between type-1 astrocytes, Schwann cells and oligodendrocytes following transplantation of glial cell cultures into demyelinating lesions in the adult rat spinal cord. *J Neurocytol,* 18, 519-28.
BLAKEMORE, W. F., GILSON, J. M., CRANG, A. J. (2003) The presence of astrocytes in areas of demyelination influences remyelination following transplantation of oligodendrocyte progenitors. *Exp Neurol.* 184, 955-63.
BLASCHUK, K. L., FROST, E. E. & FFRENCH-CONSTANT, C. (2000) The regulation of proliferation and differentiation in oligodendrocyte progenitor cells by alphaV integrins. *Development,* 127, 1961-9.
BODEGA, G., SUAREZ, I. & FERNANDEZ, B. (1987) Fine structural relationships between astrocytes and the node of Ranvier in the amphibian and reptilian spinal cord. *Neurosci Lett,* 80, 7-10.
BOGLER, O., WREN, D., BARNETT, S. C., LAND, H. & NOBLE, M. (1990) Cooperation between two growth factors promotes extended self-renewal and inhibits differentiation of oligodendrocyte-type-2 astrocyte (O-2A) progenitor cells. *Proc Natl Acad Sci U S A,* 87, 6368-72.
BOIKO, T., RASBAND, M. N., LEVINSON, S. R., CALDWELL, J. H., MANDEL, G., TRIMMER, J. S. & MATTHEWS, G. (2001) Compact myelin dictates the differential targeting of two sodium channel isoforms in the same axon. *Neuron,* 30, 91-104.
BONAFEDE, D. M., MACALA, L. J., CONSTANTINE-PATON, M. & YU, R. K. (1989) Isolation and characterization of ganglioside 9-O-acetyl-GD3 from bovine buttermilk. *Lipids,* 24, 680-4.
BONINO, M., CANTINO, D. & SASSOE-POGNETTO, M. (1999) Cellular and subcellular localization of gamma-aminobutyric acidB receptors in the rat olfactory bulb. *Neurosci Lett,* 274, 195-8.
BORLAND, C. Z., SCHUTZMAN, J. L. & STERN, M. J. (2001) Fibroblast growth factor signaling in Caenorhabditis elegans. *Bioessays,* 23, 1120-30.
BOSE, B., OSTERHOLM, J. L. & KALIA, M. (1986) Ganglioside-induced regeneration and reestablishment of axonal continuity in spinal cord-transected rats. *Neurosci Lett,* 63, 165-9.

BOSSY-WETZEL, E., SCHWARZENBACHER, R. & LIPTON, S. A. (2004) Molecular pathways to neurodegeneration. *Nat Med,* 10 Suppl, S2-9.
BOYLE, M. E., BERGLUND, E. O., MURAI, K. K., WEBER, L., PELES, E. & RANSCHT, B. (2001) Contactin orchestrates assembly of the septate-like junctions at the paranode in myelinated peripheral nerve. *Neuron,* 30, 385-97.
BREMER, E. G. & HAKOMORI, S. (1982) GM3 ganglioside induces hamster fibroblast growth inhibition in chemically-defined medium: ganglioside may regulate growth factor receptor function. *Biochem Biophys Res Commun,* 106, 711-8.
BREMER, E. G., HAKOMORI, S., BOWEN-POPE, D. F., RAINES, E. & ROSS, R. (1984) Ganglioside-mediated modulation of cell growth, growth factor binding, and receptor phosphorylation. *J Biol Chem,* 259, 6818-25.
BREMER, E. G., SCHLESSINGER, J. & HAKOMORI, S. (1986) Ganglioside-mediated modulation of cell growth. Specific effects of GM3 on tyrosine phosphorylation of the epidermal growth factor receptor. *J Biol Chem,* 261, 2434-40.
BREWER, G. J., TORRICELLI, J. R., EVEGE, E. K. & PRICE, P. J. (1993) Optimized survival of hippocampal neurons in B27-supplemented Neurobasal, a new serum-free medium combination. *J Neurosci Res,* 35, 567-76.
BROCKES, J. P., FIELDS, K. L. & RAFF, M. C. (1979) Studies on cultured rat Schwann cells. I. Establishment of purified populations from cultures of peripheral nerve. *Brain Res,* 165, 105-18.
BROWN, D. A. & LONDON, E. (1997) Structure of detergent-resistant membrane domains: does phase separation occur in biological membranes? *Biochem Biophys Res Commun,* 240, 1-7.
BROWN, D. A. & LONDON, E. (1998) Functions of lipid rafts in biological membranes. *Annu Rev Cell Dev Biol,* 14, 111-36.
BRUNJES, P. C. & FRAZIER, L. L. (1986) Maturation and plasticity in the olfactory system of vertebrates. *Brain Res,* 396, 1-45.
BUCKLAND, M. E. & CUNNINGHAM, A. M. (1999) Alterations in expression of the neurotrophic factors glial cell line-derived neurotrophic factor, ciliary neurotrophic factor and brain-derived neurotrophic factor, in the target-deprived olfactory neuroepithelium. *Neuroscience,* 90, 333-47.
BUIAKOVA, O. I., BAKER, H., SCOTT, J. W., FARBMAN, A., KREAM, R., GRILLO, M., FRANZEN, L., RICHMAN, M., DAVIS, L. M., ABBONDANZO, S., STEWART, C. L. & MARGOLIS, F. L. (1996) Olfactory marker protein (OMP) gene deletion causes altered physiological activity of olfactory sensory neurons. *Proc Natl Acad Sci U S A,* 93, 9858-63.
BUNGE, R. P. (1968) Glial cells and the central myelin sheath. *Physiol Rev,* 48, 197-251.
BUNGE, R. P. (1993) Expanding roles for the Schwann cell: ensheathment, myelination, trophism and regeneration. *Curr Opin Neurobiol,* 3, 805-9.
BUNGE, R. P., BUNGE, M. B. & ELDRIDGE, C. F. (1986) Linkage between axonal ensheathment and basal lamina production by Schwann cells. *Annu Rev Neurosci,* 9, 305-28.
BUONANNO, A. & FISCHBACH, G. D. (2001) Neuregulin and ErbB receptor signaling pathways in the nervous system. *Curr Opin Neurobiol,* 11, 287-96.
BURD, G. D. (1993) Morphological study of the effects of intranasal zinc sulfate irrigation on the mouse olfactory epithelium and olfactory bulb. *Microsc Res Tech,* 24, 195-213.
BURNETT, M. G. & ZAGER, E. L. (2004) Pathophysiology of peripheral nerve injury: a brief review. *Neurosurg Focus,* 16, E1.
BUTLER, A. B., GRAZIADEI, P. P., MONTI GRAZIADEI, G. A. & SLOTNICK, B. M. (1984) Neonatally bulbectomized rats with new olfactory-neocortical connections are anosmic. *Neurosci Lett,* 48, 247-54.

BUTT, A. M. & DINSDALE, J. (2005a) Fibroblast growth factor 2 induces loss of adult oligodendrocytes and myelin in vivo. *Exp Neurol,* 192, 125-33.
BUTT, A. M. & DINSDALE, J. (2005b) Opposing actions of fibroblast growth factor-2 on early and late oligodendrocyte lineage cells in vivo. *J Neuroimmunol,* 166, 75-87.
CAGGIANO, M., KAUER, J. S. & HUNTER, D. D. (1994) Globose basal cells are neuronal progenitors in the olfactory epithelium: a lineage analysis using a replication-incompetent retrovirus. *Neuron,* 13, 339-52.
CALDWELL, J. H., SCHALLER, K. L., LASHER, R. S., PELES, E. & LEVINSON, S. R. (2000) Sodium channel Na(v)1.6 is localized at nodes of ranvier, dendrites, and synapses. *Proc Natl Acad Sci U S A,* 97, 5616-20.
CALOF, A. L., HAGIWARA, N., HOLCOMB, J. D., MUMM, J. S. & SHOU, J. (1996) Neurogenesis and cell death in olfactory epithelium. *J Neurobiol,* 30, 67-81.
CALVACANTE, L. A. & SANTOS-SILVA, A. (2003) Olfactory ensheathing glia in organotypical cultures: modulation of their migrating and myelinating potentials. In: 33rd Meeting of the Society for Neuroscience, 2003, New Orleans. Soc Neurosci Abstract. . Washington, DC : Society for Neuroscience, .
CALVER, A. R., HALL, A. C., YU, W. P., WALSH, F. S., HEATH, J. K., BETSHOLTZ, C. & RICHARDSON, W. D. (1998) Oligodendrocyte population dynamics and the role of PDGF in vivo. *Neuron,* 20, 869-82.
CAMMER, W. & ZHANG, H. (1996) Ganglioside GD3 in radial glia and astrocytes in situ in brains of young and adult mice. *J Neurosci Res,* 46, 18-23.
CANOLL, P. D., KRAEMER, R., TENG, K. K., MARCHIONNI, M. A. & SALZER, J. L. (1999) GGF/neuregulin induces a phenotypic reversion of oligodendrocytes. *Mol Cell Neurosci,* 13, 79-94.
CANOLL, P. D., MUSACCHIO, J. M., HARDY, R., REYNOLDS, R., MARCHIONNI, M. A. & SALZER, J. L. (1996) GGF/neuregulin is a neuronal signal that promotes the proliferation and survival and inhibits the differentiation of oligodendrocyte progenitors. *Neuron,* 17, 229-43.
CAPUTTO, R., MACCIONI, H. J., ARCE, A. & CUMAR, F. A. (1976) Biosynthesis of brain gangliosides. *Adv Exp Med Biol,* 71, 27-44.
CARLSTEDT, T., CULLHEIM, S., RISLING, M. & ULFHAKE, B. (1989) Nerve fibre regeneration across the PNS-CNS interface at the root-spinal cord junction. *Brain Res Bull,* 22, 93-102.
CARLSTEDT, T., DALSGAARD, C. J. & MOLANDER, C. (1987) Regrowth of lesioned dorsal root nerve fibers into the spinal cord of neonatal rats. *Neurosci Lett,* 74, 14-8.
CARMIGNOTO, G. (2000) Reciprocal communication systems between astrocytes and neurones. *Prog Neurobiol,* 62, 561-81.
CARR, V. M. & FARBMAN, A. I. (1993) The dynamics of cell death in the olfactory epithelium. *Exp Neurol,* 124, 308-14.
CARR, W. E., GLEESON, R. A. & TRAPIDO-ROSENTHAL, H. G. (1990) The role of perireceptor events in chemosensory processes. *Trends Neurosci,* 13, 212-5.
CAU, E., CASAROSA, S. & GUILLEMOT, F. (2002) Mash1 and Ngn1 control distinct steps of determination and differentiation in the olfactory sensory neuron lineage. *Development,* 129, 1871-80.
CAU, E., GRADWOHL, G., FODE, C. & GUILLEMOT, F. (1997) Mash1 activates a cascade of bHLH regulators in olfactory neuron progenitors. *Development,* 124, 1611-21.
CECCARELLI, B., APORTI, F. & FINESSO, M. (1976) Effects of brain gangliosides on functional recovery in experimental regeneration and reinnervation. *Adv Exp Med Biol,* 71, 275-93.

CHAKRABORTY, M., LAHIRI, P. & CHATTERJEE, D. (1992) Thyroidal influence on the cell surface GM1 of granule cells: its significance in cell migration during rat brain development. *Cell Mol Neurobiol,* 12, 589-96.
CHAN, J. R., WATKINS, T. A., COSGAYA, J. M., ZHANG, C., CHEN, L., REICHARDT, L. F., SHOOTER, E. M. & BARRES, B. A. (2004) NGF controls axonal receptivity to myelination by Schwann cells or oligodendrocytes. *Neuron,* 43, 183-91.
CHANG, A., NISHIYAMA, A., PETERSON, J., PRINEAS, J. & TRAPP, B. D. (2000) NG2-positive oligodendrocyte progenitor cells in adult human brain and multiple sclerosis lesions. *J Neurosci,* 20, 6404-12.
CHANG, A., TOURTELLOTTE, W. W., RUDICK, R. & TRAPP, B. D. (2002) Premyelinating oligodendrocytes in chronic lesions of multiple sclerosis. *N Engl J Med,* 346, 165-73.
CHANG, F., LI, R. & LADISCH, S. (1997) Shedding of gangliosides by human medulloblastoma cells. *Exp Cell Res,* 234, 341-6.
CHARI, D. M. (2007) Remyelination in multiple sclerosis. *Int Rev Neurobiol,* 79, 589-620.
CHARLES, A. C., MERRILL, J. E., DIRKSEN, E. R. & SANDERSON, M. J. (1991) Intercellular signaling in glial cells: calcium waves and oscillations in response to mechanical stimulation and glutamate. *Neuron,* 6, 983-92.
CHARLES, P., TAIT, S., FAIVRE-SARRAILH, C., BARBIN, G., GUNN-MOORE, F., DENISENKO-NEHRBASS, N., GUENNOC, A. M., GIRAULT, J. A., BROPHY, P. J. & LUBETZKI, C. (2002) Neurofascin is a glial receptor for the paranodin/Caspr-contactin axonal complex at the axoglial junction. *Curr Biol,* 12, 217-20.
CHEN, H. H., FUKUMOTO, S., FURUKAWA, K., NAKAO, A., AKIYAMA, S., URANO, T. & FURUKAWA, K. (2003) Suppression of lung metastasis of mouse Lewis lung cancer P29 with transfection of the ganglioside GM2/GD2 synthase gene. *Int J Cancer,* 103, 169-76.
CHERESH, D. A., PIERSCHBACHER, M. D., HERZIG, M. A. & MUJOO, K. (1986) Disialogangliosides GD2 and GD3 are involved in the attachment of human melanoma and neuroblastoma cells to extracellular matrix proteins. *J Cell Biol,* 102, 688-96.
CHERESH, D. A., PYTELA, R., PIERSCHBACHER, M. D., KLIER, F. G., RUOSLAHTI, E. & REISFELD, R. A. (1987) An Arg-Gly-Asp-directed receptor on the surface of human melanoma cells exists in an divalent cation-dependent functional complex with the disialoganglioside GD2. *J Cell Biol,* 105, 1163-73.
CHERNAUSEK, S. D. (1993) Insulin-like growth factor-I (IGF-I) production by astroglial cells: regulation and importance for epidermal growth factor-induced cell replication. *J Neurosci Res,* 34, 189-97.
CHERNOUSOV, M. A. & CAREY, D. J. (2003) alphaVbeta8 integrin is a Schwann cell receptor for fibrin. *Exp Cell Res,* 291, 514-24.
CHERNOUSOV, M. A., KAUFMAN, S. J., STAHL, R. C., ROTHBLUM, K. & CAREY, D. J. (2007) Alpha7beta1 integrin is a receptor for laminin-2 on Schwann cells. *Glia,* 55, 1134-44.
CHIAVEGATTO, S., SUN, J., NELSON, R. J. & SCHNAAR, R. L. (2000) A functional role for complex gangliosides: motor deficits in GM2/GD2 synthase knockout mice. *Exp Neurol,* 166, 227-34.
CHIBA, A., KUSUNOKI, S., OBATA, H., MACHINAMI, R. & KANAZAWA, I. (1993) Serum anti-GQ1b IgG antibody is associated with ophthalmoplegia in Miller Fisher syndrome and Guillain-Barre syndrome: clinical and immunohistochemical studies. *Neurology,* 43, 1911-7.
CHIBA, A., KUSUNOKI, S., OBATA, H., MACHINAMI, R. & KANAZAWA, I. (1997) Ganglioside composition of the human cranial nerves, with special reference to pathophysiology of Miller Fisher syndrome. *Brain Res,* 745, 32-6.

CHUAH, M. I. & AU, C. (1991) Olfactory Schwann cells are derived from precursor cells in the olfactory epithelium. *J Neurosci Res,* 29, 172-80.
CHUAH, M. I. & TEAGUE, R. (1999) Basic fibroblast growth factor in the primary olfactory pathway: mitogenic effect on ensheathing cells. *Neuroscience,* 88, 1043-50.
CHUAH, M. I., TENNENT, R. & JACOBS, I. (1995) Response of olfactory Schwann cells to intranasal zinc sulfate irrigation. *J Neurosci Res,* 42, 470-8.
COCHRAN, F. B., JR., YU, R. K. & LEDEEN, R. W. (1982) Myelin gangliosides in vertebrates. *J Neurochem,* 39, 773-9.
COETZEE, T., FUJITA, N., DUPREE, J., SHI, R., BLIGHT, A., SUZUKI, K., SUZUKI, K. & POPKO, B. (1996) Myelination in the absence of galactocerebroside and sulfatide: normal structure with abnormal function and regional instability. *Cell,* 86, 209-19.
COHEN, J., BURNE, J. F., MCKINLAY, C. & WINTER, J. (1987) The role of laminin and the laminin/fibronectin receptor complex in the outgrowth of retinal ganglion cell axons. *Dev Biol,* 122, 407-18.
COHEN, R. I., MARMUR, R., NORTON, W. T., MEHLER, M. F. & KESSLER, J. A. (1996) Nerve growth factor and neurotrophin-3 differentially regulate the proliferation and survival of developing rat brain oligodendrocytes. *J Neurosci,* 16, 6433-42.
COLLINS, B. E., KISO, M., HASEGAWA, A., TROPAK, M. B., RODER, J. C., CROCKER, P. R. & SCHNAAR, R. L. (1997) Binding specificities of the sialoadhesin family of I-type lectins. Sialic acid linkage and substructure requirements for binding of myelin-associated glycoprotein, Schwann cell myelin protein, and sialoadhesin. *J Biol Chem,* 272, 16889-95.
COLOGNATO, H., BARON, W., AVELLANA-ADALID, V., RELVAS, J. B., BARON-VAN EVERCOOREN, A., GEORGES-LABOUESSE, E. & FFRENCH-CONSTANT, C. (2002) CNS integrins switch growth factor signalling to promote target-dependent survival. *Nat Cell Biol,* 4, 833-41.
COLOGNATO, H., RAMACHANDRAPPA, S., OLSEN, I. M. & FFRENCH-CONSTANT, C. (2004) Integrins direct Src family kinases to regulate distinct phases of oligodendrocyte development. *J Cell Biol,* 167, 365-75.
CONSTANTINE-PATON, M., BLUM, A. S., MENDEZ-OTERO, R. & BARNSTABLE, C. J. (1986) A cell surface molecule distributed in a dorsoventral gradient in the perinatal rat retina. *Nature,* 324, 459-62.
CORNELL-BELL, A. H. & FINKBEINER, S. M. (1991) Ca2+ waves in astrocytes. *Cell Calcium,* 12, 185-204.
CORNELL-BELL, A. H., FINKBEINER, S. M., COOPER, M. S. & SMITH, S. J. (1990) Glutamate induces calcium waves in cultured astrocytes: long-range glial signaling. *Science,* 247, 470-3.
COTRINA, M. L., LIN, J. H., ALVES-RODRIGUES, A., LIU, S., LI, J., AZMI-GHADIMI, H., KANG, J., NAUS, C. C. & NEDERGAARD, M. (1998) Connexins regulate calcium signaling by controlling ATP release. *Proc Natl Acad Sci U S A,* 95, 15735-40.
COUMOUL, X. & DENG, C. X. (2003) Roles of FGF receptors in mammalian development and congenital diseases. *Birth Defects Res C Embryo Today,* 69, 286-304.
CUELLO, A. C., GAROFALO, L., KENIGSBERG, R. L. & MAYSINGER, D. (1989) Gangliosides potentiate in vivo and in vitro effects of nerve growth factor on central cholinergic neurons. *Proc Natl Acad Sci U S A,* 86, 2056-60.
CUI, Q. L., ZHENG, W. H., QUIRION, R. & ALMAZAN, G. (2005) Inhibition of Src-like kinases reveals Akt-dependent and -independent pathways in insulin-like growth factor I-mediated oligodendrocyte progenitor survival. *J Biol Chem,* 280, 8918-28.

CURTIS, R., STEWART, H. J., HALL, S. M., WILKIN, G. P., MIRSKY, R. & JESSEN, K. R. (1992) GAP-43 is expressed by nonmyelin-forming Schwann cells of the peripheral nervous system. *J Cell Biol,* 116, 1455-64.
D'AZZO, A., TESSITORE, A. & SANO, R. (2006) Gangliosides as apoptotic signals in ER stress response. *Cell Death Differ,* 13, 404-14.
DANI, J. W., CHERNJAVSKY, A. & SMITH, S. J. (1992) Neuronal activity triggers calcium waves in hippocampal astrocyte networks. *Neuron,* 8, 429-40.
DAVIES, S. J., FITCH, M. T., MEMBERG, S. P., HALL, A. K., RAISMAN, G. & SILVER, J. (1997) Regeneration of adult axons in white matter tracts of the central nervous system. *Nature,* 390, 680-3.
DAVIS, J. B. & STROOBANT, P. (1990) Platelet-derived growth factors and fibroblast growth factors are mitogens for rat Schwann cells. *J Cell Biol,* 110, 1353-60.
DAVIS, J. Q., LAMBERT, S. & BENNETT, V. (1996) Molecular composition of the node of Ranvier: identification of ankyrin-binding cell adhesion molecules neurofascin (mucin+/third FNIII domain-) and NrCAM at nodal axon segments. *J Cell Biol,* 135, 1355-67.
DAWSON, M. R., LEVINE, J. M. & REYNOLDS, R. (2000) NG2-expressing cells in the central nervous system: are they oligodendroglial progenitors? *J Neurosci Res,* 61, 471-9.
DAWSON, M. R., POLITO, A., LEVINE, J. M. & REYNOLDS, R. (2003) NG2-expressing glial progenitor cells: an abundant and widespread population of cycling cells in the adult rat CNS. *Mol Cell Neurosci,* 24, 476-88.
DE CARLOS, J. A., LOPEZ-MASCARAQUE, L. & VALVERDE, F. (1995) The telencephalic vesicles are innervated by olfactory placode-derived cells: a possible mechanism to induce neocortical development. *Neuroscience,* 68, 1167-78.
DE CRISTAN, G., MORBIDELLI, L., ALESSANDRI, G., ZICHE, M., CAPPA, A. P. & GULLINO, P. M. (1990) Synergism between gangliosides and basic fibroblastic growth factor in favouring survival, growth, and motility of capillary endothelium. *J Cell Physiol,* 144, 505-10.
DECKER, L. & FFRENCH-CONSTANT, C. (2004) Lipid rafts and integrin activation regulate oligodendrocyte survival. *J Neurosci,* 24, 3816-25.
DEHAMER, M. K., GUEVARA, J. L., HANNON, K., OLWIN, B. B. & CALOF, A. L. (1994) Genesis of olfactory receptor neurons in vitro: regulation of progenitor cell divisions by fibroblast growth factors. *Neuron,* 13, 1083-97.
DEMERENS, C., STANKOFF, B., LOGAK, M., ANGLADE, P., ALLINQUANT, B., COURAUD, F., ZALC, B. & LUBETZKI, C. (1996) Induction of myelination in the central nervous system by electrical activity. *Proc Natl Acad Sci U S A,* 93, 9887-92.
DI GREGORIO, F., FERRARI, G., MARINI, P., SILIPRANDI, R. & GORIO, A. (1984) The influence of gangliosides on neurite growth and regeneration. *Neuropediatrics,* 15 Suppl, 93-6.
DIAMOND, M. S. & SPRINGER, T. A. (1994) The dynamic regulation of integrin adhesiveness. *Curr Biol,* 4, 506-17.
DONG, Z., BRENNAN, A., LIU, N., YARDEN, Y., LEFKOWITZ, G., MIRSKY, R. & JESSEN, K. R. (1995) Neu differentiation factor is a neuron-glia signal and regulates survival, proliferation, and maturation of rat Schwann cell precursors. *Neuron,* 15, 585-96.
DONG, Z., DEAN, C., WALTERS, J. E., MIRSKY, R. & JESSEN, K. R. (1997) Response of Schwann cells to mitogens in vitro is determined by pre-exposure to serum, time in vitro, and developmental age. *Glia,* 20, 219-30.

DONG, Z., SINANAN, A., PARKINSON, D., PARMANTIER, E., MIRSKY, R. & JESSEN, K. R. (1999) Schwann cell development in embryonic mouse nerves. *J Neurosci Res,* 56, 334-48.
DOUCETTE, J. R. (1984) The glial cells in the nerve fiber layer of the rat olfactory bulb. *Anat Rec,* 210, 385-91.
DOUCETTE, J. R., KIERNAN, J. A. & FLUMERFELT, B. A. (1983) The re-innervation of olfactory glomeruli following transection of primary olfactory axons in the central or peripheral nervous system. *J Anat,* 137 (Pt 1), 1-19.
DOUCETTE, R. (1991) PNS-CNS transitional zone of the first cranial nerve. *J Comp Neurol,* 312, 451-66.
DOUCETTE, R. (1993) Glial cells in the nerve fiber layer of the main olfactory bulb of embryonic and adult mammals. *Microsc Res Tech,* 24, 113-30.
DOUCETTE, R. (1996) Immunohistochemical localization of laminin, fibronectin and collagen type IV in the nerve fiber layer of the olfactory bulb. *Int J Dev Neurosci,* 14, 945-59.
DUBOIS, C., MANUGUERRA, J. C., HAUTTECOEUR, B. & MAZE, J. (1990) Monoclonal antibody A2B5, which detects cell surface antigens, binds to ganglioside GT3 (II3 (NeuAc)3LacCer) and to its 9-O-acetylated derivative. *J Biol Chem,* 265, 2797-803.
DUBOVY, P., SVIZENSKA, I., KLUSAKOVA, I., ZITKOVA, A., HOUST'AVA, L. & HANINEC, P. (2001) Laminin molecules in freeze-treated nerve segments are associated with migrating Schwann cells that display the corresponding alpha6beta1 integrin receptor. *Glia,* 33, 36-44.
DUCHEMIN, A. M., REN, Q., MO, L., NEFF, N. H. & HADJICONSTANTINOU, M. (2002) GM1 ganglioside induces phosphorylation and activation of Trk and Erk in brain. *J Neurochem,* 81, 696-707.
DUCRAY, A., BONDIER, J. R., MICHEL, G., BON, K., MILLOT, J. L., PROPPER, A. & KASTNER, A. (2002) Recovery following peripheral destruction of olfactory neurons in young and adult mice. *Eur J Neurosci,* 15, 1907-17.
DUFFY, S. & MACVICAR, B. A. (1995) Adrenergic calcium signaling in astrocyte networks within the hippocampal slice. *J Neurosci,* 15, 5535-50.
DUGANDZIJA-NOVAKOVIC, S., KOSZOWSKI, A. G., LEVINSON, S. R. & SHRAGER, P. (1995) Clustering of Na+ channels and node of Ranvier formation in remyelinating axons. *J Neurosci,* 15, 492-503.
DUPREE, J. L., COETZEE, T., BLIGHT, A., SUZUKI, K. & POPKO, B. (1998) Myelin galactolipids are essential for proper node of Ranvier formation in the CNS. *J Neurosci,* 18, 1642-9.
DUPREE, J. L., GIRAULT, J. A. & POPKO, B. (1999) Axo-glial interactions regulate the localization of axonal paranodal proteins. *J Cell Biol,* 147, 1145-52.
DUPREE, J. L., MASON, J. L., MARCUS, J. R., STULL, M., LEVINSON, R., MATSUSHIMA, G. K. & POPKO, B. (2005) Oligodendrocytes assist in the maintenance of sodium channel clusters independent of the myelin sheath. *Neuron Glia Biol,* 1, 1-14.
EDWARDS, D. A., THOMPSON, M. L. & BURGE, K. G. (1972) Olfactory bulb removal vs peripherally induced anosmia: differential effects on the aggressive behavior of male mice. *Behav Biol,* 7, 823-8.
EINHEBER, S., MILNER, T. A., GIANCOTTI, F. & SALZER, J. L. (1993) Axonal regulation of Schwann cell integrin expression suggests a role for alpha 6 beta 4 in myelination. *J Cell Biol,* 123, 1223-36.
EINHEBER, S., ZANAZZI, G., CHING, W., SCHERER, S., MILNER, T. A., PELES, E. & SALZER, J. L. (1997) The axonal membrane protein Caspr, a homologue of neurexin IV, is a component of the septate-like paranodal junctions that assemble during myelination. *J Cell Biol,* 139, 1495-506.

EISENBARTH, G. S., WALSH, F. S. & NIRENBERG, M. (1979) Monoclonal antibody to a plasma membrane antigen of neurons. *Proc Natl Acad Sci U S A,* 76, 4913-7.
ELDRIDGE, C. F., BUNGE, M. B. & BUNGE, R. P. (1989) Differentiation of axon-related Schwann cells in vitro: II. Control of myelin formation by basal lamina. *J Neurosci,* 9, 625-38.
ELDRIDGE, C. F., BUNGE, M. B., BUNGE, R. P. & WOOD, P. M. (1987) Differentiation of axon-related Schwann cells in vitro. I. Ascorbic acid regulates basal lamina assembly and myelin formation. *J Cell Biol,* 105, 1023-34.
ELLISON, J. A. & DE VELLIS, J. (1995) Amoeboid microglia expressing GD3 ganglioside are concentrated in regions of oligodendrogenesis during development of the rat corpus callosum. *Glia,* 14, 123-32.
ENG, L. F. (1985) Glial fibrillary acidic protein (GFAP): the major protein of glial intermediate filaments in differentiated astrocytes. *J Neuroimmunol,* 8, 203-14.
ENG, L. F. & GHIRNIKAR, R. S. (1994) GFAP and astrogliosis. *Brain Pathol,* 4, 229-37.
ENG, L. F., YU, A. C. & LEE, Y. L. (1992) Astrocytic response to injury. *Prog Brain Res,* 94, 353-65.
ESCARTIN, C., VALETTE, J., LEBON, V. & BONVENTO, G. (2006) Neuron-astrocyte interactions in the regulation of brain energy metabolism: a focus on NMR spectroscopy. *J Neurochem,* 99, 393-401.
ESPINOSA DE LOS MONTEROS, A., ZHANG, M. & DE VELLIS, J. (1993) O2A progenitor cells transplanted into the neonatal rat brain develop into oligodendrocytes but not astrocytes. *Proc Natl Acad Sci U S A,* 90, 50-4.
EVERS, S. M., HENDRICKS, K. R., KOTT, J. N., LEE, M. E., GREGOV, M. E. & WESTRUM, L. E. (1996) Recovery of olfactory function in thirteen-day-old rats after olfactory bulb transplantation but not after olfactory bulb ablation. *Brain Res,* 724, 129-35.
FACCI, L., SKAPER, S. D., FAVARON, M. & LEON, A. (1988) A role for gangliosides in astroglial cell differentiation in vitro. *J Cell Biol,* 106, 821-8.
FACCI, L., SKAPER, S. D., LEVIN, D. L. & VARON, S. (1987) Dissociation of the stellate morphology from intracellular cyclic AMP levels in cultured rat brain astroglial cells: effects of ganglioside GM1 and lysophosphatidylserine. *J Neurochem,* 48, 566-73.
FADDA, E., NEGRO, A., FACCI, L. & SKAPER, S. D. (1993) Ganglioside GM1 cooperates with brain-derived neurotrophic factor to protect dopaminergic neurons from 6-hydroxydopamine-induced degeneration. *Neurosci Lett,* 159, 147-50.
FANO, G., BIOCCA, S., FULLE, S., MARIGGIO, M. A., BELIA, S. & CALISSANO, P. (1995) The S-100: a protein family in search of a function. *Prog Neurobiol*, 46, 71-82.
FARBMAN, A. I. (1990) Olfactory neurogenesis: genetic or environmental controls? *Trends Neurosci,* 13, 362-5.
FARBMAN, A. I. (1994) The cellular basis of olfaction. *Endeavour,* 18, 2-8.
FARBMAN, A. I. & BUCHHOLZ, J. A. (1992) Growth of olfactory epithelial tissue in vitro: lectin staining of axons. *Microsc Res Tech,* 23, 173-80.
FARBMAN, A. I. & BUCHHOLZ, J. A. (1996) Transforming growth factor-alpha and other growth factors stimulate cell division in olfactory epithelium in vitro. *J Neurobiol,* 30, 267-80.
FARBMAN, A. I., BUCHHOLZ, J. A., WALTERS, E. & MARGOLIS, F. L. (1998) Does olfactory marker protein participate in olfactory neurogenesis? *Ann N Y Acad Sci,* 855, 248-51.
FAROOQUI, T., FRANKLIN, T., PEARL, D. K. & YATES, A. J. (1997) Ganglioside GM1 enhances induction by nerve growth factor of a putative dimer of TrkA. *J Neurochem,* 68, 2348-55.

FARRER, R. G. & QUARLES, R. H. (1996) Extracellular matrix upregulates synthesis of glucosylceramide-based glycosphingolipids in primary Schwann cells. *J Neurosci Res,* 45, 248-57.
FARRER, R. G. & QUARLES, R. H. (1999) GT3 and its O-acetylated derivative are the principal A2B5-reactive gangliosides in cultured O2A lineage cells and are down-regulated along with O-acetyl GD3 during differentiation to oligodendrocytes. *J Neurosci Res,* 57, 371-80.
FASS, B. & RAMIREZ, J. J. (1984) Effects of ganglioside treatments on lesion-induced behavioral impairments and sprouting in the CNS. *J Neurosci Res,* 12, 445-58.
FAVARON, M., MANEV, H., ALHO, H., BERTOLINO, M., FERRET, B., GUIDOTTI, A. & COSTA, E. (1988) Gangliosides prevent glutamate and kainate neurotoxicity in primary neuronal cultures of neonatal rat cerebellum and cortex. *Proc Natl Acad Sci U S A,* 85, 7351-5.
FAWCETT, J. W. (1997) Astrocytic and neuronal factors affecting axon regeneration in the damaged central nervous system. *Cell Tissue Res,* 290, 371-7.
FEDERICO, G., MAREMMANI, C., CINQUANTA, L., BARONCELLI, G. I., FATTORI, B. & SAGGESE, G. (1999) Mucus of the human olfactory epithelium contains the insulin-like growth factor-I system which is altered in some neurodegenerative diseases. *Brain Res,* 835, 306-14.
FELTRI, M. L., SCHERER, S. S., NEMNI, R., KAMHOLZ, J., VOGELBACKER, H., SCOTT, M. O., CANAL, N., QUARANTA, V. & WRABETZ, L. (1994) Beta 4 integrin expression in myelinating Schwann cells is polarized, developmentally regulated and axonally dependent. *Development,* 120, 1287-301.
FENDERSON, B. A., ANDREWS, P. W., NUDELMAN, E., CLAUSEN, H. & HAKOMORI, S. (1987) Glycolipid core structure switching from globo- to lacto- and ganglio-series during retinoic acid-induced differentiation of TERA-2-derived human embryonal carcinoma cells. *Dev Biol,* 122, 21-34.
FERNANDEZ-VALLE, C., FREGIEN, N., WOOD, P. M. & BUNGE, M. B. (1993) Expression of the protein zero myelin gene in axon-related Schwann cells is linked to basal lamina formation. *Development,* 119, 867-80.
FERNANDEZ-VALLE, C., GWYNN, L., WOOD, P. M., CARBONETTO, S. & BUNGE, M. B. (1994) Anti-beta 1 integrin antibody inhibits Schwann cell myelination. *J Neurobiol,* 25, 1207-26.
FERNANDEZ, P. A., TANG, D. G., CHENG, L., PROCHIANTZ, A., MUDGE, A. W. & RAFF, M. C. (2000) Evidence that axon-derived neuregulin promotes oligodendrocyte survival in the developing rat optic nerve. *Neuron,* 28, 81-90.
FERRARI, G., ANDERSON, B. L., STEPHENS, R. M., KAPLAN, D. R. & GREENE, L. A. (1995) Prevention of apoptotic neuronal death by GM1 ganglioside. Involvement of Trk neurotrophin receptors. *J Biol Chem,* 270, 3074-80.
FFRENCH-CONSTANT, C., MILLER, R. H., KRUSE, J., SCHACHNER, M. & RAFF, M. C. (1986) Molecular specialization of astrocyte processes at nodes of Ranvier in rat optic nerve. *J Cell Biol,* 102, 844-52.
FIELDS, K. L., BROCKES, J. P., MIRSKY, R. & WENDON, L. M. (1978) Cell surface markers for distinguishing different types of rat dorsal root ganglion cells in culture. *Cell,* 14, 43-51.
FINKBEINER, S. (1992) Calcium waves in astrocytes-filling in the gaps. *Neuron,* 8, 1101-8.
FLORES, A. I., MALLON, B. S., MATSUI, T., OGAWA, W., ROSENZWEIG, A., OKAMOTO, T. & MACKLIN, W. B. (2000) Akt-mediated survival of oligodendrocytes induced by neuregulins. *J Neurosci,* 20, 7622-30.

FOGARTY, M., RICHARDSON, W. D. & KESSARIS, N. (2005) A subset of oligodendrocytes generated from radial glia in the dorsal spinal cord. *Development,* 132, 1951-9.
FOLCH, J. & LEES, M. (1951) Proteolipides, a new type of tissue lipoproteins; their isolation from brain. *J Biol Chem,* 191, 807-17.
FONG, T. G., VOGELSBERG, V., NEFF, N. H. & HADJICONSTANTINOU, M. (1995) GM1 and NGF synergism on choline acetyltransferase and choline uptake in aged brain. *Neurobiol Aging,* 16, 917-23.
FRANCESCHINI, I. A. & BARNETT, S. C. (1996) Low-affinity NGF-receptor and E-N-CAM expression define two types of olfactory nerve ensheathing cells that share a common lineage. *Dev Biol,* 173, 327-43.
FRANCIS, A., RAABE, T. D., WEN, D. & DEVRIES, G. H. (1999) Neuregulins and ErbB receptors in cultured neonatal astrocytes. *J Neurosci Res,* 57, 487-94.
FRANKLIN, R. J., CRANG, A. J. & BLAKEMORE, W. F. (1991) Transplanted type-1 astrocytes facilitate repair of demyelinating lesions by host oligodendrocytes in adult rat spinal cord. J Neurocytol, 20, 420-30.
FRANKLIN, R. J. & BARNETT, S. C. (1997) Do olfactory glia have advantages over Schwann cells for CNS repair? *J Neurosci Res,* 50, 665-72.
FREIRE, E., GOMES, F. C., JOTHA-MATTOS, T., NETO, V. M., SILVA FILHO, F. C. & COELHO-SAMPAIO, T. (2004) Sialic acid residues on astrocytes regulate neuritogenesis by controlling the assembly of laminin matrices. *J Cell Sci,* 117, 4067-76.
FRESSINAUD, C., VALLAT, J. M. & LABOURDETTE, G. (1995) Basic fibroblast growth factor down-regulates myelin basic protein gene expression and alters myelin compaction of mature oligodendrocytes in vitro. *J Neurosci Res,* 40, 285-93.
FRIDRIKSSON, E. K., SHIPKOVA, P. A., SHEETS, E. D., HOLOWKA, D., BAIRD, B. & MCLAFFERTY, F. W. (1999) Quantitative analysis of phospholipids in functionally important membrane domains from RBL-2H3 mast cells using tandem high-resolution mass spectrometry. *Biochemistry,* 38, 8056-63.
FRISEN, J. (1997) Determinants of axonal regeneration. *Histol Histopathol,* 12, 857-68.
FROST, E. E., BUTTERY, P. C., MILNER, R. & FFRENCH-CONSTANT, C. (1999) Integrins mediate a neuronal survival signal for oligodendrocytes. *Curr Biol,* 9, 1251-4.
FRUTTIGER, M., CALVER, A. R. & RICHARDSON, W. D. (2000) Platelet-derived growth factor is constitutively secreted from neuronal cell bodies but not from axons. *Curr Biol,* 10, 1283-6.
FU, S. Y. & GORDON, T. (1997) The cellular and molecular basis of peripheral nerve regeneration. *Mol Neurobiol,* 14, 67-116.
FUJITANI, M., KAWAI, H., PROIA, R. L., KASHIWAGI, A., YASUDA, H. & YAMASHITA, T. (2005) Binding of soluble myelin-associated glycoprotein to specific gangliosides induces the association of p75NTR to lipid rafts and signal transduction. *J Neurochem,* 94, 15-21.
FUKUMOTO, S., MUTOH, T., HASEGAWA, T., MIYAZAKI, H., OKADA, M., GOTO, G., FURUKAWA, K. & URANO, T. (2000) GD3 synthase gene expression in PC12 cells results in the continuous activation of TrkA and ERK1/2 and enhanced proliferation. *J Biol Chem,* 275, 5832-8.
FURUKAWA, S., FURUKAWA, Y., SATOYOSHI, E. & HAYASHI, K. (1986) Synthesis and secretion of nerve growth factor by mouse astroglial cells in culture. *Biochem Biophys Res Commun,* 136, 57-63.
GANSER, A. L., KIRSCHNER, D. A. & WILLINGER, M. (1983) Ganglioside localization on myelinated nerve fibres by cholera toxin binding. *J Neurocytol,* 12, 921-38.

GARD, A. L. & PFEIFFER, S. E. (1990) Two proliferative stages of the oligodendrocyte lineage (A2B5+O4- and O4+GalC-) under different mitogenic control. *Neuron,* 5, 615-25.
GARD, A. L. & PFEIFFER, S. E. (1993) Glial cell mitogens bFGF and PDGF differentially regulate development of O4+GalC- oligodendrocyte progenitors. *Dev Biol,* 159, 618-30.
GARRATT, A. N., VOICULESCU, O., TOPILKO, P., CHARNAY, P. & BIRCHMEIER, C. (2000) A dual role of erbB2 in myelination and in expansion of the schwann cell precursor pool. *J Cell Biol,* 148, 1035-46.
GEBICKE-HAERTER, P. J., VAN CALKER, D., NORENBERG, W. & ILLES, P. (1996) Molecular mechanisms of microglial activation. A. Implications for regeneration and neurodegenerative diseases. *Neurochem Int,* 29, 1-12.
GEISLER, F. H., COLEMAN, W. P., GRIECO, G. & POONIAN, D. (2001) The Sygen multicenter acute spinal cord injury study. *Spine,* 26, S87-98.
GEISLER, F. H., DORSEY, F. C. & COLEMAN, W. P. (1991) Recovery of motor function after spinal-cord injury--a randomized, placebo-controlled trial with GM-1 ganglioside. *N Engl J Med,* 324, 1829-38.
GETCHELL, T. V., MARGOLIS, F. L. & GETCHELL, M. L. (1984) Perireceptor and receptor events in vertebrate olfaction. *Prog Neurobiol,* 23, 317-45.
GETCHELL, T. V., NARLA, R. K., LITTLE, S., HYDE, J. F. & GETCHELL, M. L. (2000) Horizontal basal cell proliferation in the olfactory epithelium of transforming growth factor-alpha transgenic mice. *Cell Tissue Res,* 299, 185-92.
GIRAULT, J. A. & PELES, E. (2002) Development of nodes of Ranvier. *Curr Opin Neurobiol,* 12, 476-85.
GODDARD, D. R., BERRY, M. & BUTT, A. M. (1999) In vivo actions of fibroblast growth factor-2 and insulin-like growth factor-I on oligodendrocyte development and myelination in the central nervous system. *J Neurosci Res,* 57, 74-85.
GOLDMAN, J. E. & REYNOLDS, R. (1996) A reappraisal of ganglioside GD3 expression in the CNS. *Glia,* 16, 291-5.
GOLDSTEIN, B. J. & SCHWOB, J. E. (1996) Analysis of the globose basal cell compartment in rat olfactory epithelium using GBC-1, a new monoclonal antibody against globose basal cells. *J Neurosci,* 16, 4005-16.
GOLDSTEIN, B. J., WOLOZIN, B. L. & SCHWOB, J. E. (1997) FGF2 suppresses neuronogenesis of a cell line derived from rat olfactory epithelium. *J Neurobiol,* 33, 411-28.
GOLDSTEIN, G. W. (1988) Endothelial cell-astrocyte interactions. A cellular model of the blood-brain barrier. *Ann N Y Acad Sci,* 529, 31-9.
GOMEZ-MOUTON, C., ABAD, J. L., MIRA, E., LACALLE, R. A., GALLARDO, E., JIMENEZ-BARANDA, S., ILLA, I., BERNAD, A., MANES, S. & MARTINEZ, A. C. (2001) Segregation of leading-edge and uropod components into specific lipid rafts during T cell polarization. *Proc Natl Acad Sci U S A,* 98, 9642-7.
GONG, Q., BAILEY, M. S., PIXLEY, S. K., ENNIS, M., LIU, W. & SHIPLEY, M. T. (1994) Localization and regulation of low affinity nerve growth factor receptor expression in the rat olfactory system during development and regeneration. *J Comp Neurol,* 344, 336-48.
GORDON, M. K., MUMM, J. S., DAVIS, R. A., HOLCOMB, J. D. & CALOF, A. L. (1995) Dynamics of MASH1 expression in vitro and in vivo suggest a non-stem cell site of MASH1 action in the olfactory receptor neuron lineage. *Mol Cell Neurosci,* 6, 363-79.
GORIO, A. (1986) Ganglioside enhancement of neuronal differentiation, plasticity, and repair. *CRC Crit Rev Clin Neurobiol,* 2, 241-96.
GORIO, A. (1988) Gangliosides as a possible treatment affecting neuronal repair processes. *Adv Neurol,* 47, 523-30.

GORIO, A., CARMIGNOTO, G., FACCI, L. & FINESSO, M. (1980) Motor nerve sprouting induced by ganglioside treatment. Possible implications for gangliosides on neuronal growth. *Brain Res,* 197, 236-41.
GORIO, A., FERRARI, G., FUSCO, M., JANIGRO, D., ZANONI, R. & JONSSON, G. (1984a) Gangliosides and their effects on rearranging peripheral and central neural pathways. *Cent Nerv Syst Trauma,* 1, 29-37.
GORIO, A., JANIGRO, D. & ZANONI, R. (1984b) Neuritogenesis and regeneration in the nervous system: an overview of the problem and on the promoting action of gangliosides. *Adv Exp Med Biol,* 174, 465-73.
GRATZNER, H. G. (1982) Monoclonal antibody to 5-bromo- and 5-iododeoxyuridine: A new reagent for detection of DNA replication. *Science,* 218, 474-5.
GRAZIADEI, P. P. & GRAZIADEI, G. A. (1979) Neurogenesis and neuron regeneration in the olfactory system of mammals. I. Morphological aspects of differentiation and structural organization of the olfactory sensory neurons. *J Neurocytol,* 8, 1-18.
GRAZIADEI, P. P., KARLAN, M. S., GRAZIADEI, G. A. & BERNSTEIN, J. J. (1980) Neurogenesis of sensory neurons in the primate olfactory system after section of the fila olfactoria. *Brain Res,* 186, 289-300.
GRAZIADEI, P. P. & MONTI GRAZIADEI, G. A. (1980) Neurogenesis and neuron regeneration in the olfactory system of mammals. III. Deafferentation and reinnervation of the olfactory bulb following section of the fila olfactoria in rat. *J Neurocytol,* 9, 145-62.
GREENE, L. A. & TISCHLER, A. S. (1976) Establishment of a noradrenergic clonal line of rat adrenal pheochromocytoma cells which respond to nerve growth factor. *Proc Natl Acad Sci U S A,* 73, 2424-8.
GREWAL, S. S., YORK, R. D. & STORK, P. J. (1999) Extracellular-signal-regulated kinase signalling in neurons. *Curr Opin Neurobiol,* 9, 544-53.
GRIFFIN, J. W., LI, C. Y., MACKO, C., HO, T. W., HSIEH, S. T., XUE, P., WANG, F. A., CORNBLATH, D. R., MCKHANN, G. M. & ASBURY, A. K. (1996) Early nodal changes in the acute motor axonal neuropathy pattern of the Guillain-Barre syndrome. *J Neurocytol,* 25, 33-51.
GRINSPAN, J. B., MARCHIONNI, M. A., REEVES, M., COULALOGLOU, M. & SCHERER, S. S. (1996a) Axonal interactions regulate Schwann cell apoptosis in developing peripheral nerve: neuregulin receptors and the role of neuregulins. *J Neurosci,* 16, 6107-18.
GRINSPAN, J. B., REEVES, M. F., COULALOGLOU, M. J., NATHANSON, D. & PLEASURE, D. (1996b) Re-entry into the cell cycle is required for bFGF-induced oligodendroglial dedifferentiation and survival. *J Neurosci Res,* 46, 456-64.
GUENARD, V., MONTAG, D., SCHACHNER, M. & MARTINI, R. (1996) Onion bulb cells in mice deficient for myelin genes share molecular properties with immature, differentiated non-myelinating, and denervated Schwann cells. *Glia,* 18, 27-38.
GUTNICK, M. J., CONNORS, B. W. & RANSOM, B. R. (1981) Dye-coupling between glial cells in the guinea pig neocortical slice. *Brain Res,* 213, 486-92.
HADJICONSTANTINOU, M. & NEFF, N. H. (1988) Treatment with GM1 ganglioside restores striatal dopamine in the 1-methyl-4-phenyl-1,2,3,6-tetrahydropyridine-treated mouse. *J Neurochem,* 51, 1190-6.
HADJICONSTANTINOU, M. & NEFF, N. H. (1998) GM1 ganglioside: in vivo and in vitro trophic actions on central neurotransmitter systems. *J Neurochem,* 70, 1335-45.
HAKOMORI, S. (1986) Glycosphingolipids. *Sci Am,* 254, 44-53.

HAKOMORI, S. (1990) Bifunctional role of glycosphingolipids. Modulators for transmembrane signaling and mediators for cellular interactions. *J Biol Chem,* 265, 18713-6.
HAKOMORI, S. (2000) Traveling for the glycosphingolipid path. *Glycoconj J,* 17, 627-47.
HAKOMORI, S. I. (2002) Inaugural Article: The glycosynapse. *Proc Natl Acad Sci U S A,* 99, 225-32.
HALL, A., GIESE, N. A. & RICHARDSON, W. D. (1996) Spinal cord oligodendrocytes develop from ventrally derived progenitor cells that express PDGF alpha-receptors. *Development,* 122, 4085-94.
HALL, S. M. (1986) The effect of inhibiting Schwann cell mitosis on the re-innervation of acellular autografts in the peripheral nervous system of the mouse. *Neuropathol Appl Neurobiol,* 12, 401-14.
HALSTEAD, S. K., MORRISON, I., O'HANLON, G. M., HUMPHREYS, P. D., GOODFELLOW, J. A., PLOMP, J. J. & WILLISON, H. J. (2005) Anti-disialosyl antibodies mediate selective neuronal or Schwann cell injury at mouse neuromuscular junctions. *Glia,* 52, 177-89.
HANAI, N., NORES, G. A., MACLEOD, C., TORRES-MENDEZ, C. R. & HAKOMORI, S. (1988) Ganglioside-mediated modulation of cell growth. Specific effects of GM3 and lyso-GM3 in tyrosine phosphorylation of the epidermal growth factor receptor. *J Biol Chem,* 263, 10915-21.
HARDER, T., SCHEIFFELE, P., VERKADE, P. & SIMONS, K. (1998) Lipid domain structure of the plasma membrane revealed by patching of membrane components. *J Cell Biol,* 141, 929-42.
HARDER, T. & SIMONS, K. (1997) Caveolae, DIGs, and the dynamics of sphingolipid-cholesterol microdomains. *Curr Opin Cell Biol,* 9, 534-42.
HARDING, J., GRAZIADEI, P. P., MONTI GRAZIADEI, G. A. & MARGOLIS, F. L. (1977) Denervation in the primary olfactory pathway of mice. IV. Biochemical and morphological evidence for neuronal replacement following nerve section. *Brain Res,* 132, 11-28.
HARDING, J. W., GETCHELL, T. V. & MARGOLIS, F. L. (1978) Denervation of the primary olfactory pathway in mice. V. Long-term effect of intranasal ZnSO4 irrigation on behavior, biochemistry and morphology. *Brain Res,* 140, 271-85.
HARDY, R. & REYNOLDS, R. (1991) Proliferation and differentiation potential of rat forebrain oligodendroglial progenitors both in vitro and in vivo. *Development,* 111, 1061-80.
HARDY, R. & REYNOLDS, R. (1993) Rat cerebral cortical neurons in primary culture release a mitogen specific for early (GD3+/04-) oligodendroglial progenitors. *J Neurosci Res,* 34, 589-600.
HARDY, R. J. & FRIEDRICH, V. L., JR. (1996) Oligodendrocyte progenitors are generated throughout the embryonic mouse brain, but differentiate in restricted foci. *Development,* 122, 2059-69.
HARPIN, M. L., PORTOUKALIAN, J. & BAUMANN, N. (1982) Modifications of ganglioside composition in peripheral nerve of myelin deficient Trembler mutant mouse. *Neurochem Res,* 7, 1367-73.
HART, I. K., RICHARDSON, W. D., BOLSOVER, S. R. & RAFF, M. C. (1989) PDGF and intracellular signaling in the timing of oligodendrocyte differentiation. *J Cell Biol,* 109, 3411-7.
HASHIRAMOTO, A., MIZUKAMI, H. & YAMASHITA, T. (2006) Ganglioside GM3 promotes cell migration by regulating MAPK and c-Fos/AP-1. *Oncogene,* 25, 3948-55.
HASSINGER, T. D., ATKINSON, P. B., STRECKER, G. J., WHALEN, L. R., DUDEK, F. E., KOSSEL, A. H. & KATER, S. B. (1995) Evidence for glutamate-mediated

activation of hippocampal neurons by glial calcium waves. *J Neurobiol,* 28, 159-70.
HASSINGER, T. D., GUTHRIE, P. B., ATKINSON, P. B., BENNETT, M. V. & KATER, S. B. (1996) An extracellular signaling component in propagation of astrocytic calcium waves. *Proc Natl Acad Sci U S A,* 93, 13268-73.
HEFTI, F., HARTIKKA, J. & FRICK, W. (1985) Gangliosides alter morphology and growth of astrocytes and increase the activity of choline acetyltransferase in cultures of dissociated septal cells. *J Neurosci,* 5, 2086-94.
HENDRICKS, K. R., KOTT, J. N., LEE, M. E., GOODEN, M. D., EVERS, S. M. & WESTRUM, L. E. (1994) Recovery of olfactory behavior. I. Recovery after a complete olfactory bulb lesion correlates with patterns of olfactory nerve penetration. *Brain Res,* 648, 121-33.
HILBIG, R., LAUKE, G. & RAHMANN, H. (1983) Brain gangliosides during the life span (embryogenesis to senescence) of the rat. *Dev Neurosci,* 6, 260-70.
HILDEBRAND, C. (1971a) Ultrastructural and light-microscopic studies of the developing feline spinal cord white matter. I. The nodes of Ranvier. *Acta Physiol Scand Suppl,* 364, 81-109.
HILDEBRAND, C. (1971b) Ultrastructural and light-microscopic studies of the nodal region in large myelinated fibres of the adult feline spinal cord white matter. *Acta Physiol Scand Suppl,* 364, 43-79.
HILDEBRAND, C. & WAXMAN, S. G. (1984) Postnatal differentiation of rat optic nerve fibers: electron microscopic observations on the development of nodes of Ranvier and axoglial relations. *J Comp Neurol,* 224, 25-37.
HILL-FELBERG, S. J., McINTOSH, T. K., OLIVER, D. L., RAGHUPATHI, R. & BARBARESE, E. (1999) Concurrent loss and proliferation of astrocytes following lateral fluid percussion brain injury in the adult rat. *J Neurosci Res,* 57, 271-9.
HINDS, J. W. (1968) Autoradiographic study of histogenesis in the mouse olfactory bulb. I. Time of origin of neurons and neuroglia. *J Comp Neurol,* 134, 287-304.
HO, T. W., WILLISON, H. J., NACHAMKIN, I., LI, C. Y., VEITCH, J., UNG, H., WANG, G. R., LIU, R. C., CORNBLATH, D. R., ASBURY, A. K., GRIFFIN, J. W. & MCKHANN, G. M. (1999) Anti-GD1a antibody is associated with axonal but not demyelinating forms of Guillain-Barre syndrome. *Ann Neurol,* 45, 168-73.
HOFTEIG, J. H., MENDELL, J. R. & YATES, A. J. (1981) Chemical and morphological studies on garfish peripheral nerves. *J Comp Neurol,* 198, 265-74.
HOKE, A. & SILVER, J. (1994) Heterogeneity among astrocytes in reactive gliosis. *Perspect Dev Neurobiol,* 2, 269-74.
HOLBROOK, E. H., SZUMOWSKI, K. E. & SCHWOB, J. E. (1995) An immunochemical, ultrastructural, and developmental characterization of the horizontal basal cells of rat olfactory epithelium. *J Comp Neurol,* 363, 129-46.
HOLCOMB, J. D., MUMM, J. S. & CALOF, A. L. (1995) Apoptosis in the neuronal lineage of the mouse olfactory epithelium: regulation in vivo and in vitro. *Dev Biol,* 172, 307-23.
HOLMGREN, J., ELWING, H., FREDMAN, P. & SVENNERHOLM, L. (1980) Polystyrene-adsorbed gangliosides for investigation of the structure of the tetanus-toxin receptor. *Eur J Biochem,* 106, 371-9.
HONKE, K., HIRAHARA, Y., DUPREE, J., SUZUKI, K., POPKO, B., FUKUSHIMA, K., FUKUSHIMA, J., NAGASAWA, T., YOSHIDA, N., WADA, Y. & TANIGUCHI, N. (2002) Paranodal junction formation and spermatogenesis require sulfoglycolipids. *Proc Natl Acad Sci U S A,* 99, 4227-32.
HOOPER, N. M. (1999) Detergent-insoluble glycosphingolipid/cholesterol-rich membrane domains, lipid rafts and caveolae (review). *Mol Membr Biol,* 16, 145-56.

HOULGATTE, R., MALLAT, M., BRACHET, P. & PROCHIANTZ, A. (1989) Secretion of nerve growth factor in cultures of glial cells and neurons derived from different regions of the mouse brain. *J Neurosci Res,* 24, 143-52.
HSIA, A. Y., VINCENT, J. D. & LLEDO, P. M. (1999) Dopamine depresses synaptic inputs into the olfactory bulb. *J Neurophysiol,* 82, 1082-5.
HUANG, J. Q., TRASLER, J. M., IGDOURA, S., MICHAUD, J., HANAL, N. & GRAVEL, R. A. (1997) Apoptotic cell death in mouse models of GM2 gangliosidosis and observations on human Tay-Sachs and Sandhoff diseases. *Hum Mol Genet,* 6, 1879-85.
HUARD, J. M. & SCHWOB, J. E. (1995) Cell cycle of globose basal cells in rat olfactory epithelium. *Dev Dyn,* 203, 17-26.
HUARD, J. M., YOUNGENTOB, S. L., GOLDSTEIN, B. J., LUSKIN, M. B. & SCHWOB, J. E. (1998) Adult olfactory epithelium contains multipotent progenitors that give rise to neurons and non-neural cells. *J Comp Neurol,* 400, 469-86.
HUGHES, R. A. & CORNBLATH, D. R. (2005) Guillain-Barre syndrome. *Lancet,* 366, 1653-66.
HUMPHRIES, M. J., AKIYAMA, S. K., KOMORIYA, A., OLDEN, K. & YAMADA, K. M. (1988) Neurite extension of chicken peripheral nervous system neurons on fibronectin: relative importance of specific adhesion sites in the central cell-binding domain and the alternatively spliced type III connecting segment. *J Cell Biol,* 106, 1289-97.
HUWILER, A., KOLTER, T., PFEILSCHIFTER, J. & SANDHOFF, K. (2000) Physiology and pathophysiology of sphingolipid metabolism and signaling. *Biochim Biophys Acta,* 1485, 63-99.
HYNES, R. O. (1992) Integrins: versatility, modulation, and signaling in cell adhesion. *Cell,* 69, 11-25.
HYNES, R. O. (2002) Integrins: bidirectional, allosteric signaling machines. *Cell,* 110, 673-87.
HYUGA, S., YAMAGATA, S., TAI, T. & YAMAGATA, T. (1997) Inhibition of highly metastatic FBJ-LL cell migration by ganglioside GD1a highly expressed in poorly metastatic FBJ-S1 cells. *Biochem Biophys Res Commun,* 231, 340-3.
HYUGA, S., YAMAGATA, S., TAKATSU, Y., HYUGA, M., NAKANISHI, H., FURUKAWA, K. & YAMAGATA, T. (1999) Suppression by ganglioside GD1A of migration capability, adhesion to vitronectin and metastatic potential of highly metastatic FBJ-LL cells. *Int J Cancer,* 83, 685-91.
IMAIZUMI, T., LANKFORD, K. L., WAXMAN, S. G., GREER, C. A. & KOCSIS, J. D. (1998) Transplanted olfactory ensheathing cells remyelinate and enhance axonal conduction in the demyelinated dorsal columns of the rat spinal cord. *J Neurosci,* 18, 6176-85.
INOKUCHI, J., JIMBO, M., MOMOSAKI, K., SHIMENO, H., NAGAMATSU, A. & RADIN, N. S. (1990) Inhibition of experimental metastasis of murine Lewis lung carcinoma by an inhibitor of glucosylceramide synthase and its possible mechanism of action. *Cancer Res,* 50, 6731-7.
INOUE, M., FUJII, Y., FURUKAWA, K., OKADA, M., OKUMURA, K., HAYAKAWA, T., FURUKAWA, K. & SUGIURA, Y. (2002) Refractory skin injury in complex knock-out mice expressing only the GM3 ganglioside. *J Biol Chem,* 277, 29881-8.
ISAACSON, J. S. & STROWBRIDGE, B. W. (1998) Olfactory reciprocal synapses: dendritic signaling in the CNS. *Neuron,* 20, 749-61.
ISHIBASHI, T., DAKIN, K. A., STEVENS, B., LEE, P. R., KOZLOV, S. V., STEWART, C. L. & FIELDS, R. D. (2006) Astrocytes promote myelination in response to electrical impulses. *Neuron,* 49, 823-32.
ISHIBASHI, T., DUPREE, J. L., IKENAKA, K., HIRAHARA, Y., HONKE, K., PELES, E., POPKO, B., SUZUKI, K., NISHINO, H. & BABA, H. (2002) A myelin galactolipid,

sulfatide, is essential for maintenance of ion channels on myelinated axon but not essential for initial cluster formation. *J Neurosci,* 22, 6507-14.
ISHIBASHI, T., IKENAKA, K., SHIMIZU, T., KAGAWA, T. & BABA, H. (2003) Initiation of sodium channel clustering at the node of Ranvier in the mouse optic nerve. *Neurochem Res,* 28, 117-25.
ISHIBASHI, T., DAKIN, K. A., STEVENS, B., LEE, P. R., KOZLOV, S. V., STEWART, C. L. & FIELDS, R. D. (2006) Astrocytes promote myelination in response to electrical impulses. *Neuron,* 49, 823-32.
ITOH, M., FUKUMOTO, S., BABA, N., KUGA, Y., MIZUNO, A. & FURUKAWA, K. (1999) Prevention of the death of the rat axotomized hypoglossal nerve and promotion of its regeneration by bovine brain gangliosides. *Glycobiology,* 9, 1247-52.
ITOH, M., FUKUMOTO, S., IWAMOTO, T., MIZUNO, A., ROKUTANDA, A., ISHIDA, H. K., KISO, M. & FURUKAWA, K. (2001) Specificity of carbohydrate structures of gangliosides in the activity to regenerate the rat axotomized hypoglossal nerve. *Glycobiology,* 11, 125-30.
IWABUCHI, K., HANDA, K. & HAKOMORI, S. (1998a) Separation of "glycosphingolipid signaling domain" from caveolin-containing membrane fraction in mouse melanoma B16 cells and its role in cell adhesion coupled with signaling. *J Biol Chem,* 273, 33766-73.
IWABUCHI, K., YAMAMURA, S., PRINETTI, A., HANDA, K. & HAKOMORI, S. (1998b) GM3-enriched microdomain involved in cell adhesion and signal transduction through carbohydrate-carbohydrate interaction in mouse melanoma B16 cells. *J Biol Chem,* 273, 9130-8.
JANG, W., YOUNGENTOB, S. L. & SCHWOB, J. E. (2003) Globose basal cells are required for reconstitution of olfactory epithelium after methyl bromide lesion. *J Comp Neurol,* 460, 123-40.
JANZER, R. C. (1993) The blood-brain barrier: cellular basis. *J Inherit Metab Dis,* 16, 639-47.
JENKINS, S. M. & BENNETT, V. (2002) Developing nodes of Ranvier are defined by ankyrin-G clustering and are independent of paranodal axoglial adhesion. *Proc Natl Acad Sci U S A,* 99, 2303-8.
JESSEN, K. R., BRENNAN, A., MORGAN, L., MIRSKY, R., KENT, A., HASHIMOTO, Y. & GAVRILOVIC, J. (1994) The Schwann cell precursor and its fate: a study of cell death and differentiation during gliogenesis in rat embryonic nerves. *Neuron,* 12, 509-27.
JESSEN, K. R. & MIRSKY, R. (1991) Schwann cell precursors and their development. *Glia,* 4, 185-94.
JESSEN, K. R. & MIRSKY, R. (1992) Schwann cells: early lineage, regulation of proliferation and control of myelin formation. *Curr Opin Neurobiol,* 2, 575-81.
JESSEN, K. R., MORGAN, L., STEWART, H. J. & MIRSKY, R. (1990) Three markers of adult non-myelin-forming Schwann cells, 217c(Ran-1), A5E3 and GFAP: development and regulation by neuron-Schwann cell interactions. *Development,* 109, 91-103.
JOE, E. H. & ANGELIDES, K. (1992) Clustering of voltage-dependent sodium channels on axons depends on Schwann cell contact. *Nature,* 356, 333-5.
KAFITZ, K. W. & GREER, C. A. (1997) Role of laminin in axonal extension from olfactory receptor cells. *J Neurobiol,* 32, 298-310.
KALMAN, B., LAITINEN, K. & KOMOLY, S. (2007) The involvement of mitochondria in the pathogenesis of multiple sclerosis. *J Neuroimmunol,* 188, 1-12.
KAMIMURA, Y., FURUKAWA, K., KITTAKA, D., NISHIO, M., HAMAMURA, K., FUKUMOTO, S. & FURUKAWA, K. (2005) Differential enhancing effects of alpha2,8-sialyltransferase on the cell proliferation and mobility. *Int J Oncol,* 26, 337-44.

KAN, M., WANG, F., XU, J., CRABB, J. W., HOU, J. & MCKEEHAN, W. L. (1993) An essential heparin-binding domain in the fibroblast growth factor receptor kinase. *Science,* 259, 1918-21.
KANG, J., JIANG, L., GOLDMAN, S. A. & NEDERGAARD, M. (1998) Astrocyte-mediated potentiation of inhibitory synaptic transmission. *Nat Neurosci,* 1, 683-92.
KAPLAN, M. R., CHO, M. H., ULLIAN, E. M., ISOM, L. L., LEVINSON, S. R. & BARRES, B. A. (2001) Differential control of clustering of the sodium channels Na(v)1.2 and Na(v)1.6 at developing CNS nodes of Ranvier. *Neuron,* 30, 105-19.
KAPLAN, M. R., MEYER-FRANKE, A., LAMBERT, S., BENNETT, V., DUNCAN, I. D., LEVINSON, S. R. & BARRES, B. A. (1997) Induction of sodium channel clustering by oligodendrocytes. *Nature,* 386, 724-8.
KARPIAK, S. E. (1984) Exogenous gangliosides enhance recovery from cns injury. *Adv Exp Med Biol,* 174, 489-97.
KARPIAK, S. E., LI, Y. S. & MAHADIK, S. P. (1986) Gangliosides reduce mortality due to global ischemia: membrane protection. *Clin Neuropharmacol,* 9 Suppl 4, 338-40.
KARPIAK, S. E., LI, Y. S. & MAHADIK, S. P. (1987) Ganglioside treatment: reduction of CNS injury and facilitation of functional recovery. *Brain Inj,* 1, 161-70.
KARPIAK, S. E. & MAHADIK, S. P. (1984) Reduction of cerebral edema with GM1 ganglioside. *J Neurosci Res,* 12, 485-92.
KASAI, N. & YU, R. K. (1983) The monoclonal antibody A2B5 is specific to ganglioside GQ1c. *Brain Res,* 277, 155-8.
KATOH-SEMBA, R., FACCI, L., SKAPER, S. D. & VARON, S. (1986) Gangliosides stimulate astroglial cell proliferation in the absence of serum. *J Cell Physiol,* 126, 147-53.
KAWAI, H., ALLENDE, M. L., WADA, R., KONO, M., SANGO, K., DENG, C., MIYAKAWA, T., CRAWLEY, J. N., WERTH, N., BIERFREUND, U., SANDHOFF, K. & PROIA, R. L. (2001) Mice expressing only monosialoganglioside GM3 exhibit lethal audiogenic seizures. *J Biol Chem,* 276, 6885-8.
KAWAI, K., KURODA, S., WATARAI, S., TAKAHASHI, H. & IKUTA, F. (1994) Occurrence of GD3 ganglioside in reactive astrocytes--an immunocytochemical study in the rat brain. *Neurosci Lett,* 174, 225-7.
KAWAI, K., TAKAHASHI, H., WATARAI, S., ISHIZU, H., FUKAI, K., TANABE, Y., NOSE, S. & KURODA, S. (1999a) Occurrence of ganglioside GD3 in neoplastic astrocytes. An immunocytochemical study in humans. *Virchows Arch,* 434, 201-5.
KAWAI, K., WATARAI, S., TAKAHASHI, H., ISHIZU, H., FUKAI, K., TANABE, Y., YOKOTA, O. & KURODA, S. (1999b) Demonstration of ganglioside GD3 in human reactive astrocytes. *Psychiatry Clin Neurosci,* 53, 79-82.
KAWAKAMI, Y., KAWAKAMI, K., STEELANT, W. F., ONO, M., BAEK, R. C., HANDA, K., WITHERS, D. A. & HAKOMORI, S. (2002) Tetraspanin CD9 is a "proteolipid," and its interaction with alpha 3 integrin in microdomain is promoted by GM3 ganglioside, leading to inhibition of laminin-5-dependent cell motility. *J Biol Chem,* 277, 34349-58.
KAWASHIMA, I., NAGATA, I. & TAI, T. (1996) Immunocytochemical analysis of gangliosides in rat primary cerebellar cultures using specific monoclonal antibodies. *Brain Res,* 732, 75-86.
KAZUI, A., ONO, M., HANDA, K. & HAKOMORI, S. (2000) Glycosylation affects translocation of integrin, Src, and caveolin into or out of GEM. *Biochem Biophys Res Commun,* 273, 159-63.
KIERNAN, B. W., GOTZ, B., FAISSNER, A. & FFRENCH-CONSTANT, C. (1996) Tenascin-C inhibits oligodendrocyte precursor cell migration by both adhesion-dependent and adhesion-independent mechanisms. *Mol Cell Neurosci,* 7, 322-35.

KIM, J. Y., SUN, Q., OGLESBEE, M. & YOON, S. O. (2003) The role of ErbB2 signaling in the onset of terminal differentiation of oligodendrocytes in vivo. *J Neurosci,* 23, 5561-71.
KIM, T., FIEDLER, K., MADISON, D. L., KRUEGER, W. H. & PFEIFFER, S. E. (1995) Cloning and characterization of MVP17: a developmentally regulated myelin protein in oligodendrocytes. *J Neurosci Res,* 42, 413-22.
KIM, T. & PFEIFFER, S. E. (1999) Myelin glycosphingolipid/cholesterol-enriched microdomains selectively sequester the non-compact myelin proteins CNP and MOG. *J Neurocytol,* 28, 281-93.
KISHI, K., MORI, K. & TAZAWA, Y. (1982) Three-dimensional analysis of dendritic trees of mitral cells in the rabbit olfactory bulb. *Neurosci Lett,* 28, 127-32.
KLENK, E. (1942) Uber die Ganglioside, eine neue Gruppe von zuckerhaltigen Gehirnlipoiden. *Hoppe Seylers Z Physiol Chem,* 273, 76-86.
KLESSE, L. J. & PARADA, L. F. (1999) Trks: signal transduction and intracellular pathways. *Microsc Res Tech,* 45, 210-6.
KOJIMA, H., GORIO, A., JANIGRO, D. & JONSSON, G. (1984) GM1 ganglioside enhances regrowth of noradrenaline nerve terminals in rat cerebral cortex lesioned by the neurotoxin 6-hydroxydopamine. *Neuroscience,* 13, 1011-22.
KOJIMA, N., KUROSAWA, N., NISHI, T., HANAI, N. & TSUJI, S. (1994) Induction of cholinergic differentiation with neurite sprouting by de novo biosynthesis and expression of GD3 and b-series gangliosides in Neuro2a cells. *J Biol Chem,* 269, 30451-6.
KOLTER, T., PROIA, R. L. & SANDHOFF, K. (2002) Combinatorial ganglioside biosynthesis. *J Biol Chem,* 277, 25859-62.
KONDO, T. & RAFF, M. (2000) Oligodendrocyte precursor cells reprogrammed to become multipotential CNS stem cells. *Science,* 289, 1754-7.
KORDELI, E., LAMBERT, S. & BENNETT, V. (1995) AnkyrinG. A new ankyrin gene with neural-specific isoforms localized at the axonal initial segment and node of Ranvier. *J Biol Chem,* 270, 2352-9.
KOSAKA, K., TOIDA, K., AIKA, Y. & KOSAKA, T. (1998) How simple is the organization of the olfactory glomerulus?: the heterogeneity of so-called periglomerular cells. *Neurosci Res,* 30, 101-10.
KOTICHA, D., MAUREL, P., ZANAZZI, G., KANE-GOLDSMITH, N., BASAK, S., BABIARZ, J., SALZER, J. & GRUMET, M. (2006) Neurofascin interactions play a critical role in clustering sodium channels, ankyrin G and beta IV spectrin at peripheral nodes of Ranvier. *Dev Biol,* 293, 1-12.
KRUSE, J., KEILHAUER, G., FAISSNER, A., TIMPL, R. & SCHACHNER, M. (1985) The J1 glycoprotein--a novel nervous system cell adhesion molecule of the L2/HNK-1 family. *Nature,* 316, 146-8.
KUMAR, S., KAHN, M. A., DINH, L. & DE VELLIS, J. (1998) NT-3-mediated TrkC receptor activation promotes proliferation and cell survival of rodent progenitor oligodendrocyte cells in vitro and in vivo. *J Neurosci Res,* 54, 754-65.
KUSUNOKI, S., CHIBA, A., TAI, T. & KANAZAWA, I. (1993) Localization of GM1 and GD1b antigens in the human peripheral nervous system. *Muscle Nerve,* 16, 752-6.
LAINETTI, R. D., PEREIRA, F. C. & DA-SILVA, C. F. (1998) Ganglioside GM1 potentiates the stimulatory effect of nerve growth factor on peripheral nerve regeneration in vivo. *Ann N Y Acad Sci,* 845, 415-6.
LAMBERT, S., DAVIS, J. Q. & BENNETT, V. (1997) Morphogenesis of the node of Ranvier: co-clusters of ankyrin and ankyrin-binding integral proteins define early developmental intermediates. *J Neurosci,* 17, 7025-36.
LANG, Z., GUERRERA, M., LI, R. & LADISCH, S. (2001) Ganglioside GD1a enhances VEGF-induced endothelial cell proliferation and migration. *Biochem Biophys Res Commun,* 282, 1031-7.

LE DOUARIN, N., DULAC, C., DUPIN, E. & CAMERON-CURRY, P. (1991) Glial cell lineages in the neural crest. *Glia,* 4, 175-84.
LEDEEN, R. W. (1984) Biology of gangliosides: neuritogenic and neuronotrophic properties. *J Neurosci Res,* 12, 147-59.
LEDEEN, R. W., SKRIVANEK, J. A., TIRRI, L. J., MARGOLIS, R. K. & MARGOLIS, R. U. (1976) Gangliosides of the neuron: localization and origin. *Adv Exp Med Biol,* 71, 83-103.
LEDEEN, R. W. & WU, G. (2006) GM1 ganglioside: another nuclear lipid that modulates nuclear calcium. GM1 potentiates the nuclear sodium-calcium exchanger. *Can J Physiol Pharmacol,* 84, 393-402.
LEE, M. C., LEE, W. S., PARK, C. S. & JUHNG, S. W. (1994) The biologic role of ganglioside in neuronal differentiation--effects of GM1 ganglioside on human neuroblastoma SH-SY5Y cells. *J Korean Med Sci,* 9, 179-87.
LEFCORT, F., VENSTROM, K., MCDONALD, J. A. & REICHARDT, L. F. (1992) Regulation of expression of fibronectin and its receptor, alpha 5 beta 1, during development and regeneration of peripheral nerve. *Development,* 116, 767-82.
LEHMANN, H. C., LOPEZ, P. H., ZHANG, G., NGYUEN, T., ZHANG, J., KIESEIER, B. C., MORI, S. & SHEIKH, K. A. (2007) Passive immunization with anti-ganglioside antibodies directly inhibits axon regeneration in an animal model. *J Neurosci,* 27, 27-34.
LEVI, A. D., BUNGE, R. P., LOFGREN, J. A., MEIMA, L., HEFTI, F., NIKOLICS, K. & SLIWKOWSKI, M. X. (1995) The influence of heregulins on human Schwann cell proliferation. *J Neurosci,* 15, 1329-40.
LEVI, G., GALLO, V. & CIOTTI, M. T. (1986) Bipotential precursors of putative fibrous astrocytes and oligodendrocytes in rat cerebellar cultures express distinct surface features and "neuron-like" gamma-aminobutyric acid transport. *Proc Natl Acad Sci U S A,* 83, 1504-8.
LEVISON, S. W. & MCCARTHY, K. D. (1989) Schwann cells influence the expression of ganglioside GD3 by rat dorsal root ganglion neurons. *J Neuroimmunol,* 24, 223-32.
LI, R., LIU, Y. & LADISCH, S. (2001) Enhancement of epidermal growth factor signaling and activation of SRC kinase by gangliosides. *J Biol Chem,* 276, 42782-92.
LI, R., MANELA, J., KONG, Y. & LADISCH, S. (2000) Cellular gangliosides promote growth factor-induced proliferation of fibroblasts. *J Biol Chem,* 275, 34213-23.
LIESI, P. (1985) Laminin-immunoreactive glia distinguish regenerative adult CNS systems from non-regenerative ones. *Embo J,* 4, 2505-11.
LINDHOLM, T., CULLHEIM, S., DECKNER, M., CARLSTEDT, T. & RISLING, M. (2002) Expression of neuregulin and ErbB3 and ErbB4 after a traumatic lesion in the ventral funiculus of the spinal cord and in the intact primary olfactory system. *Exp Brain Res,* 142, 81-90.
LIU, H., KOJIMA, N., KUROSAWA, N. & TSUJI, S. (1997) Regulated expression system for GD3 synthase cDNA and induction of differentiation in Neuro2a cells. *Glycobiology,* 7, 1067-76.
LIU, Y., MCCARTHY, J. & LADISCH, S. (2006) Membrane ganglioside enrichment lowers the threshold for vascular endothelial cell angiogenic signaling. *Cancer Res,* 66, 10408-14.
LLOYD, K. O. & FURUKAWA, K. (1998) Biosynthesis and functions of gangliosides: recent advances. *Glycoconj J,* 15, 627-36.
LOIS, C., GARCIA-VERDUGO, J. M. & ALVAREZ-BUYLLA, A. (1996) Chain migration of neuronal precursors. *Science,* 271, 978-81.
LUBETZKI, C., DEMERENS, C., ANGELADE, P., VILLARROYA, H., FRANKFURTER, A., LEE, V. M. & ZALC, B. (1993) Even in culture, oligodendrocytes myelinate solely axons. *Proc Natl Acad Sci U S A,* 90, 6820-4.

LU, H. Z., WANG, Y. X., LI, Y., FU, S. L., HANG, Q. & LU, P. H. (2008) Proliferation and differentiation of oligodendrocyte progenitor cells induced from rat embryonic neural precursor cells followed by flow cytometry. Cytometry A
MA, Q., KOBAYASHI, M., SUGIURA, M., OZAKI, N., NISHIO, K., SHIRAISHI, Y., FURUKAWA, K., FURUKAWA, K. & SUGIURA, Y. (2003) Morphological study of disordered myelination and the degeneration of nerve fibers in the spinal cord of mice lacking complex gangliosides. *Arch Histol Cytol,* 66, 37-44.
MACCIONI, H. J., LANDA, C., ARCE, A. & CAPUTTO, R. (1977) The biosynthesis of brain gangliosides--evidence for a "transient pool" and an "end product pool" of gangliosides. *Adv Exp Med Biol,* 83, 267-81.
MACKAY-SIMA, A. & CHUAHB, M. I. (2000) Neurotrophic factors in the primary olfactory pathway. *Prog Neurobiol,* 62, 527-59.
MACRIDES, F. & SCHNEIDER, S. P. (1982) Laminar organization of mitral and tufted cells in the main olfactory bulb of the adult hamster. *J Comp Neurol,* 208, 419-30.
MAHANTHAPPA, N. K. & SCHWARTING, G. A. (1993) Peptide growth factor control of olfactory neurogenesis and neuron survival in vitro: roles of EGF and TGF-beta s. *Neuron,* 10, 293-305.
MAIER, O., BARON, W. & HOEKSTRA, D. (2007) Reduced raft-association of NF155 in active MS-lesions is accompanied by the disruption of the paranodal junction. *Glia,* 55, 885-95.
MAIER, O., VAN DER HEIDE, T., VAN DAM, A. M., BARON, W., DE VRIES, H. & HOEKSTRA, D. (2005) Alteration of the extracellular matrix interferes with raft association of neurofascin in oligodendrocytes. Potential significance for multiple sclerosis? *Mol Cell Neurosci,* 28, 390-401.
MAJOUL, I., SCHMIDT, T., POMASANOVA, M., BOUTKEVICH, E., KOZLOV, Y. & SOLING, H. D. (2002) Differential expression of receptors for Shiga and Cholera toxin is regulated by the cell cycle. *J Cell Sci,* 115, 817-26.
MALEK-HEDAYAT, S. & ROME, L. H. (1994) Expression of a beta 1-related integrin by oligodendroglia in primary culture: evidence for a functional role in myelination. *J Cell Biol,* 124, 1039-46.
MALISAN, F. & TESTI, R. (2002) GD3 ganglioside and apoptosis. *Biochim Biophys Acta,* 1585, 179-87.
MANNION, B. A., BERDITCHEVSKI, F., KRAEFT, S. K., CHEN, L. B. & HEMLER, M. E. (1996) Transmembrane-4 superfamily proteins CD81 (TAPA-1), CD82, CD63, and CD53 specifically associated with integrin alpha 4 beta 1 (CD49d/CD29). *J Immunol,* 157, 2039-47.
MARCONI, S., DE TONI, L., LOVATO, L., TEDESCHI, E., GAETTI, L., ACLER, M. & BONETTI, B. (2005) Expression of gangliosides on glial and neuronal cells in normal and pathological adult human brain. *J Neuroimmunol,* 170, 115-21.
MARCUS, J., DUPREE, J. L. & POPKO, B. (2002) Myelin-associated glycoprotein and myelin galactolipids stabilize developing axo-glial interactions. *J Cell Biol,* 156, 567-77.
MARGOLIS, F. L. (1982) Olfactory marker protein (OMP). *Scand J Immunol Suppl,* 9, 181-99.
MARGOLIS, F. L., ROBERTS, N., FERRIERO, D. & FELDMAN, J. (1974) Denervation in the primary olfactory pathway of mice: biochemical and morphological effects. *Brain Res,* 81, 469-83.
MARO, G. S., VERMEREN, M., VOICULESCU, O., MELTON, L., COHEN, J., CHARNAY, P. & TOPILKO, P. (2004) Neural crest boundary cap cells constitute a source of neuronal and glial cells of the PNS. *Nat Neurosci,* 7, 930-8.
MARRIE, R. A. (2004) Environmental risk factors in multiple sclerosis aetiology. *Lancet Neurol*, 3, 709-18.

MARTINI, R., XIN, Y. & SCHACHNER, M. (1994) Restricted localization of L1 and N-CAM at sites of contact between Schwann cells and neurites in culture. *Glia,* 10, 70-4.
MASSA, P. T. & MUGNAINI, E. (1982) Cell junctions and intramembrane particles of astrocytes and oligodendrocytes: a freeze-fracture study. *Neuroscience,* 7, 523-38.
MATHEWS, M. B., BERNSTEIN, R. M., FRANZA, B. R. Jr.& GARRELS, J. I. (1984) Identity of the proliferating cell nuclear antigen and cyclin. *Nature,* 309, 374-6.
MATULIONIS, D. H. (1975) Ultrastructural study of mouse olfactory epithelium following destruction by ZnSO4 and its subsequent regeneration. *Am J Anat,* 142, 67-89.
MATULIONIS, D. H. (1976) Light and electron microscopic study of the degeneration and early regeneration of olfactory epithelium in the mouse. *Am J Anat,* 145, 79-99.
MCKERRACHER, L., DAVID, S., JACKSON, D. L., KOTTIS, V., DUNN, R. J. & BRAUN, P. E. (1994) Identification of myelin-associated glycoprotein as a major myelin-derived inhibitor of neurite growth. *Neuron,* 13, 805-11.
MCKINNON, R. D., MATSUI, T., DUBOIS-DALCQ, M. & AARONSON, S. A. (1990) FGF modulates the PDGF-driven pathway of oligodendrocyte development. *Neuron,* 5, 603-14.
MCMORRIS, F. A. & DUBOIS-DALCQ, M. (1988) Insulin-like growth factor I promotes cell proliferation and oligodendroglial commitment in rat glial progenitor cells developing in vitro. *J Neurosci Res,* 21, 199-209.
MCMORRIS, F. A., SMITH, T. M., DESALVO, S. & FURLANETTO, R. W. (1986) Insulin-like growth factor I/somatomedin C: a potent inducer of oligodendrocyte development. *Proc Natl Acad Sci U S A,* 83, 822-6.
MEIER, C., PARMANTIER, E., BRENNAN, A., MIRSKY, R. & JESSEN, K. R. (1999) Developing Schwann cells acquire the ability to survive without axons by establishing an autocrine circuit involving insulin-like growth factor, neurotrophin-3, and platelet-derived growth factor-BB. *J Neurosci,* 19, 3847-59.
MEIRI, K. F., BICKERSTAFF, L. E. & SCHWOB, J. E. (1991) Monoclonal antibodies show that kinase C phosphorylation of GAP-43 during axonogenesis is both spatially and temporally restricted in vivo. *J Cell Biol,* 112, 991-1005.
MEISAMI, E. & SENDERA, T. J. (1993) Morphometry of rat olfactory bulbs stained for cytochrome oxidase reveals that the entire population of glomeruli forms early in the neonatal period. *Brain Res Dev Brain Res,* 71, 253-7.
MELKONIAN, K. A., OSTERMEYER, A. G., CHEN, J. Z., ROTH, M. G. & BROWN, D. A. (1999) Role of lipid modifications in targeting proteins to detergent-resistant membrane rafts. Many raft proteins are acylated, while few are prenylated. *J Biol Chem,* 274, 3910-7.
MENDEZ-OTERO, R. & CONSTANTINE-PATON, M. (1990) Granule cell induction of 9-O-acetyl gangliosides on cerebellar glia in microcultures. *Dev Biol,* 138, 400-9.
MENDEZ-OTERO, R. & FRIEDMAN, J. E. (1996) Role of acetylated gangliosides on neurite extension. *Eur J Cell Biol,* 71, 192-8.
MENDEZ-OTERO, R. & RAMON-CUETO, A. (1994) Expression of 9-O-acetylated gangliosides during development of the rat olfactory system. *Neuroreport,* 5, 1755-9.
MENDEZ-OTERO, R. & SANTIAGO, M. F. (2003) Functional role of a specific ganglioside in neuronal migration and neurite outgrowth. *Braz J Med Biol Res,* 36, 1003-13.
MENDEZ-OTERO, R., SCHLOSSHAUER, B., BARNSTABLE, C. J. & CONSTANTINE-PATON, M. (1988) A developmentally regulated antigen associated with neural cell and process migration. *J Neurosci,* 8, 564-79.

MENON, K., RASBAND, M. N., TAYLOR, C. M., BROPHY, P., BANSAL, R. & PFEIFFER, S. E. (2003) The myelin-axolemmal complex: biochemical dissection and the role of galactosphingolipids. *J Neurochem,* 87, 995-1009.
MERZAK, A., KOOCHEKPOUR, S., MCCREA, S., ROXANIS, Y. & PILKINGTON, G. J. (1995a) Gangliosides modulate proliferation, migration, and invasiveness of human brain tumor cells in vitro. *Mol Chem Neuropathol,* 24, 121-35.
MERZAK, A., KOOCHEKPOUR, S. & PILKINGTON, G. J. (1994) Cell surface gangliosides are involved in the control of human glioma cell invasion in vitro. *Neurosci Lett,* 177, 44-6.
MERZAK, A., KOOCHEKPOUR, S. & PILKINGTON, G. J. (1995b) Adhesion of human glioma cell lines to fibronectin, laminin, vitronectin and collagen I is modulated by gangliosides in vitro. *Cell Adhes Commun,* 3, 27-43.
MEUILLET, E., CREMEL, G., HICKS, D. & DREYFUS, H. (1996) Ganglioside effects on basic fibroblast and epidermal growth factor receptors in retinal glial cells. *J Lipid Mediat Cell Signal,* 14, 277-88.
MEUILLET, E. J., KROES, R., YAMAMOTO, H., WARNER, T. G., FERRARI, J., MANIA-FARNELL, B., GEORGE, D., REBBAA, A., MOSKAL, J. R. & BREMER, E. G. (1999) Sialidase gene transfection enhances epidermal growth factor receptor activity in an epidermoid carcinoma cell line, A431. *Cancer Res,* 59, 234-40.
MEUILLET, E. J., MANIA-FARNELL, B., GEORGE, D., INOKUCHI, J. I. & BREMER, E. G. (2000) Modulation of EGF receptor activity by changes in the GM3 content in a human epidermoid carcinoma cell line, A431. *Exp Cell Res,* 256, 74-82.
MEYER, D. & BIRCHMEIER, C. (1994) Distinct isoforms of neuregulin are expressed in mesenchymal and neuronal cells during mouse development. *Proc Natl Acad Sci U S A,* 91, 1064-8.
MI, H., DEERINCK, T. J., ELLISMAN, M. H. & SCHWARZ, T. L. (1995) Differential distribution of closely related potassium channels in rat Schwann cells. *J Neurosci,* 15, 3761-74.
MI, S., MILLER, R. H., LEE, X., SCOTT, M. L., SHULAG-MORSKAYA, S., SHAO, Z., CHANG, J., THILL, G., LEVESQUE, M., ZHANG, M., HESSION, C., SAH, D., TRAPP, B., HE, Z., JUNG, V., McCOY, J. M. & PEPINSKY, R. B. (2005) LINGO-1 negatively regulates myelination by oligodendrocytes. *Nat Neurosci,* 8, 745-51.
MICHAILOV, G. V., SEREDA, M. W., BRINKMANN, B. G., FISCHER, T. M., HAUG, B., BIRCHMEIER, C., ROLE, L., LAI, C., SCHWAB, M. H. & NAVE, K. A. (2004) Axonal neuregulin-1 regulates myelin sheath thickness. *Science,* 304, 700-3.
MILJAN, E. A. & BREMER, E. G. (2002) Regulation of growth factor receptors by gangliosides. *Sci STKE,* 2002, RE15.
MILJAN, E. A., MEUILLET, E. J., MANIA-FARNELL, B., GEORGE, D., YAMAMOTO, H., SIMON, H. G. & BREMER, E. G. (2002) Interaction of the extracellular domain of the epidermal growth factor receptor with gangliosides. *J Biol Chem,* 277, 10108-13.
MILLER-PODRAZA, H. & FISHMAN, P. H. (1982) Translocation of newly synthesized gangliosides to the cell surface. *Biochemistry,* 21, 3265-70.
MILLER, R. H., DAVID, S., PATEL, R., ABNEY, E. R. & RAFF, M. C. (1985) A quantitative immunohistochemical study of macroglial cell development in the rat optic nerve: in vivo evidence for two distinct astrocyte lineages. *Dev Biol,* 111, 35-41.
MILNER, R., ANDERSON, H. J., RIPPON, R. F., MCKAY, J. S., FRANKLIN, R. J., MARCHIONNI, M. A., REYNOLDS, R. & FFRENCH-CONSTANT, C. (1997a) Contrasting effects of mitogenic growth factors on oligodendrocyte precursor cell migration. *Glia,* 19, 85-90.
MILNER, R., EDWARDS, G., STREULI, C. & FFRENCH-CONSTANT, C. (1996) A role in migration for the alpha V beta 1 integrin expressed on oligodendrocyte precursors. *J Neurosci,* 16, 7240-52.

MILNER, R. & FFRENCH-CONSTANT, C. (1994) A developmental analysis of oligodendroglial integrins in primary cells: changes in alpha v-associated beta subunits during differentiation. *Development,* 120, 3497-506.
MILNER, R., FROST, E., NISHIMURA, S., DELCOMMENNE, M., STREULI, C., PYTELA, R. & FFRENCH-CONSTANT, C. (1997b) Expression of alpha vbeta3 and alpha vbeta8 integrins during oligodendrocyte precursor differentiation in the presence and absence of axons. *Glia,* 21, 350-60.
MILNER, R., HUANG, X., WU, J., NISHIMURA, S., PYTELA, R., SHEPPARD, D. & FFRENCH-CONSTANT, C. (1999) Distinct roles for astrocyte alphavbeta5 and alphavbeta8 integrins in adhesion and migration. *J Cell Sci,* 112 (Pt 23), 4271-9.
MIRAGALL, F., KADMON, G., HUSMANN, M. & SCHACHNER, M. (1988) Expression of cell adhesion molecules in the olfactory system of the adult mouse: presence of the embryonic form of N-CAM. *Dev Biol,* 129, 516-31.
MIRSKY, R., DUBOIS, C., MORGAN, L. & JESSEN, K. R. (1990) 04 and A007-sulfatide antibodies bind to embryonic Schwann cells prior to the appearance of galactocerebroside; regulation of the antigen by axon-Schwann cell signals and cyclic AMP. *Development,* 109, 105-16.
MIRSKY, R. & JESSEN, K. R. (1996) Schwann cell development, differentiation and myelination. *Curr Opin Neurobiol,* 6, 89-96.
MIRSKY, R. & JESSEN, K. R. (1999) The neurobiology of Schwann cells. *Brain Pathol,* 9, 293-311.
MIRSKY, R., JESSEN, K. R., BRENNAN, A., PARKINSON, D., DONG, Z., MEIER, C., PARMANTIER, E. & LAWSON, D. (2002) Schwann cells as regulators of nerve development. *J Physiol Paris,* 96, 17-24.
MIRSKY, R., JESSEN, K. R., SCHACHNER, M. & GORIDIS, C. (1986) Distribution of the adhesion molecules N-CAM and L1 on peripheral neurons and glia in adult rats. *J Neurocytol,* 15, 799-815.
MITSUDA, T., FURUKAWA, K., FUKUMOTO, S., MIYAZAKI, H., URANO, T. & FURUKAWA, K. (2002) Overexpression of ganglioside GM1 results in the dispersion of platelet-derived growth factor receptor from glycolipid-enriched microdomains and in the suppression of cell growth signals. *J Biol Chem,* 277, 11239-46.
MOLANDER, M., BERTHOLD, C. H., PERSSON, H., ANDERSSON, K. & FREDMAN, P. (1997) Monosialoganglioside (GM1) immunofluorescence in rat spinal roots studied with a monoclonal antibody. *J Neurocytol,* 26, 101-11.
MOLANDER, M., BERTHOLD, C. H., PERSSON, H. & FREDMAN, P. (2000) Immunostaining of ganglioside GD1b, GD3 and GM1 in rat cerebellum: cellular layer and cell type specific associations. *J Neurosci Res,* 60, 531-42.
MOORE, S. & THANOS, S. (1996) The concept of microglia in relation to central nervous system disease and regeneration. *Prog Neurobiol,* 48, 441-60.
MORGAN, J. I. & SEIFERT, W. (1979) Growth factors and gangliosides: a possible new perspective in neuronal growth control. *J Supramol Struct,* 10, 111-24.
MOSS, J. & VAUGHAN, M. (1979) Activation of adenylate cyclase by choleragen. *Annu Rev Biochem,* 48, 581-600.
MUKHOPADHYAY, G., DOHERTY, P., WALSH, F. S., CROCKER, P. R. & FILBIN, M. T. (1994) A novel role for myelin-associated glycoprotein as an inhibitor of axonal regeneration. *Neuron,* 13, 757-67.
MUMM, J. S., SHOU, J. & CALOF, A. L. (1996) Colony-forming progenitors from mouse olfactory epithelium: evidence for feedback regulation of neuron production. *Proc Natl Acad Sci U S A,* 93, 11167-72.
MUNRO, S. (2003) Lipid rafts: elusive or illusive? *Cell,* 115, 377-88.
MURAKAMI, K., ASOU, H., ADACHI, T., TAKAGI, T., KUNIMOTO, M., SAITO, H. & UYEMURA, K. (1999) Neutral glycolipid and ganglioside composition of type-1 and type-2 astrocytes from rat cerebral hemisphere. *J Neurosci Res,* 55, 382-93.

MUTOH, T., TOKUDA, A., MIYADAI, T., HAMAGUCHI, M. & FUJIKI, N. (1995) Ganglioside GM1 binds to the Trk protein and regulates receptor function. *Proc Natl Acad Sci U S A,* 92, 5087-91.
NAN, B., GETCHELL, M. L., PARTIN, J. V. & GETCHELL, T. V. (2001) Leukemia inhibitory factor, interleukin-6, and their receptors are expressed transiently in the olfactory mucosa after target ablation. *J Comp Neurol,* 435, 60-77.
NEWMAN, E. A. (2001) Propagation of intercellular calcium waves in retinal astrocytes and Muller cells. *J Neurosci,* 21, 2215-23.
NEWMAN, M. P., FERON, F. & MACKAY-SIM, A. (2000) Growth factor regulation of neurogenesis in adult olfactory epithelium. *Neuroscience,* 99, 343-50.
NIEDERLANDER, C. & LUMSDEN, A. (1996) Late emigrating neural crest cells migrate specifically to the exit points of cranial branchiomotor nerves. *Development,* 122, 2367-74.
NIESSEN, C. M., CREMONA, O., DAAMS, H., FERRARESI, S., SONNENBERG, A. & MARCHISIO, P. C. (1994) Expression of the integrin alpha 6 beta 4 in peripheral nerves: localization in Schwann and perineural cells and different variants of the beta 4 subunit. *J Cell Sci,* 107 (Pt 2), 543-52.
NISHIO, M., FUKUMOTO, S., FURUKAWA, K., ICHIMURA, A., MIYAZAKI, H., KUSUNOKI, S., URANO, T. & FURUKAWA, K. (2004) Overexpressed GM1 suppresses nerve growth factor (NGF) signals by modulating the intracellular localization of NGF receptors and membrane fluidity in PC12 cells. *J Biol Chem,* 279, 33368-78.
NISHIYAMA, A., LIN, X. H., GIESE, N., HELDIN, C. H. & STALLCUP, W. B. (1996) Co-localization of NG2 proteoglycan and PDGF alpha-receptor on O2A progenitor cells in the developing rat brain. *J Neurosci Res,* 43, 299-314.
NOBLE, M. & MURRAY, K. (1984) Purified astrocytes promote the in vitro division of a bipotential glial progenitor cell. *Embo J,* 3, 2243-7.
NOBLE, M., MURRAY, K., STROOBANT, P., WATERFIELD, M. D. & RIDDLE, P. (1988) Platelet-derived growth factor promotes division and motility and inhibits premature differentiation of the oligodendrocyte/type-2 astrocyte progenitor cell. *Nature,* 333, 560-2.
NOJIRI, H., STROUD, M. & HAKOMORI, S. (1991) A specific type of ganglioside as a modulator of insulin-dependent cell growth and insulin receptor tyrosine kinase activity. Possible association of ganglioside-induced inhibition of insulin receptor function and monocytic differentiation induction in HL-60 cells. *J Biol Chem,* 266, 4531-7.
NOWAK, L., ASCHER, P. & BERWALD-NETTER, Y. (1987) Ionic channels in mouse astrocytes in culture. *J Neurosci,* 7, 101-9.
OHSAWA, T. (1989) Changes of mouse brain gangliosides during aging from young adult until senescence. *Mech Ageing Dev,* 50, 169-77.
OHSAWA, T. & SHUMIYA, S. (1991) Age-related alteration of brain gangliosides in senescence-accelerated mouse (SAM)-P/8. *Mech Ageing Dev,* 59, 263-74.
OKADA, S., McCREA, M. & O'BRIEN, J. S. (1972) Sandhoff's disease (GM2 gangliosidosis type 2): clinical, chemical, and enzyme studies in five patients. *Pediatr Res,* 6, 606-15.
xOKADA, E., MAEDA, T. & WATANABE, T. (1982) Immunocytochemical study on cholera toxin binding sites by monoclonal anti-cholera toxin antibody in neuronal tissue culture. *Brain Res,* 242, 233-41.
OKADA, M., ITOH MI, M., HARAGUCHI, M., OKAJIMA, T., INOUE, M., OISHI, H., MATSUDA, Y., IWAMOTO, T., KAWANO, T., FUKUMOTO, S., MIYAZAKI, H., FURUKAWA, K., AIZAWA, S. & FURUKAWA, K. (2002) b-series Ganglioside deficiency exhibits no definite changes in the neurogenesis and the sensitivity to Fas-mediated apoptosis but impairs regeneration of the lesioned hypoglossal nerve. *J Biol Chem,* 277, 1633-6.

OLSEN, I. M. & FFRENCH-CONSTANT, C. (2005) Dynamic regulation of integrin activation by intracellular and extracellular signals controls oligodendrocyte morphology. *BMC Biol,* 3, 25.
ONO, M., HANDA, K., SONNINO, S., WITHERS, D. A., NAGAI, H. & HAKOMORI, S. (2001) GM3 ganglioside inhibits CD9-facilitated haptotactic cell motility: coexpression of GM3 and CD9 is essential in the downregulation of tumor cell motility and malignancy. *Biochemistry,* 40, 6414-21.
ORENTAS, D. M. & MILLER, R. H. (1998) Regulation of oligodendrocyte development. *Mol Neurobiol,* 18, 247-59.
ORNITZ, D. M., XU, J., COLVIN, J. S., MCEWEN, D. G., MACARTHUR, C. A., COULIER, F., GAO, G. & GOLDFARB, M. (1996) Receptor specificity of the fibroblast growth factor family. *J Biol Chem,* 271, 15292-7.
OSTERHOUT, D. J., EBNER, S., XU, J., ORNITZ, D. M., ZAZANIS, G. A. & MCKINNON, R. D. (1997) Transplanted oligodendrocyte progenitor cells expressing a dominant-negative FGF receptor transgene fail to migrate in vivo. *J Neurosci,* 17, 9122-32.
OZAWA, H., KOTANI, M., KAWASHIMA, I., NUMATA, M., OGAWA, T., TERASHIMA, T. & TAI, T. (1993) Generation of a monoclonal antibody specific for ganglioside GM4: evidence for GM4 expression on astrocytes in chicken cerebellum. *J Biochem (Tokyo),* 114, 5-8.
PALLER, A. S., ARNSMEIER, S. L., CHEN, J. D. & WOODLEY, D. T. (1995) Ganglioside GT1b inhibits keratinocyte adhesion and migration on a fibronectin matrix. *J Invest Dermatol,* 105, 237-42.
PAN, B., FROMHOLT, S. E., HESS, E. J., CRAWFORD, T. O., GRIFFIN, J. W., SHEIKH, K. A. & SCHNAAR, R. L. (2005) Myelin-associated glycoprotein and complementary axonal ligands, gangliosides, mediate axon stability in the CNS and PNS: neuropathology and behavioral deficits in single- and double-null mice. *Exp Neurol,* 195, 208-17.
PANDE, G. (2000) The role of membrane lipids in regulation of integrin functions. *Curr Opin Cell Biol,* 12, 569-74.
PARENT, A. (1996) *Carpenter's Human Anatomy, 9th Edition*, Williams and Wilkin.
PARK, S. K., MILLER, R., KRANE, I. & VARTANIAN, T. (2001) The erbB2 gene is required for the development of terminally differentiated spinal cord oligodendrocytes. *J Cell Biol,* 154, 1245-58.
PARPURA, V., BASARSKY, T. A., LIU, F., JEFTINIJA, K., JEFTINIJA, S. & HAYDON, P. G. (1994) Glutamate-mediated astrocyte-neuron signalling. *Nature,* 369, 744-7.
PARPURA, V. & HAYDON, P. G. (2000) Physiological astrocytic calcium levels stimulate glutamate release to modulate adjacent neurons. *Proc Natl Acad Sci U S A,* 97, 8629-34.
PASTI, L., VOLTERRA, A., POZZAN, T. & CARMIGNOTO, G. (1997) Intracellular calcium oscillations in astrocytes: a highly plastic, bidirectional form of communication between neurons and astrocytes in situ. *J Neurosci,* 17, 7817-30.
PASTRANA, E., MORENO-FLORES, M. T., GURZOV, E. N., AVILA, J., WANDOSELL, F. & DIAZ-NIDO, J. (2006) Genes associated with adult axon regeneration promoted by olfactory ensheathing cells: a new role for matrix metalloproteinase 2. *J Neurosci,* 26, 5347-59.
PAUNESKU, T., MITTAL, S., PROTIC, M., ORYHON, J., KOROLEV, S. V., JOACHIMIAK, A. & WOLOSCHAK, G. E. (2001) Proliferating cell nuclear antigen (PCNA): ringmaster of the genome. *Int J Radiat Biol,* 77, 1007-21.
PELES, E., NATIV, M., LUSTIG, M., GRUMET, M., SCHILLING, J., MARTINEZ, R., PLOWMAN, G. D. & SCHLESSINGER, J. (1997) Identification of a novel contactin-associated transmembrane receptor with multiple domains implicated in protein-protein interactions. *Embo J,* 16, 978-88.

PELLEGRINI, L., BURKE, D. F., VON DELFT, F., MULLOY, B. & BLUNDELL, T. L. (2000) Crystal structure of fibroblast growth factor receptor ectodomain bound to ligand and heparin. *Nature,* 407, 1029-34.
PERKINS, C. S., AGUAYO, A. J. & BRAY, G. M. (1981) Schwann cell multiplication in Trembler mice. *Neuropathol Appl Neurobiol,* 7, 115-26.
PERROTEAU, I., OBERTO, M., IERACI, A., BOVOLIN, P. & FASOLO, A. (1998) ErbB-3 and ErbB-4 expression in the mouse olfactory system. *Ann N Y Acad Sci,* 855, 255-9.
PETERS, A., PALAY, S. L. & WEBSTAR, H. D. (1991) *The fine structure of the nervous system, neurons and their supporting cells. ,* New York Oxford University Press.
PFEIFFER, S. E., WARRINGTON, A. E. & BANSAL, R. (1993) The oligodendrocyte and its many cellular processes. *Trends Cell Biol,* 3, 191-7.
PIXLEY, S. K. (1992) CNS glial cells support in vitro survival, division, and differentiation of dissociated olfactory neuronal progenitor cells. *Neuron,* 8, 1191-204.
PIXLEY, S. K., DANGORIA, N. S., ODOMS, K. K. & HASTINGS, L. (1998) Effects of insulin-like growth factor 1 on olfactory neurogenesis in vivo and in vitro. *Ann N Y Acad Sci,* 855, 244-7.
POLIAK, S., GOLLAN, L., SALOMON, D., BERGLUND, E. O., OHARA, R., RANSCHT, B. & PELES, E. (2001) Localization of Caspr2 in myelinated nerves depends on axon-glia interactions and the generation of barriers along the axon. *J Neurosci,* 21, 7568-75.
POLIAK, S. & PELES, E. (2003) The local differentiation of myelinated axons at nodes of Ranvier. *Nat Rev Neurosci,* 4, 968-80.
POLIAK, S., SALOMON, D., ELHANANY, H., SABANAY, H., KIERNAN, B., PEVNY, L., STEWART, C. L., XU, X., CHIU, S. Y., SHRAGER, P., FURLEY, A. J. & PELES, E. (2003) Juxtaparanodal clustering of Shaker-like K+ channels in myelinated axons depends on Caspr2 and TAG-1. *J Cell Biol,* 162, 1149-60.
POLLOCK, G. S., FRANCESCHINI, I. A., GRAHAM, G., MARCHIONNI, M. A. & BARNETT, S. C. (1999) Neuregulin is a mitogen and survival factor for olfactory bulb ensheathing cells and an isoform is produced by astrocytes. *Eur J Neurosci,* 11, 769-80.
POPE-COLEMAN, A., TINKER, J. P. & SCHNEIDER, J. S. (2000) Effects of GM1 ganglioside treatment on pre- and postsynaptic dopaminergic markers in the striatum of parkinsonian monkeys. *Synapse,* 36, 120-8.
PORTER, J. T. & MCCARTHY, K. D. (1996) Hippocampal astrocytes in situ respond to glutamate released from synaptic terminals. *J Neurosci,* 16, 5073-81.
PREVITALI, S. C., DINA, G., NODARI, A., FASOLINI, M., WRABETZ, L., MAYER, U., FELTRI, M. L. & QUATTRINI, A. (2003a) Schwann cells synthesize alpha7beta1 integrin which is dispensable for peripheral nerve development and myelination. *Mol Cell Neurosci,* 23, 210-8.
PREVITALI, S. C., NODARI, A., TAVEGGIA, C., PARDINI, C., DINA, G., VILLA, A., WRABETZ, L., QUATTRINI, A. & FELTRI, M. L. (2003b) Expression of laminin receptors in schwann cell differentiation: evidence for distinct roles. *J Neurosci,* 23, 5520-30.
PRINGLE, N. P., MUDHAR, H. S., COLLARINI, E. J. & RICHARDSON, W. D. (1992) PDGF receptors in the rat CNS: during late neurogenesis, PDGF alpha-receptor expression appears to be restricted to glial cells of the oligodendrocyte lineage. *Development,* 115, 535-51.
PRINGLE, N. P. & RICHARDSON, W. D. (1993) A singularity of PDGF alpha-receptor expression in the dorsoventral axis of the neural tube may define the origin of the oligodendrocyte lineage. *Development,* 117, 525-33.

PROBSTMEIER, R., MICHELS, M., FRANZ, T., CHAN, B. M. & PESHEVA, P. (1999) Tenascin-R interferes with integrin-dependent oligodendrocyte precursor cell adhesion by a ganglioside-mediated signalling mechanism. *Eur J Neurosci*, 11, 2474-88.
PURPURA, D. P. & SUZUKI, K. (1976) Distortion of neuronal geometry and formation of aberrant synapses in neuronal storage disease. *Brain Res,* 116, 1-21.
QUARLES, R. H. (2007) Myelin-associated glycoprotein (MAG): past, present and beyond. *J Neurochem,* 100, 1431-48.
RAABE, T. D., CLIVE, D. R., NEUBERGER, T. J., WEN, D. & DEVRIES, G. H. (1996) Cultured neonatal Schwann cells contain and secrete neuregulins. *J Neurosci Res,* 46, 263-70.
RAABE, T. D., CLIVE, D. R., WEN, D. & DEVRIES, G. H. (1997) Neonatal oligodendrocytes contain and secrete neuregulins in vitro. *J Neurochem,* 69, 1859-63.
RABIN, S. J. & MOCCHETTI, I. (1995) GM1 ganglioside activates the high-affinity nerve growth factor receptor trkA. *J Neurochem,* 65, 347-54.
RAFF, M. C. (1989) Glial cell diversification in the rat optic nerve. *Science,* 243, 1450-5.
RAFF, M. C., ABNEY, E. R., COHEN, J., LINDSAY, R. & NOBLE, M. (1983a) Two types of astrocytes in cultures of developing rat white matter: differences in morphology, surface gangliosides, and growth characteristics. *J Neurosci,* 3, 1289-1300.
RAFF, M. C., ABNEY, E. R. & MILLER, R. H. (1984a) Two glial cell lineages diverge prenatally in rat optic nerve. *Dev Biol,* 106, 53-60.
RAFF, M. C., FIELDS, K. L., HAKOMORI, S. I., MIRSKY, R., PRUSS, R. M. & WINTER, J. (1979) Cell-type-specific markers for distinguishing and studying neurons and the major classes of glial cells in culture. *Brain Res,* 174, 283-308.
RAFF, M. C., HORNBY-SMITH, A. & BROCKES, J. P. (1978a) Cyclic AMP as a mitogenic signal for cultured rat Schwann cells. *Nature,* 273, 672-3.
RAFF, M. C., MILLER, R. H. & NOBLE, M. (1983b) A glial progenitor cell that develops in vitro into an astrocyte or an oligodendrocyte depending on culture medium. *Nature,* 303, 390-6.
RAFF, M. C., MIRSKY, R., FIELDS, K. L., LISAK, R. P., DORFMAN, S. H., SILBERBERG, D. H., GREGSON, N. A., LEIBOWITZ, S. & KENNEDY, M. C. (1978b) Galactocerebroside is a specific cell-surface antigenic marker for oligodendrocytes in culture. *Nature,* 274, 813-6.
RAFF, M. C., WILLIAMS, B. P. & MILLER, R. H. (1984b) The in vitro differentiation of a bipotential glial progenitor cell. *Embo J,* 3, 1857-64.
RAINE, C. S. (1984) On the association between perinodal astrocytic processes and the node of Ranvier in the C.N.S. *J Neurocytol,* 13, 21-7.
RAISMAN, G. (1985) Specialized neuroglial arrangement may explain the capacity of vomeronasal axons to reinnervate central neurons. *Neuroscience,* 14, 237-54.
RAITERI, M., VERSACE, P. & MARCHI, M. (1985) GM1 monosialoganglioside inner ester induces early recovery of striatal dopamine uptake in rats with unilateral nigrostriatal lesion. *Eur J Pharmacol,* 118, 347-50.
RAMER, M. S., DURAISINGAM, I., PRIESTLEY, J. V. & MCMAHON, S. B. (2001) Two-tiered inhibition of axon regeneration at the dorsal root entry zone. *J Neurosci,* 21, 2651-60.
RAMIREZ, J. J., FASS, B., KARPIAK, S. E. & STEWARD, O. (1987a) Ganglioside treatments reduce locomotor hyperactivity after bilateral lesions of the entorhinal cortex. *Neurosci Lett,* 75, 283-7.
RAMIREZ, J. J., FASS, B., KILFOIL, T., HENSCHEL, B., GRONES, W. & KARPIAK, S. E. (1987b) Ganglioside-induced enhancement of behavioral recovery after bilateral lesions of the entorhinal cortex. *Brain Res,* 414, 85-90.

RAMON-CUETO, A. & AVILA, J. (1998) Olfactory ensheathing glia: properties and function. *Brain Res Bull,* 46, 175-87.
RAMON-CUETO, A. & NIETO-SAMPEDRO, M. (1992) Glial cells from adult rat olfactory bulb: immunocytochemical properties of pure cultures of ensheathing cells. *Neuroscience,* 47, 213-20.
RAMON-CUETO, A., PLANT, G. W., AVILA, J. & BUNGE, M. B. (1998) Long-distance axonal regeneration in the transected adult rat spinal cord is promoted by olfactory ensheathing glia transplants. *J Neurosci,* 18, 3803-15.
RANSCHT, B., CLAPSHAW, P. A., PRICE, J., NOBLE, M. & SEIFERT, W. (1982) Development of oligodendrocytes and Schwann cells studied with a monoclonal antibody against galactocerebroside. *Proc Natl Acad Sci U S A,* 79, 2709-13.
RAPRAEGER, A. C., KRUFKA, A. & OLWIN, B. B. (1991) Requirement of heparan sulfate for bFGF-mediated fibroblast growth and myoblast differentiation. *Science,* 252, 1705-8.
RASBAND, M. N. (2004) It's "juxta" potassium channel! *J Neurosci Res,* 76, 749-57.
RASBAND, M. N., PELES, E., TRIMMER, J. S., LEVINSON, S. R., LUX, S. E. & SHRAGER, P. (1999a) Dependence of nodal sodium channel clustering on paranodal axoglial contact in the developing CNS. *J Neurosci,* 19, 7516-28.
RASBAND, M. N. & TRIMMER, J. S. (2001) Developmental clustering of ion channels at and near the node of Ranvier. *Dev Biol,* 236, 5-16.
RASBAND, M. N., TRIMMER, J. S., PELES, E., LEVINSON, S. R. & SHRAGER, P. (1999b) K+ channel distribution and clustering in developing and hypomyelinated axons of the optic nerve. *J Neurocytol,* 28, 319-31.
RAY, J. & GAGE, F. H. (2006) Differential properties of adult rat and mouse brain-derived neural stem/progenitor cells. *Mol Cell Neurosci,* 31, 560-73.
REBBAA, A., HURH, J., YAMAMOTO, H., KERSEY, D. S. & BREMER, E. G. (1996) Ganglioside GM3 inhibition of EGF receptor mediated signal transduction. *Glycobiology,* 6, 399-406.
REIER, P. J. & HOULE, J. D. (1988) The glial scar: its bearing on axonal elongation and transplantation approaches to CNS repair. *Adv Neurol,* 47, 87-138.
RELVAS, J. B., SETZU, A., BARON, W., BUTTERY, P. C., LAFLAMME, S. E., FRANKLIN, R. J. & FFRENCH-CONSTANT, C. (2001) Expression of dominant-negative and chimeric subunits reveals an essential role for beta1 integrin during myelination. *Curr Biol,* 11, 1039-43.
RESH, M. D. (1999) Fatty acylation of proteins: new insights into membrane targeting of myristoylated and palmitoylated proteins. *Biochim Biophys Acta,* 1451, 1-16.
REUSS, B. & VON BOHLEN UND HALBACH, O. (2003) Fibroblast growth factors and their receptors in the central nervous system. *Cell Tissue Res,* 313, 139-57.
REYNOLDS, R., CAREY, E. M. & HERSCHKOWITZ, N. (1989) Immunohistochemical localization of myelin basic protein and 2',3'-cyclic nucleotide 3'-phosphohydrolase in flattened membrane expansions produced by cultured oligodendrocytes. *Neuroscience,* 28, 181-8.
RIBONI, L., BASSI, R. & TETTAMANTI, G. (1994) Effect of brefeldin A on ganglioside metabolism in cultured neurons: implications for the intracellular traffic of gangliosides. *J Biochem (Tokyo),* 116, 140-6.
RICHARDSON, W. D., PRINGLE, N., MOSLEY, M. J., WESTERMARK, B. & DUBOIS-DALCQ, M. (1988) A role for platelet-derived growth factor in normal gliogenesis in the central nervous system. *Cell,* 53, 309-19.
RIDET, J. L., MALHOTRA, S. K., PRIVAT, A. & GAGE, F. H. (1997) Reactive astrocytes: cellular and molecular cues to biological function. *Trends Neurosci,* 20, 570-7.

RIETVELD, A., NEUTZ, S., SIMONS, K. & EATON, S. (1999) Association of sterol- and glycosylphosphatidylinositol-linked proteins with Drosophila raft lipid microdomains. *J Biol Chem,* 274, 12049-54.
RIOS, J. C., MELENDEZ-VASQUEZ, C. V., EINHEBER, S., LUSTIG, M., GRUMET, M., HEMPERLY, J., PELES, E. & SALZER, J. L. (2000) Contactin-associated protein (Caspr) and contactin form a complex that is targeted to the paranodal junctions during myelination. *J Neurosci,* 20, 8354-64.
RIOS, J. C., RUBIN, M., ST MARTIN, M., DOWNEY, R. T., EINHEBER, S., ROSENBLUTH, J., LEVINSON, S. R., BHAT, M. & SALZER, J. L. (2003) Paranodal interactions regulate expression of sodium channel subtypes and provide a diffusion barrier for the node of Ranvier. *J Neurosci,* 23, 7001-11.
ROCHEL, S. & MARGOLIS, F. L. (1980) The response of ornithine decarboxylase during neuronal degeneration and regeneration in olfactory epithelium. *J Neurochem,* 35, 850-60.
ROISEN, F. J., BARTFELD, H., NAGELE, R. & YORKE, G. (1981) Ganglioside stimulation of axonal sprouting in vitro. *Science,* 214, 577-8.
ROSATI, G. (2001) The prevalence of multiple sclerosis in the world: an update. *Neurol Sci*, 22, 117-39.
ROSKAMS, A. J., BETHEL, M. A., HURT, K. J. & RONNETT, G. V. (1996) Sequential expression of Trks A, B, and C in the regenerating olfactory neuroepithelium. *J Neurosci,* 16, 1294-307.
RUDGE, J. S., ALDERSON, R. F., PASNIKOWSKI, E., MCCLAIN, J., IP, N. Y. & LINDSAY, R. M. (1992) Expression of Ciliary Neurotrophic Factor and the Neurotrophins-Nerve Growth Factor, Brain-Derived Neurotrophic Factor and Neurotrophin 3-in Cultured Rat Hippocampal Astrocytes. *Eur J Neurosci,* 4, 459-471.
RUOSLAHTI, E. (1991) Integrins. *J Clin Invest,* 87, 1-5.
RUSNATI, M., TANGHETTI, E., URBINATI, C., TULIPANO, G., MARCHESINI, S., ZICHE, M. & PRESTA, M. (1999) Interaction of fibroblast growth factor-2 (FGF-2) with free gangliosides: biochemical characterization and biological consequences in endothelial cell cultures. *Mol Biol Cell,* 10, 313-27.
RUSNATI, M., URBINATI, C., TANGHETTI, E., DELL'ERA, P., LORTAT-JACOB, H. & PRESTA, M. (2002) Cell membrane GM1 ganglioside is a functional coreceptor for fibroblast growth factor 2. *Proc Natl Acad Sci U S A,* 99, 4367-72.
RYBAK, S., GINZBURG, I. & YAVIN, E. (1983) Gangliosides stimulate neurite outgrowth and induce tubulin mRNA accumulation in neural cells. *Biochem Biophys Res Commun,* 116, 974-80.
SAAD, B., CONSTAM, D. B., ORTMANN, R., MOOS, M., FONTANA, A. & SCHACHNER, M. (1991) Astrocyte-derived TGF-beta 2 and NGF differentially regulate neural recognition molecule expression by cultured astrocytes. *J Cell Biol,* 115, 473-84.
SABEL, B. A., DELMASTRO, R., DUNBAR, G. L. & STEIN, D. G. (1987) Reduction of anterograde degeneration in brain damaged rats by GM1-gangliosides. *Neurosci Lett,* 77, 360-6.
SABEL, B. A., DUNBAR, G. L. & STEIN, D. G. (1984a) Gangliosides minimize behavioral deficits and enhance structural repair after brain injury. *J Neurosci Res,* 12, 429-43.
SABEL, B. A., SLAVIN, M. D. & STEIN, D. G. (1984b) GM1 ganglioside treatment facilitates behavioral recovery from bilateral brain damage. *Science,* 225, 340-2.
SABEL, B. A. & STEIN, D. G. (1986) Pharmacological treatment of central nervous system injury. *Nature,* 323, 493.
SAHA, S., MOHANTY, K. C. & MALLICK, P. (2005) Gangliosides enhance migration of mouse B16-melanoma cells through artificial basement membrane alone or in presence of laminin or fibronectin. *Indian J Exp Biol,* 43, 1130-8.

SALEHI-ASHTIANI, K. & FARBMAN, A. I. (1996) Expression of neu and Neu differentiation factor in the olfactory mucosa of rat. *Int J Dev Neurosci,* 14, 801-11.
SALZER, J. L. (2002) Nodes of Ranvier come of age. *Trends Neurosci,* 25, 2-5.
SALZER, J. L. (2003) Polarized domains of myelinated axons. *Neuron,* 40, 297-318.
SALZER, J. L. & BUNGE, R. P. (1980) Studies of Schwann cell proliferation. I. An analysis in tissue culture of proliferation during development, Wallerian degeneration, and direct injury. *J Cell Biol,* 84, 739-52.
SALZER, J. L., BUNGE, R. P. & GLASER, L. (1980a) Studies of Schwann cell proliferation. III. Evidence for the surface localization of the neurite mitogen. *J Cell Biol,* 84, 767-78.
SALZER, J. L., WILLIAMS, A. K., GLASER, L. & BUNGE, R. P. (1980b) Studies of Schwann cell proliferation. II. Characterization of the stimulation and specificity of the response to a neurite membrane fraction. *J Cell Biol,* 84, 753-66.
SANCHEZ, I., HASSINGER, L., PASKEVICH, P. A., SHINE, H. D. & NIXON, R. A. (1996) Oligodendroglia regulate the regional expansion of axon caliber and local accumulation of neurofilaments during development independently of myelin formation. *J Neurosci,* 16, 5095-105.
SANDHOFF, K., ANDREAE, U. & JATZKEWITZ, H. (1968) Deficient hexozaminidase activity in an exceptional case of Tay-Sachs disease with additional storage of kidney globoside in visceral organs. *Life Sci,* 7, 283-8.
SANGO, K., YAMANAKA, S., HOFFMANN, A., OKUDA, Y., GRINBERG, A., WESTPHAL, H., MCDONALD, M. P., CRAWLEY, J. N., SANDHOFF, K., SUZUKI, K. & PROIA, R. L. (1995) Mouse models of Tay-Sachs and Sandhoff diseases differ in neurologic phenotype and ganglioside metabolism. *Nat Genet,* 11, 170-6.
SANTAFE, M. M., SABATE, M. M., GARCIA, N., ORTIZ, N., LANUZA, M. A. & TOMAS, J. (2005) Changes in the neuromuscular synapse induced by an antibody against gangliosides. *Ann Neurol,* 57, 396-407.
SANTIAGO, M. F., COSTA, M. R. & MENDEZ-OTERO, R. (2004) Immunoblockage of 9-O-acetyl GD3 ganglioside arrests the in vivo migration of cerebellar granule neurons. *J Neurosci,* 24, 474-8.
SATOH, J. & KIM, S. U. (1995) Ganglioside markers GD3, GD2, and A2B5 in fetal human neurons and glial cells in culture. *Dev Neurosci,* 17, 137-48.
SATOH, J. I., TAI, T. & KIM, S. U. (1996) Differential expression of gangliosides and galactolipids in fetal human oligodendrocytes and astrocytes in culture. *Brain Res Dev Brain Res,* 93, 172-81.
SBASCHNIG-AGLER, M., DREYFUS, H., NORTON, W. T., SENSENBRENNER, M., FAROOQ, M., BYRNE, M. C. & LEDEEN, R. W. (1988) Gangliosides of cultured astroglia. *Brain Res,* 461, 98-106.
SCHACHNER, M. & BARTSCH, U. (2000) Multiple functions of the myelin-associated glycoprotein MAG (siglec-4a) in formation and maintenance of myelin. *Glia,* 29, 154-65.
SCHACHNER, M., HEDLEY-WHYTE, E. T., HSU, D. W., SCHOONMAKER, G. & BIGNAMI, A. (1977) Ultrastructural localization of glial fibrillary acidic protein in mouse cerebellum by immunoperoxidase labeling. *J Cell Biol,* 75, 67-73.
SCHAEFFER, H. J. & WEBER, M. J. (1999) Mitogen-activated protein kinases: specific messages from ubiquitous messengers. *Mol Cell Biol,* 19, 2435-44.
SCHAFER, D. P., BANSAL, R., HEDSTROM, K. L., PFEIFFER, S. E. & RASBAND, M. N. (2004) Does paranode formation and maintenance require partitioning of neurofascin 155 into lipid rafts? *J Neurosci,* 24, 3176-85.
SCHECHTER, R., WHITMIRE, J., BEJU, D., JACKSON, K. W., HARLOW, R. & GAVIN, J. R., 3RD (1995) An immunohistochemical and in situ hybridization study of

insulin-like growth factor I within fetal neuron cell cultures. *Brain Res,* 670, 1-13.
SCHECHTER, R., WHITMIRE, J., WHEET, G. S., BEJU, D., JACKSON, K. W., HARLOW, R. & GAVIN, J. R., 3RD (1994) Immunohistochemical and in situ hybridization study of an insulin-like substance in fetal neuron cell cultures. *Brain Res,* 636, 9-27.
SCHEIFFELE, P., ROTH, M. G. & SIMONS, K. (1997) Interaction of influenza virus haemagglutinin with sphingolipid-cholesterol membrane domains via its transmembrane domain. *Embo J,* 16, 5501-8.
SCHENGRUND, C. L. (1990) The role(s) of gangliosides in neural differentiation and repair: a perspective. *Brain Res Bull,* 24, 131-41.
SCHLESSINGER, J., PLOTNIKOV, A. N., IBRAHIMI, O. A., ELISEENKOVA, A. V., YEH, B. K., YAYON, A., LINHARDT, R. J. & MOHAMMADI, M. (2000) Crystal structure of a ternary FGF-FGFR-heparin complex reveals a dual role for heparin in FGFR binding and dimerization. *Mol Cell,* 6, 743-50.
SCHNAAR, R. L., LONGO, P., YANG, L. J. & TAI, T. (1996) Distinctive ganglioside patterns revealed by anti-ganglioside antibody binding to differentiating CG-4 oligodendrocytes. *Glycobiology,* 6, 257-63.
SCHNEIDER, J. S. (1998) GM1 ganglioside in the treatment of Parkinson's disease. *Ann N Y Acad Sci,* 845, 363-73.
SCHNEIDER, J. S., POPE, A., SIMPSON, K., TAGGART, J., SMITH, M. G. & DISTEFANO, L. (1992) Recovery from experimental parkinsonism in primates with GM1 ganglioside treatment. *Science,* 256, 843-6.
SCHNEIDER, J. S., ROELTGEN, D. P., MANCALL, E. L., CHAPAS-CRILLY, J., ROTHBLAT, D. S. & TATARIAN, G. T. (1998) Parkinson's disease: improved function with GM1 ganglioside treatment in a randomized placebo-controlled study. *Neurology,* 50, 1630-6.
SCHNITZER, J. & SCHACHNER, M. (1982) Cell type specificity of a neural cell surface antigen recognized by the monoclonal antibody A2B5. *Cell Tissue Res,* 224, 625-36.
SCHNITZER, J. E., MCINTOSH, D. P., DVORAK, A. M., LIU, J. & OH, P. (1995) Separation of caveolae from associated microdomains of GPI-anchored proteins. *Science,* 269, 1435-9.
SCHOUSBOE, A., WESTERGAARD, N., SONNEWALD, U., PETERSEN, S. B., YU, A. C. & HERTZ, L. (1992) Regulatory role of astrocytes for neuronal biosynthesis and homeostasis of glutamate and GABA. *Prog Brain Res,* 94, 199-211.
SCHROEDER, R., LONDON, E. & BROWN, D. (1994) Interactions between saturated acyl chains confer detergent resistance on lipids and glycosylphosphatidylinositol (GPI)-anchored proteins: GPI-anchored proteins in liposomes and cells show similar behavior. *Proc Natl Acad Sci U S A,* 91, 12130-4.
SCHWARTZ LEVEY, M., CHIKARAISHI, D. M. & KAUER, J. S. (1991) Characterization of potential precursor populations in the mouse olfactory epithelium using immunocytochemistry and autoradiography. *J Neurosci,* 11, 3556-64.
SCHWARZ, A. & FUTERMAN, A. H. (1997) Determination of the localization of gangliosides using anti-ganglioside antibodies: comparison of fixation methods. *J Histochem Cytochem,* 45, 611-8.
SCHWOB, J. E. (2002) Neural regeneration and the peripheral olfactory system. *Anat Rec,* 269, 33-49.
SCHWOB, J. E., HUARD, J. M., LUSKIN, M. B. & YOUNGENTOB, S. L. (1994a) Retroviral lineage studies of the rat olfactory epithelium. *Chem Senses,* 19, 671-82.
SCHWOB, J. E. & MOZELL, M. M. (1999) *Olfaction. In Elsevier's Encyclopaedia of Neuroscience, 2nd Edition*

SCHWOB, J. E., SZUMOWSKI, K. E. & STASKY, A. A. (1992) Olfactory sensory neurons are trophically dependent on the olfactory bulb for their prolonged survival. *J Neurosci,* 12, 3896-919.
SCHWOB, J. E., YOUNGENTOB, S. L. & MEIRI, K. F. (1994b) On the formation of neuromata in the primary olfactory projection. *J Comp Neurol,* 340, 361-80.
SCHWOB, J. E., YOUNGENTOB, S. L. & MEZZA, R. C. (1995) Reconstitution of the rat olfactory epithelium after methyl bromide-induced lesion. *J Comp Neurol,* 359, 15-37.
SCHWOB, J. E., YOUNGENTOB, S. L., RING, G., IWEMA, C. L. & MEZZA, R. C. (1999) Reinnervation of the rat olfactory bulb after methyl bromide-induced lesion: timing and extent of reinnervation. *J Comp Neurol,* 412, 439-57.
SHEIKH, K. A., DEERINCK, T. J., ELLISMAN, M. H. & GRIFFIN, J. W. (1999a) The distribution of ganglioside-like moieties in peripheral nerves. *Brain,* 122 (Pt 3), 449-60.
SHEIKH, K. A., SUN, J., LIU, Y., KAWAI, H., CRAWFORD, T. O., PROIA, R. L., GRIFFIN, J. W. & SCHNAAR, R. L. (1999b) Mice lacking complex gangliosides develop Wallerian degeneration and myelination defects. *Proc Natl Acad Sci U S A,* 96, 7532-7.
SHERMAN, D. L. & BROPHY, P. J. (2005) Mechanisms of axon ensheathment and myelin growth. *Nat Rev Neurosci,* 6, 683-90.
SHERMAN, D. L., TAIT, S., MELROSE, S., JOHNSON, R., ZONTA, B., COURT, F. A., MACKLIN, W. B., MEEK, S., SMITH, A. J., COTTRELL, D. F. & BROPHY, P. J. (2005) Neurofascins are required to establish axonal domains for saltatory conduction. *Neuron,* 48, 737-42.
SHI, J., MARINOVICH, A. & BARRES, B. A. (1998) Purification and characterization of adult oligodendrocyte precursor cells from the rat optic nerve. *J Neurosci,* 18, 4627-36.
SHINODA, H., MARINI, A. M., COSI, C. & SCHWARTZ, J. P. (1989) Brain region and gene specificity of neuropeptide gene expression in cultured astrocytes. *Science,* 245, 415-7.
SHOU, J., MURRAY, R. C., RIM, P. C. & CALOF, A. L. (2000) Opposing effects of bone morphogenetic proteins on neuron production and survival in the olfactory receptor neuron lineage. *Development,* 127, 5403-13.
SHOU, J., RIM, P. C. & CALOF, A. L. (1999) BMPs inhibit neurogenesis by a mechanism involving degradation of a transcription factor. *Nat Neurosci,* 2, 339-45.
SIMON, B. M., MALISAN, F., TESTI, R., NICOTERA, P. & LEIST, M. (2002) Disialoganglioside GD3 is released by microglia and induces oligodendrocyte apoptosis. *Cell Death Differ,* 9, 758-67.
SIMONS, K. & IKONEN, E. (1997) Functional rafts in cell membranes. *Nature,* 387, 569-72.
SIMONS, K. & TOOMRE, D. (2000) Lipid rafts and signal transduction. *Nat Rev Mol Cell Biol,* 1, 31-9.
SIMPSON, M. A., CROSS, H., PROUKAKIS, C., PRIESTMAN, D. A., NEVILLE, D. C., REINKENSMEIER, G., WANG, H., WIZNITZER, M., GURTZ, K., VERGENELAKI, A., PRYDE, A., PATTON, M. A., DWEK, R. A., BUTTERS, T. D., PLATT, F. M. & CROSBY, A. H. (2004) Infantile-onset symptomatic epilepsy syndrome caused by a homozygous loss-of-function mutation of GM3 synthase. *Nat Genet*, 36, 1225-9.
SIMS, T. J., WAXMAN, S. G., BLACK, J. A. & GILMORE, S. A. (1985) Perinodal astrocytic processes at nodes of Ranvier in developing normal and glial cell deficient rat spinal cord. *Brain Res,* 337, 321-31.
SKAPER, S. D., FACCI, L., RUDGE, J., KATOH-SEMBA, R., MANTHORPE, M. & VARON, S. (1986) Morphological modulation of cultured rat brain astroglial cells: antagonism by ganglioside GM1. *Brain Res,* 390, 21-31.

SKAPER, S. D. & LEON, A. (1992) Monosialogangliosides, neuroprotection, and neuronal repair processes. *J Neurotrauma,* 9 Suppl 2, S507-16.
SKOFF, R. P. (1990) Gliogenesis in rat optic nerve: astrocytes are generated in a single wave before oligodendrocytes. *Dev Biol,* 139, 149-68.
SKOFF, R. P. & KNAPP, P. E. (1991) Division of astroblasts and oligodendroblasts in postnatal rodent brain: evidence for separate astrocyte and oligodendrocyte lineages. *Glia,* 4, 165-74.
SLOMIANY, B. L., LIU, J., YAO, P., PIOTROWSKI, J., GRABSKA, M. & SLOMIANY, A. (1992) Effect of GM1-ganglioside on gastric mucosal epidermal growth factor and platelet-derived growth factor receptor expression. *Biochem Int,* 27, 97-104.
SMALL, R. K., RIDDLE, P. & NOBLE, M. (1987) Evidence for migration of oligodendrocyte--type-2 astrocyte progenitor cells into the developing rat optic nerve. *Nature,* 328, 155-7.
SMIT, A. B., SYED, N. I., SCHAAP, D., VAN MINNEN, J., KLUMPERMAN, J., KITS, K. S., LODDER, H., VAN DER SCHORS, R. C., VAN ELK, R., SORGEDRAGER, B., BREJC, K., SIXMA, T. K. & GERAERTS, W. P. (2001) A glia-derived acetylcholine-binding protein that modulates synaptic transmission. *Nature,* 411, 261-8.
SMITH, C. G. (1938a) Changes in the olfactory mucosa and the olfactory nerves following intranasal treatment with one per cent zinc sulphate. *Can. Med. Assoc. J.,* 39, 138-140.
SMITH, C. G. (1938b) Pathologic change in olfactory nasal mucosa of albino rats with “stunted” olfactory bulbs. *Arch. Otolaryngol.,* 31, 131-143.
SOBUE, G., TAKI, T., YASUDA, T. & MITSUMA, T. (1988) Gangliosides modulate Schwann cell proliferation and morphology. *Brain Res,* 474, 287-95.
SOMJEN, G. G. (1988) Nervenkitt: notes on the history of the concept of neuroglia. *Glia,* 1, 2-9.
SOMMER, I. & SCHACHNER, M. (1981) Monoclonal antibodies (O1 to O4) to oligodendrocyte cell surfaces: an immunocytological study in the central nervous system. *Dev Biol,* 83, 311-27.
SON, Y. J., TRACHTENBERG, J. T. & THOMPSON, W. J. (1996) Schwann cells induce and guide sprouting and reinnervation of neuromuscular junctions. *Trends Neurosci,* 19, 280-5.
SORENSEN, A., MOFFAT, K., THOMSON, C. & BARNETT, S.C. (2008) Astrocytes, but not olfactory ensheathing cells or Schwann cells, promote myelination of CNS axons in vitro. *Glia,* 56, 750-63.
SORICE, M., PAROLINI, I., SANSOLINI, T., GAROFALO, T., DOLO, V., SARGIACOMO, M., TAI, T., PESCHLE, C., TORRISI, M. R. & PAVAN, A. (1997) Evidence for the existence of ganglioside-enriched plasma membrane domains in human peripheral lymphocytes. *J Lipid Res,* 38, 969-80.
SOUTH, S. A., DEIBLER, G. E., TZENG, S. F., BADACHE, A., KIRCHNER, M. G., MUJA, N. & DE VRIES, G. H. (2000) Myelin basic protein (MBP) and MBP peptides are mitogens for cultured astrocytes. *Glia,* 29, 81-90.
SPERO, D. A. & ROISEN, F. J. (1984) Ganglioside-mediated enhancement of the cytoskeletal organization and activity in neuro-2a neuroblastoma cells. *Brain Res,* 315, 37-48.
SPIEGEL, I. & PELES, E. (2002) Cellular junctions of myelinated nerves (Review). *Mol Membr Biol,* 19, 95-101.
STEWART, H. J., BRADKE, F., TABERNERO, A., MORRELL, D., JESSEN, K. R. & MIRSKY, R. (1996) Regulation of rat Schwann cell Po expression and DNA synthesis by insulin-like growth factors in vitro. *Eur J Neurosci,* 8, 553-64.
STEWART, H. J., ECCLESTON, P. A., JESSEN, K. R. & MIRSKY, R. (1991) Mitogenic response and phenotype of short- and long-term cultured Schwann cells. Relationship to intracellular cAMP levels. *Ann N Y Acad Sci,* 633, 537-9.

STEWART, H. J., TURNER, D., JESSEN, K. R. & MIRSKY, R. (1997) Expression and regulation of alpha1beta1 integrin in Schwann cells. *J Neurobiol,* 33, 914-28.
STOCKLI, K. A., LOTTSPEICH, F., SENDTNER, M., MASIAKOWSKI, P., CARROLL, P., GOTZ, R., LINDHOLM, D. & THOENEN, H. (1989) Molecular cloning, expression and regional distribution of rat ciliary neurotrophic factor. *Nature,* 342, 920-3.
STROMBERG, N., NYHOLM, P. G., PASCHER, I. & NORMARK, S. (1991) Saccharide orientation at the cell surface affects glycolipid receptor function. *Proc Natl Acad Sci U S A,* 88, 9340-4.
STULTS, C. L., SWEELEY, C. C. & MACHER, B. A. (1989) Glycosphingolipids: structure, biological source, and properties. *Methods Enzymol,* 179, 167-214.
SUCHY, S. F., YAMAMOTO, M., BARBERO, L. & SCHWARTING, G. A. (1988) A monoclonal antibody, WCC4, recognizes a developmentally regulated ganglioside containing alpha-galactose and alpha-fucose present in the rat nervous system. *Brain Res,* 440, 25-34.
SUN, J., SHAPER, N. L., ITONORI, S., HEFFER-LAUC, M., SHEIKH, K. A. & SCHNAAR, R. L. (2004) Myelin-associated glycoprotein (Siglec-4) expression is progressively and selectively decreased in the brains of mice lacking complex gangliosides. *Glycobiology,* 14, 851-7.
SUSUKI, K., BABA, H., TOHYAMA, K., KANAI, K., KUWABARA, S., HIRATA, K., FURUKAWA, K., FURUKAWA, K., RASBAND, M. N. & YUKI, N. (2007a) Gangliosides contribute to stability of paranodal junctions and ion channel clusters in myelinated nerve fibers. *Glia,* 55, 746-57.
SUSUKI, K., RASBAND, M. N., TOHYAMA, K., KOIBUCHI, K., OKAMOTO, S., FUNAKOSHI, K., HIRATA, K., BABA, H. & YUKI, N. (2007b) Anti-GM1 antibodies cause complement-mediated disruption of sodium channel clusters in peripheral motor nerve fibers. *J Neurosci,* 27, 3956-67.
SUZUKI, Y. (1998) Cell death, phagocytosis, and neurogenesis in mouse olfactory epithelium and vomeronasal organ after colchicine treatment. *Ann N Y Acad Sci,* 855, 252-4.
SVENDSEN, C. N., SKEPPER, J., ROSSER, A. E., TER BORG, M. G., TYRES, P. & RYKEN, T. (1997) Restricted growth potential of rat neural precursors as compared to mouse. *Brain Res Dev Brain Res,* 99, 253-8.
SVENNERHOLM, L. (1994) Designation and schematic structure of gangliosides and allied glycosphingolipids. *Prog Brain Res,* 101, XI-XIV.
SYKOVA, E., SVOBODA, J., SIMONOVA, Z. & JENDELOVA, P. (1992) Role of astrocytes in ionic and volume homeostasis in spinal cord during development and injury. *Prog Brain Res,* 94, 47-56.
TAIT, S., GUNN-MOORE, F., COLLINSON, J. M., HUANG, J., LUBETZKI, C., PEDRAZA, L., SHERMAN, D. L., COLMAN, D. R. & BROPHY, P. J. (2000) An oligodendrocyte cell adhesion molecule at the site of assembly of the paranodal axo-glial junction. *J Cell Biol,* 150, 657-66.
TAKAMIYA, K., YAMAMOTO, A., FURUKAWA, K., YAMASHIRO, S., SHIN, M., OKADA, M., FUKUMOTO, S., HARAGUCHI, M., TAKEDA, N., FUJIMURA, K., SAKAE, M., KISHIKAWA, M., SHIKU, H., FURUKAWA, K. & AIZAWA, S. (1996) Mice with disrupted GM2/GD2 synthase gene lack complex gangliosides but exhibit only subtle defects in their nervous system. *Proc Natl Acad Sci U S A,* 93, 10662-7.
TAKAMIYA, K., YAMAMOTO, A., YAMASHIRO, S., FURUKAWA, K., HARAGUCHI, M., OKADA, M., IKEDA, T., SHIKU, H. & FURUKAWA, K. (1995) T cell receptor-mediated stimulation of mouse thymocytes induces up-regulation of the GM2/GD2 synthase gene. *FEBS Lett,* 358, 79-83.
TATSUMI, K., SAITO, M., LIN, B., IWAMORI, M., ICHISEKI, H., SHIMOZAWA, N., KAMOSHITA, S., IGARASHI, T. & SAKAKIHARA, Y. (2001) Enhanced expression of a-series gangliosides in fibroblasts of patients with peroxisome biogenesis disorders. *Biochim Biophys Acta,* 1535, 285-93.

TAWIL, N., WILSON, P. & CARBONETTO, S. (1993) Integrins in point contacts mediate cell spreading: factors that regulate integrin accumulation in point contacts vs. focal contacts. *J Cell Biol,* 120, 261-71.
TAWIL, N. J., WILSON, P. & CARBONETTO, S. (1994) Expression and distribution of functional integrins in rat CNS glia. *J Neurosci Res,* 39, 436-47.
TAYLOR, C. M., COETZEE, T. & PFEIFFER, S. E. (2002) Detergent-insoluble glycosphingolipid/cholesterol microdomains of the myelin membrane. *J Neurochem,* 81, 993-1004.
TETTAMANTI, G. & RIBONI, L. (1994) Gangliosides turnover and neural cells function: a new perspective. *Prog Brain Res,* 101, 77-100.
THANT, A. A., NAWA, A., KIKKAWA, F., ICHIGOTANI, Y., ZHANG, Y., SEIN, T. T., AMIN, A. R. & HAMAGUCHI, M. (2000) Fibronectin activates matrix metalloproteinase-9 secretion via the MEK1-MAPK and the PI3K-Akt pathways in ovarian cancer cells. *Clin Exp Metastasis,* 18, 423-8.
THISSE, B. & THISSE, C. (2005) Functions and regulations of fibroblast growth factor signaling during embryonic development. *Dev Biol,* 287, 390-402.
THOMSON, C. E., ANDERSON, T. J., McCULLOCH, M. C., DICKINSON, P., VOUYIOUKLIS, D. A. & GRIFFITHS, I. R. (1999) The early phenotype associated with the jimpy mutation of the proteolipid protein gene. *J Neurocytol,* 28, 207-21.
THOMSON, C. E., HUNTER, A. M., GRIFFITHS, I. R., EDGAR, J. M. & MCCULLOCH, M. C. (2006) Murine spinal cord explants: a model for evaluating axonal growth and myelination in vitro. *J Neurosci Res,* 84, 1703-15.
TIMSIT, S., MARTINEZ, S., ALLINQUANT, B., PEYRON, F., PUELLES, L. & ZALC, B. (1995) Oligodendrocytes originate in a restricted zone of the embryonic ventral neural tube defined by DM-20 mRNA expression. *J Neurosci,* 15, 1012-24.
TOFFANO, G., SAVOINI, G., ALDINIO, C., VALENTI, G., DAL TOSO, R., LEON, A., CALZA, L., ZINI, I., AGNATI, L. F. & FUXE, K. (1984a) Effects of gangliosides on the functional recovery of damaged brain. *Adv Exp Med Biol,* 174, 475-88.
TOFFANO, G., SAVOINI, G., MORONI, F., LOMBARDI, G., CALZA, L. & AGNATI, L. F. (1983) GM1 ganglioside stimulates the regeneration of dopaminergic neurons in the central nervous system. *Brain Res,* 261, 163-6.
TOFFANO, G., SAVOINI, G. E., MORONI, F., LOMBARDI, G., CALZA, L. & AGNATI, L. F. (1984b) Chronic GM1 ganglioside treatment reduces dopamine cell body degeneration in the substantia nigra after unilateral hemitransection in rat. *Brain Res,* 296, 233-9.
TOLEDO, M. S., SUZUKI, E., HANDA, K. & HAKOMORI, S. (2005) Effect of ganglioside and tetraspanins in microdomains on interaction of integrins with fibroblast growth factor receptor. *J Biol Chem,* 280, 16227-34.
TORIGOE, K., TANAKA, H. F., TAKAHASHI, A., AWAYA, A. & HASHIMOTO, K. (1996) Basic behavior of migratory Schwann cells in peripheral nerve regeneration. *Exp Neurol,* 137, 301-8.
TRACHTENBERG, J. T. & THOMPSON, W. J. (1996) Schwann cell apoptosis at developing neuromuscular junctions is regulated by glial growth factor. *Nature,* 379, 174-7.
TRAKA, M., GOUTEBROZE, L., DENISENKO, N., BESSA, M., NIFLI, A., HAVAKI, S., IWAKURA, Y., FUKAMAUCHI, F., WATANABE, K., SOLIVEN, B., GIRAULT, J. A. & KARAGOGEOS, D. (2003) Association of TAG-1 with Caspr2 is essential for the molecular organization of juxtaparanodal regions of myelinated fibers. *J Cell Biol,* 162, 1161-72.
TRAPP, B. D., NISHIYAMA, A., CHENG, D. & MACKLIN, W. (1997) Differentiation and death of premyelinating oligodendrocytes in developing rodent brain. *J Cell Biol,* 137, 459-68.

TRINCHERA, M., PIROVANO, B. & GHIDONI, R. (1990) Sub-Golgi distribution in rat liver of CMP-NeuAc GM3- and CMP-NeuAc:GT1b alpha 2----8sialyltransferases and comparison with the distribution of the other glycosyltransferase activities involved in ganglioside biosynthesis. *J Biol Chem,* 265, 18242-7.
TURK, M. A., HENK, W. G. & FLORY, W. (1987) 3-Methylindole-induced nasal mucosal damage in mice. *Vet Pathol,* 24, 400-3.
TURNER, C. P. & PEREZ-POLO, J. R. (1993) Expression of p75NGFR in the olfactory system following peripheral deafferentation. *Neuroreport,* 4, 1023-6.
TZENG, S. F., DEIBLER, G. E. & DEVRIES, G. H. (1999) Myelin basic protein and myelin basic protein peptides induce the proliferation of Schwann cells via ganglioside GM1 and the FGF receptor. *Neurochem Res,* 24, 255-60.
TZENG, S. F., DEIBLER, G. E., NEUBERGER, T. J. & DEVRIES, G. H. (1995) Two mitogenic regions of myelin basic protein interact with different receptors to induce Schwann cell proliferation in a cAMP dependent process. *J Neurosci Res,* 42, 758-67.
USUKI, S., THOMPSON, S. A., RIVNER, M. H., TAGUCHI, K., SHIBATA, K., ARIGA, T. & YU, R. K. (2006) Molecular mimicry: sensitization of Lewis rats with Campylobacter jejuni lipopolysaccharides induces formation of antibody toward GD3 ganglioside. *J Neurosci Res,* 83, 274-84.
VABNICK, I., NOVAKOVIC, S. D., LEVINSON, S. R., SCHACHNER, M. & SHRAGER, P. (1996) The clustering of axonal sodium channels during development of the peripheral nervous system. *J Neurosci,* 16, 4914-22.
VABNICK, I. & SHRAGER, P. (1998) Ion channel redistribution and function during development of the myelinated axon. *J Neurobiol,* 37, 80-96.
VABNICK, I., TRIMMER, J. S., SCHWARZ, T. L., LEVINSON, S. R., RISAL, D. & SHRAGER, P. (1999) Dynamic potassium channel distributions during axonal development prevent aberrant firing patterns. *J Neurosci,* 19, 747-58.
VALDES-GONZALEZ, T., MORITA, Y., SUZUKI, K. & IDO, T. (2001) Excitotoxicity induces changes in rat brain gangliosides. *Neurosci Res,* 39, 197-203.
VAN BROCKLYN, J., BREMER, E. G. & YATES, A. J. (1993) Gangliosides inhibit platelet-derived growth factor-stimulated receptor dimerization in human glioma U-1242MG and Swiss 3T3 cells. *J Neurochem,* 61, 371-4.
VAN HEYNINGEN, P., CALVER, A. R. & RICHARDSON, W. D. (2001) Control of progenitor cell number by mitogen supply and demand. *Curr Biol,* 11, 232-41.
VAN HEYNINGEN, W. E. (1963) The fixation of tetanus toxin, strychnine, serotonin and other substances by ganglioside. *J Gen Microbiol,* 31, 375-87.
VARTANIAN, T., FISCHBACH, G. & MILLER, R. (1999) Failure of spinal cord oligodendrocyte development in mice lacking neuregulin. *Proc Natl Acad Sci U S A,* 96, 731-5.
VAUGHN, J. E. & PETERS, A. (1967) Electron microscopy of the early postnatal development of fibrous astrocytes. *Am J Anat,* 121, 131-52.
VERHAAGEN, J., OESTREICHER, A. B., GISPEN, W. H. & MARGOLIS, F. L. (1989) The expression of the growth associated protein B50/GAP43 in the olfactory system of neonatal and adult rats. *J Neurosci,* 9, 683-91.
VERHAAGEN, J., OESTREICHER, A. B., GRILLO, M., KHEW-GOODALL, Y. S., GISPEN, W. H. & MARGOLIS, F. L. (1990) Neuroplasticity in the olfactory system: differential effects of central and peripheral lesions of the primary olfactory pathway on the expression of B-50/GAP43 and the olfactory marker protein. *J Neurosci Res,* 26, 31-44.
VINSON, M., STRIJBOS, P. J., ROWLES, A., FACCI, L., MOORE, S. E., SIMMONS, D. L. & WALSH, F. S. (2001) Myelin-associated glycoprotein interacts with ganglioside GT1b. A mechanism for neurite outgrowth inhibition. *J Biol Chem,* 276, 20280-5.

VYAS, A. A., PATEL, H. V., FROMHOLT, S. E., HEFFER-LAUC, M., VYAS, K. A., DANG, J., SCHACHNER, M. & SCHNAAR, R. L. (2002) Gangliosides are functional nerve cell ligands for myelin-associated glycoprotein (MAG), an inhibitor of nerve regeneration. *Proc Natl Acad Sci U S A,* 99, 8412-7.
VYAS, A. A. & SCHNAAR, R. L. (2001) Brain gangliosides: functional ligands for myelin stability and the control of nerve regeneration. *Biochimie,* 83, 677-82.
WAGNER, S., TAGAYA, M., KOZIOL, J. A., QUARANTA, V. & DEL ZOPPO, G. J. (1997) Rapid disruption of an astrocyte interaction with the extracellular matrix mediated by integrin alpha 6 beta 4 during focal cerebral ischemia/reperfusion. *Stroke,* 28, 858-65.
WALKER, M. D. (1991) Acute spinal-cord injury. *N Engl J Med,* 324, 1885-7.
WALLER, A. (1850) Experiments on the section of the glossopharyngeal and hypoglossal nerves of the frog, and observations of the alterations produced thereby in the structure of their primitive fibers. *Philosophical Transactions of the Royal Society of London,* 140, 423-429.
WANG, H., KUNKEL, D. D., MARTIN, T. M., SCHWARTZKROIN, P. A. & TEMPEL, B. L. (1993) Heteromultimeric K+ channels in terminal and juxtaparanodal regions of neurons. *Nature,* 365, 75-9.
WANG, M. S., CHEN, Z. W., ZHANG, G. J. & CHEN, Z. R. (1995) Topical GM1 ganglioside to promote crushed rat sciatic nerve regeneration. *Microsurgery,* 16, 542-6.
WANG, X., SUN, P., AL-QAMARI, A., TAI, T., KAWASHIMA, I. & PALLER, A. S. (2001a) Carbohydrate-carbohydrate binding of ganglioside to integrin alpha(5) modulates alpha(5)beta(1) function. *J Biol Chem,* 276, 8436-44.
WANG, X. Q., SUN, P., O'GORMAN, M., TAI, T. & PALLER, A. S. (2001b) Epidermal growth factor receptor glycosylation is required for ganglioside GM3 binding and GM3-mediated suppression [correction of suppresion] of activation. *Glycobiology,* 11, 515-22.
WANG, X. Q., SUN, P. & PALLER, A. S. (2003) Ganglioside GM3 inhibits matrix metalloproteinase-9 activation and disrupts its association with integrin. *J Biol Chem,* 278, 25591-9.
WANG, X. Q., SUN, P. & PALLER, A. S. (2005) Gangliosides inhibit urokinase-type plasminogen activator (uPA)-dependent squamous carcinoma cell migration by preventing uPA receptor/alphabeta integrin/epidermal growth factor receptor interactions. *J Invest Dermatol,* 124, 839-48.
WANG, Z., COLOGNATO, H. & FFRENCH-CONSTANT, C. (2007) Contrasting effects of mitogenic growth factors on myelination in neuron-oligodendrocyte co-cultures. *Glia,* 55, 537-45.
WARF, B. C., FOK-SEANG, J. & MILLER, R. H. (1991) Evidence for the ventral origin of oligodendrocyte precursors in the rat spinal cord. *J Neurosci,* 11, 2477-88.
WARRINGTON, A. E., BARBARESE, E. & PFEIFFER, S. E. (1993) Differential myelinogenic capacity of specific developmental stages of the oligodendrocyte lineage upon transplantation into hypomyelinating hosts. *J Neurosci Res,* 34, 1-13.
WATABE, K., IDA, H., UEHARA, K., OYANAGI, K., SAKAMOTO, T., TANAKA, J., GARVER, W. S., MIYAWAKI, S., OHNO, K. & ETO, Y. (2001) Establishment and characterization of immortalized Schwann cells from murine model of Niemann-Pick disease type C (spm/spm). *J Peripher Nerv Syst,* 6, 85-94.
WAXMAN, S. G. (1986) The astrocyte as a component of the node of Ranvier *Trends in Neurosciences* 9, 250-253.
WAXMAN, S. G. & BLACK, J. A. (1984) Freeze-fracture ultrastructure of the perinodal astrocyte and associated glial junctions. *Brain Res,* 308, 77-87.

WAXMAN, S. G. & RITCHIE, J. M. (1993) Molecular dissection of the myelinated axon. *Ann Neurol,* 33, 121-36.
WAXMAN, S. G. & SIMS, T. J. (1984) Specificity in central myelination: evidence for local regulation of myelin thickness. *Brain Res,* 292, 179-85.
WAXMAN, S. G. & SWADLOW, H. A. (1976) Ultrastructure of visual callosal axons in the rabbit. *Exp Neurol,* 53, 115-27.
WEILER, E. & FARBMAN, A. I. (1998) Supporting cell proliferation in the olfactory epithelium decreases postnatally. *Glia,* 22, 315-28.
WEIS, F. M. & DAVIS, R. J. (1990) Regulation of epidermal growth factor receptor signal transduction. Role of gangliosides. *J Biol Chem,* 265, 12059-66.
WEWETZER, K., GROTHE, C. & CLAUS, P. (2001) In vitro expression and regulation of ciliary neurotrophic factor and its alpha receptor subunit in neonatal rat olfactory ensheathing cells. *Neurosci Lett,* 306, 165-8.
WHITLEY, M., TRELOAR, H., DE ARCANGELIS, A., GEORGES LABOUESSE, E. & GREER, C. A. (2005) The alpha6 integrin subunit in the developing mouse olfactory bulb. *J Neurocytol,* 34, 81-96.
WILKIN, G. P., MARRIOTT, D. R. & CHOLEWINSKI, A. J. (1990) Astrocyte heterogeneity. *Trends Neurosci,* 13, 43-6.
WILLIAMS, R. & RUSH, R. A. (1988) Electron microscopic immunocytochemical localization of nerve growth factor in developing mouse olfactory neurons. *Brain Res,* 463, 21-7.
WILLIAMS, S. K., FRANKLIN, R. J. & BARNETT, S. C. (2004) Response of olfactory ensheathing cells to the degeneration and regeneration of the peripheral olfactory system and the involvement of the neuregulins. *J Comp Neurol,* 470, 50-62.
WOLSWIJK, G. (1995) Strongly GD3+ cells in the developing and adult rat cerebellum belong to the microglial lineage rather than to the oligodendrocyte lineage. *Glia,* 13, 13-26.
WOLSWIJK, G. & NOBLE, M. (1989) Identification of an adult-specific glial progenitor cell. *Development,* 105, 387-400.
WOOD, P. M. & BUNGE, R. P. (1986) Evidence that axons are mitogenic for oligodendrocytes isolated from adult animals. *Nature,* 320, 756-8.
WOODHALL, E., WEST, A. K. & CHUAH, M. I. (2001) Cultured olfactory ensheathing cells express nerve growth factor, brain-derived neurotrophic factor, glia cell line-derived neurotrophic factor and their receptors. *Brain Res Mol Brain Res,* 88, 203-13.
WOODRUFF, R. H., TEKKI-KESSARIS, N., STILES, C. D., ROWITCH, D. H. & RICHARDSON, W. D. (2001) Oligodendrocyte development in the spinal cord and telencephalon: common themes and new perspectives. *Int J Dev Neurosci,* 19, 379-85.
XIE, X., WU, G. & LEDEEN, R. W. (2004) C6 cells express a sodium-calcium exchanger/GM1 complex in the nuclear envelope but have no exchanger in the plasma membrane: comparison to astrocytes. *J Neurosci Res,* 76, 363-75.
YAMAMOTO, M., SOBUE, G., LI, M., ARAKAWA, Y., MITSUMA, T. & KIMATA, K. (1993) Nerve growth factor (NGF), brain-derived neurotrophic factor (BDNF) and low-affinity nerve growth factor receptor (LNGFR) mRNA levels in cultured rat Schwann cells; differential time- and dose-dependent regulation by cAMP. *Neurosci Lett,* 152, 37-40.
YAMAMOTO, N., FUKATA, Y., FUKATA, M. & YANAGISAWA, K. (2007) GM1-ganglioside-induced Abeta assembly on synaptic membranes of cultured neurons. *Biochim Biophys Acta,* 1768, 1128-37.
YAMAMURA, S., HANDA, K. & HAKOMORI, S. (1997) A close association of GM3 with c-Src and Rho in GM3-enriched microdomains at the B16 melanoma cell

surface membrane: a preliminary note. *Biochem Biophys Res Commun,* 236, 218-22.
YAMASHITA, T., WU, Y. P., SANDHOFF, R., WERTH, N., MIZUKAMI, H., ELLIS, J. M., DUPREE, J. L., GEYER, R., SANDHOFF, K. & PROIA, R. L. (2005) Interruption of ganglioside synthesis produces central nervous system degeneration and altered axon-glial interactions. *Proc Natl Acad Sci U S A,* 102, 2725-30.
YAN, H., BUNGE, M. B., WOOD, P. M. & PLANT, G. W. (2001) Mitogenic response of adult rat olfactory ensheathing glia to four growth factors. *Glia,* 33, 334-42.
YAN, Q. & JOHNSON, E. M., JR. (1988) An immunohistochemical study of the nerve growth factor receptor in developing rats. *J Neurosci,* 8, 3481-98.
YANG, C. R., LIOUR, S. S., DASGUPTA, S. & YU, R. K. (2007) Inhibition of neuronal migration by JONES antibody is independent of 9-O-acetyl GD3 in GD3-synthase knockout mice. *J Neurosci Res,* 85, 1381-90.
YANG, Z., ZHAO, Z. & PANJWANI, N. (1996) Gangliosides of migrating and nonmigrating corneal epithelium in organ and cell culture. *Invest Ophthalmol Vis Sci,* 37, 501-10.
YATES, A. J. & RAMPERSAUD, A. (1998) Sphingolipids as receptor modulators. An overview. *Ann N Y Acad Sci,* 845, 57-71.
YATES, A. J., VANBROCKLYN, J., SAQR, H. E., GUAN, Z., STOKES, B. T. & O'DORISIO, M. S. (1993) Mechanisms through which gangliosides inhibit PDGF-stimulated mitogenesis in intact Swiss 3T3 cells: receptor tyrosine phosphorylation, intracellular calcium, and receptor binding. *Exp Cell Res,* 204, 38-45.
YAYON, A., KLAGSBRUN, M., ESKO, J. D., LEDER, P. & ORNITZ, D. M. (1991) Cell surface, heparin-like molecules are required for binding of basic fibroblast growth factor to its high affinity receptor. *Cell,* 64, 841-8.
YEH, H. J., RUIT, K. G., WANG, Y. X., PARKS, W. C., SNIDER, W. D. & DEUEL, T. F. (1991) PDGF A-chain gene is expressed by mammalian neurons during development and in maturity. *Cell,* 64, 209-16.
YIM, S. H., FARRER, R. G., HAMMER, J. A., YAVIN, E. & QUARLES, R. H. (1994) Differentiation of oligodendrocytes cultured from developing rat brain is enhanced by exogenous GM3 ganglioside. *J Neurosci Res,* 38, 268-81.
YIM, S. H., FARRER, R. G. & QUARLES, R. H. (1995) Expression of glycolipids and myelin-associated glycoprotein during the differentiation of oligodendrocytes: comparison of the CG-4 glial cell line to primary cultures. *Dev Neurosci,* 17, 171-80.
YIM, S. H., YAVIN, E., HAMMER, J. A. & QUARLES, R. H. (1991) Exogenous GM3 ganglioside stimulates process formation and glycoprotein release by cultured bovine oligodendrocytes. *J Neurochem,* 57, 2144-7.
YIN, X., CRAWFORD, T. O., GRIFFIN, J. W., TU, P., LEE, V. M., LI, C., RODER, J. & TRAPP, B. D. (1998) Myelin-associated glycoprotein is a myelin signal that modulates the caliber of myelinated axons. *J Neurosci,* 18, 1953-62.
YONEZAWA, T., OHTSUKA, A., YOSHITAKA, T., HIRANO, S., NOMOTO, H., YAMAMOTO, K. & NINOMIYA, Y. (2003) Limitrin, a novel immunoglobulin superfamily protein localized to glia limitans formed by astrocyte endfeet. *Glia,* 44, 190-204.
YU, R. K., LEDEEN, R. W. & ENG, L. F. (1974) Ganglioside abnormalities in multiple sclerosis. *J Neurochem,* 23, 169-74.
YU, R. K. & YEN, S. I. (1975) Gangliosides in developing mouse brain myelin. *J Neurochem,* 25, 229-32.
YU, W. P., COLLARINI, E. J., PRINGLE, N. P. & RICHARDSON, W. D. (1994) Embryonic expression of myelin genes: evidence for a focal source of oligodendrocyte precursors in the ventricular zone of the neural tube. *Neuron,* 12, 1353-62.

ZENG, G., GAO, L. & YU, R. K. (2000) Reduced cell migration, tumor growth and experimental metastasis of rat F-11 cells whose expression of GD3-synthase is suppressed. *Int J Cancer,* 88, 53-7.
ZHANG, B. T., HIKAWA, N., HORIE, H. & TAKENAKA, T. (1995) Mitogen induced proliferation of isolated adult mouse Schwann cells. *J Neurosci Res,* 41, 648-54.
ZHANG, H., VUTSKITS, L., CALAORA, V., DURBEC, P. & KISS, J. Z. (2004) A role for the polysialic acid-neural cell adhesion molecule in PDGF-induced chemotaxis of oligodendrocyte precursor cells. *J Cell Sci,* 117, 93-103.
ZHENG, M., FANG, H., TSURUOKA, T., TSUJI, T., SASAKI, T. & HAKOMORI, S. (1993) Regulatory role of GM3 ganglioside in alpha 5 beta 1 integrin receptor for fibronectin-mediated adhesion of FUA169 cells. *J Biol Chem,* 268, 2217-22.
ZURITA, A. R., MACCIONI, H. J. & DANIOTTI, J. L. (2001) Modulation of epidermal growth factor receptor phosphorylation by endogenously expressed gangliosides. *Biochem J,* 355, 465-72.

1 Appendix

1.1 Equipment

Axioplan 2 fluorescent microscope	Zeiss, Herts, UK
Axioskop fluorescent microscope	Zeiss, Herts, UK
Axiovert S100 time-lapse microscope	Zeiss, Herts, UK
Axioplan 200 time-lapse microscope	Zeiss, Herts, UK
Camera controller (time-lapse)	Hamamatsu Photonics Ltd, Middlesex, UK
Clifton unstirred water bath	Bennett Scientific, Devon, UK
FACSVantage SE sorter	Becton Dickinson, Oxford, UK
Halogen hot plate/stirrer	Bibby Sterilin, Stone, UK
Leica TCS SP2 confocal microscope	Leica Microsystems (UK) Ltd, Bucks, UK
Microcentaur desk top centrifuge	MSE Ltd, Kent, UK
Olympus CK2 phase microscope	Olympus, London, UK
Olympus Fluoview FV1000 confocal	Olympus, London, UK
Sigma 4K15 centrifuge (T/C)	Sigma, Osterode am Harz, Germany
Syngene Bioimaging System	Syngene, Cambridge, UK
Tissue Culture Hoods	Medical Air Technology, Oldham, UK
Vortex Genie	Scientific Industries Inc, New York, USA

1.2 General Plasticware

Bijous – 5 ml	Bibby-Sterilin, Stone, UK
Cell strainer – 70 µl	Becton Dickinson, Oxford, UK
Coverslips	BDH, Pool, UK
Eppendorfs – 0.5 ml, 1.5 ml	Eppendorf, Cambridge, UK
Falcon tube – 15 ml, 50 ml	Becton Dickinson, Oxford, UK
Filters with receiver – 250 ml	Nalge Nunc Int, Rochester, NY, USA
Flasks – T25, T75	Bibby-Sterilin, Stone, UK
Haemocytometer	Weber Scintific Int. Ltd., Middlesex, UK
ImmEdge Pen	Vector Laboratories, Burlingame, USA
Microscope slides	BDH, Poole, UK
Needles – 21G, 23G	Becton Dickinson, Oxford, UK
Pastettes	Elkay Lab products, Basingstoke, UK
Petri dishes	Bibby-Sterilin, Stone, UK
Gilson Diamond pipette tips	Gilson, France
Plates – 24-well, 6-well	Bibby-Sterilin, Stone, UK
Polystyrene round bottom tubes – 5 ml	Becton Dickinson, Oxford, UK
Scalpels	Swann-Morton Ltd, Sheffield, UK
Slide Storage File	Ted Pella, California, USA
Syringes – 5 ml, 20 ml	Becton Dickinson, Oxford, UK
Syringe Filters – 0.2 µm, 0.4 µm	PALL Live Sciences, NY, USA
Universals – 30 ml	Bibby-Sterilin, Stone, UK

1.3 Chemicals and reagents

Absolute Alcohol	James Burrough Ltd., Essex, UK
Acetic Acid	Fisher Scientific, Leicestershire, UK
Agarose, Electrophoresis Grade	Invitrogen, Inchinnan, UK

AmpliTaq Gold DNA polymerase	Applied Biosystems, California, USA
Apo-transferrin (human)	Sigma Aldrich, Dorset, UK
Avidin/HRP	DakoCytomation, Cambridgeshire, UK
Bouins Fixative	Bios Europe, Lancashire, UK
Bovine Serum Albumin	Sigma Aldrich, Dorset, UK
B27 supplement	Invitrogen, Inchinnan, UK
BSA	Sigma Aldrich, Dorset, UK
BSA path-o-cyte	Sigma Aldrich, Dorset, UK
Cholera Toxin B subunit FITC labelled	Sigma Aldrich, Dorset, UK
Collagen Type IV (human placenta)	Sigma Aldrich, Dorset, UK
Collagenase Type I	MP Biomedicals, Ohio, USA
DAB peroxidase substrate kit	Vector Laboratories, Burlingame, USA
DMEM – 1885	Invitrogen, Paisley, UK
Deoxyribonuclease	Sigma Aldrich, Dorset, UK
dNTPs (A, C, G and T)	PerkinElmer, Bucks, UK
DNA ladder 100bp	
Donkey Serum	Abcam, Cambridge, UK
EGF	Peprotech, London, UK
Eosin	Surgipath, Cambridge, UK
FBS	Autogen Bioclear, Caine, UK
FGF	Peprotech, London, UK
Forskolin	Sigma Aldrich, Dorset, UK
Gelatin (porcine skin)	Sigma Aldrich, Dorset, UK
Gentamycin	Sigma Aldrich, Dorset, UK
Glucose	Sigma Aldrich, Dorset, UK
Glutamax	Invitrogen, Paisley, UK
L-glutamine	Sigma Aldrich, Dorset, UK
Glycerol	Fisher Scientific, Leicestershire, UK
Halothane	Rhodia Organique Fine Ltd, Bristol, UK
HBSS	Invitrogen, Inchinnan, UK
Harris' Haematoxylin	Surgipath, Cambridge, UK
Heparin	Leo Laboratories, Dublin, Ireland
Heregulin	R&D systems, Abingdon, UK
Histoclear	Fisher Scientific, Leicestershire, UK
Histomount	Hughes & Hughes Ltd, Somerset UK
Hydrochloric acid	Fisher Scientific, Leicestershire, UK
Hydrocortisone	Sigma Aldrich, Dorset, UK
Hydrogen peroxide	Fisher Scientific, Leicestershire, UK
Insulin (bovine pancreas)	Sigma Aldrich, Dorset, UK
Isopropanol	Fisher Scientific, Leicestershire, UK
L-15	Invitrogen, Paisley, UK
Laminin (human placenta)	Sigma Aldrich, Dorset, UK
Methanol	Fisher Scientific, Leicestershire, UK
$MgCl_2$	Bioline, London, UK
NaOH	Fisher Scientific, Leicestershire, UK
Neurobasal media w/o L-glutamine	Invitrogen, Paisley, UK
Normal Rabbit Serum	DakoCytomation, Cambridgeshire, UK
Normal Goat Serum	Vector Laboratories, Burlingame, USA
O.C.T. compound	VWR International Ltd, Poole, UK
Orange G	Merck, Darmstadt, Germany
PCR buffer 10x	Applied Biosystems, California, USA
PCR primers	gift from Prof. Willison's lab
Paraformaldehyde	Sigma Aldrich, Dorset, UK
PBS tablets	Oxoid Ltd, Hampshire, UK

PDGF	Peprotech, London, UK
Penicillin/Streptomycin	Invitrogen, Paisley, UK
PLL	Sigma Aldrich, Dorset, UK
Progesterone	Sigma Aldrich, Dorset, UK
Proteinase K	Sigma Aldrich, Dorset, UK
Puregene Mouse Tail Kit	Gentra Systems, Minnesota, USA
Putrescine	Sigma Aldrich, Dorset, UK
Scott's Tap Water Substitute	Surgipath, Cambridge, UK
Selenium	MP Biomedicals, Ohio, USA
Sodium chloride	Fisher Scientific, Leicestershire, UK
Soyabean trypsin inhibitor	Sigma Aldrich, Dorset, UK
Sucrose	Fisher Scientific, Leicestershire, UK
Thyroxine	Sigma Aldrich, Dorset, UK
Transferrin	Sigma Aldrich, Dorset, UK
Tri-iodo-thyronine	Sigma Aldrich, Dorset, UK
Triton X-100	Sigma Aldrich, Dorset, UK
Trypsin	Invitrogen, Paisley, UK
Vectabond	Vector Laboratories, Burlingame, USA
Vectashield with DAPI	Vector Laboratories, Burlingame, USA
Vector SG peroxidase substrate kit	Vector Laboratories, Burlingame, USA
Zinc Sulphate	VWR International Ltd, Poole, UK

1.4 PCR reagents

1.4.1 Agarose gel

2 g agarose
100 ml 1% TBS
Microwave for 1.25 minutes
Add 3.5 µl ethidium bromide

1.4.2 Loading buffer

2 ml of 2x TBE
2 ml glycerol
2 µl Orange G

1.4.3 Master Mix

For 1 sample:
13.35 µl distilled water
2.5 µl 10x PCR buffer
0.5 µl of each 100 mM dNTP: A, C, G, T
0.3 µl of each primer: PAGN3, PES4-bL, ALK5-3L
2 µl of 25 mM $MgCl_2$
0.25 µl AmpliTaq Gold DNA polymerase

1.4.4 PCR primers

1. PAGN3 (Neo^r sense)
   5'–GCC TGC TTG CCG AAT ATC ATG GTG GAA AAT-3'
2. PES4-bL (anti-sense)
   5'-GAA GAA TTC AAG ACT GTC TGT GAA ATT CTG-3'
3. AK5-3L (sense)
   5'-TCC CCC GTG AGA GTC ACT CCT GTT ACT TCC-3'

1.5 Tissue culture reagents

1.5.1 10% FBS with heregulin and forskolin (10%HF)

10% FBS
2µM forskolin
20ng/ml beta-1 heregulin

1.5.2 Bottenstein-Sato's serum free media (DMEM-BS)

25 µg/ml Gentamycin
5 ng/ml Insulin
50 ng/ml Transferrin
0.011% SATO mix (see below)
100 mM Glutamine
in DMEM (1885)

1.5.3 Collagenase

1.33% Collagenase (6.6 mg/ml)
in L15

1.5.4 Differentiation Medium

47.9 ml DMEM (1885)
50 µl Biotin (10 ng/ml)
250 µl N1 medium (see below)
250 µl hydrocortisone (10 mM)
583 µl 30% glucose
1 ml Insulin (0.5 mg/ml)

After 12 DIV Insulin is withdrawn from this media

1.5.5 Dubco's Modified Eagle Medium with 10% FBS (10% FBS)

10% FBS
25 µg/ml Gentamycin
100 mM Glutamine
in DMEM (1885)

1.5.6 Dubco's Modified Eagle Medium with 1% FBS (1% FBS)

1% FBS
25 µg/ml Gentamycin
100 mM Glutamine
in DMEM (1885)

1.5.7 OEC mitogen media with FBS (OMM+5%FBS)

75% SATO
5% FBS
500 ng/ml FGF2
50 ng/ml Heregulin
$5x10^{-7}$M Forskolin
20% ACM (astrocyte conditioned medium)

1.5.8 N1 medium

1 mg/ml Apo-transferrin
3.422 mg/ml Putrescine
1.258 µg/ml Progesterone
1.038 µg/ml Selenium

1.5.9 Neurobasal/B27

24.25 ml Neurobasal media without L-glutamine
0.5 ml B27 supplement
250 µl glutamax

1.5.10 Plating medium (PM)

25% HBSS without Ca, Mg
25% horse serum
400 µl L-glutamine
in DMEM (1885)

1.5.11 SATO mix

0.01288% BSA path-o-cyte 4
72.5 µg/ml Putrescine
180.2 µg/ml Thyroxine
151.8 µg/ml Tri-iodo-thyronine
28.1 µg/ml Progesterone
17.4 µg/ml Selenium

1.5.12 Soyabean trypsin inhibitor-DNAse (SD)

0.52 mg/ml Soyabean trypsin inhibitor
0.04 mg/ml bovine pancreas deoxyribonucelase (DNAse)
3.0 mg/ml bovine serum albumin, fraction A
in L15

1.6 Immunocytochemistry reagents

1.6.1 Acid Alcohol

70 % ethanol
1% concentrated hydrochloric acid

1.6.2 Citric Acid Buffer, pH 6.0

10 mM Citric acid

1.6.3 4% paraformaldehyde

40 g paraformaldehyde
1 l PBS
Solution heated to around 53 ºC
Sodium hydroxide added until solution became clear

1.7 Macro: “percentage of BrdU positive nuclei”

```
Dapi="blue";
BrDU="green";
None="red";                                          //Sets which colour channel holds which stain
thresh = 40                                          //Value to set threshold at

iTitle=getTitle;
imageDirectory = getDirectory("image");              //get the directory where the open image is saved
print (imageDirectory);                              //record directory path to be analysed

fList=getFileList(imageDirectory);                   //save a list of all files in directory

selectWindow(iTitle);
run("Close");                                        //close the open image

for (i=0; i<fList.length; i++){                      //main loop - for each image in directory

   if (endsWith(fList[i],"tif")) {                   //check file to open is a *.tiff" image

   open(imageDirectory + fList[i]);                  //open the file
run("RGB Color");                                    //make sure image is a 24-bit RGB file

iTitle = getTitle;                                   //get the image's name
iTitleDapi = iTitle + " (" + Dapi + ")";
iTitleBrDU = iTitle + " (" + BrDU + ")";
iTitleNone = iTitle + " (" + None + ")";             //work out names of colour channels

run("RGB Split");                                    //split image into colour channels
selectWindow(iTitleNone);
run("Close");                                        //close the 3rd channel with nothing on it

selectWindow(iTitleDapi);                            //select the DAPI channel
rename("dapi");                                      //rename it to "dapi"
run("Subtract Background...", "rolling=50");         //subtract the background

setThreshold(thresh, 255);                           //set the threshold using value at the top
run("Threshold", "thresholded remaining black"); //threshold it
run("Watershed");                                    //separate nuclei that are close together
run("Analyze Particles...", "minimum=15 maximum=500 bins=20 show=Nothing display clear");
DapiCount=nResults;                                  //analyse particles and count the number of nuclei
run("Invert");                                       //invert, to allow image to be AND-ed with BrdU

selectWindow(iTitleBrDU);                            //Select BrdU channel
rename("brdu");                                      //Rename it to “BrdU”
run("Subtract Background...", "rolling=50");         //Subtract the background
setThreshold(thresh, 255);                           //Set the threshold
run("Threshold", "thresholded remaining black"); //threshold it
run("Invert");                                       //Invert to AND with DAPI
run("Image Calculator...", "image1=[brdu] operation=AND image2=[dapi]");
                                                     //AND image with DAPI
run("Threshold", "thresholded remaining black"); //Make sure the image is still thresholded
run("Analyze Particles...", "minimum=15 maximum=500 bins=20 show=Nothing display clear");
BrDUCount=nResults;                                  //analyse particles and count the number of nuclei

selectWindow("brdu");                                //Close BrdU window
run("Close");
selectWindow("dapi");                                //Close DAPI window
run("Close");

print (iTitle + "," + DapiCount + "," + BrDUCount + "," + (BrDUCount / DapiCount * 100));}}
                    //record the number of DAPI nuclei, BrdU nuclei and calculate BrdU/DAPI*100
                    //loop back and open the next image, or end the macro if all images are done
```

1.8 Macro: “quantitation of PLP labelling”

```
thresh_red = 80;
thresh_green = 67;
thresh_blue = 128;                                  //Values to set thresholds at

iTitle=getTitle;
imageDirectory = getDirectory("image");
print (imageDirectory);
print ("Image name,Red Black,Red White,Green Black,Green White,Blue Black,Blue White")
                                    //get the name of the open image, and the folder it came from
fList=getFileList(imageDirectory);              //build a list of all images in the folder
selectWindow(iTitle);
run("Close");                                   //close window

for (i=0; i<fList.length; i++){                 //start the loop to open files
if (endsWith(fList[i],"tif")) {                 //check that file is a valid image
open(imageDirectory + fList[i]);                //if it is valid, open it

iTitle=getTitle;
iTitleRed=iTitle + " (red)";
iTitleGreen=iTitle + " (green)";
iTitleBlue=iTitle + " (blue)";                  //build names of color component images

run("RGB Split");                               //split image into colour components

string="image1=["+iTitleGreen + "] operation=AND image2=[" + iTitleBlue+"] create";
run("Image Calculator...", string);
iTitleAND = getTitle;
setThreshold(thresh_blue, 255);
run("Threshold", "thresholded remaining black");
run("Invert");                                  //get red and blue areas and threshold
getStatistics(area, mean, min, max, std, histogram);
n_blue_black=histogram[0];
n_blue_white=histogram[255];                    //measure areas
selectWindow(iTitleAND);
run("Close");
selectWindow(iTitleBlue);
run("Close");                                   //close windows

selectWindow(iTitleRed);
setThreshold(thresh_red, 255);
run("Threshold", "thresholded remaining black");
run("Invert");                                  //get red threshold
getStatistics(area, mean, min, max, std, histogram);
n_red_black=histogram[0];
n_red_white=histogram[255];                     //measure areas
selectWindow(iTitleRed);
run("Close");                                   //close window

selectWindow(iTitleGreen);
setThreshold(thresh_green, 255);
run("Threshold", "thresholded remaining black");
run("Invert");                                  //get green threshold
getStatistics(area, mean, min, max, std, histogram);
n_green_black=histogram[0];
n_green_white=histogram[255];                   //measure areas
selectWindow(iTitleGreen);
run("Close");                                   //close window

print
(iTitle+","+n_red_black+","+n_red_white+","+n_green_black+","+n_green_white+","+n_blue_black+
","+n_blue_white);}}                            //display results
```